



HAL
open science

Mechanism of microglia-neuron interaction at the node of Ranvier

Rémi Ronzano

► **To cite this version:**

Rémi Ronzano. Mechanism of microglia-neuron interaction at the node of Ranvier. *Neurons and Cognition [q-bio.NC]*. Sorbonne Université, 2022. English. NNT : 2022SORUS099 . tel-03730159

HAL Id: tel-03730159

<https://theses.hal.science/tel-03730159v1>

Submitted on 20 Jul 2022

HAL is a multi-disciplinary open access archive for the deposit and dissemination of scientific research documents, whether they are published or not. The documents may come from teaching and research institutions in France or abroad, or from public or private research centers.

L'archive ouverte pluridisciplinaire **HAL**, est destinée au dépôt et à la diffusion de documents scientifiques de niveau recherche, publiés ou non, émanant des établissements d'enseignement et de recherche français ou étrangers, des laboratoires publics ou privés.



THESE DE LA FACULTE DES SCIENCES DE SORBONNE UNIVERSITE

École Doctorale Cerveau, Cognition, Comportement (ED3C)

Présentée par Rémi Ronzano

Pour obtenir le grade de docteur
Spécialité Neurosciences

Mechanism of microglia-neuron interaction at the node of Ranvier

Soutenue le 13 Janvier 2022 devant la commission d'examen formée de :

Pr Alain Trembleau
Dr Maria-Cecilia Angulo
Pr Sonia Garel
Dr Tim Czopka
Pr Pierre Gressens
Dr Anne Desmazière
Pr Catherine Lubetzki

Président du Jury
Rapportrice
Rapportrice
Examinateur
Examinateur
Directrice de thèse
Co-directrice de thèse

Remerciements

*Tout d'abord je souhaite particulièrement remercier les membres de mon jury **Dr Maria Cecilia Angulo**, **Pr Sonia Garel**, **Dr Tim Czopka**, **Pr Pierre Gressens** et **Pr Alain Trembleau** qui me font l'honneur d'évaluer ce travail de thèse.*

*Je remercie du fond du cœur **Pr Catherine Lubetzki** et **Pr Bruno Stankoff** de m'avoir permis de poursuivre mon travail de doctorat après leur chaleureux accueil au cours de mon master 2 recherche. Je les remercie pour leur soutien constant, et pour leurs nombreux conseils tout au long de ce projet. Je remercie tout particulièrement **Pr Catherine Lubetzki**, pour les échanges si précieux que nous avons eu tout au long de ce travail et pour ses encouragements permanents.*

*Je souhaite tout particulièrement remercier **Dr Anne Desmazières** qui m'a encadré durant mon stage de M2 recherche et durant ma thèse et sans qui rien de tout cela n'aurait pu voir le jour. Je la remercie pour tout ce qu'elle m'a appris, pour les discussions scientifiques enrichissantes que nous avons eu, directement liées au projet ou non. Je souhaite également la remercier pour son dévouement total à faire de moi un meilleur scientifique que celui que j'étais en commençant ce projet.*

*Merci à tous ceux qui ont contribué à ce travail directement ou indirectement, et qui ont fait que chaque jour à l'institut était un plaisir. Merci à **Thomas Roux** d'avoir partagé le projet interaction nœud-microglie et les discussions autour de celui-ci, avec des échanges toujours fructueux. Merci à **Melina Thetiot** qui m'a formé sur de nombreuses techniques lors de mon stage et avec qui nous avons initié une partie du projet. Merci pour les nombreuses discussions que nous avons eu au départ de ce projet et qui ont été toujours très enrichissantes. Un immense merci à **Marie Stéphane Aigrot** pour son soutien sans faille, et pour sa capacité à toujours gérer simultanément de multiples situations en gardant un sens de l'humour et une bonne humeur indéfectible. Merci à **Elisa Mazuir** pour toutes nos discussions scientifiques et pour sa formation sur les cultures primaires en tant que nouvelle post doctorante. Merci à **Vasiliki Pantazou** qui nous a rejoint pour cette dernière année et avec qui nous avons partagé de nombreuses discussions scientifiques autour du projet et plus largement, la relève est assurée.*

*Merci à **Bernard Zalc**, **Nathalie Sol-Foulon** et **Marc Davenne** pour leur précieux conseils et les discussions scientifiques toujours enrichissantes. Merci à **Elodie**, ma chère voisine de bureau à la bonne humeur inébranlable. Merci à **Giorgos Tsoumpikos** et **Vanessa Oliveira Moreira** pour leur bonne humeur et les nombreux moments que nous avons partagés. Merci à tous ceux, stagiaire de licence et master qui*

m'ont permis de transmettre une partie de ce que j'ai eu la chance d'apprendre, Julien, Thomas, Federico, Lucien, Fanny et Clément. Je remercie spécifiquement Clément Perrot que j'ai formé techniquement lors de son master 2 recherche et avec qui nous avons commencé la suite du projet interaction nœud-microglie. Je suis persuadé que la suite de ce projet est assurée et que les résultats intéressants que nous avons pu obtenir jusque-là ne sont qu'un début.

Je souhaite également remercier toutes les personnes extérieures au labo qui sont intervenues dans ce projet et qui ont rendu sa réalisation possible. Je souhaite remercier Eric Marty avec qui nous avons passée de nombreuses soirées de tests qui lui ont permis de construire le prototype d'optogénétique. Je remercie Pr Jean-Michel Vallat et Laurence Richard pour leur collaboration sur la partie microscopie électronique. Je souhaite aussi remercier Chiara Stringari et Bahar Asadipour avec qui nous collaborons et qui ont partagé avec moi leur passion pour l'imagerie. Je remercie chaleureusement l'ensemble des plateformes de l'ICM, ICM.Quant (Asha, Aymeric, Basile, Claire, David, Dominique), le Fablab (Pierre), Data Analysis Core (François-Xavier), Celis (Carine, Charlotte, Laetitia). Je remercie particulièrement Charlotte pour son soutien sans faille lors de ma formation au patch. Je remercie également la plateforme de l'animalerie, de génotypage, de vectorologie et Histomics. Un merci particulier à Annick pour son assistance sur le RNAscope.

Merci à tous ceux avec qui nous avons partagé des moments de vie à l'institut et en dehors, qui ont fait de cette expérience de thèse un plaisir de chaque jour, Emeric, Rana, Corentine, Jean-Baptiste, Lucas, Karim, Laurent, José, Emilie, Sandra, Nathalie, Florine, Cristina et bien d'autres...

Merci à toute l'équipe pédagogique du département de Biologie de l'ENS Paris-Saclay qui après m'avoir transmis tant quand j'étais élève, m'a accueilli à bras ouvert, m'a fait confiance et m'a tant appris lors de mon monitorat.

De façon plus générale, je souhaite dire un grand merci à tous ceux qui œuvrent pour que le monde des sciences soit un monde plus ouvert et à ce que l'ensemble des productions du monde académique soient accessibles au plus grand nombre. Je souhaite également remercier toutes les personnes qui œuvrent à la transmission des connaissances et qui sont pour chacun d'entre nous si essentielles.

Enfin je souhaiterais remercier tous mes amis et ma famille, qui chaque jour sont là pour moi et m'encouragent en embrassant mes qualités mais surtout mes défauts. Je suis si chanceux de tous vous connaître et je ne le réalise que très partiellement.

A Françoise.

Table of contents

TABLE OF CONTENTS	5
TABLE OF FIGURES	9
ABBREVIATIONS.....	11
INTRODUCTION	15
1. THE NODES OF RANVIER, DOMAINS ALTERNATING WITH MYELIN ALONG THE AXON ...	17
1.1 A brief history of myelinated fiber description	17
1.2 Organization of the myelin sheath.....	21
1.2.1 Myelin architecture.....	21
1.2.2 Myelin composition	23
1.2.2.1 Lipid composition	23
1.2.2.2 Protein composition	24
1.3 Organization of the nodal domain.....	26
1.3.1 Structural organization	26
1.3.2 Molecular organization of the node of Ranvier	28
1.3.2.1 Ion channels.....	28
Voltage-gated sodium channels (Nav).....	28
Potassium channels	30
1.3.2.2 Cell adhesion molecules	32
L1-CAMs.....	32
GPI-anchored CAMs.....	33
1.3.2.3 Scaffolding proteins.....	33
Ankyrins	34
Spectrins	34
1.3.2.4 Perinodal extracellular matrix	35
1.3.3 Paranodes	36
1.3.4 Juxtaparanodes	38
1.4 From oligodendrogenesis to myelin sheath formation and functions.....	38
1.4.1 Multiple embryonic origin of the OPCs	38
1.4.2 From OPCs to oligodendrocytes.....	40
1.4.3 Myelin sheath formation	41
1.4.4 Myelin functions in conduction and metabolic support	43
1.4.4.1 Myelin allows fast saltatory conduction.....	43
1.4.4.2 Myelin provides metabolic support to the axons.....	43
1.5 Assembly and function of nodal domains along myelinated fibers.....	45
1.5.1 Nodal domain assembly in the CNS, a multimodal mechanism.....	45
1.5.1.1 Nodal clustering is concomitant with myelination : the classic mechanism	45
Axoglial junction at the paranode.....	45
Perinodal ECM	46
Nodal cytoskeletal scaffold	46

1.5.1.2	Nodal clustering can precede myelination : an alternative mechanism	48
1.5.2	Functions of nodal domains along the axons.....	51
1.5.2.1	Function of node-like-clusters along unmyelinated axons.....	51
1.5.2.2	Function of mature nodes of Ranvier along myelinated axons.....	53
1.6	Disruption and repair of the myelinated fibers in pathological conditions; focus on multiple sclerosis .	55
1.6.1	Multiple sclerosis and its experimental models.....	55
1.6.1.1	Multiple sclerosis, an inflammatory demyelinating disease of the CNS	55
1.6.1.2	Development of animal models: toward a better understanding of MS	57
1.6.2	Disruption of nodal domains upon demyelination	58
1.6.3	Remyelination of the CNS and reclustering of nodal domains	60
1.6.3.1	Remyelination mechanism: cell of origin and restoration of myelin pattern.....	60
1.6.3.2	Nodal reclustering	63
2.	MICROGLIA SHAPE THE CNS IN DEVELOPMENT, HOMEOSTASIS AND PATHOLOGICAL CONDITIONS	65
2.1	Microglia, a sensor of the CNS	66
2.1.1	Ontogeny of microglia.....	66
2.1.2	Microglia sense their environment dynamically.....	68
2.1.2.1	Microglia motility, a parameter set by the environment	68
2.1.2.2	Microglia chemotaxis, an oriented motility toward the damaged environment	71
2.2	Microglia contact neurons and shape circuits in homeostasis	73
2.2.1	Microglia contact directly every neuronal compartments	73
2.2.2	Microglia sculpt neuronal circuits during pre and postnatal development	76
2.2.2.1	Microglial control of neurogenesis.....	76
2.2.2.2	Microglia are active players in brain wiring.....	78
2.2.3	Microglia modulate CNS plasticity	79
2.3	Microglia modulate oligodendrogenesis and myelination	80
2.3.1	Microglia modulate the proliferation and differentiation of OPCs.....	80
2.3.2	Microglia modulate myelination pattern and structure	82
2.4	Microglia modulate remyelination : focus on MS and its experimental models	84
2.4.1	Microglia activation and early event of the disease	84
2.4.1.1	Microglia activation	84
2.4.1.2	Identification of activated microglia vs monocyte derived macrophages.....	87
2.4.1.3	Microglia activation and inflammation may drive early neuronal damages	88
2.4.2	Microglia clear myelin debris following demyelination	90
2.4.3	Microglia a key player to promote remyelination	91
2.4.3.1	Microglia promote oligodendrogenesis and remyelination	91
2.4.3.2	The microglial switch is required to promote an efficient remyelination	93
2.4.4	Microglia a potential therapeutical target to promote remyelination in MS	94
3.	NEURONAL ACTIVITY MODULATES MICROGLIA AND OLIGODENDROGLIAL FUNCTIONS	95
3.1	Effect of neuronal activity on the oligodendrocyte lineage and myelination in development, homeostasis and pathological conditions.....	96
3.1.1	Oligodendrocyte progenitor cells sense neuronal activity in developmental myelination	96
3.1.2	Neuronal activity modulates developmental myelination.....	98
3.1.3	Oligodendroglial cells participate in CNS plasticity: adaptive myelination	100
3.1.3.1	Neuronal activity modulates oligodendrocyte production	100
3.1.3.2	Neuronal activity regulates myelin patterns	101
3.1.3.3	Functions of adaptive myelination	102

3.1.4	Neuronal activity also drives remyelination processes in pathological conditions	104
3.2	Neuronal activity modulates microglia functions	106
3.2.1	Microglia motility and morphology are modulated by neuronal activity	106
3.2.2	Microglial modulations of CNS circuits depend on neuronal activity	107
3.2.2.1	Synapse elimination by microglia is modulated by neuronal activity	107
3.2.2.2	Neuronal activity drives microglia modulations of CNS plasticity	109
3.2.3	Microglia regulates neuronal hyperactivity	110
3.2.4	Neuronal activity modulates activated microglia behavior in pathology	113
AIM OF THE DISSERTATION		115
RESULTS		117
1	ARTICLE: MICROGLIA-NEURON INTERACTION AT NODES OF RANVIER DEPENDS ON NEURONAL ACTIVITY THROUGH POTASSIUM RELEASE AND CONTRIBUTES TO REMYELINATION	118
2	ONGOING WORK: NEURONAL ACTIVITY PROMOTES NODE-LIKE CLUSTER FORMATION PRIOR TO MYELINATION	151
DISCUSSION		181
1	MICROGLIA-NEURON INTERACTION AT NODES OF RANVIER: MECHANISMS AND FUNCTIONS.....	183
1.1	Potassium fluxes role in microglia-neuron interaction	183
1.1.1	Potassium fluxes stabilize microglia-neuron interaction at node of Ranvier	183
1.1.2	Do potassium fluxes participate in microglia-neuron interactions at other neuronal sub-compartments?	185
1.2	Mechanism and function of microglia-node interaction	186
1.2.1	Microglial potassium fluxes modulate remyelination	186
1.2.2	Neuronal stimulation increases microglia-node interaction and modulates microglia activation ..	187
1.2.3	Microglia-node interaction is increased following neuronal stimulation and in remyelination: an additional signal?	190
2	MULTIPLE GLIA-NEURON INTERACTIONS AT THE NODES OF RANVIER: FUNCTION IN DEVELOPMENT AND HOMEOSTASIS.....	193
2.1	The nodes of Ranvier are contacted by microglia and macroglia in homeostasis	193
2.2	Microglia and astrocytes at nodes of Ranvier: complementary functions in the modulation of action potential conduction?	195
2.3	Function of glia-neuron interactions at immature nodes	199
3	FUNCTION OF NODE-LIKE CLUSTERS IN MYELINATION AND REMYELINATION	201
3.1	Node-like clusters are formed on preferentially myelinated neurons	201

3.2	Underlying mechanism(s) of neural activity dependent formation of nodal domains	202
3.3	Neuronal activity promotes node-like cluster formation: effect on action potential conduction	203
3.4	Neuronal activity promotes node-like clusters formation: effect on myelination	204
3.5	Node-like clusters are formed prior to remyelination: an impact on repair.....	205
	REFERENCES	209
	RESUME.....	253
	SUMMARY	255

Table of figures

Figure 1: The myelinated fiber, from the first definition of the axon to the discovery of oligodendrocytes.....	18
Figure 2: Discovery of the function of myelinated fibers in conduction followed by the fine description of myelin structure.....	20
Figure 3: Ultrastructure of the myelinated fiber.	22
Figure 4: Compaction of myelin and its component.	25
Figure 5: Structural organization of the node of Ranvier.	27
Figure 6: Structural organization of voltage-gated sodium channels.	30
Figure 7: Nodal channels, scaffolding proteins and CAMs expressed at the node in the CNS.	32
Figure 8: Molecular organisation of the perinodal extracellular matrix in the CNS.	35
Figure 9: Molecular organization of the nodal domain.	37
Figure 10: Multiple embryonic origin of OPCs in the forebrain and spinal cord.....	39
Figure 11: From OPC to OL, a continuum along the oligodendroglial lineage.....	41
Figure 12: Model of myelin wrapping around axon in the CNS	42
Figure 13: Myelin provide metabolic support to the axons of the CNS.	44
Figure 14: Three mechanisms contribute to the classical process of nodal assembly in the CNS.	47
Figure 15: Node-like clusters are assembled along various populations of neurons in the CNS in mouse and zebrafish.....	50
Figure 16: Node-like clusters are associated with modulations of the conduction velocity and myelination.....	52
Figure 17: Modulations of nodal molecular composition and structure modulate action potential conduction.	54
Figure 18: Anatomical lesions and clinical course of MS patients.	56
Figure 19: Disruption of nodal domain upon demyelination.	59
Figure 20: From demyelination to remyelination.	62
Figure 21: Ontogeny of microglia in mouse.	67
Figure 22: Developmental processes of the CNS and microglia invasion.....	67
Figure 23: Microglia dynamics and morphology are modulated by the environment.	70
Figure 24: Microglia chemotaxis and the receptors involved in its modulation.	72
Figure 25: Microglia interact directly with every compartments of neurons.....	74

Figure 26: Microglia shape neuronal circuits during development.	77
Figure 27: Microglia control oligodendrogenesis and myelination.	81
Figure 28: Microglia populations upon activation and modulation of their phenotype.....	86
Figure 29: MDM invasion of the node of Ranvier precedes demyelination and induces nodal pathology.	89
Figure 30: Pro-remyelinating functions of microglia following demyelination.....	91
Figure 31: Neuronal activity modulates developmental myelination.....	98
Figure 32: Adaptive myelination induced by neuronal activity changes participates in CNS plasticity.....	103
Figure 33: Microglia modulation of CNS circuits depends on neuronal activity.	108
Figure 34: Microglia dampen neuronal hyperactivity.	112
Figure 35: Aim of the dissertation.....	116
Figure 36: Decrease of microglia-node interaction by the inhibition of Kv7 and Kca3.1.....	184
Figure 37: Neuronal activity stimulation promotes microglia-neuron interactions at nodes in myelinated and remyelinating cerebellar organotypic slices.....	188
Figure 38: Chemogenetic stimulation of neuronal activity promotes microglia expression of IGF-1 in remyelinating cerebellar organotypic slices.	189
Figure 39: Nodes of Ranvier are contacted by microglia and macroglia in homeostasis.....	194
Figure 40: Microglia might participate to modulations of nodal length and myelin thickness at nodes.....	196
Figure 41: Microglia might also participate to the astrocytic dependant reduction of conduction velocity at nodes of Ranvier.	198
Figure 42: Node-like clusters are formed prior to myelination in the dorsal column of the spinal cord in mouse.....	202
Figure 43: Node-like clusters are observed prior to remyelination in mouse organotypic cerebellar slices.	206

Abbreviations

ADP	Adenosine diphosphate
AIS	Axon initial segment
AMP	Adenosine monophosphate
AMPA	α -amino-3-hydroxy-5-methyl-4-isoxazolepropionic acid
Ank	Ankyrin
ApoE	Apolipoprotein E
ATP	Adenosine triphosphate
BDNF	Brain-derived neurotrophic factor
BTK	Bruton's tyrosine kinase
CAM	Cells adhesion molecules
cAMP	Cyclic adenosine monophosphate
Caspr	Contactin-associated protein
CCR2	C-C Motif Chemokine Receptor 2
Cd11c	Integrin subunit alpha X
CD39	Cluster of differentiation 39
ChR2	Channelrhodopsin-2
Clec7a	C-type lectin domain family 7 member A
CNO	Clozapine N-oxide
CNPase	The 2',3'-cyclic nucleotide 3'-phosphodiesterase
CNS	Central nervous system
CX3CR1	C-X3-C motif chemokine receptor 1
DAP12	DNAX activating protein of 12kDa
DIV	Days in vitro
dLGN	Dorsal lateral geniculate nucleus
DMSO	Dimethyl sulfoxide
DREADD	Designer Receptors Exclusively Activated by Designer Drugs
E	Embryonic day
EAE	Experimental autoimmune encephalomyelitis
ECM	Extracellular matrix
FN14	Fibroblast growth factor-inducible 14
GABA	Gamma-aminobutyric acid
GAD	Glutamic acid decarboxylase
GM	Grey matter
HAPLN2	Proteoglycan link protein 2
Hexb	Hexosaminidase subunit beta

Ig	Immunoglobuline
IGF1	Insulin growth factor 1
IL1-b	Interleukin 1 beta
K2P	Two pore domain potassium channels
Kca	Calcium activated potassium channel
KIF5	Kinesin Family Member 5
Kv	Voltage-gated potassium channels
LPC	Lysophosphatidylcholine
LPL	Lipoprotein Lipase
LXR	Liver X receptor
MBP	Myelin Basic Protein
MDM	Monocyte derived macrophage
MDM	Monocyte derived macrophage
MOG	Myelin/oligodendrocyte glycoprotein
MS	Multiple sclerosis
Nav	Voltage-gated sodium channel
Nfasc	Neurofascin
NMDA	N-methyl-D-aspartate
OCM	Oligodendrocyte conditioned medium
OL	Oligodendrocyte
OPC	Oligodendrocyte progenitor cell
P	Post-natal day
PDGFR α	Platelet derived growth factor receptor α
PLP	Proteolipid protein
PNS	Peripheral nervous system
RGC	Retinal ganglion cell
Spp1	Secreted phosphoprotein 1
STED	Stimulated emission depletion
t-SNE	t-distributed stochastic neighbor embedding projection
TEA	Tetraethylammonium
Thik-1	TWIK-related halothane-inhibited K ⁺ channel 1
TLR	Toll like receptor
Tmem119	Transmembrane Protein 119
TNF	Tumor Necrosis Factor
TNFR	Tumor Necrosis Factor receptor
TPA	Tetrapentylammonium
TRAAK	Potassium channel subfamily K member 4
TREK-1	Potassium channel subfamily K member 2

TREM2	Triggering receptor expressed on myeloid cells-2
TTX	Tetrodotoxine
TWEAK	TNF-associated weak inducer of apoptosis
WM	white matter

Introduction

Between the end of the 19th and the beginning of the 20th century, many anatomists dedicated their work to the description of the main central nervous system cell types. From their observations, the major types of glia (astrocytes, oligodendrocytes and microglia) could be defined and some of their functions suggested. However, the limited amount of tools that they could use let them with only hypothetical answers to the question: “what is the function of glia?” (Ramón y Cajal, 1909). In the following decades and until the end of the 20th century, the field of neuroscience mainly focused on deciphering the function of the signaling units of the circuits, neurons. It is not until the beginning of the 21st century that technological advances allowed glial functions to be assessed more consistently. Seminal studies could notably demonstrate the role of glial cells in neurogenesis, cell migration, chemotaxis, metabolic support and insulation most of which had been suggested upon glia first observation (Somjen, 1988). As we have known for more than a century in the case of neurons, it is now becoming evident that each main population of glial cells is made of heterogeneous subpopulations that show functional diversity (Marques et al., 2016; Zhang et al., 2016; Li et al., 2019; Masuda et al., 2019; Bruggen et al., 2021).

In the two last decades, it has been demonstrated that glial cells communicate with neurons and participate to their development and function throughout life. These communications are made through the secretion of molecular cues or directly by membrane to membrane contacts, and modulate neuronal survival, wiring, plasticity and activity (Marín-Teva et al., 2004; Parkhurst et al., 2013; Squarzoni et al., 2014; Badimon et al., 2020). Lastly, growing evidence show that glial cell functions are also modulated by neuronal activity, and take part into the plasticity of the central nervous system by refinement of brain wiring with for instance, synaptic pruning or adaptive myelination (Schafer et al., 2012; Gibson et al., 2014). In pathological conditions, glial communications with neurons are disrupted and lead to neuronal dysfunctions. Recently, the development of cutting-edge technologies allowed to demonstrate the role of neuronal activity in repair. These methods further give the opportunity to neuroscientists to assess how neuronal activity modulates neuroglial communication and promotes efficiently repair. Therefore, the study of neuroglial interactions through the lens of glial diversity and neuronal activity may pave the way for a better understanding of the central nervous system in development, homeostasis and pathology.

1. The nodes of Ranvier, domains alternating with myelin along the axon

1.1 A brief history of myelinated fiber description

In the mid-16th century, a physician considered as the father of the modern anatomy, Andreas Vesalius (1514-1564), distinguished for the first time the grey and white matter (Vesalius, 1543). In the beginning of the 18th century, Antoni van Leeuwenhoek (1632-1723), using the spinal nerve of a ruminant, discovered that nerve were made of “vessels of an indescribable fineness” with a diameter that is “a third larger than the canal” (van Leeuwenhoek, 1719). The description of the myelinated fiber was further refined by Felice Gaspar Fontana (1730-1805), who noted that elementary structures of the nerves were made of cylinders “endowed by an envelope in the shape of an outer sheath” (Fontana, 1781). In the first part of the 19th century, Christian Gottfried Ehrenberg (1795-1876) suggested a continuity between grey and white matter and specify for the first time that “nerve marrow” strictly refer to the sheath and not the entire nerve fiber (Ehrenberg, 1833). Ehrenberg observations paved the way for Robert Remak (1815-1865) first description of the axon as a primitive band (Remak, 1836) followed by Theodor Schwann (1810-1882) who adopted Remark’s theory describing two types of fibers, white nervous fibers and grey fibers named organic fibers (Schwann, 1839)(Figure 1A-B).

In 1854, the German pathologist Rudolf Ludwig Virchow (1821-1902), proposed for the first time that the nervous system is comprised of an independent non-neuronal elements named neuroglia (Virchow, 1858). Although he did not associate it strictly to the nervous system, Virchow also coined the term of myelin that derives from the Greek term *myelos* standing for “marrow”. Only in 1872, Louis-Antoine Ranvier (1835-1922) using osmium based staining observed Schwann cells nuclei along myelin sheath (Ranvier, 1872). Later on, using carmine, Louis-Antoine Ranvier showed that axonal membrane was accessible at the site of regularly spaced “annular constrictions”, the nodes of Ranvier (Ranvier, 1878)(Figure 1C). He observed that, the internodes alternating with “annular constrictions” nested the nucleus of one Schwann cell per internode located at equal distance from each myelin interruption. Although, his initial hypothesis that myelin was “essentially a liquid material” was proved wrong, he postulated that the organisation of myelinated nerve could allow a “more perfect” transmission by acting has electrical insulation (Ranvier, 1878; see review in Lubetzki et al., 2020a). An hypothesis that would take several decades to be experimentally tested by Ralph Stayner Lillie (1875-1952), using an iron wire covered by glass insulant with periodic breaks (Lillie, 1925).

While the nodes of Ranvier had been identified by Louis Antoine Ranvier in the PNS, he postulated that these structures were absent from the CNS. Thus, even though constrictions were

observed soon after his work along myelinated axons in the spinal cord (Tourneux and Le Goff, 1875), the idea that nodes were also formed along myelinated axons of the CNS was accepted in the scientific community only after several decades when Santiago Ramon y Cajal, described nodes in the CNS (Ramón y Cajal, 1909)(Figure 1D).

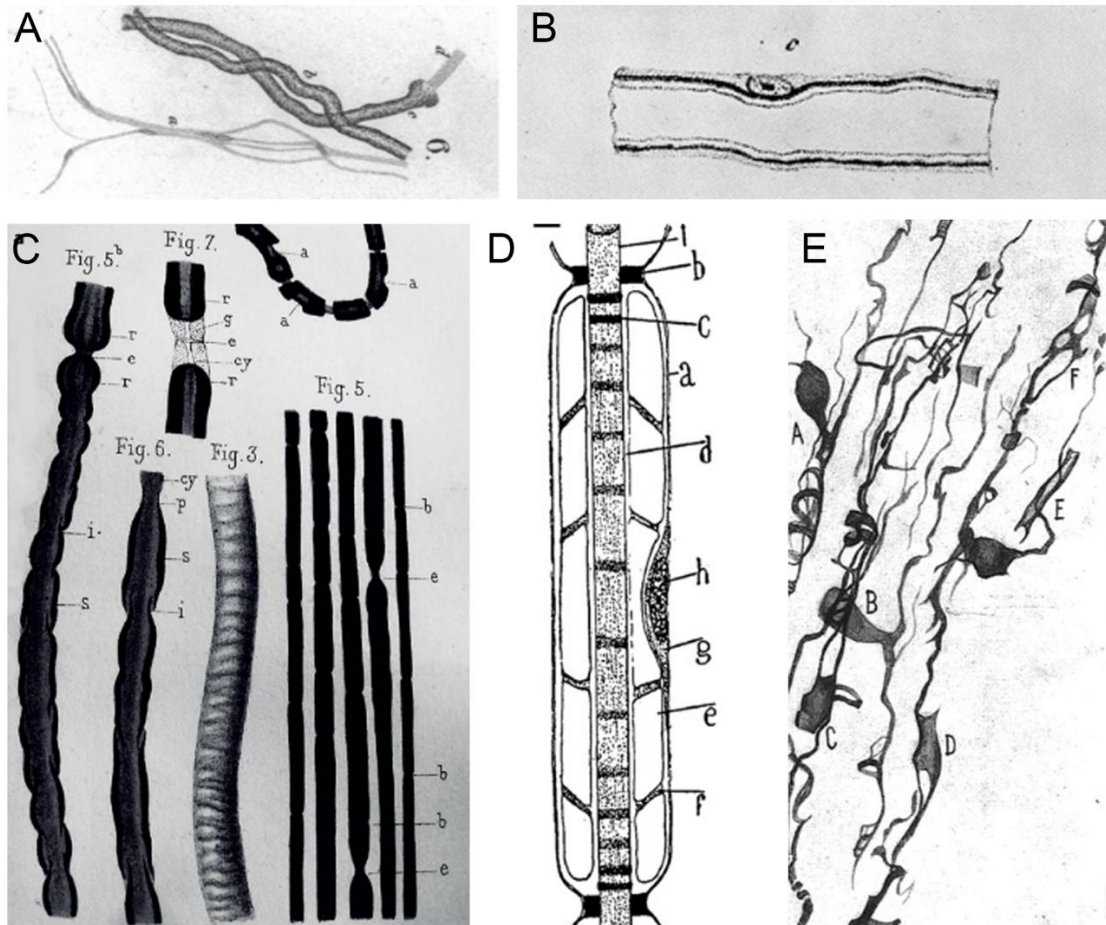


Figure 1: The myelinated fiber, from the first definition of the axon to the discovery of oligodendrocytes.

(A) Drawing by Robert Remak of two myelinated fibers with axons emerging on the right and unmyelinated fibers ("organic fibers") at the bottom. (B) Original drawing from Theodor Schwann showing a nucleus in Schwann sheath of a calf nerve fiber. (C) Drawings of the "annular constrictions" along sciatic nerve fibers stained using silver nitrate by Louis-Antoine Ranvier. (D) Schematic of a peripheral internode by Santiago Ramon y Cajal. (E) The "third element", oligodendrocytes, stained using silver carbonate with fine processes that spirals around invisible myelin sheaths. Drawing by Pio del Rio Hortega. Figure adapted from Boullerne, 2016 and Lubetzki et al, 2020.

Although the worldwide known Spanish histologist Santiago Ramon y Cajal could confirm the neuron doctrine using improved Golgi staining techniques (Cajal, 1894), and identified astrocytes as the first non-neuronal cells of the central nervous system (Ramón y Cajal, 1911), he could not visualize what he named “the third element”. The development of new staining protocols using silver carbonate by Pio del Rio Hortega (1882-1945) led him to identify “the third element” unravelling not only microglia, but also oligodendroglia (del Río-Hortega, 1919d, 1921, 1928)(Figure 1E). Since silver carbonate left myelin unstained, it is only one year later that Rio-Hortega together with Wilder Penfield (1891-1976) postulated that oligodendroglia were the myelinating cells of the CNS (del Río-Hortega, 1922; Penfield, 1924).

In the mid-20th century, the development of electrophysiology and microscopy allowed a better understanding of the structure, composition and function of the myelinated nerve in the propagation of action potential. First, Ichiji Tasaki (1910-2009), showed using anaesthetic along defined portion of an isolated nerve fiber that the conduction of an electrical stimuli was blocked when at least three nodes were exposed. This observation led him to suggest that action potentials could jump from one node to another, describing for the first time the saltatory conduction along myelinated nerve (Tasaki, 1939). Andrew Fielding Huxley (1917-2012) one of the two fathers of modern electrophysiology together with Alan Lloyd Hodgkins (1914-1998), further described, in a collaborative work with Robert Stampfli (1914-2002), the propagation of an electrical stimuli along a myelinated fiber. In their study, the two scientists showed, using isolated sciatic nerves from frogs, the saltatory conduction of an electrical stimuli from one node to the next (Huxley and Stampfli, 1949)(Figure 2A), a finding that was soon confirmed on intact myelinated frog fibers by Bernhard Frankenhaeuser (1915-1994) (Frankenhaeuser, 1952).

On the way to a better understanding of myelin organisation and structure, the development of electronic microscopy allowed the visualization of myelin spirals in the PNS by Betty Ben Geren (Geren, 1954)(Figure 2B). The observation of compacted spirals of plasma membrane in the PNS was followed in 1962, by the work of Mary Barlett and her husband Richard Paul Bunge that produced micrograph of myelin spirals around axons of the CNS (Bunge et al., 1962; Bunge, 1968)(Figure 2C-D). Geren observations of Schwann cells myelination further led her to hypothesize that the inner mesaxon of Schwann cells could wrap the axons while excluding the cytoplasm from myelin allowing its compaction, a mechanism that stayed debated for CNS myelination until a recent seminal work by Snaidero and collaborators (Snaidero et al., 2014).

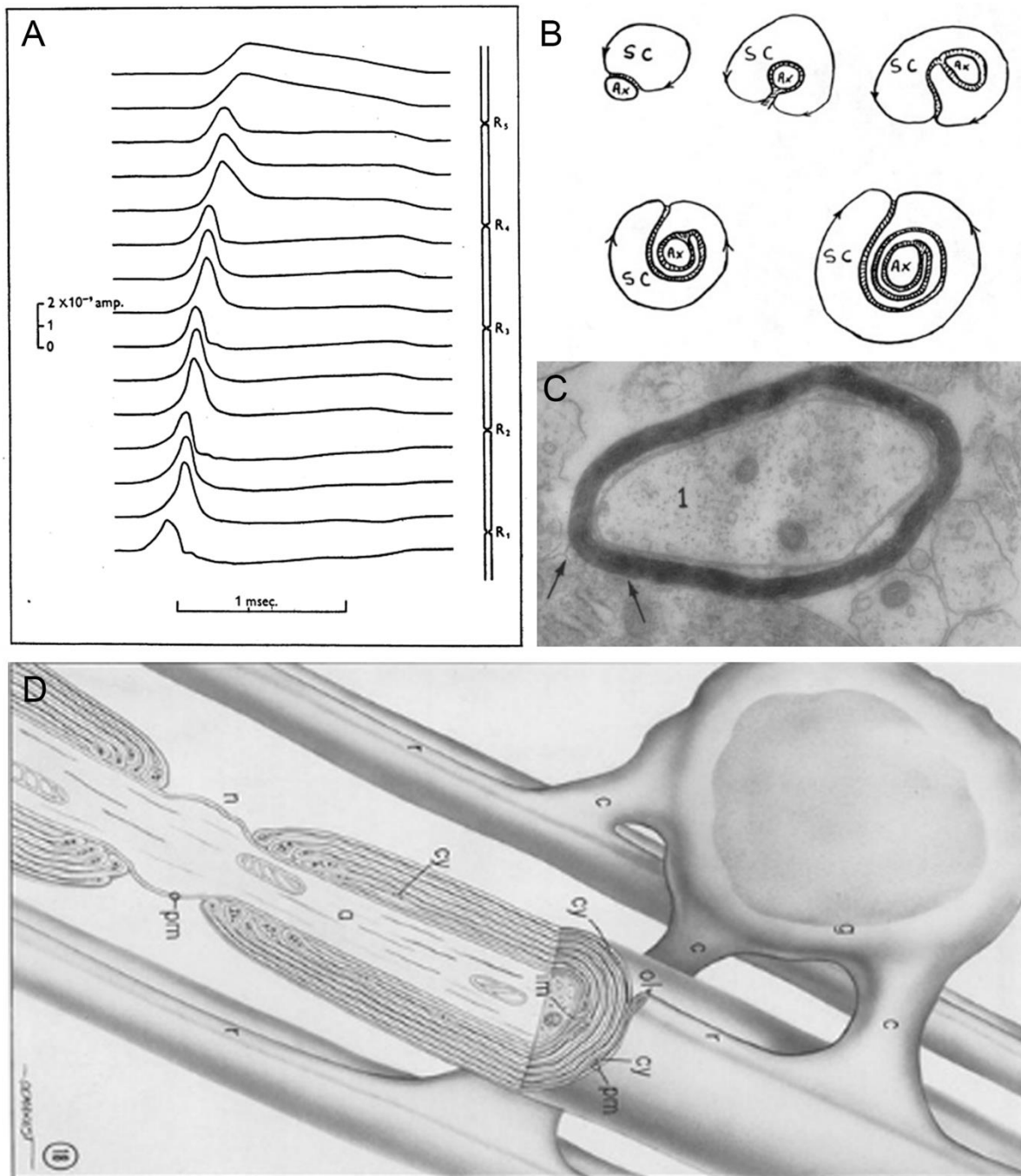


Figure 2: Discovery of the function of myelinated fibers in conduction followed by the fine description of myelin structure. (A) Original tracing of recordings obtained by Andrew Fielding Huxley and Robert Stampfli, showing the propagation of a stimulus along an isolated fiber of a frog sciatic nerve. (B) Original drawing by Betty Ben Geren showing a Schwann cell forming spirals around an axon. (C) Original micrograph of myelin sheath surrounding an axon in the CNS. (D) Bunge's drawing, showing with an impressive accuracy an oligodendrocyte wrapping axons. Figure adapted from Huxley and Stampfli, 1949; Bunge et al, 1962 and Boullerne, 2016.

1.2 Organization of the myelin sheath

Although glial cells enwrapping axons are shared by the clade of bilaterians (Hartline, 2011), the compact myelin is present only in jawed vertebrates (Zalc et al., 2008) and few invertebrate taxa (Hartline and Colman, 2007). Myelin is a lipid-rich structure formed by the wrapping of multiple compact layers of plasma membrane around axons. This evolutive innovation increasing drastically local radial resistance allowed the increase of action potential conduction velocity by a factor up to 50 folds. Such a conduction speed would otherwise have required to increase drastically the size of the nervous fibers (Salzer and Zalc, 2016). Although the “giant axon” strategy has been selected in several taxa of invertebrates (e.g cephalopods and their giant axons), the development of a nervous system as intricately wired as, for instance in mammals, would not have been possible without myelin (Hartline and Colman, 2007; Zalc et al., 2008). Across the nervous system, two types of cells are producing myelin, the Schwann cells restricted to the PNS and the oligodendrocytes (OLs) that myelinate axons in the CNS. While Schwann cells myelinate only one internode of a unique fiber, oligodendrocytes are able to form a range of 20 to 60 internodes along different axons in mice (Matthews and Duncan, 1971; Chong et al., 2012).

1.2.1 Myelin architecture

Owing to the tight compaction of myelin, it is thanks to the development of electronic microscopy that the fine structure of myelin has been described. Indeed, compact myelin shows a periodicity of about 12nm with an alternation of electron dense and electron light layers named respectively “major dense line” and “intraproduct line” (Aggarwal et al., 2011a) (Figure 3B). The “major dense line” corresponds to the tight apposition of the two cytoplasmic layers of the myelin membrane whereas the “intraproduct line” corresponds to the apposition of the two outer layers of the membrane. The great compaction of myelin excludes cytoplasmic materials from the internode, leaving small uncompacted regions, the innermost and outermost tongues, the paranodal loops and in the PNS the Schmidt-Lanterman incisures (Figure 3). Myelin sheaths length often exceed 500 microns in the PNS (Hildebrand et al., 1994) and range from 50 to 200 microns in the CNS (Tomassy et al., 2014; Stedehouder et al., 2017, 2019), making uncompacted structures along internode necessary paths from OL cytoplasm to their sheaths. Uncompacted regions of the myelin sheath are essential for lipids and proteins transport along the growing internode during development. In fully myelinated fibers, the uncompacted regions may play an essential role in the distribution of metabolites and ions, providing a necessary route for the myelinating cell to metabolically support to the axon (Arroyo and Scherer, 2000; Simons and Nave, 2016). The visualization of the uncompacted regions of the myelin

sheath with a better accuracy was allowed in the last decade, by the development of high pressure freezing electronic microscopy (Möbius et al., 2010). The accurate measure of the myelin (including inner tongue) and periaxonal space thickness using this methodology was used by Cohen et al, to demonstrate the important contribution made by the periaxonal and paranodal submyelin spaces in action potential conduction along myelinated fibers (Cohen et al., 2019).

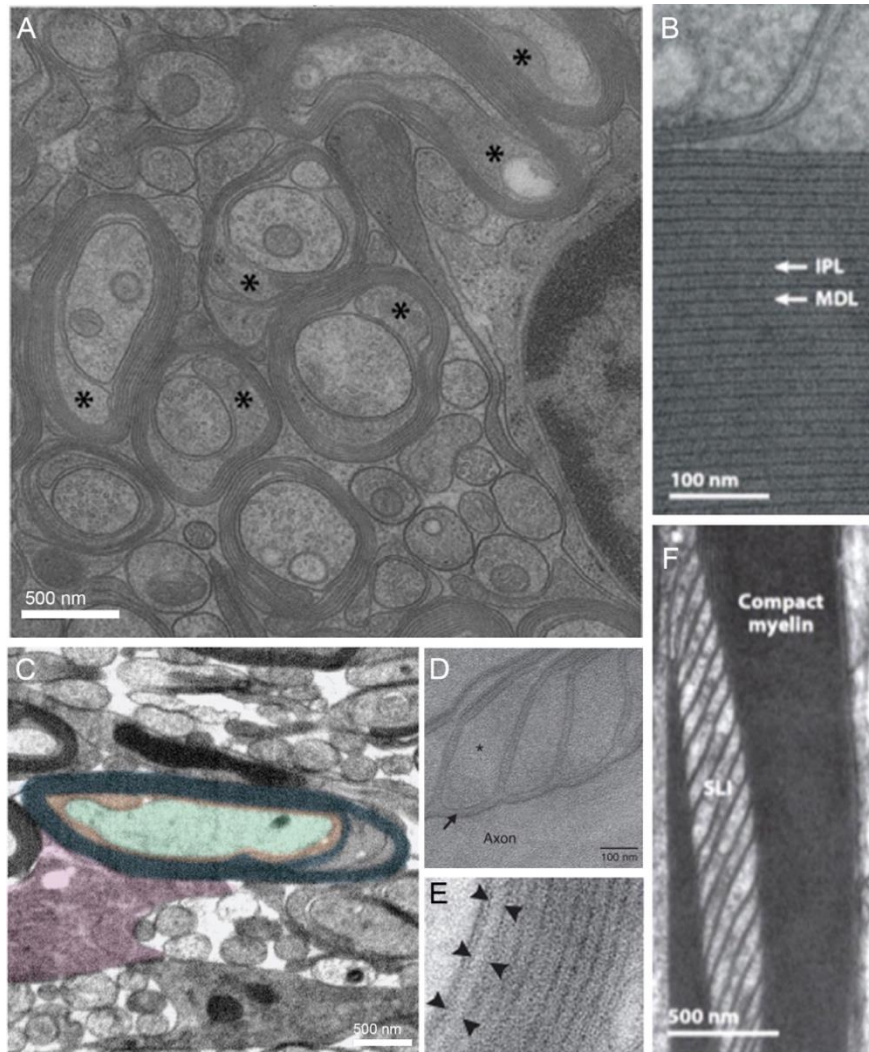


Figure 3: Ultrastructure of the myelinated fiber.

(A) Ultrastructure of a fresh mouse optic nerve at post-natal day 14. The asterisks show the large inner tongue at this age, resolved with a better accuracy using high pressure freezing electronic microscopy. (B) Higher magnification of the dense myelin showing its periodicity with the alternation of major dense line (MDL) and intraperiod line (IPL). (C) Cross section of an axon of the optic nerve showing the axolemma (filled in green), the inner tongue (filled in orange), the dense myelin (filled in blue) and the outer tongue (filled in purple). (D) Micrograph showing with a high magnification the paranodal loop (asterisk), another uncompacted structure of the myelin. (E) High pressure freezing electronic microscopy, allows the fine visualization of the periaxonal space an important modulator of action potential conduction. (F) In the PNS, Schmidt-Lanterman incisures are specific structures of uncompacted myelin that allow to connect the Schwann cells cytoplasm to the myelin inner layers. Figure adapted from Möbius et al, 2010; Nave and Werner, 2014; Snaidero et al, 2014 and Cohen et al, 2019.

1.2.2 Myelin composition

The global composition of myelin was analysed following the improvement of CNS membranes purification methods by William Norton, which gave access to purified fraction of CNS myelin (Norton and Poduslo, 1973). Using purified myelin, it was found that the dry weight of myelin is made of 70 to 85% of lipids and only 15 to 30% of proteins (Norton and Cammer, 1984) giving to myelin its insulating function.

1.2.2.1 Lipid composition

Myelin lipid composition is unusual compare to other membranes, with three major categories: cholesterol, phospholipids and glycosphingolipid with an approximate molar ratio of 2:2:1 (O'Brien and Sampson, 1965; Norton and Poduslo, 1973), that is greatly conserved between PNS and CNS myelin. This ratio allows for myelin lipids a high lateral mobility, the percentage of cholesterol being a key parameter to modulate membrane's fluidity (Rawlins, 1973; Demel and De Kruffy, 1976).

Cholesterol constitutes 25% of myelin lipids, which represent a twofold enrichment compared to other plasma membranes. Cholesterol, is necessary for myelin formation and constitute a limiting factor for myelin growth (Saher et al., 2005; Mathews et al., 2014). Interestingly, preventing cholesterol synthesis in OL does not entirely prevent cholesterol incorporation to myelin sheath, probably due to the horizontal transfer of cholesterol from astrocytes (Nave and Werner, 2014). In the formed myelin sheath, cholesterol limits membrane fluidity, and further interacts with major myelin protein to improve membranes compaction both in the PNS (Saher et al., 2009) and the CNS (Simons et al., 2000; Werner et al., 2013).

Two key phospholipids of the myelin sheath are plasmalogens and phosphoinositides. Although their functions are not yet fully understood, plasmalogens deficient mice produce a reduced amount of myelin in the CNS (Rodemer et al., 2003). Plasmalogens are also known to prevent oxydations of unsaturated membrane lipid (Lessig and Fuchs, 2009) and constitute the source of lipid mediators of inflammation (Wallner and Schmitz, 2011). Given their potential function in modulating inflammation, plasmalogens might be implicated in demyelinating diseases. Furthermore, the phosphoinositide phosphatidylinositol-(3,4,5)-triphosphate (PI(3,4,5)P3), although it represents a very small proportion of myelin lipids, is enriched at the leading edge of the inner tongue and regulates myelin growth (Snaidero et al., 2014).

Galactosylceramides and sulfatides, two sub-groups of glycosphingolipids, are the most specific lipids of myelin. Mice unable to synthetize them are able to synthetize myelin but display a higher proportion of myelin unfolding and vacuole formation, underlying the importance of glycosphingolipid in myelin structure (Coetzee et al., 1996). Moreover, these mice suffer from action

potential conduction defect associated with a higher accessibility of juxtaparanodal potassium channels indicating paranodal disruptions (Bosio et al., 1996; Coetzee et al., 1996).

1.2.2.2 Protein composition

As indicated above, proteins comprise a rather low fraction of myelin composition. Nonetheless, they are necessary to allow myelination, myelin compaction and maintenance. Even though the use of cutting edge mass spectrometry technologies on myelin fraction led to the identification of more than a thousand proteins in the PNS and CNS of mice and zebrafish (Jahn et al., 2020; Siems et al., 2020, 2021), myelin has the particularity to be highly enriched in a relatively small diversity of main proteins. This section will focus on the main proteins of myelin in the CNS, the identity of which partially overlap with the PNS. However, two of the main PNS myelin proteins, myelin protein zero (PO, 50-70% of myelin protein) and peripheral myelin protein 22 (PMP-22, 2-5% of myelin protein), are totally absent from myelin in the CNS (Garbay et al., 1988, 1989, 2000; Snipes et al., 1992; Notterpek et al., 1999).

The proteolipid protein (PLP) and its smaller splice isoform DM20 are the most abundant proteins of myelin in the CNS and comprise 30 to 45% of its protein content. While PLP is expressed in mature OLs, DM20 is expressed as early as in OPCs (Timsit et al., 1995; Spassky et al., 2001). PLP/DM-20 deficient mice do not show a strong impairment of myelin structure with only subtle ultrastructural changes observed (Klugmann et al., 1997). Nonetheless, whereas PLP/DM-20 deficient mice assemble compact myelin, they subsequently show axonal swelling and degeneration, phenomena that were also observed in patients with PLP mutations. These defects highlight the importance of PLP/DM-20 in myelin maintenance, and their potential role in the stabilisation of axonal local support (Griffiths et al., 1998; Garbern et al., 2002).

The myelin basic protein (MBP) is the second most abundant protein of myelin in the CNS and account for 22 to 35% of myelin protein content (Jahn et al., 2009). The well-known mouse mutant missing functional MBP named *shiverer*, shows uncompacted myelin and hypomyelination throughout the CNS (A.Privat et al., 1979; Rosenbluth, 1980). The lack of myelin compaction results in the development of tremor in the second postnatal week, a typical symptom for conduction failure in the spinal cord. A similar phenotype is found in Evan *shaker* rats in which MBP is mutated (Carré et al., 2002). MBP is localised between the intracellular layer of the plasma membrane. While self-repulsive in solution, MBP interaction with negatively charged membrane phospholipids neutralizes its charges and triggers its polymerisation (Aggarwal et al., 2013). MBP polymerisation joins together the two intracellular layers of the plasma membrane in a zipping like mechanism leading to membrane compaction and to the formation of a diffusion barrier (Aggarwal et al., 2011b, 2013).

2',3'-cyclic nucleotide 3'-phosphodiesterase (CNPase) is a membrane anchored protein that consist of two folded domains with a lipidated tail (Myllykoski et al., 2016). Amongst the highly enriched myelin protein, CNPase is the only protein that localizes at the non-compacted myelin (Trapp et al., 1988), a property that is in line with the defect observed in CNPase deficient mice. Indeed, CNPase-deficient mice show a defect in the formation of the inner tongue, and a decrease in the amount of uncompact myelin (Edgar et al., 2009; Snaidero et al., 2014). Conversely, CNPase overexpression leads to an increased formation of uncompact myelin (Gravel et al., 1996; Yin et al., 1997). Recent studies showed that it is actually the balance between MBP and CNPase that control myelin compaction (Snaidero et al., 2014, 2017). CNPase interaction with the actin cytoskeleton, is necessary to maintain uncompact myelin (e.g inner tongue, paranodal loops) and allows for the metabolic support of axons (Snaidero et al., 2017), preventing the axonal degeneration observed in CNPase deficient mice (Lappe-Siefke et al., 2003; Edgar et al., 2009).

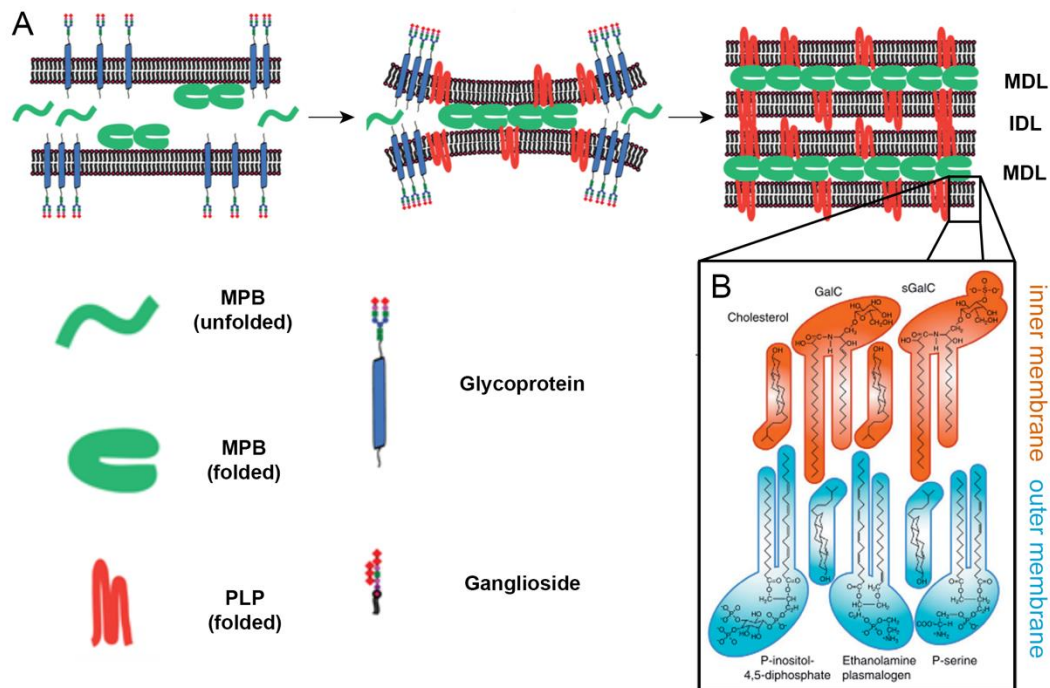


Figure 4: Compaction of myelin and its component.

(A) Model of myelin compaction showing the interactions at the extracellular and cytoplasmic side of the membrane. The polymerisation of MBP leads to the very close apposition of the two inner membranes whereas interactions between PLP extracellular domains tight outer membranes together. This organisation leads to the formation of major dense line (MDL) and intraperiod line (IPL). (B) Schematic of the myelin lipid bilayer showing its asymmetric composition with examples of the main lipids that myelin comprises. Figure adapted from Aggarwal et al, 2011 and Bakhti et al, 2014.

1.3 Organization of the nodal domain

Since the first description of “annular constrictions” by Louis-Antoine Ranvier back in the late 19th century, the development of electronic microscopy, electrophysiology and more recently the considerable progress of molecular biology has extended our knowledge about nodes of Ranvier. While nodes are restricted to about 1% of the length of the myelinated fiber, they are responsible for the rapid depolarization and repolarization of the axolemma and sustain electrical impulses thanks to the dense clustering of sodium and potassium channels at their level.

1.3.1 Structural organization

Nodes of Ranvier are small unmyelinated domains with a typical length ranging from 1 to 2 microns with variation that can extend from 0.5 to 4 microns (Arancibia-Cárcamo et al., 2017). The variation of nodal length is partly explained by neuronal identity, with for instance in the neocortex, GABAergic neurons having shorter nodal gap than excitatory neurons independently from the axonal diameter (Micheva et al., 2016, 2018). However, neuronal identity explains only partly nodal length variation, and nodal length varies to a factor up to 4 along individual axons (Arancibia-Cárcamo et al., 2017). Nodes of Ranvier form along the axon periodic constrictions, where the diameter of the axon is reduced compared to its diameter at the internode (Landon and Williams, 1963). These constrictions are notably due to the reduction of both the number and the phosphorylation of neurofilaments at the nodes (Peters et al., 1991; Salzer, 2003). Beneath the axolemma, there is an electron dense layer that must correspond to the dense network of cytoskeletal scaffold that anchor nodal proteins (Rosenbluth, 1983). The use of freeze fracture technique has provided an estimate of sodium channels density of 1000 to 2000 channels/ μm^2 at the nodes (Rosenbluth, 1976), in line with electrophysiological recordings which allowed to estimate a density of 1500 channels/ μm^2 by measuring gating current (Chiu, 1980). The first ultrastructural observations of sodium channels at the node further showed that the channel distribution was not homogenous suggesting a more complex organisation by the cytoskeleton (Waxman and Ritchie, 1993). Recently, the use of super resolution light microscopy (stimulated emission depletion, STED), allowed to further describe the fine spatial organisation of the nodal proteins in the CNS as well as in the PNS. Intriguingly, nodal proteins showed a conserved 200 nm lateral periodicity with an alignment of transmembrane proteins with the actin cytoskeleton (D’Este et al., 2016, 2017).

The repolarisation of the axolemma at the node requires an important amount of energy, which led scientists to study the localisation of mitochondria along the axons (Fabricius et al., 1993).

Using electronic microscopy early studies showed their presence at the nodal domain, with more recently the description of an enrichment of this organelle at nodal domains compared to internodes in the PNS (Perkins and Ellisman, 2011). In the CNS however, there is no enrichment of mitochondria at nodes and rather a decreased density compared to the internode (Edgar et al., 2008; Ohno et al., 2011). In the CNS, it was further observed using live imaging that neuronal activity modulates the transport of mitochondria along the axons with a stabilisation of these organelles at nodal domains when the activity is increased (Ohno et al., 2011). The mechanism of activity dependent recruitment of mitochondria at nodes has been further suggested, with a major role played by Ca²⁺ signalling (Zhang et al., 2010; Ohno et al., 2011).

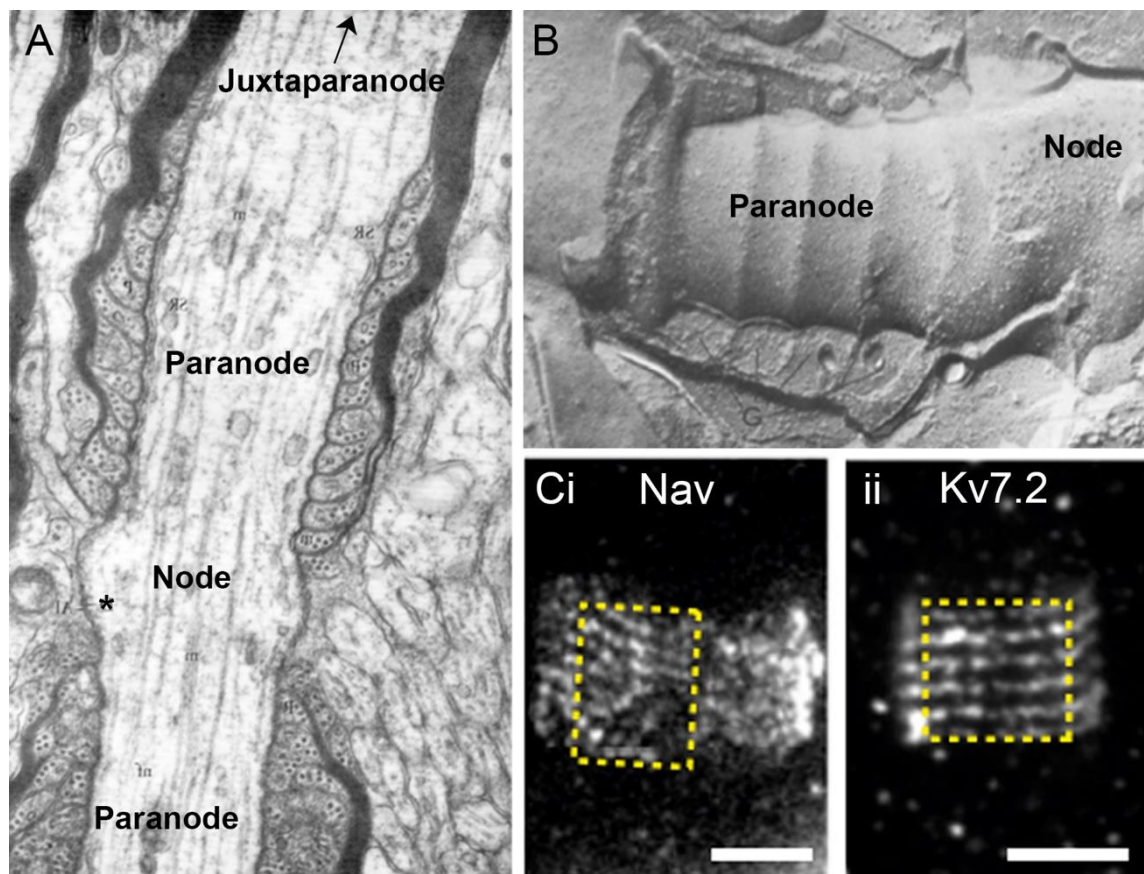


Figure 5: Structural organization of the node of Ranvier.

(A) Ultrastructure of the nodal domain along the axon of a rat basal ganglion. The nodal axolemma shows a dense coating (highlighted with an asterisk), and is flanked by the paranodes identified thanks to the paranodal loops. (B) Freeze fracture of an axon from the CNS of a frog. The apparent roughness at the nodal axolemma are densities corresponding to intramembraneous proteins. (C) Organization of Kv7.2 and Nav channels along the node of the sciatic nerve showing a periodic alignment of nodal proteins visualized using STED microscopy. (C) Scale bars: 1 μ m. Adapted from Peter et al, 1976; Rosenbluth et al, 1976 and D'Este et al, 2017.

1.3.2 Molecular organization of the node of Ranvier

The ability of the nodes of Ranvier to generate a depolarization of the axolemma followed by its repolarisation requires an important enrichment of ion channels at these short domains of the axon. The clustering of ion channels is allowed by the interaction of these channels with, a large range of cell adhesion molecules (CAMs), scaffolding protein anchored to the cytoskeleton and by the perinodal ECM. This section, focusing on the CNS of mammals, will describe each of these protein classes and their distribution at the node of Ranvier.

1.3.2.1 Ion channels

In a seminal study for which they won the Nobel prize in 1963, Andrew Fielding Huxley and Alan Lloyd Hodgkins, demonstrated the basis for action potential in the squid giant axon (Hodgkin and Huxley, 1952). In their study, using voltage-clamp, they showed that the depolarisation of the axolemma results from a sodium current generated in a voltage dependent manner, followed by a potassium voltage-dependant current allowing the repolarisation of the axolemma. This description, made using a non-myelinated axon, paved the way for the subsequent description of the conduction in myelinated fibers, along which nodes of Ranvier enable action potential regeneration. While sodium voltage-gated channels responsible for the depolarisation of the axolemma are restricted to the nodal domains (Black et al., 1989; Caldwell et al., 2000), potassium channels that mediate the repolarisation are more diverse and localize at nodes, juxtaparanodes and more rarely at paranodes (Wang et al., 1993; Devaux et al., 2003; Devaux, 2004; Battefeld et al., 2014; Hirono et al., 2015; Brohawn et al., 2019; Kanda et al., 2019).

Voltage-gated sodium channels (Nav)

The axolemma at the node of Ranvier is highly enriched in Nav channels (see above). Owing to their voltage-gated activation, they critically regulate neuronal excitability and are responsible for the rising depolarisation phase of the action potential. Nav channels are self-inactivating with a kinetic of few milliseconds (William A. Catterall, 2000), and selective for sodium (Na⁺) with a small permeability to calcium ions (Hanemaaijer et al., 2020). The structural organization of this channel consist of a central pore-forming α -subunit of 260 kDa, associated with one or more isoform of the 30 to 40 kDa auxiliary β -subunits (Goldin et al., 2000)(Figure 6). The pore-forming α -subunit is sufficient for the functional expression of the channel, and its association with β -subunits modulates its kinetic, voltage dependence and membrane targeting (Namadurai et al., 2015).

In mammals, ten genes of the Scna family encode α -subunits, Nav1.1 to Nav1.9 and one atypical Na_x (Goldin et al., 2000; Namadurai et al., 2015). Of these ten α -subunits, the main subunits found at the nodes in the CNS are Nav1.1, Nav1.2 and Nav1.6. The main α -subunit expressed at nodes of Ranvier are Nav1.2 and Nav1.6. Nav1.2 is localized mainly at the immature nodal domain and is further replaced by Nav1.6 in mature node as myelination is completed (Boiko et al., 2001). The switch from Nav1.2 to Nav1.6 requires myelination to proceed and could allow nodal domains to sustain higher frequency of action potential as it has been described in regards to the axonal initial segment (Hu et al., 2009). The expression of Nav1.1 is sparser and depends on neuronal populations. Nav1.1 was in particular detected at the nodes of Ranvier of Purkinje cells, motoneurons and GABAergic interneurons of the neocortex and hippocampus (Ogiwara et al., 2007; Duflocq et al., 2008; Freeman et al., 2015)(Figure 7A).

There are four β -subunits genes, Scn1b to Scn4b, that encode β 1- β 4 subunits respectively. The primary sequence of β 1-Nav and β 3-Nav subunits are more closely related than the sequence of β 2 and β 4. Moreover, the association with the α -subunit is made through non-covalent bounds in the case of β 1-Nav and β 3-Nav whereas a disulphide covalent bound links the α -subunit with whether β 2-Nav or β 4-Nav (Namadurai et al., 2015; O'Malley and Isom, 2015). The β -subunits belong to the immunoglobulin domain family of the cell-adhesion molecule (CAM) superfamily. The immunoglobulin domain of β -subunits allow them to develop homophilic as well as heterophilic interactions (O'Malley and Isom, 2015). At the nodes of Ranvier, three of the four β -subunits have been identified, β 1, β 2 and β 4-Nav (Ratcliffe et al., 2001; Chen et al., 2002; Chen, 2004; Buffington and Rasband, 2013)(Figure 6 and 7A), and their immunoglobulin domain allow them to interact with other nodal CAMs (e.g contactin, neurofascin 186) and perinodal ECM through tenascin (Srinivasan et al., 1998; Ratcliffe et al., 2001). β 1-Nav and β 2-Nav subunits can further interact through their intracellular domain with AnkyrinG, one of the main scaffold protein of the nodal domain (Malhotra et al., 2000). These interactions with other nodal protein allow β -subunits to control the clustering and the trafficking of alpha subunit at the nodes. For instance, β 1-Nav and β 2-Nav have been involved in the control of α -subunit density at the node (Chen et al., 2002; McEwen and Isom, 2004) and β 2 is a key regulator of the early clustering of α -subunit along axons of hippocampal GABAergic neurons (Thetiot et al., 2020).

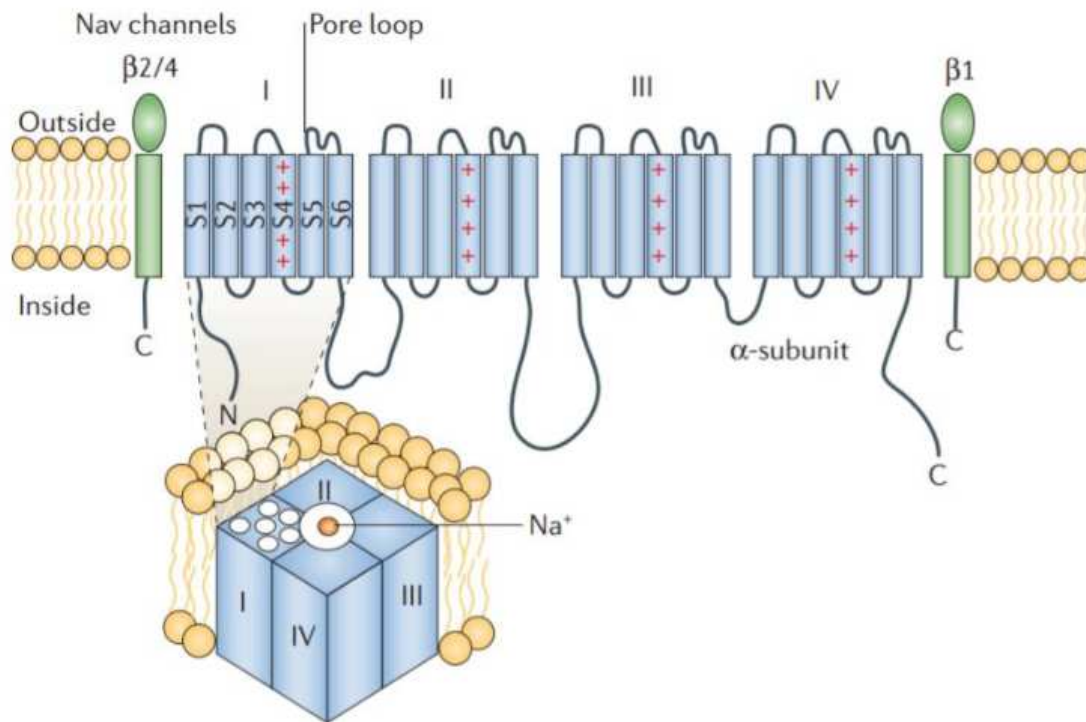


Figure 6: Structural organization of voltage-gated sodium channels.

Schematic of the ultrastructure of α Nav subunits associated with β Nav subunits. The α Nav subunits contain four repeats (domains I-IV), each domain has 6 α -helix transmembrane segments. β 2 and 4 are linked to the α subunit by a disulphide bounds whereas β 1 interacts with the pore loop of the domain IV. Adapted from Lai and Jan, 2006.

Potassium channels

Potassium channels are much more diverse than sodium channels and comprise by far the most diverse group of mammalian ion channels, with 80 genes encoding their α -subunits (Trimmer, 2015). Early electrophysiological recordings suggested a more complex organisation of potassium channels than sodium channels along the myelinated fibers, with fast potassium channels covered by the myelin sheath and slow potassium channels exposed at the node (Waxman and Ritchie, 1993). Further investigation showed a large diversity of potassium channels expressed at the nodes (directly exposed) and, beneath the myelin sheath at the juxtaparanode and more rarely at the paranode (see below, 1.3.3 paranode and 1.3.4 juxtaparanode). Indeed, at nodes, several families of potassium channels are clustered including, voltage-gated potassium channels (Kv), constitutively open two pore domain potassium channels (K2P) and calcium activated potassium channel (Kca).

Two main subtypes of Kv channels have been first identified at nodes, Kv3 and Kv7. Kv3 is a family of four members, one of which, Kv3.1b (splicing variant of Kv3.1) has been reported at the nodes of Ranvier (Devaux et al., 2003). However, its expression at nodes depends on the neuronal population

considered. It has been described solely in a subset of nodes in the spinal cord and the optic nerve in the CNS, and at even fewer nodes in the PNS (Devaux et al., 2003). Of the five Kv7 subunits, Kv7.2 and Kv7.3 have been reported at the nodes of several neuronal populations of the CNS (e.g Purkinje cells, pyramidal cortical neurons) as well as along sciatic nerve fibers in the PNS (Devaux, 2004; Pan et al., 2006; Schwarz et al., 2006; Cooper, 2011; Battefeld et al., 2014)(Figure 7B and 9B). Kv7.2 and Kv7.3 are partially open at the resting membrane potential and mediate a potassium outward current (M-current) that stabilizes the resting membrane potential (Battefeld et al., 2014). The stabilization of the resting potential at a lower value increase Nav channel availability leading to an increase of the action potential amplitude (Devaux, 2004; Battefeld et al., 2014).

The second family of nodal potassium channels, recently observed at nodes is the constitutively open two pore domain potassium channels (K2P). Primarily named 'leak current' because their properties resemble a mere potassium selective pore in the membrane (Enyedi and Czirják, 2010), recent studies have shown that their activity is regulated by diverse parameter including temperature, membrane stretch, pH and membrane potential (Renigunta et al., 2015). The development of specific antibody as well as the development of patch-clamp methods allowing a direct access to the node of Ranvier led to the identification of two K2P channels at the node, TRAAK and TREK-1 (Brohawn et al., 2019; Kanda et al., 2019) (Figure 7B and 9B). A first study by Brohawn et al, identified the mechanosensitive channel TRAAK as a nodal component throughout several structures of the CNS including the cortex, the hippocampus, the optic nerve and the spinal cord, as well as in the PNS along sciatic nerve fibers (Brohawn et al., 2019). This study was followed by the work of Kanda et al, that described the clustering of TREK-1 a temperature sensitive K2P channel at nodes of the afferent trigeminal nerves, motor nerve as well as myelinated fibers of the dorsal and ventral column of the spinal cord (Kanda et al., 2019). Assessing the functional role of TRAAK along sciatic nerves, Brohawn et al. observed that it accounts for 20% of the total leak current and participate in stabilizing the membrane resting potential (Brohawn et al., 2019). Kanda et al. further showed that TREK-1 and TRAAK in combination accelerate action potential repolarization phase and are required for high frequency saltatory conduction along afferent nerves (Kanda et al., 2019).

Lastly, the calcium activated potassium channel Kca3.1 has been identified at the nodes along Purkinje cell axons (Gründemann and Clark, 2015). Purkinje cells can securely transmit action potentials at a maximal frequency of about 250 Hz (Monsivais et al., 2005; Khaliq and Raman, 2006), a frequency that implies a fast repolarisation of the axolemma. In this context, it has been showed that Kca3.1 provides a repolarizing potassium current and has a key role in securing action potential conductance along a large range of firing frequencies (Gründemann and Clark, 2015).

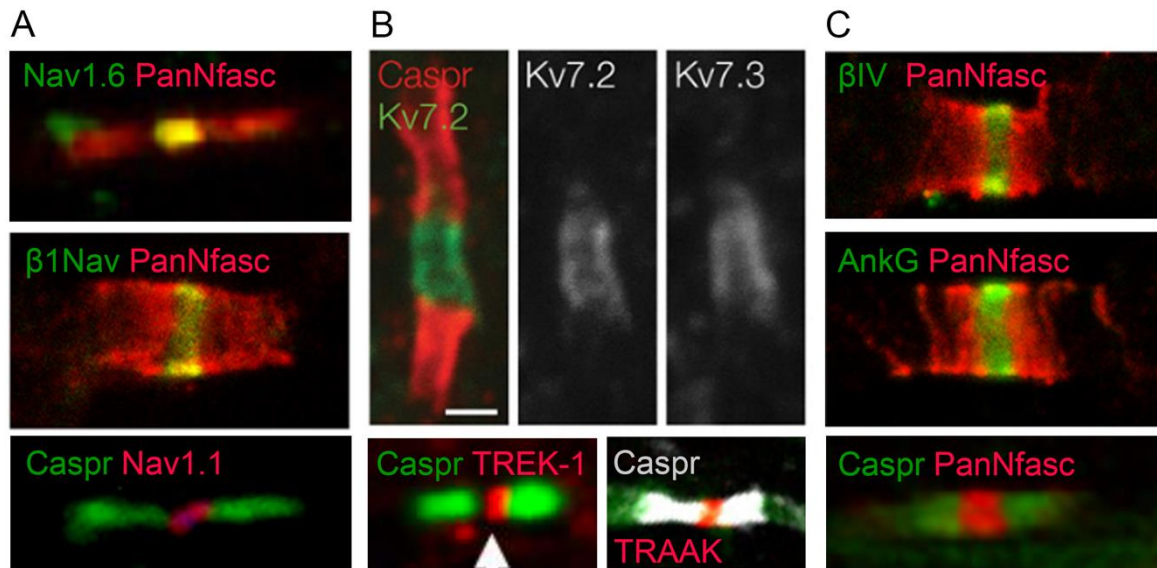


Figure 7: Nodal channels, scaffolding proteins and CAMs expressed at the node in the CNS.

(A) Three examples of sodium voltage-gated channels protein expressed at the node in the spinal cord. (B) Four examples of potassium channels expressed at the node, Kv7.2 and Kv7.3 in the cortex, TREK-1 and TRAAK in the spinal cord. (B) Three examples of the main scaffolding proteins and CAMs expressed at the node in the spinal cord. On the last row, the use of Pan neurofascin staining show its expression at node (Nfasc 186) and paranode (Nfasc 155). In all other images Caspr and PanNfasc are used to delineate the paranodal domains from the nodal domain. Adapted from Desmazières et al, 2014; Amor et al, 2017; Brohawn et al, 2019; Kanda et al, 2019; Dufolcq et al, 2008 ; Battefeld et al, 2014.

1.3.2.2 Cell adhesion molecules

Cell adhesions molecules (CAMs) are an important family of proteins modulating cell-cell interactions. CAMs gather a large diversity of proteins subdivided in several groups such as integrins, netrins, selectins, cadherins and the superfamily of immunoglobulins (Igs). At nodes, CAMs are highly enriched and stabilize ion channels by interacting with scaffolding proteins and ECM (Freeman et al., 2016).

L1-CAMs

L1-CAMs is a highly enriched family in the nervous system, with NrCAM and Neurofascin (Nfasc) that are main components of nodal domains. The Ig domains enable homophilic and heterophilic interactions with various nodal components such as sodium channels subunits, ECM and other CAMs (Hortsch et al., 2009).

Amongst the nodal L1-CAMs, neurofascin possesses 4 isoforms generated through alternative splicing in mammals. Three of them, Nfasc 186, 180 and 140 are expressed in neurons whereas Nfasc 155 is restricted to myelinating glia (Davis et al., 1996; Tait et al., 2000). At nodes, only Nfasc 186 and 140 have been observed (Figure 6C) (Lambert et al., 1997; Lustig et al., 2001; Zhang et al., 2015). Nfasc

140 is expressed early in the development and its expression declines after the onset of myelination (Hassel et al., 1997; Zhang et al., 2015). At nodes, Nfasc 140 may participate to the assembly of nodal proteins and further stabilize nodal complex. Later in the development, its expression at nodes is further replaced by Nfasc 186 while myelination proceeds, with a complete loss of nodal Nfasc 140 in adults (Zhang et al., 2015). Nfasc 186, is expressed at nodes in the PNS as well as in the CNS along the course of the development and in adulthood. Nfasc 186 interacts with multiple partners (e.g Contactin, β 1Nav, NrCAM) and participate to the assembly and the stabilization of nodal proteins (Ratcliffe et al., 2001; Sherman et al., 2005; Zonta et al., 2008; Labasque and Faivre-Sarrailh, 2010; Desmazieres et al., 2014) (Figure 7A, C and 9B).

Another important nodal protein of the L1-CAM family is NrCAM. NrCAM is a 200 kDa protein, expressed by both neurons and glia, that can be cleaved at two domains giving rise to a 170 and 140 kDa sub-products (Grumet et al., 1991). NrCAM, once cleaved interacts with other nodal CAMs and with the perinodal ECM in the CNS and in the PNS (Feinberg et al., 2010; Susuki et al., 2013). Although it has been described in the PNS that NrCAM participates to the heminodal clustering of sodium channels (Feinberg et al., 2010), its function in the CNS remains elusive (Rasband and Peles, 2021).

GPI-anchored CAMs

Glycosylphosphatidylinositol (GPI)-anchored CAMs are part of the Ig superfamily and are attached to the membrane through a GPI tail. An important nodal GPI-anchored CAM is contactin (Figure B). This protein is expressed both in glia and neurons and localizes at the nodal domains (Einheber et al., 1997; Koch et al., 1997; Kazarinova-Noyes et al., 2001). In the PNS contactin is restricted to the paranodes, but its expression in the CNS extend both to nodal and paranodal domains (Rios et al., 2000; Kazarinova-Noyes et al., 2001). In the CNS, mice lacking contactin display a reduction in the number of nodes, a decrease of Nav1.6 positive nodes and a paranodal disruption (Colakoglu et al., 2014). In addition to its role in node stabilization in the CNS, the study of the formation of node-like clusters identified contactin as one of the main component modulating the initiation of nodal clustering along axons prior to myelination (Dubessy et al., 2019).

1.3.2.3 Scaffolding proteins

Scaffold proteins are required at the nodes of Ranvier to assemble and organize nodal membrane proteins and anchor them to the axonal actin cytoskeleton. Two families of scaffolding proteins are expressed at the nodes, ankyrins and spectrins (Bennett and Lorenzo, 2016).

Ankyrins

The family of ankyrins (Ank) comprises three *ank* genes that encode AnkR (*ank1*), B (*ank2*) and G (*ank3*). Although AnkB expression is restricted to the paranode, AnkG and more sparsely AnkR are expressed at nodes in the CNS (Kordeli et al., 1995; Chang et al., 2014; Ho et al., 2014). In the CNS, AnkR is only found in a very small subset of nodes during the development and, AnkG is the only Ankyrin highly enriched at nodes throughout the CNS (Ho et al., 2014) (Figure 7C and 9B). In the CNS, several isoforms of AnkG exist, the ones clustered at node being the 270kD and 480kD isoforms (Kordeli et al., 1995). At nodes, AnkG interacts and anchors to the actin cytoskeleton (through its interaction with β IV-spectrin) virtually all major nodal proteins such as α and β subunits of Nav channels, potassium channels Kv7 and neurofascin 186 (Davis et al., 1996; Zhang and Bennett, 1998; Malhotra et al., 2000, 2002; Garrido et al., 2003; Lemaillet et al., 2003; Pan et al., 2006). One exception to this rule might be the recently identified nodal K2P channels that are devoid of AnkG binding domain (Brohawn et al., 2019; Kanda et al., 2019). In the CNS, mice depleted in AnkG show a compensatory mechanism by AnkR but the double knock-out AnkG/AnkR leads to a complete block of nodal clustering (Ho et al., 2014). Therefore, AnkG alone is not required to form nodes of Ranvier in the CNS, but it is only due to a compensatory mechanism that the large variety of nodal proteins can cluster in its absence, demonstrating the major role of ankyrins in nodal formation.

Spectrins

The other family of scaffolding proteins expressed at nodes of the CNS is the family of spectrins. Spectrins assemble in tetrameric complex, with heterodimerized α and β subunits. In mammals, the two subunits α and β are respectively encoded by two and five genes (Bennett and Lorenzo, 2016). The primary spectrin enriched at the nodes of Ranvier is β IV-spectrin, where two of its six isoforms are clustered, β IV Σ 1 and β IV Σ 6 (Figure 7C and 9B) (Berghs et al., 2000; Lacas-Gervais et al., 2004). In mice lacking the longest isoform β IV Σ 1, the architecture of the nodal structure in the cerebellum and the optic nerve is deeply affected (Lacas-Gervais et al., 2004). The complete knock-out of β IV-spectrin further disrupts the architecture of the nodes in the optic nerve, suggesting an additional function of the β IV Σ 6 isoform at the nodes (Uemoto et al., 2007). Interestingly, the deletion of β IV-spectrin leads to an increase of β I-spectrin expression and to its clustering at the nodes of the corpus callosum (Ho et al., 2014; Liu et al., 2020). To avoid this compensation mechanism at nodes, mice lacking both β I and β IV-spectrins have been generated. In these mice, nodes of the corpus callosum are formed but the clustering of Nav channel decreases with time, which demonstrates the necessary function of spectrins in the stabilization of nodal protein in the CNS (Liu et al., 2020).

1.3.2.4 Perinodal extracellular matrix

The nodal domain is surrounded by a dense ECM, named perinodal nets. This ECM forms around nodes a network comprising a large diversity of component such as proteoglycan link protein 2 (HAPLN2 also named Bral1), tenascin-R and chondroitin sulfate proteoglycans (e.g brevican, versican and neurocan) (Oohashi et al., 2002; Hedstrom et al., 2007; Bekku et al., 2009; Dours-Zimmermann et al., 2009)(Figure 8A). This dense network interacts notably with neurofascin 186 and β -subunits of Nav channels (Srinivasan et al., 1998; Hedstrom et al., 2007)(Figure 8B). The interactions between ECM and neurofascin 186 participate to the stabilization of nodal proteins (Bekku et al., 2009; Susuki et al., 2013). Once node are mature, the perinodal ECM is thought to create a “ion-sink” or diffusion barrier that allows for a faster conduction of the action potential (Hunter et al., 1988; Bekku et al., 2009). The perinodal ECM does not form in HAPLN2 deficient mice, which allowed to test perinodal ECM function in fiber conduction (Bekku et al., 2010). In the white matter of these mice, there was no reduction of Nav channel density at nodes. However, there was a decrease in nerve conduction associated with the perturbation of the diffusion barrier at nodes suggesting that perinodal ECM accelerates action potential velocity (Bekku et al., 2010).

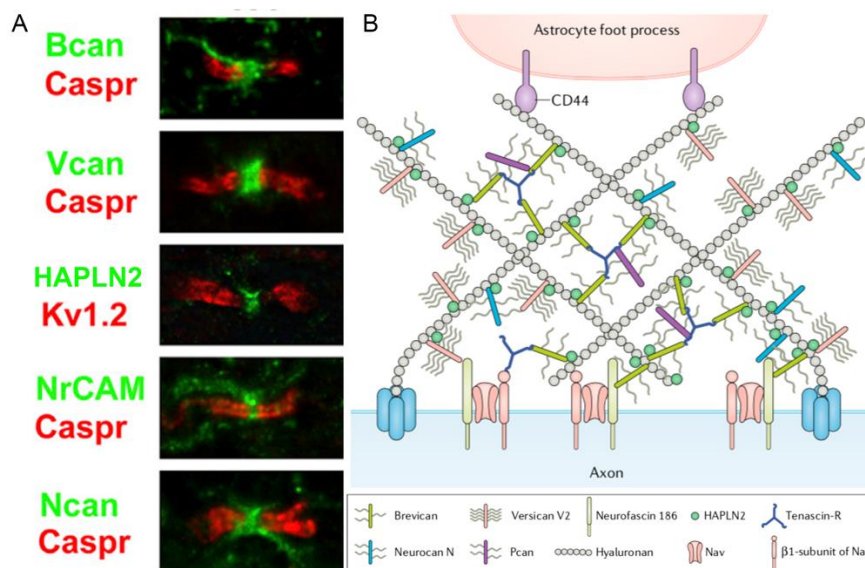


Figure 8: Molecular organisation of the perinodal extracellular matrix in the CNS.

(A) The components of the perinodal extracellular matrix (in green) localises at the nodal domain flanked on both side by paranodes (Caspr, red) in mouse spinal cord. The images show the following protein of the perinodal ECM: Brevican (Bcan), Versican V2 (Vcan), HAPLN2 and Neurocan N (Ncan). (B) Schematic representing the molecular organisation and the interactions at the perinodal matrix in the CNS. Adapted from Susuki et al, 2013 and Fawcett et al, 2019.

1.3.3 Paranodes

The node is flanked on both side by the paranodes, where tight axo-glial junctions attach the axolemma with the paranodal loops (Figure 5A). The axo-glial junctions restrict molecule diffusion, stabilize nodal components and increase the axial resistivity allowing saltatory conduction (Rosenbluth, 2009; Cohen et al., 2019; Rasband and Peles, 2021). These functions of the paranodes are intrinsically related to the tightness of the axogial junction, with a tight apposition of the axolemma and glial membranes, their distance ranging from 3 to 7 nm (Salzer, 2003; Nans et al., 2011). To reach this proximity, a dense clustering of three major CAMs is observed at the paranode, the axonal Caspr (also named Caspr1 or Paranodin), contactin and the glial neurofascin 155 (Figure 9B).

The molecular description of the septate-like junctions at the paranode, started with the study of similar septate junctions established by glial cells in *Drosophila* (Baumgartner et al., 1996). Indeed, the first required component identified at these junctions neurexin IV, had close similarities with the mammalian protein Caspr (Peles et al., 1997a), that was soon identified at the paranodal domains (Einheber et al., 1997; Menegoz et al., 1997). Caspr is a glycoprotein of the neurexin family that was identified through its interaction with the GPI-anchored CAM, contactin (Peles et al., 1997b). Contrarily to contactin that is expressed both in neurons and glia, Caspr is exclusively expressed by neurons (Einheber et al., 1997; Menegoz et al., 1997). During the development, Caspr is expressed diffusely along the axons that are not yet myelinated. As myelination proceeds, Caspr clusters together with contactin at the junction between the myelin sheath and the axolemma (Einheber et al., 1997; Faivre-Sarrailh et al., 2000; Bonnon et al., 2003). In Caspr deficient mice, there is an extensive disruption of the axogial function, with the absence of contactin at the paranodes and Kv1 voltage-gated potassium channels invading the paranodal domains (Bhat et al., 2001). Consequently, in these mice a strong decrease of the conduction velocity is observed, that may be due to the mislocalisation of potassium channels (Koles and Rasminsky, 1972; Bhat et al., 2001). The localization of the Caspr/contactin complex at the paranodal junction need the adaptive protein 4.1B that connect the complex to the actin cytoskeleton through its interaction with the α II- β II spectrin (Gollan et al., 2002)(Figure 9B). The Caspr/contactin complex forms a tripartite complex with the glial Nfasc 155, by interacting with the Ig domains of Nfasc 155 (Tait et al., 2000; Charles et al., 2002)(Figure 9B). These interactions between Caspr/contactin and Nfasc 155 seal the two membranes together linking the actin cytoskeleton of the axon with its glial counterpart (Chang et al., 2014).

In Purkinje cells, BK potassium channels are clustered at paranodes (Hirono et al., 2015). The activation of BK channels is controlled by an allosteric effect between membrane depolarisation and Ca^{2+} binding (Sausbier et al., 2006; Lorenzo-Ceballos et al., 2019). Their activation at the paranodes at high firing frequencies secures action potential propagation along Purkinje cell axons (Hirono et al., 2015).

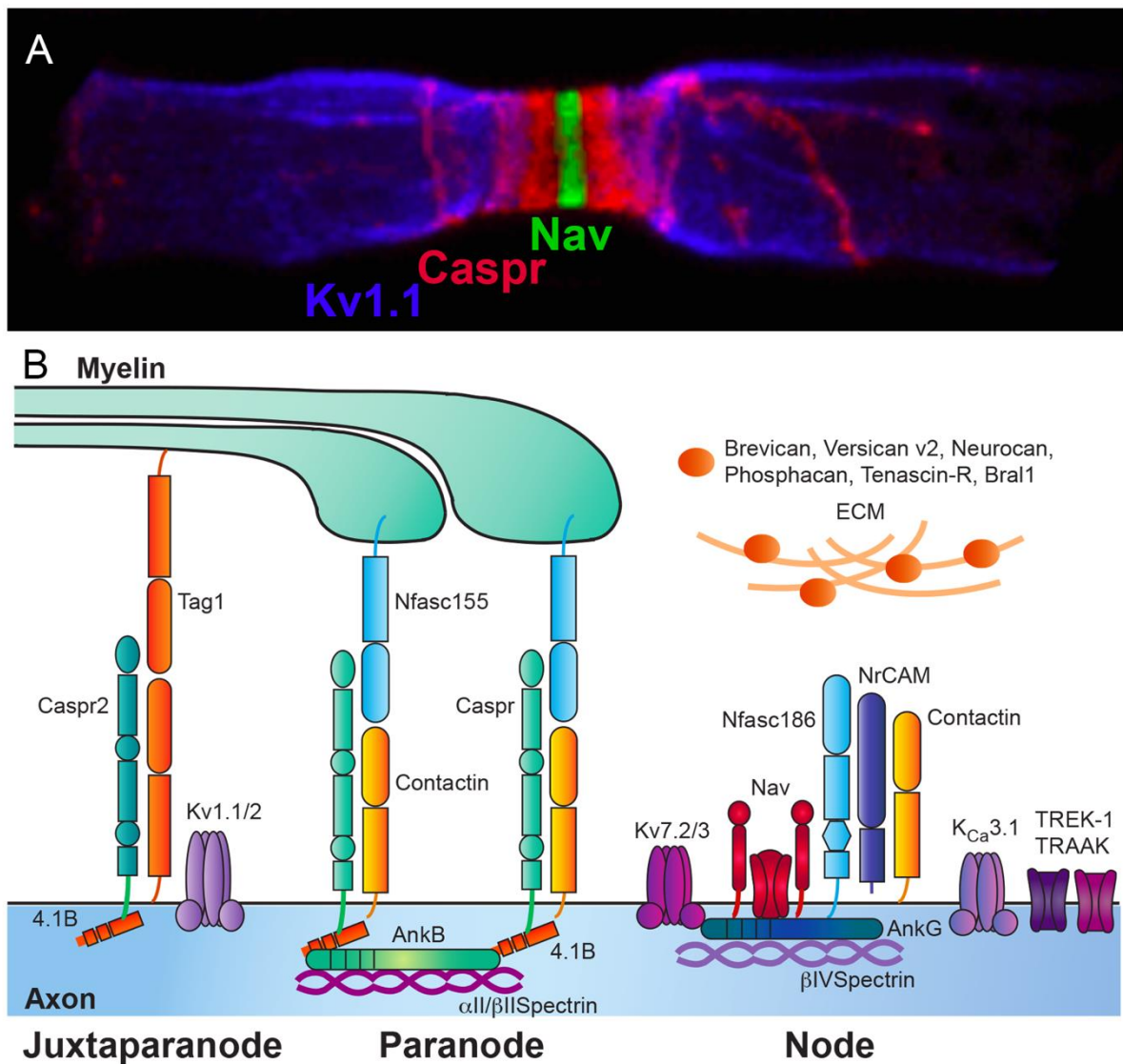


Figure 9: Molecular organization of the nodal domain.

(A) Image of a teased fiber of the ventral funiculus of the spinal cord showing the nodal (Nav, in green), paranodal (Caspr, in red) and juxtapanodal (Kv1.1, in blue) domains. (B) Schematics of the molecular organisation and the interactions between proteins at the nodal domain in the CNS. Adapted from Desmazières et al., 2014; Lubetzki et al., 2020.

1.3.4 Juxtaparanodes

Neighbouring the paranodes are the juxtaparanodes which are localized under the compact myelin. Juxtaparanodes are characterized by the clustering of voltage-gated potassium channels, Kv1.1 and 1.2 being the predominant subunits (Wang et al., 1993; Rasband et al., 1998)(Figure 9B). Although their function at this site is still unclear, they might shunt the depolarisation of the axolemma (Arancibia-Carcamo and Attwell, 2014). Indeed, a recent study by Cohen and colleagues has suggested that the depolarisation at the juxtaparanode reaches about 80 mV of amplitude, which is virtually sufficient to transiently activate the majority of Kv1.1 and 1.2 channels (Scholle et al., 2004; Hao et al., 2013; Cohen et al., 2019).

The clustering of Kv channels at the juxtaparanodes relies on the paranodal junction, and the disruption of paranodal loops leads to the mislocalisation of the Kv channels (Bhat et al., 2001; Zonta et al., 2008). The juxtaparanodal Kv channels are further stabilized by the complex comprising the neuronal protein Caspr2 and TAG-1 (also named contactin-2) expressed by both neuron and glia (Traka et al., 2003)(Figure 9B). Indeed, in mice lacking TAG-1, there is no clustering of Caspr2 at the juxtaparanode and the accumulation of Kv channels is severely disrupted (Traka et al., 2003). This phenotype, is further recapitulated by the deletion of Caspr2, demonstrating that both Caspr2 and TAG-1 are required to properly cluster Kv channels at the juxtaparanode (Poliak et al., 2003). Similarly to the Caspr/contactin complex at the paranode, the Caspr2/TAG-1 complex is anchored to the axonal cytoskeleton through its interaction with the 4.1 adaptator and α II- β II spectrin (Gollan et al., 2002; Denisenko-Nehrbass et al., 2003; Ogawa, 2006)(Figure 9B).

1.4 From oligodendrogenesis to myelin sheath formation and functions

In the CNS, the myelinating cells are the OLs, each of them enwrapping several tens of axons (Matthews and Duncan, 1971; Chong et al., 2012). Therefore, the membrane of OLs reaches a level of complexity that stands above any other cell of the body (Simons and Nave, 2016). OLs originate from the differentiation of oligodendrocyte progenitor cells (OPCs) that proliferate, migrate and then differentiate into myelinating oligodendrocytes. Once differentiated in myelinating OL, these cells start to enwrap axons which include several steps, recognition of the axons to target, production and trafficking of the myelin components and ultimately myelin compaction (Nave and Werner, 2014).

1.4.1 Multiple embryonic origin of the OPCs

The origin of OPCs has been a long standing debate in the scientific community from the 90s until a seminal study by Kessaris et al, in 2006 (Richardson et al., 2000, 2006; Spassky et al., 2000).

Indeed, back in the 90s, there were evidences supporting a single ventral source of the OPCs (Pringle and Richardson, 1993). However, this result was challenged by the team of JL. Thomas and B. Zalc, using LacZ expression under the control of the *plp* promoter. Their observations suggested a plural origin of the oligodendroglial lineage, from restricted domains of the dorsal and ventral ventricular zone both in the spinal cord and forebrain (Spassky et al., 1998, 2001). The study of Kessaris et al, in 2006 described in more details OPCs origin using a Cre-lox fate mapping approach. Using this approach, it was shown that OPCs are generated in three successive waves. At E12.5, a first wave of OPCs is generated from *nkx2.1* expressing precursors localized in the medial ganglionic eminences of the ventral forebrain and populates the entire telencephalon. The second wave arises at E15.5 from precursors expressing *Gsh2* in the lateral and caudal ganglionic eminences. And lastly, at birth, a third wave arises from *Emx1* positive precursor in the ventricular zone of the cortex (Kessaris et al., 2006) (Figure 10A). More recent work suggested that the third wave might start as early as E17.5 (Winkler et al., 2018).

In the spinal cord, OPCs are also generated from ventral as well as dorsal progenitor domains in two successive waves. The first wave starts at E12.5 and generates the majority of the spinal OPCs arising from the same ventral progenitor domain than motoneurons. The second dorsal wave, arises around E15 from the dorsal progenitor domains dP3, 4 and 5 and colonize the dorsal part of the spinal cord (Cai et al., 2005; Vallstedt et al., 2005) (Figure 10B).

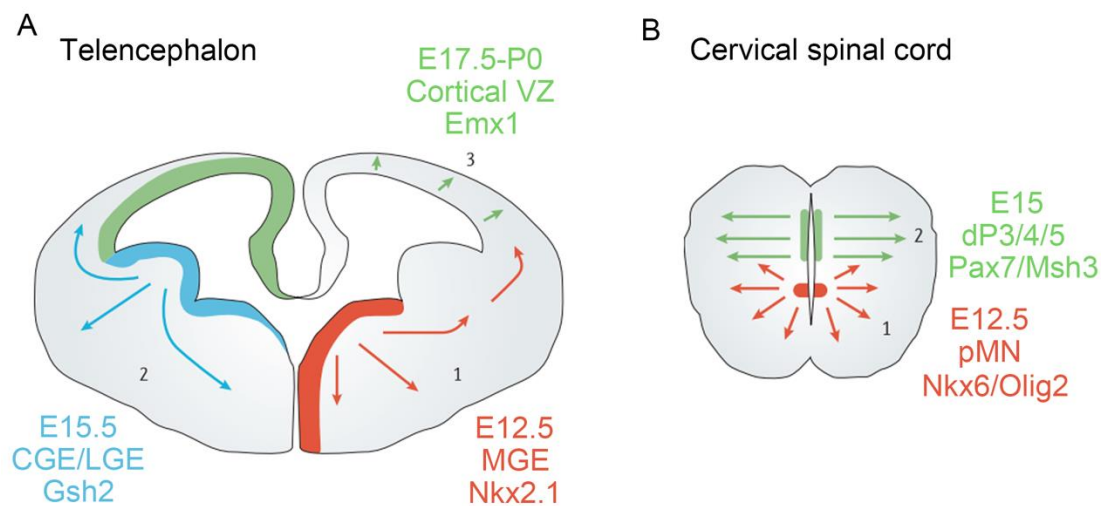


Figure 10: Multiple embryonic origin of OPCs in the forebrain and spinal cord.

(A) Schematic of the three sequential waves of OPCs in the telencephalon. The ventral wave originates from the *Nkx2.1* positive progenitor in the medial ganglionic eminences at E12.5. The second wave arises from *Gsh2* expressing progenitor in the lateral and caudal ganglionic eminence at E15.5. The third wave was suggested to arise at birth (P0) but could start around E17.5. This last wave originates from the *Emx1* positive progenitor of the cortical ventricular zone (VZ). (B) Schematics of the two sequential waves of OPCs in the cervical spinal cord. The ventral wave originates from the *Nkx6* positive, *Olig2* positive pMN progenitor domain at E12.5. The dorsal wave arises from the *Pax7*, *Msh3* expressing dorsal progenitor domains (dP3, dP4 and dP5). Adapted from Richardson et al, 2006.

1.4.2 From OPCs to oligodendrocytes

Following their generation during the embryonic development, OPCs invade the whole parenchyma and continue to proliferate. Although their proliferation extends to adulthood, OPCs undergo a maximal proliferation in the first week of postnatal development. Their differentiation into OLs starts in the first week of postnatal development and peaks between the second and the third week postnatally, simultaneously with developmental myelination (Rivers et al., 2008; Zhu et al., 2011; Young et al., 2013). To form OLs, OPCs undergo several steps of a continuous differentiation that have been recently characterized in details by the team of G. Castello-Branco using single-cell RNA sequencing (Marques et al., 2016)(Figure 11A). When looking at the state of cells along the oligodendroglial lineage, some markers are commonly used. OPCs are generally characterized by their expression of NG2 and PDGFR α . While they start to differentiate, the expression of NG2 and PDGFR α decreases and committed OPCs start to express sulfatide (O4) at their membrane and grow multiple processes (Bansal and Pfeiffer, 1989)(Figure 11B). Pursuing their differentiation, committed OPCs lose their proliferative capacities, grow a very complex arborization of processes and become newly formed OLs characterized by their expression of markers such as GalC (O1) or CNPase (Zalc et al., 1981). While growing their arborization, OLs start to express myelin specific proteins (e.g Opalin, PLP/DM20, MBP) and are defined as myelin-forming OLs (Marques et al., 2016). Lastly, while they myelinate, OLs start to express the protein MOG that is commonly used to characterize the last step of mature OLs (Solly et al., 1996)(Figure 11B). This continuum of differentiation is highly active during the first weeks of postnatal development and the intermediate states of OLs differentiation persist but are rare in adult (Marques et al., 2016). Nevertheless, the OPCs persist in adulthood where they represent 5 to 8% of the total cells and keep proliferating (Chang et al., 2000; Horner et al., 2000; Dawson et al., 2003). This pool of OPC is widely distributed in the CNS and is thought to participate to the generation of OLs during remyelination (see 1.6.3)

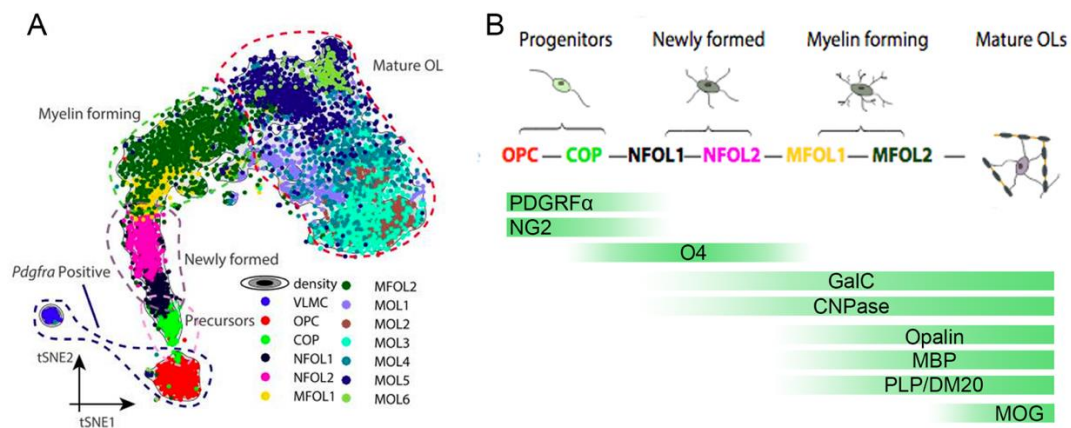


Figure 11: From OPC to OL, a continuum along the oligodendroglial lineage.

(A) t-SNE plot of single cell RNAseq data showing a continuum of the oligodendroglial lineage from OPCs to mature OLs in mouse. This continuum is uniform in the CNS and heterogeneity arises at the mature oligodendrocyte state. The colors match the colors used in (B) to identify the different maturation stage. (B) Schematics of the progression along the oligodendroglial lineage, and expression of the classical protein markers used to identify oligodendroglial cells along their differentiation. Adapted from Marques et al, 2016.

1.4.3 Myelin sheath formation

In the CNS, there is a very restricted time window of about 1 or 2 days between the oligodendrocyte starting to myelinate and the generation of all the fully compacted and stable myelin sheaths generated by this cell (Watkins et al., 2008; Czopka et al., 2013). Within this short period of time, OLs need first to identify the axons to myelinate. In the zebrafish, pre-myelinating OLs, grow a large number of motile processes that contact various axons, and initiate myelination on a subset of these axons (5 hours)(Czopka et al., 2013). Along the course of myelination, about 20% of these processes are retracted, the other 80% being stabilized as compact myelin sheath wrapped around axons (1-2 days after myelination start)(Czopka et al., 2013). The mechanisms that restrain myelination to only a subset of axons is still not fully understood. Indeed, fixed axons or more recently, synthetic nanofibers have been used to demonstrate the ability of OLs to myelinate inert material without any other clue than their diameters (Rosenberg et al., 2008; Lee et al., 2012a). However, in the CNS, some axons with similar diameters are either myelinated or not, and the “diameter” rule cannot explain on its own myelination patterns. These results led to the hypothesis that the targeting of axons by OL must be driven by inhibitory cues expressed at the membrane of unmyelinated structures (soma, dendrites, axon initial segment, nodes of Ranvier and axons with a sufficient diameter that remain unmyelinated). Aiming to identify these cues, a study by the team of J. Chan described junction adhesion molecule 2 (JAM2) as an inhibitory signal for the myelination of the somatodendritic compartment of Pax2 positive interneurons in the dorsal horn of the spinal cord (Redmond et al., 2016). However, as the expression of JAM2 is restricted to some interneurons, other cues may exist as

hallmarks of the myelination pattern later formed by OLs. Furthermore, a genetic screening in zebrafish identified that neurofascin B (predicted to encode a protein analogous to Nfasc 155) prevents the mistargeting of myelination to cell bodies (Klingseisen et al., 2019). However, questioning the view that unmyelinated portion of neurons must express inhibitory signals to prevent mistargeted myelination, a recent study showed that the homeostasis of myelin production is an important parameter for the specificity of myelination (Almeida et al., 2018). Indeed, increasing pharmacologically (in zebrafish) or genetically (in mice) the number of OLs or reducing the number of axons using kif1-binding protein (kf1bp) mutants in zebrafish led to an increased ratio of OLs over axons. This manipulation triggered mistargeted myelination of neuronal cell body, and suggested that the pattern of myelination also depends on the fine regulation of OLs production (Almeida et al., 2018). Thus, the balance between OL number and axonal density, might allow the specific myelination of axons depending on their diameter (Mayoral et al., 2018), neuronal identity (Nelson et al., 2019) or neuronal activity (see 3.2.2).

Once OLs have identified their target, they need to wrap and form compact sheath around them. The growth of the myelin sheath proceeds through the extension of the inner tongue underneath the previously wrapped membranes. The extension of the newly formed layers along the axon occurs simultaneously and ultimately the uncompacted edges form the paranodal loops (Snaidero et al., 2014)(Figure 12). The membrane layers are compacted from the outer to the inner layers, leaving cytoplasmic channels of uncompacted myelin to allow for the transport of myelin components toward the edges of the inner tongue that concentrate myelin extension (Snaidero et al., 2014, 2017) (Figure 12). Although the compaction is triggered by the actin cytoskeleton depolymerization concomitantly with MBP polymerization, F-actin interacting with CNPase prevents the compaction at the inner tongue and along the cytoplasmic channels (Zuchero et al., 2015; Snaidero et al., 2017).

Figure 12

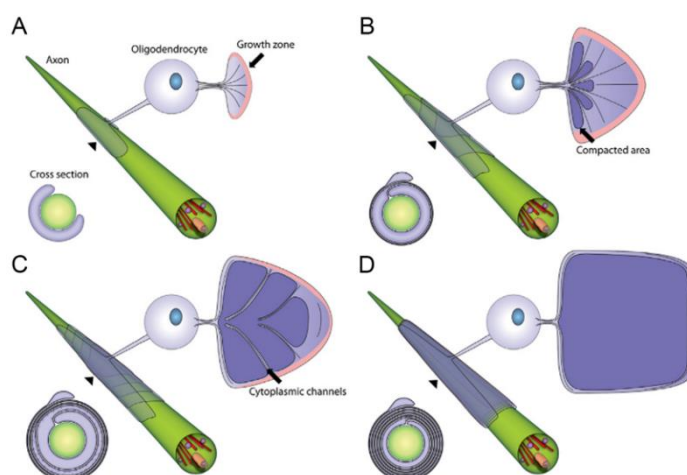


Figure 12: Model of myelin wrapping around axon in the CNS. (A-D) Schematic of the developing myelin sheath along an axon in the CNS. The flattened configuration is shown to emphasize the organisation of the myelin sheath and the cytoplasmic channels along it. It shows the inner tongue where the membrane extends (in pink) and the compacted myelin (in dark violet). The wrapped representation shows the extension of myelin layers along the axon. Lastly, the cross-section representation highlights the compaction of the myelin layers while myelination is ongoing. Snaidero et al, 2014.

1.4.4 Myelin functions in conduction and metabolic support

1.4.4.1 Myelin allows fast saltatory conduction

Myelin allows to increase by a factor up to 50 the conduction velocity without increasing axonal diameter, by increasing local radial resistance and reducing axonal membrane capacitance. Myelination of the axon theoretically enables to increase conduction with diameters as low as 0.2 μm (Waxman and Bennett, 1972). Experimentally, CNS axons with a diameter above (but not below) 0.4 μm can be myelinated (Hildebrand et al., 1993). At a fixed diameter, two main parameters of the myelin sheath are modulating conduction velocity. First, the thickness of myelin that is often characterized by the g-ratio (the axonal diameter divided by the total outer diameter of the fiber). The g-ratio is optimal for conduction velocity between 0.75 and 0.80 in the CNS (Smith and Koles, 1970; Waxman and Swadlow, 1976; Chomiak and Hu, 2009). The second physical parameter of the myelin sheath that participates in setting conduction velocity is the internodal length (Huxley and Stampfli, 1949). Indeed, conduction velocity increases together with the increase of the internodal length until a plateau at about 1000 μm (Brill et al., 1977; Moore et al., 1978). In the CNS, internodes are usually between 50 and 150 μm long (Tomassy et al., 2014; Stedehouder et al., 2017) and changes in their length modify conduction velocity (Etxeberria et al., 2016). Along myelinated fibers, other parameters and in particular nodal structure can modulate the conduction velocity (see 1.5).

1.4.4.2 Myelin provides metabolic support to the axons

Besides its function in action potential conduction, myelin has been recently studied for its function in metabolic support of the axon. Indeed, axons are very long structures that can reach their targets several meters away in mammals, hence metabolite diffusion from the soma cannot provide a sufficient source of energy. The first clues suggesting a function of myelin in metabolic support of the axons came along with the study of myelin specific proteins deficient mice (CNPase, PLP) (Griffiths et al., 1998; Edgar et al., 2008). These mice showed normal myelination but develop early axonal defects indicative of axonal energy deficits (Griffiths et al., 1998; Edgar et al., 2008). Further investigations, using mice with mitochondrial respiration deficiency, showed that lactate produced in OLs is transported to the axon and used for ATP production. This metabolic support is allowed by the monocarboxylate transporters MCT1 and MCT2 respectively expressed by OLs and axons (Fünfschilling et al., 2012; Lee et al., 2012b)(Figure 12). OLs are also involved in ion homeostasis underneath myelin sheath, with notably potassium clearance at the periaxonal space (Larson et al., 2018; Marshall-Phelps et al., 2020). Potassium concentration in the periaxonal space depends on neuronal activity, and its clearance by myelin sheaths might control the activity dependent metabolic support of myelin to the

axons (Hamilton et al., 2016). Indeed, potassium concentration increase in the periaxonal space could trigger calcium signaling (Hamilton et al., 2016), a mechanism that may also be mediated by oligodendroglial NMDA receptors activation (Saab et al., 2016; Saab and Nave, 2017)(Figure 13).

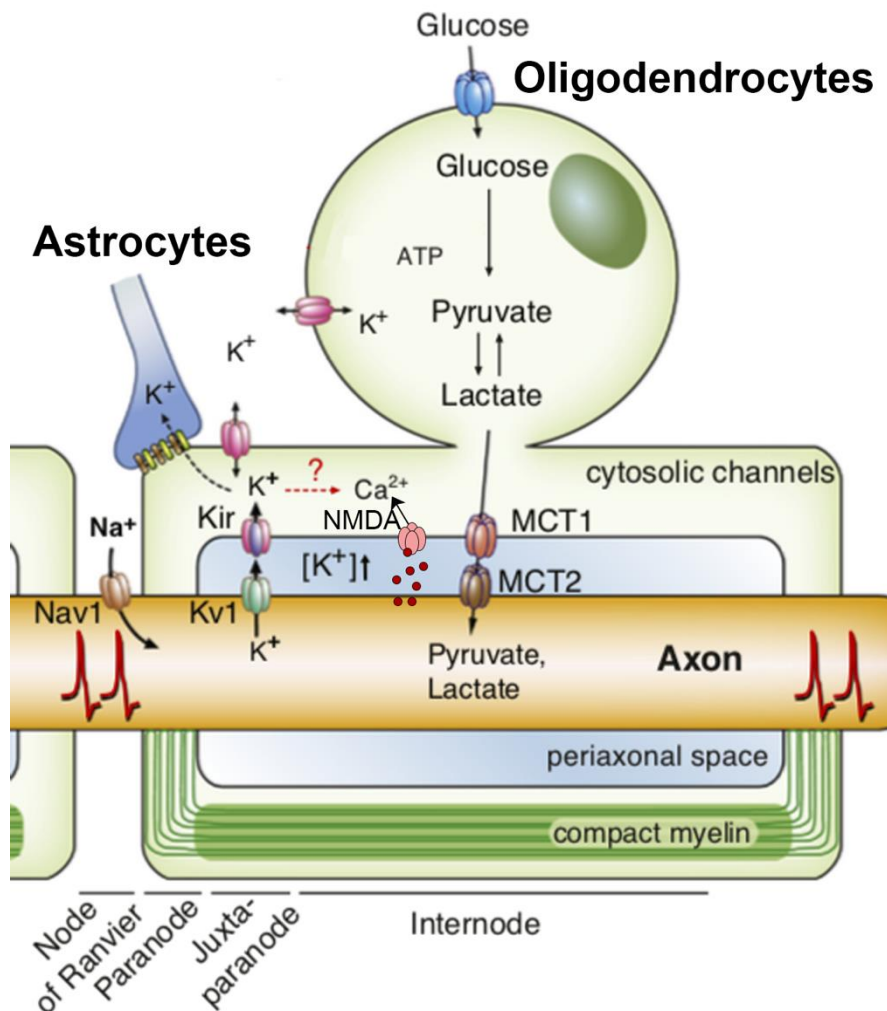


Figure 13: Myelin provide metabolic support to the axons of the CNS.

Schematic showing the metabolic support provided by oligodendrocytes through the myelin sheath to the axon. The metabolic support is provided by the transport of lactate from the soma of OL to the myelin sheath through the cytosolic channels and then diffuse to the inner tongue where MCT1 transport it to the periaxonal space. Once in the periaxonal space, lactate is imported in axons through MCT2, and is used to produce ATP. This mechanism is further activated by ATP release at the axon upon neuronal activity. Potassium ions are released in the periaxonal space by the Kv1 channels at the juxtaparanode and subsequently cleared by OLs. This mechanism could lead to the raise of calcium concentration and participate together with NMDA receptor activation to the activity dependant metabolic support. Adapted from Saab and Nave, 2017.

1.5 Assembly and function of nodal domains along myelinated fibers

1.5.1 Nodal domain assembly in the CNS, a multimodal mechanism.

In the PNS the mechanisms responsible for the clustering of nodal protein are well established and rely on two complementary processes, heminodal clustering and restrictions of proteins at nodes by the paranodal junctions (Vabnick et al., 1996; Ching et al., 1999; Pedraza et al., 2001; Eshed et al., 2005; Schafer et al., 2006; Feinberg et al., 2010). In the CNS, the exact mechanisms leading to the assembly of the nodes of Ranvier are less well understood. The loss of function strategies used to decipher this process showed the existence of mechanisms that can compensate with three main actors, the paranodal junctions, the axonal cytoskeletal scaffold and the extracellular matrix (Susuki et al., 2013; Amor et al., 2017).

1.5.1.1 Nodal clustering is concomitant with myelination : the classic mechanism

Axoglial junction at the paranode

At the onset of myelination, it has been shown in the CNS that axo-glial junctions can be formed prior to the clustering of Nav channels or nodal CAMs like Nfasc 186 (Rasband et al., 1999). The study of the optic nerve myelination in rodents, showed that this structure starts to be myelinated at the beginning of the second week of postnatal development (Skoff et al., 1976; Black et al., 1982). At P7, few axo-glial junctions are observed (identified by clusters of Caspr) in the optic nerve whereas nodal proteins are not clustered yet (Rasband et al., 1999). The clustering of nodal proteins such as Nfasc186, Nav channels and scaffold protein (β IV-spectrin) was detected only after P9 at heminodes (Rasband et al., 1999; Susuki et al., 2013), whereas perinodal ECM was observed as late as P20 a timepoint at which virtually all nodal structures are flanked by myelin (Susuki et al., 2013). This observation suggested that the axo-glial junction formation is an early event of nodal domain assembly and could participate to the clustering of nodal proteins while myelination is ongoing. It was proposed that while the heminodes (juxtapose to myelin only on one side) are moving forward with myelination, the paranodal junction “pushes” nodal proteins and play the role of a diffusion barrier eventually restricting all the nodal proteins to the mature node (Rasband et al., 1999; Pedraza et al., 2001; Susuki et al., 2013). To explore further the function of paranodal junction as a diffusion barrier, several groups started to look at the nodal domains of mice missing proper paranodal junctions. However, in Caspr and Nfasc155 deficient mice that lack proper paranodal loops, Nav channels are still clustered at nodes suggesting that paranodal junctions participate in nodal clustering but are not required and can be

compensated by over mechanism in the CNS (Bhat et al., 2001; Rios et al., 2003; Zonta et al., 2008; Pillai et al., 2009; Susuki et al., 2013; Amor et al., 2017) (Figure 14).

Perinodal ECM

In the CNS, another important mechanism is the stabilization of nodal proteins by the perinodal ECM. Indeed, *in vitro*, the overexpression of perinodal ECM proteins leads to the formation of Nfasc 186 clusters along axons in absence of myelin (Susuki et al., 2013). Moreover, in mice lacking both paranodal junctions and perinodal ECM proteins, the number of nodal domains with Nav clustering is deeply reduced whereas this parameter is not affected in single mutant lacking whether paranodal junction (Caspr deficient) or perinodal ECM proteins (Versican and Brevican double knock-out or HAPLN2 knock out) (Weber et al., 1999; Bekku et al., 2009; Dours-Zimmermann et al., 2009; Susuki et al., 2013; Amor et al., 2017). However, since the perinodal ECM is formed late in the development, when most of the nodes are formed, ECM proteins may not participate to the initiation of node assembly but rather take part in the stabilization of nodal domains by interacting with Nfasc 186 and β Nav subunits (Srinivasan et al., 1998; Hedstrom et al., 2007)(Figure 8, Figure 14).

Nodal cytoskeletal scaffold

As described previously, nodal scaffolding proteins interact with most of the nodal proteins and anchor them to the cytoskeleton (see section 1.3.2.3). In the optic nerve, AnkG is clustered at heminodes as early as P9, prior to Nav channels and Nfasc 186 (Jenkins and Bennett, 2002). Furthermore, Nav binding to AnkG is necessary and sufficient to cluster Nav channels (Gasser et al., 2012; Barry et al., 2014), and the deletion of AnkG binding motif of Nfasc186 prevents its clustering to nodal domains (Susuki et al., 2013). Thus, AnkG (or AnkR, see 1.3.2.3) is required for the clustering of nodal proteins (Barry et al., 2014; Ho et al., 2014), however its connection to the axonal cytoskeleton through β IV-spectrin is not necessary. Indeed, β IV-spectrin deficient mice form nodal structures (Yang, 2004; Yang et al., 2007; Susuki et al., 2013), and it is only upon double deletion of β IV-spectrin and paranodal junctions or β IV-spectrin and perinodal ECM that Nav clustering at nodes is affected (Susuki et al., 2013). Nevertheless, the nodal domains become elongated in older β IV-spectrin deficient mice (1.5 vs 6 months), and Nav distribution as well as density seem disrupted (Lacas-Gervais et al., 2004; Yang, 2004; Yang et al., 2007). The anchoring to the nodal cytoskeletal scaffold is therefore involved in the stabilization of nodal proteins but is not directly involved in the initiation of its formation in this model (Figure 14).

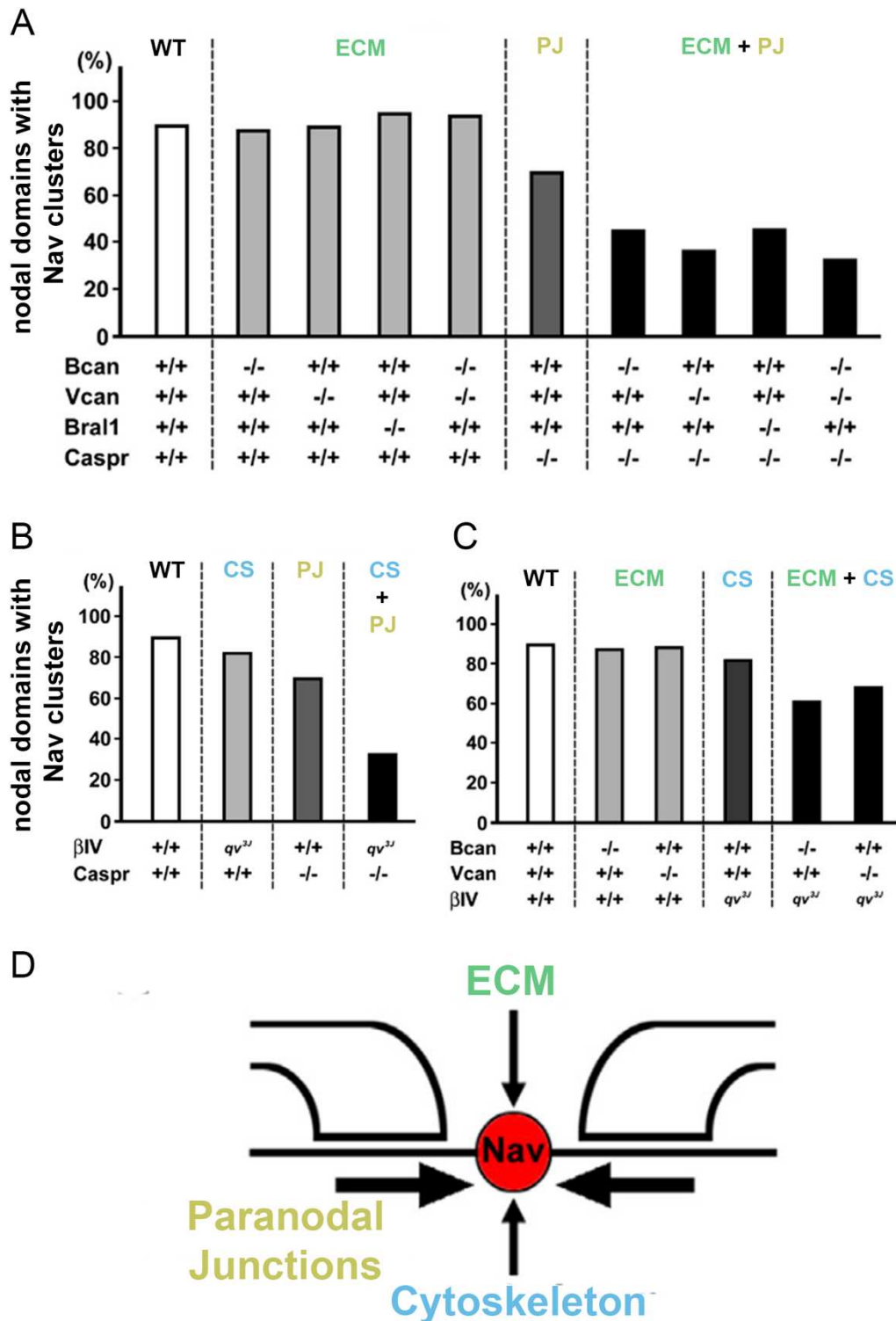


Figure 14: Three mechanisms contribute to the classical process of nodal assembly in the CNS.

(A-C) Proportion of nodes in the optic nerve that shows Nav clustering in WT mice, in mice deficient for the paranodal junctions (PJ, Caspr^{-/-}), for perinodal ECM (ECM, Bcan^{-/-}, Vcan^{-/-}, Bral1^{-/-} (also named HAPLN2)) and for the anchoring to the cytoskeletal scaffold (CS, β IVspectrin^{-/-}). (D) Schematic showing the main actors participating in the nodal clustering and its stabilization in the CNS. Paranodal junctions restrict Nav channels to the nodes while perinodal ECM and anchoring to the cytoskeleton stabilize Nav clusters. Adapted from Susuki et al, 2013.

1.5.1.2 Nodal clustering can precede myelination : an alternative mechanism

In the CNS, clusters of Nav channels along unmyelinated axons were first reported in rat optic nerve at P10 (Waxman and Ritchie, 1993) and along axons of the ganglia of *Aplysia* (the CNS in this organism is made of fused ganglia)(Johnston et al., 1996). Moreover, although axoglial junctions have been described to initiate the mechanism of nodal assembly in the optic nerve, at P9-P10, 12% of the nodal structures were characterized by an isolated cluster of Nav channels without any paranodal junction at their vicinity (Rasband et al., 1999). Similarly, experiments performed by several groups *in vitro* on retinal ganglion cells (RGCs) and *in vivo* in the optic nerve and hippocampal GABAergic neurons showed that Nav channels can cluster prior to myelination and form “node-like-clusters” (Kaplan et al., 1997, 2001; Freeman et al., 2015; Dubessy et al., 2019; Thetiot et al., 2020). More recently, node-like clusters were described along Purkinje cells axons, and isolated clusters of neurofascin were observed on commissural primary ascending and circumferential descending neurons of the zebrafish (Lubetzki et al., 2020a; Vagionitis et al., 2021)(Figure 15A-C). Since these clusters are formed prior to the formation of paranodal junctions and perinodal ECM, the observation of these structures led to the conclusion that other mechanisms of nodal formation may exist. The study of the formation of node-like clusters along unmyelinated axons led to the identification of two main mechanisms that are required for their formation. First the oligodendroglial secreted factors and second the involvement of the scaffolding proteins and β 2-Nav subunits (Kaplan et al., 1997; Freeman et al., 2015; Dubessy et al., 2019; Thetiot et al., 2020).

The mechanism leading to Nav clustering prior to myelination could be addressed using RGCs culture (Meyer-Franke et al., 1995). Indeed, culture of isolated RGCs failed to cluster Nav channels along axons except at the axon initial segment (AIS). However, the same culture, with all glia from the optic nerve or over a conditioning layer of isolated OLs induced Nav channels clustering whereas co-culture with isolated astrocytes failed to induce Nav channels clustering (Kaplan et al., 1997). This first experiment led to the conclusion that OLs might secrete factors that induce the clustering of Nav channels along unmyelinated RGC axons (Kaplan et al., 1997). These secreted factors were shown to lose their clustering activity following a treatment with high temperatures or protease leading to the conclusion that the clustering factor was at least partially a protein (Kaplan et al., 1997). The same group headed by B. Barres, further described the mechanism leading to node-like clustering. They could show that the disruption of actin cytoskeleton, protein synthesis or vesicular trafficking in neurons led to the inhibition of Nav clustering (Kaplan et al., 2001). In this study, the authors could not identify precisely the protein(s) secreted responsible for the clustering activity but suggested its approximate size to be between 30 and 50 kDa (Kaplan et al., 2001). Whereas studies on node assembly focused on the role of paranodal junctions for the next fifteen years following Rasband and

colleagues' seminal work in 1999, it is only in 2015 that Freeman et al. showed node-like clustering along unmyelinated axons of the hippocampus both *in vitro* and *in vivo* (Freeman et al., 2015)(Figure 15A-B). This study showed that hippocampal neurons form node-like clusters along their unmyelinated axons and confirmed that oligodendroglial conditioned medium (OCM) is required for the clustering (Figure 15A). Investigating further the identity of node-like cluster forming neurons, they could show that node-like clusters are restricted to GABAergic hippocampal neurons, the vast majority being parvalbumin (PV) and/or somatostatin (SST) positive. Contrarily to GABAergic neurons, pyramidal neurons from the hippocampus failed to form any node-like cluster suggesting that this mechanism is restricted to some of the neuronal sub-populations of the CNS (Freeman et al., 2015; Lubetzki et al., 2020a). Node-like clusters along axons showed a clustering of α -Nav1.1 and 1.2 channels together with AnkG and β 2-Nav, followed later by the clustering of other nodal CAMs and Nav1.6 channels (Freeman et al., 2015; Thetiot et al., 2020)(Figure 15D). The study demonstrated that AnkG is required for node-like clustering whereas Nfasc 186 is not necessary for this assembly (Freeman et al., 2015). Furthermore, β 2-Nav knockdown was shown to induce a 2-fold inhibition of node-like cluster formation (Thetiot et al., 2020). Altogether these results shed light on nodal proteins clustering, establishing that node-like clustering is an alternative mechanism of early assembly, distinct from the "classical" mechanism in which Nfasc 186 together with paranodal junctions are required to form nodal clusters (Rasband et al., 1999; Susuki et al., 2013; Amor et al., 2017). Using a live imaging approach, Thetiot et al showed that proteins expressed at node like clusters can pre-assemble and are partially co-transported along the axon (Thetiot et al., 2020), with a key role of molecular motors KIF5A and C (kinesin-1 family) and dynein/dynactin-1 (Thetiot et al., 2020). Lastly, Dubessy et al, identified, using a proteomic approach that contactin (released by oligodendrocytes and therefore present in OCM) was accounting for a large part of OCM clustering activity (Dubessy et al., 2019). They further showed the involvement of the ECM in Nav clustering, identifying Tenascin-R and phosphacan as critical partner of contactin for node-like clustering (Dubessy et al., 2019).

Very recently, clusters of Nav channels were observed prior to myelination in the PNS, raising the possibility that this alternative mechanism in which nodal proteins are clustered prior to the formation of paranodal junctions and to myelination could be extended in some cases to the PNS (Malavasi et al., 2021).

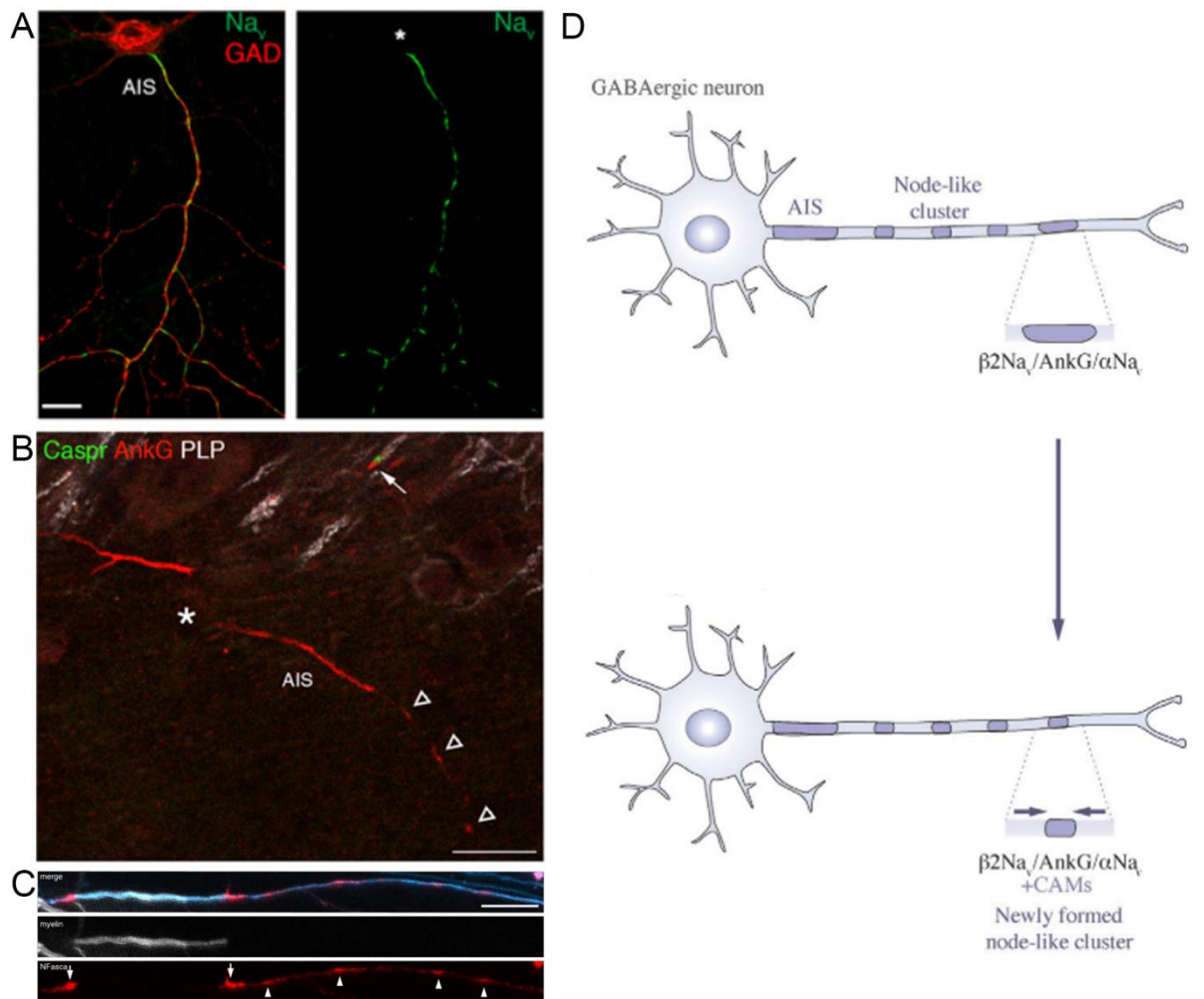


Figure 15: Node-like clusters are assembled along various populations of neurons in the CNS in mouse and zebrafish.

(A-C) Images of unmyelinated axons with node-like clusters along them. (A) In cultures of purified hippocampal neurons treated with OCM, GABAergic neurons (GAD+, in red) form node-like clusters (Nav, in green) along their axon showing that secreted factors from OLs are required for node-like clustering. (B) *In vivo*, in P12 mouse hippocampus, node-like clusters (AnkG, in red, arrowheads) can be observed prior to myelination (PLP, in grey), and their formation does not require paranodal junction (Caspr, in green, arrow). (C) In zebrafish, *in vivo*, neurofascin A (in red) forms node-like clusters along unmyelinated segment of axons (in cyan, arrowhead). (D) *In vitro*, in mixed hippocampal culture Nav, AnkG and β2-Nav are first clustered and later on, other nodal CAMs are recruited at node-like clusters and participate to the restriction of these domains. Scale bars: (A) 25μm, (B) 20μm; (C) 10μm. Adapted from Freeman et al, 2015; Vagionitis et al, 2021; Thetiot et al, 2020.

1.5.2 Functions of nodal domains along the axons

Axonal Nav channels are responsible for the regeneration of the action potential along the axon, and their organization in clusters at nodal domains allow fast saltatory conduction. Therefore by regulating the action potential arrival, nodal structure distribution, length and composition tune the function of neuronal circuits (Pajevic et al., 2014; Ford et al., 2015).

1.5.2.1 Function of node-like-clusters along unmyelinated axons

The role of node-like clusters along axons is still unclear, but some evidence suggested two potential functions so far. First, the presence of node-like clusters along axons has been correlated with a higher conduction velocity (Freeman et al., 2015), and second they may guide myelination initiation as well as define hallmarks for the future pattern of myelination (Thetiot et al., 2020; Vagionitis et al., 2021).

Concerning their role on conduction velocity, Freeman et al. were able to assess through simultaneous recordings of the soma and the axon distally the conduction speed along the axons. Using an immunostaining of Nfasc on live hippocampal neurons in culture, enabling to distinguish neurons on the presence or absence of node-like clusters along their axons, they showed that node-like clusters are associated with an approximate 2 fold increase of action potential conduction velocity (Freeman et al., 2015)(Figure 16A-B).

Regarding the fate of node-like clusters as well as their potential role in myelination, a study using co-culture of rat hippocampal neurons with murine OLs (Thetiot et al., 2020), and another work performed *in vivo* in zebrafish (Vagionitis et al., 2021), showed that the majority of node-like clusters either participate to the heminodal assembly or to mature nodes (in zebrafish). Thetiot et al. further showed that pre-myelinating OLs can contact node-like clusters and start to myelinate at their vicinity suggesting that these structures might guide myelination (Thetiot et al., 2020). In zebrafish, there are two neurofascin encoding loci, neurofascin a that localizes at the nodes of Ranvier and neurofascin b that is predicted to be analogous to mammalian neurofascin 155 (Auer et al., 2018; Klingseisen et al., 2019). Vagionitis and colleagues followed isolated clusters of neurofascin A throughout the myelination process using live-imaging on zebrafish. They found that one third of these clusters remained at the same position after myelination becoming either mature node or stable heminode. When using neurofascin A mutants, they further showed that the pattern of myelination was altered with an increased variability of intermodal length in mutant compared to WT animals. This result led them to the hypothesis that node-like clusters may prefigure mature nodes of Ranvier position along the axons to be myelinated (Vagionitis et al., 2021). Of note, the space between clusters is usually

almost twice shorter than the internodal space, meaning that some of the clusters (about a half), are overlaid by myelin sheath or become heminodes and move with myelination, the former phenomenon being observed in both (rodents and zebrafish) live imaging studies (Thetiot et al., 2020; Vagionitis et al., 2021)(Figure 16C-F).

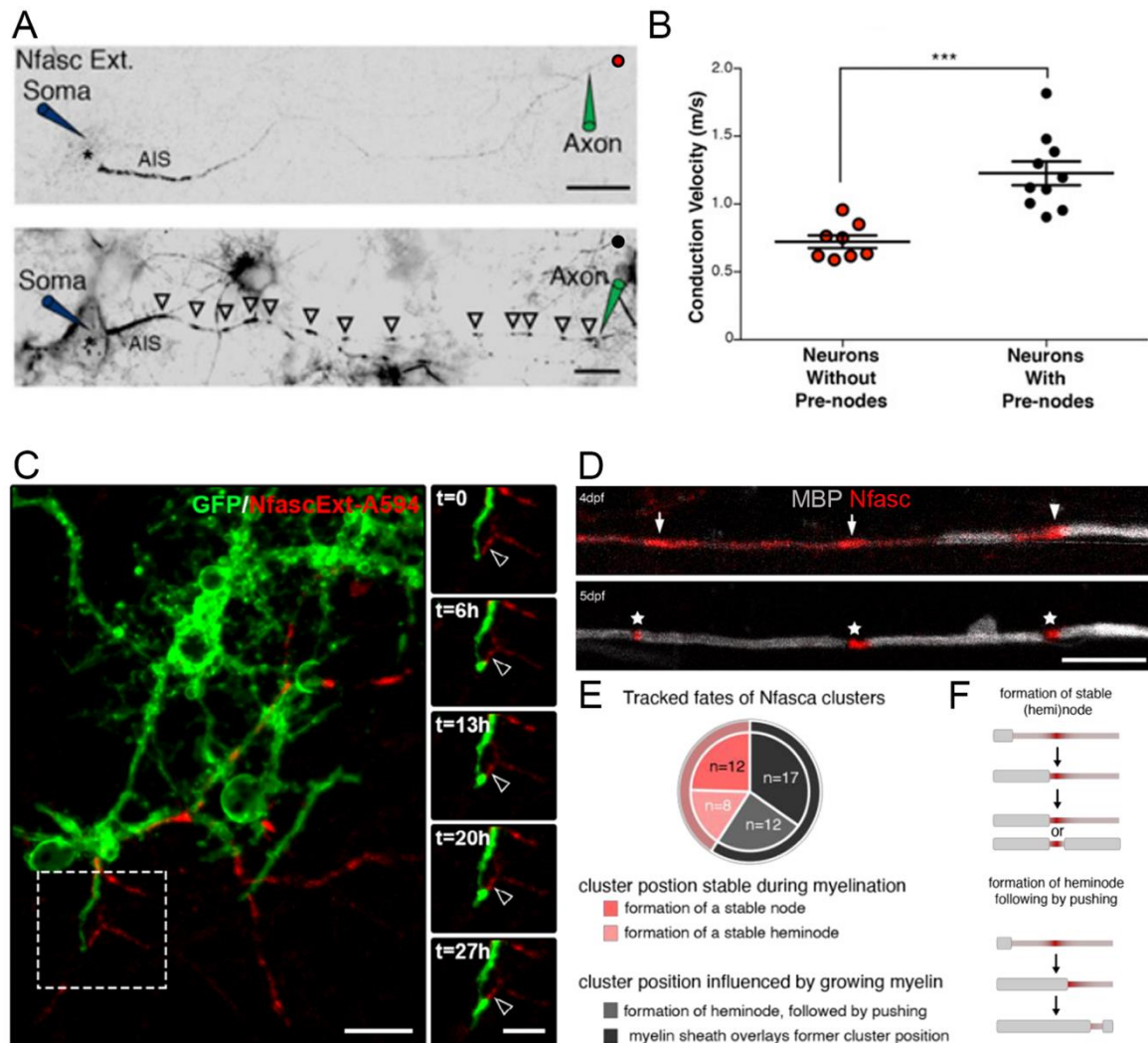


Figure 16: Node-like clusters are associated with modulations of the conduction velocity and myelination.

(A) Image of a live immunostaining with an antibody against the extracellular domain of Nfasc (in grey) showing axons without (above) or with node-like clusters (arrowhead, below). Spontaneous activity was recorded simultaneously from the soma (blue coloured pipette) and from the axon distally (green coloured pipette). (B) The conduction velocity calculated from the simultaneous recordings, show that the conduction velocity is higher along axons with node-like clusters compared to axons without cluster. (C) Live-imaging in mixed hippocampal cultures from rat co-cultured with PLP-GFP OLs, showing the initiation of myelination (GFP positive process, in green) at the direct vicinity of a node-like cluster (Nfasc, in red, arrowhead). (D) Live-imaging *in vivo* in zebrafish, showing node-like clusters (Nfasc, in red, arrow) at day post fertilization 4 that keep their position once the axon is fully myelinated (MBP, in grey) at day post fertilization 5 (stars). (E) Possible fates of node like clusters in zebrafish *in vivo*. Most of node-like clusters either stay stable to form a nodal structure or form a heminode and later move along the axon as myelination proceeds. About a third of the node-like clusters disappear. (F) Schematics of the possible fate of node-like clusters when they take part to nodal domain formation. Scale bars: (A) 25 μ m, (C) 15 μ m and zoom 10 μ m (E) 10 μ m. Adapted from Freeman et al, 2015; Thetiot et al, 2020; Vagionitis et al, 2021.

1.5.2.2 Function of mature nodes of Ranvier along myelinated axons

Along myelinated fibers, the conduction velocity is not exclusively modulated by myelin pattern and structure (see 1.4.4.1). The structure and the molecular composition of nodes also affect conduction velocity. First, the identity of Nav channels expressed at nodes can modulate the firing pattern and the conduction velocity. For instance, Nav1.2 expressed at nodes during development have a higher threshold of activation than Nav1.6 and inactivate at high frequency (20-100 Hz)(Rush et al., 2005; Hu et al., 2009). The higher threshold of inactivation together with the smaller currents triggered by Nav1.2 compare to Nav1.6 may increase the amount of time necessary to depolarize nodal membrane hence slowdown action potential conduction velocity (Rush et al., 2005; Hu et al., 2009)(Figure 17A).

In addition to Nav channel identity, several structural parameters of nodes have been shown to modulate the conduction velocity: the density of Nav channels at the node, the nodal length and the nodal diameter (Ford et al., 2015; Arancibia-Cárcamo et al., 2017). Although the density of Nav channels at nodes seems rather constant, it has been shown experimentally that both the length and the diameter of the nodal domains can vary along myelinated axons (Rios et al., 2003; Ford et al., 2015; Arancibia-Cárcamo et al., 2017; Stange-Marten et al., 2017). The modulations of the conduction velocity by the nodal length and nodal diameters are both related to the modifications of membrane capacitance, axial resistance and number of nodal Nav channels. Indeed, an increase in nodal length or diameter increase the surface of membrane at node hence increasing the capacitance and the number of nodal Nav channels. Furthermore, an increase of nodal length increases the intracellular axial resistance of the node whereas an increase of the nodal diameter decreases it (Figure 17B-C). As a consequence, although a higher resistance or capacitance tend to decrease conduction velocity whereas the increase of the number of Nav channels increases conduction, experimentally there is no simple correlation between one of these parameters and the conduction velocity. It is rather the combination of these three parameters that modulates conduction and can optimize it depending on the other properties of the myelinated fiber (Ford et al., 2015; Arancibia-Cárcamo et al., 2017). Experimentally, it has been shown in gerbil that the variation of nodal diameter in the auditory system ensure a precisely timed arrival of action potentials at the calyx of Held (Ford et al., 2015). In the cortex and optic nerve the variation in nodal length could result in a modulation of action potential conduction velocity by 20% (Arancibia-Cárcamo et al., 2017). This range of modulation is equivalent to the modulations induced by a change in the myelin thickness or internodal length but nodal modifications are more efficient regarding their energy cost (Arancibia-Cárcamo et al., 2017). Lastly, changes in nodes of Ranvier morphology could be relatively fast, and might adapt the conduction

velocity dynamically which is believed to profoundly affect neural circuits processing (Pajevic et al., 2014; Dutta et al., 2018; Cullen et al., 2021).

Although the mechanisms leading to modulation of nodal structure remain to be further described, astrocytes and neuronal activity have been suggested to modulate nodal length (Dutta et al., 2018; Cullen et al., 2021). Astrocytes have been shown to release the thrombin-protease inhibitors SERPINE2 that prevents the detachment of paranodal loops and maintain nodal length (Dutta et al., 2018). The inhibition of astrocytic exocytosis led to inhibition of SERPINE2 release and correlated with a nodal lengthening and a decrease of conduction speed (Dutta et al., 2018). Moreover, the modulation of neuronal activity using repetitive transcranial magnetic stimulations induced a decrease of nodal length (Cullen et al., 2021). This modulation is further reversible, since the mean nodal length one week after the stimulation is similar to the mean nodal length of unstimulated animals (Cullen et al., 2021).

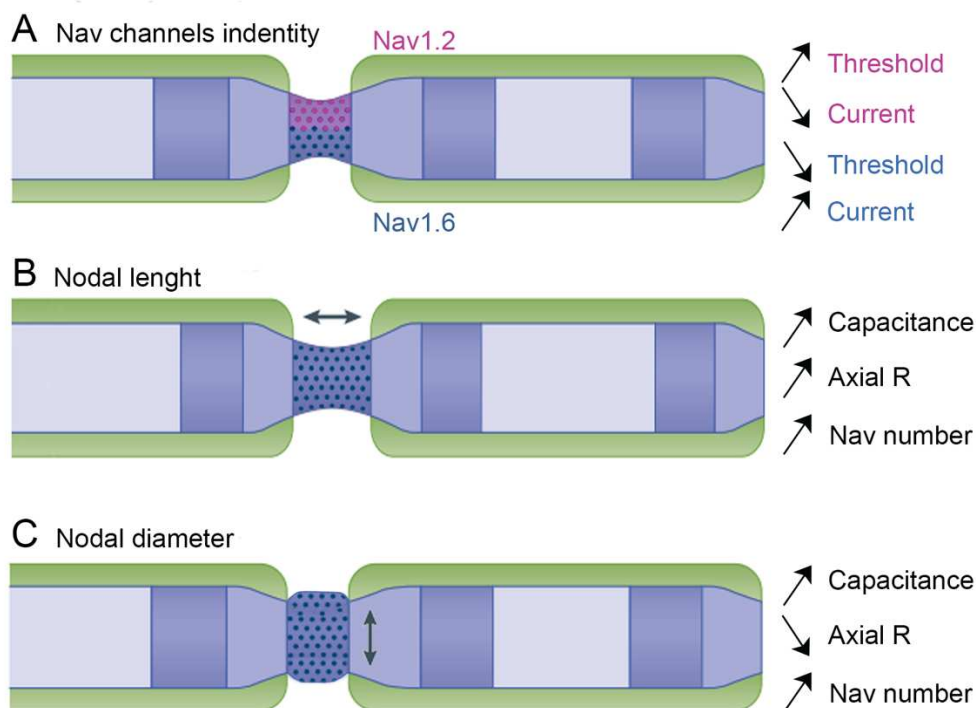


Figure 17: Modulations of nodal molecular composition and structure modulate action potential conduction.

(A) The identity of nodal Nav channels modulates the activation threshold and current flow at the node. Nav1.2 has a higher threshold and trigger lower current than Nav1.6. The properties of Nav1.6 channels may lead to a higher conduction velocity than Nav1.2. (B) The lengthening of the node increases axial resistance (Axial R) and capacitance. At a constant number of channels, it would slow down conduction velocity. However, concomitantly with nodal length increase there is an increase of the number of Nav channels at the node that also modulates conduction, leading to a complex modulation of the conduction taking into account the three parameters. (C) The increase of the nodal diameter increases nodal capacitance, decreases axial resistance and increases the number of nodal Nav channels. This leads to the same complex modulation of conduction velocity than nodal lengthening. Adapted from Lubetzki et al, 2020.

1.6 Disruption and repair of the myelinated fibers in pathological conditions; focus on multiple sclerosis

1.6.1 Multiple sclerosis and its experimental models

1.6.1.1 Multiple sclerosis, an inflammatory demyelinating disease of the CNS

Disseminated lesions of white matter were described almost simultaneously between 1835 and 1838 by Jean Cruveilhier (1791-1874) and Robert Carswell (1793-1857). However, the link between the clinical symptoms and the anatomical lesions was made in 1868 by the famous neurologist Jean-Martin Charcot (1825-1893) that named this pathology, multiple sclerosis. Using this name, he referred to the anatomical features of the disease, characterized by multifocal demyelinated plaques in the CNS (Charcot, 1868)(Figure 18A). MS is an inflammatory demyelinating and neuro-degenerative disease of the CNS characterized by focal areas of demyelination distributed throughout the CNS in both white and grey matter. Spontaneous remyelination can occur and are identified as shadow plaques using myelin staining, but the remyelination is incomplete in most cases, and further decreases with time, which leads to axonal degeneration (Chang et al., 2002; Frischer et al., 2015; Lubetzki et al., 2020b). Worldwide, MS as a prevalence of 300 to 500 cases per 100 000 individuals, with a ratio male/female of 1/3 (Thompson et al., 2018). The diagnosis is typically made in young adult with patient suffering from blurred vision, vertigo, loss of balance and sensitive or motor defects among other symptoms. In the relapsing-remitting phase of the disease, these symptoms usually last few weeks before recovery (Waxman, 2006). However, some patients (about 15%), do not recover from the first deficit and show accumulation of disability from the onset of the disease, which is commonly described as a primary progressive form of MS (Thompson et al., 2018). Along the course of the disease, patients will either remain in a relapsing-remitting form of the disease or develop a secondary progressive form of the disease in which they stop to recover from the symptoms. Lastly, some patients recover but not completely from the onset of the disease and develop a progressive-relapsing form of MS (Lublin and Reingold, 1996; Thompson et al., 2018)(Figure 18B). Although the causes of MS are still unclear, several parameters have been identified, genetic, epigenetic and environmental, with ongoing studies on their relative weight in MS etiology (Thompson et al., 2018; Factor et al., 2020).

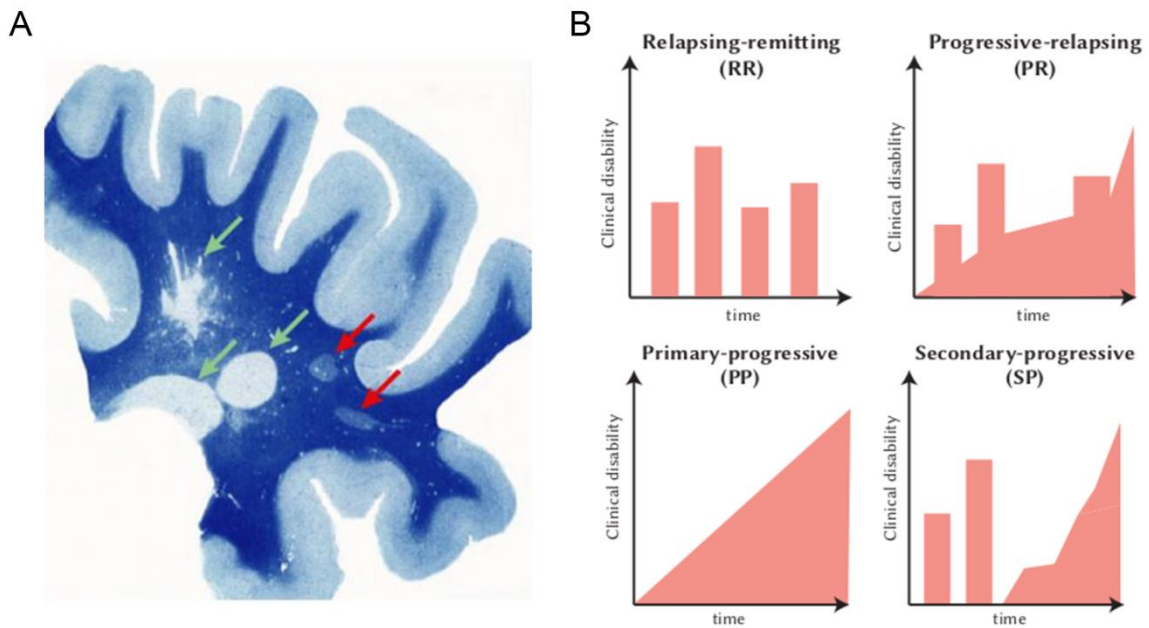


Figure 18: Anatomical lesions and clinical course of MS patients.

(A) Image of a forebrain section from a MS patient stained with luxol fast blue showing two different types of lesions found in MS patients with demyelinated regions (green arrows) and remyelinated lesions named shadow plaques (red arrows). (B) Schematics representing the progression of the disease along the course of the different form of MS. Adapted from Franklin, 2002 and Lublin and reingold, 1996.

MS is considered to be an autoimmune disease, with an adaptive immune response characterized by the invasion of the CNS by T and B lymphocytes. Even if the identification of a specific antigen has failed so far, T and B cells are suggested to be directed against CNS antigens driving the pathogenesis (Lubetzki et al., 2020b). The innate immune system is also at play in MS and might be particularly involved in disability progression (Dendrou et al., 2015). So far, most of the available treatments for MS act on the inflammatory component of the disease. If this strategy has proved very efficient to reduce the symptoms of the relapsing-remitting phase of MS, efficient treatment to stop the progression of the disease are still an unmet need (Feinstein et al., 2015). Furthermore, while inflammation is also an important component of the progressive phase of the disease, it has been suggested that tissue damage could depend independently of the inflammatory component (Trapp and Nave, 2008; Cree et al., 2019). Indeed, demyelinated axons may become more vulnerable leading to neurodegeneration. In particular, demyelinated axons display a redistribution of sodium channels along axons, a defect in potassium clearance and a lack of metabolic support from the OLs (Craner et al., 2004b; Waxman et al., 2004; Friese et al., 2014; Schirmer et al., 2014). These results highlight the importance of a better understanding of the neurodegenerative process, and the need for identification of mechanisms that would allow to promote remyelination and neuroprotection.

1.6.1.2 Development of animal models: toward a better understanding of MS

Animal models have been of major value towards a better understanding of MS and allowed to identify key parameters that could promote recovery in MS patients. Although animal models are not perfect, they allow to study the de- and remyelination mechanisms taking into account the existence or absence of inflammatory component (Lassmann and Bradl, 2017). Three main models of remyelination exist, experimental autoimmune encephalomyelitis (EAE) mainly based on inflammation, toxin-based model that are useful to study the mechanism of de and remyelination and viral models that recapitulate some aspects of the disease but are very complex and make the pathological process difficult to study.

EAE is an autoimmune disease induced in the animal by immunization with myelin components. EAE is usually triggered by injecting a specific myelin peptide to sensitize the animal together with an adjuvant used as a massive immune stimulant (Kabat et al., 1951; Mendel et al., 1995). Depending on the myelin peptide used, different features of MS can be mimicked, the most extensively used peptide being MOG₃₅₋₅₅ in mice (Lassmann and Bradl, 2017). This peptide, allow to induce a reliable chronic or acute EAE mainly restricted to the spinal cord. However, it shows a primary axonal injury mediated by auto-reactive MHC class II T CD4+ cells with only sparse primary demyelination restricted to the spinal cord (Soulika et al., 2009; Nikić et al., 2011). In other species, like rats or guinea pigs, the peptide MOG₁₋₁₂₅ can overcome this issue and triggers large plaques of primary demyelination similar to what is seen in MS (Lassmann, 1979; Storch et al., 1998). One major limitation of EAE models is their difficulty to reproduce the complexity of immune cells at play in MS (Lassmann and Bradl, 2017). Nonetheless, EAE is a largely used model notably to test the efficiency of immunomodulatory treatments and to validate pro-remyelinating strategies in animal models.

Another strategy largely applied to study more precisely the mechanisms of de- and remyelination is toxin-induced demyelination. These models generally mimic the primary demyelination seen in MS, but largely lack the inflammatory component. The most extensively used is cuprizone which induces a large depletion of OLs and demyelination, predominantly in the corpus callosum, but that can extent to the cortex with longer treatment duration. In this model, spontaneous remyelination occurs after the removal of cuprizone diet (Blakemore, 1972, 1973). Moreover, if the diet is maintained for several months, a model of chronic demyelination is established (Ludwin, 1980), which allows to mimic partially the characteristics of MS lesions diversity. Remyelination in the cuprizone model is very efficient and starts soon after the demyelination is complete (Matsushima and Morell, 2006). Although this model is largely devoid of inflammatory component, demyelination with cuprizone activates microglia and triggers astrogliosis which allows to study along the myelination processes, the glial interactions during de- and remyelination (Skripuletz et al., 2013; Gudi et al., 2014).

Another strategy is the injection of lysophosphatidylcholine (LPC) in the white matter track of adult rodents. Typically injected in the corpus callosum, cerebellum or spinal tracks, LPC induces a focal demyelination due to the primary effect of detergent on the lipid-rich membrane of myelin (Hall, 1972; Jeffery and Blakemore, 1995). The demyelination is rapidly followed by spontaneous remyelination and the timeline of repair is well described allowing to precisely follow the mechanisms of remyelination (Jeffery and Blakemore, 1995; Woodruff and Franklin, 1999). This model like the cuprizone, induces an astrogliosis and microglia activation but also exhibit some infiltration from the bone marrow (monocytes derived macrophages and brief influx of T cells) (Ousman and David, 2000; Ghasemlou et al., 2007; Plemel et al., 2020). It can also be used *ex vivo* on organotypic slices, which allows to access the tissue more easily, performing for instance pharmacological tests or live-imaging (Birgbauer et al., 2004; Thetiot et al., 2019).

1.6.2 Disruption of nodal domains upon demyelination

In MS tissues and its experimental models, demyelination triggers deep alterations of nodal domains. These alterations lead to nodal clusters disruption and participates in conduction failure of the action potential, that are directly causing disabilities in patients (McDonald and Sears, 1970; Bostock and Sears, 1978; Felts et al., 1997; Craner et al., 2004b; Coman et al., 2006; Crawford et al., 2009). At nodes several forms of alteration have been described, i.e mislocalization of ions channels at nodes, changes in Nav channel identity and a decrease of channel density up to a complete loss of ion channels clusters.

It was shown using a cuprizone model that most of the Nav clusters along axons were lost upon demyelination (Dupree et al., 2004). Similarly, in EAE it was observed in the optic nerve and spinal cord that demyelination triggers a strong decrease of Nav clusters associated with a diffused distribution of Nav channels along demyelinated axons (Craner et al., 2003, 2004a). In post-mortem tissue of MS patients, there is also a diffusion of Nav channels with few Nav aggregates remaining in demyelinated lesions (Craner et al., 2004b; Coman et al., 2006). Following demyelination, the loss of Nav clustering go along with changes in the α -Nav subunits expressed at nodes. Indeed, in various models of demyelination as well as in tissue from MS patients, a reduced expression of Nav1.6 was reported, with fewer Nav1.6 positive nodes. Conversely, Nav1.2 channels, typically found at immature nodes during the development or along unmyelinated axons (Boiko et al., 2001), are detected in higher proportion at nodal domains following demyelination (Craner et al., 2003, 2004b; Rasband et al., 2003; Pfeiffer et al., 2019). Investigating the origin of the increase of Nav1.2 positive nodes, it was shown in EAE that demyelination triggers *de novo* expression of Nav1.2 channels associated with an increase in the level of Nav1.2 mRNA (Craner et al., 2003). In Purkinje cells, following EAE induction, the expression

of α -Nav subunits was disturbed with an ectopic expression of Nav1.8 channels, an α -Nav subunit that is usually absent from these neurons (Black et al., 2000). In grey matter, the distribution of Nav channels following cuprizone demyelination is also affected, with a lower number of nodal regions expressing Nav1.6 channels and a lengthening of the remaining Nav1.6 clusters (Hamada and Kole, 2015). This redistribution of Nav channels together with a diffusion of Kv7 channels along the axons induce a strong decrease of conduction speed along the main branch of the axon and the generation of ectopic action potentials (Hamada and Kole, 2015). Investigating further the arborization of the axons and its physiological properties, Hamada and colleagues showed that demyelination also lead to frequency-dependent conduction failure in axons collaterals (Hamada et al., 2017). Thus, the perturbations of circuits functions are not only due to lesions in the white matter but also arise from demyelination of the grey matter (Kutzelnigg et al., 2005; Rinaldi et al., 2010; Hamada and Kole, 2015).

A disruption of paranodal junctions prior to demyelination has been reported as an early event in demyelinating models such as EAE and cuprizone (Howell et al., 2010; Zoupi et al., 2013). The disruption of paranodal junctions has a dramatic effect since it leads to a mislocalization of Kv1.1 and 1.2 channels at the paranode (Jukkola et al., 2012; Bagchi et al., 2014). Indeed, Kv1.1 and 1.2 channels adjacent to Nav have been reported in EAE mice and this mislocalization induces a stronger activation upon action potential that participates to conduction defects (Arancibia-Carcamo and Attwell, 2014) (Figure 19).

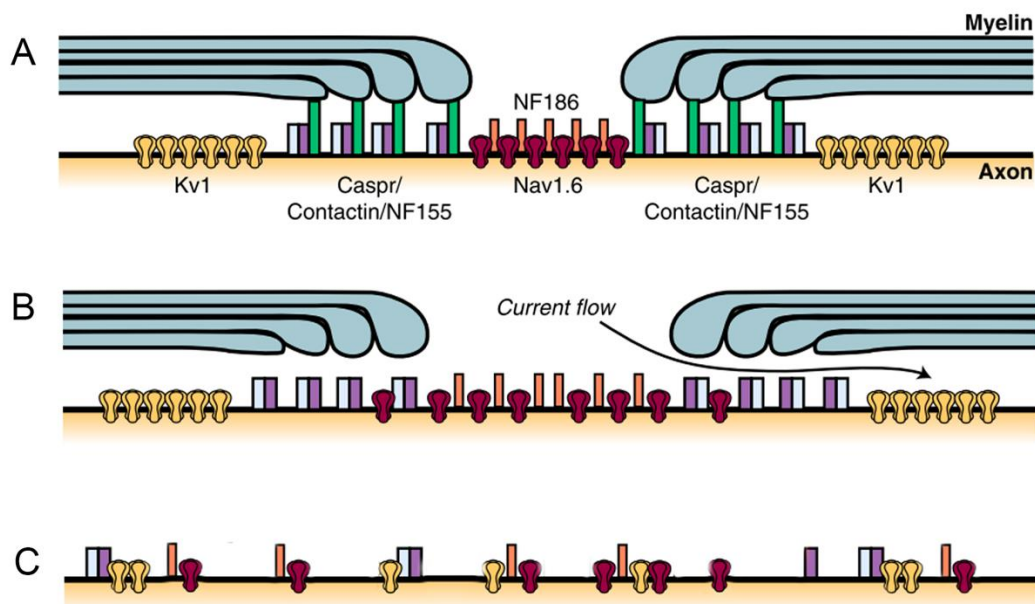


Figure 19: Disruption of nodal domain upon demyelination.

(A-C) Schematics showing the nodal disruptions following demyelination. (A) Diagram of the node in control conditions. (B) The node of Ranvier is enlarged and the paranodal junctions are detached leading to a decrease of conduction velocity and conduction failure. (C) When the myelin sheaths are completely lost, the nodal proteins diffuse along the axons which blocks saltatory conduction. Adapted from Arancibia-Carcamo and Attwell, 2014.

1.6.3 Remyelination of the CNS and reclustering of nodal domains

Remyelination can occur spontaneously in the CNS, restoring the conduction of action potential along axons as well as metabolic support. In 1961, it was observed that myelin can be regenerated after the induction of demyelination in cat spinal cord, with detection by electron microscopy of new myelin sheaths enwrapping axons (Bunge et al., 1961). The main differences between developmental myelin and regenerative myelin are the reduced thickness and the shorter myelin sheaths (Blakemore, 1974; Prineas et al., 1993). Although remyelination was described as early as in the 60s, the demonstration that it promotes axonal survival is rather recent with the work of Irvine and Blakemore. They demonstrated using a model of cuprizone that the inhibition of remyelination with X-irradiation led to the increase of axonal degeneration, which was partially restored by exogenous myelinating cells (Irvine and Blakemore, 2008). This seminal result supporting the causal link between remyelination and axonal survival was further confirmed, in particular by Mei et al. using a conditional knock-out of *Chrm1* (muscarinic acetylcholine receptor subtype 1) (Mei et al., 2016). Indeed, *Chrm1* is a potent inhibitor of OPC differentiation into OL and its genetic inactivation or pharmacological inhibition (with clemastine) promotes remyelination and prevents axonal loss with no effect on inflammation (Mei et al., 2016). In addition to the enwrapping of denuded axons by myelin, the remyelination process is also characterized by a reclustering of nodal proteins, and notably ion channels, that are required to restore saltatory conduction (Dupree et al., 2004; Coman et al., 2006).

1.6.3.1 Remyelination mechanism: cell of origin and restoration of myelin pattern

It was considered as established that remyelination was made by newly generated OLs. This hypothesis was based on several studies in experimental model of MS, showing that first the OPCs are recruited in the area of remyelination, and then differentiate in remyelinating OLs (Carroll and Jennings, 1994; Franklin et al., 1997; Gensert and Goldman, 1997; Carroll, 1998). This hypothesis was further strengthened by the use of cell fate mapping in transgenic mice expressing YFP following an inducible recombination under the control of OPCs specific promotor PDGFR α and NG2 (Tripathi et al., 2010; Zawadzka et al., 2010). Using this method, it was showed that OPC following a demyelination were able to proliferate and differentiate into remyelinating OLs. Following demyelination there is an activation of OPCs that induces their proliferation and the expression of genes involved in OPCs differentiation (Arnett, 2004; Fancy et al., 2004; Watanabe et al., 2004; Shen et al., 2008). Several pathways have been described to either promote or inhibit OPCs differentiation leading to a modulation of remyelination efficiency. For instance, Wnt pathway (Dai et al., 2014), Notch signaling

(Mathieu et al., 2019) and fibrinogen (Petersen et al., 2017) have been described to inhibit OPCs differentiation and limit remyelination efficiency. In contrast, the activation of retinoid X receptor (Huang et al., 2011) or the use of thyroid hormones (Hartley et al., 2019) allow to promote differentiation and remyelination in toxin induced demyelination model. In addition to the control of proliferation and differentiation some factors have been described to guide OPC migration toward demyelinating lesions. For instance, class 3 semaphorins have been involved in the recruitment of OPCs at demyelinated lesions (Williams et al., 2007; Piaton et al., 2011).

Although remyelination is thought to rely on the generation of new OLs, the question of the cell responsible for remyelination and the relative involvement of surviving OLs in repair has been a long standing debate that is still ongoing in the field (Franklin et al., 2020). Recently, a study using the quantification of C^{14} (from atomic bomb tests in the mid 1950s of the last century) for birthdating brain cells, gave new insight into this question by analysis of OLs ages in normal appearing white matter and remyelinated lesions of post-mortem tissue from MS patients (Yeung et al., 2019). These measures gave access to the dynamic of OL generation, and a very low rate of renewal that was further decreased in shadow plaques was found leading to the hypothesis that remyelination in MS patients is primarily made by surviving OLs (Yeung et al., 2019). The generation of myelin sheath by surviving OLs during repair was further observed in animal model of demyelination to a variable extent between animal species and demyelination models (Duncan et al., 2018; Bacmeister et al., 2020; Neely et al., 2020). However, surviving OLs although they seem to participate to remyelination have been shown to make a low number of new sheaths compared to newly generated OLs. Furthermore, using live-imaging *in vivo*, it was shown that the surviving OLs had a higher probability to make mistargeted myelin, e.g myelin on a domain that should not be myelinated (Neely et al., 2020). The participation of both surviving as well as newly generated OLs to remyelination is now the current view, but the topic is still debated (Franklin et al., 2020). However, the relative balance between these two mechanisms remains unknown and may constitute one of the main difference between remyelination in human and large animals (species with a long life expectancy and insufficient remyelination) compared to small animal models (species with short lifespan and robust remyelination) (Franklin et al., 2020).

The development of *in vivo* live imaging recently allowed the assessment of the ability of remyelination to restore preceding pattern of myelination. A study using the cuprizone model coupled to longitudinal imaging of the cerebral cortex could show that following demyelination the pattern of remyelination was deeply changed compared to the preexisting one (Orthmann-Murphy et al., 2020). There was after remyelination about 50% of the preexisting sheaths that were replaced whereas about half of the newly formed internode were mistargeted to previously unmyelinated segments (Orthmann-Murphy et al., 2020). Investigation using either cuprizone model or single cell laser ablation further showed that the remyelination pattern was more reliably regenerated along axons that were

fully myelinated than axons displaying a discontinuous pattern of myelination prior to demyelination. This result suggests that the signals guiding discontinuous myelination are not preserved upon demyelination (Orthmann-Murphy et al., 2020; Snaidero et al., 2020). Lastly, using the cuprizone model, the capacity to regenerate an accurate pattern of remyelination was tested depending on the neuronal population remyelinated. The authors showed that whereas the pattern of myelination was changed along a single axon, the global amount of axonal length covered by myelin was conserved between neuronal populations (Call and Bergles, 2021). Thus, it suggests that the pattern of myelin is changed upon remyelination but that the amount of myelinated axons amongst each neuronal population can be restored (Call and Bergles, 2021). However, although the amount of myelin wrapped along each neuronal population is preserved after demyelination, promoting globally remyelination might fail to restore completely neural functions owing to the modifications of myelin pattern along individual axons.

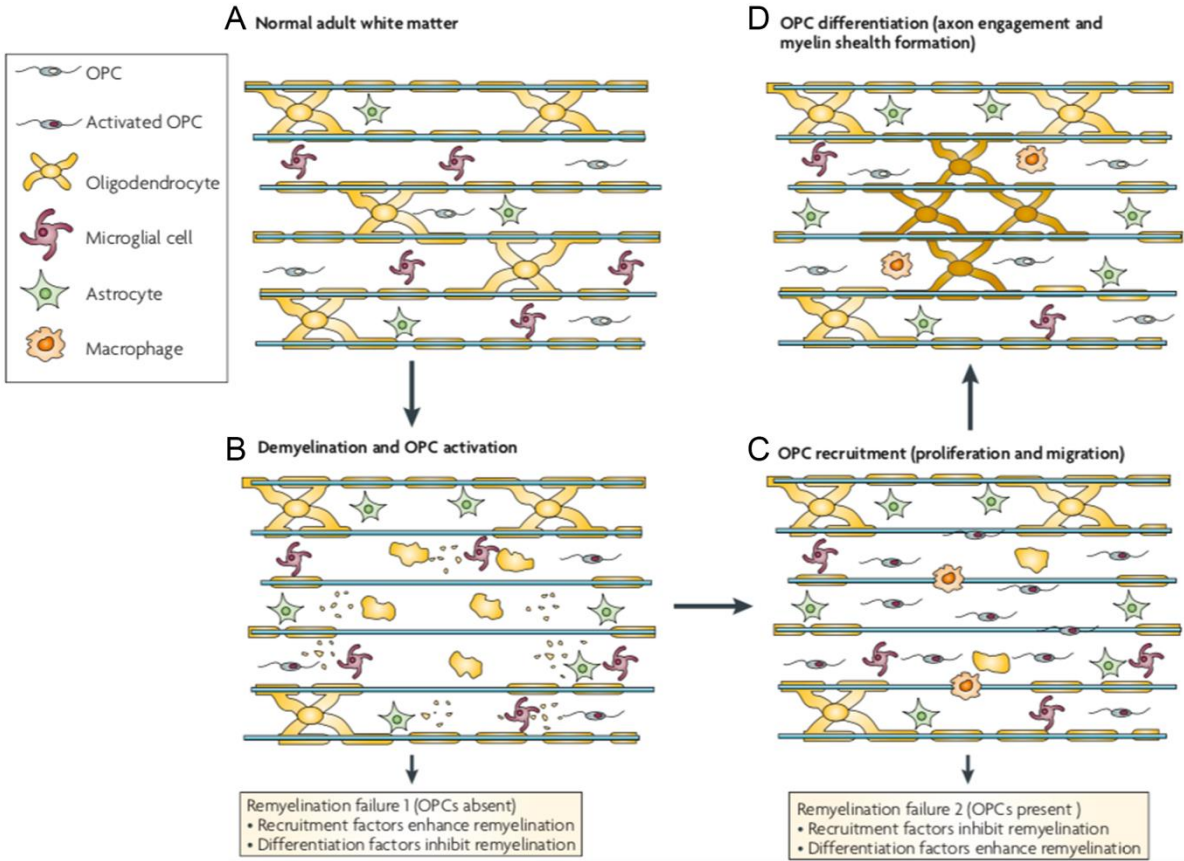


Figure 20: From demyelination to remyelination.

(A-D) Schematics showing the different steps from demyelination to remyelination and the different actors of remyelination mechanisms. Adapted from Franklin and Ffrench-Constant, 2008.

1.6.3.2 Nodal recluster

Another important parameter to restore the function of the circuits is the clustering of nodal protein along remyelinated axons. Investigating nodal protein distribution in post mortem tissues of MS patients, Coman et al. showed that remyelination process is associated with a recluster of proteins at nodal domains, with Nav at nodes, Caspr at the paranode and Kv channels and Caspr2 at juxtaparanodes (Coman et al., 2006). Intriguingly, it was shown that isolated clusters of Nav channels and independent clusters of Caspr are found along axons lacking myelin staining. Furthermore, the quantification of these isolated clusters in periplaques and partially remyelinated plaques showed that whereas isolated Caspr clusters were found in the same proportion, the density of Nav isolated clusters was deeply increased in partially remyelinated plaques. This result suggested that Nav clustering is an early event in remyelination that could precede the formation of paranodal junctions and the clustering of paranodal proteins (Coman et al., 2006). It further corroborated results obtain in the PNS, showing that saltatory conduction could appear prior to remyelination due to foci of inward current at what was named ϕ -nodes (Smith L et al., 1982). These isolated clusters of Nav channels formed prior remyelination may represent the counterpart of node-like clusters formed along axons prior to myelination (Kaplan et al., 1997; Freeman et al., 2015; Bonetto et al., 2019; Dubessy et al., 2019; Thetiot et al., 2020; Vagionitis et al., 2021). In contrast with the early clustering of nodal and paranodal proteins, isolated clusters of Kv channels were virtually absent along unmyelinated axons, which suggest that clusters at juxtaparanode are formed only once remyelination has started (Coman et al., 2006). In a cuprizone model of demyelination, it was found that after a chronic demyelination, component of the cytoskeleton (β IV-spectrin) remained clustered along demyelinated axons (Orthmann-Murphy et al., 2020). Furthermore, when the remyelination occurred along portions of axons previously myelinated, the positions of nodal domains were frequently kept. This observation suggested that the axonal cytoskeleton might keep landmarks used to guide the pattern of remyelination (Orthmann-Murphy et al., 2020).

The function of persistent cytoskeleton landmarks as well as isolated Nav clusters formed prior to remyelination remain to be resolved. The description of the mechanisms leading to their formation and how these structures could modulate remyelination is of great interest to further allow the development of pro-remyelinating strategies.

2. Microglia shape the CNS in development, homeostasis and pathological conditions

Microglia have been described as an independent cell type in 1919 by Pio del Río-Hortega. Using silver staining method Río-Hortega hypothesized a mesodermic origin of microglia, and described their ability to phagocytose debris (del Río-Hortega, 1919a, 1919c, 1919d, 1939; Sierra et al., 2016). His observation of tissue in development led him to suggest that microglia could phagocytose neuronal debris including soma of neurons and fine neuronal processes (del Río-Hortega, 1919d). Lastly, studying pathological tissue, he observed that microglia could proliferate and undergo morphological changes only several hours after injury (del Río-Hortega, 1919b; Sierra et al., 2016). The colonization of the brain by microglia was studied in humans, when John Kershman observed their infiltration in the developing CNS during embryonic development (Kershman, 1939). After these initial discoveries, the field of microglia has been largely neglected for two decades. It was not until the late 60s that the group of Goerg Kreutzberg studied microglia in the facial nucleus following facial nerve lesions. Using this model, his group showed that microglia were involved in the reorganization of the neuronal circuits in the facial nucleus playing a role in the removal of synaptic terminals on motoneurons (Blinzinger and Kreutzberg, 1968). The establishment of microglial culture in the late 80s allowed the first functional studies of these cells (Giulian and Baker, 1986). Using cell culture, it became evident that microglial cells had a prominent role in the release of cytokines like IL1- β or TNF- α in pathological conditions, hence regulating neuroinflammation (Hetier et al., 1988; Sawada et al., 1989). Electrophysiology applied to isolated microglia further allowed to differentiate them from peripheral macrophages, with notably specific properties of potassium currents (Kettenmann et al., 1990). Until the beginning of the 21st century, most of the studies were restricted to isolated microglia. The development of *in vivo* live-imaging led to the observation of the striking dynamics of microglia in the brain parenchyma in homeostatic conditions (Davalos et al., 2005; Nimmerjahn et al., 2005). These two seminal studies launched a growing interest in the scientific community for microglial cells, interest that have been constantly growing since then with the demonstration of the involvement of microglia in development, homeostasis and pathological conditions. This chapter will describe microglia function in the CNS, their role in shaping circuits from development to adulthood in homeostatic condition. It will further focus on the functional impact of microglia on myelination and remyelination in pathological conditions.

2.1 Microglia, a sensor of the CNS

2.1.1 Ontogeny of microglia

When Pio Del Rio-Hortega first identified microglia, he hypothesized that they were from a mesodermic origin contrary to neurons and macroglia (comprising astrocytes and oligodendroglia) that were from neuroectodermic origin (del Río-Hortega, 1919c, 1932, 1939). Microglia origin was then debated for many decades with the majority of the scientists that joined the mesodermic hypothesis based on the morphologic similarities and the expression of common antigen (Murabe and Sano, 1982, 1983; Hume et al., 1983; Perry et al., 1985). The other hypothesis was supporting a neuroectodermic origin of microglia that would differentiate from the same tissue than the other cells of the brain (Kitamura et al., 1984; Hao et al., 1991; Fedoroff et al., 1997). The dominant hypothesis until recently was that microglia arose from the embryonic and perinatal wave of hematopoietic cells that would invade the CNS and differentiate in the parenchyma. The observation that the developing brain already contain apparent microglia at E9.5 in mice suggested that the primitive hematopoiesis occurring at E8.5 participated to microglia formation that would originate from the yolk sac (Alliot et al., 1991, 1999). Indeed, the definitive hematopoiesis occurs at E10.5, a time that was incompatible with microglia colonizing the brain at E9.5 (Bertrand et al., 2005; Cumano and Godin, 2007; Prinz et al., 2019). Between 2010 and 2013, three studies firmly demonstrated the yolk sac origin of microglia using cell fate mapping (Ginhoux et al., 2010; Schulz et al., 2012; Kierdorf et al., 2013)(Figure 21). By labelling primitive macrophages between E6.5 and E10.5, Ginhoux and colleagues demonstrated that labeled primitive macrophage were produced between E6.5 and E8.5, and persisted in the CNS into adulthood (Ginhoux et al., 2010). Although the ontogeny of microglia seem to differ between species and in particular in zebrafish (Xu et al., 2015; Ferrero et al., 2018; Sharma et al., 2021), recent single cell RNA sequencing approach in human tissue suggested a yolk sac origin for microglia similarly to what has been described in mice (Bian et al., 2020).

The early invasion of the brain by microglia, before the differentiation of neurons and other glial cell types allow them to regulate many processes of the CNS development such as neurogenesis, neuronal migration, circuit wiring and later synaptogenesis, oligodendrogenesis and myelination (see 2.2 and 2.3) (Figure 22). Furthermore, microglial cells persist into adulthood through their proliferation within the CNS and self-renew, thus maintaining a constant density without any contribution of the peripheral circulating monocytes (Askew et al., 2017; Réu et al., 2017; Tay et al., 2017).

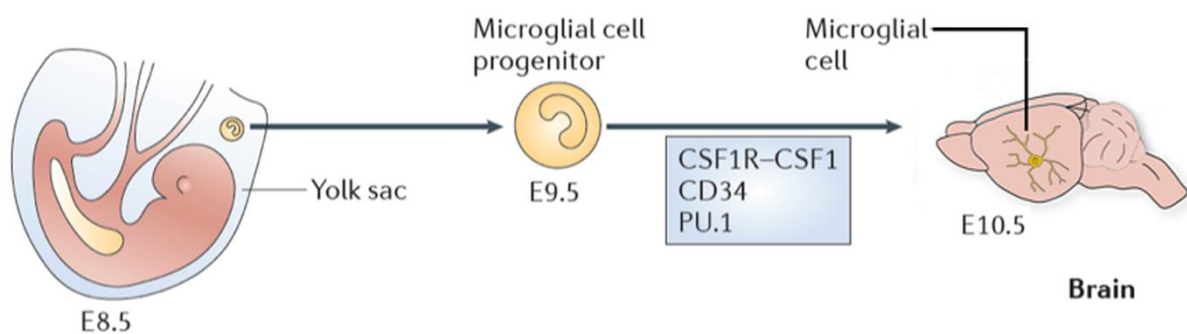


Figure 21: Ontogeny of microglia in mouse.

Schematics showing the developmental origin of microglia. Microglia start to invade the developing CNS as early as E9.5-E10.5. Adapted from Saijo and Glass, 2011.

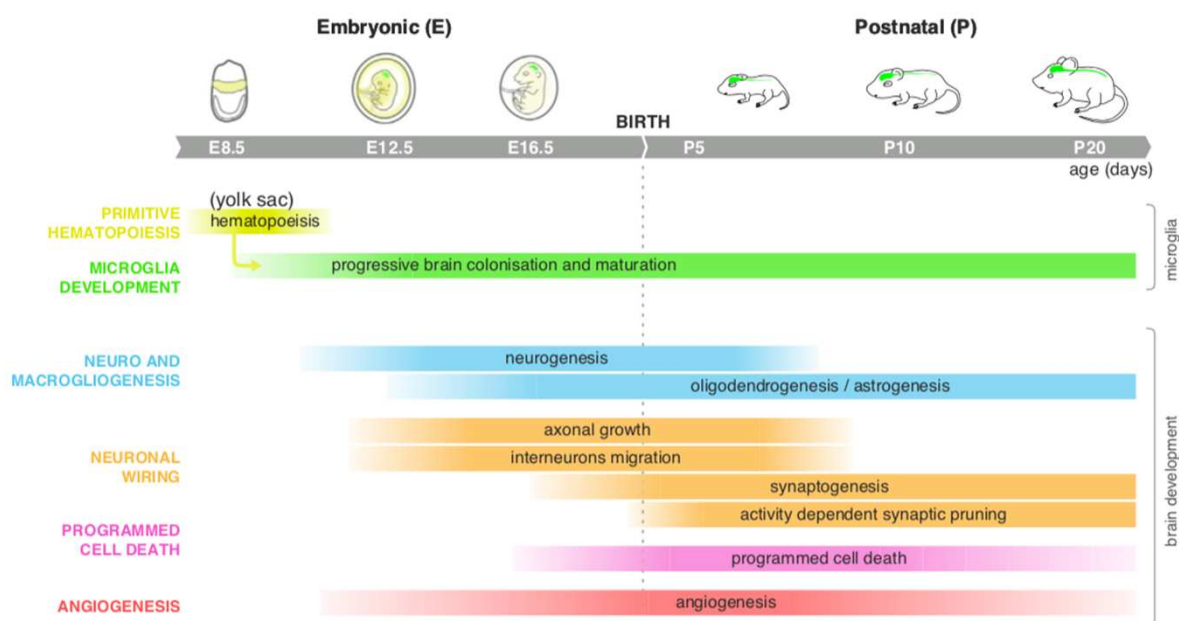


Figure 22: Developmental processes of the CNS and microglia invasion.

Schematics showing the timeline of microglia development in mice and the other main developmental processes occurring in the CNS that are modulated by microglia cells. From Thion and Garel, 2017.

2.1.2 Microglia sense their environment dynamically

2.1.2.1 Microglia motility, a parameter set by the environment

The development of *in vivo* live imaging using two photon microscopy (Svoboda et al., 1997; Grutzendler et al., 2002) and microglia reporter mice (CX3CR1^{GFP})(Jung et al., 2000) allowed to assess the dynamics of microglial cells in the parenchyma (Davalos et al., 2005; Nimmerjahn et al., 2005)(Figure 23A). In this context, two seminal studies described that homeostatic microglia are very dynamic cells extending and retracting their process at about 1.5 $\mu\text{m}/\text{min}$ (Davalos et al., 2005; Nimmerjahn et al., 2005). Moreover, in homeostatic condition each microglial cell has a non-overlapping territory in the brain, and their density is maintained from postnatal development throughout life due to a spatial and temporal balance between proliferation and apoptosis (Nimmerjahn et al., 2005; Jinno et al., 2007; Askew et al., 2017). Although the soma of microglia are rather stable, it has been shown that 10% of the microglial somata move daily in the somatosensory cortex which increases at a long temporal scale the volume of tissue explored (Eyo et al., 2018). Furthermore, additionally to their main dynamic processes described initially, it has been recently shown that microglia display filopodia (Bolasco et al., 2018; Bernier et al., 2019). These actin-dependent structures allow the screening of microglia direct environment with a faster time scale, their extension and retraction velocity being on average about 8 $\mu\text{m}/\text{min}$ (Bernier et al., 2019). This strategy of space screening with different time and space scales (fast scanning of the direct environment and slower scanning distally) is a highly efficient behavior used by other immune cell types to monitor and sense their environment (Viswanathan et al., 1999; Shlesinger, 2006; Harris et al., 2012).

The tissue screening by microglia is further modulated by several environmental parameters that regulate their morphology and dynamics. It has been recently shown that the resting potential of microglia, modulated by the tonic active potassium channel Thik-1 (TWIK-related halothane-inhibited K⁺ channel 1), regulates microglia morphology and process dynamics (Madry et al., 2018b, 2018a). Consequently, a depolarization of microglia membrane by Thik-1 inhibition or by raising K⁺ extracellular concentration induces a diminution of microglia motility and ramification in both rodents and human tissue (Madry et al., 2018b, 2018a; Izquierdo et al., 2021b)(Figure 23B). Interestingly, in the substantia nigra pars reticulata, microglia show a more hyperpolarized resting membrane potential than microglia elsewhere in the basal ganglia, which correlate with their more complex morphology (De Biase et al., 2017). Microglia monitoring of the tissue is also modulated by cyclic AMP (cAMP) intracellular concentration and compartmentalization. The increase of intracellular cAMP concentration induces an increase of microglial filopodia and a retraction of the microglial processes (Bernier et al., 2019)(Figure 23B). Conversely, reduction of cAMP concentration results in collapse of

filopodia and tends to promote large microglial processes extension (Bernier et al., 2019). As a result, several microglial G protein-coupled receptors induce respectively an increase (Gs-coupled) or a decrease (Gi-coupled) of intracellular cAMP concentration modulating microglial dynamics and ramification (Kalla et al., 2003; Haynes et al., 2006; Liang et al., 2009; Orr et al., 2009; Gyoneva and Traynelis, 2013; Gyoneva et al., 2014; Sipe et al., 2016). One of the Gi receptors highly expressed by homeostatic microglia is the P2Y12 receptor (Sasaki et al., 2003). Its activation by ATP release following damage in the CNS induces microglial process extension towards the injured site (Davalos et al., 2005; Haynes et al., 2006). In addition to the inhibition of cAMP production by the adenylyl cyclase, P2Y12 receptor activation also potentiates Thik-1 channels that trigger an hyperpolarization of the membrane potential (Madry et al., 2018b). These modulations both lead to an increase of process extension together with a retraction of microglial filopodia (Haynes et al., 2006; Fontainhas et al., 2011; Madry et al., 2018b; Bernier et al., 2019). Other Gi-coupled receptors are expressed by microglia and have been shown to modulate microglial dynamics. P2Y13 is an adrenergic receptor highly similar to P2Y12 (Pérez-Sen et al., 2017), its deficiency in mice induces a decrease of microglia dynamics and ramification, most probably due to an increase in basal cAMP level in microglia (Kyrargyri et al., 2019). Similarly, in mice deficient for the Gi-coupled receptor CX3CR1 receptor, a reduced screening behavior and a decrease of microglial morphological complexity has been described (Liang et al., 2009; Pagani et al., 2015)(Figure 23B). Lastly, tyrosine kinase receptors have been suggested to promote microglia dynamics *in vivo*. Indeed, in mice with specific microglial deficiency of TAM tyrosine kinase receptors Axl and Mer, there is a decreased microglia dynamics (Fourgeaud et al., 2016), that might be due to the regulation of Thik-1 activity by tyrosine phosphorylation (Gierten et al., 2008)(Figure 23B).

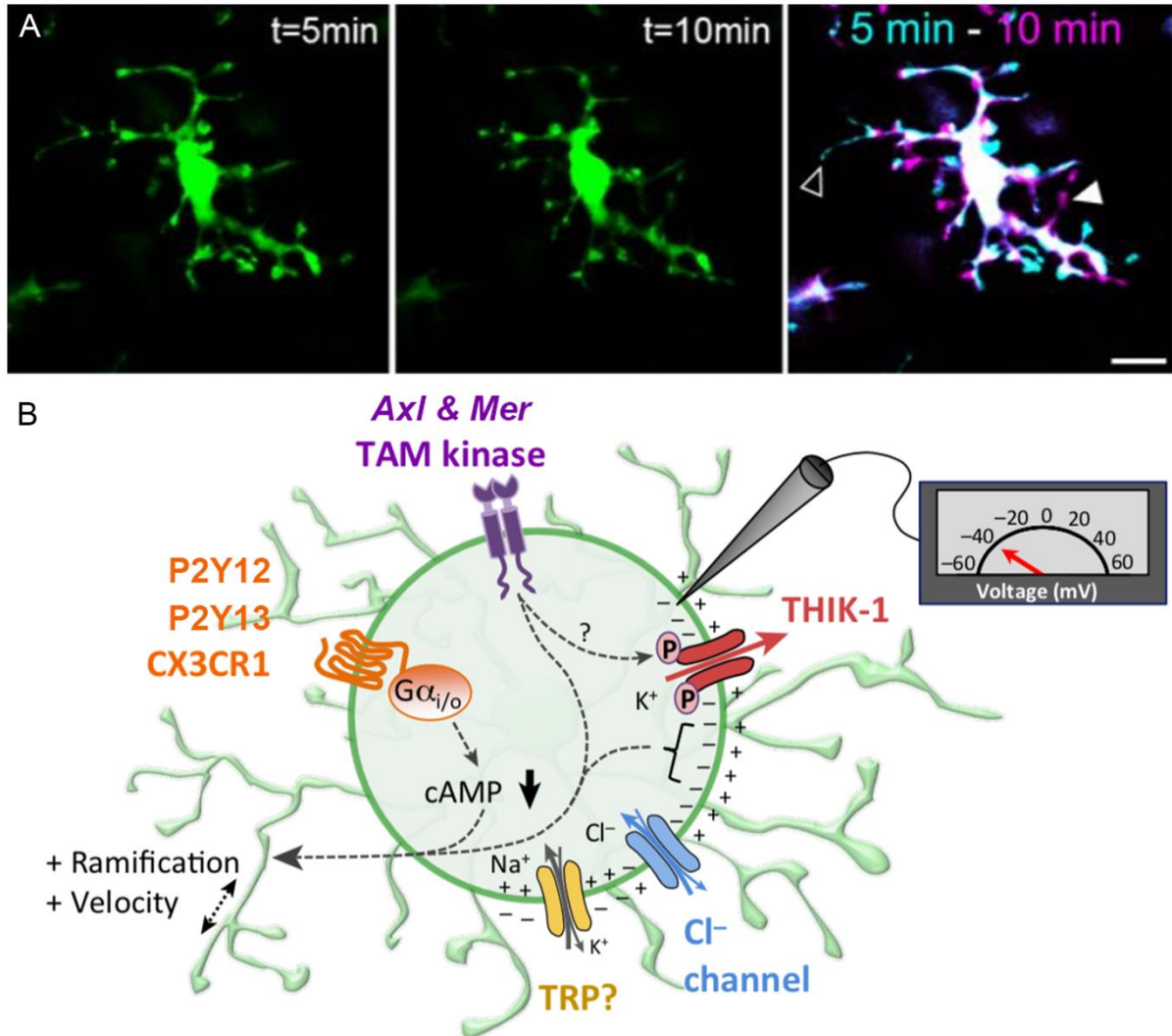


Figure 23: Microglia dynamics and morphology are modulated by the environment.

(A) Live imaging of microglia showing its morphology and dynamics. The overlap highlight extending processes (in magenta) and retracting processes (in cyan). (B) Schematics showing the parameters that set microglia morphology and dynamics. Ion channels set the membrane potential that is responsible for the modulation of surveillance and morphology of microglia. Primarily the tonic active channel Thik-1 is responsible for the regulation of membrane potential. Other ion channels might be involved in setting microglia membrane potential, Cl⁻ channels and depolarizing cation channels like TRP. Gi-coupled proteins like CX3CR1, P2Y12 and P2Y13 when activated induce a low concentration of cAMP and promote ramification and surveillance. The Mer and Axl TAM tyrosine kinase receptors promote surveillance and ramification of microglia through a mechanism that may involve Thik-1 phosphorylations. Scale bar: 10μm. Adapted from Izquierdo et al, 2019.

2.1.2.2 Microglia chemotaxis, an oriented motility toward the damaged environment

Microglial cells survey the CNS parenchyma and adapt their dynamics to the local environment. This primary function of sensing the brain is fundamentally related to their capacity to react as a first line to prevent or restrain brain injuries and dysfunctions. Following damage, microglia can rapidly extend processes specifically toward the lesion in order to restrict it (Davalos et al., 2005; Haynes et al., 2006)(Figure 24A). This process while also modulating global microglial surveillance, is regulated differently by chemotaxis and is mainly modulated by purinergic receptors (Haynes et al., 2006; Kurpius et al., 2007; Sipe et al., 2016; Madry et al., 2018b). Amongst purinergic receptors, two main categories are expressed by microglia, the ionotropic P2X and the metabotropic P2Y receptors. These purinergic receptors are directly activated by ATP (P2X4, P2X7) or by the quickly produced byproduct ADP (P2Y12, P2Y13) (Madry and Attwell, 2015). As a result of brain injury, the main nucleotide released is ATP. The main purinergic receptor involved in ATP/ADP guided chemotaxis is P2Y12, that is expressed at the surface of microglia with an enrichment at the tip of the extending process during chemotaxis (Honda et al., 2001; Davalos et al., 2005; Haynes et al., 2006; Dissing-Olesen et al., 2014a)(Figure 24B). Following its activation, P2Y12 induces process extension toward the ADP gradient and increases the expression of β -integrin that interacts with the ECM and participates in process extension (Ohsawa et al., 2010; Meller et al., 2017)(Figure 24B). The stimulation of the integrin receptor CD11b/CD18 is also involved in microglial chemotaxis. Its activation by fibrinogen released upon blood brain barrier destabilization in EAE, leads to microglial process extension followed by microglia clustering at the site of release (Davalos et al., 2012). Other receptors like CX3CR1 and TAM tyrosine kinase have also been described to participate in chemotaxis (Figure 24B). In mice deficient for these receptors, there is a slowdown of process extension toward laser-induced injury or local ATP release (Liang et al., 2009; Pagani et al., 2015; Fourgeaud et al., 2016).

Other microglial receptors participate in sensing the environment but do not directly modulate microglia dynamics. These other signaling pathways are in particular involved in microglia activation and regulation of phagocytosis. These signaling are at play in the regulation of neurogenesis, oligodendrogenesis and brain wiring (see 2.2 and 2.3) and in pathological conditions, following demyelination for instance (see 2.4).

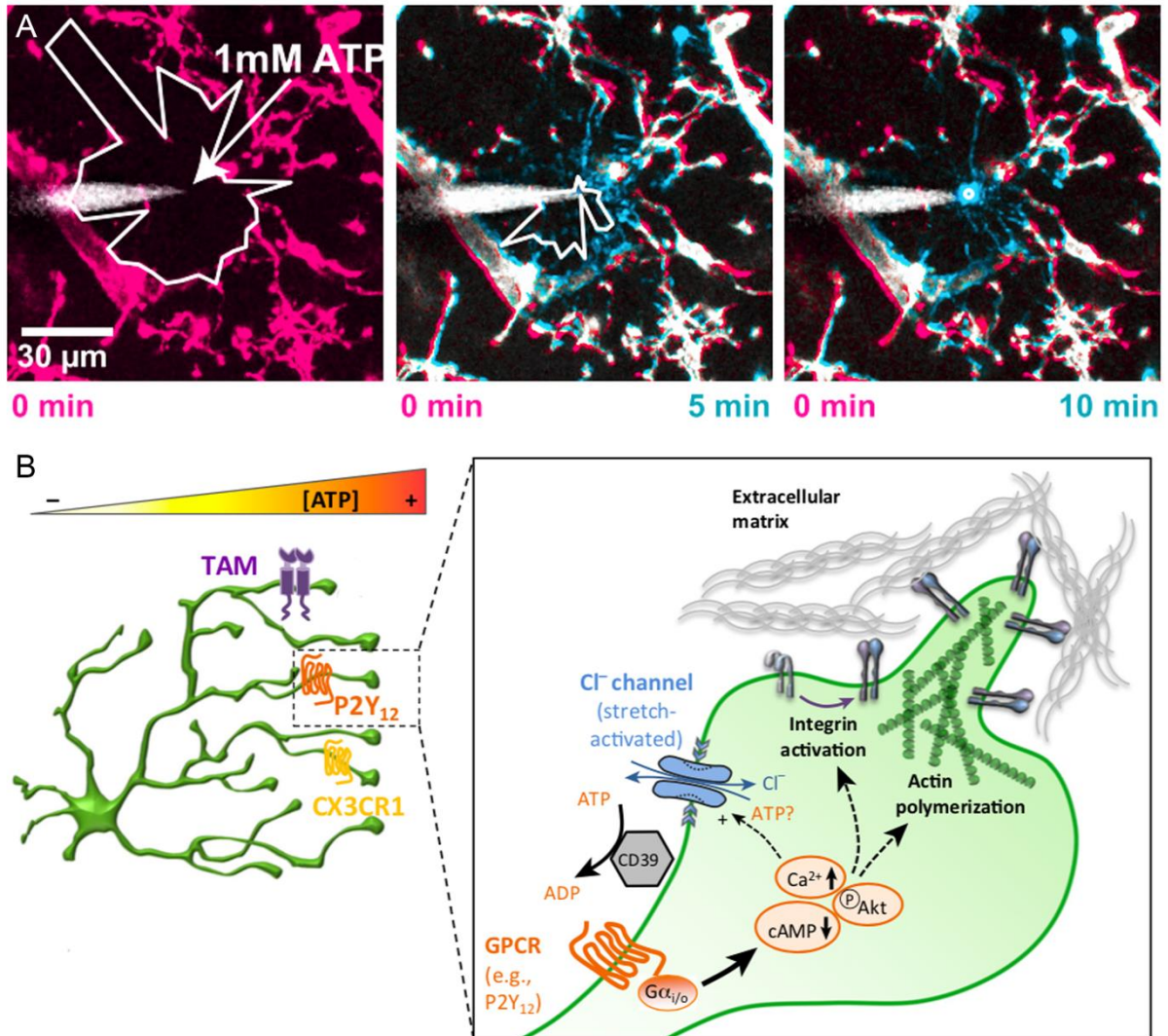


Figure 24: Microglia chemotaxis and the receptors involved in its modulation.

(A) Images of live imaging of microglia showing process extension toward the site of ATP release. The overlap highlights extending processes that converge toward the site of ATP release (in cyan). (B) Schematics showing the receptors that modulate chemotaxis. The right part of the schematics highlights the molecular mechanisms responsible for process outgrowth following P2Y₁₂ activation. Adapted from Madry et al, 2018 and Izquierdo et al, 2019.

2.2 Microglia contact neurons and shape circuits in homeostasis

The modulations of neuronal function by microglia are made directly by contact (Li et al., 2012; Schafer et al., 2012; Cserép et al., 2020) as well as by secretion of soluble factors (Parkhurst et al., 2013; Eyo et al., 2014; Badimon et al., 2020), or indirectly through intermediate glial cells (Pascual et al., 2012; Liddel et al., 2017). Through these interactions microglia modulate neuronal fate and shape circuits with growing evidence of microglia control of neuronal functions.

2.2.1 Microglia contact directly every neuronal compartments

Neurons have a very complex morphology, with functions that are restricted to specific compartments of their elaborated structure (Matsuda et al., 2009; Bolam and Pissadaki, 2012; Donato et al., 2019). As a consequence, to monitor the homeostatic brain functions and further modulate them, microglial cells contact directly each of their functional units (Cserép et al., 2021a).

The most studied contact between microglia and neurons is the one established by microglia at synapses with both the pre- and postsynaptic compartments (Wake et al., 2009; Tremblay et al., 2010) (Figure 25A-C). In the CA1 region of the hippocampus in mice and in the forebrain of rats, about 3% of the dendritic spines were found to be contacted by microglia (Sogn et al., 2013; Weinhard et al., 2018). Complementary to light microscopy, correlative light and electron microscopy further confirmed the direct interaction for more than 80% of the contacts observed using light microscopy (Weinhard et al., 2018). Although not focusing their work of microglia-synapses interaction Cserép et al. observed in the cortical layer II and III of the cortex in mouse, using neurotransmitter specific markers, that both glutamatergic and GABAergic synapses were in close contact with microglial processes in similar proportions (Cserép et al., 2020). A proportion of 3% of contacted synapses might appear low but these contacts are not long lasting. In the somatosensory and visual cortex on average the apposition was shown to last about 5 minutes with about one contact per hour on a given dendritic spine (Wake et al., 2009). Therefore, the proportion of synapses contacted over time might be much larger (Uweru and Eyo, 2019). Taking into account the stability and frequency of contact on synapse from Wake et al., a rough estimate would for instance lead to 35% of the synapses contacted over one hour (Wake et al., 2009). Several molecular mechanisms have been involved in the modulation of microglia-neuron contact at synapses and are mainly involved in synaptic pruning (see below 2.2.2.2). However, synapse pruning is modulated by direct contact as well as by diffusive factors secreted in the extracellular medium (Paolicelli et al., 2011; Hoshiko et al., 2012; Vainchtein et al., 2018). So far, two molecular signalings, the complement components C3 that interact with the complement receptor CR3, and SIRP α activation by CD47, have been shown to control synapse pruning by direct contact between microglia and synapses (Schafer et al., 2012; Lehrman et al., 2018).

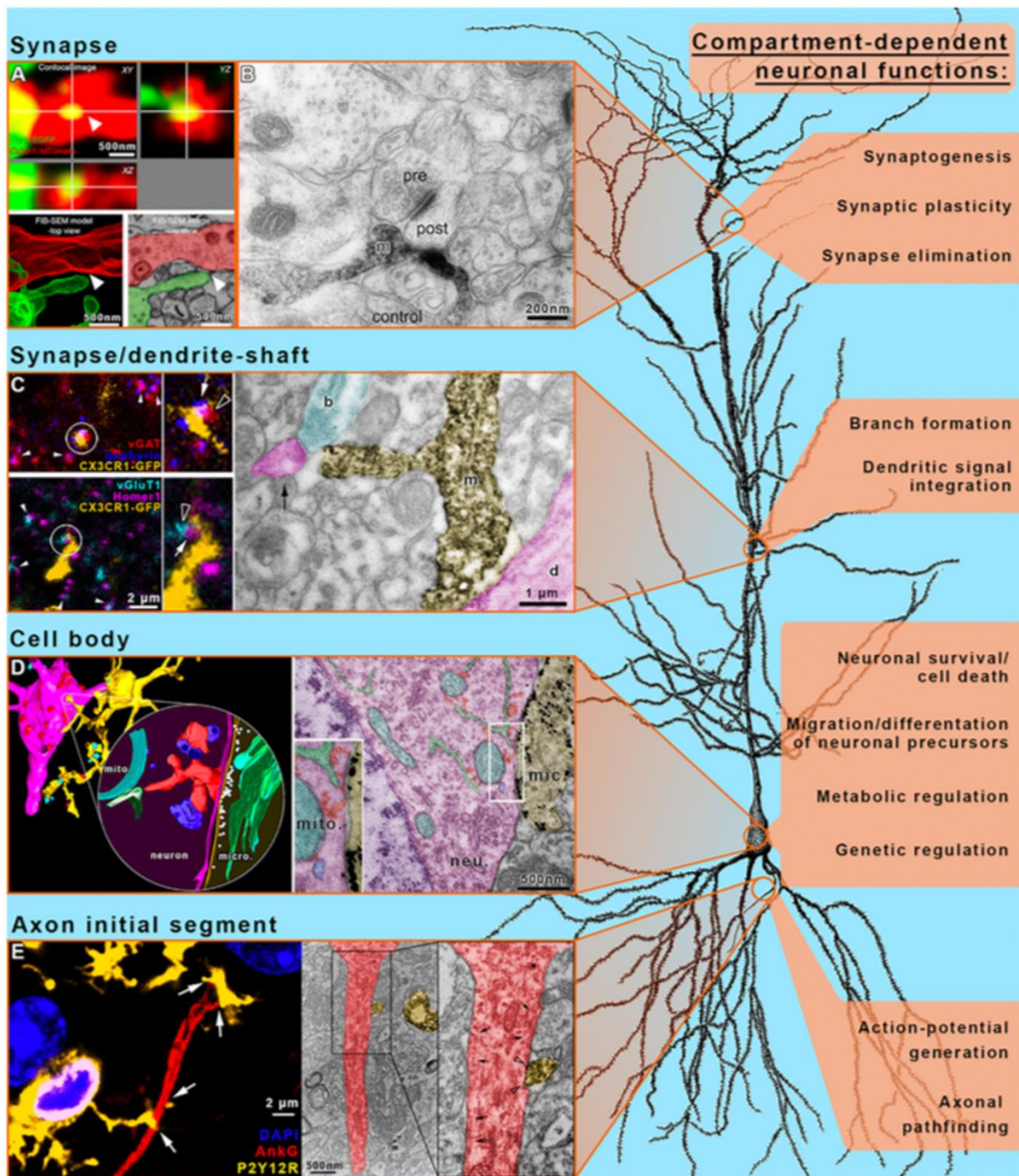


Figure 25: Microglia interact directly with every compartment of neurons.

(A-E) Schematics showing the different types of contacts established directly on neurons by microglia. The potential functions of these direct interactions with microglia are shown on the right of the figure. (A) Example of a close apposition between a dendritic spine (in green) and a microglial process (in red). The two structures are apparently in contact, but the correlated electronic microscopy shows that there is no direct contact between the two structures highlighting the importance of electron microscopy to show membrane to membrane appositions. (B) Example of a transmission electron micrograph from a mouse cerebral cortex showing a microglial cell (m, dark precipitate) interacting with the pre and post-synaptic compartment of a glutamatergic synapse (the asymmetric densities allow to identify the glutamatergic nature of the synapse). (C) Confocal images showing that microglial processes (in yellow) are closely apposed to both GABAergic (Vgat presynaptic and gephyrin postsynaptic) and glutamatergic (vGluT1 presynaptic and Homer1 postsynaptic) specific markers of synapses. Transmission electron micrograph showing a close contact between a microglial process (m, dark precipitate) and a presynaptic bouton (filled with cyan, b) of a glutamatergic synapse. (The figure legend continues on the next page)

(D) 3D reconstruction of a confocal volume scan showing microglia (in yellow) contacting the soma of a neuron (in magenta). The insert shows the 3D electron tomographic reconstruction of a microglial contact with a neuronal cell body and highlight the close apposition of the microglia membrane (yellow) with the membrane of the neuron (magenta). On the right, an electron microscopy micrograph shows a direct contact of microglial process (filled with yellow, mic) in direct contact with the membrane of a neuronal soma (filled with magenta, neu). (E) Confocal image showing a microglial process (P2Y12R, in yellow) that contact the axon initial segment (AnkG, in red) of a neuron. On the right the transmission electron micrograph shows the direct contact established by a microglial process (filled in yellow) on the axonal initial segment (filled in red). Figure from Cserep et al, 2021a.

Direct contacts between the soma of neurons and microglia were observed in pathological conditions, in particular in the stripping of cell body from axon terminals following microglia activation (Blinzinger and Kreutzberg, 1968; Trapp et al., 2007). Later on, microglial contacts with the neuronal soma have been observed in various areas of the developing and homeostatic CNS in zebrafish, rodents and human tissues (Li et al., 2012; Stowell et al., 2018; Cserep et al., 2020, 2021b; Hughes and Appel, 2020) (Figure 25D). In the developing optic tectum of the zebrafish and neocortical area of the mouse, the direct contact of microglia with the soma of neurons has been characterized using electronic microscopy (Li et al., 2012; Cserep et al., 2020). The use of live imaging allowed the observation of long lasting direct contact during the development and in adulthood which suggested a role of microglia in monitoring neuronal state throughout lifetime (Li et al., 2012; Cserep et al., 2020, 2021b). In the mouse, it has been shown that about 90% of neuronal somata are contacted by microglia in cortical layer II and III (Cserep et al., 2020). These contacts are established by microglia at sites of Kv2.1/2.2 clustering on soma membrane and are stabilized with on average a lifetime of 25 minutes (Cserep et al., 2020). The inhibition of P2Y12 receptors abolishes the stabilization of this interaction and inhibits the formation of additional junctions upon neuronal activity stimulation, showing the involvement of this receptor in the direct somatic contact establish by microglia (Cserep et al., 2020).

Microglia directly contact the axolemma of neurons. During the postnatal development of the mouse cortex, the layer V neurons promote microglia accumulation along their subcortical projections. This accumulation supports neuronal survival and is mediated by the membrane GPI-anchored netrin-G1 expressed by neurons that interacts with the transmembrane protein NGL1 expressed by microglia (Fujita et al., 2020). During the embryonic development of the dopaminergic axons microglia have been shown to interact directly with these axons and limit their growth (Squarzoni et al., 2014). The microglial receptor CX3CR1 is involved in this mechanism, however its implication in the signals mediating the direct contact between microglia and axons remains unknown (Squarzoni et al., 2014). Direct contacts between microglia and the highly specialized membrane of the axon initial segment have been described in mouse, rats and non-human primates (Baalman et al., 2015; Cserep et al.,

2021a) (Figure 25E). These contacts are established early in the postnatal development and remain into adulthood with a preferential interaction with axon initial segments of non-GABAergic neurons (Baalman et al., 2015). Lastly, microglia in the corpus callosum have been shown to contact the nodes of Ranvier, excitable domains with a similar molecular composition than the axonal initial segment (Zhang et al., 2019). However, the contact in the corpus callosum were shown at the node and on the myelin sheath but not quantified. Thus, considering the very high density of nodal structures in this area, nodes of Ranvier might be contacted randomly by microglial cells while they are screening their environment (Zhang et al., 2019). Therefore, the mechanism mediating direct contact between microglia and the excitable domains of the axons remain unknown, and the specificity of these contacts, particularly in the case of nodes of Ranvier, remains to be deciphered.

2.2.2 Microglia sculpt neuronal circuits during pre and postnatal development

2.2.2.1 Microglial control of neurogenesis

The first studies of neuron-microglia interactions and capacity of microglia to modulate neuronal survival used *ex vivo* models. In the retina of the chicken embryo, there is a process of cell death occurring in the normal development (Martín-Partido et al., 1988). However, when the retina was separated from the surrounding tissue prior to microglia invasion of the developing CNS, there was a reduction by a factor of 60% of cell death, that was further restored by adding isolated microglia to the explant (Frade and Barde, 1998). In a different system, consisting of organotypic culture of cerebellar slices, it was further shown that the depletion of microglia using clodronate loaded liposomes increases Purkinje cells survival (Marín-Teva et al., 2004). The authors also showed that microglia produce superoxide ions directly responsible for the induction of Purkinje cells death (Marín-Teva et al., 2004). In the hippocampus it was shown that microglial integrin CD11b and the immunoreceptor DAP12 trigger superoxide ions production that induces developmental neuronal death (Wakselman et al., 2008)(Figure 26A). Later on, Cunningham et al. showed that depletion of microglia *in utero* leads to an increase of the number of neural progenitors in the developing cerebral cortex. Conversely over-activated microglia, following maternal immune activation, induce a reduction of the neural progenitor (Cunningham et al., 2013). These results further supported the role of microglia in regulating developmental neurogenesis. Microglia are not only involved in promoting neuronal death but can also promote neuronal survival (Ueno et al., 2013; Fujita et al., 2020). For instance, in the cortex, layer V and to a lesser extent layer II- IV neurons survival is promoted by microglia secretion of IGF1 in a CX3CR1 dependent mechanism (Ueno et al., 2013)(Figure 26D).

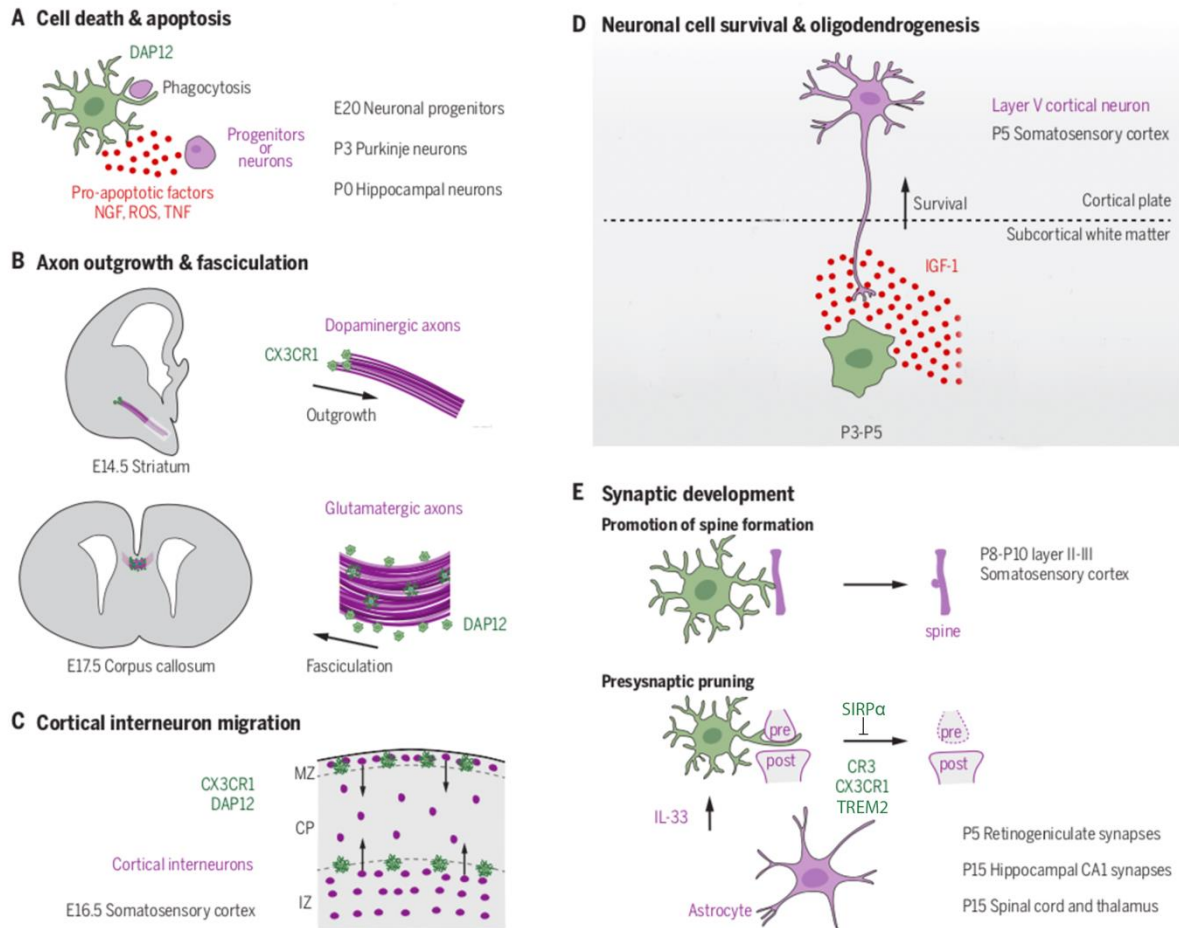


Figure 26: Microglia shape neuronal circuits during development.

(A-E) Schematics showing the different types of microglial functions that participate in shaping neuronal circuits in the pre and postnatal development. In each panel microglia are in green and their target in purple. (A) Microglia modulate neurogenesis by promoting apoptosis and phagocytosis of progenitor or differentiated neurons. (B) Microglia control the growth and the fasciculation of axonal tracts. (C) Microglia can regulate migration of interneurons in the somatosensory cortex. (D) Microglia in the subcortical white matter release IGF-1 and promote pyramidal neuron survival. (E) In postnatal development, microglia are involved in promoting dendritic spine formation and participate to synaptic pruning. Synaptic pruning by microglia can be further promoted by astrocytic release of IL-33. Figure adapted from Thion et al, 2018.

2.2.2.2 Microglia are active players in brain wiring

The control of neuronal circuits by microglia is not restricted to their modulation of neuronal death and survival. Indeed, microglia have been shown to modulate axonal tracts formation and synapse elimination by synaptic pruning, taking part to the wiring and refinement of neuronal circuits during development (Paolicelli et al., 2011; Hoshiko et al., 2012; Schafer et al., 2012; Pont-Lezica et al., 2014; Squarzoni et al., 2014).

First, during development, microglia regulate the formation of axonal tracts and neuronal migration (Pont-Lezica et al., 2014; Squarzoni et al., 2014). At E14.5 of the mouse embryonic development, the association of microglia with the growing dopaminergic axons restricts their extension in the striatum. This mechanism is disrupted in mice deficient for the CX3CR1 receptor with an abnormal expansion of the axons in the subpallium, showing that this receptor is involved in the control of axonal tract formation (Squarzoni et al., 2014)(Figure 26B). In the same study, Squarzoni et al. showed that the migration of Lhx6-positive interneurons, that in particular gives rise to somatostatin and parvalbumin interneurons (Liodis et al., 2007), is controlled by microglial cells (Squarzoni et al., 2014). Indeed, by depleting microglia they showed that microglia depletion disrupts parvalbumin interneurons distribution embryonically, and that the disruption remains postnatally. Using mice deficient for CX3CR1 or DAP12, it was further shown that these two receptors are involved in the control of interneurons migration by microglia (Squarzoni et al., 2014)(Figure 26C). DAP12 has been further involved in the development of the corpus callosum, DAP12 inactivation leading to axonal defasciculation (Pont-Lezica et al., 2014)(Figure 26B).

In addition to the regulation of axonal tracts formation by microglia, it has also been shown that microglia control brain wiring during the postnatal development by removing synaptic elements by synaptic pruning (Paolicelli et al., 2011; Schafer et al., 2012). This mechanism has been well characterized in the development of the retinogeniculate system. Postnatally between P10 and P30 in the dorsal lateral geniculate nucleus (dLGN), there is a segregation between the synaptic input of retinal ganglion cells from the ipsilateral and the contralateral eye (Rakic, 1976; Levay et al., 1978; Hooks and Chen, 2006). This segregation is made by the pruning of mistargeted synapses by microglia. This mechanism depends on the expression of C3 at presynaptic boutons and CR3 in microglial cells (Schafer et al., 2012). The disruption of either C3 or CR3 leads to sustained deficits in the segregation of the connections coming from the ipsilateral vs contralateral eye (Schafer et al., 2012). In the same paradigm, it has been shown by Beth Stevens' laboratory that the transmembrane immunoglobulin protein CD47 by activating SIRP α on microglia acts as an opposite mechanism that prevent an excessive synaptic pruning during the refinement of the dLGN circuits (Lehrman et al., 2018). In addition to these modulations by direct contacts, the signaling between the chemokine fractalkine

CX3CL1 secreted by neurons and the receptor CX3CR1 also modulates microglial synaptic pruning. In mice deficient for CX3CR1, there is a disruption of microglial dendritic spine engulfment in the hippocampus and a delayed maturation of thalamocortical synapses (Paolicelli et al., 2011; Hoshiko et al., 2012). Recently, it was further shown that mice deficient for Thik-1 receptor have a decreased synaptic pruning activity in the hippocampus, that could be partly due to the important reduction of microglia ramification and dynamics in these mice (Izquierdo et al., 2021a). Synaptic pruning by microglia has also been shown to depend on TREM2 receptor in the hippocampus (Filipello et al., 2018), and on the IL-33 released by astrocytes in the thalamus and spinal cord (Vainchtein et al., 2018)(Figure 26E). Very recently, it was shown that a subpopulation of microglia expressing GABA_B receptors are involved in the specific synaptic pruning of inhibitory synapses during the development of the mouse somatosensory cortex (Favuzzi et al., 2021). This seminal work demonstrated for the first time that subpopulations of microglial cells may be responsible for the refinement of specific circuits (Favuzzi et al., 2021). Lastly, in addition to synaptic pruning, microglia have also been suggested to promote directly the formation of dendritic spine, however the molecular signaling involved in this mechanism remains elusive (Miyamoto et al., 2016; Weinhard et al., 2018)(Figure 26E).

2.2.3 Microglia modulate CNS plasticity

The involvement of microglia in neuronal circuits function is not restricted to the development and extends into adult CNS where microglia are active players in the control of plasticity (Roumier et al., 2004; Parkhurst et al., 2013; Cantaut-Belarif et al., 2017; Nguyen et al., 2020; Wang et al., 2020a).

In adult mice, although neurogenesis is continuous and provides new neurons throughout adulthood, only a small proportion of these neurons are eventually integrated to neuronal circuits (Ma et al., 2009). In the subgranular zone of the dentate gyrus, an active area of adult neurogenesis in mice, microglia phagocyte up to 90% of the apoptotic cells (Sierra et al., 2010). In mice deficient for the microglial Mer and Axl TAM receptors, there is an accumulation of apoptotic cells in the adult neurogenic niches. The phagocytosis of apoptotic cells is induced by the microglial TAM tyrosine kinase receptors activation by Gas6 and Protein S (Fourgeaud et al., 2016). The neuronal secretion of IL-33 has also been involved in the modulation of adult neurogenesis in the dentate gyrus (Nguyen et al., 2020). This modulation is suggested to act through the activation of the microglial receptor of IL-33, IL1RL1, that may control microglia engulfment of newly generated neurons (Nguyen et al., 2020).

In mice deficient for TNF receptor or TNF α , CD200 and CX3CR1, alterations of synaptic plasticity have been described but could indirectly result from a modulation of microglia activation following gene inactivation (Stellwagen and Malenka, 2006; Costello et al., 2011; Rogers et al., 2011). More recently, several mechanisms by which microglia can modulate synaptic plasticity in an

homeostatic state have been described (Parkhurst et al., 2013; Nguyen et al., 2020; Wang et al., 2020a). Since synaptic plasticity is fundamentally dependent on neural activity and allows neural system to adapt permanently (Turrigiano, 2012; Kandel et al., 2014; Nicoll, 2017), these results suggest that microglia could also modulate plasticity depending on neuronal activity (see 3.1.2.2).

2.3 Microglia modulate oligodendrogenesis and myelination

In addition to its role in modulating neurogenesis, brain wiring, and brain plasticity in homeostatic conditions, microglia also control the development of the myelinating cells of the CNS and shape myelination (Shigemoto-Mogami et al., 2014a; Hagemeyer et al., 2017; Wlodarczyk et al., 2017; Giera et al., 2018; Hughes and Appel, 2020; Nemes-baran et al., 2020; Djannatian et al., 2021).

2.3.1 Microglia modulate the proliferation and differentiation of OPCs

In the first week of post-natal development, there is an accumulation of microglia in the corpus callosum first reported as the “fountain of microglia” (Imamoto and Leblond, 1978; Ling, 1979). This enrichment in microglia has been further investigated and it has been shown that microglia with an amoeboid morphology proliferate and accumulate transiently in the corpus callosum and in the white matter of the cerebellum (Hagemeyer et al., 2017). This transient population of microglia has been described consistently as a very specific subpopulation characterized by the expression of CD11c, Spp1, IGF1 and Clec7a markers (Hagemeyer et al., 2017; Wlodarczyk et al., 2017; Hammond et al., 2019; Li et al., 2019). Interestingly these markers are usually expressed by microglia in the context of injury, and correlate with both detrimental and pro-regenerative function (Krasemann et al., 2017; Hammond et al., 2019; Lloyd et al., 2019; Masuda et al., 2019). Since the presence of this specific population of microglia in white matter structures correlated with the onset of their myelination (Barres et al., 1992; Trapp et al., 1997), several groups assessed the role of this subpopulation of microglia in myelination. First by using minocycline, Shigemoto-Mogami et al. showed that the disruption of microglial activation in the first postnatal week leads to a decrease of oligodendrocyte density suggesting that microglia modulate oligodendrogenesis (Shigemoto-Mogami et al., 2014a). The depletion of microglia in the first week of postnatal development supported this hypothesis, showing a drastic reduction of OPC numbers. Further investigation at P20 showed that microglia depletion leads to a decrease of OL number and a reduced percentage of myelinated axons in the corpus callosum and cerebellar white matter tracts (Hagemeyer et al., 2017). Amoeboid microglia are usually associated with a phagocytic state of microglia (Ling and Wong, 1993). Consequently, the phagocytic activity of this subpopulation of microglial cells was assessed, and it was shown that they actively phagocyte newly formed oligodendrocyte regulating oligodendrogenesis in white matter tracts (Li et al., 2019)(Figure 27). Mice

deficient for the CX3CR1 receptor display a decreased engulfment of newly generated OLs and an increase of OLs density in the corpus callosum at P7 (Nemes-baran et al., 2020). Thus, the phagocytosis of newly generated oligodendrocytes depends on CX3CR1 receptor and is a key mechanism in OL homeostasis during early postnatal development.

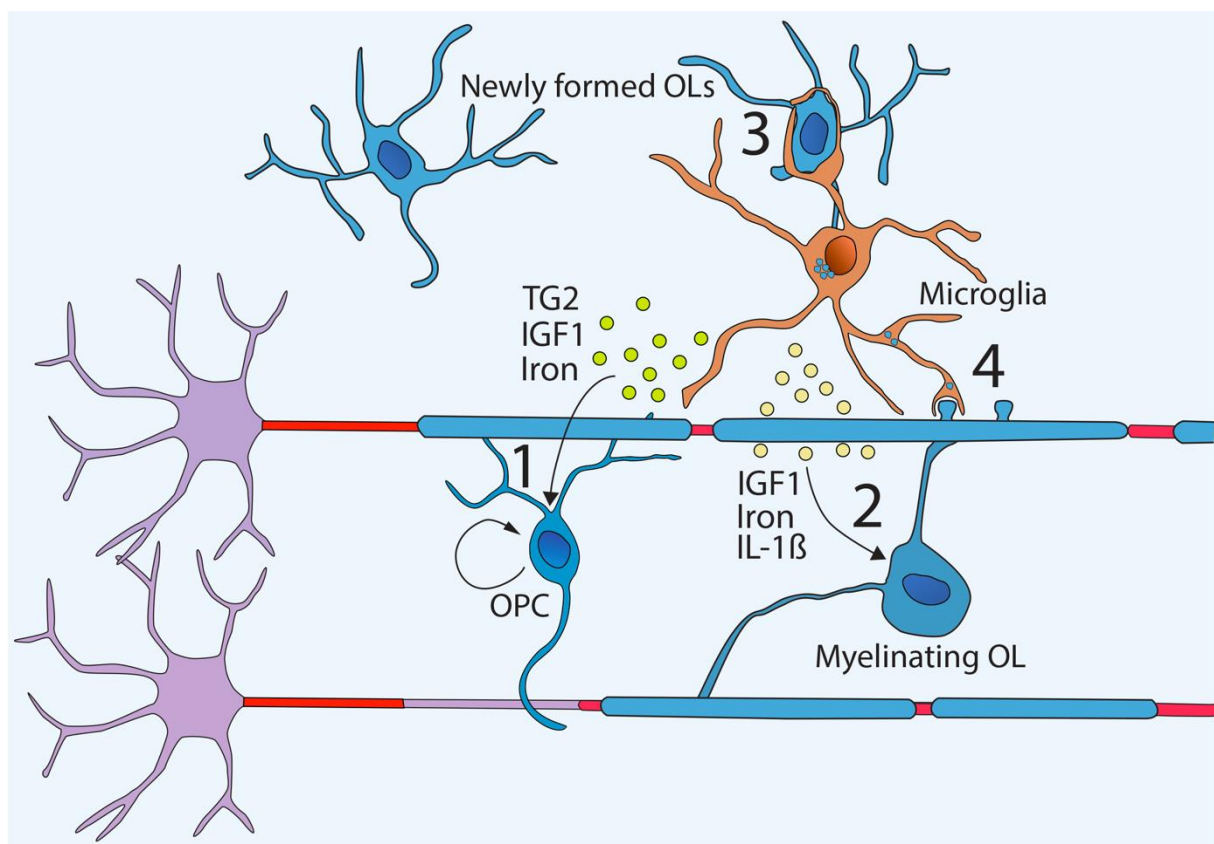


Figure 27: Microglia control oligodendrogenesis and myelination.

Schematics showing the different types of microglial functions that participate in regulating oligodendrogenesis and myelination. Microglia release factors that promote OPCs proliferation (1), and support OPC differentiation into OLs (2). Microglia during myelination phagocyte newly formed OLs (3) and eliminate misfolded myelin and myelin fragments during myelin biogenesis and throughout life (4). Drawings adapted from Ronzano et al, 2020.

Several factors secreted by microglia modulate oligodendrogenesis (Figure 27). First, it has been consistently found that microglia associated to white matter in postnatal development express high level of IFG-1 (Wlodarczyk et al., 2017; Hammond et al., 2019; Li et al., 2019), a factor that is involved in promoting OPC proliferation and differentiation *in vitro* and *in vivo* (Butovsky et al., 2006a; Zeger et al., 2007). Furthermore, the secretion of transglutaminase-2 (TG2) by microglia has been found to participate in oligodendrogenesis by activating the adhesion G protein-coupled receptor ADGRG1 (Giera et al., 2018). Indeed, the inactivation of TG2 specifically in microglia led to the decrease of OL density in the corpus callosum (Giera et al., 2018). The decrease of OL density originates from a lack of OPCs proliferation, that is normally activated by TG2 together with the ECM protein laminin-111 (Giera et al., 2018). The disruption of microglia activation by minocycline injection during the first week of postnatal development has been shown to trigger the downregulation of IL-1 β and IL-6 (Shigemoto-Mogami et al., 2014a). Although these factors have not been shown to directly control oligodendrogenesis in this study, *in vitro* experiments have shown their involvement in the modulation of OPC proliferation and differentiation (Valerio et al., 2002; Vela et al., 2002). Microglia are also thought to be the main supplier of iron in the CNS, which is critical to promote OPC proliferation (Connor and Menzies, 1996; Cheepsunthorn et al., 1998; Zhang et al., 2006; Todorich et al., 2009). Interestingly, iron management proteins such as Ferritin, are enriched in amoeboid microglia that localizes at the white matter tracts characterized by a highly active oligodendrogenesis (Cheepsunthorn et al., 1998).

2.3.2 Microglia modulate myelination pattern and structure

Microglia have also been involved in the regulation of myelination by oligodendrocyte. Through the release of growth factors and by phagocytosing myelin, microglia modulate myelin sheath thickness, myelin pattern and structure (Wlodarczyk et al., 2017; Hughes and Appel, 2020; Marschallinger et al., 2020; Nemes-baran et al., 2020; Djannatian et al., 2021).

First, CD11c positive microglia in the first postnatal week of development were shown to be involved in the regulation of the thickness of myelin sheaths (Hagemeyer et al., 2017; Wlodarczyk et al., 2017; Nemes-baran et al., 2020). Indeed, the ablation of microglia in the first week of postnatal development results in the thinning of myelin sheaths in the corpus callosum (Hagemeyer et al., 2017). Furthermore, based on the fact that CD11c microglial cells highly express IFG-1 previously involved in oligodendrogenesis (Zeger et al., 2007), Wlodarczyk and colleagues inactivated IGF1 expression specifically in CD11c positive cells (Wlodarczyk et al., 2017). This inactivation, induced a hypomyelination of the corpus callosum together with the thinning of myelin sheaths at P21

(Wlodarczyk et al., 2017). Thus, IGF-1 released by microglia at this stage not only promotes neuronal cell survival but also foster myelination (Ueno et al., 2013; Wlodarczyk et al., 2017)(Figure 27). A thinning of myelin sheath in the corpus callosum has also been reported at P30 in mice deficient for the CX3CR1 receptor (Nemes-baran et al., 2020). However, this latter effect might be due to an indirect consequence of CX3CR1 inactivation that may impact microglia activation.

In the zebrafish, it has been shown that microglia survey axon tracts during myelination and contact closely myelin sheaths in the optic tectum (Hughes and Appel, 2020). Furthermore, the depletion of microglia, resulted in the development of a higher number of sheaths per OL, which on average were shorter. Some models of microglia depletion also triggered a higher proportion of mistargeted myelination, with OLs wrapping neuronal somata, a feature also observed when the ratio OL/axon number was disrupted (see 1.4.3, (Almeida et al., 2018)). It was suggested using live-imaging that the modulation by microglia was triggered by a direct phagocytosis of growing myelin sheaths rather than by a modulation of myelin sheaths retraction during myelination (Hughes and Appel, 2020). A very recent study identified that myelination is associated with the production of small misfolded membrane structures that are subsequently removed by microglia phagocytosis in mouse and zebrafish (Djannatian et al., 2021)(Figure 27). Microglia phagocytosis of these structures depends on the expression of phosphatidyl-serine, a well described “eat-me” signal (Takahashi et al., 2005), at the outer leaflet of myelin membrane (Djannatian et al., 2021). Therefore, microglia is suggested to control developmental myelination pattern (Hughes and Appel, 2020), and finely regulate myelin structure (Wlodarczyk et al., 2017; Djannatian et al., 2021), which is expected to play an important role in action potential conduction and circuit functions (Pajevic et al., 2014).

Microglia functions related to myelin are not restricted to developmental myelination and can extend to adulthood and aging brain (Safaiyan et al., 2016; Hill et al., 2018). Indeed, in aging mice (24 months), there is an increase of abnormal multilamellar myelin fragments in the white matter (Safaiyan et al., 2016). Microglia at this stage appear to have internalized myelin protein suggesting that they participate to abnormal myelin fragments removal through lifetime. Moreover, in mice with specific deficiency in microglial lysosomal functions, there is an accumulation of myelin fragments earlier in aging and a higher proportion of microglia containing myelin fragments. These results support the hypothesis that microglia is responsible for the removal of aberrant myelin structures throughout life, leading to the accumulation of lysosomal inclusions in microglia and to immune dysfunction in aging (Safaiyan et al., 2016). Lastly, it is now widely accepted that myelin sheaths are added in the CNS of adult mice and take part to the mechanism of adaptive myelination (see 3.2.3). In this context, microglia activation has been shown to impact adaptive myelination (Geraghty et al., 2019). Furthermore, one of the identified molecular mechanisms promoting adaptive myelination is the neuronal release of BDNF (Geraghty et al., 2019). Although the involvement of microglial BDNF in

this mechanism has not been assessed, it is possible that microglial secretion of BDNF also support adaptive myelination (Parkhurst et al., 2013; Hughes, 2021).

2.4 Microglia modulate remyelination : focus on MS and its experimental models

In the last decade it has become evident that microglia are key modulators in neurodegenerative diseases like Alzheimer, Parkinson, amyotrophic lateral sclerosis and MS (Butovsky and Weiner, 2018; Hickman et al., 2018). In these pathologies, there are common changes that are observed in microglia with in particular, the loss of expression of their homeostatic markers along with the acquisition of a pro-inflammatory signature (Holtman et al., 2015; Krasemann et al., 2017; Zrzavy et al., 2017; Jordão et al., 2019; Masuda et al., 2019). However, MS differs from the other pathologies by a process of neurodegeneration which partly results from demyelination and by its important regenerative component (Franklin and Ffrench-Constant, 2008). Consequently, following demyelination microglia have a dual role, promoting damage and repair. At first they promote inflammation, and then switch to a pro-regenerative phenotype in which microglia promote OL differentiation and remyelination (Miron et al., 2013; Locatelli et al., 2018; Lloyd and Miron, 2019). However, if microglial cells adopt a chronic inflammatory signature, this leads to the inhibition of remyelination and to neuronal damages (Franklin and Ffrench-Constant, 2008; Miron et al., 2013; Lloyd et al., 2019).

2.4.1 Microglia activation and early event of the disease

2.4.1.1 Microglia activation

Upon demyelination microglia are activated, proliferate and retract their processes to adopt an amoeboid morphology (Bö et al., 1994; Rinner et al., 1995; Zhang et al., 2001; Foote and Blakemore, 2005; Plemel et al., 2020). At a transcriptomic level microglia lose or downregulate strongly their homeostatic markers such as P2Y12 receptor, CX3CR1 or Tmem119 and start to express transcripts of chemokines (e.g Ccl2, Ccl4), phagocytes markers (e.g CD68) and apolipoprotein E (ApoE) (Holtman et al., 2015; Krasemann et al., 2017; Hammond et al., 2019; Jordão et al., 2019; Masuda et al., 2019)(Figure 28). The homeostatic signature specific to microglia is regulated by TGF- β , the expression of which is dramatically decreased following microglial activation (Butovsky et al., 2014; Gosselin et al., 2014; Krasemann et al., 2017). The regulation of this switch from homeostatic to activated microglia has been shown to depend on TREM-2 which activates ApoE signaling responsible for the induction of the activation (Krasemann et al., 2017; Mazaheri et al., 2017). TREM2 is a phospholipid sensing receptor, activated upon demyelination by myelin debris (Poliani et al., 2015). In mice deficient for TREM2, there is a defect in the activation of microglial cells that prevents the development of a

phagocytic phenotype and maintains the homeostatic signature (Poliani et al., 2015; Krasemann et al., 2017; Cignarella et al., 2020). This inhibition prevents microglia to clear myelin debris (see 2.4.2.1) and also disrupt their pro-inflammatory functions. Indeed, following demyelination, activated microglia initially start to secrete pro-inflammatory cytokines like TNF- α , IL-1 β and to express the inducible nitric oxidase synthetase (iNOS) (Arnett et al., 2001; Miron et al., 2013; Locatelli et al., 2018; Cunha et al., 2020). Subsequently, microglia shift toward a pro-regenerative phenotype at the onset of OL differentiation and remyelination and express factors like IGF1, Arg1 and TGF- β receptor (Butovsky et al., 2006a; Miron et al., 2013; Krasemann et al., 2017). The inhibition of the emergence of this second population of activated microglia leads to the disruption of remyelination (Miron et al., 2013; Lloyd et al., 2019). Traditionally categorized between the wide categories M1 (pro-inflammatory) and M2 (pro-regenerative), it has been shown that these M1 and M2 markers are sometimes express within the same cells (Morganti et al., 2016; El Behi et al., 2017; Locatelli et al., 2018). Furthermore, recent transcriptomic studies have demonstrated that upon demyelination several phenotypes of microglia emerge and form subpopulations with various signatures (Ransohoff, 2016; Hammond et al., 2019; Jordão et al., 2019; Masuda et al., 2019)(Figure 28C). Although the function of each of these clusters remains unknown, these data raise the necessity to use microglia markers in relation with their function in a specific paradigm more than as a marker for a global microglial status. A better understanding of each microglial signature following demyelination may further pave the way for a better understanding of their function in repair (Butovsky and Weiner, 2018).

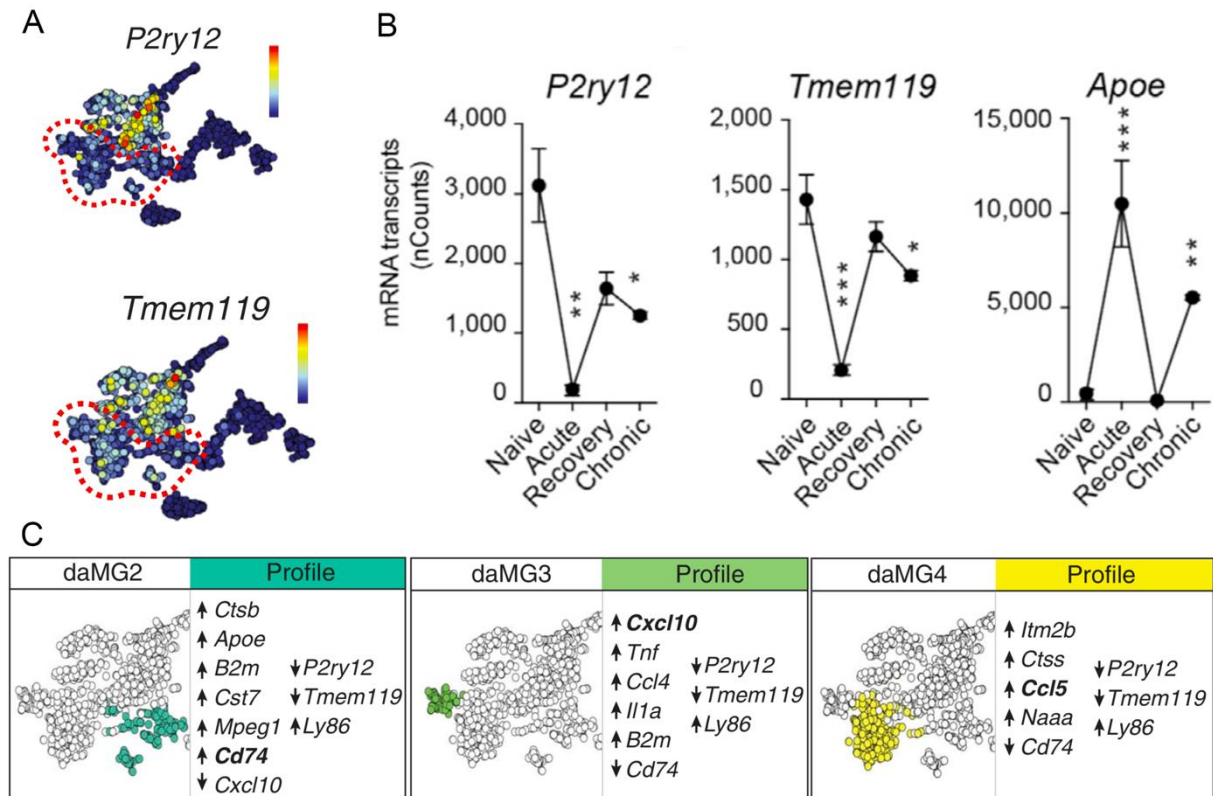


Figure 28: Microglia populations upon activation and modulation of their phenotype.

(A) t-SNE plots, showing the suppression of P2Y12 receptor and the downregulation of Tmem119 in activated microglia (highlighted by the red dotted line) following EAE induction. (B) Plot showing the decrease of the mRNA quantity of P2Y12 receptor and Tmem119 in microglial cells following acute demyelination in EAE. The amount of mRNA transcripts for homeostatic genes is upregulated at the time point of remyelination. In chronic inflammation, homeostatic genes tend to be downregulated compared to remyelination conditions. (C) Transcriptomic profile of the 3 clusters of activated microglia detected in EAE. The lists of genes, display the up- and downregulated genes in each cluster. A group of genes allows to define each cluster, and none of them can alone identify a single cluster. Moreover, none of the cluster corresponds to the initial definition of M1 and M2 activated microglia. These data are extracted from demyelinating models in mice. The results were largely reproduced in single RNAseq data from post-mortem tissue of MS patients. Adapted from Jordão et al., 2019 and Krasemann et al., 2017.

2.4.1.2 Identification of activated microglia vs monocyte derived macrophages

Following demyelination, blood monocytes are recruited to the CNS, and differentiate into monocyte derived macrophages (MDMs). There is a large recruitment in MS and although it is rather limited in toxin based model of demyelination, all the main demyelination models (EAE, LPC, Cuprizone) are characterized by the invasion of MDMs (Ousman and David, 2000; McMahon et al., 2002; Remington et al., 2007; Yamasaki et al., 2014; Plemel et al., 2020). Therefore, it is of critical importance to be able to distinguish these two populations to understand their distinct functions. However, upon activation it is impossible to differentiate microglia from MDMs based on their morphology, or classical markers commonly used like CX3CR1 or Iba1 which are expressed in both microglia and MDMs (Ito et al., 1998; Jung et al., 2000; Saederup et al., 2010; Bennett et al., 2016). Furthermore, the specific markers of microglia Tmem119, and P2Y12 receptor enriched in microglia, are both downregulated upon demyelination and are impossible to use to distinguish specifically microglia (at least in mice) (Butovsky et al., 2014; Bennett et al., 2016; Zrzavy et al., 2017; Hammond et al., 2019; Masuda et al., 2019)(Figure 28A-B).

Therefore, only few approaches have so far been used to successfully differentiate microglia from MDM following demyelination. The first one is the use of FACS to sort MDMs with CD45 that is 10 fold higher in MDMs compared to microglia (Yamasaki et al., 2014; O’Koren et al., 2016). This strategy have been used even in human tissue, in which MDMs have been distinguished from microglia by mass spectrometry using CD45 expression (Böttcher et al., 2019). However, this strategy suffers from two major limitations. First, CNS-associated macrophages, specific macrophage populations present at the CNS boarder (Kierdorf et al., 2019), express low level of CD45 and cannot be distinguished from microglia using this technic alone (Mrdjen et al., 2018). And second, this technic loses spatial localization. Two other strategies based on transgenic reporters have overcome this later limitation for studies in mice. The first one uses the specific expression of the transgenic reporter CCR2 in MDMs (Saederup et al., 2010; Yamasaki et al., 2014). However, with time there is a downregulation of CCR2 expression in MDMs limiting the duration of the study. The second strategy uses the inducible Cre recombinase under the control of CX3CR1. Upon induction microglia and monocyte are labelled, but due to the short life time of monocytes, the labelled monocytes disappear almost completely after a month and only microglia remain labelled (Goldmann et al., 2013; Plemel et al., 2020). However, CNS-associated macrophages also expresses CX3CR1, have a long lifetime and self-renew making them indistinguishable from microglia using this latter strategy (Goldmann et al., 2016). Recently models of Hexb-TdTomato mice and inducible Cre recombinase expression under the promotor of Hexb have been developed (Masuda et al., 2020). These two mouse lines are supposed to override the latter

limitation with CNS-associated macrophages, since Hexb is exclusively expressed in microglia and is not downregulated upon microglia activation (Masuda et al., 2020).

The capacity to distinguish microglia from MDMs is critical to understand the different functions of these two populations in remyelination. One recent example illustrates this need of distinction. Plemel and colleagues, using inducible Cre recombinase under the control of CX3CR1 could show that microglia restrict spatially the infiltration of MDM at the center of the lesion and limit their toxicity in a model of LPC induced focal demyelination (Plemel et al., 2020). Moreover, the distinction between MDMs and microglia is of primary importance for therapeutic strategies. Indeed, depending on the cells to target, drug design could for instance focus on molecules able to cross the blood brain barrier (to target microglia) or not (targeting MDMs) (see 2.4.4, (Lloyd and Miron, 2019)).

2.4.1.3 Microglia activation and inflammation may drive early neuronal damages

In the inflammatory environment, microglia and MDMs have been involved in neuronal damages prior to a significant demyelination. Several neuronal compartments appear to be particularly sensitive to the inflammatory environment, like synapses, axon initial segments and nodes of Ranvier (Howell et al., 2010; Nikić et al., 2011; Yamasaki et al., 2014; Clark et al., 2016; Werneburg et al., 2019; Gallego-Delgado et al., 2020). In MS tissue, in normal appearing white matter (NAWM) and in various model of EAE in marmoset and mice, there is an increase of complement component C3 expression associated with an abnormal synaptic pruning of microglia (Ramaglia et al., 2012; Werneburg et al., 2019). In EAE model, the expression of C3 component has been further characterized and localizes at synapses prior to significant demyelination. The overexpression of Crry, a complement inhibitor, leads to the inhibition of synaptic pruning by microglia and restore cognitive defect in EAE (Werneburg et al., 2019). These results show that a synaptic loss is mediated by microglial prior to demyelination in an inflammatory environment. Furthermore, microglia contact axon initial segments (AISs) in both homeostatic (Baalman et al., 2015) and inflammatory conditions (Clark et al., 2016). These contacts are further increased following demyelination in EAE and after cuprizone diet (Clark et al., 2016). However, in a model of EAE there is a disruption of AIS that is not present in the cuprizone model. Consequently, this work suggest that the disruption of AISs is the result of the inflammation and does not correlate with the demyelination itself (Clark et al., 2016).

Another excitable domain of the myelinated axon, the node of Ranvier is disrupted by inflammation prior to demyelination. A live imaging study of the spinal cord of EAE mice has suggested that the initial disruption of axonal integrity is often occurring at nodes and correlates with activated microglia/MDM contacts (Nikić et al., 2011)(Figure 29A). Furthermore, in the normal appearing white matter (NAWM) in MS tissue and in a model of EAE in mice, it was further shown that microglia/MDMs

inflammatory profile precedes significant demyelination and correlates with the disruption of nodal and paranodal domains (Howell et al., 2010; Gallego-Delgado et al., 2020). The disruption of the paranodal domains, characterized by the lengthening of Caspr and Nfasc 155 clusters, was associated with a paranodal invasion of the potassium channels normally restricted at juxtaparanodes (Howell et al., 2010; Gallego-Delgado et al., 2020). At the nodal domain the clustering of Nav1.6 was lost at some nodes both in NAWM and EAE, and in EAE up to a two-fold increase of nodal structures without Nav1.6 clustering was evidenced (Howell et al., 2010). These abnormalities at nodes before demyelination were predicted to alter action potential conduction (Gallego-Delgado et al., 2020). The inhibition of microglia/MDMs activation by minocycline injections in rodents following EAE induction, decreased nodal disruption suggesting a role of microglia and/or MDMs activation in the initiation of axonal disruption at nodes (Howell et al., 2010). At the onset of demyelination Yamasaki and colleagues found that preceding demyelination MDMs induced a nodal pathology by invading about 10% of the nodes of Ranvier in the mouse EAE spinal cord (Yamasaki et al., 2014)(Figure 29B-C). However, microglia were not involved in this nodal pathology and did not seem to play a role in this early pathological mechanism (Yamasaki et al., 2014). These findings have identified the nodes of Ranvier as an early target of innate immune cells, and more presumably of MDMs but not of microglia, in inflammatory conditions (Figure 29).

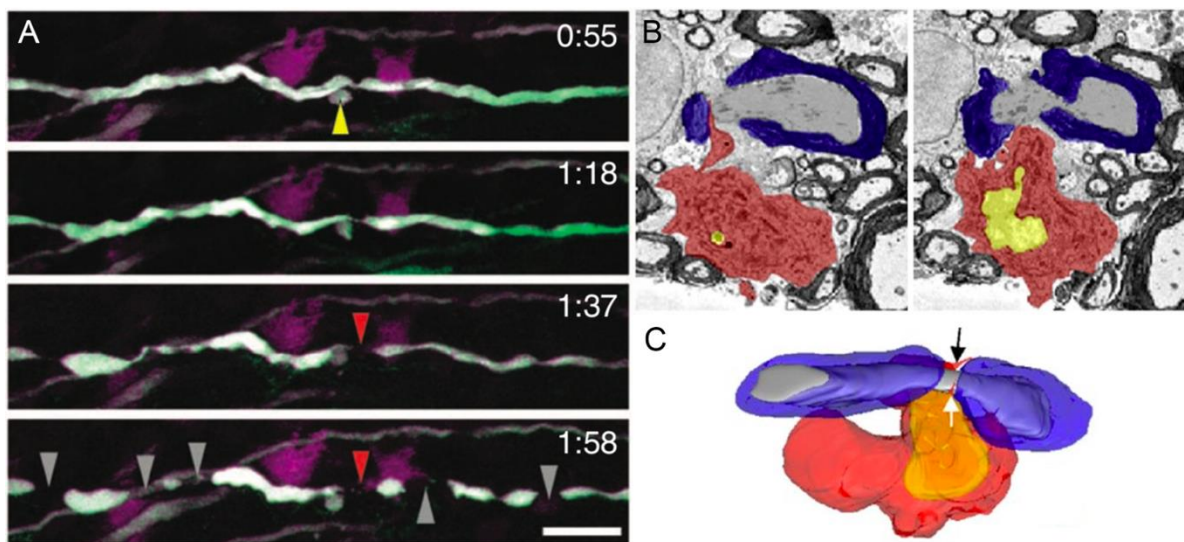


Figure 29: MDM invasion of the node of Ranvier precedes demyelination and induces nodal pathology.

(A) Images extracted from a live imaging performed in the spinal cord of an EAE mouse. They show an axon (in white) first break (red arrowhead) happening near a putative node of Ranvier with a small swelling (yellow arrowhead). An activated microglial cell or MDM (in magenta, third line), contacts the axon at the initial break point where the putative node of Ranvier could be observed earlier. This event is followed by the fragmentation of the axon (grey arrowhead). The time is shown as h:min. Scale bar: 25 μ m. (B) Images of serial micrographs showing a MDM (filled in red) invading a node of Ranvier (interruption of the myelin sheaths, depicted in blue). The area filled in yellow correspond to the MDM nucleus. (C) 3D reconstruction of the MDM invasion of the node. MDM is filled in red, with its nucleus in yellow. Myelin is filled in blue. The two arrows show MDM microvillus invading the paranodes. Adapted from Nikić et al, 2011 and Yamasaki et al, 2014.

2.4.2 Microglia clear myelin debris following demyelination

One critical function of microglia following demyelination is the clearance of myelin debris which inhibit OPCs recruitment and production of newly generated OLs (Graca and Blakemore, 1986; Gilson and Blakemore, 1993; Ousman and David, 2000; Shields et al., 2000; Kotter et al., 2005, 2006; Cantuti-Castelvetri et al., 2018; Cignarella et al., 2020; Cunha et al., 2020). One of the receptors highly expressed by microglia, CX3CR1, has been involved in this mechanism. In CX3CR1 global knockout, there is an alteration of myelin debris clearance (Lampron et al., 2015)(Figure 30). However, this effect could be indirect in these mice characterized by an altered activation and a decrease of TREM2 expression, a key receptor modulating myelin debris removal (Cantoni et al., 2015; Lampron et al., 2015)(Figure 30). Indeed, in TREM2 deficient mice, there is a lack of myelin debris clearance that leads to a decreased number of oligodendrocytes, a persistent demyelination and an axonal dystrophy (Cantoni et al., 2015; Poliani et al., 2015). Conversely, the activation of TREM2 with an agonistic antibody promotes myelin debris clearance (Cignarella et al., 2020). Moreover, TREM2 signaling upregulates the expression of Axl receptor involved in myelin debris phagocytosis. It further upregulates the expression of proteins involved in lipid transport and metabolism like Apo E and lipoprotein lipase (LPL), which facilitates myelin debris clearance (Hoehn et al., 2008; Krasemann et al., 2017; Bruce et al., 2018; Hammond et al., 2019). Toll like receptors (TLRs), expressed by both microglia and MDMs have also been involved in promoting myelin debris removal (Church et al., 2016; Cunha et al., 2020). Indeed, in zebrafish and mice deficient for MyD88, an adapter protein required for the induction of downstream inflammatory cytokine of almost all TLRs (except TLR3, (Kawai and Akira, 2007)), myelin debris phagocytosis is impaired (Cunha et al., 2020). Other microglial receptors involved in myelin debris removal have been identified, such as the retinoid X receptor- α and the protein tyrosine kinase MER which represent potential therapeutical targets (see 2.4.4, (Natrajan et al., 2015; Healy et al., 2016)). In addition to their direct modulation of myelin debris clearance receptors like TREM2 and TLRs also trigger the secretion of pro-inflammatory factors that promote remyelination (Krasemann et al., 2017; Cunha et al., 2020).

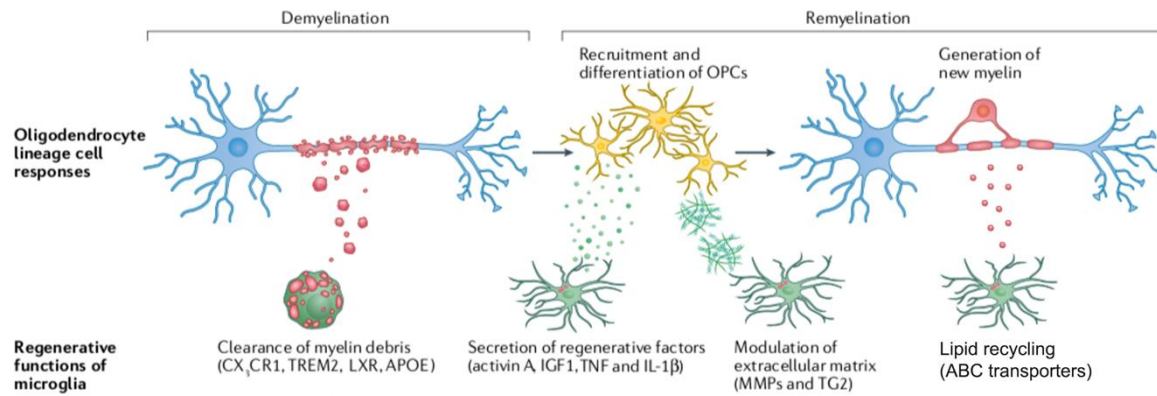


Figure 30: Pro-remyelinating functions of microglia following demyelination.

Schematics showing the microglial regulation of the different steps of remyelination following demyelination. Microglia drive remyelination by clearing myelin debris which facilitates OPCs recruitment. Microglia secrete factors that promote the recruitment, proliferation and differentiation of OPCs in OLCs. Lastly, by recycling and releasing cholesterol, microglia increase cholesterol availability and promote myelin synthesis by OLCs. Adapted from Lloyd et al., 2019.

2.4.3 Microglia a key player to promote remyelination

2.4.3.1 Microglia promote oligodendrogenesis and remyelination

Following demyelination, activated microglia start to secrete pro-inflammatory factors (Foote and Blakemore, 2005; Butovsky et al., 2006a; Miron et al., 2013; Cunha et al., 2020). The induction of this inflammatory phase is essential to promote oligodendrogenesis (Foote and Blakemore, 2005). Several factors released by microglia have been identified. $TNF\alpha$, a pro-inflammatory cytokine is upregulated in microglia following demyelination (Arnett et al., 2001; Voss et al., 2012; Miron et al., 2013; Cunha et al., 2020). $TNF\alpha$ has two receptors, TNFR1 and TNFR2 with different functions. Whereas TNFR1 is mainly thought to mediate cell death, TNFR2 also promotes cell proliferation (Declercq et al., 1998; Locksley et al., 2001). Inducing a model of cuprizone dependent demyelination in mice knockout for TNFR1 or TNFR2 respectively, it has been shown that TNFR2 activated by $TNF\alpha$ promotes OPCs proliferation and production of new OLCs (Arnett et al., 2001). Furthermore, in microglia inactivated for MyD88, adaptor protein of TLRs, following an LPC induced demyelination there is a reduction of $TNF\alpha$ secretion (Cunha et al., 2020). $TNF\alpha$ secretion by microglia in this model has been shown to promote the generation of premyelinating OLCs, which allows a more efficient remyelination (Cunha et al., 2020). The pro-inflammatory cytokine IL-1 β is mainly expressed in activated microglia and MDMs following demyelination (Bauer et al., 1993; Mason et al., 2001), and its expression by microglia is regulated by THIK-1 (Madry et al., 2018b). *In vitro*, it has been shown that IL-1 β inhibits OPC proliferation and promote their differentiation into OLCs (Vela et al., 2002). *In vivo*, mice deficient

for IL-1 β show a defect of OL differentiation that leads to remyelination defects (Mason et al., 2001). In IL-1 β deficient mice, there is an alteration of IGF-1 upregulation following demyelination that might cause OL differentiation defects (Mason et al., 2001). Therefore, IL-1 β may modulate the oligodendroglial lineage via the activation of IGF-1 expression.

Once microglia switch toward a more pro-regenerative phenotype, they start to express various factors that promote OPC differentiation and remyelination. Activin A, a member of the TGF β superfamily is expressed in microglia with a pro-regenerative signature (Miron et al., 2013; Yu et al., 2015). The treatment of demyelinated organotypic cerebellar slices with Activin A at the onset of remyelination has been shown to promote OL production (Miron et al., 2013). Conversely, the inhibition of Activin A receptor following demyelination prevented efficient remyelination (Dillenburg et al., 2018). Thus, Activin A expressed by microglia displaying a pro-regenerative phenotype, promotes OPC differentiation and allows an efficient remyelination. Microglia, as they switch towards a pro-regenerative signature also start to express IGF1 (Miron et al., 2013; Wlodarczyk et al., 2015). This factor has been found to promote remyelination and OLs survival (Mason et al., 2000; Hlavica et al., 2017). Although IGF-1 effect in remyelination has not been studied in details, its secretion by microglia could promote oligodendrogenesis and myelin production in repair as it has been reported during developmental myelination (Butovsky et al., 2006b; Zeger et al., 2007; Wlodarczyk et al., 2017). As for IGF1, the microglial secretion of transglutaminase-2 (TG2) is involved in both developmental myelination and remyelination (Giera et al., 2018). Its expression in microglia is maintained after EAE induction in mice (Wlodarczyk et al., 2017; Giera et al., 2018). Furthermore, TG2 knockout mice exhibit an impaired remyelination following cuprizone diet, and the treatment ex vivo of demyelinated slices with recombinant TG2 further promote remyelination (Van Strien et al., 2011; Giera et al., 2018). Therefore, microglia secretion of TG2 by promoting OPC proliferation and differentiation enhances remyelination (Van Strien et al., 2011; Giera et al., 2018).

Galectin-3, a receptor that recognizes glycan, is expressed by microglia following cuprizone induced demyelination (Hoyos et al., 2014). In galectin-3 deficient mice, there is an inhibition of OL differentiation and defects in remyelination capacities (Pasquini et al., 2011; Hoyos et al., 2014). However, this effect may be indirectly due to the disruption of microglia activation following demyelination in galectin-3 deficient mice. Indeed, in these mice, it has been shown that microglia do not activate normally, with phagocytic defects and a lack of TREM-2 upregulation following demyelination (Hoyos et al., 2014). Therefore, since TREM2 modulates microglia activation, debris clearance and is required to promote an efficient remyelination, the defects observed in galectin-3 deficient mice could be rather indirect (see 2.4.2, (Poliani et al., 2015; Krasemann et al., 2017; Mazaheri et al., 2017; Cignarella et al., 2020)).

2.4.3.2 The microglial switch is required to promote an efficient remyelination

Following a first phase of activation with a pro-inflammatory phenotype, the switch of the microglial cell population towards a pro-regenerative phenotype is necessary to promote an efficient remyelination (Miron et al., 2013; El Behi et al., 2017; Lloyd et al., 2019). In MDMs, a live imaging study in the spinal cord of EAE mice showed that individual cell can switch from one state to another gradually forming a spectrum of activation from iNOS positive exclusively to Arginase-1 positive only MDMs (Locatelli et al., 2018). However, the mechanism by which microglia adopt a pro-regenerative phenotype is more elusive (Lloyd and Miron, 2019). In mice with EAE induction, the microglial expression of the ionotropic purinergic receptor P2X4 is upregulated at the peak and later during recovery (Zabala et al., 2018). In mice treated with a P2X4 receptor antagonist, there are defects in myelin debris removal and oligodendrocyte differentiation. Furthermore, the inhibition of P2X4 receptor maintains microglia in a pro-inflammatory state and inhibits the microglial expression of pro-regenerative factors. Potentiating pharmacologically P2X4 receptors activation further ameliorates the course of the disease and promotes *in vitro* the expression of pro-regenerative markers while inhibiting pro-inflammatory signature (Zabala et al., 2018). Therefore, P2X4 receptor activation could participate in the microglial switch necessary to promote efficiently remyelination. Following myelin phagocytosis, it has been shown that microglia start to synthesize desmosterol which activate microglial liver X receptor (LXR) (Berghoff et al., 2021). Preventing either desmosterol synthesis or transport in microglia and MDMs enhanced the pro-inflammatory signature of microglia/MDMs and disrupted the induction of a pro-regenerative signature. Moreover, the administration of exogenous squalene that can be converted in desmosterol in mice deficient for desmosterol synthesis, suppressed the inhibition of the microglial/MDM switch and promoted remyelination. Thus the synthesis of post-squalene-sterol following microglia phagocytosis of myelin debris may guide the microglial switch towards pro-regenerative signature through the activation of LXR signaling in microglia (Berghoff et al., 2021). Furthermore, this study suggested that microglia recycle cholesterol and release it to promote directly myelin production by remyelinating OLs (Berghoff et al., 2021)(Figure 30). The adaptive immune system has also been described to modulate microglial switch (El Behi et al., 2017). Using supernatant of human lymphocytes in culture, it was shown that lymphocytes from MS patients secrete factors that increase OPCs proliferation but fail to induce their differentiation into OLs (El Behi et al., 2017). Lastly, using a model of focal demyelination, the group of Veronique Miron demonstrated that the pro-inflammatory microglia go through necroptosis at the onset of remyelination, followed by a repopulation of pro-regenerative microglia (Lloyd et al., 2019). The authors have shown that inhibiting necroptosis delays the switch towards pro-regenerative microglia and impairs remyelination (Lloyd et

al., 2019). Thus, several mechanisms could be at play to promote the subsequent switch from pro-inflammatory to pro-regenerative microglia after myelin debris removal and may require a replacement of a subpopulation of microglia.

2.4.4 Microglia a potential therapeutical target to promote remyelination in MS

Currently there is a lack of efficient drug to promote remyelination, and although there are several drugs being tested to promote OPC differentiation into remyelinating OLs none of these drugs are specifically targeting microglia (Stangel et al., 2017; Lubetzki et al., 2020b). However, some experimental studies showed that the efficiency of some molecules may be due to off target beneficial effect on microglial cells (Lloyd and Miron, 2019; Lubetzki et al., 2020b). For instance, the bexarotene that is a retinoid X receptor (RXR) agonist has been recently studied (Brown et al., 2021). Although its tolerance by MS patients is weak, partially positive results on MRI and electrophysiological parameters, suggestive of increased remyelination was provided by the recently published phase 2 study in MS patients (Brown et al., 2021). In experimental model, it has been found that the activation of RXR led to a better clearance of myelin debris by macrophages derived from MS patients (Natrajan et al., 2015), which could partly account for the biological effect of RXR agonists. Clemastine, which is an anti-muscarinic drug has been identified to promote remyelination in a large drug screening *in vitro* and its pro-remyelinating effect further confirmed in different models of neurogenerative pathologies in mice (Mei et al., 2014, 2016; Chen et al., 2021). A clinical phase 2 trial, in patients suffering from chronic optic neuritis, showed that a treatment with clemastine fumarate could improve remyelination, evaluated by the latency of visual evoked potentials (Green et al., 2017). Although the primary target of clemastine is the oligodendroglial lineage (Mei et al., 2016), it has been shown *in vitro* and *in vivo* in a mouse model of amyotrophic lateral sclerosis that clemastine treatment also induces an anti-inflammatory phenotype of microglia (Apolloni et al., 2016). Thus, clemastine treatment could also modulate microglial activation status as an off-target effect. As a last example, another family of molecules tested by several pharmaceutical groups and currently in phase 3, target the inhibition of Bruton's tyrosine kinase (BTK) (Montalban et al., 2019; Dolgin, 2021; Reich et al., 2021). These inhibitors could modulate both the adaptive and the innate immune system, and ongoing works suggest that BTK inhibitors can modulate microglial behavior and favor remyelination in experimental model of demyelination (Dolgin, 2021; Albrecht et al, submitted).

3. Neuronal activity modulates microglia and oligodendroglial functions

The activity of neurons regulates the formation of neural circuits and controls their plasticity throughout life. The formation of neuronal circuits during development starts as a diffuse mechanism and is further refined depending on neuronal activity (Shatz, 1990; Katz and Shatz, 1996; Martini et al., 2021). In early brain development, neuronal activity modulates a broad range of processes from neurogenesis and neuronal migration to synapse formation and elimination (Komuro and Rakic, 1993; Crair and Malenka, 1995; Penn et al., 1998; Hanson and Landmesser, 2004; Berg et al., 2011; Chang et al., 2021). Adaptive changes in neuronal circuits are later on continuously ongoing, and their modulation is greatly dependent on neuronal activity in adulthood (Bliss and Lømo, 1973; Hawkins et al., 1983; Turrigiano et al., 1998; Abbott and Nelson, 2000). In the last two decades, it became evident that glial cells sense neuronal activity expressing a broad range of receptors to neurotransmitters and neuromodulators (Bergles et al., 2000; Lin and Bergles, 2004; Davalos et al., 2005; Káradóttir et al., 2008; Fontainhas et al., 2011; Zhang et al., 2014; Spitzer et al., 2019). Furthermore, glia not only sense but also respond to neuronal activity. Indeed, it was in particular shown that glia takes part to neuronal activity dependent mechanisms modulating synapse elimination, synapse plasticity, circuits synchrony, developmental and adaptive myelination (Demerens et al., 1996; Stevens et al., 2002; Tremblay et al., 2010; Schafer et al., 2012; Parkhurst et al., 2013; Gibson et al., 2014; McKenzie et al., 2014; Nguyen et al., 2020). Very recently, it was further demonstrated that glia takes part to the direct modulation of neuronal activity, thus impacting animal behaviors (Mu et al., 2019; Badimon et al., 2020; Steadman et al., 2020).

In pathological conditions glial cells are important modulators of recovery processes. In this context, their physiology is impacted and the modulation of neuronal activity directly or by sensory stimulations has emerged in experimental models as an efficient strategy to promote repair (Iaccarino et al., 2016; Jensen et al., 2018; Adaikkan et al., 2019; Andoh et al., 2019; Martorell et al., 2019; Ortiz et al., 2019; Bacmeister et al., 2020). This pro-regenerative effect of neuronal activity is notably promising to improve remyelination in MS patients, and clinical trials are currently ongoing to test the effect of visual stimulation on the treatment of optic neuritis (Lubetzki et al., 2020b). Therefore, the detailed description of the impact of neuronal activity on glial cells is of primary importance to better understand how neuroglial communications could be manipulated to potentiate recovery.

This chapter will focus on the effect of neuronal activity on the oligodendroglial lineage and microglia in homeostatic conditions, and describe further how neuronal activity modulations could be used in a pathological context to promote repair.

3.1 Effect of neuronal activity on the oligodendrocyte lineage and myelination in development, homeostasis and pathological conditions

The role of neuronal activity in myelination was first suggested in the optic nerve of mouse by the fact that sensory deprivation leads to alteration of myelination (Gyllenstein and Malmfors, 1963). Later on, pharmacological agents modulating neuronal activity and electrophysiological stimulations were used *in vitro* and *in vivo* to show that OPCs proliferation, differentiation and myelination are modulated by neuronal activity (Barres and Raff, 1993; Demerens et al., 1996; Stevens et al., 2002). More recently, the role of neuronal activity in developmental myelination has been described more precisely and some cellular and molecular mechanisms underlying these regulations have been identified (Gibson et al., 2014; Hines et al., 2015; Mensch et al., 2015; Wake et al., 2015; Etxeberria et al., 2016; Krasnow et al., 2018; Almeida et al., 2021; Swire et al., 2021). Furthermore, in the last decade the concept of adaptive myelination has emerged. Whereas myelin was previously seen as a rather static structure after the end of postnatal myelination in juvenile animals, new evidence showed that myelin is continuously added to the CNS in adulthood and its regulation by neuronal activity participates in some neuronal circuits functions (Rivers et al., 2008; Gibson et al., 2014; McKenzie et al., 2014; Geraghty et al., 2019; Pan et al., 2020; Steadman et al., 2020; Wang et al., 2020b).

3.1.1 Oligodendrocyte progenitor cells sense neuronal activity in developmental myelination

The study of the electrophysiological properties of OPCs uncovered their expression of functional receptors to neurotransmitters such as glutamate receptors (AMPA, NMDA, Kainate) and GABA receptors (Gilbert et al., 1984; Barres et al., 1990; Steinhäser et al., 1994; Gallo et al., 1996; Káradóttir et al., 2005; Salter and Fern, 2005; Kukley and Dietrich, 2009). The expression of these receptors is modulated along the oligodendroglial lineage and within OPC populations depending on their proliferative or quiescent status (De Biase et al., 2010; Spitzer et al., 2019). Furthermore, OPCs are the only glial cells that have been described to form *bona fide* synapses with neurons in both rodent and human tissues (Bergles et al., 2000; Lin and Bergles, 2004; Gallo et al., 2008)(Figure 32). At these synapses AMPA and early after GABA receptors have been described but NMDA and Kainate receptors have never been found at these structures so far (Bergles et al., 2000; Lin and Bergles, 2004). The synapses formed on OPCs have been described in several region of the CNS such as the corpus callosum, cerebral cortex and hippocampus (Bergles et al., 2000; Chittajallu et al., 2004; Lin and Bergles, 2004; Lin et al., 2005; Kukley et al., 2007; Ziskin et al., 2007; Orduz et al., 2015; Zonouzi et al., 2015). Recently the use of retrograde monosynaptic tracing of neuron-OPC synapses allowed to describe anatomically the connectivity between neurons and OPCs. Using this method, the group of

M.Monje determined that these neuron-OPC synapses are widespread in the brain, and that neurons make synapses on OPCs in the regions where they functionally project (Mount et al., 2019).

Functionally, glutamatergic synapses on OPCs have been suggested to slow down their proliferation (Mangin et al., 2012). However, OPCs receiving glutamatergic input keep proliferating (Kukley et al., 2008) and mice deficient for AMPA receptor subunits in OPC do not show any defect in their proliferation (Kougioumtzidou et al., 2017). Thus, the exact functions of glutamatergic synapses on OPCs are still debated and remain to be clarified. GABAergic synapses on OPCs trigger their depolarization and increases intracellular calcium concentration through voltage-gated calcium channels activation (Lin and Bergles, 2004; Tanaka et al., 2009; Velez-Fort et al., 2010). However, although calcium signaling in OPCs have been described to modulate their fate (Wake et al., 2011, 2015; Marisca et al., 2020), the specific role of GABAergic synaptic inputs in calcium signaling is unclear (Balía et al., 2017). The inactivation of the $\gamma 2$ subunit of GABA_A receptors inhibits synaptic inputs receive by OPCs from fast spiking interneurons in the somatosensory cortex and allows to assess specifically the role of synaptic GABAergic inputs in this area (Orduz et al., 2015). Surprisingly, mice deficient for this receptor in the oligodendroglial lineage display no disruption of OPC proliferation and differentiation and only show a decreased survival of OPCs (Balía et al., 2017)(Figure 31). Further investigations on these mice, showed that the physiological and morphological properties of fast-spiking interneurons are modified, as well as their myelination pattern and nodes of Ranvier length leading to cognitive defects (Benamer et al., 2020). Thus, GABAergic synapses of interneurons on OPCs are critical for circuits functions, at least in the somato-sensory cortex (Benamer et al., 2020).

OPC-neuron synapses are eliminated while OPCs differentiate into OLs and correlates with the downregulations of AMPA expression in mature OLs (De Biase et al., 2010; Kukley et al., 2010). Following the first weeks of postnatal development, synaptic GABAergic signaling on OPC is deeply decreased (Velez-Fort et al., 2010). However, non-synaptic mode of communications are also involved in neuron-OPC communications and modulate their fate (Wake et al., 2015)(Figure 31). Although AMPA expression is downregulated while OPCs differentiate, NMDA receptors are expressed along the oligodendroglial lineage and have been involved in the control of neuronal activity dependent OPC proliferation and differentiation (Káradóttir et al., 2005; Micu et al., 2006; Lundgaard et al., 2013). Furthermore, OPCs respond to neuronal activity in a pattern dependent manner (Nagy et al., 2017). Indeed, in mouse, electrical stimulations of the corpus callosum *in vivo* at 5Hz promoted OPCs differentiation into pre-myelinating OLs whereas stimulation at higher frequency (25 Hz) mainly promoted their proliferation (Nagy et al., 2017).

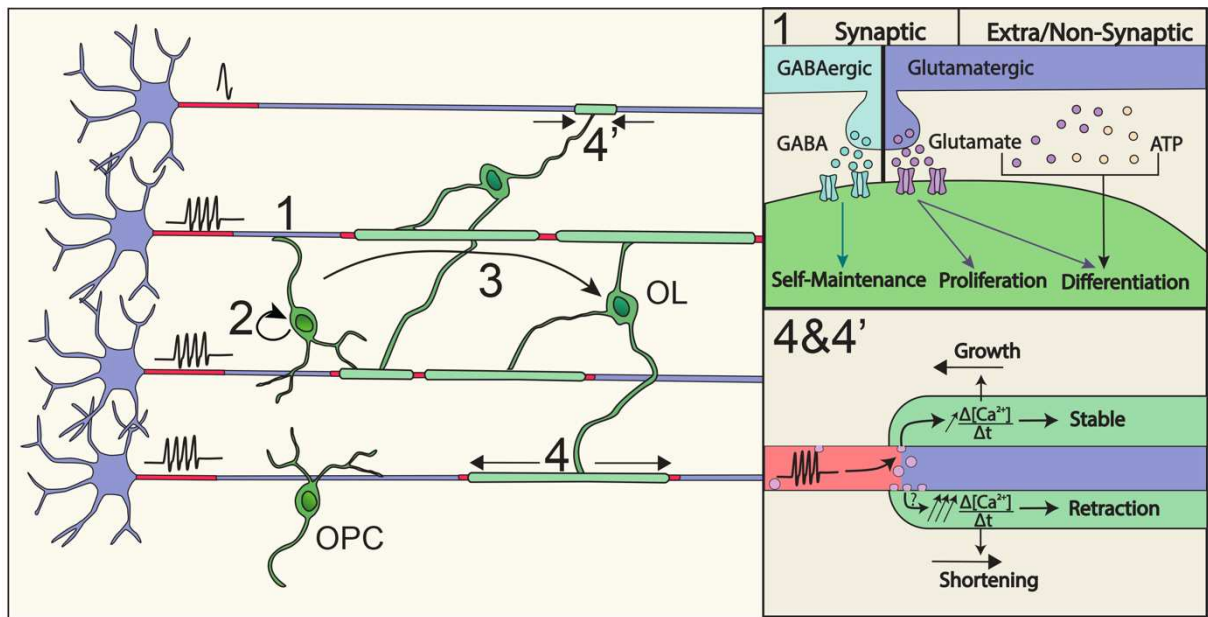


Figure 31: Neuronal activity modulates developmental myelination.

Schematics showing the different steps of developmental myelination and their modulation by neuronal activity. Neuronal activity is sensed by OPC, and modulation of OPCs proliferation (2) and differentiation (3) is modulated by synaptic signals at GABAergic as well as glutamatergic synapses. Non/Extra-synaptic release, is also modulating the fate of OPC depending on neuronal activity. Neuronal activity also modulates myelin sheath growth and stability (4&4'). Activity triggers synaptic vesicles exocytosis with an enrichment at heminode. Calcium transients in newly forming myelin sheaths are partly driven by neuronal activity. Fast frequent calcium transients promote myelin sheath stability and growth whereas high amplitude long-lasting calcium transients facilitate sheath retractions. Drawings adapted from Ronzano et al., 2020.

3.1.2 Neuronal activity modulates developmental myelination

During developmental myelination, there is a fast selection of the axonal domains to be myelinated, and myelin sheaths remain stable later on (Watkins et al., 2008; Czopka et al., 2013). Amongst the signals that have been described to influence axonal choice for myelination targeting is neuronal activity, together with axonal morphology and neuronal identity (see 1.4.3). Early works on the effects of neuronal activity on oligodendroglial lineage, showed a modulation of myelin biogenesis by neuronal activity (Demerens et al., 1996; Stevens et al., 2002). More recently, expressing the tetanus toxin (TeNT) in neurons of zebrafish which inhibit synaptic vesicle release, two different groups showed that the amount of myelinated axons was reduced specifically on axons expressing TeNT, with a decreased number of myelin sheath per OL (Hines et al., 2015; Mensch et al., 2015)(Figure 31). Furthermore, on TeNT expressing neurons there was a higher rate of myelin sheath retraction than on non-inhibited neurons (Hines et al., 2015). Using pharmacological agents, it was found that a global increase of neuronal activity led to an increased number of myelin sheaths per OL, that are on average slightly shorter (Hines et al., 2015; Mensch et al., 2015). These results suggested that neuronal activity

modulates specifically myelin deposition on activated axons, the number of myelin sheaths per OL and their length. The inhibition of synaptic release along a subpopulation of dorsal root ganglion neurons from rodents *in vitro* showed that axons that were not inhibited were preferentially myelinated, supporting the role of neuronal activity on axon selection during myelination (Wake et al., 2015). Furthermore, the inhibition of glutamate synaptic release in the retinal ganglion cells using a conditional knock-out of vGLUT2 led to the shortening of internode length in the optic nerve (Etxeberria et al., 2016), extending to rodents this result initially obtained in zebrafish. Recently, using a reporter with a pH dependent fluorescence in synaptic vesicle (SypHy, (Zhu et al., 2009)), the group of D. Lyons visualized *in vivo* in zebrafish, the exocytosis of synaptic vesicles along the axons while myelination was ongoing (Almeida et al., 2021). Using this approach, it was shown that vesicle release coincides with the onset of myelination. Moreover, it was found that the exocytosis of vesicles is highly enriched at the unmyelinated part of the axons with a further enrichment at heminodes. The inhibition of vesicles fusion decreased the growth speed of the myelin sheath and increased the proportion of retraction, which confirmed previous results. Lastly, using a chemogenetic approach, it was shown that an increase of neuronal activity promotes vesicle release and myelin sheath growth along axons (Almeida et al., 2021). Thus, this last result allowed to describe the direct link between neuronal activity, vesicles release and modulation of the myelination process. However, although glutamate is a good candidate, the molecule loaded in the vesicle remain unknown. ATP, that is loaded in synaptic vesicle with other neurotransmitters such as glutamate and GABA (Pankratov et al., 2006), and has been described to promote myelination *in vitro* (Stevens et al., 2002), might also participate in this process (Figure 31).

Downstream of this mechanism, it has been described in the zebrafish *in vivo* that the stability and growth of the newly forming sheaths on axons depend on their transient calcium activity (Baraban et al., 2018; Krasnow et al., 2018)(Figure 31). Pre-myelinating and myelinating OLs show transient calcium activity that decline with OLs maturation (Krasnow et al., 2018). Using electrical stimulation at 50Hz and inhibition of neuronal activity using TTX, it was shown that the calcium transients in the myelin sheaths and neuronal activity were correlated, with about 50% of calcium transients that were activity dependent (Krasnow et al., 2018). Furthermore, the growth of the myelin sheath was correlated with calcium activity (Baraban et al., 2018; Krasnow et al., 2018). It was further shown that high-amplitude long-duration calcium transients mediated sheath retractions (Baraban et al., 2018; Krasnow et al., 2018). However, the involvement of neuronal activity in this latter type of calcium transients was not tested and it remains unknown whether for instance, a neuronal hyperactivity could trigger myelin sheath retraction. So far, together these results showed that neuronal activity promotes myelin sheath growth through vesicular release, by modulating calcium activity in newly forming sheaths. Intriguingly, half of the calcium transients were independent of neuronal activity and could in

some populations be completely uncorrelated to neuronal activity as observed in the mouse cortex (Battefeld et al., 2019). Therefore, other mechanisms might be at play to modulate myelination and in particular activity independent processes (see 1.4.3). Indeed, it must be noted that myelination of some neuronal populations is not activity dependent. For instance, zebrafish commissural primary ascending neurons do not regulate their myelination by neuronal activity (Koudelka et al., 2016; Almeida et al., 2021). Indeed, these neurons are myelinated during the early development while they are largely silent (Auer, 2019), and do not modulate their myelination through vesicular synaptic release (Koudelka et al., 2016).

3.1.3 Oligodendroglial cells participate in CNS plasticity: adaptive myelination

In adult mice, OPCs account for 3 to 10% of the cells of the adult brain (von Bartheld et al., 2016). Furthermore, they keep proliferating and differentiating in OLs, with 5 to 20% of OLs produced in adulthood (Rivers et al., 2008; Kang et al., 2010; Simon et al., 2011; Young et al., 2013). Consequently, since it has been described that the turnover of OLs is very slow with at 8 month a survival rate of about 90%, the production of new OLs in adult mice may rather participates in the production of new myelin sheaths (Tripathi et al., 2017). Indeed, longitudinal studies of cortical myelination in mice, showed that oligodendrocytes accumulate in adulthood and add new myelin sheaths on unmyelinated or partially myelinated axons (Hill et al., 2018; Hughes et al., 2018). Myelination in adult has been shown to depend on neuronal activity that regulates the progression of the oligodendroglial lineage, OLs survival and the production of new myelin sheaths, giving rise to the concept of adaptive myelination (Gibson et al., 2014; McKenzie et al., 2014; Hughes et al., 2018; Steadman et al., 2020).

3.1.3.1 Neuronal activity modulates oligodendrocyte production

The role of neuronal activity in activating OPCs proliferation and differentiation into OLs is not restricted to the postnatal development and extends to adulthood (Sampaio-Baptista et al., 2013; Gibson et al., 2014; McKenzie et al., 2014; Xiao et al., 2016; Mitew et al., 2018)(Figure 32A). In two seminal studies using motor training and direct optogenetic stimulation of neuronal activity, it was shown that neuronal activity promotes OPCs proliferation and differentiation into OLs (Gibson et al., 2014; McKenzie et al., 2014). Genetically blocking oligodendrogenesis prior to motor training further disrupted motor learning, showing for the first time that adaptive myelination participate in learning (McKenzie et al., 2014). Furthermore, these results were reproduced in various paradigms modulating neuronal activity either directly by chemogenetic or optogenetic, or indirectly through different

behavioral tasks (Hughes et al., 2018; Geraghty et al., 2019; Bacmeister et al., 2020; Pan et al., 2020; Steadman et al., 2020). Conversely, it was shown in two different paradigms that promoting oligodendrogenesis either genetically or by treatment with clemastine improves memory (Pan et al., 2020; Wang et al., 2020b). Therefore, the production of new OLs in adaptive myelination participates in mechanisms of memory and learning in adult mice.

3.1.3.2 Neuronal activity regulates myelin patterns

Neuronal activity promotes the production of new OLs allowing the production of new myelin sheaths that remain stable along time (Hughes et al., 2018)(Figure 32A). Indeed, in mice sensory enrichment has been shown to increase the number of mature OLs that are integrated stably in cortical circuits. Moreover, memory tasks induce an increase in the proportion of myelinated axons in the prefrontal cortex (Pan et al., 2020) and the corpus callosum (Steadman et al., 2020). In the corpus callosum of mice, it was further shown that a direct stimulation of neuronal activity in a subpopulation of neurons by chemogenetic increases specifically their myelination compared to the non-activated axons (Mitew et al., 2018). Thus, neuronal activity in adult not only promotes globally myelination but also guides adaptive myelination specifically to activated axons (Mitew et al., 2018).

Furthermore, adaptive myelination changes are not restricted to the production of new myelin sheaths, and several parameters of the myelinated fibers that contribute to the conduction velocity of action potential are also modulated (see 1.4.4.1 and 1.5.2.2), such as myelin thickness, internodal length, periaxonal space size and nodal length (Liu et al., 2012; Gibson et al., 2014; Mitew et al., 2018; Geraghty et al., 2019; Bacmeister et al., 2020; Yang et al., 2020; Cullen et al., 2021)(Figure 32B). The first demonstration of myelin sheath plasticity in adult mice has been reported following social isolation (Liu et al., 2012). In these mice, there was a thinning of myelin sheath and transcriptional changes in OLs specifically in the prefrontal cortex (Liu et al., 2012). Conversely, the activation of neuronal activity by optogenetic in the motor cortex (Gibson et al., 2014; Geraghty et al., 2019), and by chemogenetic in the corpus callosum induced an increase of the g-ratio, specifically along activated axons (Mitew et al., 2018). Modulation of another important parameter along myelin fiber, internodal length, has been observed upon specific experience (Bacmeister et al., 2020, 2021; Yang et al., 2020). Motor training as well as monocular deprivation induced dynamic length changes in preexisting internode in the motor and visual cortex respectively (Bacmeister et al., 2020; Yang et al., 2020). It has been further found in the visual cortex that the dynamic changes of intermodal length were neuron populations specific (Yang et al., 2020). Following monocular deprivation, dynamic changes of myelin sheaths' length were observed along parvalbumin interneuron axons, whereas internodes on excitatory callosal projection neurons remained unchanged (Yang et al., 2020). Lastly, it has been

recently reported that spatial learning and transcranial magnetic stimulation modulate nodes' of Ranvier length and the size of the periaxonal space which leads together to conduction velocity modulations (Cullen et al., 2021).

In humans, it has been shown by several imaging studies that motor and memory tasks trigger white matter structural changes that may account for myelin addition (Scholz et al., 2009; Takeuchi et al., 2010). Nevertheless, owing to the limitations of diffusion imaging, these changes might also result from axonal remodeling and might not reflect myelination per se (Zatorre et al., 2012). Furthermore, in human, the origin of the newly produced myelin sheaths is still debated. Indeed, although there is evidence of OPC proliferation in the adult human brain (Geha et al., 2010), recent data suggest that this mechanism may be limited (Yeung et al., 2014). Thus, to which extend adaptive myelination stems from the production of new OLs or from new myelin sheaths synthesized by pre-existing OLs remains unknown.

3.1.3.3 Functions of adaptive myelination

The encoding of learning and memory tasks depends on the fine temporal control of inputs' arrival on the post synaptic structures, and involves coordinated neuronal activities between different areas of the CNS (Hawkins et al., 1983; Siapas and Wilson, 1998; Feldman, 2012; Maingret et al., 2016). Thus, adaptive myelination was hypothesized to impact these mechanisms (Pajevic et al., 2014). Later on, it was shown that inhibiting adaptive myelination by blocking oligodendrogenesis prior to training, disrupts activity of the prefrontal cortex (Pan et al., 2020), and its coordination with hippocampus activity (Steadman et al., 2020)(Figure 32C). Consequently, it was shown that the disruption or the inhibition of adaptive myelination lead to various memory and learning impairments (McKenzie et al., 2014; Geraghty et al., 2019; Pan et al., 2020; Steadman et al., 2020). Thus, adaptive myelination is an activity dependent mechanism that participates in central nervous plasticity and is required to achieve some behavioral tasks. However, adaptive myelination when disrupted by pathological patterns of activity such as epileptic crisis, may be maladaptive and by synchronizing the activity may disrupt further the function of neuronal circuits leading to a worsening of the pathology (Knowles et al., 2020).

Another potential function of adaptive myelination would be to provide metabolic support to the active axons, a mechanism that further depend on neuronal activity (Fünfschilling et al., 2012; Lee et al., 2012b; Saab et al., 2016; Meyer et al., 2018). Indeed, high level of activity requires more energy from the axons to maintain its membrane potential, and metabolic support from the myelin sheath might be necessary for some neuronal population such as fast-spiking interneurons and neurons of the auditory system (Micheva et al., 2016; Moore et al., 2020).

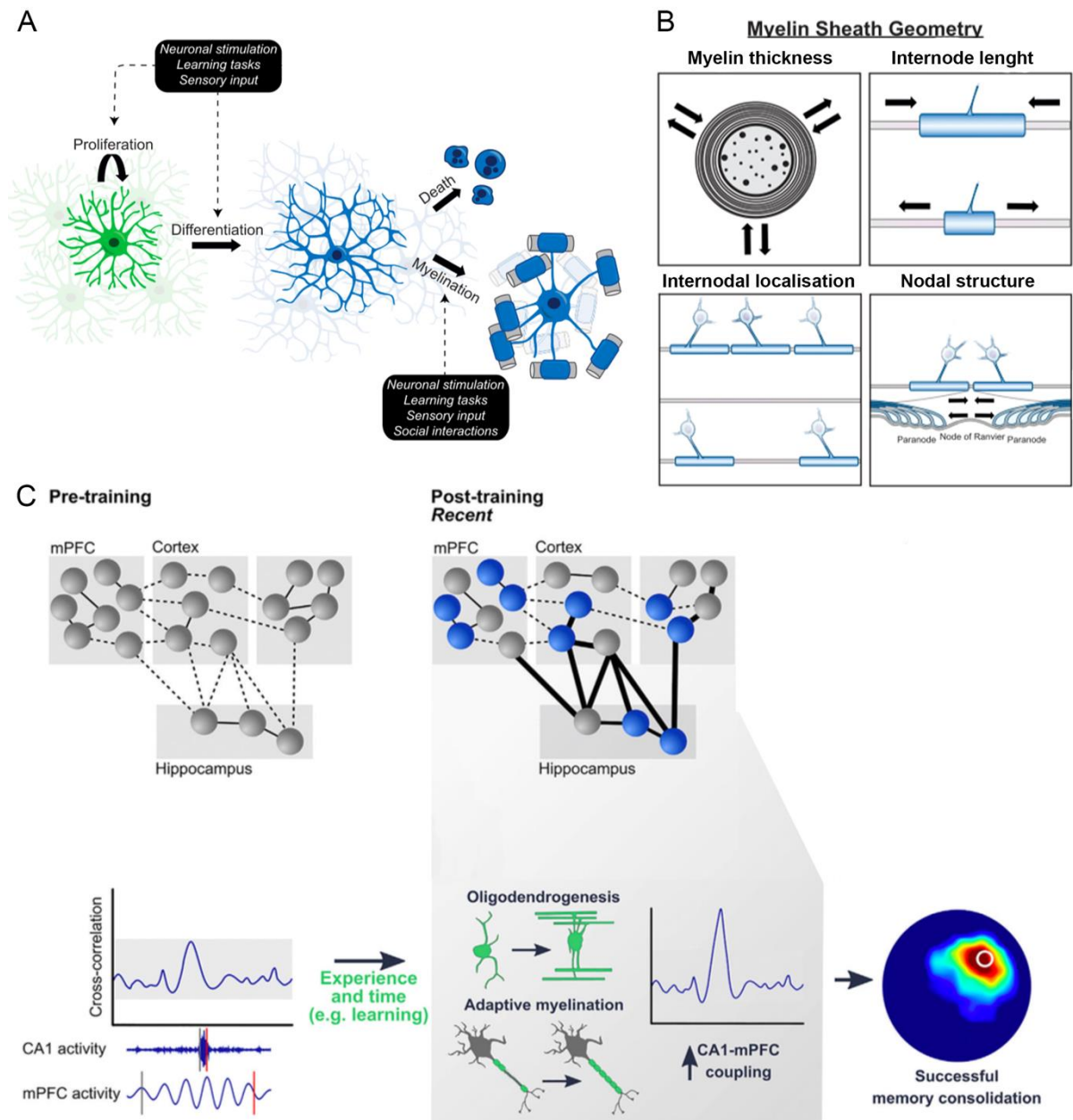


Figure 32: Adaptive myelination induced by neuronal activity changes participates in CNS plasticity.

(A) Schematics showing the different steps of adaptive myelination modulated by neuronal activity. (B) Schematics showing the different modulation of myelin sheaths that allow adaptive myelination to regulate action potential conduction. (C) Model showing how adaptive myelination coordinates neuronal circuits activity to consolidate spatial memory. Following training, there is an activation of oligodendrogenesis and adaptive myelination that induces a higher coupling between the prefrontal cortex (mPFC) and the hippocampus. This mechanism reinforces the connexions used to memorise a task of spatial memory and allows later on a better localization of the target (white circle). The density map illustrates the probability of presence of the mouse in space from very low (blue) to high (red). Adapted from Pease-Raissi et al, 2021 and Steadman et al, 2020.

3.1.4 Neuronal activity also drives remyelination processes in pathological conditions

Owing to the effect of neuronal activity on developmental and adaptive myelination, the possibility to improve remyelination using neuronal activity stimulation has been explored recently. The involvement of neuronal activity in remyelination efficiency was first shown in a model of focal demyelination in the caudal cerebellar peduncle of rats (Gautier et al., 2015). It was shown following demyelination that functional glutamatergic synapses were formed *de novo* by demyelinated axons on OPCs. Although the specific function of these synapses in remyelination could not be tested, it was further shown on human tissues from MS patients that synaptic boutons were more densely distributed in lesions with some of them apposed on OPCs. In rats, Gautier and colleagues showed that the infusion of blockers of neuronal activity, synaptic release or AMPA receptors locally in the demyelinated lesion decreased the efficiency of remyelination. Furthermore, the inhibition of neuronal activity following TTX infusion triggered an inhibition of the oligodendrogenesis, and a thinning of the myelin sheath. Lastly, it was shown that the inhibition of neuronal activity had an effect on remyelination when it was applied during the phase of oligodendrogenesis but not afterwards, once OLs had been produced (Gautier et al., 2015). Although this study suggested for the first time the involvement of neuronal activity in remyelination, the pharmacological agents used may have also altered more directly the oligodendroglial lineage that express the targets of the different molecules used (Spitzer et al., 2019). The use of optogenetic stimulation allowed to specifically activate neuronal activity and demonstrated its potential in promoting remyelination (Ortiz et al., 2019). In mice with a focal demyelination in the corpus callosum, a single protocol of stimulation at 20Hz at the onset of OPCs differentiation is sufficient to increase OPCs proliferation one hour after the stimulation. However, it was shown that daily stimulations along the period of OPCs differentiation into oligodendrocytes were necessary to promote OPCs differentiation and increase the OLs population in the lesion. This increase was further associated with a global increase of remyelination. Interestingly, the recording of compound action potentials from the corpus callosum demonstrated that the repeated stimulations induced a better functional recovery, with a mean conduction velocity that was similar to the one in the normal appearing white matter (Ortiz et al., 2019). These data showed that the activation of neuronal activity may represent a valuable strategy to improve remyelination and help to decipher the protocol of stimulation that could promote repair efficiently.

In two other studies, the efficiency of remyelination was assessed following motor learning or physical activity (Jensen et al., 2018; Bacmeister et al., 2020). Following a demyelination triggered by cuprizone diet, it was shown that motor learning promotes oligodendrogenesis in a time-dependent manner (Bacmeister et al., 2020). In the early phase following cuprizone diet, there is a spontaneous

neuronal hyperactivity and motor learning during this period does not improve oligodendrogenesis and even delays the production of new OLs. However, a delayed motor training after the period of neuronal hyperactivity due to the demyelination leads to an increase of OLs production and a higher number of myelin sheaths produced. Furthermore, it was shown that the delayed motor training also promoted remyelination by surviving OLs, with a higher proportion of surviving OLs that added new myelin sheaths. Intriguingly, following motor training the surviving OLs were suggested to remyelinate more efficiently segments that were previously myelinated and added a lower proportion of myelin sheaths on previously unmyelinated axons compared to newly generated OLs. Overall, the delayed motor training induced a better remyelination and a higher pattern conservation than remyelination in untrained mice (Bacmeister et al., 2020). A second study, using focal demyelination of the spinal cord by LPC injection, showed that physical exercise following demyelination promotes oligodendrogenesis, increases the density of remyelinated axons and the thickness of the sheath produced during remyelination (Jensen et al., 2018). These effects were further associated with effects on innate immune cells (see 3.1.4) and had an additive effect with a treatment by clemastine (Jensen et al., 2018).

In human, several strategies exist to promote neuronal activity. The first one that is currently under clinical trial is the transorbital electrical stimulation (Lubetzki et al., 2020b). This technic performed on patients with recent optic neuritis allows to access a clear readout of the remyelination efficiency by measuring visual evoked potentials. However, this latter method is restricted to the optic nerve and more global stimulation of neuronal activity may be necessary to efficiently enhance remyelination in MS patients. For instance, repetitive transcranial magnetic stimulations (TMS) are used to treat neuropsychiatric diseases with light side effects (Brunoni et al., 2017), and have been shown to trigger myelin plasticity in mice (Cullen et al., 2021). However, none of these TMS strategy has shown a positive effect on remyelination in MS. Trials are in their early phases and further investigations are necessary to define the type of protocols and the strategies that may give the most efficient results with minimal invasion for patients. Furthermore, additional investigations are necessary to decipher the exact role of the different types of cells at play in repair, in particular oligodendroglial and microglial cells that are influenced by neuronal activity and modulate directly or indirectly myelin production.

3.2 Neuronal activity modulates microglia functions

3.2.1 Microglia motility and morphology are modulated by neuronal activity

The first description *in vivo* of microglia surveillance showed that process extensions were mediated by ATP upon laser induced lesions (Davalos et al., 2005; Haynes et al., 2006). Since ATP was known to be co-released with other neurotransmitters at synapses or following the activation of receptor to neurotransmitter, these first results on microglia dynamics suggested that microglial processes may be oriented by ATP release upon neuronal activity (Díaz-Hernández et al., 2002; Fujii et al., 2002; Jo and Role, 2002). However, the use of TTX application to inhibit neuronal activity failed to show any modulation of microglia motility (Nimmerjahn et al., 2005). This apparent lack of modulation may have arisen from the isoflurane mediated anesthesia that was used for this experiment, and later on was shown to inhibit drastically microglia dynamics (Madry et al., 2018b). Supporting a modulation of microglia motility by neuronal activity, treatments with GABA antagonists, agonists of glutamate inotropic receptors or electrophysiological induction of high frequency firing induced a modulation of microglia morphology and dynamics (Nimmerjahn et al., 2005; Fontainhas et al., 2011; Pfeiffer et al., 2016). The modulation of sensory experience in the retina led to microglia motility modulations supporting these latter results (Tremblay et al., 2010). However, these approaches were rather global and none of the molecular mechanism at play were described.

NMDA receptors were also involved in the control of microglial process outgrowth that was shown to be indirectly triggered by ATP release following NMDA activation (Dissing-Olesen et al., 2014b). Recently the use of live imaging *in vivo* in awake mice versus mice that were anesthetized has allowed to confirm the importance of neuronal activity in microglia dynamics (Liu et al., 2019; Stowell et al., 2019; Umpierre et al., 2020). Two of these last studies could identify the role of locus coeruleus (LC) activity in the modulation of microglia surveillance. The release of norepinephrine by neurons from the LC was shown to activate β 2-adrenergic receptor, highly expressed by microglia (Zhang et al., 2014), leading to a decrease of microglia motility (Liu et al., 2019; Stowell et al., 2019). These last results further confirmed the involvement of adrenergic receptor in microglia motility previously suggested in acute slice (Gyoneva and Traynelis, 2013), and showed the importance of studying microglia dynamics *in vivo* in awake mice to preserve microglia motility. However, the downstream signaling that link β 2-adrenergic receptor activation to the reduction of microglia motility remains hypothetical. This control may rely on their function of Gs-coupled receptors, that act as a counterpart of the Gi-coupled protein receptors such as P2Y12 (Gyoneva and Traynelis, 2013). The modulation of K⁺ concentration in the extracellular space upon high frequency firing might also modulate microglia surveillance via Thik-1 activity modulation (Madry et al., 2018b, 2018a). Indeed, it was shown that an important increase of K⁺ concentration in the extracellular medium of 20 to 25mM,

has a direct effect on microglia motility via Thik-1 activity (Madry et al., 2018a). Although physiologic range of K^+ variation have not been tested, K^+ released locally may modulate microglia motility in a neuronal activity dependent manner. Furthermore, upon high frequency firing, for instance following epileptic crisis or spreading depolarization, the important increase of extracellular K^+ up to 60mM (Lux and Heinemann, 1978; Lauritzen et al., 2011) is expected to reduce microglia ramifications and motility. Supporting this hypothesis, it was shown that following spreading depolarization the number of microglial main processes was decreased by 20% (Varga et al., 2020). Furthermore, the decrease of microglia motility by about 30%, observed by Badimon et al. in the striatum following neuronal stimulation by chemogenetic, might be partly due to the K^+ extracellular concentration elevation following the global hyperactivity induced by the stimulation (Badimon et al., 2020).

3.2.2 Microglial modulations of CNS circuits depend on neuronal activity

3.2.2.1 Synapse elimination by microglia is modulated by neuronal activity

The two seminal studies demonstrating that microglia contact synapses *in vivo* further showed, using either pharmacological inhibition or sensory deprivation, that microglia synapse interaction depends on neuronal activity (Wake et al., 2009; Tremblay et al., 2010). During the first phase of maturation of the dorsal lateral geniculate nucleus (dLGN), the synaptic pruning by microglia depends on a balance between the expression of the complement component C3 (that activates CR3) and C47 (activating SIRP α) at synaptic boutons (see 2.2.2.2). This first phase depends on the spontaneous activity of the retina and not on the sensory experience (Hooks and Chen, 2006). It has been shown that the inhibition of the spontaneous neuronal activity of retinal ganglion cells leads to a preferential synaptic pruning of microglia at terminal that have been inhibited (Schafer et al., 2012). Moreover, the expression of CD47 at these terminal is modulated by spontaneous activity, with a decrease of its expression specifically at the terminals of retinal ganglion cell blocked with TTX (Lehrman et al., 2018). Thus, in combination, these two signals allow the activity dependent synaptic pruning by microglia during the first phase of dLGN maturation (Figure 33A). Later in the development of dLGN, there is a further refinement of synaptic connections that depends on sensory experience (Hooks and Chen, 2006). In this second phase, it has been recently shown that the expression of the TNF family cytokine TWEAK by microglia, depends on neuronal activity triggered by visual experience (Cheadle et al., 2020)(Figure 33B). The fixation of TWEAK to its receptor FN14 expressed at the post-synaptic compartment, promotes its elimination and allow to further mature circuits of the dLGN (Cheadle et al., 2020). Thus, microglia participate in brain wiring in the dLGN throughout both phases of postnatal refinement with a control by neuronal activity (Lehrman et al., 2018; Cheadle et al., 2020).

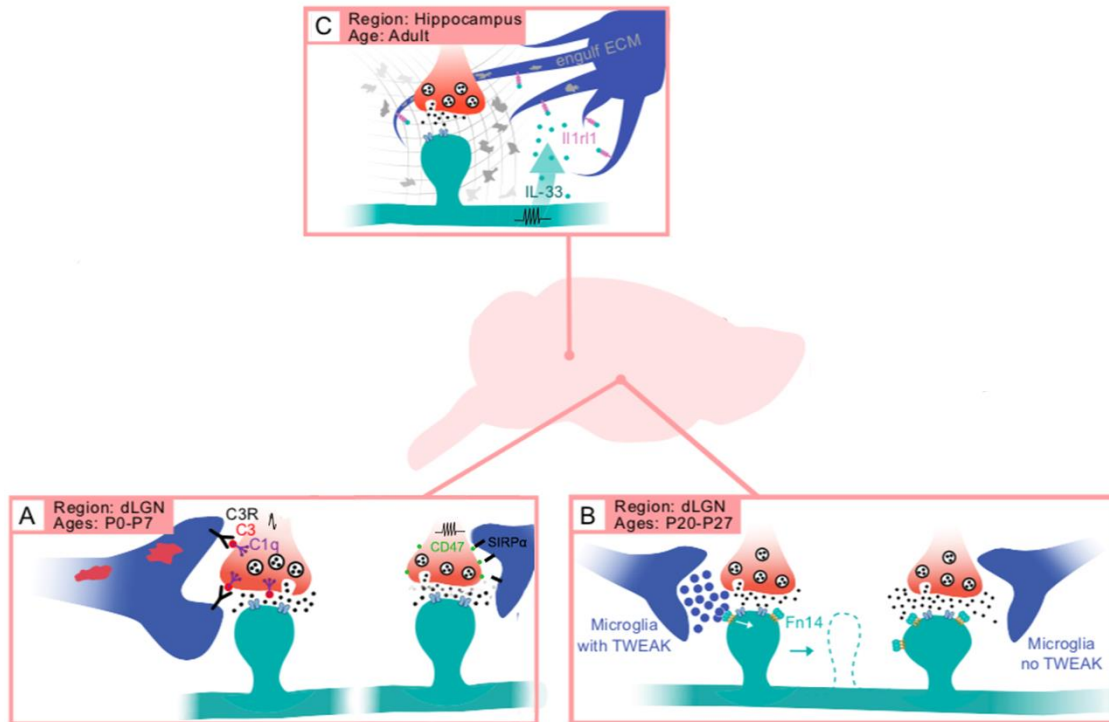


Figure 33: Microglia modulation of CNS circuits depends on neuronal activity.

Schematics showing the different types of neuronal activity dependent regulation mediated by microglia at synapses in mouse CNS, and the molecular mechanisms involved. (A) In the first phase of maturation of the dorsal lateral geniculate nucleus (dLGN) spontaneous neuronal activity modulates the expression of CD47 at synaptic boutons. CD47 activates the microglial receptor SIRP α and acts as a “don’t eat me” signal. The expression at other synapses of C3 and C1q activates CR3 microglial receptor and lead to synaptic pruning. (B) In a second phase of maturation of the dLGN, microglial expression of TWEAK is modulated by the neuronal activity triggered by sensory experience. TWEAK released by microglia binds the receptor FN14 and promotes the elimination of the dendritic spine in a non-phagocytic mechanism. (C) In the adult hippocampus of mouse, the activity dependant secretion of IL-33 by neurons, activates IL1RL1 receptors on microglia and promotes the engulfment of ECM. The engulfment of the ECM by microglia facilitates structural plasticity of dendrites and activates dendritic spine formation. Adapted from Ferro et al, 2021.

3.2.2.2 Neuronal activity drives microglia modulations of CNS plasticity

Microglia modulate CNS plasticity and in particular it was shown that microglia modulate synaptic plasticity (see 2.2.3, (Roumier et al., 2004; Parkhurst et al., 2013; Cantaut-Belarif et al., 2017; Nguyen et al., 2020; Wang et al., 2020a)). For instance, the inactivation of DAP12 in mice led to the observation that long-term potentiation was disrupted and associated with an alteration of the BDNF signaling (Roumier et al., 2004). The involvement of BDNF specifically released by microglia in spine plasticity was further confirmed using a conditional knockout CX3CR1^{creER/+} crossed with BDNF^{fl/fl} mice (Parkhurst et al., 2013). Indeed, preventing BDNF expression specifically in microglia triggered an inhibition of spine formation upon training, a modulation of NMDA receptor subunits expression and a disruption in motor learning (Parkhurst et al., 2013). Thus, these results suggested that microglia control synaptic plasticity by its facilitation, however there was no direct modulation of microglia behavior by neuronal activity.

It is only recently that neuronal activity was shown to directly modulate microglia behavior resulting in modulations of synaptic plasticity. In the hippocampus of mice the neuronal expression of IL-33 is neuronal activity dependent (Nguyen et al., 2020). Moreover, the obligatory receptor of IL-33, IL1RL1 is mainly expressed by microglia in the hippocampus and its specific inactivation in microglia leads to the reduction of dendritic spine formation. Investigating further this mechanism, the authors showed that the dendritic spines formation was promoted by microglia by engulfment of the presynaptic extracellular matrix (Nguyen et al., 2020). Thus, in this mechanism, microglia are the sensor of an activity dependent signaling and promote dendritic spine formation (Figure 33C). It was further shown in this study that the activity dependent secretion of IL-33 promotes adult neurogenesis in the dentate gyrus. Therefore, microglia that are the main cell expressing IL-33 receptor might also participate to the mechanism of activity dependent integration of new neurons to circuits in adult mice (Nguyen et al., 2020).

3.2.3 Microglia regulate neuronal hyperactivity

Several studies recently showed that the activation of neuronal activity leads to reinforced interaction between microglia processes and neurons and further results in the regulation of neuronal activity by microglia (Li et al., 2012; Eyo et al., 2014; Kato et al., 2016; Akiyoshi et al., 2018; Peng et al., 2019; Badimon et al., 2020; Merlini et al., 2021)(Figure 34A). In zebrafish, neuronal activity promotes microglial processes interaction with neuron somata in the optic tectum (Li et al., 2012; Hughes and Appel, 2020). It was shown that the contact of the microglial processes downregulates the activity of the contacted neuron (Li et al., 2012). This result, showed for the first time a reciprocal regulation between neuronal activity and microglial contacts (Li et al., 2012). A similar mechanism has been suggested in mouse (Eyo et al., 2014; Cserép et al., 2020; Merlini et al., 2021). In adult mice, it was shown that a chemogenetic activation of neuronal activity using the DREADD receptor hM3Dq (Roth, 2016), increases the area of neuron somata covered by microglial processes (Cserép et al., 2020). Furthermore, the same group showed that this contact is strengthened following spreading depolarization, a wave of depolarization invading the grey matter and silencing neuronal activity (Varga et al., 2020). In mice with microglia depletion, the amplitude of stimulation to trigger a spreading depolarization is lower than in control, and trigger a higher increase of extracellular K⁺, suggesting that microglia-neuron interactions at neuronal soma may modulate neuronal excitability (Varga et al., 2020). Similarly to what was shown by chemogenetic stimulation, following whisker stimulations, it was observed in the barrel cortex of mice *in vivo* that microglial cells contact preferentially the soma of neurons that have been specifically activated by the stimulation (Merlini et al., 2021). The inhibition of microglial processes recruitment at activated neuron somata further led to a higher synchronization and an hyperactivity in the barrel cortex of mice following whisker stimulation (Merlini et al., 2021). These later results suggest that microglial processes prevent neuronal hyperactivity through their interaction with neuron somata.

The regulation of neuronal hyperactivity by microglia was also observed along the axon (Kato et al., 2016). Following the stimulation of single pyramidal neurons of the cortex with a train of action potentials on acute slices, microglial processes were recruited specifically along the axon of the stimulated neuron. Furthermore, the stimulation triggered a long lasting depolarization of the membrane that was further increased by blocking microglial process recruitment at the axon (Kato et al., 2016). Thus, these results suggest that the recruitment of microglial process at axons can dampen the effect of hyperactivity specifically along hyperactive neurons.

In both interactions along axons as well as at neuron somata, ATP release and the purinergic receptor P2Y₁₂ were involved in the activity dependent recruitment of the microglial processes (Li et al., 2012; Eyo et al., 2014; Kato et al., 2016; Cserép et al., 2020; Varga et al., 2020). Interestingly, the

inhibition of the downstream signaling of Gi coupled proteins (such as P2Y12 receptor) specifically in microglia, showed an inhibition of microglial recruitment by neuronal activity but for the fewer neurons that were contacted by microglia the aberrant activity was still reduced. Thus, the Gi signaling and in particular P2Y12 is required for the recruitment of microglial processes at the neuron soma but the activity dampening of microglial cells may not depend on it (Merlini et al., 2021).

Hence, the molecular mechanism resulting in the microglial dampening of neuronal hyperactivity at neuronal somata and axons remain unknown. A clarification of this molecular mechanism may arise from the seminal study by Badimon and colleagues that showed the molecular signaling involved in the neuronal activity dampening following microglial processes recruitment at synapses (Badimon et al., 2020). In the striatum of mice, following an activation of neuronal activity using DREADDs, microglial processes are recruited by ATP release at synapses through the activation of P2Y12 receptors. The recruitment at synapses put microglial processes expressing CD39 at their surface, in close apposition to synapses. CD39 is an ATP/ADP-hydrolysing enzyme that catalyzes ATP hydrolysis in AMP and is expressed mostly by microglia in the brain. The AMP is further converted to adenosine and activates the protein Gi/o coupled adenosine A1 receptor that dampen D1 neurons response in the striatum (Figure 34B). Consequently, the genetic inactivation or pharmacological inhibition of P2Y12 receptor, the microglia inactivation of CD39 and the inactivation or pharmacological inhibition of the adenosine receptor A1, all led to an increased susceptibility of mice to seizure following a treatment with D1 agonist. The effect of P2Y12 and CD39 inactivation or inhibition was further reversed by a treatment with adenosine A1 receptor agonist supporting the involvement of this molecular mechanism (Badimon et al., 2020). This molecular mechanism described in the striatum at synapses on D1 neurons may also be at play in the microglia dependent dampening of neuron activity described above at neuron somata and axons. Indeed, A1 receptor expression has been observed broadly in the CNS, at the pre and postsynaptic compartments, apical dendrites, axon initial segment and soma of neurons (Ochiishi et al., 1999; Hackett, 2018). Furthermore, this mechanism is compatible with the observation that P2Y12 receptor is not involved in the dampening of neuronal activity but mediates solely the recruitment of microglial processes.

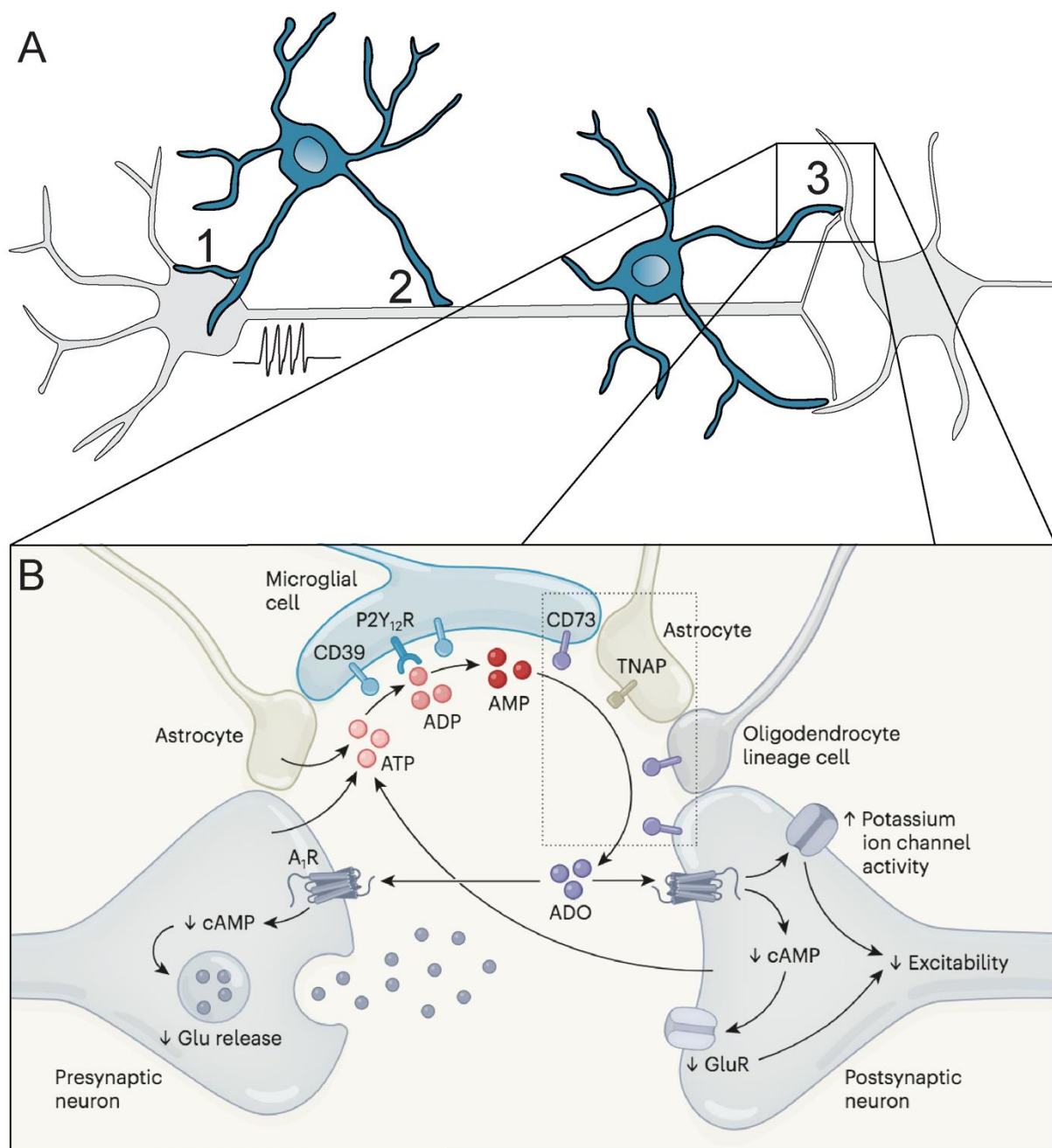


Figure 34: Microglia dampen neuronal hyperactivity.

(A) Schematics showing microglia (blue) contacts on neuronal compartments (grey), soma (1), axon (2) and synapses (3) at which they are recruited upon hyperactivity. At each of these compartments, microglia are involved in activity dampening following hyperactivity. (B) Molecular mechanism described for the dampening of neuronal activity by microglia at the synapse in the striatum. ATP is released by the pre-synaptic compartment (and astrocytes, (Pascual et al., 2005; Corkrum et al., 2020)), hydrolysed into ADP and then AMP by CD39 expressed by microglia and further converted into adenosine by CD73 and TNAP. Adenosine activates A₁ adenosine receptors expressed at the pre- and postsynaptic compartment and dampened the neuronal excitability. This molecular mechanism may be involved at the other compartments of neuron (soma and axon) that are contacted by microglial cells upon activation of neuronal activity. Adapted from Pfeiffer and Attwell, 2020.

3.2.4 Neuronal activity modulates activated microglia behavior in pathology

In pathological conditions, microglial cells are activated and downregulate the expression of multiple markers. Among them P2Y12, CD39 and CX3CR1 (Krasemann et al., 2017; Hammond et al., 2019; Jordão et al., 2019; Badimon et al., 2020) are involved in the neuronal activity dependent modulation of microglial cells (see 3.2.2 and 3.2.3). Therefore, some of the mechanisms described above that depend on microglial sensing of neuronal activity might be deficient following microglia activation in pathological conditions. However, it has been shown that the state of activation of microglial cells can be modulated by neuronal activity, suggesting that they still sense neuronal activity. In a mouse model of Alzheimer disease (5XFAD), the optogenetic stimulation of neurons at 40 Hz in the hippocampus or in the visual and auditory cortex by sensory stimulation increases the phagocytosis of A β peptide by microglia (Iaccarino et al., 2016; Martorell et al., 2019). It was further shown in the same model of Alzheimer disease in mice that optogenetic stimulation at 40 Hz in the hippocampus, modulates the expression of several genes involved in the phagocytic activity of microglia such as CD68 (Iaccarino et al., 2016). In two other mouse models of Alzheimer disease, CK-p25 and P301S, auditory stimulations triggering gamma oscillations in the auditory cortex modified microglial signature related to immune response, antigen presentation and interferon response (Adaikkan et al., 2019).

Following demyelinating lesions, activity dependent modulations of phagocytic capacity and regulations of inflammation may promote remyelination. However, so far most of the studies that triggered neuronal activity to promote remyelination focused on the modulations of the oligodendroglial lineage and on the efficiency of remyelination (see 3.1.4, (Gautier et al., 2015; Ortiz et al., 2019; Bacmeister et al., 2020)). Although not focusing only on microglia, a study using local demyelination of the ventral column of the spinal cord with LPC, has shown some effect of physical exercise on microglia/MDMs activation (Jensen et al., 2018). Using CD16/32 and CD206 markers to segregate respectively pro-inflammatory and anti-inflammatory microglia, they found that physical exercise which enhances neuronal activity, promoted the upregulation of CD206 earlier following demyelination than in demyelinated untrained mice. Furthermore, the expression of CD16/32 was downregulated in the early phase of demyelination. These results were further supported by the increase of IGF-1 signaling - a pro-remyelinating factor in particular expressed by microglia - in the lesion of trained animals (Miron et al., 2013; Jensen et al., 2018). These results suggested that neuronal activity may modulate the switch of the activation state of microglia/MDMs from more pro-inflammatory to more pro-regenerative functions. Furthermore, in the lesions, myelin debris were cleared more efficiently in the group of mice doing physical exercise suggesting a better clearance of myelin debris by microglia/MDMs (Jensen et al., 2018). Thus, although further investigations are needed, the activation of neuronal activity following demyelination may allow to promote myelination by regulation of both microglial and oligodendroglial lineage cells (see 3.1.4).

Aim of the dissertation

The dialog between neuron and microglia is involved in several function in homeostasis as well as pathological conditions. Considering the various contacts made directly on neurons by microglia and their important function in regulating brain functions, we aimed at studying the potential contact of microglia at the node of Ranvier. In the CNS, the contacts of microglia at synapses and on neuronal somata have been well described, however the contacts of microglia on the axonal excitable domains and their function(s), remained elusive. Furthermore, nodes of Ranvier are the only directly accessible neuronal domains along myelinated axons and could constitute a preferential target for microglia to sense the physiology of the neurons while their soma is distant. Thus, the first aim of my project was to characterize the contacts between microglia and nodes of Ranvier through their occurrence and dynamics in homeostasis and during remyelination. Then, we investigated the underlying mechanism that could attract and/or stabilize microglial processes at nodes. Taking advantage of the accessibility of organotypic cerebellar slices, we tested the role of neuronal activity in the interaction and analyzed molecular mechanisms that might participate in microglia-neuron interaction at nodes of Ranvier. The identification of a signal – related to potassium fluxes - mediating the interaction further allowed us to modulate it. Thus, the project next focused on the potential function of this contact in remyelination and how microglia interactions with node could modulate microglial phenotype to promote repair. The results of this work, which has been recently published are presented page 111. These observations raise the question of the consequences of a reinforcement of the interaction on remyelination. To investigate this question, we developed two models of neuronal activity stimulations - chemogenetic and optogenetic - on cerebellar organotypic slices. This allowed to explore the role of neuronal activity on microglia-node interaction in remyelination, and how the reinforcement of the interaction modulate microglia phenotype. Due to their preliminary nature, these unpublished results will be part of the discussion (page 176).

In addition, in an ongoing project we addressed the role of neuronal activity in node-like cluster formation prior to myelination. We first we aimed at determining if these structures were formed *in vivo* and in which proportion. Having confirmed that node-like clusters are similarly formed *ex vivo* and *in vivo* along Purkinje cell axons, we took advantage of our newly developed approaches to modulate neuronal activity and investigated *in vitro* and *ex vivo* whether neuronal activity could modulate node-like clustering prior to myelination. The results of this ongoing work are detailed starting on page 145.

Homeostasis & Remyelination

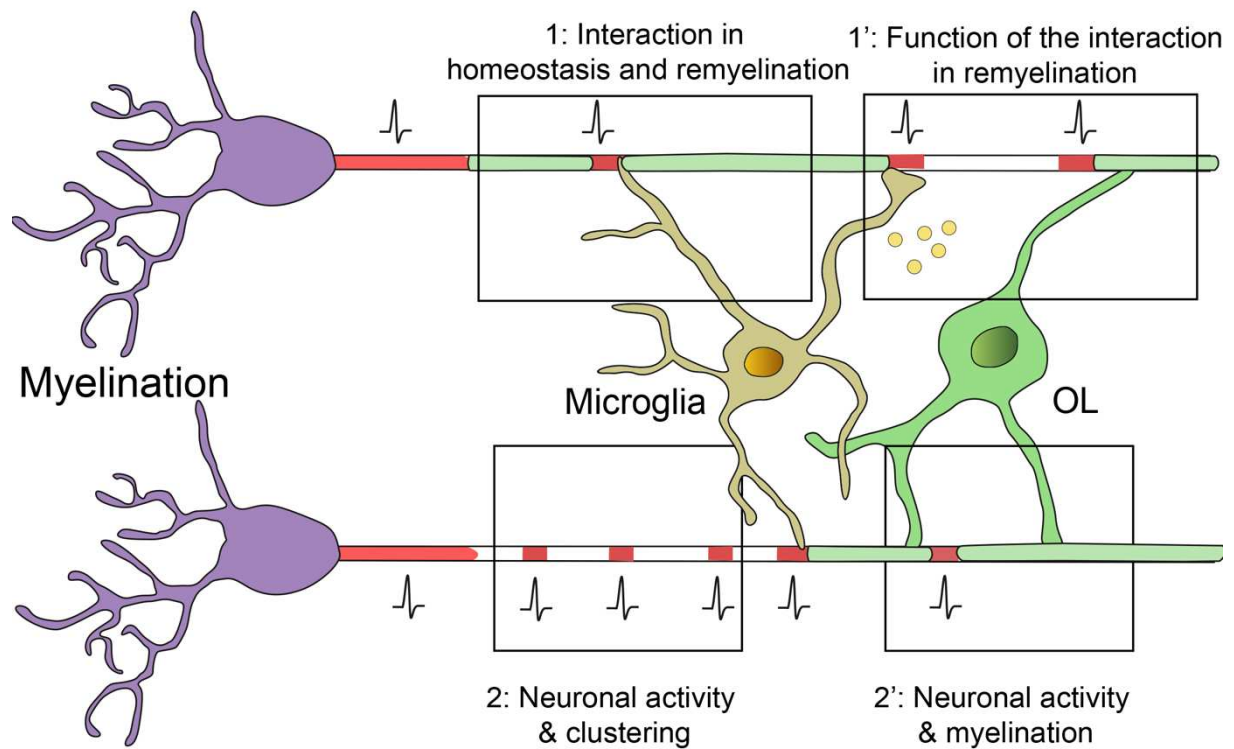


Figure 35: Aim of the dissertation.

The first aim of the project was to characterize the occurrence and the stability of microglial contacts on nodes of Ranvier in myelinated (homeostasis) and remyelinating conditions (1). Then, we aimed at investigating the underlying mechanism(s) modulating microglia-node of Ranvier contact (1'). By inhibiting microglia-node contact in remyelination, we further assessed whether microglia-node interaction could modulate remyelination or not (1'). In an ongoing project, we first investigated the function of neuronal activity in node-like cluster formation (2) and second assessed the role of neuronal activity in myelination along Purkinje cell axons (2').

Results

1 Article: Microglia-neuron interaction at nodes of Ranvier depends on neuronal activity through potassium release and contributes to remyelination

Ronzano R.^{1#}, Roux T.^{1,2#}, Thetiot M.¹, Aigrot M.S.¹, Richard L.³, Lejeune F.X.¹, Mazuir E.¹, Vallat J.M.³, Lubetzki C.^{1,2#}, Desmazières A.^{1#*}

¹ Paris Brain Institute, ICM, Sorbonne University, Inserm U1127, CNRS UMR 7225, Pitié-Salpêtrière hospital, Paris, France.

² Assistance Publique des Hôpitaux de Paris (APHP), Neurology Department, Pitié-Salpêtrière hospital, Paris, France.

³ Centre de Référence National des Neuropathies Périphériques Rares et Département de Neurologie, Hopital Universitaire, Limoges, France

These authors contributed equally to this work

*Corresponding author : Anne Desmazieres; anne.desmazieres@icm-institute.org

Summary

Microglia, the resident immune cells of the central nervous system, are key players in healthy brain homeostasis and plasticity. In homeostasis as well as in pathological condition microglia contact several neuronal compartments. The existence of microglial contacts at nodes of Ranvier was recently described – without data on mechanism and function – albeit without distinguishing targeted contact from a random interaction (Zhang et al., 2019). Furthermore, both the mechanism and the function of microglia-neuron contacts at the node of Ranvier remain unknown.

We thus assessed the existence of this contact and quantified their occurrence in homeostasis, and in remyelinating conditions using both *in vivo* and *ex vivo* models. As an *in vivo* model, we used the dorsal column of the spinal cord where focal demyelination can be performed. Following demyelination, the lesion spontaneously remyelinate with a timeline that is well described. Furthermore, the dorsal location of the lesion allows to perform longitudinal live-imaging of the demyelinated area using a spinal glass window. We further used a model of organotypic cerebellar slices that myelinate spontaneously. Once fully myelinated, it is possible to trigger a demyelination of the entire cerebellar cortex using lysophosphatidylcholine (LPC) and then study its spontaneous remyelination. This model gives a better access to the tissue and allowed us to investigate the dynamic of the contact with a better spatial and temporal resolution. Furthermore, in this model the molecular mechanism at play in the interaction could be investigated more easily. It also allowed us to study further the impact of microglia-node interaction in remyelination.

This study was carried out together with Dr Thomas Roux, who performed the mouse *in vivo* study (apart from the functional study in mouse *in vivo*, Figure 8) and the human tissue study, while I focused on the *ex vivo* part of this work and the functional study *in vivo*.

Studying this contact throughout the CNS, we found that microglia interact with nodes of Ranvier in white as well as grey matter. Further investigation in human tissue showed that this contact is also present in human in similar proportions. Using demyelination with LPC, we could further show both *in vivo* in the white matter of the spinal cord and *ex vivo* in the cerebellar cortex that a higher proportion of nodal structures are contacted by microglia at the onset of remyelination than in myelinated tissue suggesting a reinforcement of these contacts associated with myelin regeneration.




Since microglia are motile and screen their environment permanently, these contacts may result from the random screening of the tissue. By performing live imaging both *in vivo* and *ex vivo* we could show that the contacts are stable. Moreover, quantifying the stability of the contact of microglial cell on the myelin sheath or at nodes, we could show that contacts at nodes were more stable than on the myelin sheaths suggesting the existence of a signal between microglia and nodes.

Investigating further the mechanism that stabilizes microglia interaction with nodes, we showed that this contact depends on neuronal activity and potassium fluxes. Pharmacological blockade or stimulation of electrical activity influenced the proportion of nodes contacted by microglia. Blocking potassium channels along the axon or on microglial cells altered the interaction.

We then analyzed this interaction during remyelination and showed that inhibiting microglia interaction with node led to a higher proportion of microglia expressing the pro-inflammatory factor iNOS, and to a decreased expression of the pro-remyelinating factor IGF-1, by microglial cells. These results suggested that microglia interaction with nodes may promote the switch of microglial phenotypes that is necessary to promote an efficient remyelination. In addition, the inhibition of the interaction was associated with reduced capacity of remyelination.

Taken together, these findings identify the node of Ranvier as a site for microglia-neuron interaction, that participates in microglia-neuron communication and that may mediate pro-remyelinating effect of microglia after myelin injury. Since neuronal activity modulates the interaction, this latter result suggests that neuronal activity also promotes remyelination through its effect on microglia. Lastly, microglia-neuron interaction at node of Ranvier might also modulate the structure and/or the electrophysiological properties of node in homeostasis and it will be important to investigate the function of this interaction in homeostasis in the future.

Microglia-neuron interaction at nodes of Ranvier depends on neuronal activity through potassium release and contributes to remyelination

R. Ronzano ^{1,5}, T. Roux^{1,2,5}, M. Thetiot¹, M. S. Aigrot¹, L. Richard³, F. X. Lejeune^{1,4}, E. Mazuir ¹, J. M. Vallat³, C. Lubetzki^{1,2,5} & A. Desmazières ^{1,5}✉

Microglia, the resident immune cells of the central nervous system, are key players in healthy brain homeostasis and plasticity. In neurological diseases, such as Multiple Sclerosis, activated microglia either promote tissue damage or favor neuroprotection and myelin regeneration. The mechanisms for microglia-neuron communication remain largely unknown. Here, we identify nodes of Ranvier as a direct site of interaction between microglia and axons, in both mouse and human tissues. Using dynamic imaging, we highlight the preferential interaction of microglial processes with nodes of Ranvier along myelinated fibers. We show that microglia-node interaction is modulated by neuronal activity and associated potassium release, with THIK-1 ensuring their microglial read-out. Altered axonal K⁺ flux following demyelination impairs the switch towards a pro-regenerative microglia phenotype and decreases remyelination rate. Taken together, these findings identify the node of Ranvier as a major site for microglia-neuron interaction, that may participate in microglia-neuron communication mediating pro-remyelinating effect of microglia after myelin injury.

¹Sorbonne Université, Paris Brain Institute (ICM), INSERM U1127, CNRS UMR 7225, Hôpital Pitié-Salpêtrière, Paris, France. ²Assistance Publique des Hôpitaux de Paris (APHP), Hôpital Pitié-Salpêtrière, Département de Neurologie, Paris, France. ³Centre de Référence National des Neuropathies Périphériques Rares et Département de Neurologie, Hôpital Universitaire, Limoges, France. ⁴Paris Brain Institute's Data and Analysis Core, University Hospital Pitié-Salpêtrière, Paris, France. ⁵These authors contributed equally: R. Ronzano, T. Roux, C. Lubetzki, A. Desmazières. ✉email: anne.desmazieres@icm-institute.org

Microglial cells are the resident immune cells of the central nervous system (CNS), where they represent 5–10% of the cells¹. This is an heterogeneous population, which participates in normal brain development, homeostasis, and maintenance of neuronal function, as well as learning and memory, by modulating neurogenesis, neuronal survival, wiring, and synaptic plasticity^{2–4}.

In the healthy brain, microglia dynamically survey their environment with their motile processes, as well as with nanoscale sensing filopodia^{5–7}. Process motility is modulated by ATP, chemokines, neurotransmitters, extracellular potassium concentration^{5,8–10}, among other cues, and integrated through microglia receptors, in particular the purinergic P2Y12 receptor and the fractalkine receptor CX3CR1, and the recently identified two-pore domain potassium channel THIK-1^{10–12}.

Microglia are activated in most neurological pathologies, including neurodegenerative diseases, epilepsy, autism, psychiatric disorders, and stroke^{2,4}. In multiple sclerosis (MS), a CNS inflammatory, demyelinating and neurodegenerative disease, activated microglia can contribute to neuronal loss, but they are also important to favor myelin regeneration, in particular through removal of myelin and neuron debris^{13–16}. Remyelination depends on the phenotype of activated microglial cells, with a polarization from M1 (pro-inflammatory) to alternatively activated M2 (pro-regenerative) microglia, though this vision of a M1/M2 polarization is clearly oversimplified^{17–20}. The pro-inflammatory signature is observed early following injury and is associated with deleterious microglial activity if maintained inappropriately^{14,21,22}. However, cells with a pro-inflammatory signature also stimulate proliferation and recruitment of oligodendrocyte precursor cells (OPCs) towards the lesion, whereas pro-regenerative microglial cells promote OPCs differentiation into myelinating oligodendrocytes^{14–16,22}. These experimental data are consistent with results showing an enrichment in pro-regenerative microglia in remyelinating lesions^{14–16}.

It is established that microglia sense neuron activity and can modulate neuron function or detect early neuronal damage^{9,11,23–29}. Aside from neuronal synapses, neuronal soma has recently been identified as a site of microglial interaction, relying on purinergic signaling and possibly involved in microglia-induced neuroprotection^{11,28,29}. The axon initial segment (AIS) has also been identified as a site of microglia–neuron contact, with description of microglial processes overlapping AIS in healthy brain, which vary following brain injury and inflammation^{30,31}.

Along myelinated fibers, the nodes of Ranvier are short unmyelinated domains allowing action potential regeneration and propagation. Astrocytic processes have been described to contact nodes of Ranvier, with a role in nodal length modulation and in ionic buffering³². OPCs processes also contact nodes, although the prevalence of these contacts as well as their physiological role remain elusive³². Direct contacts of microglia on myelin sheaths and nodes of Ranvier have recently been observed in rat corpus callosum³³. We therefore tested, in control and demyelinated CNS, the hypothesis that nodes of Ranvier might be a preferential site for axon–microglia communication.

Here we identify nodes of Ranvier as a site for microglia–neuron communication, in mouse and human CNS, suggesting they could play the role of a “neuro–glial communication hub”. We show that microglia–node interactions are modulated by neuronal activity and potassium ion release, and provide evidence of their influence in microglia-dependent remyelination capacity after experimental demyelination.

Results

Microglia contact nodes of Ranvier in vivo in mouse and human tissues. The nodes of Ranvier, short unmyelinated axonal domains, allow direct access to the axonal surface of myelinated

axons. We thus addressed whether microglia can contact axons at the nodes of Ranvier.

By performing immunostainings and 3D reconstruction on adult mouse fixed tissue, we first observed that microglia (Iba1⁺ cells) contact nodes of Ranvier (AnkyrinG⁺ structures surrounded by paranodal Caspr⁺ staining) in CNS gray (cortex and cerebellum, Fig. 1Ai–ii) as well as white matter (corpus callosum and cortico–spinal tract, Fig. 1Aiii–iv), thus confirming and extending a previous observation in rat corpus callosum³³. The vast majority of microglial cells contact multiple nodes, through cell soma or processes (at the tip or “en–passant”), with the preferential area of contact being along the node and extending to the junction of the node and the paranode (Fig. 1A). This was confirmed by an electron microscopy study following immunostaining with Iba1 antibody, to visualize microglial processes. Longitudinal views of nodes delineated by the paranodal loops on both sides and contacted by microglial processes show that these processes directly contact the nodal axolemma (Fig. 1B) and that the microglial process sometimes extends towards the first paranodal loops (Fig. 1Bii–ii’).

Knowing that nodes can also be contacted by astrocytes and OPCs, we next addressed whether a single node could be contacted by multiple glial cell types. We performed co–stainings in adult mouse spinal cord tissue for microglia (Iba1) and astrocytes (GFAP, Fig. 1C) or OPCs (PDGFR α , Fig. 1D). Our results, showing that a single node can be contacted simultaneously by multiple glial processes, suggest that the node of Ranvier could be a neuro–glial “hub”.

Microglia–node contacts were further detected in human post-mortem hemispheric white matter of healthy donors (Fig. 2), as shown using a specific marker for resident microglia (TMEM119, Fig. 2A, B) and a marker of homeostatic microglia (P2Y12R, Fig. 2C), with 20% of the nodes contacted by microglia (Fig. S1).

Microglia–node of Ranvier contacts are durable and their frequency increases during remyelination.

To assess the extent of microglia–neuron contacts at nodes, we first quantified the percentage of nodal structures contacted by microglial cells in adult mouse dorsal spinal cord. As shown in Fig. 3B, E, $26.3 \pm 3.7\%$ of nodes are contacted by microglia. To assess whether these contacts correspond to microglial cell random scanning of the local environment or to a directed and/or controlled interaction, we then quantified the stability of the contacts, using *in vivo* live-imaging of mouse dorsal spinal cord³⁴ from CX3CR1^{GFP/+}/Thy1–Nfasc186mCherry double-transgenic mice allowing to detect both microglia (GFP) and nodes of Ranvier (Nfasc186mCherry; Fig. 3H, I). We confirmed that microglia are dynamic cells, with motile processes and that their whole morphology can vary over long periods of time (Movie 1). However, when selecting nodes initially contacted by microglia (Figs. 3J, S2A–C, and Movies 1–4), we observed that the microglia–node contacts were maintained along the vast majority of 1-h movies, as well as 3-h movies (Figs. 3K, L and S2D–E respectively). This suggests that microglia–node contact is a specific interaction rather than a random scanning.

We then used the same methods to assess microglia–node interaction following a demyelinating insult (focal demyelination induced by lysophosphatidylcholine, LPC, Fig. 3A). As nodes are deeply disrupted by demyelination³⁵, we excluded demyelinated areas and instead analyzed the perilesional area (i.e., the periphery of a demyelinated lesion, where nodal structures are preserved despite paranodal abnormalities; 7 DPI). Remyelinating lesions (11 DPI) and corresponding Shams, injected with LPC carrier (NaCl 9%), were also analyzed (Figs. 3C–G and S2).

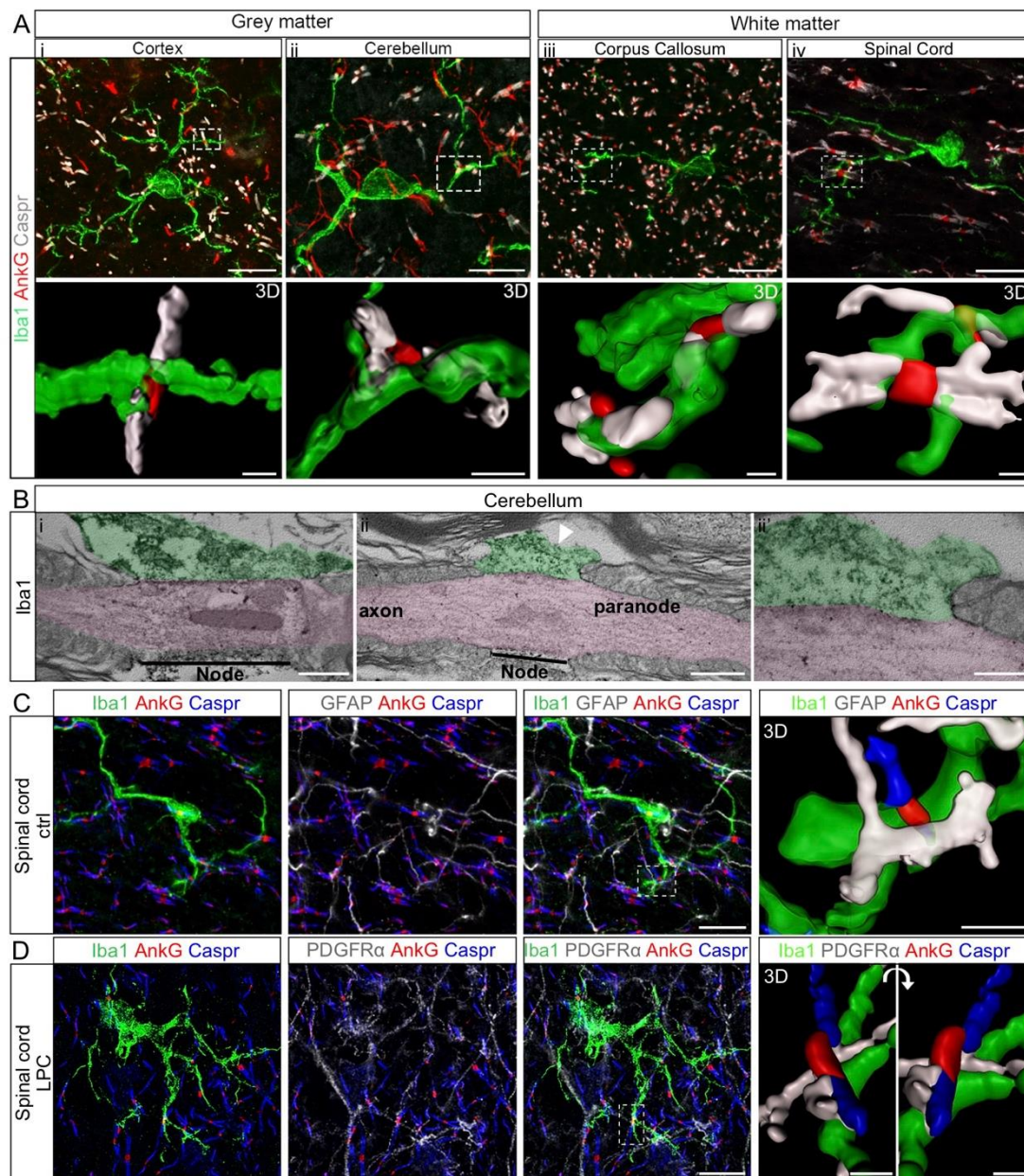


Fig. 1 Microglial cells contact nodes of Ranvier in mouse central nervous system. **A** In adult mouse nervous tissue, microglial cells (Iba1, green) contact nodes of Ranvier (AnkyrinG, indicated as AnkG in the figures, red) in grey matter (i, cortex and ii, cerebellum) and white matter (iii, corpus callosum and iv, dorsal spinal cord, cortico-spinal tractus). **Ai-iv** 3D reconstruction of boxed area in i to iv respectively. **Bi-ii'** Transmission electron micrographs showing microglial processes (Iba1⁺, green) contacting directly the nodal axolemma (pink) in adult mouse cerebellum. **ii'** Higher magnification of the micrograph (ii), showing the interaction between the microglial process, the axolemma and first paranodal loop. **C, D** Immunofluorescent stainings of adult mouse dorsal spinal cord showing nodes of Ranvier (AnkyrinG, red) contacted by both a microglial cell (Iba1, green) and an astrocyte (GFAP, white) in control condition (ctrl) (**C**) and a microglial cell (Iba1, green) and an oligodendrocyte progenitor cell (PDGFR α , white) in remyelinating condition (LPC) (**D**). 3D reconstructions correspond to the boxed area. Scale bars: **A, C, D** 2D: 10 μ m; 3D: **A** 1 μ m, **C, D** 2 μ m; **Bi-ii'** 500 nm, **Biii** 200 nm. **A, C, D**: $n = 4$ animals, **B**: $n = 3$ animals.

We found that the frequency of interaction (i.e. the percentage of nodes contacted by microglia) was unchanged in the perilesional area (perilesional: $37.6 \pm 2.7\%$ vs sham: $31.8 \pm 3.5\%$; Fig. 3C–E). In contrast, the stability of the interaction was significantly decreased in perilesional tissue at the peak of demyelination (1-h movies, $88.4 \pm 3.1\%$ of timepoints with contact) compared to control and 7 DPI Sham ($98.9 \pm 1.1\%$ and $100 \pm 0.0\%$ respectively, Fig. 3K). Similar results were obtained with the longest sequence of consecutive timepoints with contact, with a reduction of 25% of contact stability (Fig. 3L). In contrast, the

frequency of interaction was significantly increased during remyelination ($60.9 \pm 1.9\%$ of nodes of Ranvier contacted; Fig. 3E, G) compared to control and 11 DPI Sham ($18.2 \pm 1.6\%$; Fig. 3E, F), which was not due to changes in microglial cell or node numbers (see statistical analysis table). Furthermore, there was a restoration of long-lasting interactions during remyelination, similar to controls (1-hour movies, Figs. 3K, L and S2 Movies 2–4). The 3-h acquisition study showed similar tendencies (Fig. S2D–E).

The increased frequency of interaction upon remyelination suggests that microglia-node communication might play a role in

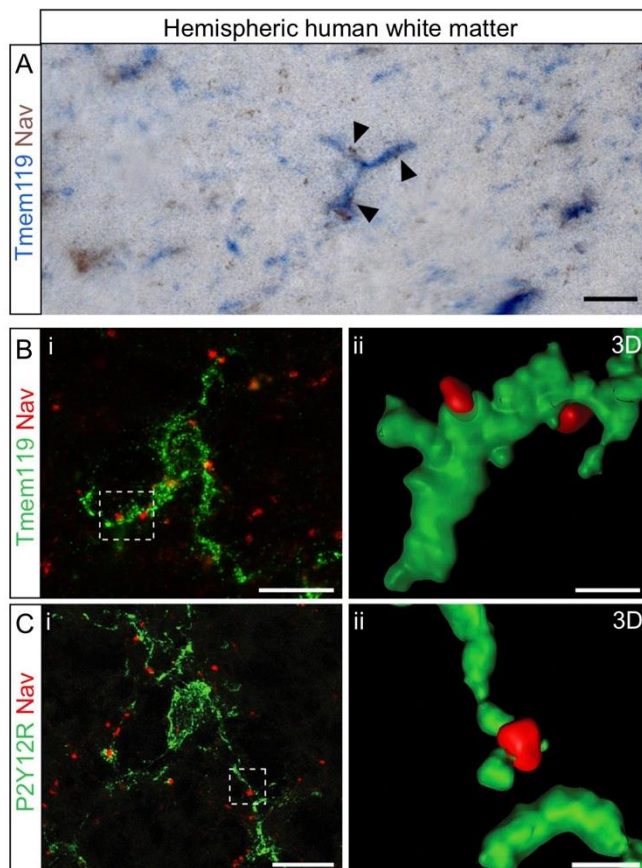


Fig. 2 Microglial cells contact nodes of Ranvier in human central nervous system. **A** Immunohistostainings of post-mortem human hemispheric white matter tissue (healthy donor) showing microglial cells (blue, resident microglia, TMEM119) contacting nodes of Ranvier (Nav , brown). **B, C** Immunofluorescent stainings of post-mortem human hemispheric white matter tissue (healthy donor) showing microglial cells (green; **B**, resident microglia, TMEM119, and **C**, homeostatic microglia, P2Y12R) contacting nodes of Ranvier (Nav , red). **Bii, Cii** 3D reconstructions correspond to the boxed area in **Bi** and **Ci** respectively. Scale bars: (2D) **A, B, C** 10 μm ; (3D), **B, C** 2 μm . **A**: $n = 6$ samples, **B, C**: $n = 5$ samples.

the repair process, whereas the decreased stability in the perilesional area (where demyelination is not yet detected) might be an early event preceding demyelination.

Microglial processes interact preferentially with the nodes of Ranvier compared to the internodes. We next studied microglia-node interaction over shorter periods of time to determine whether the contacts were stable along time or could correspond to back and forth microglial contacts. Microglial cell bodies and thick processes contacting nodes were mostly non moving during short periods of time and we thus focused on contacts between nodes and the thin microglial process tips, which are very motile. We in particular wanted to address whether the contact at nodes by these processes corresponded to a random screening of the environment or whether they would preferentially interact with the nodal area. To obtain the increased temporal and spatial resolution needed to visualize microglial thin process tips and to explore this question in myelinated as well as (re)myelinating contexts, we used organotypic cultures of mouse cerebellar slices, a model which presents a preserved cytoarchitecture and is highly accessible for spinning-disk confocal live-imaging^{36,37}. It is

further adapted for electrophysiology studies and pharmacological treatments.

In fully myelinated $\text{CX3CR1}^{\text{GFP/+}}$ slices (Fig. S3F), the percentage of nodes of Ranvier contacted by microglia is comparable to in vivo ($23.9 \pm 4.0\%$, Fig. S3H).

Microglia also contact nodes of Ranvier during developmental myelination, both in vivo and ex vivo (Fig. S3B, C, respectively). In myelinating tissue ex vivo, the percentage of nodal structures contacted is similar to adult myelinated tissue ($21.8 \pm 3.4\%$, Fig. S3D), with no significant bias towards mature nodes of Ranvier or immature nodal structures (node-like clusters and heminodes, Fig. S3A, E). Following LPC treatment, and in agreement with our in vivo observations, the percentage of nodal structures contacted in remyelinating slices (Fig. S3G) is increased compared to control condition ($46.0 \pm 3.2\%$, Fig. S3H), without any bias towards mature or immature structures (Fig. S3I).

Having established the similarity of ex vivo and in vivo models for the analysis of microglia-node interaction, we then used $\text{CX3CR1}^{\text{GFP/+}}$ cerebellar slices transduced to visualize nodal structures ($\beta 1\text{Nav}$ -mCherry neuronal expression, Fig. S4A, B) along Purkinje cell axons (10-min movies; Fig. S4C, D and Movies 5–7), to gain deeper insight into the dynamics of microglia processes at nodes. We first compared microglial process tip dynamics when contacting an internodal or a nodal area along the axon in myelinated slices (Fig. 4A, Control, Movies 5 and 6, respectively). The rate of microglial process contact is significantly increased at nodes compared to internodes ($81 \pm 8\%$ of timeframes per movie with contact at nodes, vs $52 \pm 5\%$ at internodes, Fig. 4B) as well as the maximum number of consecutive timeframes with contact (14.0 ± 2.2 frames at nodes vs 8.2 ± 1.1 frames at internodes, Fig. 4C). Similarly, the number of consecutive timeframes without contact is increased at internodes (8.5 ± 1.2 frames vs 3.9 ± 1.6 frames at nodes, Fig. S4E). Regarding microglial contacts at nodes, these parameters are similar in remyelinating slices (rem) compared to control slices (Fig. 4A, F, G, Movie 7 and Fig. S4G).

Microglial process behavior is modified at the nodes of Ranvier. To further assess how microglial process motility and behavior could be modified at the vicinity of a node, we further analyzed the trajectory of process tips with nodal contact or without contact (wo contact) at imaging onset (Fig. 4D, E). The total length of the trajectory was unchanged along 10 min (wo contact $28.1 \pm 4.0 \mu\text{m}$ vs nodal contact $26.1 \pm 4.4 \mu\text{m}$, Fig. 4D), as well as the mean instantaneous velocity (wo contact: $2.6 \pm 0.4 \mu\text{m}/\text{min}$ vs nodal contact: $2.2 \pm 0.4 \mu\text{m}/\text{min}$, Fig. 4E). However, the microglial process tip remained in the direct vicinity of the node contacted compared to non-contacting tips, which frequently move away from their initial position (mean distance from origin, wo contact: $3.06 \pm 0.4 \mu\text{m}$ vs nodal contact: $1.77 \pm 0.4 \mu\text{m}$, Figs. 4D and S4F).

In remyelinating slices, the mean distance from origin was also reduced for processes contacting nodes (wo contact: $2.88 \pm 0.7 \mu\text{m}$ and with nodal contact: $1.20 \pm 0.5 \mu\text{m}$, Figs. 4H and S4H). Interestingly, the mean velocity was in that case significantly decreased by a half for process tips contacting a node compared to non-contacting ones (wo contact: $2.1 \pm 0.3 \mu\text{m}/\text{min}$ vs node: $1.2 \pm 0.3 \mu\text{m}/\text{min}$, Fig. 4I). Hence, the total length of the trajectory covered in 10 min was decreased when contacting a node (wo contact: $24.9 \pm 3.7 \mu\text{m}$ vs node $15.8 \pm 4.2 \mu\text{m}$).

Taken together, these data suggest the existence of (an) underlying mechanism(s) attracting and/or stabilizing microglia at nodes of Ranvier, including the very motile microglial processes. Microglial interaction at the node is further

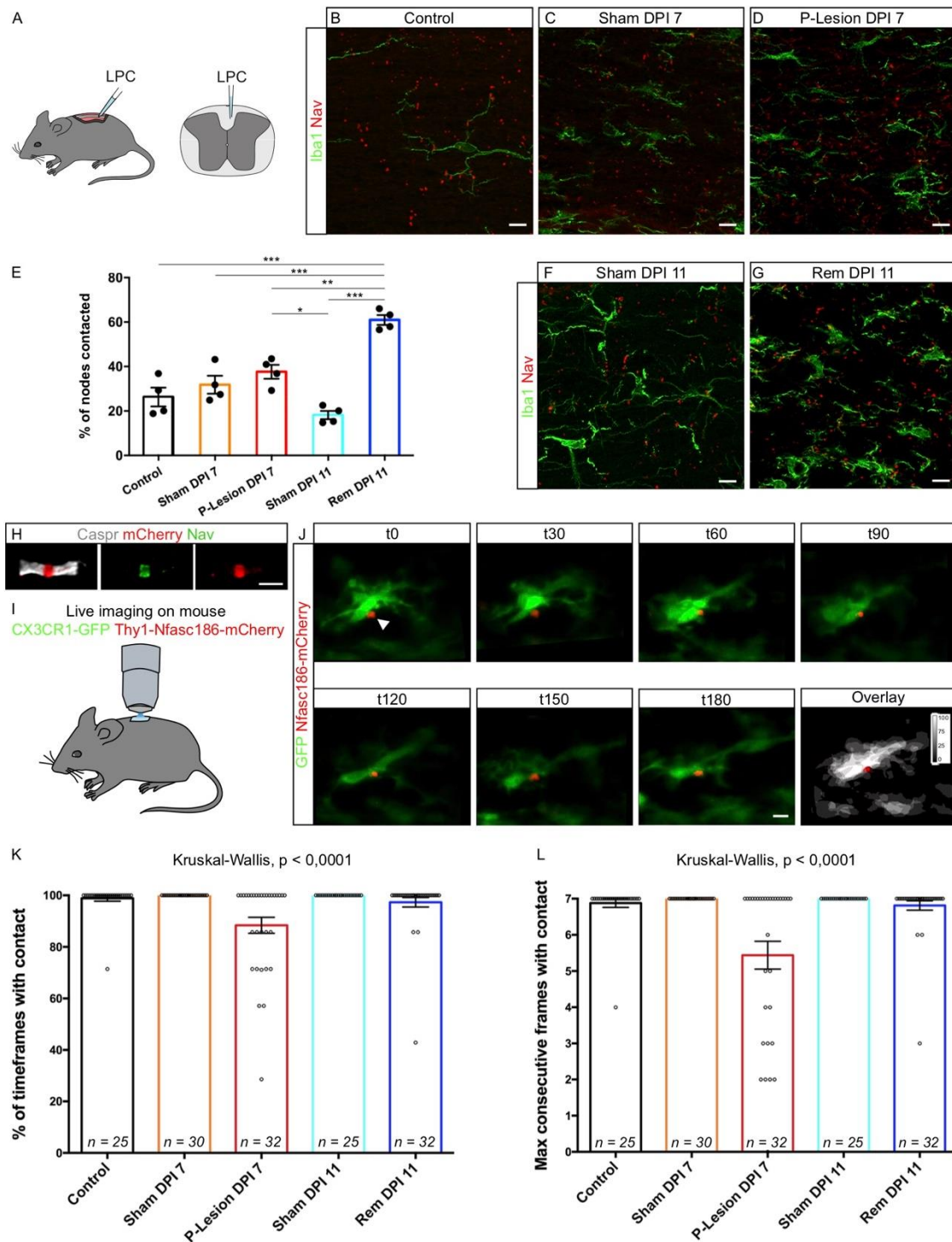


Fig. 3 Microglial cell contacts at nodes of Ranvier are stable in vivo and increase in remyelination. **A** LPC injection in mouse spinal cord (cortico-spinal tractus). **B–G** Contacts are observed between nodes of Ranvier (Nav, red) and microglia (Iba1, green) in control (without injection) (**B**), Sham 7 and 11 days post-NaCl injection (Sham DPI 7 and 11) (**C, F**, respectively), in perilesional tissue 7 days post LPC injection (P-Lesion DPI 7) (**D**) and in remyelinating tissue 11 days post-LPC injection (rem DPI 11) (**G**). **E** Corresponding quantifications of the percentage of nodes contacted. **B–G:** $n = 4$ animals per condition; 4–6 areas per animal, 42 nodes minimum per area. **H** Nfasc186mCherry colocalizes with Nav at the node of Ranvier in Thy1-Nfasc186mCherry mouse dorsal spinal cord ($n = 3$ animals). **I** Glass-window system above dorsal spinal cord for 2-Photon live-imaging. **J** Images from a 3-h movie (Movie 1) from a CX3CR1-GFP/Thy1-Nfasc186mCherry mouse shows a stable interaction between a microglial cell (green) and a node of Ranvier (red) (arrow head). scale bar: 10 μm . **K** Percentage of time in contact in 1-h movies, with one acquisition every 10 min. **L** Longest sequence of consecutive timepoints with contact in 1-h movies. Each dot is a microglia-node pair. The number of node-microglia pairs imaged is indicated on each bar. **J–L** $n = 6$ –11 animals per condition. Scale bars: (**B–D, F, G, J**) 10 μm . **E** ANOVA with post hoc Tukey test; **K, L** Two-sided Kruskal-Wallis test. * $P < 0.05$, ** $P < 0.01$, *** $P < 0.001$, **** $P < 0.0001$, ns not significant. Bars and error bars represent the mean \pm s.e.m. For detailed statistics, see Supplementary Table.

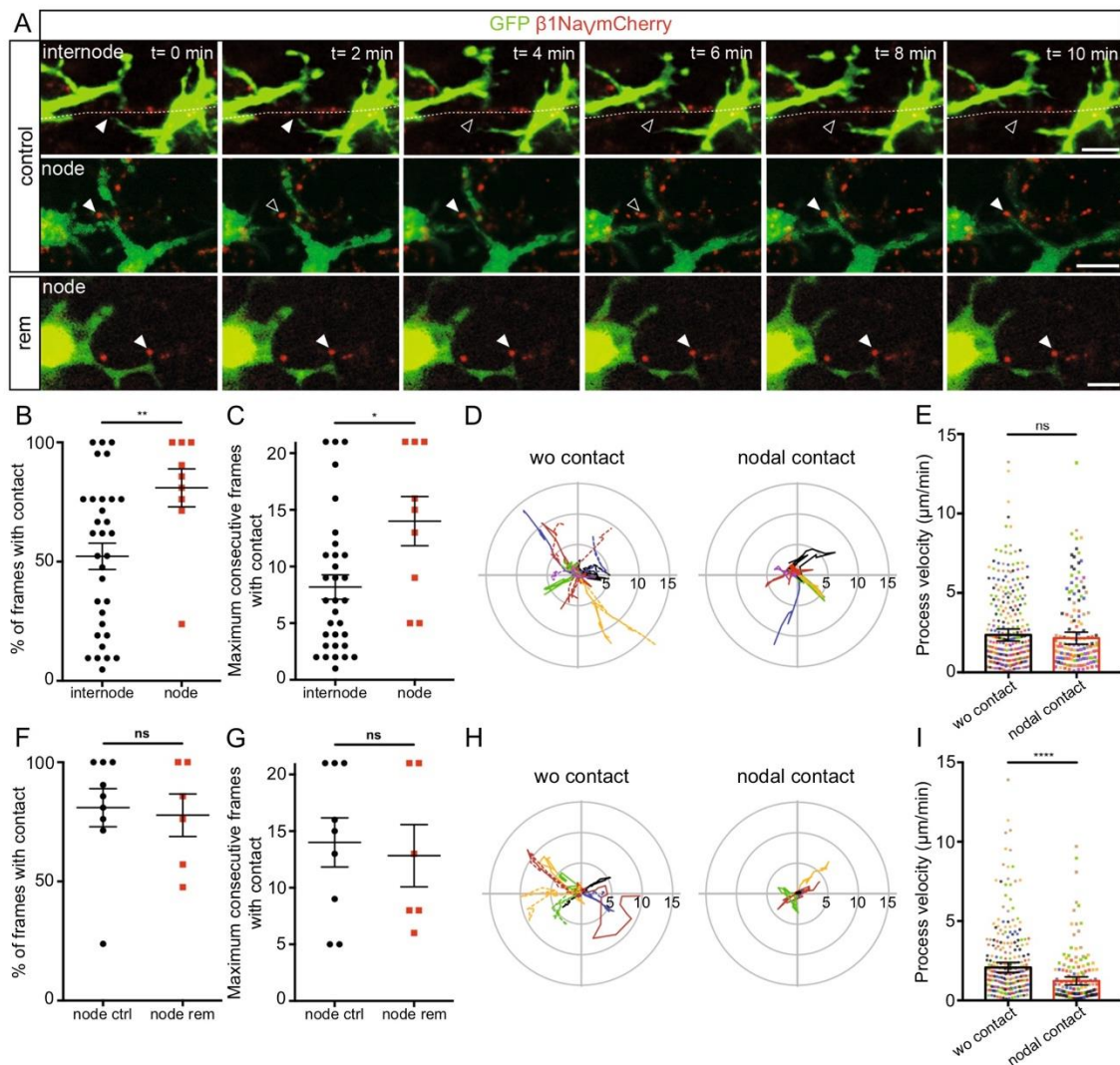


Fig. 4 Microglia process dynamics are modified by nodal structure vicinity in myelinated and remyelinating cultured slices. **A** Microglial cells (green) initially contacting an internode or a node (red) in myelinated slices (control), or a node in a remyelinating slice (rem). Arrowheads show the initial contact position (filled: contact, empty: no contact). (Control: internode: $n = 32$ contacts from 16 animals, node: $n = 9$ contacts from 8 animals; rem: $n = 6$ contacts from 6 animals). **B, C** Dynamics of microglial processes contacting an internode vs a node in myelinated slices (internode: $n = 32$ contacts from 16 animals, node: $n = 9$ contacts from 8 animals). **D** Trajectories (with t_0 position as reference, distance in μm) of microglial process tips in myelinated slices, initially contacting a node (nodal contact) or not (wo contact). wo contact: $n = 14$, nodal contact: $n = 7$, from 7 color coded animals. Type II Wald χ^2 (two-sided analysis), $p = 1.679 \times 10^{-8}$ (for quantification, see Fig. S4F). **E** Instantaneous process velocity in myelinated slices. wo contact: 280 measures from 14 trajectories in 7 animals, nodal contact: 140 measures from 7 trajectories in 7 color coded animals. **F, G** Dynamics of microglial processes contacting a node in control (node ctrl) or remyelinating slices (node rem). ctrl: $n = 9$ contacts from 8 animals, rem: $n = 6$ contacts from 6 animals. **H** Trajectories (with t_0 position as a reference, distance in μm) of microglial process tips in remyelinating slices, initially contacting a node or not. wo contact: $n = 12$, nodal contact: $n = 6$, in 6 color coded animals. Type II Wald χ^2 test (two-sided analysis), $p = 2.2 \times 10^{-16}$ (for quantification, see Fig. S4H). **I** Instantaneous process velocity in remyelinating slices. wo contact: 240 measures from 12 trajectories in 6 animals, nodal contact: 120 measures from 6 trajectories in 6 color coded animals. Scale bars: **A** 10 μm . **B, C, F, G** Two-sided Mann-Whitney test, **E, I** Type II Wald χ^2 test (two-sided analysis). * $P < 0.05$, ** $P < 0.01$, *** $P < 0.001$, **** $P < 0.0001$, ns not significant; bars and error bars represent the mean \pm s.e.m. For detailed statistics, see Supplementary Table.

strengthened in the remyelinating context. We thus questioned which signal(s) could be regulating this interaction.

CX3CR1, P2Y12, and P2Y13 are not required for microglia-node interaction in physiological condition. Various signaling pathways mediating neuron-microglia crosstalk have been uncovered in physiological and pathological contexts³⁸. Among them, we first focused on CX3CR1 pathway, taking advantage of the fact that CX3CR1-GFP mouse strain corresponds to a knock-in of GFP into the CX3CR1 gene locus, leading to a loss of function of this gene in homozygous mice. By comparing

CX3CR1^{GFP/GFP} with CX3CR1^{GFP/+} littermates in myelinated cultured slices, we found no significant difference in the percentage of nodes contacted ($25.1 \pm 2.5\%$ vs $20.8 \pm 2.6\%$ respectively, Fig. S5A–B). We confirmed these results in vivo, where no significant difference was observed in the mean percentage of contacted nodes between CX3CR1^{GFP/GFP} and control mice (Fig. S5C–D).

The microglial P2Y12 purinergic receptor has also been involved in multiple microglia-neuron interactions, and is highly expressed by microglia in myelinated cerebellar slices ex vivo (Fig. S6A). In order to address whether this pathway was required for microglia-node

contact, we first inhibited the P2Y₁₂R receptor specifically using PSB0739 (1 μ M), a highly potent P2Y₁₂ antagonist, and found that it is not required for microglia-node interaction ($15.1 \pm 1.2\%$ of nodes contacted in control vs $15.5 \pm 1.7\%$ following treatment, Fig. S6B–C). To further assess the potential role of the P2Y receptor family and exclude any compensatory mechanisms, we also inhibited P2Y₁₃R, which participates in microglia dynamics control³⁹, concomitantly to P2Y₁₂R by using the MRS2211 inhibitor (50 μ M). Again, there was no significant variation in the number of nodes contacted in control vs treated slices ($15.1 \pm 1.5\%$ vs $14.3 \pm 1.3\%$ respectively, Fig. S6D–E), confirming that P2Y₁₂R and P2Y₁₃R are not required for microglia-node interactions in physiological condition.

Neuronal electrical activity modulates microglia-node interaction. As reciprocal interactions between electrically active neurons and microglia have been established, we then addressed whether changes in neuronal activity might impact microglia-node contacts. Purkinje cells are spontaneously active in organotypic cerebellar slices, as assessed by loose-cell attached recordings ($n = 13$ cells from 9 animals, Fig. S7A). To modulate neuronal activity, we used two pharmacological agents, Apamin (Apa, 500 nM) and Tetrodotoxin (TTX, 500 nM). Apamin is a blocker of SK2 channels, which leads to a specific increase of Purkinje cells firing in the cerebellum⁴⁰, while TTX is a well described blocker of action potential generation through voltage-gated sodium channel inhibition⁴¹. Apamin treatment lead to a 60% increase of Purkinje cell instantaneous firing frequency (Ctrl: 16.09 ± 3.47 Hz; Apamin: 26.12 ± 7.14 Hz, Fig. S7B–C), whereas TTX completely blocked their activity (Fig. S7A–B). We first confirmed that both TTX and Apamin do not affect global morphology and dynamics of microglial cells (Fig. S8). We then addressed whether microglia-node contacts were modified following these pharmacological treatments. Following 1-h TTX treatment of myelinated slices, microglia-node contacts were significantly decreased by 20% ($21.3 \pm 2.4\%$ nodes contacted in control vs $16.9 \pm 2.0\%$ in treated slices, Fig. 5A–C), while a 1-h Apamin treatment on myelinated slices significantly increased by 20% the percentage of nodes contacted ($16.9 \pm 1.7\%$ nodes contacted in control vs $20.4 \pm 1.2\%$ in treated slices, Fig. 5D–F).

Taken together, these data demonstrate that microglial contacts at nodes are modulated by neuronal activity, adding further insight into the role of microglia as a neuronal activity sensor.

Microglia-node interaction is modulated by potassium release at nodes. Recent works suggest that microglia dynamics can be modulated by extracellular potassium concentration^{10,42}. To assess the potential involvement of nodal potassium flux in microglia-node interaction, we treated myelinated cultured slices with the large spectrum inhibitor of potassium channels tetraethylammonium (TEA, 30 mM, Fig. 6A) for 1 h. We first confirmed that TEA does not affect global morphology and dynamics of microglial cells (Fig. S8). This treatment however resulted in a 40% decrease of microglia-node interaction, with $11.4 \pm 1.1\%$ of the nodes contacted in the treated slices, compared to $18.8 \pm 1.1\%$ in control condition (Fig. 6B, C). High concentration of TEA is expected to decrease Purkinje cells activity, which would lead to reduced interaction. We thus compared the normalized effects of TEA and TTX and observed that the reduction of microglia-node interaction is significantly more pronounced after TEA treatment than after TTX treatment (40 and 20% decrease respectively), suggesting that the outward potassium current existing at axonal resting potential may also participate in modulating microglia-node interaction.

We then addressed how TEA impacts the dynamics of microglial process in myelinated slices, by comparing processes contacting a node or an internode (Fig. 6D–I and Movie 8). Contrary to the preferential interaction of microglial processes at nodes found in untreated slice cultures (Fig. 4), in the TEA treated slices, the dynamics of contact was similar between processes with internodal or nodal contact ($49.7 \pm 4.9\%$ of timeframes with contact at internodes vs $55.2 \pm 9.3\%$ at nodes, Fig. 6E) and consecutive number of timeframes with contact was comparable (internode: 8.5 ± 0.9 frames; node: 10.0 ± 1.8 frames; Fig. 6F). Similarly, in myelinated slices treated with TEA, the process trajectory and velocity are not significantly different for processes with and without nodal contacts (Fig. 6G–I).

The two-pore domain channel THIK-1 was recently identified as the main K⁺ channel expressed in microglia¹⁰. We first showed that THIK-1 mRNA is expressed by microglial cells in myelinated and remyelinating condition in our slice model (Fig. S9A, C respectively), and that it is not expressed by Purkinje cells (Fig. S9B, D). We detected THIK-1 mRNA expression in the majority of microglial cells, with $76.4 \pm 3.2\%$ of microglial cells clearly expressing this marker in myelinated tissue and $66.5 \pm 8.0\%$ in remyelinating condition (Fig. S9E, F, $n = 3$ animals per condition, $n = 200$ and $n = 209$ total cells analyzed respectively). To confirm the role of K⁺ flux in microglia-node interaction, we treated myelinated cultured slices for 1 h with tetrapentylammonium (TPA, 50 μ M), a blocker of THIK-1, (Fig. 6J). We observed a significant 36% decrease of microglia-node interaction, with $10.8 \pm 1.2\%$ of the nodes contacted in the treated slices, compared to $17.1 \pm 1.4\%$ in control condition (Fig. 6K–L), an effect which is similar in amplitude to the effect of TEA treatment.

Taken together, these results confirm that microglia preferential interaction with nodes of Ranvier depends on potassium level within the nodal area, with a key role of microglial THIK-1 K⁺ channel.

The alteration of microglia-node interaction by K⁺ channel inhibitors impairs the microglial switch towards a pro-regenerative phenotype and decreases remyelination. Having confirmed that node-microglia communication also depends on K⁺ flux in remyelination (Fig. 7A–C), we next addressed whether altering microglia-node interaction at remyelination onset could affect the repair process in LPC-demyelinated cultured cerebellar slices. To address this question, we thus treated cerebellar slices with either TEA or TPA at the onset of remyelination and studied whether this could affect the microglial switch from pro-inflammatory towards pro-regenerative phenotype, by quantifying the percentage of microglial cells expressing the pro-regenerative marker IGF1 (Fig. 7D, E, TEA and Fig. 7H, I, TPA) and the pro-inflammatory marker iNOS (Fig. S9G, H, TEA and Fig. S9I, J, TPA). We observed a significant 22% decrease in IGF1 population following TEA treatment (ctrl: $74.2 \pm 2.8\%$; TEA: $57.5 \pm 1.9\%$; Fig. 7E), and a significant 25% decrease following TPA treatment (ctrl: $79.7 \pm 2.2\%$; TPA: $60.0 \pm 1.0\%$; Fig. 7I). Conversely, we observed a significant 21% increase in iNOS⁺ population following TEA treatment (ctrl: $57.2 \pm 0.9\%$; TEA: $69.5 \pm 1.7\%$; Fig. S9H), and a significant 26% increase following TPA treatment (ctrl: $60.0 \pm 1.0\%$; TPA: $75.9 \pm 2.2\%$; Fig. S9J). Microglia-node K⁺ signaling dysregulation at onset of remyelination thus results in altered microglial phenotypic switch.

We next quantified the rate of remyelination of Purkinje axons in demyelinated slices treated with TEA or TPA, compared to untreated slices (Fig. 7F–G, J–K). We observed a significant 24% decrease of the remyelination rate following TEA treatment (ctrl:

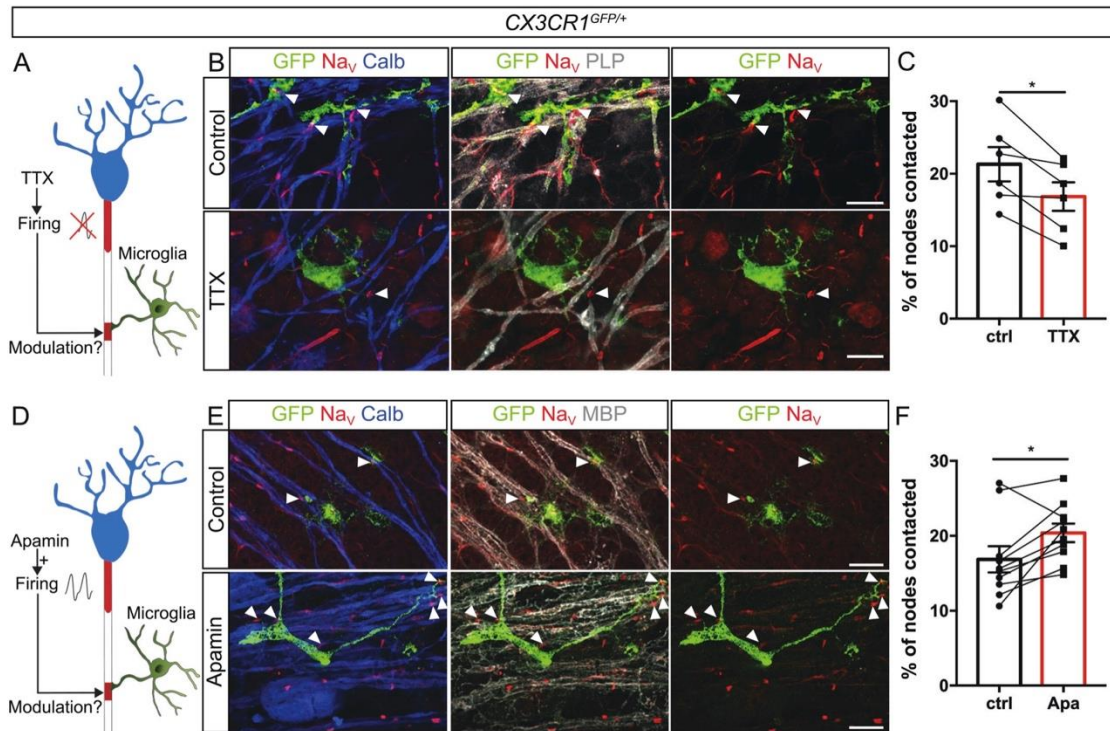


Fig. 5 Neuronal activity modulates microglia-node of Ranvier interaction. **A, D** Experimental designs. **B, C** In myelinated CX3CR1^{GFP/+} cerebellar organotypic slices, microglia (GFP, green) contacts with nodes (Nav_v, red) are reduced following electrical activity inhibition with tetrodotoxin (TTX). **E, F** They are conversely increased following electrical activity activation using apamin (Apa). Arrowheads show the nodes of Ranvier contacted by microglia. **C, F** Percentage of nodes of Ranvier contacted by microglial cells in control (ctrl) vs 1-h treated slices from the same animal (**B–C**) TTX (500 nM, $n = 6$ animals), **E, F** Apamin (500 nM, $n = 10$ animals). Scale bars: **B, E** 10 μm . **C** Two-sided Paired t-test; **F** Two-sided Wilcoxon matched pairs test. * $P < 0.05$, ** $P < 0.01$, *** $P < 0.001$, **** $P < 0.0001$, ns not significant; bars and error bars represent the mean \pm s.e.m. For detailed statistics, see Supplementary Table.

$47.7 \pm 2.6\%$; TEA: $36.4 \pm 2.5\%$; Fig. 7G), and a significant 23% decrease following TPA treatment (ctrl: $37.5 \pm 2.7\%$; TPA: $28.9 \pm 1.7\%$; Fig. 7K).

To confirm these observations in vivo, we induced demyelination in mouse dorsal spinal cord by LPC focal injection and placed at 9 DPI a pump allowing the delivery of TPA (50 μM) or its carrier solution directly above the lesion (Fig. 8A). The animals were perfused 2 days later and the microglial cell phenotype (using IGF1 stainings) and the remyelination rate were assessed (Fig. 8B–E). We observed a significant 15% decrease of IGF1⁺ microglia (Fig. 8B, C) and a significant 2.6 fold increase of the non remyelinated area (Fig. 8D, E) within the lesions in TPA treated animals compared to controls.

These results are further supported by our observation that, in remyelinating mouse dorsal spinal cord lesion following LPC-induced focal demyelination, microglia contacting nodal structures have a more pro-regenerative phenotype, with a 31% increase of IGF1⁺ pro-regenerative cells and a 35% decrease of iNOS⁺ pro-inflammatory cells in node-contacting microglial population compared to non-contacting cells (Fig. S9K–M).

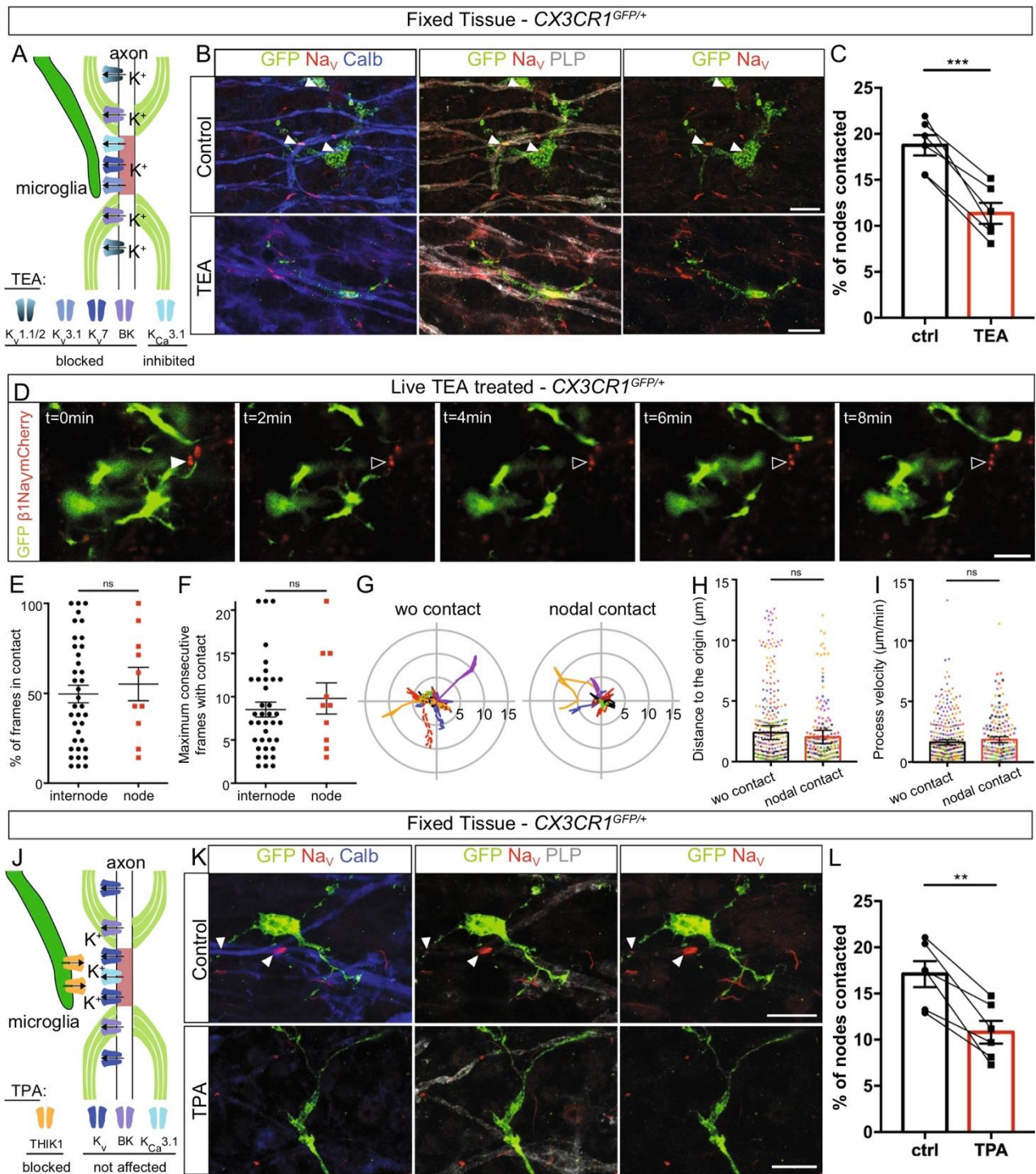
Taken together these data demonstrate that nodal K⁺ modulates the remyelination process, by promoting the pro-regenerative phenotype of microglia after myelin injury. This effect is associated and likely mediated by changes in microglia-node of Ranvier interaction.

Discussion

Here we show that microglia establish direct contacts at nodes of Ranvier both in mouse and human tissue. These microglial contacts co-exist on a given node with contacts from astrocytes and

OPCs processes, establishing the node as a privileged site for axons to interact with their glial environment. Using in vivo and ex vivo mouse models, we show that this interaction is stable in healthy tissue but also during remyelination, with an increased percentage of nodes contacted in this latter situation. In addition, we provide evidence that microglial process contacting nodes of Ranvier have reduced dynamics compared to processes moving freely or contacting internodal areas, reinforcing the hypothesis of a specific interaction rather than a random “surveilling” contact between microglia and nodes of Ranvier. This preferential interaction at the nodes of Ranvier depends on neuron activity and potassium ion release. When altering this interaction during remyelination by disrupting nodal K⁺ flux or blocking microglial K⁺ channels, microglial cells acquire a more pro-inflammatory phenotype, which associates with reduced remyelination (model Fig. 9).

Microglial contact at nodes is stable and depends on neuronal activity and physiological status of the tissue. We show that the nodes of Ranvier are specific sites for neuron-microglia interaction, this interaction likely corresponding to microglial sensing of neuronal activity, mediated through specific signaling. We first observed that the majority of microglial cells interact with nodes of Ranvier, regardless of the CNS area considered, with about a fifth to a fourth of the nodes contacted in healthy condition in spinal cord and cerebellar mouse tissue. The increased rate of contact in remyelinating condition could be linked to neuronal transient hyperactivity⁴³. Whether frequency of nodal contacts depends on the neuronal subtype or activity pattern is unknown.



Using live-imaging we were able to demonstrate for the first time the stability of these microglia-nodes contacts, strongly arguing for a specific interaction rather than a random survey of the local environment by microglial processes. Whether the reduced interaction stability in perilesional tissue relates to altered axonal physiology or increased local inflammatory signals remains uncertain.

When addressing the mechanisms supporting these microglia-nodes interactions, we demonstrate that neuronal electrical activity and nodal efflux of potassium are playing a key role, by showing that pharmacological inhibition of nodal and perinodal potassium channels leads to a 40% decrease of the contact, and

that blocking THIK-1, the main microglial potassium channel linked with K^+ homeostasis¹⁰ reproduces this effect. Various potassium channels have been suggested to be at play at the node, depending on the neuronal subtype considered, with $K_{Ca}3.1$ being present at nodes of Ranvier in Purkinje cells⁴⁴ and TRAAK and TREK channels recently described as playing a major role at PNS nodes, and in several CNS areas, such as the cortex, hippocampus and spinal cord^{45,46}. Thus, the microglia-node interaction may be modulated through axonal potassium efflux mediated by various players depending of the neuron considered, with the microglial THIK-1 channel allowing the read-out of this signal.

Fig. 6 Microglia preferential contact with nodes depends on potassium fluxes. **A** Experimental design. **B** In myelinated CX3CR1^{GFP/+} cerebellar organotypic slices, microglia (GFP, green) contacts with nodes (Nav, red) are reduced following potassium channel inhibition by tetraethylammonium (TEA). Arrowheads indicate the nodes of Ranvier contacted. **C** Percentage of nodes of Ranvier contacted in control condition or following 1-h TEA treatment (**B, C**, 30 mM, $n = 6$ animals); the mean values per animal are individually plotted. **D** Microglial cell (green) initially contacting a node (red) in a myelinated slice treated with TEA. Arrowheads show the initial contact position (filled: contact, empty: no contact). **E, F** Dynamics of microglial tips contacting an internode vs a node in myelinated slices treated with TEA (**D-F**, internode: $n = 37$ contacts from 12 animals, node: $n = 10$ contacts from 8 animals). **G** Trajectories (with t0 position as reference, distance in μm) of microglial process tips whether they were initially contacting a node (nodal contact) or not (wo contact) at t0 (wo contact: $n = 14$; nodal contact: $n = 7$; from 7 color coded movies from 6 animals). **H** Distance between the process tip and its position at t0 for each timepoint in myelinated slices treated with TEA (wo contact: 280 measures from 14 trajectories in 6 animals, nodal contact: 140 measures from 7 trajectories from 7 color coded movies in 6 animals). **I** Instantaneous process velocity in myelinated slices (wo initial contact: 280 measures from 14 trajectories in 7 animals, initial nodal contact: 140 measures from 7 trajectories in 7 color coded animals). **J** Schematic of the experimental design. **K** Microglia (GFP, green) contacts at nodes (Nav, red) are importantly reduced following THIK-1 inhibition by tetrapentylammonium (TPA). **L** Percentage of nodes of Ranvier contacted by microglial cells in control condition or following 1-h TPA treatment (**K, L**, 50 μM , $n = 6$ animals); the mean values per animal are individually plotted. Scale bars: (**B, D, K**) 10 μm . **C, L** Two-sided Paired t-test; **E, F** Two-sided Mann-Whitney test; **H, I** Type II Wald χ^2 test (two-sided analysis). * $P < 0.05$, ** $P < 0.01$, *** $P < 0.001$, **** $P < 0.0001$, ns not significant; bars and error bars represent the mean \pm s.e.m. For detailed statistics, see Supplementary Table.

Although some molecular mechanisms underlying microglia-node contact remain to be further deciphered, our results highlight a novel way of axo-glial interaction.

The node of Ranvier: a neuron-glia communication hub? It has previously been described that OPCs and perinodal astrocytes contact nodes of Ranvier³², and that these cells might interact at a given node⁴⁷. We now show that microglia can also form multipartite contacts with these other glial cell types, which suggests that nodes of Ranvier may act as a hub of intercellular communication in the CNS. This is further supported by our 3D reconstruction data showing that microglia establish a physical contact both with the nodal constituents and the other contacting glial cell.

This nodal “communication hub” could in particular participate in transmitting information on neuronal function and neuronal health to the glial environment and glia could in return modulate neuronal physiology. Oligodendroglial lineage cells have been shown to sense neuronal activity, which modulates their proliferation, differentiation and the myelination process^{41,48,49}. Furthermore, electrophysiological paired recordings show that OPCs adjacent to neurons can sense their discharge, and extracellular stimulation induces slow K^+ currents in OPCs, showing they could sense K^+ variations linked with activity⁵⁰. This suggests that both OPCs and microglia could have a read-out of neuronal activity at nodes through similar signaling pathways. Nodal protein clusters could further guide myelination initiation along some axons both in development and repair^{51,52}.

In addition to this node-OPC dialog, astrocyte-node interaction has been implicated in buffering K^+ at the node⁵³, but also recently in the regulation of axonal conduction velocity, by modulating nodal gap length and myelin thickness. This later effect relies on the secretion of Serpine2⁵⁴, a thrombin inhibitor also expressed by microglial cells in mice^{19,55}. This neuronal crosstalk with multiple glial cells at node could be of importance for network synchronization and adaptive plasticity in healthy condition, as well as adequate repair in disease⁴⁹.

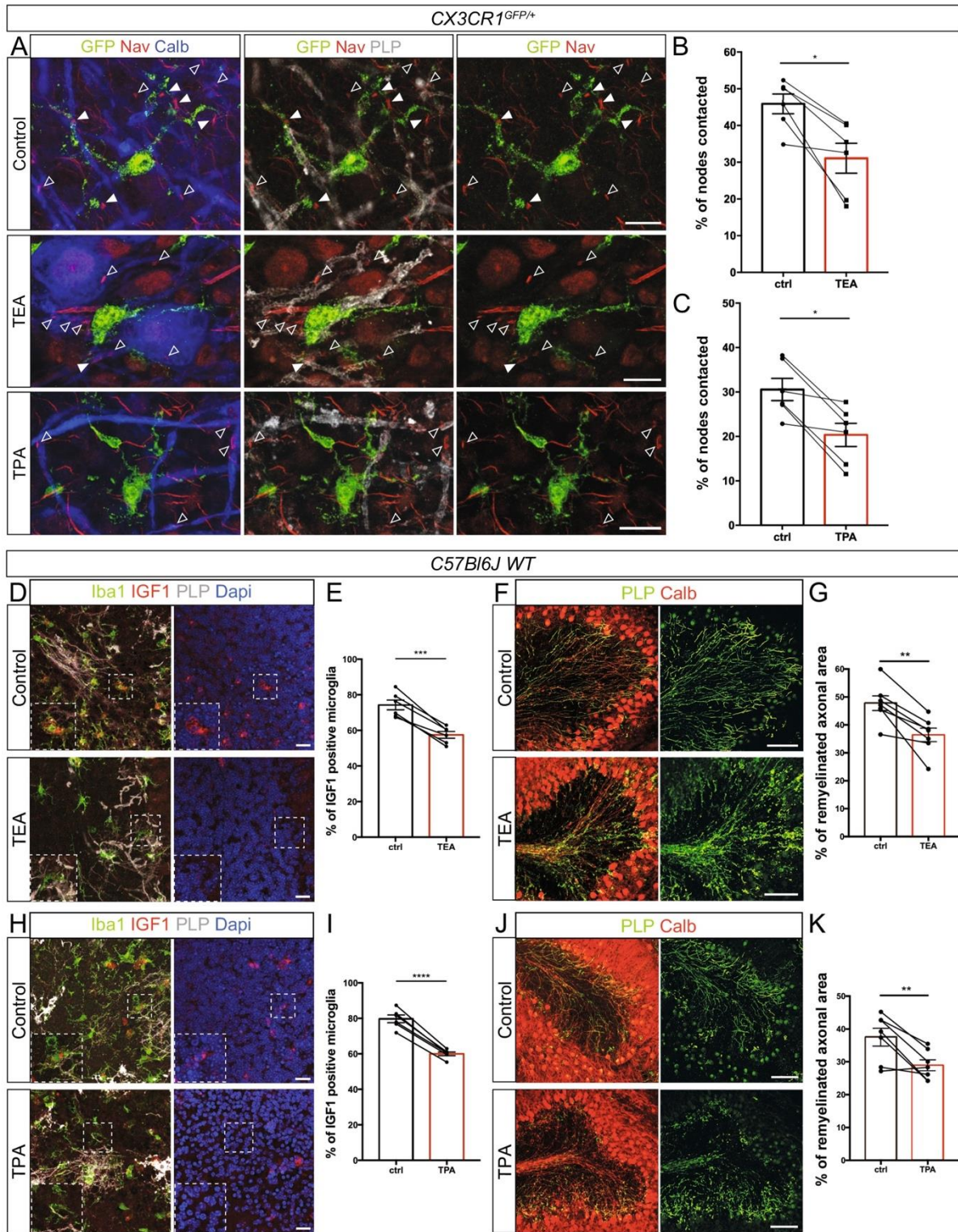
Microglia-node of Ranvier interaction in disease: damaging or protective? Activated microglia are known to have a dual role in disease, with a deleterious impact in case their pro-inflammatory phenotype is maintained inappropriately, and an active role in repair, in particular when they acquire a pro-regenerative phenotype^{14,21}. Activated microglia have been observed in normal appearing white matter (NAWM) in MS tissue and MS models, together with nodal area alteration^{56–58}. In addition,

some nodes of Ranvier are contacted by macrophages even prior demyelination and it has been hypothesized that they might be an early site of axonal damage⁵⁷. It appears however that the cells actively attacking nodal domains are rather monocyte derived macrophages than microglial cells⁵⁹. Our observation that microglial-node contact is destabilized in perilesional area at the peak of demyelination is compatible with this observation.

An increased microglia-node interaction might favor remyelination. In both our in vivo and ex vivo models, we report that microglia contact nodal structures, including heminodes and node-like clusters at the onset of remyelination. Strikingly, as observed in our ex vivo model, the microglial cell processes at nodes are less motile during ongoing remyelination compared to control myelinated tissue. This reinforced attraction/stability could be linked to increased potassium release at the sites where nodal structures reaggregate or to increased microglial sensitivity to this K^+ signal in a remyelinating condition. Regarding K^+ flux in remyelination, it is described that a transient neuronal hyperactivity can be observed in the first phasis of remyelination⁴⁴, suggesting K^+ efflux might be increased at that time. Furthermore, this pathway and other(s) could synergize, such as P2Y12R, which is known to potentiate THIK-1¹⁰.

Nodes of Ranvier disruption and reassembly following demyelination have a major impact on neuronal physiology. In addition, several lines of evidence have shown that neuronal activity affects the (re)myelination process^{41,60,61}. Early nodal reclustering along axons might lead to restored saltatory-like (or “microsaltatory”) axonal conduction³² and generate a local increase of K^+ efflux. This local modulation might trigger microglial behavior changes and participate in the regulation of microglial activation state by neuronal activity^{62,63}, including the pro-inflammatory to pro-repair switch observed concomitantly to the onset of remyelination^{14,64,65}. Intracellular K^+ decrease has been associated with microglial inflammasome expression^{10,66}. The axonal K^+ locally released at nodal structures when they reassemble could thus contribute to modulate microglial K^+ flux and subsequently limit inflammasome expression in the microglial cells with nodal contacts. Conversely, the restoration of stable microglial contacts at nodal structures could allow for microglia to buffer reassembled nodal area and modulate activity at nodes, as neurons may be transiently hyperexcitable at onset of remyelination^{43,67}.

To address the functional role of microglia-node interaction in repair, we took advantage of the modulation of the microglia-node interaction by potassium flux. We first inhibited potassium efflux at onset of remyelination and further targeted THIK-1, the



main channel implicated in microglial K^+ conductance¹⁰. Interestingly, THIK-1 channel is expressed in microglial cells in the CNS in healthy as well as MS tissues^{55,68}. These different pharmacological approaches affect the microglial switch towards a pro-regenerative profile, associated with decreased remyelination. This suggests that neuron dialog with microglia through K^+ signaling might influence myelin regeneration capacity.

Microglia contact at nodal structures could allow for a read-out of the neuron physiological status and orientate microglial

phenotype, which in turn could modulate neuronal survival and remyelination. This reciprocal interaction might be of importance in different pathological contexts in the CNS.

Recent data suggest that the impact of neuronal activity on OPCs recruited at the lesion follows a two-step mechanism, with consecutive time windows, first facilitating proliferation of OPCs, then promoting OLs differentiation and myelination^{43,60,61,69}. This parallels the biphasic activation of microglial cells following demyelination, with a switch from the pro-inflammatory to the

Fig. 7 Altered K^+ fluxes following demyelination leads to a reduced number of pro-regenerative microglia and impairs remyelination ex vivo. **A** In remyelinating CX3CR1^{GFP/+} cerebellar organotypic slices, microglial (GFP, green) contacts with nodes (Na_v, red) are importantly reduced following potassium channels inhibition by TEA and TPA treatments. Arrowheads show the nodal structures (filled: contacted by microglia; empty: not contacted). **B, C** Percentage of nodal structures contacted by microglial cells in control remyelinating condition or following 1-h TEA (**A, B**, 30 mM, $n = 6$ animals) or TPA treatment (**A, C**, 50 μ M, $n = 6$ animals); the mean values per animal are shown as dots. **D–H** In remyelinating C57bl6/J cerebellar organotypic slices, the number of microglial cells expressing IGF1 is decreased following potassium channel inhibition by TEA (**D**) or THIK-1 inhibition by TPA treatment (**H**). **E–I** Percentage of IGF1⁺ microglial cells at remyelination onset, with no treatment (ctrl) or with TEA (**D, E**, 2 h, 30 mM, $n = 6$ animals) or TPA treatment (**H, I**, 2 h, 50 μ M, $p = 2.195 \times 10^{-5}$, $n = 6$ animals), the mean values per animal are shown as dots and paired with the corresponding control. **F, J** In remyelinating C57bl6/J cerebellar organotypic slices, remyelination is reduced following TEA (**F**) or TPA (**J**) treatment. **G, K** Percentage of axonal area remyelinated in LPC-demyelinated slices without (ctrl) or with TEA (**F, G**, 2 h, 30 mM, $n = 7$ animals) or TPA treatment (**J, K**, 2 h, 50 μ M, $n = 7$ animals). Scale bars: **A** 10 μ m; **D, H** 20 μ m; **F, J** 100 μ m. **B, C, E, G, I, K** Two-sided Paired t-test. * $P < 0.05$, ** $P < 0.01$, *** $P < 0.001$, **** $P < 0.0001$, ns not significant; bars and error bars represent the mean \pm s.e.m. For detailed statistics, see Supplementary Table.

pro-regenerative state, with recently published data suggesting that both stages are required for optimal repair^{14,16,65}. Our results show that the recovery of a stable microglia-node interaction at onset of remyelination could influence the microglial phenotypic switch and contribute to accumulation of pro-regenerative microglia. Neuronal activity could then play a role in remyelination both through direct OL lineage regulation and indirectly through modulating microglial phenotypic orientation.

The preferential interaction of the main glial cell types at nodes of Ranvier forming a “neuro-glial communication hub” may thus contribute to efficient repair orchestration.

Methods

Animal care and use. The care and use of mice conformed to institutional policies and guidelines (UPMC, INSERM, French and European Community Council Directive 86/609/EEC). The following mouse strains were used: C57bl6/J (Janvier Labs), CX3CR1-GFP (gift from Prof S. Jung, Weizmann Institute of Science, Israel⁷⁰) and Thy1-Nfasc186mCherry (gift from Prof P.J. Brophy, University of Edinburgh, UK).

Focal demyelination of mouse spinal cord. Following intraperitoneal injection of Ketamin/Xylazine in NaCl 9‰ (respectively 110/25 mg/kg, Centravet), a small incision was made between thoracic and lumbar vertebrae to access the spine and inject with a glass capillary 1 μ l of lysophosphatidylcholine diluted into NaCl 9‰ (LPC, 10 mg/ml; Sigma-Aldrich) or NaCl 9‰ for the sham condition. Following surgery, mice were stitched and placed into warming chambers (Vet tech solution LTD, HE011). At either 7-day post-injection (7 DPI peak of demyelination) or 10–11 DPI (early remyelination phase), the mice were euthanized with Euthasol (Centravet) and transcardially perfused with 2% PFA (Electron Microscopy Services).

Osmotic pump surgery. The surgery to place the micro-osmotic pump (Alzet, 1003D) above the demyelinating spinal cord lesion was made 9 days post LPC injection. The day before surgery, the pumps were pre-filled with NaCl 9‰ (Ctrl) or TPA diluted in NaCl 9‰ (TPA, 50 μ M). The pumps were subsequently connected to a cannula with three depth-adjustment spacers (Alzet, brain infusion kit III) and incubated overnight at 37 °C in sterile saline solution. Prior to surgery, the mice received an intraperitoneal injection of Ketamin/Xylazine in NaCl 9‰ (respectively 110/25 mg/kg, Centravet) and a small incision was made in the skin above the site of LPC injection. The pre-filled pump connected to the cannula was inserted subcutaneously and the spinal cord meninges were carefully removed above the lesion. The extremity of the cannula connected to the pump was placed above the lesion without touching the surface of the spinal cord and fixed with glue. The skin incision was stitched and the animals were monitored closely 24 h post-surgery. After 2 days, the animals were intracardially perfused with 4% PFA and the spinal cord was collected through a ventral laminectomy. The tissue was then processed as described in the Tissue Preparation section.

Spinal glass window surgery. Surgery protocol was adapted from Fenrich et al.³⁴. Briefly, following an intraperitoneal injection of Ketamin/Xylazine as described above, the dorsal skin and muscles were incised, and the spine immobilized with two spinal forks placed at T12 and L2 vertebrae, with Tronothane 1% (Lisa-Pharm) applied at the point of junction with the forks. Two staples were then fixed along the transverse processes of the vertebrae as a support for a reshaped paperclip, stabilized with glue (Cyanolite) and dental cement (Unifast Trad 250 mg/250 mg, GC Dental Products Corp). A dorsal laminectomy was performed using a high-speed drill with a carbide bur. Spinal cord was then hydrated with a solution PBS/penicillin-streptomycin/Naquadem (Dexaméthasone 0.05%, Intervet) and LPC (or

NaCl) was injected as described above. A glass window cut from a glass coverslip (Menzel-Glaser, 0.13–0.16 mm) was cleaned, dried and placed above silicon (Kwik-Sil, World Precision Instruments) directly applied on the spinal cord. The window was fixed with glue and dental cement. Finally, the animal received a subcutaneous injection of Buprenorphine (0.1 mg/kg, Centravet) and was placed in a warming chamber.

Cerebellum organotypic slice culture. Ex vivo culture protocol was adapted from^{36,37}. Briefly, P8 to P10 mouse cerebella were dissected in ice cold Gey’s balanced salt solution complemented with 4.5 mg/ml D-Glucose and penicillin-streptomycin (100 IU/mL, Thermo Fisher Scientific). They were cut into 250 μ m parasagittal slices using a McIlwain tissue chopper and the slices placed on Millicell membrane (3–4 slices per membrane, 2 membranes per animal, 0.4 μ m Millicell, Merck Millipore) in 50% BME (Thermo Fisher Scientific), 25% Earle’s Balanced Salt Solution (Sigma), 25% heat-inactivated horse serum (Thermo Fisher Scientific), supplemented with GlutaMax (2 mM, Thermo Fisher Scientific), penicillin-streptomycin (100 IU/mL, Thermo Fisher Scientific), and D-Glucose (4.5 mg/ml; Sigma). Cultures were maintained at 37 °C under 5% CO₂ and medium changed every two to three days. Experiments were analyzed at 4 days in vitro (DIV) for myelinating condition and at 10 to 11 DIV for myelinated control and remyelinating conditions.

Lentiviral transduction of cerebellar slices. For live-imaging ex vivo, nodes of Ranvier were detected using β 1Na_vmCherry expressed under the control of the Synapsin promoter. Briefly, the pEntr- β 1Na_vmCherry plasmid was recombined with the pDestSynAS (generated by Philippe Ravassard, ICM), using the Gateway LR clonase kit from Thermo Fisher Scientific³⁷; detailed description on demand) and the corresponding lentivirus produced by the ICM vectorology platform. Transduction was performed immediately following slice generation by addition of the lentiviral solution directly onto the slices placed on Millicell membranes (1 μ l/slice at a final concentration of $\approx 10^9$ VP/ μ l).

Ex vivo treatments. As culture systems may lead to increased variability between animals, we always cultured the slices from a given animal on two membranes. One of these membrane was treated, while the second one was kept untreated. This allowed us to minimize the potential variability and to do paired experiments.

To induce demyelination, for each animal, the slices on one membrane were incubated overnight at 6 DIV in 0.5 mg/ml LPC added to fresh culture medium, while the other membrane was kept as control.

To study microglia-node interaction in myelinated tissue, for each animal, the myelinated slices (10–11 DIV) on one membrane were left untreated (control), while the ones on the other membrane were treated with tetrodotoxin (TTX, 1 h, 500 nM, Tocris) or apamin (1 h, 500 nM, Sigma-Aldrich), to inhibit or activate neuronal activity respectively. Similarly, PSB0739 (3 h, 1 μ M, Tocris) or MRS2211 (3 h, 50 μ M, Tocris) were used to inhibit the microglial purinergic receptors P2Y₁₂R and P2Y₁₂R/P2Y₁₃R respectively. Tetraethylammonium (TEA, 1 h, 30 mM, Sigma) was used to neuronal inhibit potassium channels and tetrapentylammonium (TPA, 1 h, 50 μ M, Sigma) to inhibit the microglial THIK-1 channel. To study microglia-node interaction in remyelination, for each animal, the two membranes were demyelinated using LPC, and one of the demyelinated membranes was treated at 10–11 DIV with TEA (1 h, 30 mM) or TPA (1 h, 50 μ M), while the other membrane was kept untreated as control.

To evaluate the functional impact of the perturbation of microglia-node interaction, demyelinated slices were treated at the very onset of remyelination (9.5 DIV) with 30 mM TEA or 50 μ M TPA for 2 h and fixed 2 h or 15 h post-treatment (together with untreated demyelinated slices as control), to evaluate microglial phenotype and remyelination rate, respectively.

Electrophysiology. Myelinated cultured slices (10–13 DIV) were transferred to a recording chamber and continuously superfused with oxygenated (95% O₂ and 5% CO₂) aCSF containing (in mM): 124 NaCl, 3 KCl, 1.25 NaH₂PO₄, 26 NaHCO₃, 1.3

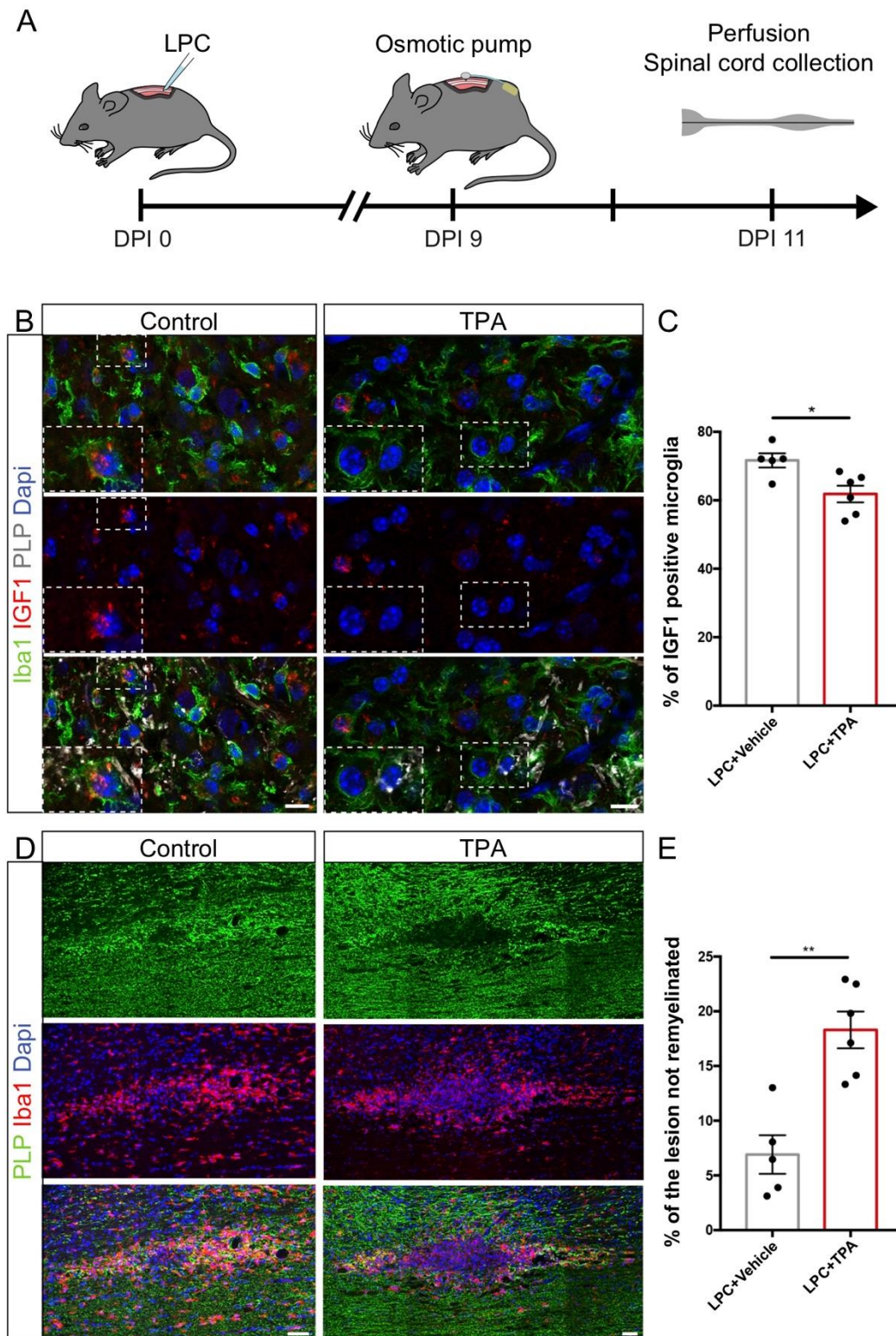


Fig. 8 Altered K^+ flux read-out by microglia following demyelination leads to a reduced number of pro-regenerative microglia and impairs remyelination *in vivo*. **A** Osmotic pumps were placed 9 days post LPC-injection to deliver NaCl 9‰ (Ctrl) or 50 μ M TPA at the lesion site and the spinal cords were collected 2 days later. **B** In remyelinating dorsal spinal cord lesion, the number of microglial cells expressing IGF1 is decreased following TPA treatment. **C** Percentage of IGF1⁺ microglial cells at 11 DPI in the remyelinating lesion, in control (Ctrl) or TPA condition (**B–C**, Ctrl: $n = 5$ animals, TPA: $n = 6$ animals). **D** Remyelination is reduced following TPA delivery at the lesion. **E** Percentage of the lesion devoid of myelin at 11 DPI, in control or TPA condition (**D–E**, Ctrl: $n = 5$ animals, TPA: $n = 6$ animals). Scale bars: **B** 10 μ m, **D** 50 μ m. **C**, **E** Two-sided Mann-Whitney tests. * $P < 0.05$, ** $P < 0.01$, *** $P < 0.001$, **** $P < 0.0001$, ns not significant. Bars and error bars represent the mean \pm s.e.m. For detailed statistics, see Supplementary Table.

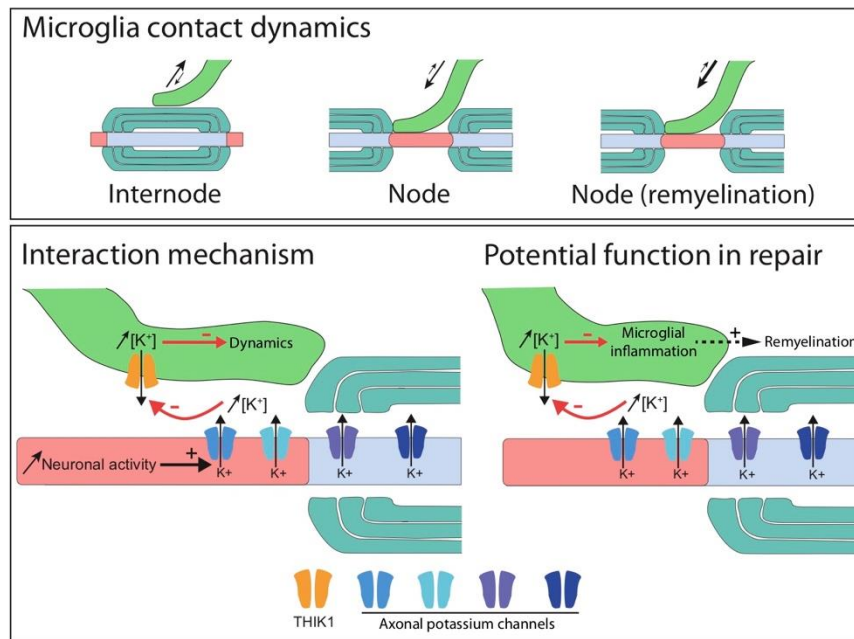


Fig. 9 Model for microglial interaction at nodes of Ranvier. Microglial contact with nodes of Ranvier depends on the tissular context. The interaction is in particular reduced in perilesional area at the peak of demyelination, and increased in remyelination compared to healthy myelinated tissue. Neuronal activity and nodal K^+ efflux promote the interaction, with microglial read-out depending on THIK-1. Altering K^+ efflux or THIK-1 activity in remyelination correlates with more pro-inflammatory microglia and decreased remyelination.

$MgSO_4$, 2.5 $CaCl_2$, and 15 glucose (pH 7.4). Purkinje cells were visualized under differential interference contrast optics using a 63X N.A 1 water immersion objective. Loose patch voltage clamp recordings of the spontaneous firing activity was performed at 32–34 °C with a borosilicate glass pipette filled with aCSF. Signals were amplified with a Multiclamp 700B amplifier (Molecular devices), sampled and filtered at 10 kHz with a Digidata 1550B (Molecular Devices). Data were acquired with the pClamp software (Molecular devices). To avoid any alteration of the spontaneous firing frequency of the cell by the patch procedure⁷¹, the holding membrane potential was set to the value at which zero current is injected by the amplifier. The resistance of the seal (R_{seal}) was controlled and calculated every minute from the current response to a voltage step (50 ms; -10 mV). Only recordings with a R_{seal} in the range of 10 to 200 M Ω and stable during the all recording procedure were included in the analysis. Spontaneous activity was tested in control condition and consecutively in the presence of apamin and TTX applied by bath perfusion. The firing rate was analyzed over a two minutes recording time window using a threshold crossing spike detection in Clampfit (Molecular devices) and calculated as the number of action potential current divided by the duration of the recording. The instantaneous frequency was reported since apamin treatment triggered clear bursts of the cells and calculated as the inverse of the interspike interval.

Tissue preparation

Ex vivo cerebellar slices. Cultured slices were fixed while attached to the membrane with either 4% or 1% PFA for 30 min at room temperature (RT) and washed with PBS.

In vivo mouse brain and spinal cord. For spinal cord preparation, the tissue was dissected following perfusion and post-fixed in PFA 2% for 30 min, washed in PBS and incubated in PBS, 15% sucrose for 3 days at 4 °C. Spinal cords were then embedded in OCT (Tissue-Tek, Sakura) or PBS, 15% Sucrose, 4% gelatin, and frozen in isopropanol onto carbonic ice.

For adult as well as P12 myelinating mouse brain tissue, animals were perfused with PFA 2% and the brain was dissected and post-fixed in PFA 2% for 30 min, washed in PBS, and incubated in PBS with successively 7, 15, and 30% sucrose for 3 days at 4 °C for cryoprotection. The tissues were then embedded in O.C.T (Tissue-Tek, Sakura).

Mouse spinal cords and brains were cut longitudinally and sagittally respectively. Human tissues were obtained after informed consent (healthy donors, UK MS Society Tissue Bank at Imperial College, London, under ethical approval by the National Research Ethics Committee 08/MRE09/31) as snap frozen blocks. Sections were cut using a cryostat Leica CM 1950 (30 and 15 μ m thick for mouse and human respectively), collected on Superfrost+ slides and stored at -80 °C until used.

Electron microscopy. Mice were transcardially perfused with PB 0.2 M, 4% PFA, and 0.5% glutaraldehyde (Electron Microscopy Services). Following 30 min post-fixation, the cerebellum was embedded in PB (0.2 M), 4% agarose (Sigma). Sagittal sections (50 μ m thick) were generated using a VT1200S vibratome (Leica). The sections were then incubated in Ethanol 50% for 30 min, washed in PBS, and incubated with anti-Iba1 antibody (1:1000; Wako), in PBS, 3% NGS, 0.05% Triton-X, for 48 h on a rotating apparatus at room temperature (RT). The tissue was then washed in PBS and incubated for 1 h in biotinylated anti-rabbit IgG (1:200; Vector Labs, Burlingame, CA, USA), rotating at RT, further washed in PBS and incubated for 1 h in ABC (Vector Labs) solution, under rotation at RT. Following incubation, sections were washed 20 min with PBS and developed by incubating in 0.025% diaminobenzidine (DAB) and 0.002% hydrogen peroxide, in PBS. Sections were then processed for electron microscopy. Briefly, sections were post-fixed in 1% osmium tetroxide for 60 min, and dehydrated by ethanol and acetone immersion. A flat-embedding procedure was used, after which a semi-thin section was cut to find the area of interest and then ultrathin (60–80 nm) sections were cut with an ultramicrotome (Leica EM UC7, Wetzlar, Germany). The sections were stained with uranyl acetate and lead citrate to enhance contrast. Sections were examined with a Jeol Flash 1400 transmission electron microscope. Images of Iba1 immunolabeled microglial cells were captured with a Radius Morada digital camera. Once acquired, the brightness and contrast of the images were adjusted and structures of interest were highlighted using Photoshop software (Adobe, version CC).

Antibodies. Primary antibodies: mouse IgG2a anti-AnkyrinG (clone N106/36; 1:100), mouse IgG2b anti-AnkyrinG (clone N106/65; 1:75), and mouse IgG1 anti-Caspr (1:100), all from Neuromab; mouse IgG1 anti-Pan Na_v (clone K58/35; 1:150; Sigma); mouse anti-Calbindin (1:500; Sigma), rabbit anti-Calbindin (1:300; Swant), rabbit anti-Caspr (1:300; Abcam), rat anti-PLP (1:10; kindly provided by Dr. K. Ikenaka, Okasaki, Japan), mouse IgG2b anti-MBP (1:200; SMI99, Sigma), rabbit IgG anti-Iba1 (1:500; Wako), chicken anti-GFAP (1:500; Aves Labs), rat anti-PDGFR α (1:100; BD Biosciences), rabbit IgG anti-TMEM119 (1:100; Sigma), rabbit IgG anti-P2Y12r (1:300; Alomone, human tissue), rabbit anti-P2Y12R (1:300; Anaspec, mouse tissue), chicken anti-GFP (1:250; Millipore), mouse IgG2a anti-iNOS (1:100; BD Biosciences), goat anti-IGF1 (1:50; R&D System), and chicken anti-mCherry (1:1000; Abcam). Secondary antibodies corresponded to goat or donkey anti-chicken, goat, mouse IgG2a, IgG2b, IgG1, rabbit and rat coupled to Alexa Fluor 488, 594, 647, or 405 from Invitrogen (1:500), or goat anti-mouse IgG1 DyLight from Jackson Immuno Research (1:600).

Immunohistostainings

Immunofluorescent stainings. Human sections were first fixed in paraformaldehyde (PFA) 4% for 5 min. For myelin protein staining, tissues were pre-incubated in absolute ethanol at -20 °C for 20 min. Tissues were blocked in PBS, 5–10%

Normal Goat Serum (50-062Z; Thermo Fisher Scientific), 0.2–0.4% Triton X-100 (Sigma), then incubated with primary antibodies in blocking solution overnight at room temperature, washed in PBS, and incubated with secondary antibodies for 1–3 h at RT in the dark. When applicable, tissues were immersed for 30 s in Hoechst solution (10 µg/ml, Euromedex). They were finally mounted under coverslip (VWR) with Fluoromount (Southern Biotech).

Chromogenic immunohistochemistry on post-mortem brain tissues. Snap frozen tissue blocks were rehydrated with PBS. Sections were then subjected to paraformaldehyde 4% for 10 min before elimination of endogenous peroxidase activity with 0.1% H₂O₂ (Sigma Aldrich) in PBS for 20 min. Blocking was performed using 5% normal sera before incubation with primary antibodies diluted in PBS containing 0.05% Triton 100-X and 5% sera. Binding of biotinylated secondary antibodies (Vector Laboratories) was visualized with the avidin-biotin horseradish peroxidase complex (Dako, Biotin Blocking System) followed by 3,3'-diaminobenzidine (DAB) (Vector Laboratories) as substrate. Primary antibody 2 was detected using the ABC-alkaline phosphatase detection system (Vector Laboratories), using Vector Blue as the substrate. Images were captured with a QICAM digital camera (QImaging Inc.).

RNAscope mRNA detection. RNAscope was performed on myelinated and remyelinating CX3CR1^{GFP/+} organotypic slices according to the supplier instructions, using RNAscope multiplex fluorescent detection reagents v2 kit (ACD, 323110), H₂O₂ and protease reagents (ACD, 322381) and kcnk13 (THIK-1), negative and positive control probes (respectively ACD, 535411, 320871, and 320881). Myelinated cultured slices (10 DIV) were fixed with 4% PFA for 30 min and washed with PBS. They were then treated 10 min with H₂O₂, transferred in target retrieval reagent for 10 min at 95 °C, followed by a 3 min treatment in ethanol. Slices were dried and treated with Protease III for 30 min, before being incubated with probes for 6 h at 40 °C. Amplification steps were subsequently performed at 40 °C using amplification solutions alternating with washes as follow: Amp1 for 30 min, Amp2 for 30 min and Amp3 for 15 min. The signal was then revealed using RNAscope multiplex FL v2 HRP-C1 signal for 15 min at 40 °C, followed by 30 min at 40 °C with a solution of Opal 650 (PerkinElmer, FP1496001KT, 1:1000) diluted in RNAscope multiplex TSA Buffer (ACD, 322809), and finally the reaction was stopped using RNAscope multiplex FL v2 blocker for 15 min at 40 °C. Immunofluorescence staining was then performed as described before to detect microglia and Purkinje cells using respectively anti-Iba1 (1:500; Wako) and anti-Calbindin (1:300; Swant) antibodies.

Imaging

Confocal microscopy for ex vivo cultured slices. Confocal microscopy was performed using an FV-1200 Upright Confocal Microscope and a Leica inverted SP8 with ×63 oil immersion objectives with 1.40 numerical aperture, using respectively metamorph and LasX software. For each acquisition, stacks of 1024 × 1024 pixel images (160.61 µm × 160.61 µm), including at least 10 Z-series with a z-step of 0.30 µm, were acquired using 405, 488, 552, and 638 laser lines or a white laser with optimized wavelengths at the peak of excitation for each fluorophore.

Confocal microscopy for in vivo tissue. Confocal microscopy was performed using an inverted Leica SP8 with ×40 or ×63 oil immersion objectives with 1.30 and 1.40 numerical aperture respectively, using LasX software. For quantification, 1024 × 1024 pixel images were acquired using a ×40 oil objective with a numerical zoom of 2, corresponding to a 0.0211 mm² final area, and 10 sections were acquired with a step of 0.30 µm. For 3D reconstruction, images were acquired using the 63x oil immersion objective, and a z-step of 0.20 µm. Deconvolution was carried out using Huygens software (v.17.10). Following deconvolution, the surface of each structure was reconstructed in 3D using Imaris software (GraphPad, Bitplane, v.9.2). Figures were made using Photoshop (Adobe, version CC).

Live-imaging

Live-imaging study ex vivo. Prior to imaging, the slices were mounted onto 35 mm glass-bottom dishes (Ibidi, BioValley) and incubated with a phenol-red free medium consisting of: 75% DMEM, 20% 1X HBSS, supplemented with HCO₃⁻ (0.075 g/L final), HEPES Buffer (10 mM final), GlutaMax (2 mM final), penicillin-streptomycin (100 IU/mL each), 5% heat-inactivated horse serum, all from Thermo Fischer Scientific, and D-Glucose (4.5 g/L final; Sigma). Imaging was performed using a Yokogawa CSU-X1 M Spinning Disk, on an inverted Leica DMi8 microscope, with a X40 NA 1.30 oil immersion objective, using the 488 nm and 561 nm laser lines and a Hamamatsu Flash 4 LT camera. Images were acquired at 37 °C in a temperature-controlled chamber under 5% CO₂ using Metamorph software (Molecular Devices), for periods of 10 min with a confocal Z-series stack of 10 µm (921 × 1024 pixels, 177.8 × 197.7 µm) acquired for both GFP and mCherry every 30 s, using a Z-interval of 0.5 µm between optical slices. The faint mCherry signal along Purkinje cells axons allowed to follow them during live acquisition (see Fig. S4Dii). Nodal structures were detected as the non-moving β1Nav-mCherry clusters along these axons.

Longitudinal live-imaging study in vivo. At 7 DPI (peak of demyelination) or 11 DPI (early phase of remyelination), the mice were anesthetized as described before and anesthesia was maintained by reinjection of Ketamin/Xylazin (respectively 11/2.5 mg/kg) when needed along the experiment. Imaging was performed in a heated chamber at 34 °C using an upright 2-photon microscope Zeiss 710 NLO with a X20 water objective (NA 1,0) and a Coherent Vision II laser. Z-series stack (1024 × 1024 pixels, 170 × 170 µm) were acquired with a Z-interval of 0.78 µm at an excitation wavelength of 940 nm every 10 or 30 min (15 to 20 images per stack). Focal lesions were identified by the visualization of microglial activation and acquisitions were made at lesion direct vicinity (<250 µm) at 7 DPI and in the remyelinating area at 11 DPI (nodal structures were selected within the lesion border). We selected nodes initially contacted by microglia for acquisitions and performed 1 h movies (one stack every 10 min) and 3-h movies (one stack every 30 min). Following imaging, the mice at 7 DPI were placed in a warming chamber until awoken and re-imaged at 11 DPI. Post-acquisition image processing was carried out using ImageJ (NIH, Bethesda, Maryland), Zen (Zeiss, 2010). Briefly, images were realigned using StackReg in ImageJ (<http://bigwww.epfl.ch/thevenaz/stackreg/>). Filter Median (3,0 X and Y) was used in Zen and Subtract Background (100 pixels in green) in ImageJ.

Analysis

Quantification of microglia-node contacts. For the ex vivo fixed slices, using ImageJ software, the brightness and contrast of the images were adjusted and the total number of nodal structures, as well as the number of nodal structures contacted by microglial cells were quantified per field using the middle plan of each Z-series, the rest of the serie being used to confirm the nature of the contacted structure, and exclude potential granule cell axon initial segment. A contact was defined by at least one positive pixel for the microglial marker juxtaposed to at least one pixel positive for the nodal marker. Three to five images were analyzed per animal with at least four animals per condition and the mean percentage of contacted nodes per condition was calculated by doing the mean of the mean percentage of contact per animal.

For the in vivo fixed tissue study, imageJ software was used to adjust the brightness and contrast of the images and to quantify the total number of nodal structures and the number of structures contacted per field using the middle plan of each Z-series, the rest of the serie being used to confirm the nature or the contacted structure. A contact was defined by at least one positive pixel for the microglial marker juxtaposed to at least one pixel positive for the nodal marker. Three to five images were analyzed per animal with four animals per condition and the mean percentage of contact per condition was calculated by doing the mean of the mean percentage of contact per animal. For the study of IGF-1 and iNOS expression in “non contacting” and “contacting” microglial cells during remyelination, we used ImageJ software to detect IBA1 + microglial cells entirely located within the stack. Each cell was then sorted as “contacting” or “non contacting” nodes and as iNOS +/- or IGF1 +/- expressing cells.

Quantification of microglial phenotype and remyelination. To analyze the effect of TEA and TPA treatments on remyelination ex vivo, five images of an entire folium were acquired per condition for each animal (1900 × 1900 pixels, ~550 × 550 µm). The myelination index was calculated semi-automatically using a custom written script on ImageJ, from Baudouin et al.⁷². Briefly, a region of interest including Purkinje cells axon (excluding soma and white matter tracks) was first selected. A mask for axonal area (Calbindin signal) and a mask for myelinated axonal area (PLP signal overlapping with Calbindin signal) were then generated, and the myelination index was calculated from the quotient of the area of the two respective masks (myelin/axon). Myelination indexes of the five images were averaged to give the mean myelination index per animal for each condition. The microglial phenotype was further analyzed by calculating the amount of Iba1⁺ cells expressing IGF-1 (pro-regenerative microglia) or iNOS (pro-inflammatory microglia) on the total number of Iba1⁺ cells (using five images per condition for each animal, 1024 × 1024 pixels, 290.9 × 290.9 µm). For each experiment, at least six animals were analyzed, with paired control and treated slices from each animal.

For the in vivo study following LPC-induced demyelination, microglial expression of IGF1 was analyzed by calculating the amount of Iba1⁺ IGF1⁺ cells on the total number of Iba1⁺ cells (using three images for each animal taken at the border of the remyelinating area, 1024 × 1024 pixels, 145.5 × 145.5 µm). To assess the percentage of the lesion not remyelinated, a mosaic image of the whole lesion was acquired with X20 oil objective (NA 0.75) for each animal on the section on which the lesion was the largest (enrichment in Iba1 positive cells). Tiles were stitched using LasX software and analysis performed on ImageJ software. The total area of the lesion (Activated microglia, Iba1 + signal, with high DAPI density) and the area without myelin signal (PLP) were measured. The percentage of the lesion not remyelinated was calculated by dividing the area without myelin signal by the total area of the lesion for each animal.

Time-lapse imaging analysis. For ex vivo time-lapse acquisitions, the field of interest was defined by selecting a node (i-e β1Nav_m-mCherry cluster along an axon) or an internodal area initially contacted by the tip of a microglial process. ImageJ software was used to adjust the brightness and contrast of the images of each movie and ImageJ stabilizer Plugins was used to realign the different timeframes using the nodes as stationary reference (red channel) and subsequently applying the same

corrections to the green channel (microglia, moving). For each timepoint, the contact was defined by at least one positive pixel for the microglial marker juxtaposed to at least one pixel positive for the nodal marker. The percentage of frames with contact and the maximum number of consecutive frames with and without contact were then calculated.

To analyze the dynamics of microglial process tips initially contacting a node or not, the images were first realigned automatically and the exact coordinates of the node (or original location of tips without contacts) were measured. For each movie, the microglial process tip contacting the node and of two non-contacting microglial process tips chosen randomly were tracked manually to get their coordinates at each timepoint. For each time point, the t0 coordinates were subtracted from the coordinates of the microglial process tips to get the coordinates relative to their initial position (fixed). Lastly, for each microglial tip independently, the position at t0 was set in Cartesian coordinates at (0, 0). Representation of the trajectories in Rose plots were generated using R and the distance between two successive timepoints t_n and t_{n+1} in the Cartesian coordinates were calculated using the following formula:

$$t_{n+1}t_n = \sqrt{(x_{n+1} - x_n)^2 + (y_{n+1} - y_n)^2} \quad (1)$$

For the in vivo live-imaging study of the microglia-node contact in dorsal spinal cord, image fields were chosen where we had initially a clear contact between at least one node and one microglial cell. In case of multiple initial contacts between node(s) and microglia on the first timeframe, each microglia-node pair was considered independently. ImageJ software was used to adjust the brightness and contrast of the images for each movie. The Z-series were then used to assess whether the nodal structure(s) were contacted by the microglial cell(s) or not. A contact was defined when at least one pixel positive for a microglial signal was juxtaposed to at least one pixel positive for the nodal signal. Whether the contact was maintained or lost for each microglia-node pair was assessed along each movie and the percentages of timeframes with contact per movie, as well as the longest sequence of consecutive timepoints with contact, were calculated for each microglia-node pair.

Microglial surveillance and ramification analysis. Movies were acquired as described above. Computation of microglia surveillance index and ramifications index were performed using custom written Matlab script from Madry et al., available at <https://github.com/AttwellLab/Microglia>. Briefly, movies were registered in ImageJ and realigned using the stabilizer plugin and “subtract Background” was applied with a ball size of 30 pixels. Each image within stacks was then filtered using a 3 pixels median filter. A maximum intensity orthogonal projection was made and individual cells of interest were selected by drawing a region of interest that included all process extensions along the full movie. Each cell was then manually binarized and registered as an independent file.

The index of ramification R was calculated as the ratio of the perimeter to the area normalized by the similar ratio calculated for a circle of this area and subsequently normalized with control conditions:

$$R = \left(\frac{\text{perimeter}}{\text{area}} \right) / \left(2 \times \sqrt{\pi/\text{area}} \right) \quad (2)$$

To quantify the surveillance index, for each movie, the frame $n-1$ was subtracted to the frame n and two binarized movies were generated. The first one containing only the pixels explored by process extension (PE) and the second the pixels associated to process retraction (PR), the unchanged pixels being set at 0. The surveillance index S was then calculated as indicated below and subsequently normalized with control conditions:

$$S = \sum_{\text{pixels}} \text{PE} + \text{PR} \quad (3)$$

Statistical analysis. All statistical analysis and data visualization were performed using Prism (GraphPad, version 7) and R (R Foundation for Statistical Computing, Vienna, Austria, 2005, <http://www.r-project.org>, version 3.5.2).

For all the experiments, the group size and statistical tests applied are indicated in the text or in the figure legends. Detailed information is further available in the statistical analysis table (supplementary data). Graphs and data are reported as the mean \pm SEM. The level of statistical significance was set at $p < 0.05$ for all tests. Asterisk denote statistical significance as follow: * $p < 0.05$, ** $p < 0.01$, *** $p < 0.001$, **** $p < 0.0001$, ns. indicates no significance.

For the fixed ex vivo cultured slices, the treated and untreated groups were compared using two-sided paired test. Parametric tests (paired Student's t tests) were used when a sample size $n \geq 6$ and the distributions passed the normality test (Shapiro–Wilk test). Otherwise, non-parametric tests were applied (Wilcoxon matched pairs tests).

For ex vivo live-imaging, when measuring the percentage of frames in contact and the maximum consecutive frames with or without contact, two-sided Mann–Whitney tests were used.

The study of the dynamics of process tips contacting a nodal structure or without contact, involved repeated measure design. The statistical analysis was thus performed with linear mixed models using lmer function from lme4 package (R software). Significance of the main effect was evaluated with the Anova function using Type II Wald χ^2 tests. When necessary, to better match the model

assumptions (normality and constant variance of residuals), the data were square root transformed prior to modeling. For data representation, the estimated marginal means and model based standard errors were extracted for each condition using emmeans package (R software).

For the in vivo fixed tissue study regarding the percentage of nodes contacted, comparisons involving five conditions in a repeated measure design were conducted with linear mixed models using the lmer function in the lme4 package. Significance of the main effect was evaluated with the Anova function in the car package in R using Type II Wald χ^2 tests. Two-sided Tukey's post hoc pairwise comparisons were then performed using the emmeans and pairs functions in the emmeans package.

For the in vivo live-imaging studies, as the condition of normal distribution was not fulfilled within the groups, we used non-parametric tests. The differences between the groups were estimated using the non-parametric Kruskal–Wallis test followed by two-sided post hoc Dunn's test with further p -value adjustment by the Benjamini–Hochberg false discovery rate method.

For the in vivo fixed tissue study coupling LPC-induced demyelination with osmotic pump implantation, Grubbs' test was used to identify potential outliers ($n = 6$ in each group, distribution passed Shapiro–Wilk normality test), one outlier was removed of all the analysis in the LPC+Vehicle group ($p = 0.0316$), no outliers were detected in the group treated with LPC+TPA. The two groups were then compared using two-sided Mann–Whitney tests. For the in vivo fixed tissue study regarding the “contacting/non contacting” iNOS/IGF1 expressing microglial cells, a compute Cochran–Mantel–Haenszel χ^2 test of the null hypothesis that two nominal variables (“contact” and “protein expression”) are conditionally independent in each animal was performed.

Reporting summary. Further information on research design is available in the Nature Research Reporting Summary linked to this article.

Data availability

Raw source data files and detailed plasmid description are available upon request. Source data are provided with this paper.

Code availability

The codes used are referenced in the methods.

Received: 14 September 2020; Accepted: 11 August 2021;

Published online: 01 September 2021

References

- Lawson, L. J., Perry, V. H., Dri, P. & Rlksn, S. G. Heterogeneity in the distribution and morphology of microglia in the normal adult mouse brain. *Neuroscience* **39**, 151–170 (1990).
- Colonna, M. & Butovsky, O. Microglia function in the central nervous system during health and neurodegeneration. *Annu. Rev. Immunol.* **35**, 441–468 (2017).
- Thion, M. S., Ginhoux, F. & Garel, S. Microglia and early brain development: an intimate journey. *Science* **362**, 185–189 (2018).
- Hammond, T. R., Robinton, D. & Stevens, B. Microglia and the brain: complementary partners in development and disease. *Annu. Rev. Cell Dev. Biol.* **34**, 523–544 (2018).
- Davalos, D. et al. ATP mediates rapid microglial response to local brain injury in vivo. *Nat. Neurosci.* **8**, 752–758 (2005).
- Nimmerjahn, A., Kirchhoff, F. & Helmchen, F. Resting microglial cells are highly dynamic surveillants of brain parenchyma in vivo. *Science* **308**, 1314–1318 (2005).
- Bernier, L. P. et al. Nanoscale surveillance of the brain by microglia via cAMP-regulated filopodia. *Cell Rep.* **27**, 2895–2908.e4 (2019).
- Fontainhas, A. M. et al. Microglial morphology and dynamic behavior is regulated by ionotropic glutamatergic and GABAergic neurotransmission. *PLoS ONE* **6**, e15973 (2011).
- Stowell, R. D. et al. Noradrenergic signaling in the wakeful state inhibits microglial surveillance and synaptic plasticity in the mouse visual cortex. *Nat. Neurosci.* **22**, 1782–1792 (2019).
- Madry, C. et al. Microglial ramification, surveillance, and interleukin-1 β release are regulated by the two-pore domain K⁺ Channel THIK-1. *Neuron* **97**, 299–312.e6 (2018).
- Cserép, C. et al. Microglia monitor and protect neuronal function through specialized somatic purinergic junctions. *Science* **367**, 528–537 (2020).
- Szepesi, Z., Manouchehrian, O., Bachiller, S. & Deierborg, T. Bidirectional microglia–neuron communication in health and disease. *Front. Cell. Neurosci.* **12**, 1–26 (2018).

13. Voet, S., Prinz, M. & van Loo, G. Microglia in central nervous system inflammation and multiple sclerosis pathology. *Trends Mol. Med.* **25**, 112–123 (2019).
14. Miron, V. E. et al. M2 microglia and macrophages drive oligodendrocyte differentiation during CNS remyelination. *Nat. Neurosci.* **16**, 1211–1218 (2013).
15. Lloyd, A. F. & Miron, V. E. The pro-remyelination properties of microglia in the central nervous system. *Nat. Rev. Neurol.* <https://doi.org/10.1038/s41582-019-0184-2> (2019).
16. Cunha, M. I. et al. Pro-inflammatory activation following demyelination is required for myelin clearance and oligodendrogenesis. *J. Exp. Med.* **217**, e20191390 (2020).
17. Ransohoff, R. M. A polarizing question: do M1 and M2 microglia exist? *Nat. Neurosci.* **19**, 987–991 (2016).
18. Masuda, T. et al. Spatial and temporal heterogeneity of mouse and human microglia at single-cell resolution. *Nature* **566**, 388–392 (2019).
19. Hammond, T. R. et al. Single-cell RNA sequencing of microglia throughout the mouse lifespan and in the injured brain reveals complex cell-state changes. *Immunity* **50**, 253–271.e6 (2019).
20. Wolf, S. A., Boddeke, H. W. G. M. & Kettenmann, H. Microglia in physiology and disease. *Annu. Rev. Physiol.* **79**, 619–643 (2017).
21. El Behi, M. et al. Adaptive human immunity drives remyelination in a mouse model of demyelination. *Brain* **140**, 967–980 (2017).
22. Butovsky, O. et al. Microglia activated by IL-4 or IFN- γ differentially induce neurogenesis and oligodendrogenesis from adult stem/progenitor cells. *Mol. Cell. Neurosci.* **31**, 149–160 (2006).
23. Liu, Y. U. et al. Neuronal network activity controls microglial process surveillance in awake mice via norepinephrine signaling. *Nat. Neurosci.* **22**, 1771–1781 (2019).
24. Nebeling, F. C. et al. Microglia motility depends on neuronal activity and promotes structural plasticity in the hippocampus. *bioRxiv* <https://doi.org/10.1101/515759> (2019).
25. Tremblay, M. É., Lowery, R. L. & Majewska, A. K. Microglial interactions with synapses are modulated by visual experience. *PLoS Biol.* **8**, e1000527 (2010).
26. Wake, H., Moorhouse, A. J., Jinno, S., Kohsaka, S. & Nabekura, J. Resting microglia directly monitor the functional state of synapses in vivo and determine the fate of ischemic terminals. *J. Neurosci.* **29**, 3974–3980 (2009).
27. Paolicelli, R. C. et al. Synaptic pruning by microglia is necessary for normal brain development. *Science* **333**, 1456–1458 (2011).
28. Li, Y., Du, X. F., Liu, C. S., Wen, Z. L. & Du, J. L. Reciprocal regulation between resting microglial dynamics and neuronal activity in vivo. *Dev. Cell* **23**, 1189–1202 (2012).
29. Hughes, A. N. & Appel, B. Microglia phagocytose myelin sheaths to modify developmental myelination. *Nat. Neurosci.* **215**, 41–47 (2020).
30. Baalman, K. et al. Axon initial segment–associated microglia. *J. Neurosci.* **35**, 2283–2292 (2015).
31. Clark, K. C. et al. Compromised axon initial segment integrity in EAE is preceded by microglial reactivity and contact. *Glia* **64**, 1190–1209 (2016).
32. Lubetzki, C., Sol-Foulon, N. & Desmazières, A. Nodes of Ranvier during development and repair in the CNS. *Nat. Rev. Neurol.* **1871**, 426–439 (2020).
33. Zhang, J., Yang, X., Zhou, Y., Fox, H. & Xiong, H. Direct contacts of microglia on myelin sheath and Ranvier’s node in the corpus callosum in rats. *J. Biomed. Res.* **33**, 192–200 (2019).
34. Fenrich, K. K. et al. Long-term in vivo imaging of normal and pathological mouse spinal cord with subcellular resolution using implanted glass windows. *J. Physiol.* **590**, 3665–3675 (2012).
35. Coman, I. et al. Nodal, paranodal and juxtapanodal axonal proteins during demyelination and remyelination in multiple sclerosis. *Brain* **129**, 3186–3195 (2006).
36. Birgbauer, E., Rao, T. S. & Webb, M. Lysolecithin induces demyelination in vitro in a cerebellar slice culture system. *J. Neurosci. Res.* **78**, 157–166 (2004).
37. Thetiot, M., Ronzano, R., Aigrot, M. S., Lubetzki, C. & Desmazières, A. Preparation and immunostaining of myelinating organotypic cerebellar slice cultures. *J. Vis. Exp.* <https://doi.org/10.3791/59163> (2019).
38. Paolicelli, R. C., Bisht, K. & Tremblay, M.-É. Fractalkine regulation of microglial physiology and consequences on the brain and behavior. *Front. Cell. Neurosci.* **8**, 129 (2014).
39. Kyrargyri, V. et al. P2Y₁₃ receptors regulate microglial morphology, surveillance, and resting levels of interleukin 1 β release. *Glia* <https://doi.org/10.1002/glia.23719> (2019).
40. Zonouzi, M. et al. GABAergic regulation of cerebellar NG2 cell development is altered in perinatal white matter injury. *Nat. Neurosci.* **18**, 674–682 (2015).
41. Demerens, C. et al. Induction of myelination in the central nervous system by electrical activity. *Proc. Natl Acad. Sci. USA* **93**, 9887–9892 (1996).
42. Madry, C. et al. Effects of the ecto-ATPase apyrase on microglial ramification and surveillance reflect cell depolarization, not ATP depletion. *Proc. Natl Acad. Sci. USA* **115**, E1608–E1617 (2018).
43. Bacmeister, C. M. et al. Motor learning promotes remyelination via new and surviving oligodendrocytes. *Nat. Neurosci.* <https://doi.org/10.1038/s41593-020-0637-3> (2020).
44. Gründemann, J. & Clark, B. A. Calcium-activated potassium channels at nodes of Ranvier secure axonal spike propagation. *Cell Rep.* **12**, 1715–1722 (2015).
45. Brohawn, S. G. et al. The mechanosensitive ion channel TRAAK is localized to the mammalian node of Ranvier. *Elife* **8**, e50403 (2019).
46. Kanda, H. et al. TREK-1 and TRAAK are principal K⁺ channels at the nodes of Ranvier for rapid action potential conduction on mammalian myelinated afferent. *Neuron* <https://doi.org/10.1016/j.neuron.2019.08.042> (2019).
47. Serwanski, D. R., Jukkola, P. & Nishiyama, A. Heterogeneity of astrocyte and NG2 cell insertion at the node of Ranvier. *J. Comp. Neurol.* <https://doi.org/10.1002/cne> (2016).
48. Mount, C. W. & Monje, M. Wrapped to adapt: experience-dependent myelination. *Neuron* **95**, 743–756 (2017).
49. Ronzano, R., Thetiot, M., Lubetzki, C. & Desmazières, A. Myelin plasticity and repair: neuro-glial choir sets the tuning. *Front. Cell. Neurosci.* **14**, 1–11 (2020).
50. Maldonado, P. P., Vélez-Fort, M., Levavasseur, F. & Angulo, M. C. Oligodendrocyte precursor cells are accurate sensors of local K⁺ in mature gray matter. *J. Neurosci.* **33**, 2432–2442 (2013).
51. Thetiot, M. et al. An alternative mechanism of early nodal clustering and myelination onset in GABAergic neurons of the central nervous system. *Glia* **68**, 1891–1909 (2020).
52. Orthmann-Murphy, J. et al. Remyelination alters the pattern of myelin in the cerebral cortex. *Elife* **9**, 1–61 (2020).
53. Black, J. A. & Waxman, S. G. The perinodal astrocyte. *Glia* **1**, 169–183 (1988).
54. Dutta, D. J. et al. Regulation of myelin structure and conduction velocity by perinodal astrocytes. *Proc. Natl Acad. Sci. USA* **115**, 11832–11837 (2018).
55. Butovsky, O. et al. Identification of a unique TGF- β -dependent molecular and functional signature in microglia. *Nat. Neurosci.* **17**, 131–143 (2014).
56. Howell, O. W. et al. Activated microglia mediate axoglial disruption that contributes to axonal injury in multiple sclerosis. *J. Neuropathol. Exp. Neurol.* **69**, 1017–1033 (2010).
57. Nikić, I. et al. A reversible form of axon damage in experimental autoimmune encephalomyelitis and multiple sclerosis. *Nat. Med.* **17**, 495–499 (2011).
58. Zrzavy, T. et al. Loss of ‘homeostatic’ microglia and patterns of their activation in active multiple sclerosis. *Brain* **140**, 1900–1913 (2017).
59. Yamasaki, R. et al. Differential roles of microglia and monocytes in the inflamed central nervous system. *J. Exp. Med.* **211**, 1533–1549 (2014).
60. Gautier, H. O. B. et al. Neuronal activity regulates remyelination via glutamate signalling to oligodendrocyte progenitors. *Nat. Commun.* **6**, 8518 (2015).
61. Ortiz, F. C. et al. Neuronal activity in vivo enhances functional myelin repair. *JCI Insight* **4**, e123434 (2019).
62. Iaccarino, H. F. et al. Gamma frequency entrainment attenuates amyloid load and modifies microglia. *Nature* **540**, 230–235 (2016).
63. Umpierre, A. D. et al. Microglial calcium signaling is attuned to neuronal activity in awake mice. *Elife* **9**, e56502 (2020).
64. Lloyd, A. F. et al. Central nervous system regeneration is driven by microglia necroptosis and repopulation. *Nat. Neurosci.* **22**, 1046–1052 (2019).
65. Locatelli, G. et al. Mononuclear phagocytes locally specify and adapt their phenotype in a multiple sclerosis model. *Nat. Neurosci.* **21**, 1196–1208 (2018).
66. Muñoz-Planillo, R. et al. K⁺ efflux is the common trigger of NLRP3 inflammasome activation by bacterial toxins and particulate matter. *Immunity* **38**, 1142–1153 (2013).
67. Hamada, M. S. & Kole, M. H. P. Myelin loss and axonal ion channel adaptations associated with gray matter neuronal hyperexcitability. *J. Neurosci.* **35**, 7272–7286 (2015).
68. Jäkel, S. et al. Altered human oligodendrocyte heterogeneity in multiple sclerosis. *Nature* **566**, 543–547 (2019).
69. Lundgaard, I. et al. Neuregulin and BDNF induce a switch to NMDA receptor-dependent myelination by oligodendrocytes. *PLoS Biol.* **11**, e1001743 (2013).
70. Jung, S. et al. Analysis of fractalkine receptor CX3CR1 function by targeted deletion and green fluorescent protein reporter gene insertion. *Mol. Cell. Biol.* **20**, 4106–4114 (2000).
71. Perkins, K. L. Cell-attached voltage-clamp and current-clamp recording and stimulation techniques in brain slices. *J. Neurosci. Methods* **154**, 1–18 (2006).
72. Baudouin, L. et al. Co-culture of exogenous oligodendrocytes with unmyelinated cerebella: Revisiting ex vivo models and new tools to study myelination. *Glia* **69**, 1916–1931 (2021).

Acknowledgements

We thank Prof P.J. Brophy, University of Edinburgh, UK and Prof S. Jung, Tel Aviv, Israel for kindly providing the Thy1-Nfasc186mCherry and the CX3CR1-GFP mouse line and Dr P. Ravassard for the gift of the pTriP-Syn plasmid. We thank Prof G. Rougon and Dr F. Debarbieux, INT, France, for the in vivo spinal cord window technique, and Dr Roberta Magliozzi, University of Verona, Italy, for the immunohistostaining

technique on human post-mortem tissue. We thank Dr B. Zalc, Dr N. Sol-Foulon, and Dr B. Stankoff for insights and fruitful discussions. We thank the MS Society Tissue Bank at Imperial College London and Dr. Gveric for the provision of the MS brain samples (supported by grant 007/14 from the UK MS Society). We thank the icm.Quant imaging platform, ICM biostatistics platform (iCONICS), CELIS, electrophysiology, histology, vectorology and genotyping ICM platforms, and PhenoICMice ICM facilities. All animal work was conducted at the PHENO-ICMice facility (supported by ANR-10- IAIHU-06 and ANR-11-INBS-0011-NeurATRIS and FRM). This work was funded by INSERM, ICM, ARSEP Grants (to C.L. and A.D.), FRM fellowships (SPF20110421435, to A.D. and FDT20170437332, to M.T.), APHP and ARSEP travel grant fellowship to T.R., Prix Bouvet-Labruyère - Fondation de France (to A.D.), BBT (ICM; to A.D.), ANR JC (ANR-17-CE16-0005-01; to A.D.), and FRC (Espoir en tête, Rotary Club).

Author contributions

A.D., R.R., T.R., and C.L. designed research. R.R., T.R., M.S.A., and A.D. performed research and analyzed data. L.R. and J.M.V. generated electron microscopy data. T.R. and A.D. designed and performed the human study. F.X.L., R.R., T.R., and A.D. designed and did the biostatistical analysis. M.T. and E.M. participated in project initiation and experimental design. A.D., R.R., T.R., and C.L. wrote the paper.

Competing interests

The authors declare no competing interests.

Additional information

Supplementary information The online version contains supplementary material available at <https://doi.org/10.1038/s41467-021-25486-7>.

Correspondence and requests for materials should be addressed to A.D.

Peer review information *Nature Communications* thanks Veronique Miron and the other anonymous reviewer(s) for their contribution to the peer review of this work. Peer reviewer reports are available.

Reprints and permission information is available at <http://www.nature.com/reprints>

Publisher's note Springer Nature remains neutral with regard to jurisdictional claims in published maps and institutional affiliations.



Open Access This article is licensed under a Creative Commons Attribution 4.0 International License, which permits use, sharing, adaptation, distribution and reproduction in any medium or format, as long as you give appropriate credit to the original author(s) and the source, provide a link to the Creative Commons license, and indicate if changes were made. The images or other third party material in this article are included in the article's Creative Commons license, unless indicated otherwise in a credit line to the material. If material is not included in the article's Creative Commons license and your intended use is not permitted by statutory regulation or exceeds the permitted use, you will need to obtain permission directly from the copyright holder. To view a copy of this license, visit <http://creativecommons.org/licenses/by/4.0/>.

© The Author(s) 2021

Supplementary Figures

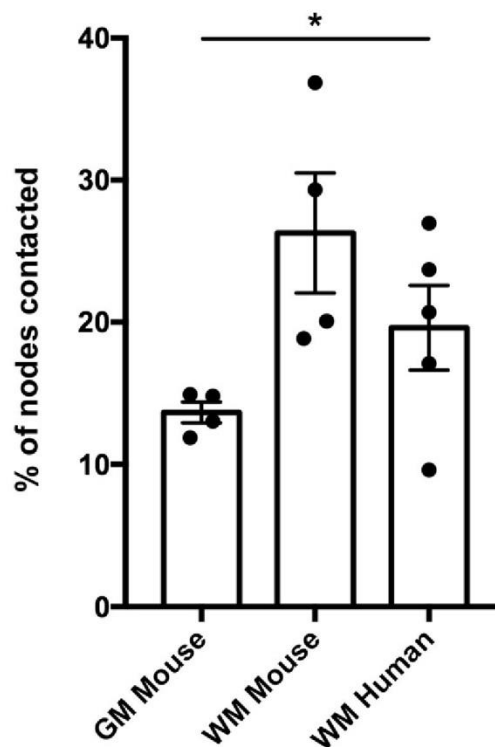


Figure S1: Percentage of nodes contacted by microglial cells in central nervous tissues. GM Mouse = mouse grey matter (cerebellum); WM Mouse = mouse white matter (spinal cord) and WM Human: human hemispheric white matter. The mean values per individual are plotted as dots. Bars and error bars represent the mean \pm s.e.m. Two-sided Kruskal-Wallis test. For detailed statistics, see Supplementary Table.

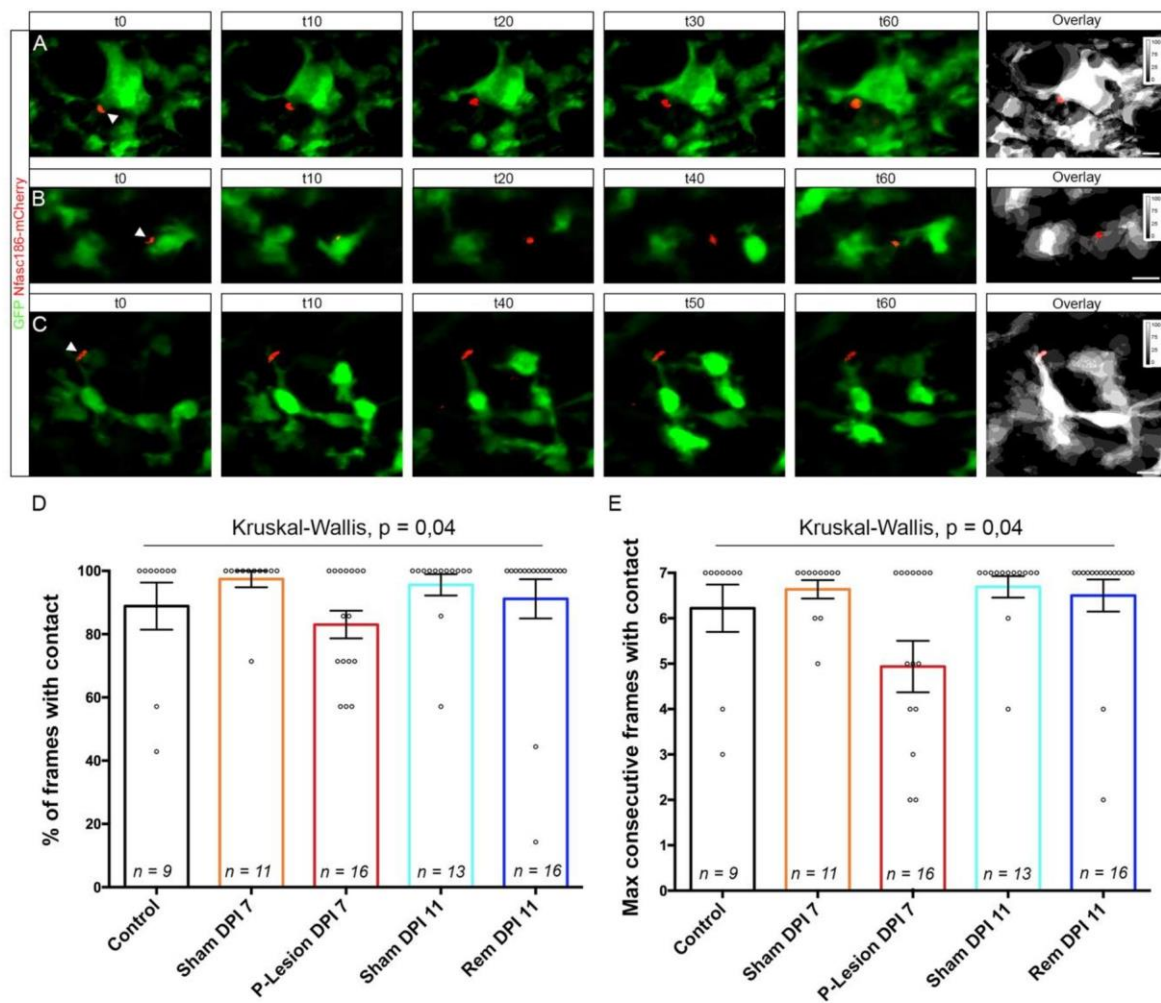


Figure S2. Microglial contacts with nodes of Ranvier are less stable during demyelination.

(A-C): *In vivo* live-imaging from CX3CR1-GFP/Thy1-Nfasc186mCherry mouse dorsal spinal cord with an initial contact between microglia (green) and nodes of Ranvier (red, arrowheads); 1-hour movies with an acquisition every 10 minutes. Scale bar 10 μ m; (A): Sham animal (NaCl injection) imaging at 7 DPI (corresponding to Movie 2 and condition Sham DPI7, n=11 animals); (B): LPC-injected animal imaged at 7 DPI (demyelination, corresponding to Movie 3 and P-Lesion DPI7, n=16 animals); (C): LPC-injected animal at 11 DPI (remyelination, corresponding to Movie 4 and Rem DPI11, n=16 animals). (D) Percentage of frames with microglia-node contact in 3-hour movies. (E) Longest sequence of consecutive timepoints with microglia-node contact in 3-hour movies. Each dot is a microglia-node pair. The number of microglia-node pairs imaged is indicated on each bar (n=4 to 7 animals per condition). Two-sided Kruskal-Wallis test. Bars and error bars represent the mean \pm s.e.m. For detailed statistics, see Supplementary Table.

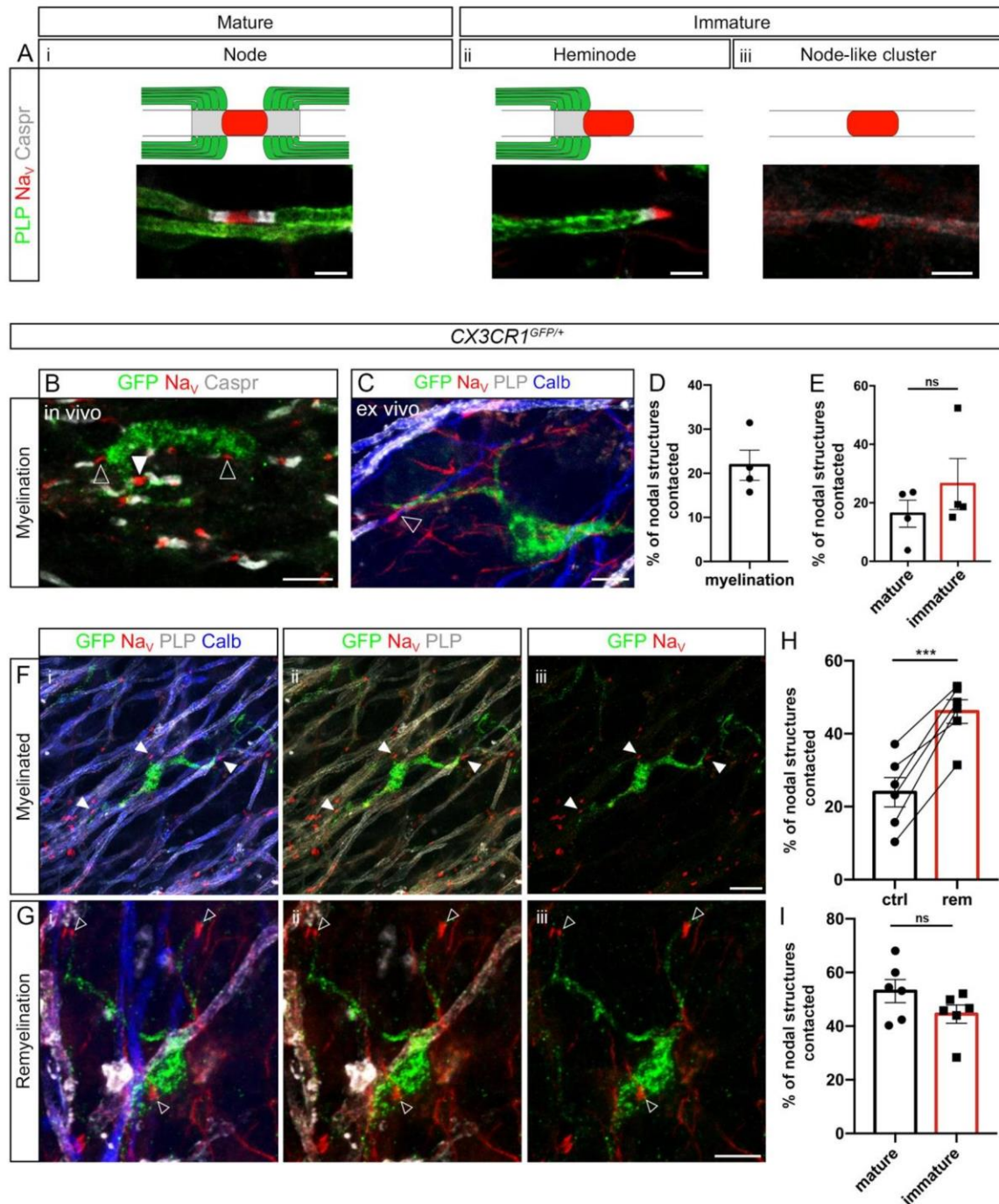


Figure S3. Microglial cells contact nodal structures in *ex vivo* organotypic cerebellar slice culture.

(A) Images and corresponding schematics illustrating a mature node (i) and immature nodal structures (heminode, ii and node-like-cluster, iii) in organotypic cerebellar slices (n=4 animals). (B, C) Microglia contact nodal structures during myelination in *CX3CR1*^{GFP/+} mouse cerebellum *in vivo* (B, P12, n=3 animals) and *ex vivo* (C, 4 DIV, n=4 animals). Both mature nodes of Ranvier (filled arrowheads) and immature nodal structures (node-like clusters and

heminodes, empty arrowheads) are contacted. (D) Percentage of nodal structures contacted by microglia in myelinating slices *ex vivo* (n=4 animals). (E) Percentage of mature and immature nodal structures contacted in myelinating condition *ex vivo* (n=4 animals per condition). (F, G) Microglia also contact nodal structures in myelinated (F) and remyelinating slices (G) *ex vivo* (11 DIV). Arrowheads indicate the nodes of Ranvier contacted by microglia. (H) Percentage of nodal structures contacted by microglia in myelinated (ctrl) vs remyelinating (rem) slices. $p=0.0006$ (I) Percentage of mature and immature nodal structures contacted in remyelinating condition (F-I: n=6 animals per condition). Scale bars: (A) 3 μm , (B, C) 5 μm , (F, G) 10 μm . (E) Two-sided Wilcoxon matched pairs test; (H, I) Two-sided Paired t-test. * $P < 0.05$, ** $P < 0.01$, *** $P < 0.001$, **** $P < 0.0001$, ns: not significant; bars and error bars represent the mean \pm s.e.m. For detailed statistics, see Supplementary Table.

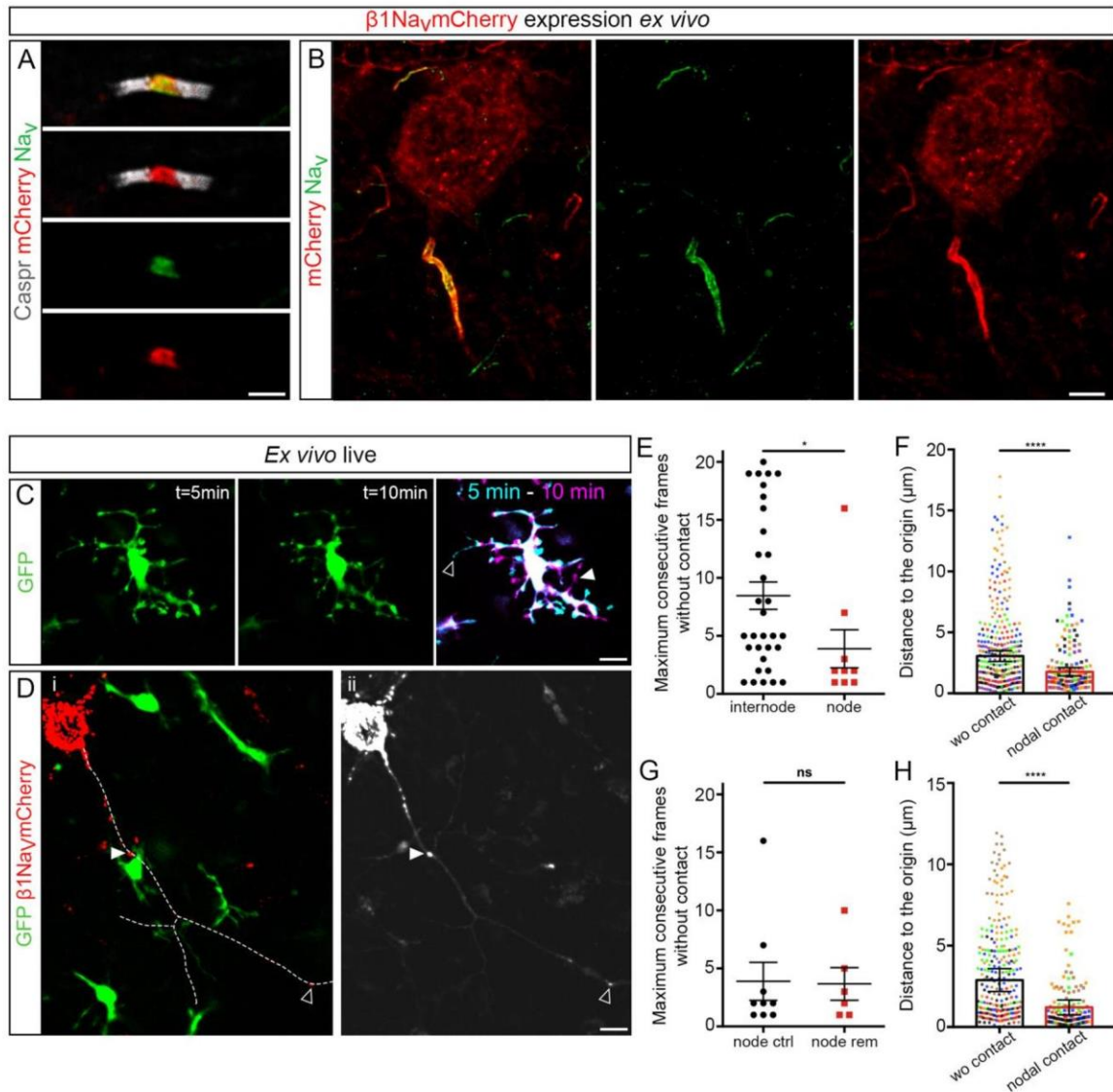


Figure S4. Live-imaging of microglia-node contact in organotypic cerebellar slice culture. (A-B) $\beta 1\text{NavmCherry}$ axonal expression is restricted to the nodes of Ranvier (A) and AIS (B) in Purkinje neurons *ex vivo*, as shown by its colocalization with Nav_v ($n=3$ animals). (C) Live images of a microglial cell (GFP^+) at two different timepoints, and the corresponding overlay showing the dynamics of the microglial cell, with extending (magenta) and retracting (cyan) processes (arrowheads: most dynamic processes, $n=59$ microglial cells in $n=6$ animals). (D) Myelinated $\text{CX3CR1}^{\text{GFP}/+}$ cerebellar slice with a Purkinje cell expressing $\beta 1\text{NavmCherry}$ following lentiviral transduction. (i) Live image showing a node (mCherry^+ , filled arrowhead) contacted by a microglial cell, and a non-contacted node (empty arrowhead). (ii) Summed projection of a movie showing the axon trajectory ($n=24$ animals). (E) Maximum duration

without contact between a microglial process and an internode or a node in myelinated slices (10 minutes acquisition, internode: n=32 contacts from 16 animals, node: n=9 contacts from 8 animals). (F) Distance between the process tip and its initial position for each frame, whether the process was initially contacting a node (nodal contact) or without contact (myelinated slices; wo contact: 280 measures from 14 trajectories, n=7 animals; nodal contact: 140 measures from 7 trajectories, n=7 color coded animals, $p=1.679e-08$). (G) Maximum duration without contact between the tip of a microglial process and the node in myelinated (node ctrl) vs remyelinating (node rem) slices (10 minutes acquisition, ctrl: n=9 contacts from 8 animals, rem: n=6 contacts from 6 color coded animals). (H) Distance between the process tip and its initial position for each frame (remyelinating slices; wo contact: 240 measures from 12 trajectories, n=6 animals, nodal contact: 120 measures from 6 trajectories, n=6 animals, $p=2.2e-16$). Scale bars: (A) 2 μm , (B) 5 μm , (C, D) 10 μm (E, G) Two-sided Mann-Whitney test; (F, H) Two-sided difference in means is indicated by Type II Wald chi-square test. * $P < 0.05$, ** $P < 0.01$, *** $P < 0.001$, **** $P < 0.0001$, ns: not significant; bars and error bars represent the mean \pm s.e.m. For detailed statistics, see Supplementary Table.

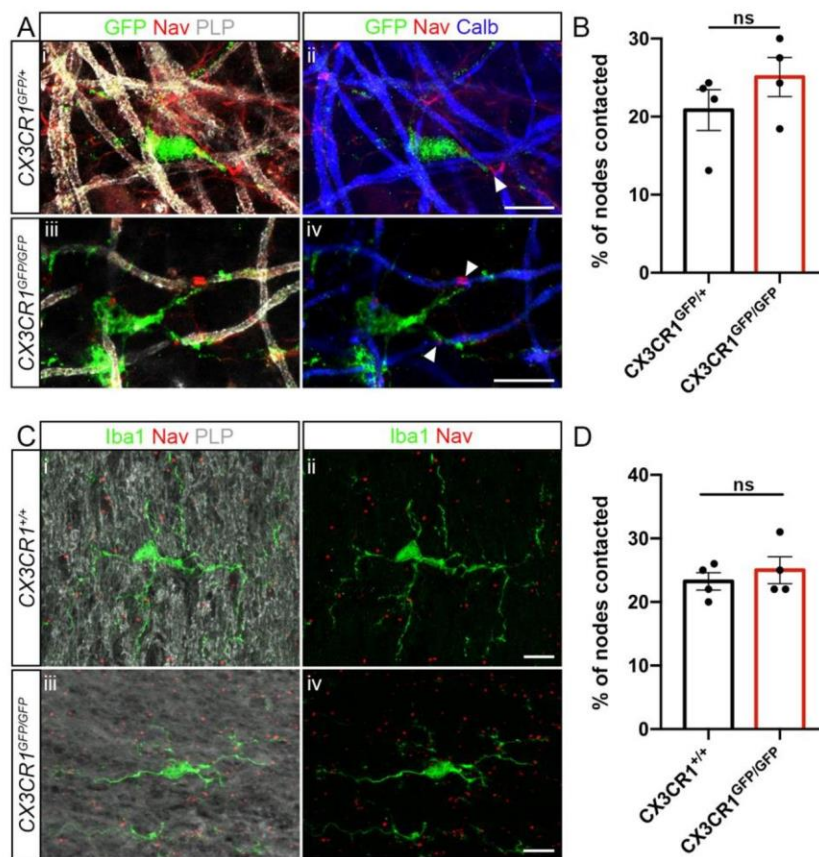


Figure S5. The microglial receptor CX3CR1 is not required for microglia-node interaction. (A) Microglia (GFP, in green) contact nodes of Ranvier (Nav, in red) both in CX3CR1^{GFP/+} and CX3CR1^{GFP/GFP} myelinated cerebellar slices. (B) Percentage of nodes of Ranvier contacted by microglia in CX3CR1^{GFP/+} vs CX3CR1^{GFP/GFP} littermate slices (A-B, n=4 animals per condition). (C) Microglia (Iba1, in green) contact nodes (Nav, in red) *in vivo* in CX3CR1^{GFP/GFP} mouse spinal cord as in wild-type littermates. (D) Percentage of nodes of Ranvier contacted by microglia in CX3CR1^{+/+} vs CX3CR1^{GFP/GFP} littermate animals (C-D, n=4 animals per condition). Scale bars: (A, C) 10 μ m. (B, D) Two-sided Mann-Whitney rank test. *P < 0.05, **P < 0.01, ***P < 0.001, ****P < 0.0001, ns: not significant; bars and error bars represent the mean \pm s.e.m. For detailed statistics, see Supplementary Table.

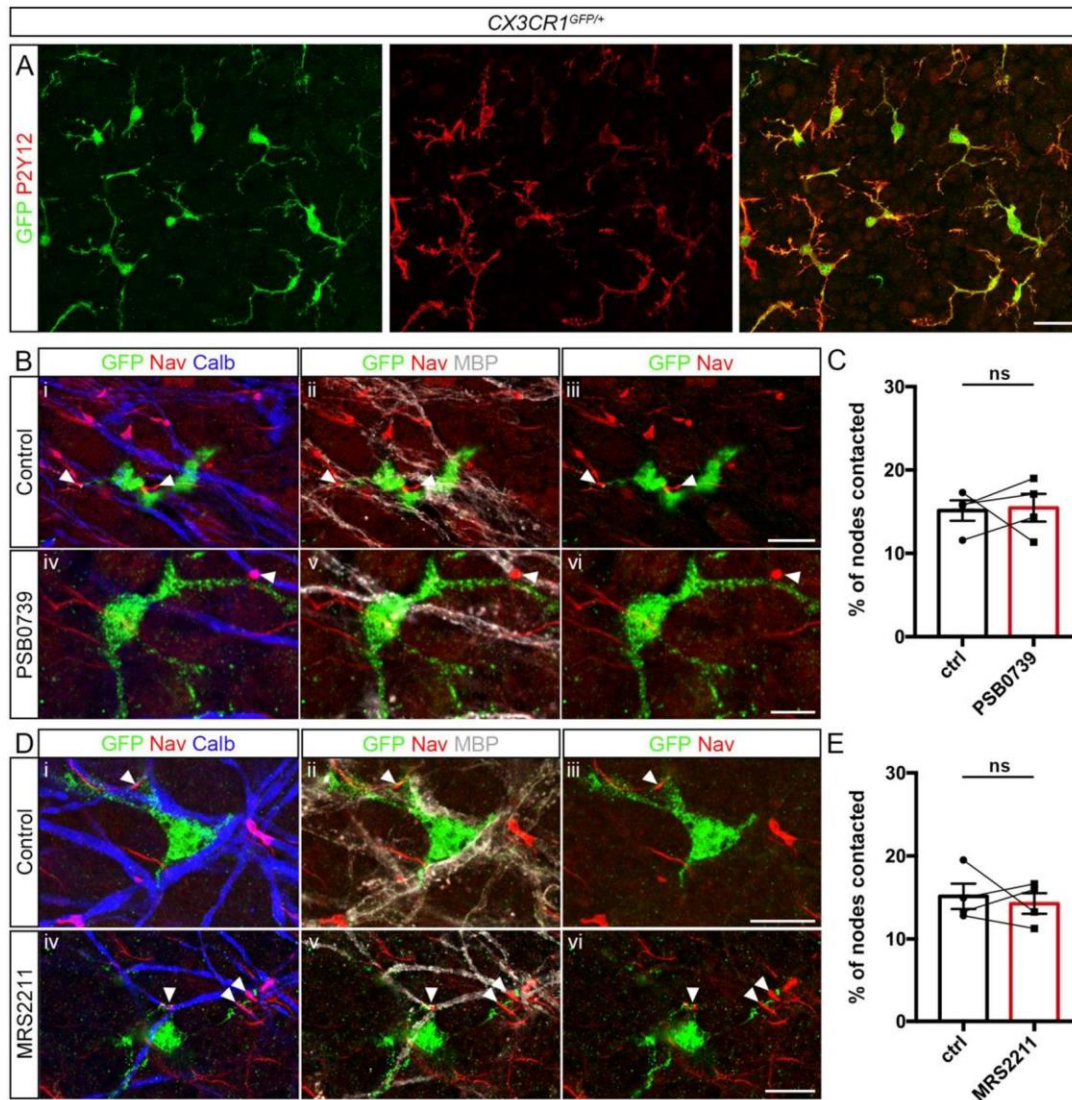


Figure S6. The microglial receptors P2Y12R and P2Y13R are not required for microglia-node interaction.

(A) Microglia express P2Y12R *ex vivo* in cerebellar organotypic cultures. (n=2 animals). (B, D) Illustration of microglia-node contacts in myelinated slices treated with PSB0739 (B, P2Y12R inhibitor, 1 μ M, 3-hour treatment) or MRS2211 (D, P2Y12R/P2Y13R inhibitor 50 μ M, 3-hours treatment). (C, E) Percentage of nodes contacted by microglial cells in *CX3CR1^{GFP/+}* myelinated slices in control (ctrl) vs treated condition, with PSB0739 (C, 1 μ M) or MRS2211 (E, 50 μ M). (B-E): n=4 animals per condition. Arrowheads show the nodes of Ranvier contacted by microglial cells. Scale bars: (A) 20 μ m, (Biii, D) 10 μ m, (Bvi) 5 μ m. (C, E) Two-sided Wilcoxon matched pairs test. *P < 0.05, **P < 0.01, ***P < 0.001, ****P < 0.0001, ns: not significant; bars and error bars represent the mean \pm s.e.m. For detailed statistics, see Supplementary Table.

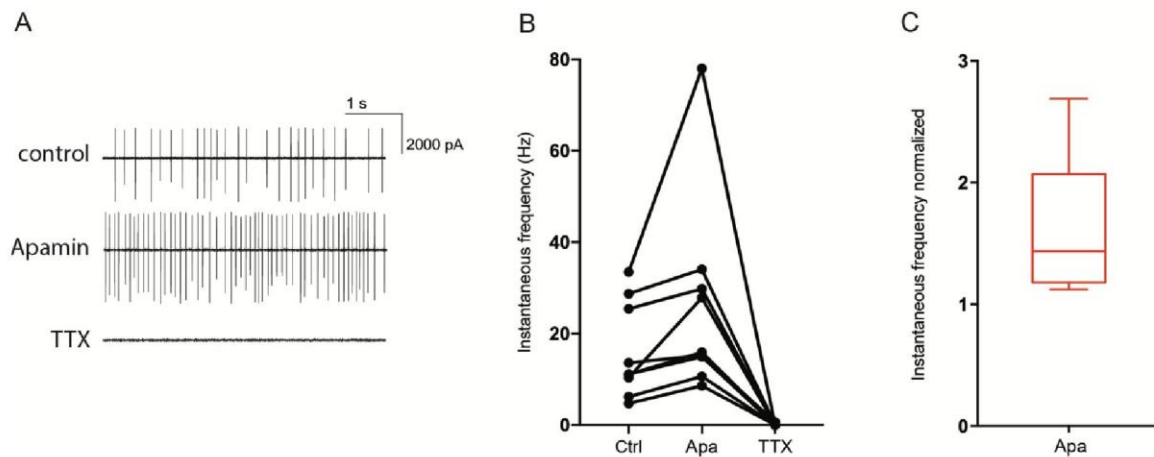


Figure S7. Purkinje cells present spontaneous activity in myelinated organotypic cerebellar slices.

(A) Representative example of loose-cell attached recordings on a Purkinje cell, in control condition followed by Apamin (Apa, 500 nM) and TTX (500 nM) consecutive treatments. (B) Instantaneous firing frequencies recorded in Purkinje cells of myelinated cerebellar organotypic slices (A-B, $n=9$ cells, $n=7$ animals, $p=1.234e-4$, Two-sided Friedman test). (C) Instantaneous firing frequencies recorded in Purkinje cells in myelinated cerebellar organotypic slices after Apamin treatment (500 nM), normalized by their matching control. The increased ratio of instantaneous frequencies ranges from 1.12 to 2.69, box-and-whiskers plot shows min, max, 25th and 75th percentiles and median ($n=9$ cells, $n=7$ animals). * $P < 0.05$, ** $P < 0.01$, *** $P < 0.001$, ns: not significant; bars and error bars represent the mean \pm s.e.m. For detailed statistics, see Supplementary Table.

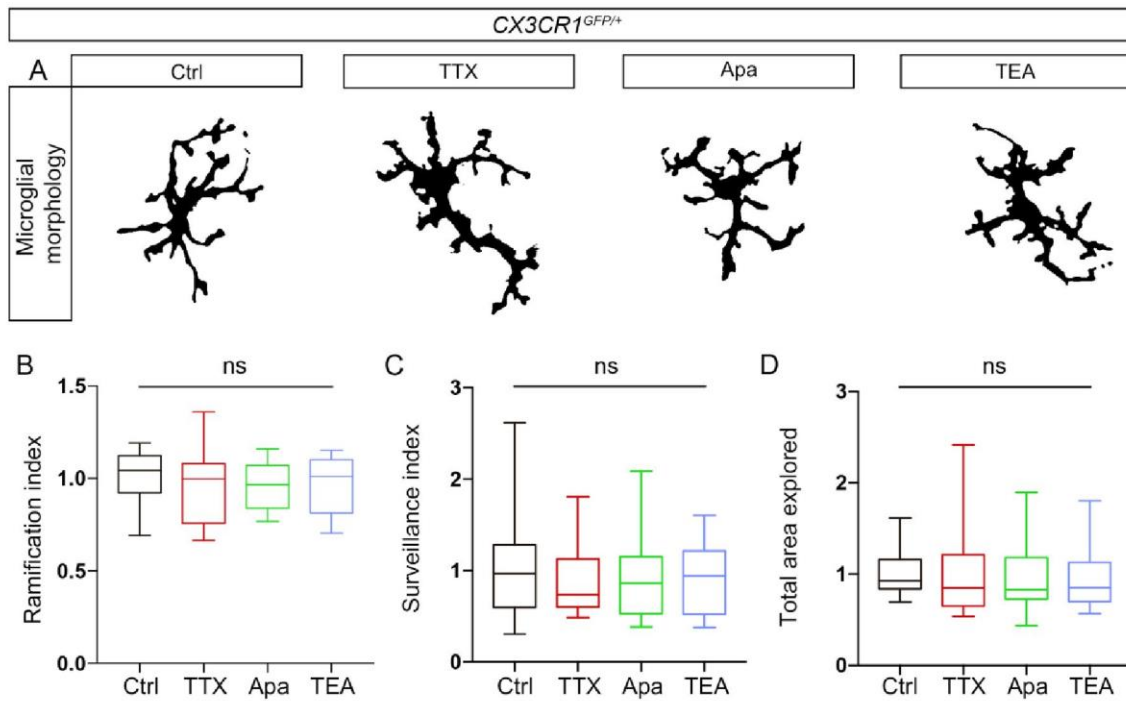


Figure S8. The dynamics and morphology of microglia are unchanged following TTX, Apamin and TEA treatments.

(A) Example of microglial morphology in control (ctrl) condition and following TTX, Apamin (Apa) or TEA treatments. (B-D) Microglia ramification (B) is unchanged after treatment, as well as their surveillance activity (C) and total area explored in 10 minute movies (D) (A-D, ctrl n=15 microglial cells, TTX: n=13 microglial cells, Apa n=15 microglial cells and TEA n=15 microglial cells, n=5 animals for each condition). Data are normalized by control values, box-and-whiskers plots show min, max, 25th and 75th percentiles and median. Two-sided Kruskal-Wallis test followed by Dunn's multiple comparison test, *P < 0.05, **P < 0.01, ***P < 0.001, ****P < 0.0001, ns: not significant; bars and error bars represent the mean \pm s.e.m. For detailed statistics, see Supplementary Table.

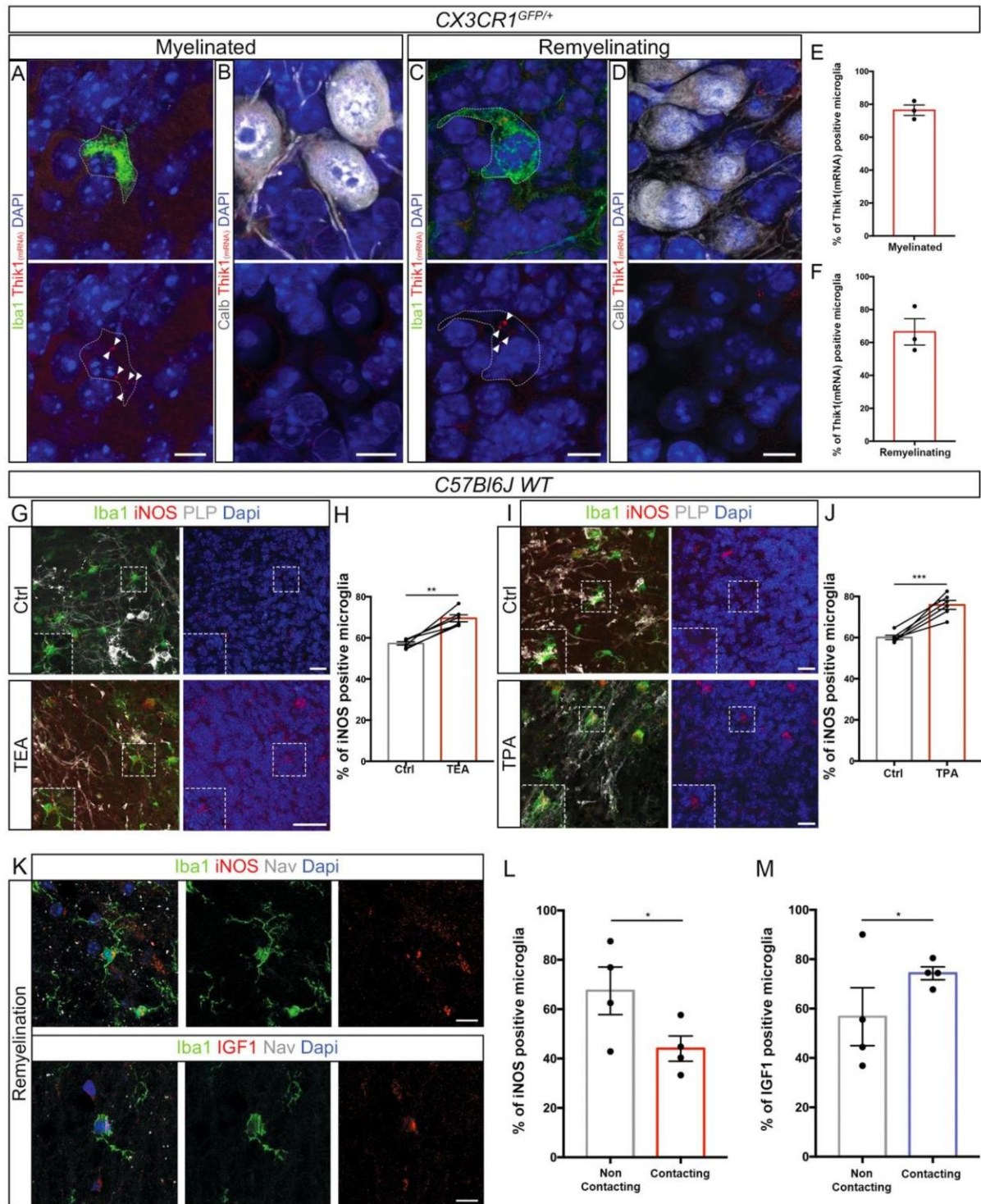


Figure S9. Microglia-node interaction influences microglial phenotype during remyelination. (A-F) THIK-1 mRNA (red) is expressed by microglia (Iba1, in green) but not Purkinje cells in myelinated as well as remyelinating organotypic cerebellar slices. Percentage of microglia with a clear expression of THIK-1 mRNA in myelinated and remyelinating slices. n=3 animals per condition. (G, I) In remyelinating C57bl6/J organotypic cerebellar slices, microglial expression

of iNOS is increased following neuronal potassium channel inhibition by TEA (G) or THIK-1 inhibition by TPA treatment (I). (H, J) Percentage of iNOS⁺ microglial cells at remyelination onset, with no treatment (ctrl) or with TEA (H, 2 hours, 30 mM) or TPA treatment (J, 2 hours, 50 μ M). The mean values per animal are individually plotted and paired with the corresponding control. (G-J, n=6 animals per condition). (K) Both iNOS⁺ and IGF1⁺ microglial cells contact nodes of Ranvier in remyelinating mouse dorsal spinal cord *in vivo*. (L, M) Percentage of iNOS (L) and IGF1 (M) positive microglial cells amongst “contacting” or “non-contacting” microglial cells. The mean values per animal are shown as dots (K-M, n=6 animals per condition). Scale bars: (A-D) 10 μ m, (G, I) 50 μ m, (K) 10 μ m; (H, J) Two-sided Paired t-test. (L, M) Two-sided Cochran-Mantel-Haenszel chi-squared test. *P < 0.05, **P < 0.01, ***P < 0.001, ****P < 0.0001, ns: not significant; bars and error bars represent the mean \pm s.e.m. For detailed statistics, see Supplementary Table.

2 Ongoing work: Neuronal activity promotes node-like cluster formation prior to myelination

Summary

The formation of node-like clusters prior to myelination in the central nervous system has been characterized by our team and others along retinal ganglion cells, GABAergic neurons of the hippocampus and two populations of spinal neurons in zebrafish (Kaplan et al., 1997, 2001; Freeman et al., 2015; Bonetto et al., 2019; Dubessy et al., 2019; Thetiot et al., 2020; Vagionitis et al., 2021). Recently, we have observed node-like clusters in cerebellar organotypic slice cultures, prior to myelination and remyelination (Lubetzki et al, 2020a; Thetiot and Desmazières, unpublished). Taking advantage of various models available in the laboratory, we investigated the role of neuronal activity on the formation of these nodal clusters using stimulations of neuronal activity by both chemogenetic and optogenetic approaches *in vitro* and *ex vivo*.

First using an *in vitro* model of mixed hippocampal culture that has been previously used to characterize node-like cluster formation, we found that neuronal activity stimulation with chemogenetic promotes the formation of node-like clusters. Furthermore, using chemogenetic and optogenetic stimulations *ex vivo* on cerebellar organotypic cultures, we observed that neuronal stimulation promotes both node-like cluster formation and myelination in an axon specific manner along Purkinje cell axons. Thus, neuronal activity in population of node-like cluster forming neurons may promote node-like cluster formation and myelination. Lastly, investigating the formation of node of Ranvier in the cerebellum *in vivo*, we observed that node-like clusters are formed prior to myelination along Purkinje axons, which indicates that the observations made *ex vivo* may similarly apply to the *in vivo* postnatal development of the cerebellum.

Neuronal activity promotes node like cluster formation prior to myelination

Introduction

Along myelinated fiber, the propagation of the nerve influx relies on the alternation of myelinated domains, the internodes and small unmyelinated domains the nodes of Ranvier. It is commonly thought that the formation of nodes during myelination starts with the assembly of the axoglial paranodal junction that acts as a lateral diffusion barrier for nodal proteins (Rasband et al., 1999; Pedraza et al., 2001; Susuki et al., 2013; Amor et al., 2017). However, more than twenty years ago, it had originally been proposed that the formation of nodes along retinal ganglion cell axon might start with the clustering of nodal proteins prior to any myelin deposition (Kaplan et al., 1997, 2001). Recently, this mechanism of node-like clustering has been described in several populations of neurons both of the central and peripheral nervous system in mice and in zebrafish (Freeman et al., 2015; Bonetto et al., 2019; Dubessy et al., 2019; Lubetzki et al., 2020a; Thetiot et al., 2020; Malavasi et al., 2021; Vagionitis et al., 2021). These clusters may have a functional impact on neuron physiology since their presence correlates with an acceleration of action potentials conduction (Freeman et al., 2015; Eshed-Eisenbach et al., 2020). Moreover, it has been shown that node-like clusters very often participate in the formation of mature node of Ranvier or heminodes once axons get myelinated (Thetiot et al., 2020; Vagionitis et al., 2021). Thus, in node-like cluster forming neurons, their formation is a first step in the transition from an unmyelinated to a myelinated fiber and may impact myelin deposition.

The role of neuronal activity in modulating myelination mechanisms has been described more than two decades ago and recently numerous studies have demonstrated the key function of neuronal activity in the modulation of myelination in development, adulthood and in pathological conditions (Barres and Raff, 1993; Demerens et al., 1996; Stevens et al., 2002; Gibson et al., 2014; McKenzie et al., 2014; Hines et al., 2015; Mensch et al., 2015; Mitew et al., 2018; Ortiz et al., 2019; Geraghty et al., 2019; Bacmeister et al., 2020; Almeida et al., 2021). This neuronal activity-dependent myelination, driven by experience is involved in various mechanisms of central nervous system development and function allowing to finely tune coordinated activity between different areas of the CNS (Etxeberria et al., 2016; Pan et al., 2020; Steadman et al., 2020; Teissier et al., 2020). However, these studies mainly focused on the effect of neuronal activity on the production of new oligodendrocytes, the production of myelin and on the modulation of the myelination pattern.

Amongst neuronal populations with a characterized activity-dependent myelination (Etxeberria et al., 2016; Demerens et al., 1996), retinal ganglion neurons have been shown to form node-like clusters (Kaplan et al., 1997, 2001; Dubessy et al., 2019). Moreover parvalbumin interneurons myelination in the cortex is activity dependent (Stedehouder et al., 2018; Yang et al., 2020), and parvalbumin interneurons from the hippocampus form node-like clusters (Freeman et al., 2015; Bonetto et al., 2019; Dubessy et al., 2019; Thetiot et al., 2020). Interestingly, it has been suggested that node-like clusters participate in the mechanism of myelination by either guiding myelination or by prefiguring mature node of Ranvier position along myelinated axons (Thetiot et al., 2020; Vagionitis et al., 2021). Therefore, as the formation of node-like clusters precedes and is suggested to regulate myelination, we wondered whether the formation of node-like clusters may be modulated by neuronal activity.

Here, we tested this hypothesis by investigating the role of neuronal activity on two neuronal populations that form node-like clusters: hippocampal GABAergic neurons and Purkinje cells. Stimulating by chemogenetic as well as optogenetic approaches neuronal activity, we showed *in vitro* and *ex vivo* that it promotes node-like clusters formation along unmyelinated axons. Furthermore, along Purkinje axons, neuronal activity increases both node-like cluster formation and myelination in an axon specific manner suggesting that activity may orchestrate the formation of both nodal domains and myelin sheaths along individual axons.

Methods

Animals

The care and use of mice conform to institutional policies and guidelines (UPMC, INSERM, French and European Community Council Directive 86/609/EEC). The following mouse strains were used in this study: C57bl6/J wild type (Janvier Labs), L7-ChR2-eYFP with a C57bl6/J genetic background (Kind gift from Pr C. Lena, IBENS, PSL University, Paris, France; Chaumont Joseph et al., 2013). Wistar pregnant rat females were purchased from Janvier Labs.

Hippocampal mixed culture

Mixed hippocampal cultures (containing neurons and glial cells) were prepared from rat embryo at E18 according to the protocol developed previously in the laboratory, as described in (Freeman et al., 2015). Hippocampi from embryo of the same litter were dissected and subsequently pooled and dissociated enzymatically in a trypsin (0.1%; Worthington)/DNase (50 µg/mL) solution for 20 min. Following trypsin neutralization, cells were mechanically dissociated, centrifuged at 400 × g

for 5 min, resuspended, and seeded on polyethylenimine precoated glass coverslips at a density of 50 000 cells/well in 24 well plates (surface of 35mm² per well, TPP). Cultures were maintained for 24 h in a 1:1 mixture of DMEM (11880; Gibco) with 10% fetal calf serum (100 IU/mL), penicillin-streptomycin (100 IU/mL), and neuron culture medium (NCM). Culture medium was replaced by a 1:1 mixture of Bottenstein–Sato (BS) medium with PDGF-A (0.5%) and NCM, and then, half of the medium was removed every 3 days and replaced by NCM. The NCM contained neurobasal medium (21103–049; Gibco) supplemented with 0.5 mM L-glutamine, B27 (1×; Invitrogen), and penicillin-streptomycin (100 IU/mL each). The BS medium was made of DMEM Glutamax supplemented with transferrin (50 µg/mL), albumin (50 µg/mL), insulin (5 µg/mL), progesterone (20 nM), putrescine (16 µg/mL), sodium selenite (5 ng/mL), T3 (40 ng/mL), and T4 (40 ng/mL). Differentiation medium: DMEM Glutamax supplemented with transferrin (50 µg/mL), albumin (50 µg/mL), insulin (5 µg/mL), putrescine (16 µg/mL), sodium selenite (5 ng/mL), T3 (40 ng/mL), T4 (40 ng/mL), biotin (10 ng/mL), vitamin B12 (27.2 ng/mL), ceruloplasmin (100 ng/mL), hydrocortisone (0.05 µM), CNTF (0.1 ng/mL), and sodium pyruvate (1 mM).

Cerebellum organotypic slice culture

Cerebellar slice cultures were prepared based on published protocols (Birgbauer et al., 2004; Thetiot et al., 2019). Briefly, P8-9 mouse cerebella were dissected in ice cold Gey's balanced salt solution complemented with 4.5 mg/ml D-Glucose and 1X penicillin-streptomycin (100 IU/mL), before being cut into 250µm parasagittal slices using a McIlwain tissue chopper and placed on Millicell membrane (2 membranes with 3 to 4 slices each per animal, 0.4 µm membranes, Merck Millipore) in 50% BME (Thermo Fisher Scientific), 25% Earle's Balanced Salt Solution (Sigma), 25% heat-inactivated horse serum (Thermo Fisher Scientific) medium, supplemented with GlutaMax (2 mM, Thermo Fisher Scientific), penicillin-streptomycin (100 IU/mL, Thermo Fisher Scientific) and D-Glucose (4.5 mg/ml; Sigma). Cultures were maintained at 37°C under 5% CO₂ and medium changed every two to three days.

Transduction on *in vitro* and *ex vivo* culture

The adenovirus used to express hM3Dq or hM4Di fused to the reporter mCherry under the control of the human Synapsin promoter, AAV8-hSyn-hM3D(Gq)-mCherry and AAV8-hSyn-hM4D(Gi)-mCherry are available commercially (Addgene, #50474-AAV8 and #50475-AAV8 respectively) and allowed the expression of DREADDs receptors specifically in neurons. In hippocampal mixed culture the transduction was performed at 6 DIV, by adding the virus at a final concentration of ~10⁹ when renewing half of the medium. Regarding organotypic slices the transduction was performed immediately following slice preparation by addition of the solution with adeno-associated viruses

directly onto the slices placed on milicell membranes (1 μl /slice at a final concentration of about 10^{11} VP/ μl).

Electrophysiology

Organotypic cerebellar slices were obtained from P9-P10 mice. Organotypic cerebellar slices (from 9 to 11 DIV) were transferred to a recording chamber and continuously superfused with oxygenated (95% O₂ and 5% CO₂) aCSF containing (in mM): 124 NaCl, 3 KCl, 1.25 NaH₂PO₄, 26 NaHCO₃, 1.3 MgSO₄, 2.5 CaCl₂, and 15 glucose (pH 7.4) (all powders were purchased from Sigma Aldrich). The Purkinje cells were visualized under differential interference contrast optics using a 63X water immersion (N.A. 1) lens and recognized morphologically. Loose cell-attached voltage clamp recordings of the spontaneous firing activity were performed at 30-34°C with a borosilicate glass pipette filled with aCSF. Signals were amplified with a Multiclamp 700B amplifier (Molecular devices), sampled and filtered at 10 kHz with a Digidata 1550B (Molecular Devices). Data were acquired with the pClamp software (Molecular devices). To avoid any alteration of the spontaneous firing frequency of the cell by the patch procedure (Perkins, 2006), the holding membrane potential was set to the value at which zero current was injected by the amplifier. The resistance of the seal (R_{seal}) was controlled and calculated every minute from the current response to a voltage step (200 ms; -10 mV). Only recordings with a R_{seal} in the range of 10 to 100M Ω and stable during the recording procedure were included in the analysis. To test chemogenetic modulation of the activity, recordings were performed in control conditions by adding DMSO (solvent of the N-clozapine) in the bath perfusion. The perfusion was then switched to a bath with 0.5 μM of N-clozapine (CNO) while recording the same neuron. To test optogenetic stimulation, the LED with an excitation filter 482/35 was calibrated to stimulate the field of view at 1.5mW/mm² and individual neurons were successively recorded with no stimulation and with pulses of 10 millisecond at 10Hz. The mean firing rate was analyzed over 110 seconds recording time window using a threshold crossing spike detection in Clampfit (Molecular devices) and calculated as the number of action potential current divided by the duration of the recording. The instantaneous frequency is also reported for optogenetic stimulations recordings and calculated as the inverse of the interspike interval i.e the time between a given detected spike and the preceding one.

Treatments with N-Clozapin

To activate the DREADD receptor hM3Dq or hM4Di, the culture medium was renewed with a culture medium containing 0.5 μM of CNO diluted in DMSO (Cayman Chemical) or a culture medium with an equivalent volume of DMSO (1 μL in 1 mL of medium) in control conditions. On hippocampal mixed culture the treatment was applied at 8 DIV and maintained until the fixation of the culture. On

organotypic slices the treatment was applied for 6 hours (for hM3Dq) and 8 hours (for hM4Di) at 3 DIV and the slices were fixed 1 hour after the end of the treatment to assess for the effect on node-like cluster formation, and 17 hours (hM3Dq) or 24 hours (hM4Di) after the treatment to assess the effect on myelination.

Optogenetic stimulations on organotypic slices

Optogenetic stimulations were performed on the organotypic slices with a custom set up that allow stimulation with light at 470nm directly on 6 well plates (Ronzano, Marty, Ballbé and Desmazières, unpublished). Each well is illuminated by 1 LED, each LED is individually calibrated to allow a stimulation at a power of 1.5mW/mm² in the center of the membrane where the slices are placed. An electronic box allows to control the pattern of stimulation by the 6 LED using an Arduino (10 ms long pulses at 10Hz for 6 hours). To avoid cytotoxicity, prior to stimulation the membrane were transferred in a medium free of phenol-red consisting of: 75% DMEM (Gibco, Thermo Fisher Scientific), 20% 1X HBSS (Gibco, Thermo Fisher Scientific) supplemented with HCO₃⁻ (0.075 g/L final; Gibco, Thermo Fisher Scientific), 5% heat-inactivated horse serum (Thermo Fisher Scientific, HEPES Buffer (10 mM final; Gibco, Thermo Fisher Scientific), D-Glucose (4.5 g/L final; Sigma), GlutaMax (2 mM final; Gibco, Thermo Fisher Scientific) and penicillin-streptomycin (100 IU/mL each; Thermo Fisher Scientific). The slices were fixed one hour after the end of the stimulation to assess the effect on node-like cluster formation, and 17 hours after the stimulation to assess the effect on myelination.

Fixation and immunohistochemistry

In vitro cultured hippocampal neurons

Cell cultures transduced with the viruses allowing the expression of hM3Dq or hM4Di were fixed at 14 and 17 DIV respectively with 1% PFA, for 10 min at room temperature and then incubated with methanol for 10 min at -20°C. Coverslips were then washed three times with PBS. After fixation, cells were incubated with blocking buffer made of PBS, 5% Normal Goat Serum (50-062Z; Thermo Fisher Scientific), 0,1% Triton X-100 (Sigma Aldrich) for 15 min and then with the solution of primary antibodies diluted in the blocking solution for 2 hours at room temperature. Coverslips were then washed three times and incubated with the secondary antibodies at room temperature in the dark for 1 hour. After two washes in PBS followed by one wash in H₂O, coverslips were mounted with Fluoromount-G with DAPI (Southern Biotech).

Ex vivo cultured cerebellar slices

Cerebellar slices were fixed as described before (Thetiot et al., 2019), with 4% PFA (Electron Microscopy, Thermo Fisher Scientific) for 5 minutes followed by 1% PFA for 25 minutes at room

temperature and then washed three times in PBS. Subsequently, the slices were incubated in absolute ethanol (Sigma Aldrich) at -20°C for 20 minutes and washed three times in PBS. Tissues were blocked for 1 hour in PBS, 5% Normal Goat Serum, 0,3% Triton X-100 and incubated with primary antibodies diluted in blocking solution overnight at room temperature. Slices were then washed three times in PBS, incubated with secondary antibodies diluted in blocking solution for 3 hours at room temperature in the dark. The slices were washed three times in PBS and mounted between a glass slide and a coverslip (VWR) with Fluoromount G (Southern Biotech).

Mouse central nervous tissues

At P10 the animals were perfused with 2% PFA and the brains were dissected and post-fixed in PFA 2% for 30 minutes, washed in PBS three times and incubated in PBS with 30% sucrose (Sigma Aldrich) for 3 days at 4°C for cryoprotection. The tissues were then included in O.C.T (Tissue-Tek, Sakura). The brains were cut sagittally in 30µm thick sections using a cryostat (Leica CM 1950). Sections were collected on Superfrost+ glass slides (VWR). For immunohistochemistry, the slides were first placed in absolute ethanol at -20°C for 20 minutes. They were then incubated with a blocking solution containing PBS, 5% Normal Goat Serum and 0.2% Triton X-100 for at least 30 minutes at room temperature. Following PBS washes, the slides were incubated with the primary antibodies diluted in blocking solution overnight at room temperature and the next day with the secondary antibodies diluted in blocking solution for 2 hours in the dark at room temperature. The slides were mounted with a glass coverslip (VWR) using Fluoromount (Sigma-Aldrich), and left to dry at room temperature before being stored at 4°C.

Antibodies

The following primary antibodies were used: mouse IgG2a anti-AnkyrinG (clone N106/36; 1:100, Neuromab), mouse IgG2b anti-AnkyrinG (clone N106/65; 1:75, Neuromab), mouse IgG1 anti-Pan Na_v (clone K58/35; 1:150, Sigma), rabbit anti-Caspr (1:300, Abcam), mouse anti-Calbindin (1:500; Sigma), rabbit anti-Calbindin (1:300; Swant), rat anti-PLP (1:10; hybridoma, kindly provided by Dr. K. Ikenaka, Okasaki, Japan), chicken anti-GFP (1:250, Millipore), chicken anti-mCherry (1:1000, EnCor Biotechnology), mouse IgG2a anti-GAD67 (clone 1G10.2; 1:400, Millipore). Secondary antibodies corresponded to goat or donkey anti-chicken, mouse IgG2a, IgG2b, IgG1, rabbit, rat coupled to Alexa Fluor 488, 594, 647 or 405 from Invitrogen (1:500).

Imaging

Confocal microscopy was performed using a FV-1200 Upright Confocal Microscope and a Leica inverted SP8 with 40x and 63x oil immersion objectives with 1.30 and 1.40 numerical aperture

respectively, controlled by Metamorph (FV-1200) or LasX (SP8) softwares. To test the effect of neuronal activity on node like cluster formation for each acquisition, 387.69 μm x 387.69 μm of 2048x2048 pixels image stacks, with a z-step of 0,35 μm were acquired with the 40x objective using 405, 488, 565 and 647 laser lines. For imaging of mixed hippocampal cultures, to avoid bias in the imaging, fields of view were randomly chosen and when a GAD67 positive cell was in the field of view the whole thickness of the soma and its proximal axon (at least along 100 μm) was imaged. For imaging of the organotypic culture slices, fields of view with Purkinje cells expressing whether mCherry (for chemogenetic experiment) or YFP (for optogenetic experiment) were chosen. A stack sufficient to follow their axons, together with the axons of an equal number of mCherry or YFP negative Purkinje cells was taken. When imaging to quantify the density of node like clusters a minimal field of view of 123.14 μm x 123.14 μm of 1024x1024 pixels image stack, including at least 10 Z-series with a z-step of 0,30 μm was acquired with a 63x objective.

Analysis

Quantification

For hippocampal mixed culture, transduced GABAergic neurons were labelled with GAD67 and mCherry. The number of GAD67+/mCherry+ neurons with node-like clusters along their axons was quantified. A Nav cluster was defined by a length between 1 and 8 μm and a mean intensity twice higher than the diffuse signal along the axon. A neuron was counted as positive for node like clusters when at least 2 Nav clusters were observed along its axon. On average about 60 GAD67 positive, mCherry positive neurons were counted per experiment per condition, and at least three independent experiments were performed (biological replicates).

For the organotypic culture of cerebellar slices at 3-4 DIV and for the sections from cerebellum at P10, the number of node-like clusters taking the same definition than above were quantified on one optical section of the middle of the image stack. The rest of the stack was used to make sure that the structures corresponded to a node-like cluster and not to an axon initial segment perpendicular to the imaging plan. The quantification was performed on 5 fields of view per animal, the number of node-like clusters per area unit was averaged to give the value for one animal. The analysis was performed in at least 4 animals per condition.

Following neuronal activity stimulation with both chemogenetic and optogenetic, the number of node-like clusters and the proportion of the axon that was myelinated was assessed along the first 130 μm of the axon starting from the distal end of the axon initial segment (see the full design of the analysis Figure S1). For node-like clusters quantification, at the time point used, a small part of the axon was sometimes myelinated, therefore the number of structures were further normalized to obtain a mean number of structures per length unit of unmyelinated axon. When the axon had a

branch point along these 130 μm , the analysis was made along the main branch going toward the white matter tract. The analysis was reduced to this part of the axon to restrain the quantification to the area where myelination was ongoing. Indeed, during cerebellar development the myelination proceeds in an ascending manner along Purkinje axons from the white matter tract toward the soma (Gianola et al., 2003). The number of node-like clusters and the proportion of axon myelinated were quantified along 10 reporter-positive (mCherry+ or YFP+) and 10 reporter-negative (mCherry- or YFP-) Purkinje axons per condition (stimulated or non-stimulated) per animal. Furthermore, the same number of cells positive and negative for the reporter were analyzed in a given field of view, to compare node-like cluster formation and myelination on neighboring cell. The mean number of node-like clusters and the mean rate of myelination was then calculated amongst Purkinje cells positive for mCherry-hM3Dq/4Di or YFP-ChR2, and amongst the ones that were negative. The ratio of node-like cluster number and myelin rate were reported for each animal in stimulated (CNO or light pulses) and non-stimulated conditions (DMSO or no light). A minimum of 4 animals per condition were analyzed. See Figure S1 for the schematics of the complete design.

Statistics

All statistical analysis and data visualization were carried out using Prism (GraphPad, version 7). For all the experiments, the number of biological replicates and statistical tests applied are reported in the text or in the figure legends. Graphs and data in the text are reported as the mean \pm SEM, each biological replicate is individually plotted. The level of statistical significance was set at $p < 0.05$ for all tests. Asterisks denote statistical significance as follow: * $p \leq 0.05$, ** $p \leq 0.01$, ns. indicates no significance.

For the analysis of the effect of neuronal activity on node-like cluster formation and myelination *in vitro* and *ex vivo*, the design involved a pairing, therefore groups were compared using two-sided paired tests. For the quantification of node-like clusters density *in vivo* and *ex vivo*, two-sided unpaired tests were used. When the sample size was $n \geq 6$, we assessed for the normality of the distribution using a Shapiro–Wilk test and used accordingly parametric tests when the distribution was not significantly different than a normal distribution and non-parametric tests were applied otherwise. When the sample size was $n < 6$, parametric tests were used assuming the normality of the distributions since in these cases each individual sample represented a large number of repeated measures.

Results

Neuronal activity promotes node-like clustering along GABAergic hippocampal axons *in vitro*

To address the effect of neuronal activity on the formation of node-like clusters, we first used a model of mixed hippocampal culture from rat embryos (with neurons both glutamatergic and GABAergic, oligodendroglial cells and astrocytes). In these cultures as well as *in vivo* in mice and rats, it has previously been shown that node-like clusters are formed specifically along some GABAergic neurons in the hippocampus (Freeman et al., 2015; Bonetto et al., 2019; Dubessy et al., 2019; Thetiot et al., 2020). The clustering starts at 14 DIV and the number of GABAergic neurons with node-like clusters increases until it reaches a plateau between 17 and 21 DIV (Freeman et al., 2015). The first data obtained regarding this question were performed in the team by pharmacological inhibition of neuronal activity on hippocampal cultures using tetrodotoxin and showed a reduced number of GABAergic neurons with node-like clusters following the tetrodotoxin treatment (Sol-Foulon and Mazuir, unpublished). To address the impact of neuronal activity on node-like clusters formation, we further transduced neurons with adenovirus inducing the expression of hM3Dq or hM4Di fused with the reporter mCherry, and subsequently treated them with N-clozapine (CNO, 0.5 μ M) starting at 8 DIV until culture were fixed (Figure 1A). Neurons were first transduced with the hM4Di construction, allowing to decrease their firing activity upon CNO treatment. We assessed for the proportion of transduced GABAergic neurons with node-like clusters at 17 DIV (when this number normally approaches its plateau) following treatment compared to control. Following treatment with CNO, we found a significant decrease of 15% of the proportion of transduced GABAergic neurons that formed node-like clusters compared to DMSO treated controls ($p=0.0011$, $n=3$, Figure 1B-D). The hippocampal mixed cultures transduced with hM3Dq, which increases the excitability upon CNO treatment, were fixed at 14 DIV when GABAergic neurons start to form node-like clusters. Following CNO treatment, we found that the proportion of transduced GABAergic neurons with node-like clusters was significantly increased by about 30% compared to DMSO treated controls ($p=0.0483$, $n=4$, Figure 1C-D). Furthermore, these effects were restricted to GABAergic neurons, and the stimulation of the neuronal activity did not trigger node-like clustering in non-GABAergic neurons showing that the effect was restricted to neurons which spontaneously form node-like clusters without stimulation (Figure S2). Together, these results suggest that node-like clusters formation is promoted by neuronal activity along the axons of GABAergic hippocampal neurons.

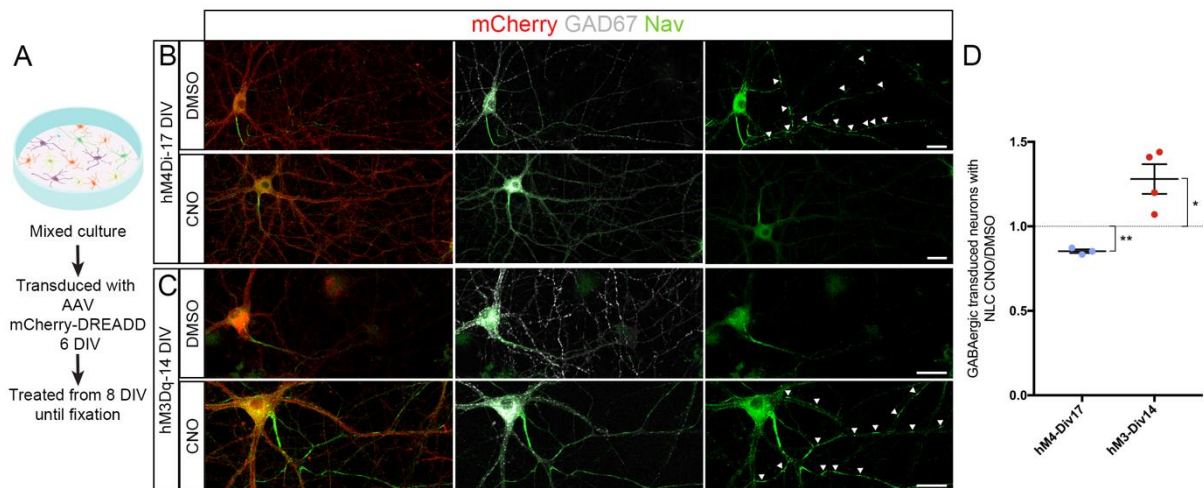


Figure 1: The formation of node-like clusters along axons of GABAergic neurons is modulated by chemogenetic control of neuronal activity. (A) Schematics of the experimental design. (B-C) Orthogonal projections showing GABAergic neurons (GAD67 positive, gray) efficiently transfected (mCherry positive, red). (B) On the first line at 17 DIV the transfected neuron in control condition (DMSO) has node-like clusters along its axon (Nav positive, green, white arrowheads) whereas in the same condition after a CNO treatment activating hM4Di receptors, the formation of node-like clusters is inhibited (second row). (C) At 14 DIV, a higher proportion of GABAergic neurons expressing hM3Dq form node-like clusters along their axons following a treatment with CNO (second row) than without activation of hM3Dq (DMSO, first row). (D) Plot showing the ratio between the proportion of transduced GABAergic neurons with node-like clusters following a stimulation with CNO and following a control treatment with DMSO. Each value individually plotted correspond to 1 biological replicate, (hM4Di) n=3, (hM3Dq) n=4 different experiments, 60 GAD67+mCherry+ neurons quantified on average. Two-sided paired t-tests were used to assess differences of the proportion of node-like clusters forming GABAergic neurons following control treatment with DMSO or treatment with CNO (0.5 μ M). Scale bars: 30 μ m.

Purkinje cell axons also form node-like clusters prior to myelination both *in vivo* and *ex vivo*

To gain insight into the function of neuronal activity in node-like cluster formation, we looked for another more integrated paradigm with a neuronal population that would form node-like clusters prior to myelination. We previously described that node-like clusters are formed prior to the spontaneous myelination of Purkinje cells axons, in organotypic cerebellar slices (Lubetzki et al., 2020a; Ronzano et al., 2021). We first assessed whether node-like clusters also form along Purkinje axons *in vivo*. The granular layer of the cerebellum starts to be myelinated between P10 and P12 and is almost completely myelinated by P15 (Gianola et al., 2003). Therefore, we assessed the presence of node-like clusters along Purkinje cell axons using sagittal sections of the cerebellum from P10 animals. We found clusters of Nav channels along unmyelinated axons in the cerebellar cortex upstream to the front of myelination (Figure 2A-B). These clusters were mainly found in the areas to be myelinated, with several clusters that can form along the same axon (Figure 2B). We then quantified these clusters and found on average 340 ± 61 cluster/mm² (n=4 animals, Figure 2C), which is similar to what we observed

previously *ex vivo* at the onset of myelination (426 ± 67 , $n=5$ animals, 3-4 DIV, $p=0.3913$, Figure 2C-E). Furthermore, in some cases several node-like clusters were found along the same individual axon or faced heminode like it was previously described in other models (Figure 2D-E) (Freeman et al., 2015; Thetiot et al., 2020; Vagionitis et al., 2021). Thus, in the cerebellum node-like clusters are formed prior to myelination *in vivo* and *ex vivo* in similar proportions. This results further validate the *ex vivo* model as suitable model to investigate node-like cluster formation.

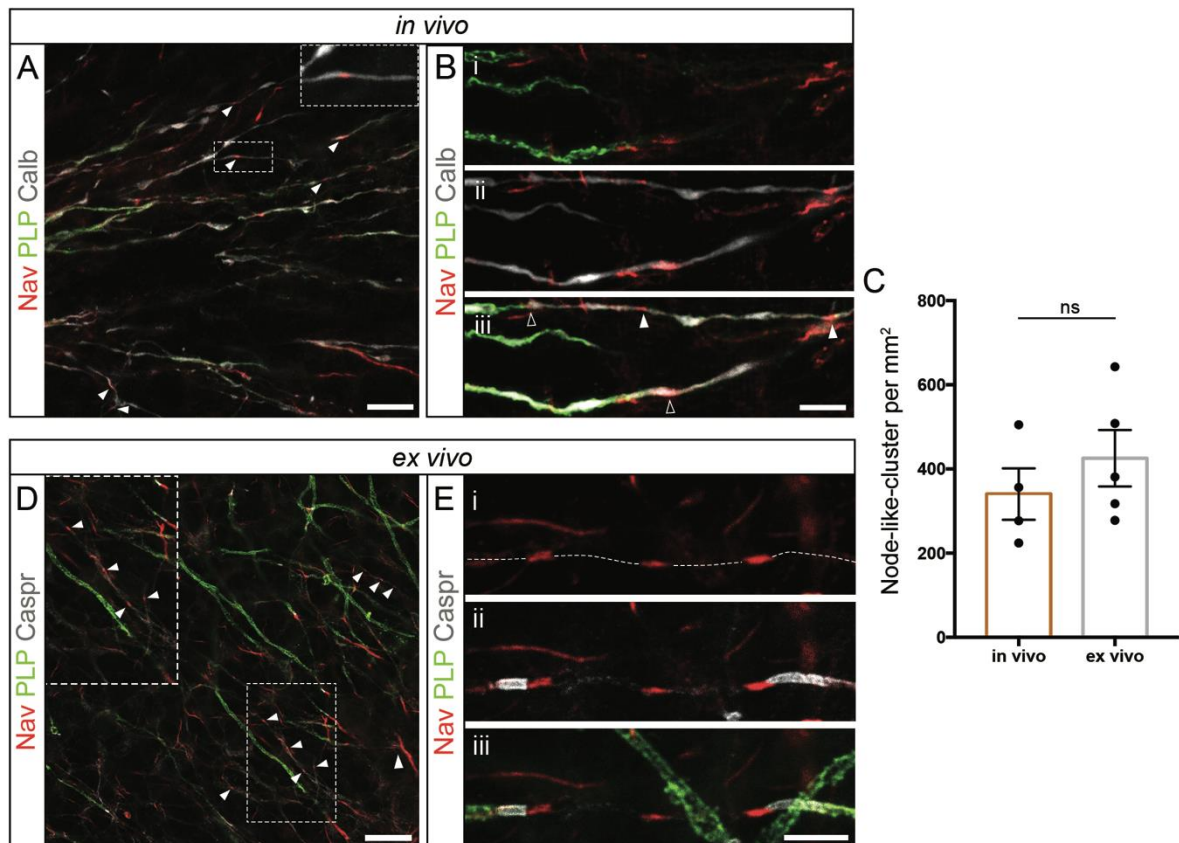


Figure 2 : Node-like clusters are formed prior to myelination along Purkinje cells axons *in vivo* and *ex vivo*. (A) Orthogonal projection of a section of cerebellum at P10 showing Purkinje cells axons (Calbindin, in gray), with clusters of Nav channels (red, white filled arrowhead) along unmyelinated part of their axons (myelin stained by PLP, green). (B) Orthogonal projection showing at a higher magnification two Nav clusters (filled arrowhead) along an unmyelinated portion of the same axon and heminodes at the extremity of the myelin sheaths (contour arrowhead). (C) Quantification of node-like clusters in the cerebellum *in vivo* at P10 and *ex vivo* at 3-4 DIV show similar densities of node-like structures, each value individually plotted correspond to 1 animal, *in vivo* $n=4$ and *ex vivo* $n=5$ animals. (D) Immunohistostainings on a cerebellar organotypic slices at 4 DIV showing Nav clusters (in red, filled arrowheads) along unmyelinated axons (PLP, in green) without paranodal clustering (gray, Caspr). The diffused Caspr signal allow to follow unmyelinated Purkinje axons. (E) Example of a Nav cluster isolated surrounded by two heminodes along the same axons (dashed line traced using the faint diffuse Caspr staining). (C) Two-sided unpaired t-test. Scale bars: (A) 10 μm , (B,E) 5 μm , (D) 20 μm . The quantification *ex vivo* was made by M.Thetiot and A.Desmazières (unpublished data).

Chemogenetic stimulation of Purkinje neurons promotes node-like cluster formation prior to myelination along their axons

To assess the role of neuronal activity in the clustering of node-like structures along Purkinje cell axons, we first used a chemogenetic strategy. As *in vivo* chemogenetic manipulations of Purkinje cells activity in young postnatal animals might be aversive, we used cerebellar organotypic cultures in which node-like cluster formation is similar to what is observed *in vivo*. We first transduced Purkinje cells with the constructs previously used *in vitro*, inducing the expression of hM3Dq or hM4Di fused with the reporter mCherry. We then recorded the firing activity of transduced Purkinje cells in control conditions and upon treatment with CNO (0.5 μ M). Recording from Purkinje cells expressing hM3Dq-mCherry, we found that in control condition the firing frequency was on average 4.5 ± 1.0 Hz and was multiplied by 4 upon CNO treatment 18.4 ± 4.0 Hz (n=8 cells, p=0.0156, Figure S3A-C). Although the activity was strongly increased following hM3Dq receptor activation, the firing frequency of Purkinje cells stayed in a range of frequency close to what was reported in postnatal development *in vivo* (Arancillo et al., 2015). We then recorded from hM4Di-mCherry positive Purkinje cells and found a mild inhibition of the firing frequency following CNO treatment (2.4 ± 0.5 Hz in DMSO vs 1.7 ± 0.4 Hz in CNO, p=0.0250, n=16 cells, Figure S3D-E). This mild inhibition might come from the fact that Purkinje cells tend to be less active *ex vivo* than *in vivo*.

In the cerebellum, it was previously described that neuronal activity of local interneurons in the molecular layer and white matter but not Purkinje cell activity modulates oligodendrogenesis (Zonouzi et al., 2015). Therefore, to determine whether Purkinje cell activity could rather modulate myelin deposition, we quantified myelination along neighboring Purkinje cells that had been differentially stimulated. We took advantage of the sparse expression of hM3Dq-mCherry amongst Purkinje cells and found that the length of axons covered by myelin was higher on cells that had been stimulated with CNO than on their non-transduced neighbors (ratio 1.53 ± 0.09 , n=4 animals, Figure S4A-B). Furthermore, the ratio of myelin length between hM3Dq-mCherry positive vs negative neighboring cells was significantly higher in CNO treated slices than in control conditions (0.66 ± 0.07 DMSO vs 1.53 ± 0.09 CNO, p=0.0100, n=4 animals, Figure S4C-D). Conversely, when we quantified the ratio of myelination along hM4Di-mCherry positive vs negative Purkinje cells, we found that CNO treatment tended to decrease myelination (0.99 ± 0.05 DMSO vs 0.77 ± 0.08 CNO, p=0.0594, n=8 animals, Figure S4E-G). In this latter experiment, the effect might have been reduced owing to the minor inhibition of firing activity in hM4Di positive Purkinje cells treated with CNO. Altogether these results suggest that neuronal activity of Purkinje cells promotes myelination in an axon specific manner.

Once we had characterized the modulation of Purkinje cells firing by chemogenetic and the role of their activity in the process of myelination, we aimed at testing the effect of the stimulation on node-like clusters formation. To do so, we used hM3Dq stimulation to increase Purkinje cell activity. One hour after the end of stimulation, we assessed the number of node-like clusters and myelination along the same domain of axon than previously (Figure 3A). At this time point, about 30% of the distance measured was myelinated on average and there was no difference in the ratio of myelination between hM3Dq-mCherry positive and negative cells following CNO or control treatment (2.05 ± 1.47 DMSO vs 1.18 ± 0.29 CNO, $p=0.5944$, paired t-test, $n=5$ animals). However, when we quantified the number of node-like clusters along Purkinje cell axons, we found that the ratio between hM3Dq-mCherry positive and negative cells was increased by almost a factor of 2 following CNO treatment (0.80 ± 0.11 DMSO vs 1.48 ± 0.19 CNO, $p=0.0470$, $n=5$ animals, Figure 3B-E). Thus, it suggests that neuronal activity of Purkinje axons increases node-like clusters formation specifically along stimulated cells prior to its effect on myelination.

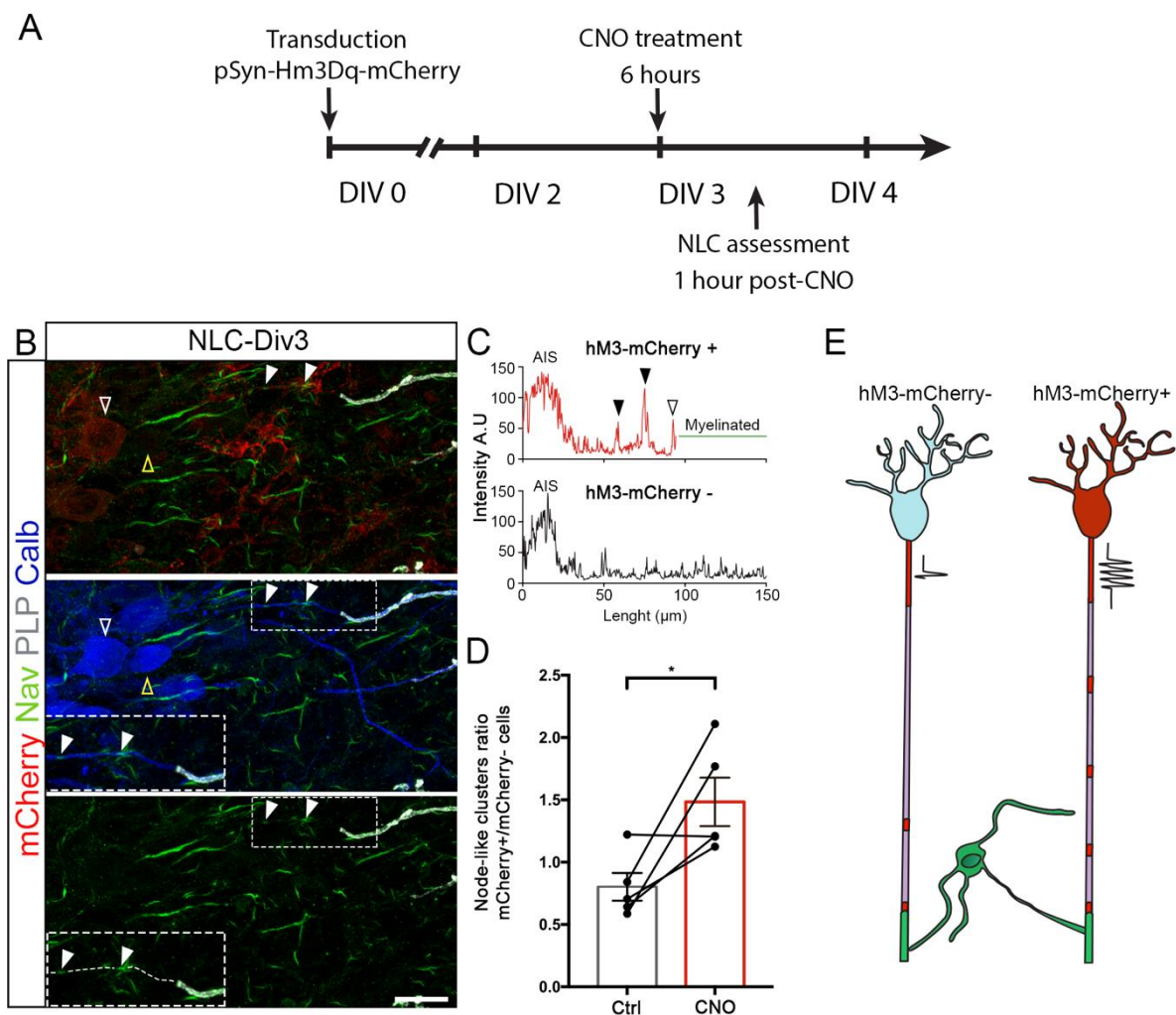


Figure 3: The formation of node-like clusters along Purkinje cell axons is promoted by chemogenetic stimulation of neuronal activity. (A) Schematics of the timeline of the experimental design. (B) Immunohistostaining on a cerebellar organotypic slice transduced with hM3Dq-mCherry and fixed at 3 DIV one hour after the end of the CNO treatment (0.5 μ M) showing two neighbor Purkinje cells and their axon (Calb, blue), one expressing mCherry (red, contour white arrowhead) and the other not (yellow contour arrowhead). Along the axon of the mCherry positive cell two node-like clusters have been formed (green, filled white arrowheads) but none has been formed along the axon of the mCherry negative neuron. (C) Plot profiles of the intensity of Nav staining along the axon of the mCherry positive and mCherry negative Purkinje cells in (B). The black filled arrowheads show the position of node-like clusters and the contour arrowhead the position of the heminode. (D) Quantification of the ratio of the number of node-like clusters along mCherry positive vs mCherry negative Purkinje axons in slices treated with CNO or its solvent DMSO (ctrl), each value individually plotted correspond to 1 animal, n=5 animals. (E) Schematics summarizing the observations. (D) Two-sided paired t-test. Scale bar: (B) 20 μ m.

Optogenetic stimulations of Purkinje neurons recapitulates the results obtained with the chemogenetic approach

The modulation of neuronal activity with DREADDs used previously is based on muscarinic mutant receptors, G-couple proteins that upon activation modulate activity but also lead to the activation of Gi and Gq canonical pathways (Sternson and Roth, 2014; Roth, 2016). To confirm that the formation of node-like clusters depends on neuronal activity itself, we used optogenetic as a second method to stimulate neuronal activity. Furthermore, using organotypic slices from L7-ChR2-YFP mice, ChR2-YFP was expressed specifically in Purkinje cells which allow their specific stimulation. To stimulate Purkinje cells with a firing frequency that is close to what we had obtained using chemogenetic activation, we set a stimulation pattern at 10Hz with 10ms long light pulses. Following this pattern of light stimulation, Purkinje cells fired on average at 15.2 ± 2.9 Hz with 1 to 3 action potentials triggered by a single pulse of light (Figure S5) a firing activity close to the one obtained following chemogenetic activation (~ 18 Hz).

Due to the late onset of L7 promoter expression during the postnatal development only a subpart of the cells was ChR2-YFP positive at the time of the experiment, therefore we could as previously compare myelination and node-like clustering on Purkinje cells stimulated or not within the same slice. First by using the same timeline than previously with hM3Dq activation, we measured myelination along ChR2-YFP positive and negative Purkinje cells on stimulated and non-stimulated slices (Figure S4A). Following optogenetic stimulation, the ratio of myelination was significantly increased by about 50% on stimulated compared to non-stimulated slices (0.84 ± 0.06 non-stimulated vs 1.26 ± 0.10 stimulated, $p=0.0072$, $n=7$ animals, Figure S4H-J). This result supports a role of Purkinje cell neuronal activity in promoting myelination in an axon specific manner.

Next, we aimed at studying the effect of the stimulation on node-like clusters formation. To do so, we used the same protocol of stimulation and quantified the number of node-like clusters one hour after the end of the stimulation (Figure 4A). At this time point, about 20% of the distance measured was myelinated on average and there was no difference in the ratio of myelination between ChR2-YFP positive and negative cells in stimulated vs non stimulated slices (1.51 ± 0.25 non stimulated vs 1.63 ± 0.60 stimulated, $p=0.8125$, Wilcoxon paired test, $n=5$ animals). However, when we quantified the number of node-like structures, we found that the ratio of their number was increased by 50% following optogenetic stimulation compared to non-stimulated slices (1.00 ± 0.09 DMSO vs 1.49 ± 0.19 CNO, $p=0.0489$, $n=5$ animals, Figure 4B-E). Taken together, these observations corroborate the results obtained using chemogenetic stimulations and confirmed that neuronal activity itself promotes node-like clustering along Purkinje cell axons prior to its effect on myelination.

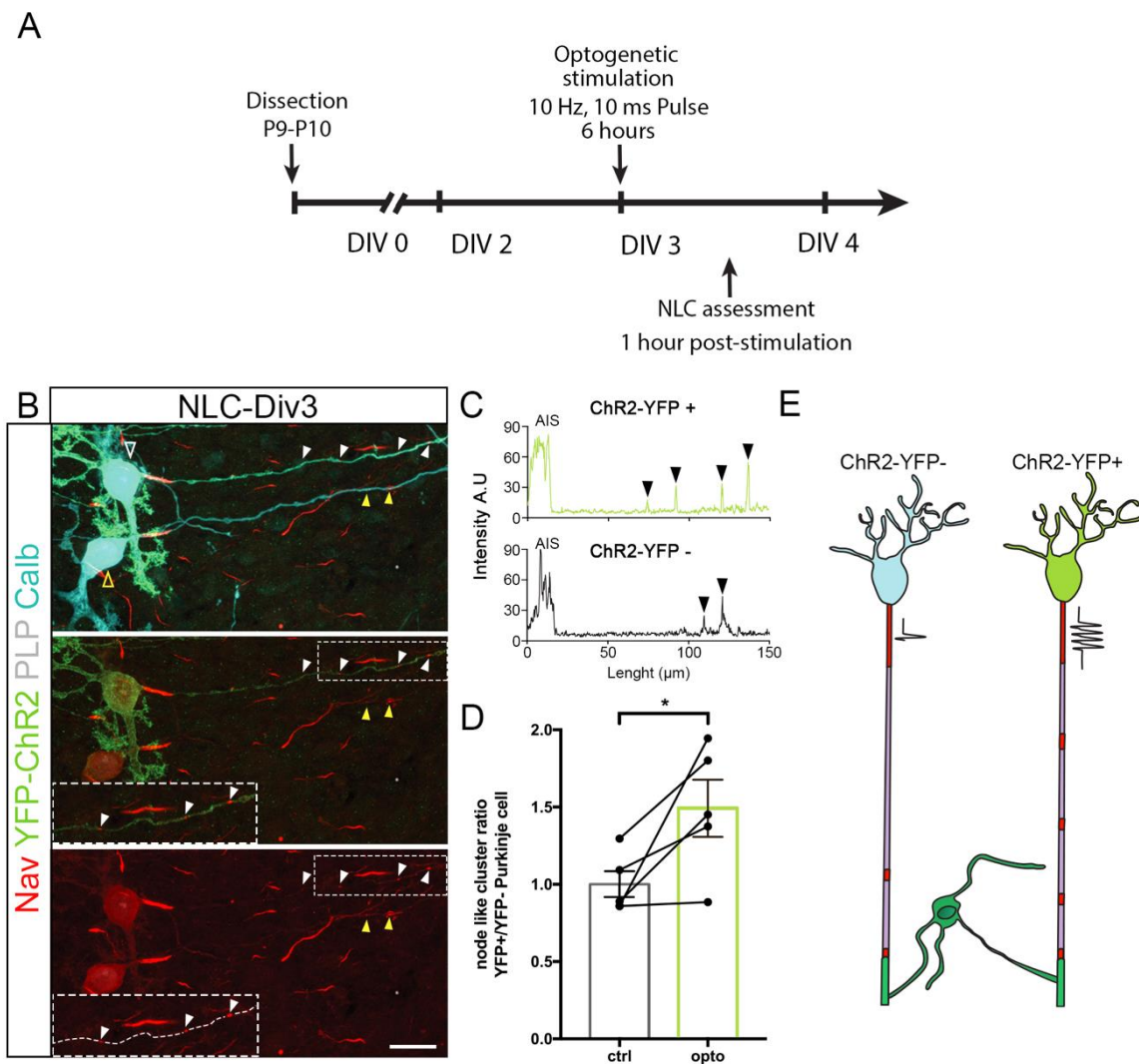


Figure 4: The formation of node-like clusters along Purkinje cells axons is promoted by optogenetic stimulation of neuronal activity. (A) Schematics of the timeline of the experimental design. (B) Immunohistostaining on a L7-ChR2-YFP cerebellar organotypic slices fixed at 3 DIV one hour after the end of the optogenetic stimulation showing two neighbor Purkinje cells and their axon (Calb, cyan), one expresses YFP (green, contour white arrowhead) and the other does not (yellow contour arrowhead). Along the axon of the YFP positive cell four node-like clusters have been formed (red, filled white arrowheads) and two of them have been formed along the axon of the YFP negative neuron (filled yellow arrowheads). (C) Plot profiles of the intensity of Nav staining along the axon of the YFP positive and YFP negative Purkinje cells in (B). The black filled arrowheads show the position of node-like clusters. (D) Quantification of the ratio of the number of node-like clusters along YFP positive vs YFP negative Purkinje axons in slices stimulated by optogenetic or not (ctrl), each value individually plotted correspond to 1 animal, n=5 animals. (E) Schematics summarizing the observations. (D) Two-sided paired t-test. Scale bar: (B) 20 μm .

Discussion

In this study, we showed *in vitro* and *ex vivo* that node-like cluster formation is promoted by neuronal activity. We further showed on a model of cerebellar organotypic slices using chemogenetic and optogenetic stimulations that both node-like clustering and myelination depend on neuronal activity along Purkinje cell axons, in an axon specific manner. Lastly, node-like clusters are formed along Purkinje cell axons *in vivo* prior to myelination with a similar density than *ex vivo*, therefore this mechanism of neuronal activity dependent node-like clustering may be at play *in vivo* and might constitute a priming step in the process of myelination.

Mechanism of node-like clustering

Our experiments provide first evidence that the formation of node-like clusters is promoted by neuronal activity. However, the exact mechanism involved in this modulation remains to be investigated. It has been previously described that the expression of AnkyrinG, $\beta 2\text{Nav}$ and oligodendroglial secreted factors are necessary to form node like clusters (Kaplan et al., 2001; Freeman et al., 2015; Dubessy et al., 2019; Thetiot et al., 2020). Thus, the effect of neuronal activity could modulate oligodendroglial secretions and indirectly promote node-like clusters formation. This possibility is rather unlikely since the effect of neuronal activity is axon specific. However, to determine the possible participation of oligodendroglial cells to this neuronal activity-dependent mechanism, experiments using purified neuron cultures treated with oligodendrocyte conditioned medium (Kaplan et al., 2001; Freeman et al., 2015; Dubessy et al., 2019), will be necessary. Another possibility is that the effect of neuronal activity promotes node-like clusters formation by acting directly on the synthesis of nodal proteins or on their transport and targeting along axons, two essential mechanisms for node-like clustering *in vitro* (Kaplan et al., 2001; Thetiot et al., 2020). Indeed, neuronal activity modifies neuronal transcriptome (Lacar et al., 2016; Hu et al., 2017; Hrvatin et al., 2018; Yap and Greenberg,

2018), but to our knowledge there are no clear data yet on nodal protein transcripts changes upon electrical stimulation in the two models used in this study. Neuronal activity has also been shown to modulate trafficking along the axon and therefore might modulate nodal proteins transport (Ohno et al., 2011; Chen and Sheng, 2013). Lastly, neuronal activity promotes synaptic vesicular release with an enrichment at the heminodes and along unmyelinated segments of axons (Almeida et al., 2021), thus neuronal activity might also promote the release of nodal proteins transporting vesicles at specific sites, further resulting in clustering of nodal proteins. This hypothesis is supported by the early expression of calcium channels along unmyelinated axon of the optic nerve (Alix et al., 2008), the small permeability of Nav channels to calcium (Hanemaaijer et al., 2020) and by the observation of calcium signals along unmyelinated Purkinje cell axons upon neuronal stimulation (Callewaert et al., 1996). Calcium transients triggered by action potential might activate fusion of nodal proteins loaded vesicles and promote the clustering in these two populations of node-like clusters forming neurons. Further investigations will be needed to gain insight into the participation of each of these mechanisms in the regulation of node-like clusters formation by activity.

Role of node-like clusters formation in myelination

The formation of node like clusters along axons prior to myelination has been shown to participate to mature node formation (Thetiot et al., 2020; Malavasi et al., 2021; Vagionitis et al., 2021). Furthermore, these clusters have been suggested to modulate myelination by two main mechanisms. First, a study from our team on hippocampal cultures from rodents shown that node-like clusters might guide myelination, with the initiation of myelination occurring at the direct vicinity of the clusters (Thetiot et al., 2020). Furthermore, *in vivo* in zebrafish it has been shown that the location of some node-like clusters often predefine the future localization of a mature node of Ranvier, suggesting that a subset of node-like clusters along axons might be landmarks for the future pattern of myelination (Vagionitis et al., 2021). Here we have shown that the effect of neuronal activity on the formation of node-like clusters precedes the effect on myelination. Indeed, one hour after the end of the stimulation, we observed that the number of node-like clusters along stimulated axons is increased whereas myelination is increased only more than half a day later. This raises the possibility that node-like cluster formation participates in activity-dependent myelin deposition. In particular, the presence of node-like clusters might promote the fusion of synaptic vesicles, like it has been previously described at the heminode (Almeida et al., 2021). Although the release of synaptic vesicles has often been associated with myelin sheath stabilization and growth (Hines et al., 2015; Mensch et al., 2015; Koudelka et al., 2016; Almeida et al., 2021), synaptic vesicle release along the axon at close contacts between pre-myelinating oligodendrocyte and electrically active axons has also been shown to

promote MBP local synthesis at the contact and may promote the initiation of myelination (Wake et al., 2015).

Node-like clusters in remyelination

Node-like clusters have been observed along axons prior to remyelination both along Purkinje cell axons in mouse and on partially remyelinated plaques from MS patients (Coman et al., 2006; Lubetzki et al., 2020a). The function of node-like cluster formation prior to remyelination remains elusive, and it is in particular not known whether they could directly promote remyelination. Extrapolating what has been suggested in developmental myelination (Vagionitis et al., 2021), it can be hypothesized that node like clusters might participate in defining the pattern of remyelination that is highly conserved in remyelination along previously continuously myelinated axons (Auer et al., 2018; Orthmann-Murphy et al., 2020; Snaidero et al., 2020). Furthermore, it has been shown that neuronal activity is a key modulator of remyelination and repeated neuronal stimulation allow a more efficient remyelination (Gautier et al., 2015; Jensen et al., 2018; Ortiz et al., 2019; Bacmeister et al., 2020). In this context, it would be interesting to assess the role of neuronal activity in node-like cluster formation and the function of these structures in remyelination. Of note, it has been described that following demyelination with cuprizone the scaffolding nodal protein spectrin β IV remains clustered at the site of former nodes of Ranvier (Orthmann-Murphy et al., 2020). These clusters were suggested to serve as landmarks for remyelination pattern which indicates that repair mechanisms might differ from developmental myelination during which nodal domains are formed *ex nihilo*. Thus, future studies will have to determine how remyelination restores the pattern of myelination and whether node-like clusters are at play in this mechanism.

Supplementary figures

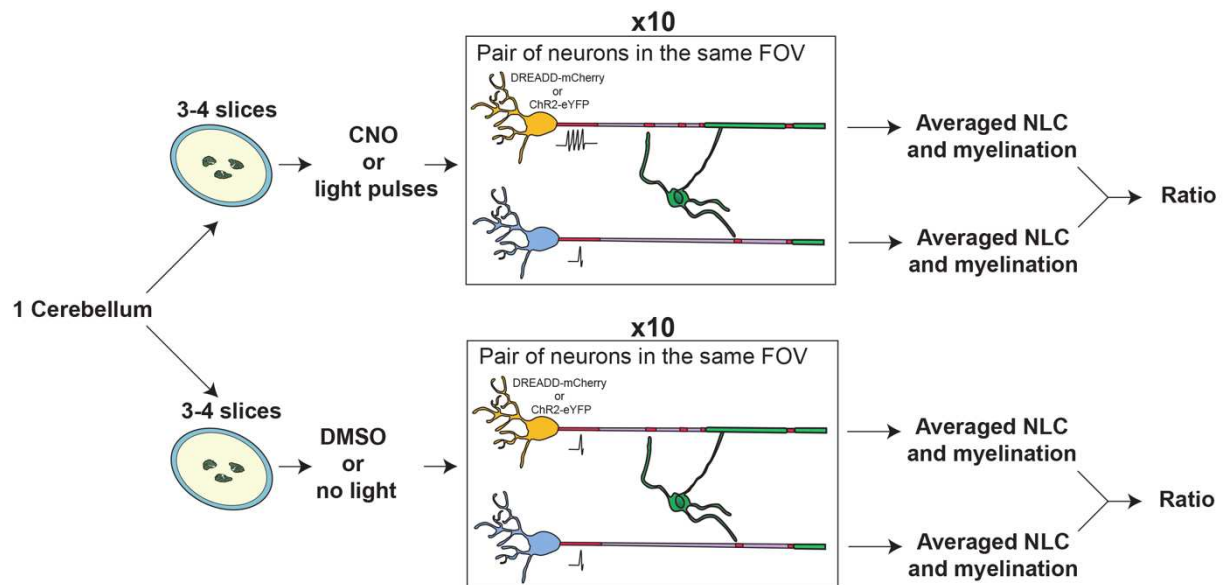


Figure S1 : Experimental design used to assess the effect of neuronal activity on node-like cluster formation and myelination on neighboring Purkinje neurons. From one cerebellum 6 to 8 slices from the vermis are splitted in two groups and put in culture on porous membrane. From these two sets of slices, 1 is treated with CNO or stimulated with light and the other one is treated with DMSO or only transferred in the medium for light stimulation but is not exposed to it. On fixed slices, depending on the set of experiment, the number of node-like clusters (NLC) along the axons or the proportion of axons myelinated is assessed in 10 pairs of neurons, one expressing either mCherry-DREADD or ChR2-eYFP (in orange) and one negative for these markers (in blue). These pairs are taken within the same field of view (FOV) of $387.69 \mu\text{m} \times 387.69 \mu\text{m}$ to avoid effect of the environment. The parameter measured is then averaged among each population separately and the ratio between the two populations is reported for the stimulated and non-stimulated slices. This design allows to compare the effect of the stimulation with an internal control within the slice, and to isolate the effect of this simulation from the effect of mCherry-DREADD or ChR2-eYFP expression without light stimulation.

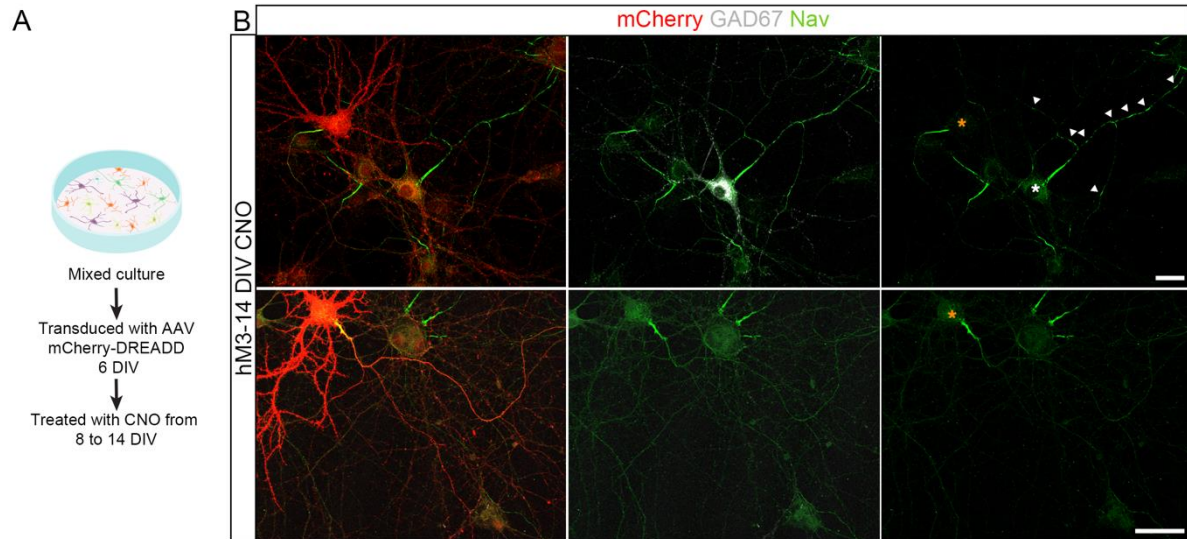


Figure S2: Neuronal activity stimulation does not trigger node-like clustering along non-GABAergic neurons. (A) Schematics of the experimental design. (B) Orthogonal projections showing GABAergic (GAD67 positive, gray) and non-GABAergic hM3Dq-mCherry transfected neurons (red) stimulated from 8 to 14 DIV with CNO (0.5 μ M). The first line shows one GABAergic neuron (white asterisk) with node-like clusters (white arrowheads) along its axon and one non-GABAergic neuron (orange asterisk) with no node-like cluster. On the second line, another example of a hM3Dq-mCherry transfected non-GABAergic neuron at 14 DIV following CNO treatment is shown with no node-like cluster along its axon. Scale bars: 30 μ m.

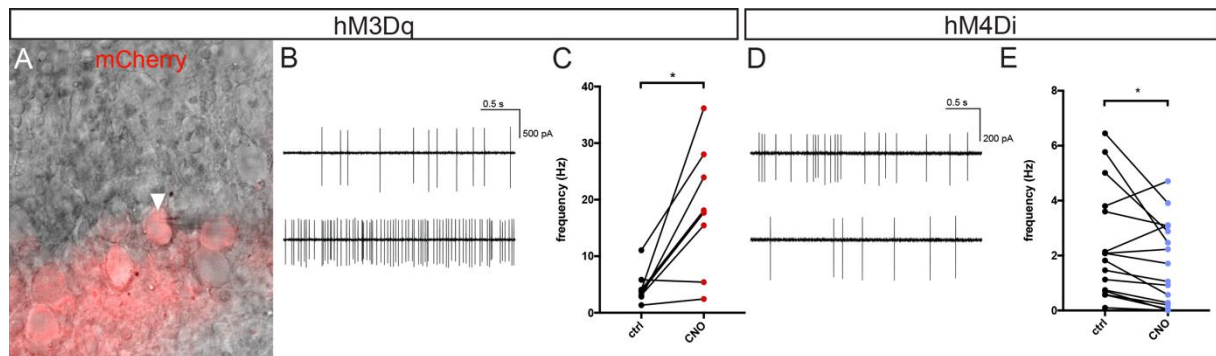


Figure S3: Chemogenetic allows modulations of the firing activity of Purkinje cells in organotypic cerebellar slices. (A) Example of a hM3Dq-mCherry transduced Purkinje cell (filled white arrowhead) recorded in loose cell-attached voltage clamp. (B, D) Representative examples of loose-cell attached voltage clamp recordings on hM3Dq-mCherry (B) or hM4Di-mCherry (D) transduced Purkinje cells, in control condition (DMSO, first row) followed by CNO treatment (0.5 μ M, second row). (C, E) Quantification of the mean firing frequency of hM3Dq-mCherry (C) or hM4Di-mCherry (E) transduced Purkinje cells in control condition (ctrl) and following addition of CNO. Each individual points represent the mean for 1 recorded cell, hM3Dq: n=8 cells from 4 animals; hM4Di: n=16 cells from 9 animals.

A

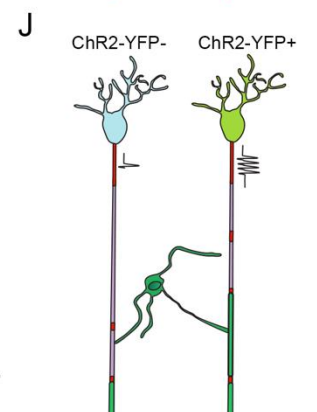
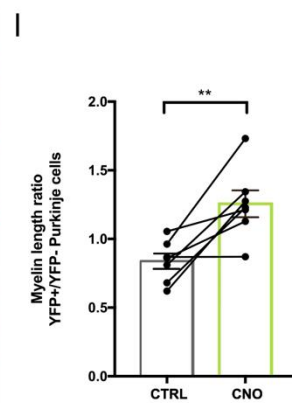
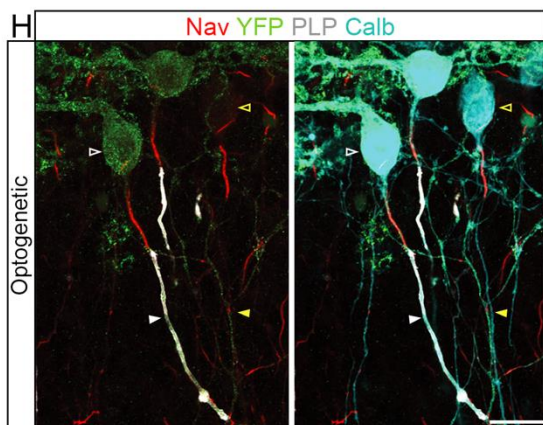
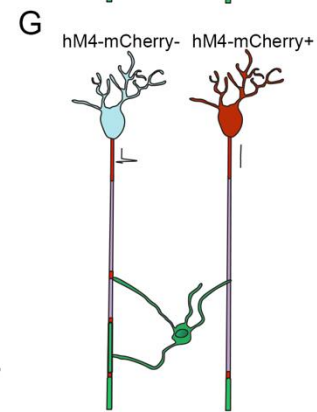
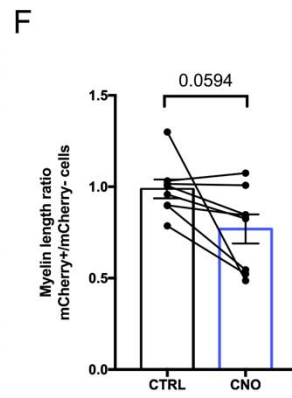
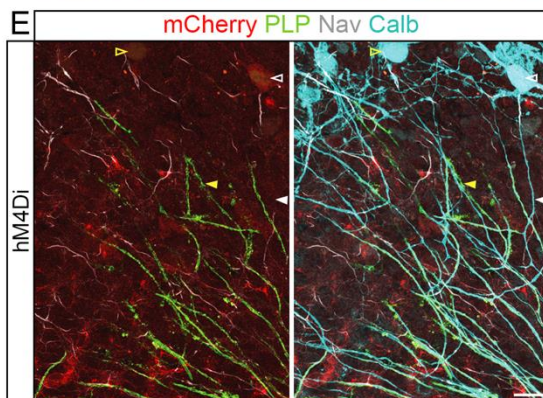
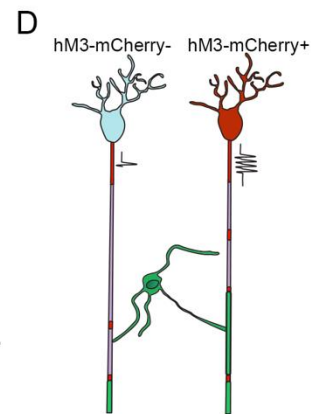
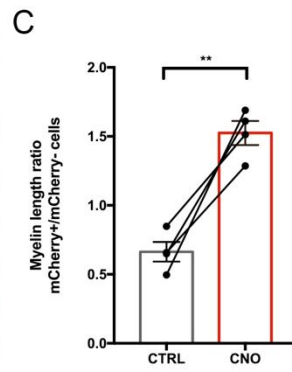
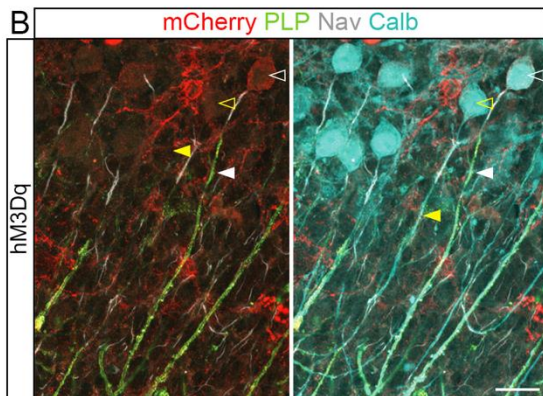
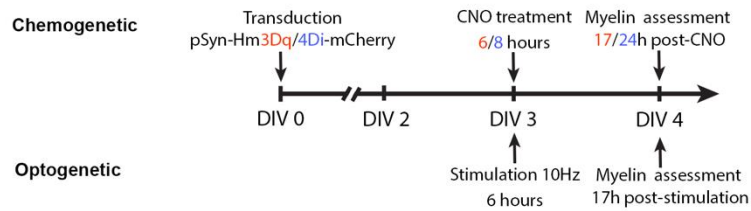


Figure S4: Chemogenetic and optogenetic modulations of neuronal activity regulate myelination in an axon specific manner. (A) Schematics of the timeline of the experimental design for chemogenetic and optogenetic experiments. (B, E) Immunohistostaining on a cerebellar organotypic slices transduced with hM3Dq-mCherry (B) or hM4Di-mCherry (E) and fixed at 4 DIV, 17 (B) or 24 (E) hours after the end of the CNO treatment (0.5 μ M) showing two neighbor Purkinje cells and their axon (Calb, cyan), one expresses mCherry (red, contour white arrowhead) and another does not (yellow contour arrowhead).

Along the axon of the mCherry positive cell myelination is promoted (B) or delayed (E) (PLP, in green, filled white arrowhead) compared to the mCherry negative axons (filled yellow arrowhead). (C, F) Quantification of the ratio of myelination along mCherry positive vs negative Purkinje axons in slices transduced with hM3Dq-mCherry (C) or hM4Di-mCherry (F) and treated with CNO or its solvent DMSO (ctrl). (H) Immunohistostaining on a L7-ChR2-YFP cerebellar organotypic slice fixed at 4 DIV, 17 hours after the end of the optogenetic stimulation showing two neighbor Purkinje cells and their axon (Calb, Cyan), one expresses YFP (green, contour white arrowhead) and another does not (yellow contour arrowhead). On the YFP positive cell the proximal part of the axon is myelinated (gray, filled white arrowheads) but no myelin has been formed along the proximal part of the YFP negative axon (filled yellow arrowheads). (I) Quantification of the ratio of myelination along YFP positive vs negative Purkinje axons in slices stimulated optogenetically or not. (C, F, I) Each value individually plotted corresponds to 1 animal, (C) n=4, (F) n=8, (I) n=7 animals. (D, G, J) Schematics summarizing the observations. (C, F, I) Two-sided Paired t-tests. Scale bars: (B) 50 μm , (E, H) 20 μm .

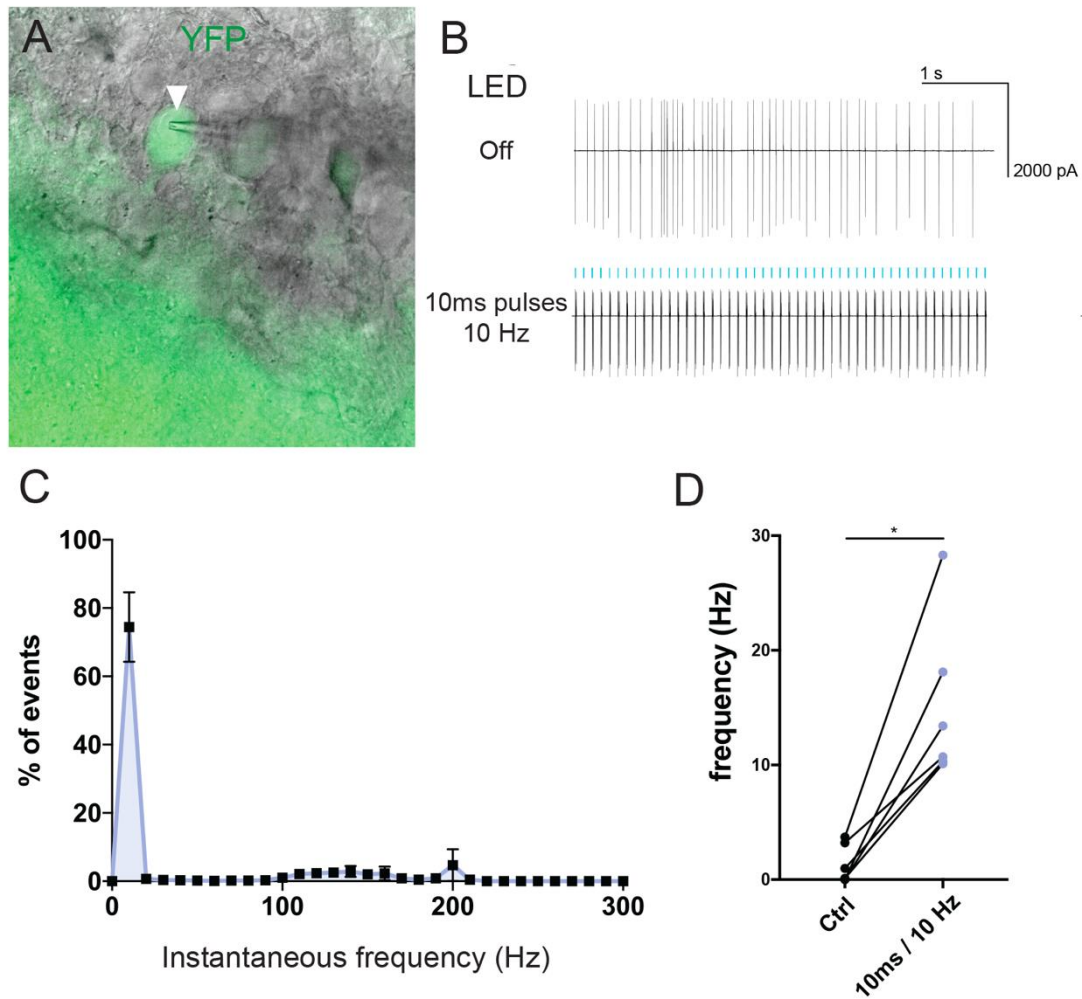


Figure S5: Optogenetic stimulations precisely set the firing activity of Purkinje cells in L7-ChR2-YFP organotypic cerebellar slices. (A) Example of a ChR2-YFP expressing Purkinje cell (in green, filled white arrowhead) recorded in loose cell-attached voltage clamp. (B) Representative examples of loose-cell attached voltage clamp recordings on a ChR2-YFP expressing Purkinje cells, in control condition (LED off) followed by stimulation at 10Hz with 10ms long light pulses at 1,5mW/mm². The pattern of activity (in black) follows the pattern of light (light pulses are indicated with the blue rectangles). (C) Distribution of the instantaneous firing frequency of stimulated Purkinje cells. Most of the light pulses trigger 1 action potential which results in the peak at 10Hz, following some light pulses few cells fire twice or three times with an instantaneous frequency between 100 and 200Hz. Average of n=6 cells from 4 animals. (D) Quantification of the mean firing frequency of Purkinje cells in control condition and following stimulation. Each individual points represent the mean for 1 cell recorded, n=6 cells from 4 animals. Wilcoxon paired test, p=0.0312.

References

- Alix, J. J. P., Dolphin, A. C., and Fern, R. (2008). Vesicular apparatus, including functional calcium channels, are present in developing rodent optic nerve axons and are required for normal node of Ranvier formation. *J. Physiol.* 586, 4069–4089. doi:10.1113/jphysiol.2008.155077.
- Almeida, R. G., Williamson, J. M., Madden, M. E., Talbot, W. S., Bianco, I. H., Lyons, D. A., et al. (2021). Myelination induces axonal hotspots of synaptic vesicle fusion that promote sheath growth. *Curr. Biol.*, 1–12. doi:10.1016/j.cub.2021.06.036.
- Amor, V., Zhang, C., Vainshtein, A., Zhang, A., Zollinger, D. R., Eshed-Eisenbach, Y., et al. (2017). The paranodal cytoskeleton clusters Na⁺ channels at nodes of Ranvier. *Elife* 6, 1–15. doi:10.7554/eLife.21392.
- Arancillo, M., White, J. J., Lin, T., Stay, T. L., and Sillitoe, R. V. (2015). In vivo analysis of Purkinje cell firing properties during postnatal mouse development. *J. Neurophysiol.* 113, 578–591. doi:10.1152/jn.00586.2014.
- Auer, F., Vagionitis, S., and Czopka, T. (2018). Evidence for Myelin Sheath Remodeling in the CNS Revealed by In Vivo Imaging. *Curr. Biol.* 28, 549-559.e3. doi:10.1016/j.cub.2018.01.017.
- Bacmeister, C. M., Barr, H. J., McClain, C. R., Thornton, M. A., Nettles, D., Welle, C. G., et al. (2020). Motor learning promotes remyelination via new and surviving oligodendrocytes. *Nat. Neurosci.* 23, 819–831. doi:10.1038/s41593-020-0637-3.
- Barres, B. A., and Raff, M. C. (1993). Proliferation of oligodendrocyte precursor cells depends on electrical activity in axons. *Nature* 361, 258–260. doi:10.1038/361258a0.
- Birgbauer, E., Rao, T. S., and Webb, M. (2004). Lysolecithin induces demyelination in vitro in a cerebellar slice culture system. *J. Neurosci. Res.* 78, 157–166. doi:10.1002/jnr.20248.
- Bonetto, G., Hivert, B., Goutebroze, L., Karageos, D., Crépel, V., and Faivre-Sarrailh, C. (2019). Selective axonal expression of the Kv1 channel complex in pre-myelinated GABAergic hippocampal neurons. *Front. Cell. Neurosci.* 13, 1–17. doi:10.3389/fncel.2019.00222.
- Callewaert, G., Eilers, J., and Konnerth, A. (1996). Axonal calcium entry during fast “sodium” action potentials in rat cerebellar Purkinje neurones. *J. Physiol.* 495, 641–647.
- Chaumont Joseph, Guyon, N., Valera, A. M., Dugué, G. P., Popa, D., Marcaggi, P., et al. (2013). Clusters of cerebellar Purkinje cells control their afferent climbing fiber discharge. *Proc. Natl. Acad. Sci. U. S. A.* 110, 16223–16228.
- Chen, Y., and Sheng, Z.-H. (2013). Kinesin-1–syntrophin coupling mediates activity-dependent regulation of axonal mitochondrial transport. *J. Cell Biol.* 202, 351–364. doi:10.1083/jcb.201302040.
- Coman, I., Aigrot, M. S., Seilhean, D., Reynolds, R., Girault, J. A., Zalc, B., et al. (2006). Nodal, paranodal and juxtaparanodal axonal proteins during demyelination and remyelination in

- multiple sclerosis. *Brain* 129, 3186–3195. doi:10.1093/brain/awl144.
- Demerens, C., Stankoff, B., Logak, M., Anglade, P., Allinquant, B., Couraud, F., et al. (1996). Induction of myelination in the central nervous system by electrical activity. *Proc. Natl. Acad. Sci. U. S. A.* 93, 9887–9892. doi:10.1073/pnas.93.18.9887.
- Dubessy, A. L., Mazuir, E., Rappeneau, Q., Ou, S., Abi Ghanem, C., Piquand, K., et al. (2019). Role of a Contactin multi-molecular complex secreted by oligodendrocytes in nodal protein clustering in the CNS. *Glia* 67, 2248–2263. doi:10.1002/glia.23681.
- Eshed-Eisenbach, Y., Devaux, J., Vainshtein, A., Golani, O., Lee, S.-J., Feinberg, K., et al. (2020). Precise Spatiotemporal Control of Nodal Na⁺ Channel Clustering by Bone Morphogenetic Protein-1/Tolloid-like Proteinases. *Neuron* 106, 806-815.e6. doi:10.1016/j.neuron.2020.03.001.
- Etxeberria, A., Hokanson, K. C., Dao, D. Q., Mayoral, S. R., Mei, F., Redmond, S. A., et al. (2016). Dynamic modulation of myelination in response to visual stimuli alters optic nerve conduction velocity. *J. Neurosci.* 36, 6937–6948. doi:10.1523/JNEUROSCI.0908-16.2016.
- Freeman, S. A., Desmazières, A., Simonnet, J., Gatta, M., Pfeiffer, F., Aigrot, M. S., et al. (2015). Acceleration of conduction velocity linked to clustering of nodal components precedes myelination. *Proc. Natl. Acad. Sci. U. S. A.* 112, E321–E328. doi:10.1073/pnas.1419099112.
- Gautier, H. O. B., Evans, K. A., Volbracht, K., James, R., Sitnikov, S., Lundgaard, I., et al. (2015). Neuronal activity regulates remyelination via glutamate signalling to oligodendrocyte progenitors. *Nat. Commun.* 6. doi:10.1038/ncomms9518.
- Geraghty, A. C., Gibson, E. M., Ghanem, R. A., Greene, J. J., Ocampo, A., Goldstein, A. K., et al. (2019). Loss of Adaptive Myelination Contributes to Methotrexate Chemotherapy-Related Cognitive Impairment. *Neuron* 103, 250-265.e8. doi:10.1016/j.neuron.2019.04.032.
- Gianola, S., Savio, T., Schwab, M. E., and Rossi, F. (2003). Cell-autonomous mechanisms and myelin-associated factors contribute to the development of Purkinje axon intracortical plexus in the rat cerebellum. *J. Neurosci.* 23, 4613–4624. doi:10.1523/jneurosci.23-11-04613.2003.
- Gibson, E. M., Purger, D., Mount, C. W., Goldstein, A. K., Lin, G. L., Wood, L. S., et al. (2014). Neuronal Activity Promotes Oligodendrogenesis and Adaptive Myelination in the Mammalian Brain. *Science (80-)*. 344, 1252304–1252304. doi:10.1126/science.1252304.
- Hanemaaijer, N. A. K., Popovic, M. A., Wilders, X., Grasman, S., Arocas, O. P., and Kole, M. H. P. (2020). Ca²⁺ entry through nav channels generates submillisecond axonal ca²⁺ signaling. *Elife* 9, 1–75. doi:10.7554/eLife.54566.
- Hines, J. H., Ravanelli, A. M., Schwindt, R., Scott, E. K., and Appel, B. (2015). Neuronal activity biases axon selection for myelination in vivo. *Nat. Neurosci.* 18, 683–689. doi:10.1038/nn.3992.
- Hrvatin, S., Hochbaum, D. R., Nagy, M. A., Cicconet, M., Robertson, K., Cheadle, L., et al. (2018). Single-cell analysis of experience-dependent transcriptomic states in the mouse visual cortex. *Nat. Neurosci.* 21, 120–129. doi:10.1038/s41593-017-0029-5.

- Hu, P., Fabyanic, E., Kwon, D. Y., Tang, S., Zhou, Z., and Wu, H. (2017). Dissecting Cell-Type Composition and Activity-Dependent Transcriptional State in Mammalian Brains by Massively Parallel Single-Nucleus RNA-Seq. *Mol. Cell* 68, 1006-1015.e7. doi:10.1016/j.molcel.2017.11.017.
- Jensen, S. K., Michaels, N. J., Ilyntskyy, S., Keough, M. B., Kovalchuk, O., and Yong, V. W. (2018). Multimodal Enhancement of Remyelination by Exercise with a Pivotal Role for Oligodendroglial PGC1 α . *Cell Rep.* 24, 3167–3179. doi:10.1016/j.celrep.2018.08.060.
- Kaplan, M. R., Cho, M. H., Ullian, E. M., Isom, L. L., Levinson, S. R., and Barres, B. A. (2001). Differential control of clustering of the sodium channels Nav1.2 and Nav1.6 at developing CNS nodes of Ranvier. *Neuron* 30, 105–119. doi:10.1016/S0896-6273(01)00266-5.
- Kaplan, M. R., Meyer-Franke, A., Lambert, S., Bennett, V., Duncan, I. D., Levinson, S. R., et al. (1997). Induction of sodium channel clustering by oligodendrocytes. *Nature* 386, 724–728. doi:10.1038/386724a0.
- Koudelka, S., Voas, M. G. G., Almeida, R. G. G., Baraban, M., Soetaert, J., Meyer, M. P. P., et al. (2016). Individual Neuronal Subtypes Exhibit Diversity in CNS Myelination Mediated by Synaptic Vesicle Release. *Curr. Biol.* 26, 1447–1455. doi:10.1016/j.cub.2016.03.070.
- Lacar, B., Linker, S. B., Jaeger, B. N., Krishnaswami, S. R., Barron, J. J., Kelder, M. J. E., et al. (2016). Nuclear RNA-seq of single neurons reveals molecular signatures of activation. *Nat. Commun.* 7, 11022. doi:10.1038/ncomms11022.
- Lubetzki, C., Sol-Foulon, N., and Desmazières, A. (2020). Nodes of Ranvier during development and repair in the CNS. *Nat. Rev. Neurol.* 16, 426–439. doi:10.1038/s41582-020-0375-x.
- Malavasi, E. L., Ghosh, A., Booth, D. G., Zagnoni, M., Sherman, D. L., and Brophy, P. J. (2021). Dynamic early clusters of nodal proteins contribute to node of Ranvier assembly during myelination of peripheral neurons. *Elife* 10. doi:10.7554/eLife.68089.
- McKenzie, I. A., Ohayon, D., Li, H., De Faria, J. P., Emery, B., Tohyama, K., et al. (2014). Motor skill learning requires active central myelination. *Science (80-)*. 346, 318–322. doi:10.1126/science.1254960.
- Mensch, S., Baraban, M., Almeida, R., Czopka, T., Ausborn, J., El Manira, A., et al. (2015). Synaptic vesicle release regulates myelin sheath number of individual oligodendrocytes in vivo. *Nat. Neurosci.* 18, 628–630. doi:10.1038/nn.3991.
- Mitew, S., Gobius, I., Fenlon, L. R., McDougall, S. J., Hawkes, D., Xing, Y. L., et al. (2018). Pharmacogenetic stimulation of neuronal activity increases myelination in an axon-specific manner. *Nat. Commun.* 9, 1–16. doi:10.1038/s41467-017-02719-2.
- Ohno, N., Kidd, G. J., Mahad, D., Kiryu-Seo, S., Avishai, A., Komuro, H., et al. (2011). Myelination and axonal electrical activity modulate the distribution and motility of mitochondria at CNS nodes of Ranvier. *J. Neurosci.* 31, 7249–7258. doi:10.1523/JNEUROSCI.0095-11.2011.
- Orthmann-Murphy, J., Call, C. L., Molina-Castro, G. C., Hsieh, Y. C., Rasband, M. N., Calabresi, P. A., et

- al. (2020). Remyelination alters the pattern of myelin in the cerebral cortex. *Elife* 9, 1–61. doi:10.7554/eLife.56621.
- Ortiz, F. C., Habermacher, C., Graciarena, M., Houry, P.-Y., Nishiyama, A., Oumesmar, B. N., et al. (2019). Neuronal activity in vivo enhances functional myelin repair. *JCI Insight* 4. doi:10.1172/jci.insight.123434.
- Pan, S., Mayoral, S. R., Choi, H. S., Chan, J. R., and Kheirbek, M. A. (2020). Preservation of a remote fear memory requires new myelin formation. *Nat. Neurosci.* 23, 487–499. doi:10.1038/s41593-019-0582-1.
- Pedraza, L., Huang, J. K., and Colman, D. R. (2001). Organizing Principles of the Axoglial Apparatus. *Neuron* 30, 335–344. doi:10.1016/S0896-6273(01)00306-3.
- Perkins, K. L. (2006). Cell-attached voltage-clamp and current-clamp recording and stimulation techniques in brain slices. *J. Neurosci. Methods* 154, 1–18. doi:10.1016/j.jneumeth.2006.02.010.
- Rasband, M. N., Peles, E., Trimmer, J. S., Levinson, S. R., Lux, S. E., and Shrager, P. (1999). Dependence of nodal sodium channel clustering on paranodal axoglial contact in the developing CNS. *J. Neurosci.* 19, 7516–7528. doi:10.1523/jneurosci.19-17-07516.1999.
- Ronzano, R., Roux, T., Thetiot, M., Aigrot, M. S., Richard, L., Lejeune, F. X., et al. (2021). Microglia-neuron interaction at nodes of Ranvier depends on neuronal activity through potassium release and contributes to remyelination. *Nat. Commun.* 12, 5219. doi:10.1038/s41467-021-25486-7.
- Roth, B. L. (2016). DREADDs for Neuroscientists. *Neuron* 89, 683–694. doi:10.1016/j.neuron.2016.01.040.
- Snaidero, N., Schifferer, M., Mezydło, A., Zalc, B., Kerschensteiner, M., and Misgeld, T. (2020). Myelin replacement triggered by single-cell demyelination in mouse cortex. *Nat. Commun.* 11. doi:10.1038/s41467-020-18632-0.
- Steadman, P. E., Xia, F., Ahmed, M., Mocle, A. J., Penning, A. R. A., Geraghty, A. C., et al. (2020). Disruption of Oligodendrogenesis Impairs Memory Consolidation in Adult Mice. *Neuron* 105, 150-164.e6. doi:10.1016/j.neuron.2019.10.013.
- Stedehouder, J., Brizee, D., Shpak, G., and Kushner, S. A. (2018). Activity-dependent myelination of parvalbumin interneurons mediated by axonal morphological plasticity. *J. Neurosci.* 38, 3631–3642. doi:10.1523/JNEUROSCI.0074-18.2018.
- Sternson, S. M., and Roth, B. L. (2014). Chemogenetic Tools to Interrogate Brain Functions. *Annu. Rev. Neurosci.* 37, 387–407. doi:10.1146/annurev-neuro-071013-014048.
- Stevens, B., Porta, S., Haak, L. L., Gallo, V., and Fields, R. D. (2002). Adenosine: A neuron-glial transmitter promoting myelination in the CNS in response to action potentials. *Neuron* 36, 855–868. doi:10.1016/S0896-6273(02)01067-X.
- Susuki, K., Chang, K. J., Zollinger, D. R., Liu, Y., Ogawa, Y., Eshed-Eisenbach, Y., et al. (2013). Three mechanisms assemble central nervous system nodes of ranvier. *Neuron* 78, 469–482.

doi:10.1016/j.neuron.2013.03.005.

- Teissier, A., Le Magueresse, C., Olusakin, J., Andrade da Costa, B. L. S., De Stasi, A. M., Bacci, A., et al. (2020). Early-life stress impairs postnatal oligodendrogenesis and adult emotional behaviour through activity-dependent mechanisms. *Mol. Psychiatry* 25, 1159–1174. doi:10.1038/s41380-019-0493-2.
- Thetiot, M., Freeman, S. A., Roux, T., Dubessy, A., Aigrot, M., Rappeneau, Q., et al. (2020a). An alternative mechanism of early nodal clustering and myelination onset in GABAergic neurons of the central nervous system. *Glia* 68, 1891–1909. doi:10.1002/glia.23812.
- Thetiot, M., Freeman, S. A., Roux, T., Dubessy, A. L., Aigrot, M. S., Rappeneau, Q., et al. (2020b). An alternative mechanism of early nodal clustering and myelination onset in GABAergic neurons of the central nervous system. *Glia* 68, 1891–1909. doi:10.1002/glia.23812.
- Thetiot, M., Ronzano, R., Aigrot, M. S., Lubetzki, C., and Desmazières, A. (2019). Preparation and Immunostaining of Myelinating Organotypic Cerebellar Slice Cultures. *J. Vis. Exp.*, 1–7. doi:10.3791/59163.
- Vagionitis, S., Auer, F., Xiao, Y., Almeida, R. G., Lyons, D. A., and Czopka, T. (2021). Clusters of neuronal Neurofascin prefigure node of Ranvier position along single axons. *bioRxiv*, 1–29.
- Wake, H., Ortiz, F. C., Woo, D. H., Lee, P. R., Angulo, M. C., and Fields, R. D. (2015). Nonsynaptic junctions on myelinating glia promote preferential myelination of electrically active axons. *Nat. Commun.* 6. doi:10.1038/ncomms8844.
- Yang, S. M., Michel, K., Jokhi, V., Nedivi, E., and Arlotta, P. (2020). Neuron class-specific responses govern adaptive myelin remodeling in the neocortex. *Science* (80-.). 370. doi:10.1126/science.abd2109.
- Yap, E.-L., and Greenberg, M. E. (2018). Activity-Regulated Transcription: Bridging the Gap between Neural Activity and Behavior. *Neuron* 100, 330–348. doi:10.1016/j.neuron.2018.10.013.
- Zhang, J., Yang, X., Zhou, Y., Fox, H., and Xiong, H. (2019). Direct contacts of microglia on myelin sheath and Ranvier's node in the corpus callosum in rats. *J. Biomed. Res.* 33, 192–200. doi:10.7555/JBR.32.20180019.
- Zonouzi, M., Scafidi, J., Li, P., McEllin, B., Edwards, J., Dupree, J. L., et al. (2015). GABAergic regulation of cerebellar NG2 cell development is altered in perinatal white matter injury. *Nat. Neurosci.* 18, 674–682. doi:10.1038/nn.3990.

Discussion

Microglial cells are the resident immune cells of the brain. In the last two decades our understanding of microglia biology has grown deeply. In this context, it was shown that microglia interact with several neuronal sub-compartments in homeostatic conditions and through these interactions, shape and modulate neuronal circuit functions. The study of microglia-neuron interactions started with the description of their interaction with synapses (Wake et al., 2009; Tremblay et al., 2010). Further investigations of microglia interactions with neurons led to the identifications of contact established by microglia at neuronal somata and axon initial segments (Li et al., 2012; Baalman et al., 2015; Cserép et al., 2020). Microglia interactions with neurons allow them in particular to sense the activity in the circuits and respond to it (Li et al., 2012; Eyo et al., 2014; Badimon et al., 2020; Cserép et al., 2020; Nguyen et al., 2020; Umpierre et al., 2020). Along myelinated fibers, most of the axon is isolated from the environment by the myelin sheaths and is directly accessible only at nodes of Ranvier, which are unmyelinated. Thus, we hypothesized that microglia may sense neuronal state through close interaction at the nodes. The aim of my dissertation was to participate in the identification and the description of microglia-neuron interaction at nodes of Ranvier. We showed that microglia interact with nodes of Ranvier throughout the CNS and found that these contacts are stabilized compared to contacts made by microglia on myelin sheaths. Microglia-neuron interaction at nodes was further modulated by neuronal activity and inhibited when potassium fluxes were blocked. Furthermore, during remyelination a higher proportion of the nodes are contacted by microglia and the contacts are further reinforced. The inhibition of microglia interaction with node during remyelination correlates with a decreased remyelination. Thus, these first results show that microglia-neuron interactions at nodes of Ranvier may modulate microglial function in remyelination.

In the first part of the discussion, I will discuss the molecular mechanisms at play in microglia-node interaction and the potential function of microglia interaction with nodes of Ranvier. In homeostasis, the function of microglia contact remains unknown, but hypothesis can be elaborated from the role of microglia at other neuronal sub-compartments and from the function of other glial cells at nodes. Therefore, in a second part of my discussion, I will focus on the potential role of neuron-microglia interactions at node of Ranvier in homeostasis and the implication of glial mechanisms in the modulation of action potential conduction and nodal formation. In the third part, I will focus on the potential functions of node-like clusters.

1 Microglia-neuron interaction at nodes of Ranvier: mechanisms and functions

1.1 Potassium fluxes role in microglia-neuron interaction

1.1.1 Potassium fluxes stabilize microglia-neuron interaction at node of Ranvier

We demonstrated using organotypic cerebellar slices that the interaction between microglia and nodes of Ranvier depends on the potassium fluxes at the node. Along Purkinje cells axons, Kv7.2/3 and K_{Ca}3.1 are localized at the node and BK channels were described at the paranode (Pan et al., 2006; Gründemann and Clark, 2015; Hirono et al., 2015). Functionally, it was shown that K_{Ca}3.1 allows the repolarization of the membrane and is necessary to secure action potential propagation at frequencies as low as 20Hz (Gründemann and Clark, 2015). BK channels were relevant functionally only at frequencies above 100Hz and were suggested to have a complementary effect with K_{Ca}3.1 during high frequency firing (Hirono et al., 2015). Lastly, Kv7.2/3 and K_{Ca}3.1 are expected to regulate the resting membrane potential at node in absence of firing activity and therefore to modulate Nav channels availability (Battefeld et al., 2014; Gründemann and Clark, 2015). Thus, a high concentration of the broad spectrum blocker of potassium channels, tetraethylammonium (TEA) was used to inhibit all these nodal potassium channels (Lang and Ritchie, 1990; Devaux, 2004; Wei et al., 2005). To verify that TEA did not block channels expressed on microglia, we first verified that the global microglia dynamics and morphology were not changed following the treatment. Since potassium currents are known to modulate microglia morphology and motility (Madry et al., 2018a, 2018b; Izquierdo et al., 2021b), the absence of modification of these parameters following TEA treatment allowed us to confirm that the treatment had no direct detectable effect on microglia potassium channels modulating microglia resting potential, in particular that TEA did not directly inhibit THIK-1 channel. Furthermore, we used specific blockers of Kv7 (XE991, Wang et al., 1998, 2000) and K_{Ca}3.1 (TRAM-34, Wulff et al., 2000) and found in both cases a significant decrease (14%), of the proportion of nodes contacted by microglia supporting the involvement of nodal potassium fluxes in the stabilization of the interaction (Figure 36). These latter results further suggest that the effect of each channel is additional since the inhibitions of a specific channel leads to a lower decrease of microglia-node interaction than the inhibition of all channels at the same time. Furthermore, since different potassium channels are involved in the modulation of the interaction, the interaction is most likely mediated by the potassium fluxes themselves and not by the activation of a specific channel. Therefore, the interaction observed in other areas of the CNS with different neuronal populations might be modulated by the activation of other nodal potassium channels and in particular the recently described two-pore-domain potassium channels TREK-1 and TRAAK (Brohawn et al., 2019; Kanda et al., 2019). Indeed, depending on the

population of neurons considered, the potassium channels expressed at nodes vary (Devaux et al., 2003; Devaux, 2004; Gründemann and Clark, 2015; Brohawn et al., 2019; Kanda et al., 2019). In particular, the K2P channels TREK-1 and TRAAK have been described at nodes in various area of the CNS, and in particular participate in axolemma repolarization and modulation of its resting potential (Brohawn et al., 2019; Kanda et al., 2019). Thus, it would be interesting to test in different areas of the CNS which potassium channels are involved in regulating microglia-node interaction and assess whether this molecular mechanism is similar throughout the CNS.

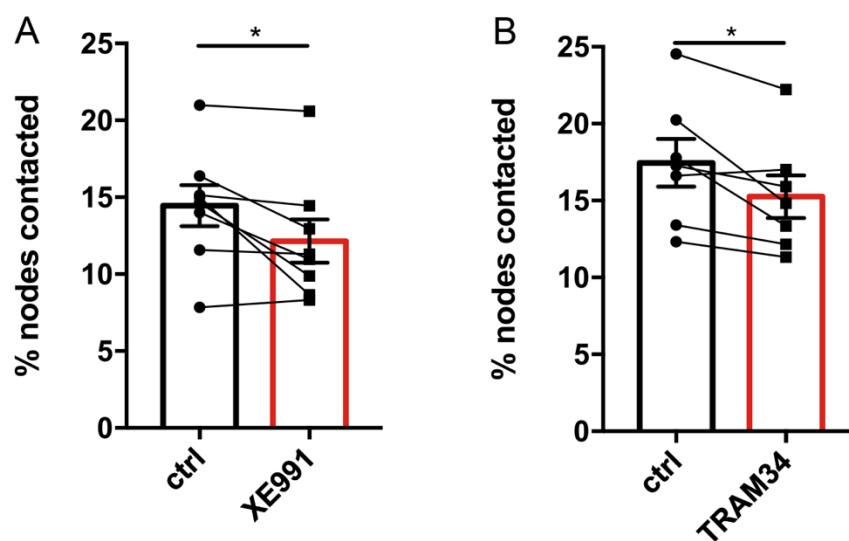


Figure 36: Decrease of microglia-node interaction by the inhibition of Kv7 and Kca3.1.

(A) Quantification of the percentage of nodes contacted by microglial cells in myelinated cerebellar slices following the inhibition of Kv7 with XE991 (100 μ M). (B) Quantification of the percentage of nodes contacted by microglial cells in myelinated cerebellar slices following the inhibition of Kca3.1 with TRAM-34 (1 μ M). (A) Wilcoxon paired test, n=8 animals, p=0.0391, (B) Two-sided paired t-test, n=7 animals, p=0.0295.

In our study, we observed that the inhibition of potassium fluxes leads to the alteration of the stability of node-microglia interaction. However, although it is expected that the concentration of extracellular potassium is locally higher at nodes and that this concentration is further increased by neuronal activity, the amplitude of this increase is unknown. Computational modeling of the electrodiffusion of sodium and potassium ions at node of Ranvier after a single action potential has suggested that locally, the concentration of extracellular potassium varies significantly following the simulation of one action potential (Lopreore et al., 2008). The variation of potassium concentration calculated following an unique action potential was limited to less than a millimolar (Lopreore et al., 2008). However, in this model, the perinodal ECM and other physical constraints around the node

were neglected whereas it is known that perinodal ECM plays an important role in ion diffusion in the CNS (Weber et al., 1999; Bekku et al., 2010). At synaptic clefts, taking into account the spatial constraints a local variation of several millimolars was calculated (Attwell and Iles, 1979). Thus, the increase of potassium concentration induced by an action potential is expected to be greater at nodes in the CNS than what was calculated (Lopreore et al., 2008), and experimental data are lacking to precisely estimate the concentration of potassium ions locally around the extracellular leaflet of the nodal axolemma. The use of potassium sensitive reporters (Wellbourne-Wood et al., 2017) might allow to estimate the local changes in potassium concentration induced at nodes by neuronal activity. This would further allow to assess the effect of a local potassium concentration increase on microglia dynamics by a local application of controlled concentration of potassium ions, a method that has been previously used to investigate other mechanisms (Hamada and Kole, 2015). Lastly, since potassium fluxes through THIK-1 maintain microglia resting potential (Madry et al., 2018b), it would be of great interest to use the recently design genetically encoded voltage indicators to investigate the changes of membrane potential locally at microglial processes, as it has recently been performed in astrocytes (Armbruster et al., 2021). Local membrane potential changes at the microglia-node contact would definitely establish a direct local microglia-neuron dialog at the node of Ranvier and would unravel a new form of neuron-microglia communication.

1.1.2 Do potassium fluxes participate in microglia-neuron interactions at other neuronal sub-compartments?

It is the first time to our knowledge that potassium fluxes are involved directly in the stabilization of microglia-neuron interaction. Thus, an intriguing question is what is the function of potassium in microglia-neuron contact at other neuronal sub-compartments like axon initial segment or neuron somata? First, axon initial segments and nodes of Ranvier are excitable domains of the axon with very similar molecular compositions (Nelson and Jenkins, 2017; Huang and Rasband, 2018). Therefore, it is possible that the contact of microglial processes with axon initial segments previously identified (Baalman et al., 2015) is modulated like the contact at the node of Ranvier. Indeed, when neurons fire, it triggers an outward current of potassium that could stabilize contact at the axon initial segment similarly to what we observed at the node. Thus, it would be interesting to study the underlying molecular mechanism that remains unknown, and address whether it is similar or not.

At the site of interaction between microglia and neuron somata, it was identified that microglial processes form very stable contacts (mean lifetime of about 25 minutes) with domains of neuronal membrane enriched in clusters of Kv2.1 and Kv2.2 (Cserép et al., 2020). Although the study focused on the role of these channels in the activation of exocytosis (Cserép et al., 2020), they also take part in the repolarization of neuronal membrane and mediate potassium outward currents upon neuronal

firing (Du et al., 2000; Palacio et al., 2017). Therefore, locally at clusters of Kv2.1 and Kv2.2 channels that are contacted by microglial processes, the concentration of potassium is expected to rise upon firing and may stabilize further the highly stable interaction of microglia with neuron somata. When testing for the effect of Kv2 channels in the interaction, the authors used HEK cells in co-culture with primary microglia (Cserép et al., 2020). They found that HEK cells (which do not express Kv2 endogenously (Jiang et al., 2002)), when transfected with Kv2, were contacted by microglia processes. Furthermore, HEK cells transfected with a mutant of Kv2 channels which is not targeted to the membrane were rarely contacted by microglia processes (Cserép et al., 2020). In primary microglial culture, the P2Y12 receptor which is involved in microglia-neuron contact at the soma (Cserép et al., 2020), is expressed at very low level (Butovsky et al., 2014). Therefore, in this co-culture experiment, the contact might have been partly mediated by an additional signal and in particular the fluxes of potassium at Kv2 channels. Taking into account all these aspects, it would be interesting to investigate this type of interaction in THIK-1 knock-out mice to assess whether potassium fluxes could participate together with P2Y12 receptor activation to microglia-neuron interaction at neuron somata.

The microglial receptor P2Y12 has been identified as a key player in the interaction between microglia and neurons (Li et al., 2012; Eyo et al., 2014; Sipe et al., 2016; Badimon et al., 2020; Cserép et al., 2020). This receptor has been shown to potentiate THIK-1 channel on microglia, the main potassium channel on homeostatic microglia (Madry et al., 2018b). Thus, the activation of P2Y12 receptor may directly modulate the recruitment of microglial processes at neuronal sub-compartments by triggering process outgrowth and modulate the stabilization of the interaction indirectly through its effect on THIK-1 channel.

1.2 Mechanism and function of microglia-node interaction in remyelination

1.2.1 Microglial potassium fluxes modulate remyelination

The inhibition of microglia-node interaction was also observed when potassium fluxes were inhibited during remyelination. First, we used TEA to inhibit the potassium channels expressed at nodes and found that further to its effect on the interaction, the treatment altered microglial expression of pro-remyelinating factor IGF1 and decreased remyelination. Reciprocally, the inhibition with tetrapentylammonium (TPA) treatment of THIK-1, the potassium channel responsible for most of the potassium conductance in microglia, allowed us to test the involvement of microglia potassium homeostasis in remyelination (Madry et al., 2018b). During remyelination, the treatment with TPA led to a similar effect on microglia and remyelination than the treatment with TEA. Thus, microglial potassium fluxes are of primary importance in the mechanism of microglia activation and repair during remyelination. However, these pharmacological approach are not totally specific (Grissmer et al.,

1994; Jarolimek et al., 1995; Hadley et al., 2000; Madry et al., 2018b), and further investigations will be necessary to confirm that defects in microglial switch and remyelination were only due to the inhibition of microglia-node interactions through alteration of potassium fluxes. Nevertheless, on the cerebellar slices, the similar effect of the treatment with TEA (that does not inhibit THIK-1) and of TPA (that does not inhibit Kca3.1 or BK nodal channels at the concentration used) suggests that the defects observed on microglia were at least partly due to a loss of communication between neurons and microglia through potassium fluxes (Augustine et al., 1988; Carl et al., 1993; Julio-Kalajzić et al., 2018). Microglia when activated express other potassium channels (Schilling and Eder, 2007, 2015). For instance, Kv1.3 have been shown to modulate the potassium conductance and the phenotype of activated microglia (Di Lucente et al., 2018; Sarkar et al., 2020). Thus, future studies using a specific inducible deletion of THIK-1 in microglia, a model that is not yet available, would allow to more specifically test the involvement of microglial THIK-1 channel in microglia activation and repair during remyelination. Alternatively, since THIK-1 transcripts are mainly expressed in microglia in the CNS (Butovsky et al., 2014), the use of the available constitutive THIK-1 deficient strain, would allow to gain insights in the role of microglial potassium homeostasis in remyelination. However, THIK-1 is involved in the regulation of phagocytosis (Izquierdo et al., 2021a), therefore the use of a constitutive knock-out model may also disrupt remyelination through the disruption of myelin debris clearance.

1.2.2 Neuronal stimulation increases microglia-node interaction and modulates microglia activation

As discussed previously, the disruption of microglia-node interaction and of potassium fluxes led to the disruption of microglia switch of phenotype. Therefore, the increase of microglia-node interaction may promote the switch of microglia activation toward a pro-remyelinating state. Since we had shown that the activation of neuronal activity promotes the interaction, we tested this hypothesis using chemogenetic and optogenetic stimulations. First, we showed on myelinated and on remyelinating cerebellar slices that activity stimulations promote microglia-node interactions (Ronzano, Perrot and Desmazières, unpublished, Figure 37). We further showed that the stimulation of neuronal activity on remyelinating slices by chemogenetic promotes the expression of the pro-remyelinating factor IGF-1 by microglia (Ronzano, Perrot and Desmazières, unpublished, Figure 38) and promotes remyelination (data not shown). Thus, the increase of the interaction between microglia and nodes also correlates with an increase of the expression of the pro-remyelinating factor IGF-1 by microglia in remyelination. Although it remains a correlation and the demonstration of the implication of microglia-node interaction in repair is not definitive, this latter experiment support further the

involvement of this interaction in the modulation of microglia phenotype during remyelination. Therefore, increasing microglia-node interaction may be efficient to promote repair.

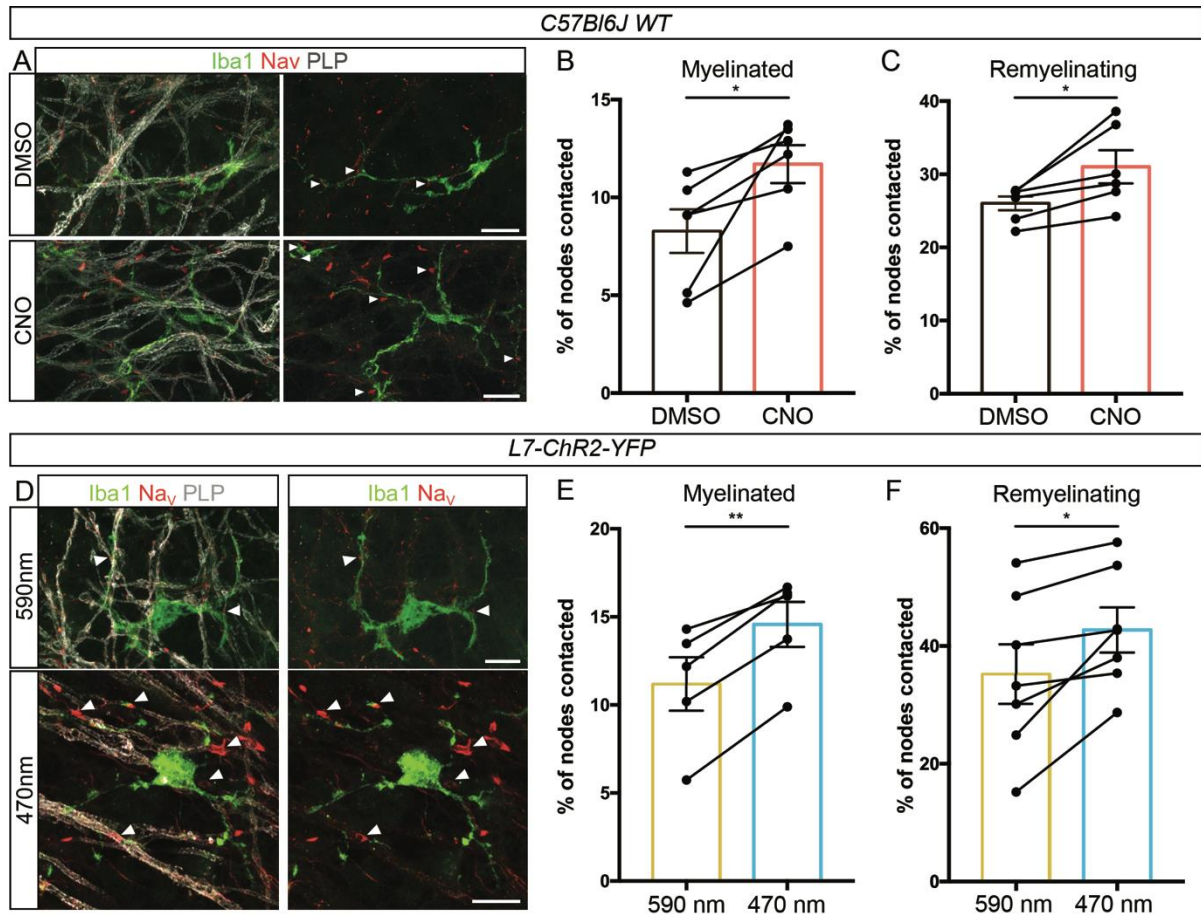


Figure 37: Neuronal activity stimulation promotes microglia-neuron interactions at nodes in myelinated and remyelinating cerebellar organotypic slices.

(A) Immunohistochemistry showing microglia contacts on nodes of Ranvier in myelinated slices with (CNO) or without (DMSO) chemogenetic stimulation. The white arrowheads highlight contacted nodes of Ranvier. (B-C) Quantification of the proportion of nodal structures contacted by microglia in myelinated (B) and remyelinating (C) organotypic cerebellar slices. The quantifications have been performed in areas of the slices with on average more than 70% of the neuron that were transfected by AAV8-hM3Dq-mCherry following one hour of treatment with CNO (0.5 μ M) or an equivalent volume of DMSO. (D) Immunohistochemistry showing microglia contacts on nodes of Ranvier in myelinated slices from L7-ChR2-YFP animals, following stimulation at 10Hz with 10ms long pulses for one hour. The stimulation at 470nm activates ChR2 whereas the stimulation at 590 at the same power of 1.5mW/mm² does not (control condition). The white arrowheads highlight contacted nodes of Ranvier. (E-F) Quantification of the proportion of nodal structures contacted by microglia in myelinated (E) and remyelinating (F) organotypic cerebellar slices. The quantifications have been performed in areas of the slices with on average more than 70% of the neuron that were YFP positive, following one hour of stimulation at 590 (control) or 470 nm. (B, C, E, F) Two-sided paired t-tests, values are individually plotted per animal. (B, C, F) n=6, (E) n=5. Scale bars: 10 μ m.

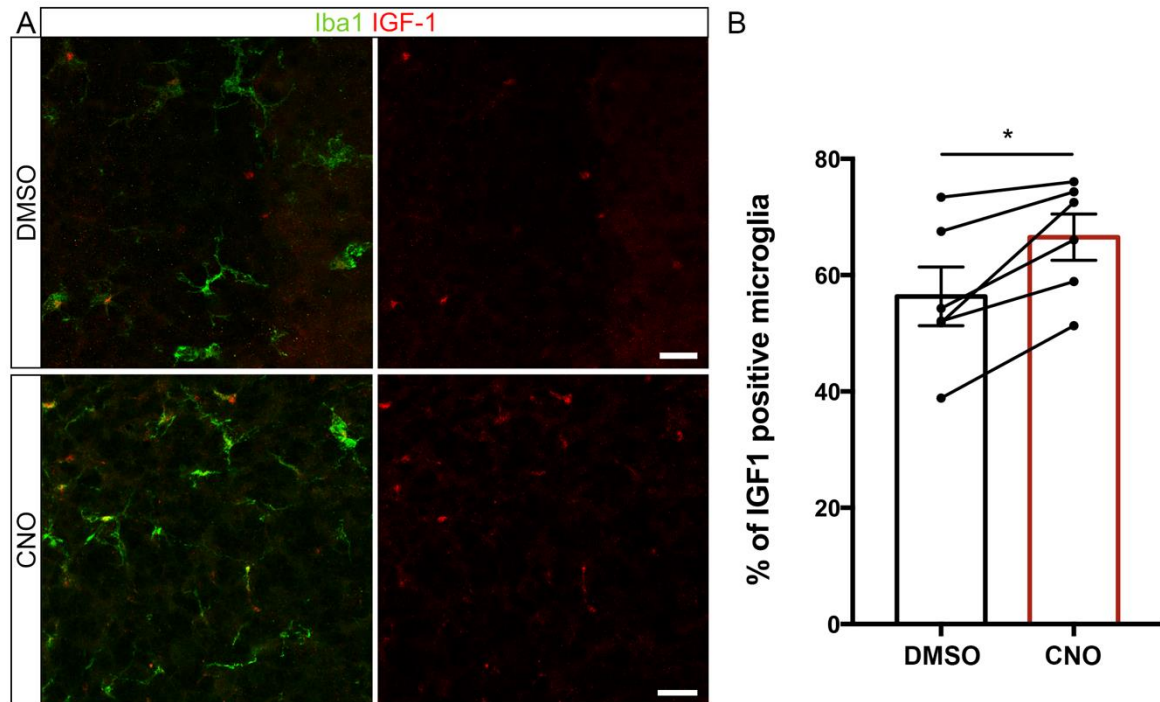


Figure 38: Chemogenetic stimulation of neuronal activity promotes microglia expression of IGF-1 in remyelinating cerebellar organotypic slices.

(A) Immunohistochemistry showing microglia expression of IGF-1 in remyelinating slices following 6 hours with (CNO) or without (DMSO) chemogenetic stimulation. (B) Quantification of the proportion of microglia cells positive for IGF-1 staining in remyelinating slices following 6h stimulation with CNO (0.5 μ M) or without stimulation (DMSO). The quantifications have been performed in area of the slices with on average more than 70% of Purkinje neurons that were transfected by AAV8-hM3Dq-mCherry. (B) Two-sided paired t-test, values are individually plotted per animal, n=6. Scale bars: 20 μ m.

Importantly, this latter results also show that neuronal activity stimulations might promote remyelination through its effects on microglia and not only directly through effect on the oligodendroglial lineage. These latter results, and in particular the increase of IGF-1 expression in microglia following neuronal activity stimulation corroborates the results obtained by Jensen et al., who showed *in vivo* that physical exercise promotes IGF-1 signaling following focal demyelination in the spinal cord (Jensen et al., 2018). Furthermore, potassium efflux through THIK-1 have been shown to modulate phagocytosis and calcium transients in microglia (Izquierdo et al., 2021a). Therefore, since calcium transients in microglia depend on neuronal activity (Umpierre et al., 2020) and are thought to modulate phagocytosis (Gronski et al., 2009; Nunes and Demareux, 2010), it is possible that neuronal activity modulations not only modulate microglia phenotype, but also promote the phagocytosis of myelin debris following demyelination. Thus, the role of neuronal activity, on the modulation of microglia activation and phagocytosis are prominent questions and will need to be addressed further in the future. Indeed, microglial activation state and phagocytosis are of primary importance in

remyelination and also impact developmental and adaptive myelination (Miron et al., 2013; Shigemoto-Mogami et al., 2014b; Geraghty et al., 2019; Lloyd et al., 2019; Cunha et al., 2020; Hughes and Appel, 2020; Djannatian et al., 2021). Thus, the description of the exact effect of neuronal activity stimulation on microglia will help to understand how neural stimulation may allow to promote repair via modulation of microglia, an issue that has been mainly tackled in Alzheimer models so far (Iaccarino et al., 2016; Adaikkan et al., 2019; Martorell et al., 2019).

In addition to the potential application of direct neuronal stimulations in repair, the description of the underlying molecular mechanisms involved is necessary to identify the signaling pathways to be targeted for promoting remyelination. Our study suggest that potassium fluxes are of primary importance in microglia phenotype modulation during remyelination. These results extended to remyelination, what has been shown on microglia as well as macrophages in other paradigms (Muñoz-Planillo et al., 2013; Madry et al., 2018b). The inhibition of THIK-1 on human microglia has been shown to trigger similar effect on microglial morphology and phagocytosis than in mouse (Izquierdo et al., 2021b). In this context, it would be interesting to further confirm the involvement of THIK-1 in microglia activation and myelin debris phagocytosis following demyelination and during remyelination. The use of neuronal stimulations on THIK-1 deficient mice (inducible and microglia-specific if possible, constitutive by default) may allow to either confirm or invalidate the direct role of THIK-1 in neuronal activity dependent modulations of microglia. If the primary importance of THIK-1 in these mechanisms is further confirmed, the conception of molecules aiming at modulating potassium homeostasis of microglia might be of great interest. Indeed, the modulation of THIK-1 might allow to regulate two of the main processes conditioning efficient remyelination, myelin debris clearance and microglia activation switch (Miron et al., 2013; Lloyd et al., 2019; Cunha et al., 2020). It is interesting to note that the administration of voltage-gated channels blockers (such as 4-amidopyridine) have been tested in patients suffering from demyelinating diseases, with some effects on motor fatigue (Horton et al., 2013; Schniepp et al., 2013). However, the treatments used have multiple consequences and are expected to modulate neuronal activity, nerve conduction and glial mechanisms. Further investigations are therefore needed to develop strategies aiming at modulating potassium fluxes more accurately to promote repair.

1.2.3 Microglia-node interaction is increased following neuronal stimulation and in remyelination: an additional signal?

Following neuronal stimulations and during remyelination, we showed that a higher proportion of nodes of Ranvier are contacted by microglia. Moreover, in remyelination microglia-node interaction is further stabilized. There are two main possibilities to explain this reinforced interaction.

First the potassium fluxes are reinforced, and so is the interaction between node and microglia. Another possibility, that could be complementary to the first one, is the existence of an additional signal.

First, following neuronal stimulation, there is an increase of potassium efflux from the nodes that is expected to stabilize further the contact. Furthermore, following demyelination with cuprizone, at the onset of remyelination there is a neuronal hyperactivity (Bacmeister et al., 2020). In EAE, the firing pattern of Purkinje cells is modified with an increase of phasic activity (Saab et al., 2004), which as we observed leads to an increase of microglia-node interaction. Therefore, in remyelination the increased stabilization of the microglia-node interaction may be partly explained by an increase of neuronal activity.

In myelinated organotypic cerebellar slices, we did not detect any disruption of microglia-node interaction following P2Y₁₂ receptor inhibition. However, as discussed previously, Purkinje cells are firing at lower frequencies in this model than *in vivo*. Therefore, *in vivo* the higher neuronal activity might promote ATP release and activates P2Y₁₂ receptors to attract microglial processes toward the nodal domains, as it has been described for interactions with other neuronal sub-compartments in homeostatic condition or following sustained stimulation (Eyo et al., 2014; Badimon et al., 2020; Cserép et al., 2020). Supporting this hypothesis, it has been suggested that following stimulations of the optic nerve at 20Hz, ATP is released along the axon (Hamilton et al., 2010). The authors of this study further hypothesized that the release of ATP might occur at nodes of Ranvier (Hamilton et al., 2010). Furthermore, a sustained stimulation of neuronal activity (30Hz, 10 seconds) triggers calcium signals in astrocytes that have been shown to induce ATP release at the node of Ranvier (Lezmy et al., 2021). Thus, ATP might recruit microglial processes at node upon sustained neuronal firing. Since neuronal stimulation increases microglia-neuron interaction at nodes of Ranvier (Figure 37), it would be interesting to stimulate neuronal activity and at the same time inhibit P2Y₁₂ receptors. In that case, the involvement of P2Y₁₂ receptor in the interaction would result in an absence or in a reduction of the increased interaction induced by the stimulation. During remyelination, P2Y₁₂ receptor is again expressed by microglia and might participate to the reinforcement of the interaction (Krasemann et al., 2017). Thus, it would be interesting to study the interaction during remyelination in P2Y₁₂ knock-out mouse or to use a pharmacological approach *in vivo* allowing to diffuse P2Y₁₂ inhibitors on the top of the lesion similarly to what we have done for TPA local diffusion on the dorsal spinal cord. Furthermore, in remyelination other signals specific of pathological conditions might be at play and remain to be further investigated.

2 Multiple glia-neuron interactions at the nodes of Ranvier: function in development and homeostasis.

2.1 The nodes of Ranvier are contacted by microglia and macroglia in homeostasis

In homeostasis, both astrocytes and OPCs have been shown to contact nodes of Ranvier (Hildebrand and Waxman, 1983; Ffrench-Constant et al., 1986; Butt et al., 1994, 1999; Huang et al., 2005; Hamilton et al., 2010; Serwanski et al., 2016; Lindsay M. De Biase et al., 2017)(Figure 39). Astrocytes have first been observed in close apposition with the axolemma at nodes of Ranvier in the optic nerve and spinal cord white matter (Hildebrand, 1971; Ffrench-Constant et al., 1986; Black and Waxman, 1988). More recently, the proportion of nodes contacted by astrocytes was quantified in several areas of the white matter and about 95% of the nodes were found in close apposition with astrocytic processes (Serwanski et al., 2016). When first observed, several hypothesis had been drawn regarding the function of astrocyte contacts at nodes, in particular they were thought to stabilize nodal structure and regulate ions homeostasis (Hildebrand, 1971; Black and Waxman, 1988). Supporting this hypothesis, a recent report showed that the perinodal astrocytes stabilize paranodal loops leading to the regulation of nodal length and myelin structure in the optic nerve and corpus callosum (Dutta et al., 2018). This stabilization is made through the secretion of SERPINE2 (also named PN1 or nexin-1) that inhibits the cleavage of neurofascin 155 by thrombin at the paranode. Thus, the detachment of the outermost paranodal loop is inhibited by astrocytic secretion contributing to the regulation of nodal length and myelin sheath. The inhibition of this mechanism led to nodal lengthening and to a slowing down of action potential conduction (Dutta et al., 2018). Furthermore, it has been recently reported that perinodal astrocyte processes release ATP along axons of the cortical pyramidal neurons (Lezmy et al., 2021). It was further shown that adenosine receptor A2a are clustered at both nodes of Ranvier and axon initial segments. The activation of A2a receptors at nodes of Ranvier has been reported to decrease axonal conduction velocity (Lezmy et al., 2021). Thus, the contact of astrocytes at nodes may through both structural and electrophysiological modulations regulate the conduction of action potentials.

OPCs have also been observed to contact directly the axolemma at nodes of Ranvier in white matter (Butt et al., 1999; Serwanski et al., 2016). Between 15 and 35% of the node were observed to be contacted by OPCs in white matter tracts (Serwanski et al., 2016; Lindsay M. De Biase et al., 2017). It was further estimated from the quantification of contacts made by OPCs on nodes vs on a random simulated distribution of nodes, that half of the interactions were specific, suggesting a function played by OPCs at nodes (Lindsay M. De Biase et al., 2017). Functionally, these contacts were suggested to

prevent collateral sprouting from the node (Huang et al., 2005) but their exact function at nodes in adult remains unclear. It was also hypothesized that during developmental myelination OPCs might promote the clustering of nodal domains (Butt et al., 1999), a mechanism that may be at play in node-like clustering through OPCs local secretions (discussed below in 2.3).

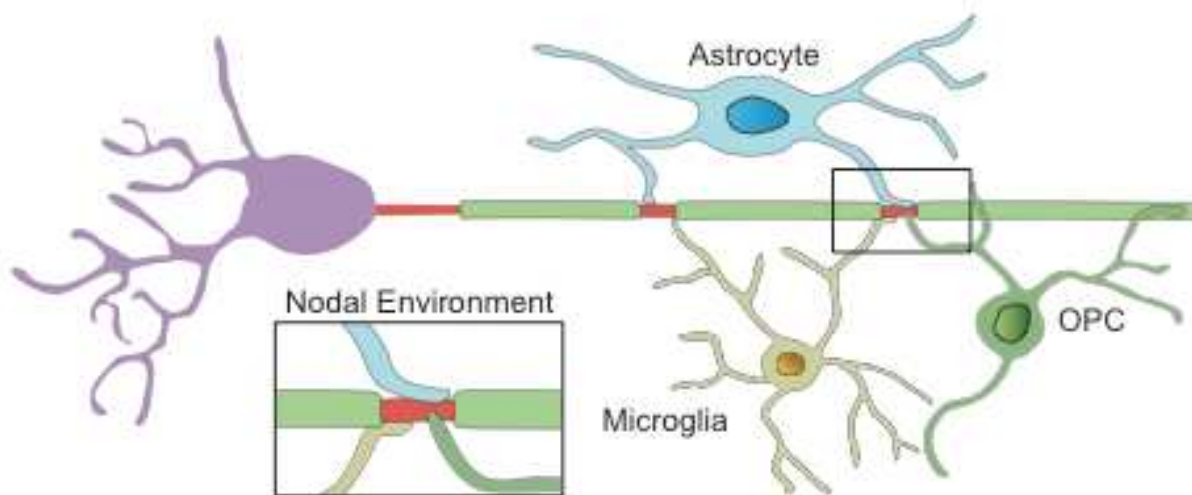


Figure 39: Nodes of Ranvier are contacted by microglia and macroglia in homeostasis.

Schematic representation of neuroglial contacts at the node of Ranvier in the CNS. In homeostasis, nodes of Ranvier are contacted by perinodal astrocytes, oligodendrocyte precursor cells (OPCs) and microglia. However, this scheme is speculative since it has never been assessed if the same node can be contacted simultaneously by the three cell types, only double simultaneous contacts have been observed so far. Drawings adapted from Lubetzki et al, 2020.

2.2 Microglia and astrocytes at nodes of Ranvier: complementary functions in the modulation of action potential conduction?

In homeostasis, astrocytes at nodes of Ranvier have been so far related to the modulation of action potential conduction. This modulation might also involve microglia, directly or by taking part to mechanisms mediated by astrocytes. Indeed, microglia also express SERPINE2 and the quantity of SERPINE2 transcripts in microglia was shown to be higher than in other glial cells (Butovsky et al., 2014)(Figure 40A). Thus, microglia in addition to astrocyte might participate to the regulation of paranodal loop stabilization and might control nodal structure, in addition to astrocytes (Figure 40B). This hypothesis is further supported by our observation of the close apposition between microglia processes and the outermost paranodal loop at nodal domains using electronic microscopy. Therefore, it would be interesting to study the effect on nodal structure, of the specific deletion of SERPINE2 in microglia. Alternatively, a model of microglia depletion such as $Csfr1^{\Delta FIRE/\Delta FIRE}$ recently developed (Rojo et al, 2019), would allow to evaluate the involvement of microglia in the regulation of nodal structures, and in particular nodal length. Since the regulation of nodal length by astrocyte has been shown to regulate conduction velocity (Dutta et al., 2018), microglia may also participate to conduction velocity regulation in homeostasis. This mechanism would be a way to modulate conduction velocity with a lower energy cost than the one needed for myelin sheath plasticity (Arancibia-Cárcamo et al., 2017). Furthermore, this mechanism of plasticity may be faster than changes in myelin pattern.

Very recently, it has been reported from a single-nucleus RNA sequencing study that in homeostatic conditions as well as in tissues from MS patients, some microglia are enriched in transcripts of nodal proteins, in particular neurofascin and AnkyrinG (Absinta et al., 2021). Although this population of microglia has not been studied further, it was interpreted that these transcripts correspond to material that has been phagocytosed by microglia in close interaction with nodes (Absinta et al., 2021). Therefore, it is possible that microglia are modulating nodal structures through partial phagocytosis (or trogocytosis) as it has been reported at axons and presynaptic boutons (Weinhard et al., 2018). However, since this result is based on RNA sequencing, this interpretation would mean that transcripts of nodal proteins are localized at nodes and translated locally by ribosomes. Although enrichment of ribosomes has been described at nodes (Walker et al., 2012), the presence of nodal proteins transcripts at node has not been observed so far, therefore this mechanism remains speculative. The mechanism of phagocytosis by microglia might also regulate action potential conduction by modelling the perinodal ECM similarly to what has been shown at synapses in the hippocampus (Nguyen et al., 2020). Indeed, perinodal ECM has been shown to affect conduction velocity along axons (Weber et al., 1999; Bekku et al., 2010). Thus, if the mechanism recently described at synapses is taking place at the node of Ranvier, the neuronal activity dependent IL-33 signaling might trigger the remodeling of perinodal ECM and indirectly modulate action potential conduction (Nguyen et al., 2020).

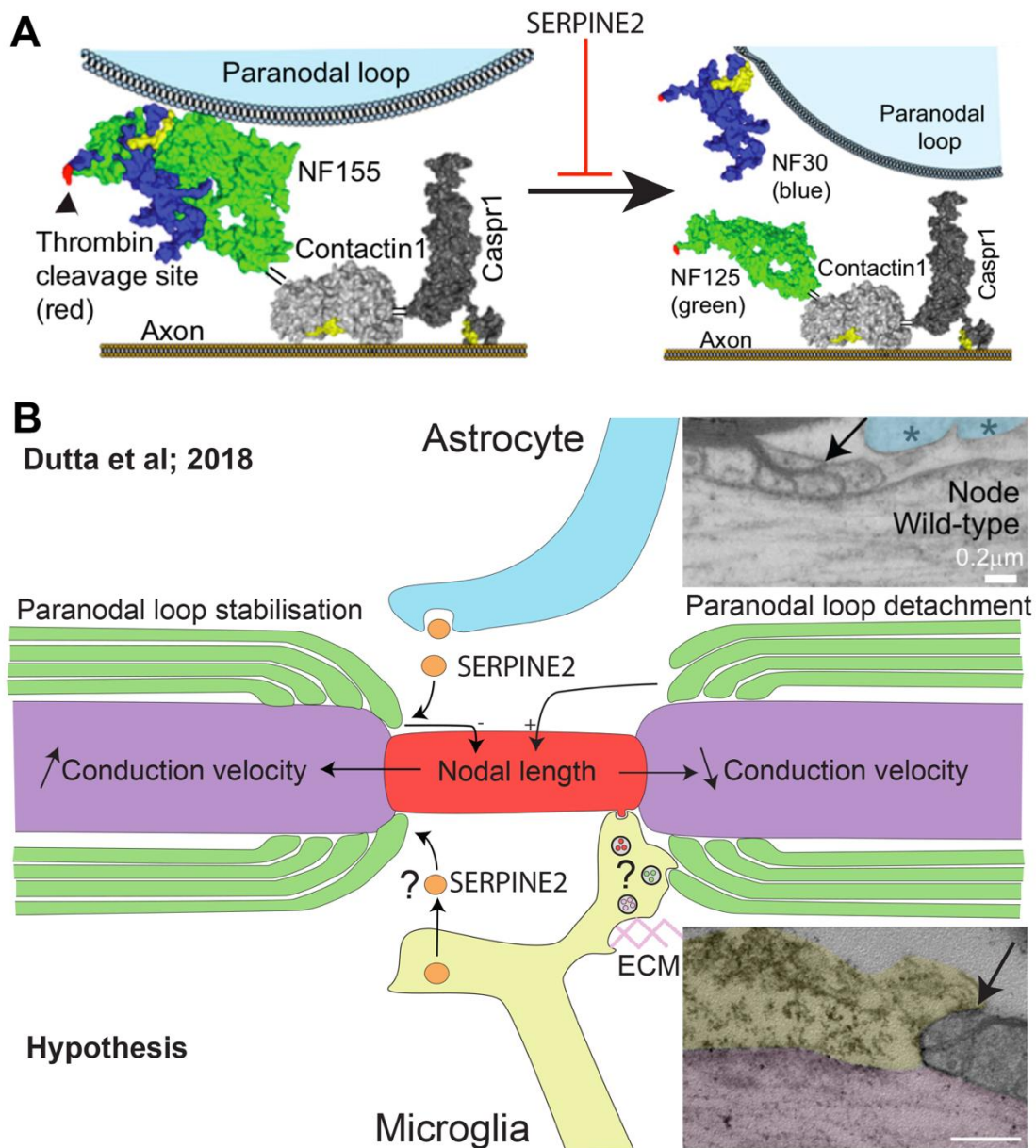


Figure 40: Microglia might participate to modulations of nodal length and myelin thickness at nodes.

(A) Paranodal loop and the axolemma form the axoglial junction through the interaction of neurofascin 155 (NF155), Contactin1 and Caspr1. On NF155 there is a site of cleavage by thrombin that disassembles the complex formed by these three proteins and leads to the paranodal loop detachment. SERPINE2 released by astrocyte and also expressed by microglia inhibits the protease activity of thrombin and stabilizes the outermost paranodal loop. (B) Since microglia also express SERPINE2 transcript, it is possible that the secretion of SERPINE2 by microglia also modulates the structure of nodal domains. The paranodal loop detachment leads to an increase of nodal length that induces a decrease of conduction velocity. Thus, astrocytes and maybe microglia inhibit this mechanism preventing the slowdown of action potential conduction. Transmission electron micrographs showing that similarly to astrocyte processes (filled in blue), microglial processes (filled in yellow) can be closely associated with paranodal loops at the node of Ranvier (black arrows). It was suggested that microglia phagocytose nodal components. However, this mechanism is speculative since the hypothesis is based on RNAsequencing data and implies that nodal proteins are locally translated at nodes of Ranvier. Lastly, microglia could also phagocytose component of the perinodal ECM like it has been observed at synapses. Adapted from Dutta et al, 2018 and Ronzano et al, 2021.

Very recently, it has been suggested that astrocytes slow down conduction along myelinated axons through ATP release and adenosine receptor activation (see 2.1, (Lezmy et al., 2021)). To activate adenosine receptor, ATP need to be hydrolyzed in ADP then AMP and finally adenosine. The enzyme CD39, mainly expressed at the surface of microglial cells, is the rate limiting enzyme for the conversion of ATP in adenosine (Braun et al., 2000; Butovsky et al., 2014; Badimon et al., 2020). In our study, we further showed that some nodes are contacted simultaneously by astrocytes and microglia. Therefore, microglia may participate to the hydrolysis of ATP released at the nodes by astrocytes and allow for the activation of A2a adenosine receptor, as it has been shown for A1 receptor at synapses (Badimon et al., 2020)(Figure 41). Astrocytic ATP release is triggered by calcium transients that are neuronal activity dependent in astrocytes (Hirase et al., 2004; Stobart et al., 2018; Semyanov et al., 2020; Lezmy et al., 2021). Interestingly, calcium transients in astrocytic processes close to axons were triggered only following a prolonged stimulation (30Hz, 10 seconds) but not after a brief stimulation (1 second) (Lezmy et al., 2021). Thus, it is possible that a mechanism similar to what has been described at synapses is also occurring at nodes. Indeed, after an abnormal sustained hyperactivity, the ATP released would attract microglial processes (activation of P2Y12), CD39 would then allow the efficient hydrolysis of ATP to adenosine and eventually adenosine by A2a activation at nodes would slow down action potential conduction (Badimon et al., 2020)(Figure 41). In this mechanism, high neuronal activity would increase potassium concentration in the extracellular medium surrounding the node and further stabilizes microglial processes (Figure 41). Hence, it will be critical for future studies to test whether microglial P2Y12 receptor is involved in microglia-node interaction when hyperactivity occurs. The model of cerebellar organotypic slices that we used might offer an accessible model to investigate further the involvement of microglia in this mechanism, since clusters of adenosine receptor A2a have been observed at about 70% of the nodes in the cerebellum (Lezmy et al., 2021).

It is interesting to note that ATP release by astrocytes has also been shown to occur at AIS where A2a receptors are also clustered (Lezmy et al., 2021). Moreover, A2a receptors activation at AIS has been shown to decrease neuron excitability. Thus, microglia associated with AIS could with a similar molecular mechanism than at node, participate to the decrease of excitability upon hyperactivity. Interestingly, it has been further suggested that A2a receptors in the cortex are clustered at AIS of excitatory neurons (Lezmy et al., 2021), which are also the neurons that more frequently show microglia associated with their AIS (Baalman et al., 2015).

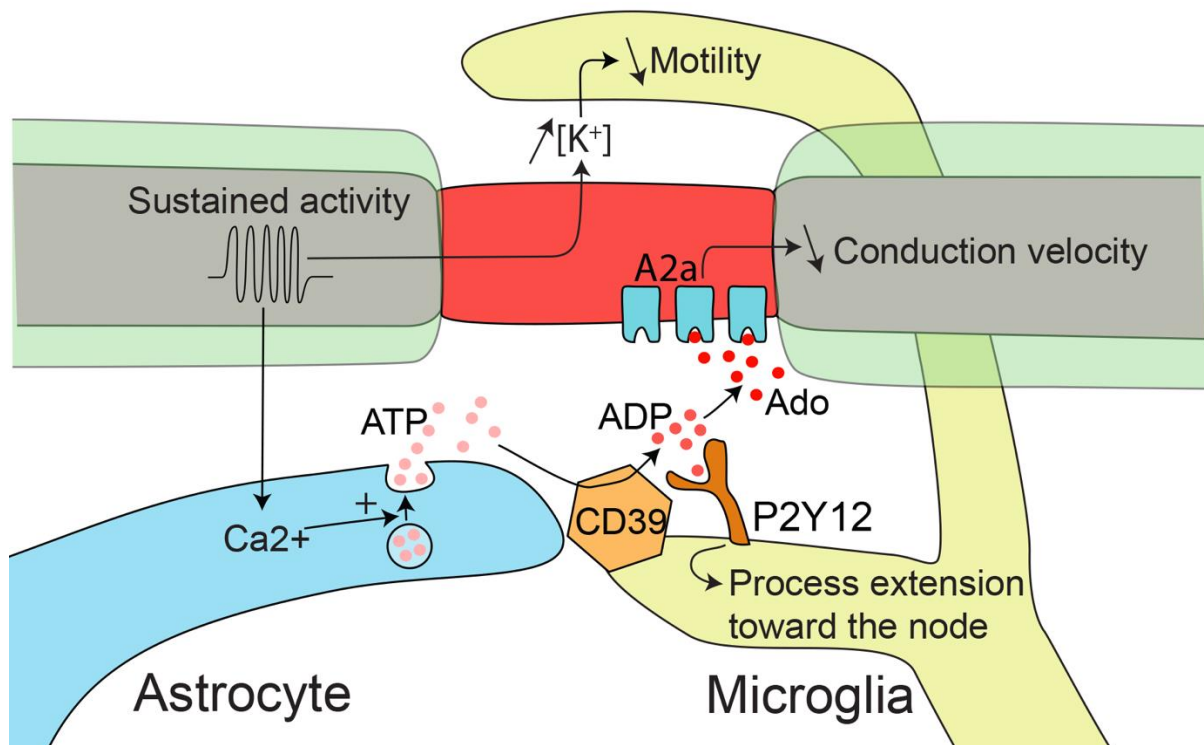


Figure 41: Microglia might also participate to the astrocytic dependant reduction of conduction velocity at nodes of Ranvier.

Schematics showing a potential molecular mechanism at play at the nodes of Ranvier. Following sustained neuronal activity, calcium transients in astrocytes trigger ATP release at nodes of Ranvier (Lezmy et al, 2021), ATP is hydrolysed spontaneously in ADP that attracts microglial processes that further catalyses ATP hydrolysis in ADP with CD39 (Badimon et al, 2020). ADP is further transformed in adenosine (Ado) and activates A2a receptors at nodes that slow down conduction velocity (Lezmy et al, 2021). The neuronal activity increases outward currents of potassium at nodes which further stabilizes microglial processes at nodes vicinity and allows microglia to participate to the regulation of hyperactivity.

2.3 Function of glia-neuron interactions at immature nodes

Microglia-neuron interaction at nodes is not restricted to mature nodes of Ranvier. Indeed, in the cerebellum, we observed that microglia contact both mature and immature nodal structures *in vivo* and *ex vivo*. *Ex vivo*, we further quantified the proportion of immature nodal structures contacted by microglia in myelination and remyelination and found that immature and mature nodal structures were contacted by microglia in similar proportions. However, the function of this contact is unknown. In white matter, during developmental myelination it has been shown that microglia present a pseudo-activated phenotype, close to what is observed in certain pathological condition (Hagemeyer et al., 2017; Wlodarczyk et al., 2017; Hammond et al., 2019; Li et al., 2019). In particular, during the myelination of Purkinje cell in the white matter of the cerebellum microglia express IGF-1 at a high level, enhance oligodendrogenesis and are highly phagocytic (Shigemoto-Mogami et al., 2014b; Hagemeyer et al., 2017; Wlodarczyk et al., 2017; Li et al., 2019). The interaction of microglia with immature nodal domains, part of which are node-like clusters, might regulate the pseudo-activated state of microglia or the expression of factor like IGF-1 during development, similarly to what we observed during remyelination. Therefore, in mice deficient for THIK-1 in microglia, it would be interesting to test if developmental myelination is altered and whether there are defects in microglia state, oligodendrogenesis and/or clearance of apoptotic cells.

OPCs have also been shown to contact immature nodes. *In vitro* in co-culture the interaction of pre-myelinating OLs with node-like clusters was suggested to promote the initiation of myelination at the vicinity of the node (Thetiot et al., 2020). *In vivo* in zebrafish, it was shown that OPC processes contact about 25% of node-like clusters mainly “en passant” and rarely with the tip of the process (Vagionitis et al., 2021). However, these contacts were transients and never lasted more than 2h30 (Vagionitis et al., 2021). Furthermore, *in vitro*, node-like clusters formation requires the secretion of oligodendroglial factors. Within the tissue, since the spatial constraints are much more important, these factors might be secreted locally at the vicinity of the axolemma. Thus, it is possible that at sites of close interaction between axons and OPCs or premyelinating OLs, the secretion of oligodendroglial factors induces the formation of node-like clusters. To support this hypothesis, it was observed using live-imaging *ex vivo* that oligodendroglial process can interact closely with unmyelinated Purkinje axons (Thetiot and Desmazières, unpublished data). Following the close apposition node-like clusters were formed along the axons while the oligodendroglial process was retracted (Thetiot and Desmazières, unpublished data). Future studies will be needed to understand better the role of the contacts between axons and oligodendroglial cells in the formation and fate of node-like clusters.

3 Function of node-like clusters in myelination and remyelination

The mechanisms of node of Ranvier formation in the central nervous system are not completely understood, and may differ between neuronal populations (Freeman et al., 2015). So far, node-like clusters have been suggested to play a role in action potential conduction, myelination and might even be at play in remyelination. However, further investigations are needed to identify their exact functions in these mechanisms.

3.1 Node-like clusters are formed on preferentially myelinated neurons

Node-like clusters are formed along axons of several populations of neurons, but not all of them. For instance, in the hippocampus of rodents, GABAergic neurons form node-like clusters whereas pyramidal neurons do not (Freeman et al., 2015). Similarly in zebrafish, commissural primary ascending and circumferential descending neurons form clusters of neurofascin prior to myelination whereas Rohon-Beard neurons do not (Auer, 2019; Vagionitis et al., 2021). However, it is unknown why some populations start to cluster nodal proteins prior to myelination and others do not. Thus, what are the common characteristics of node-like cluster forming neurons that may lead to this alternative mechanism? First, the neurotransmitter does not define population of node-like cluster forming neurons. Indeed, both glutamatergic (retinal ganglion cells, commissural primary ascending and circumferential descending neurons) and GABAergic (hippocampal parvalbumin or somatostatin interneurons, Purkinje cells) neurons have been observed to form node-like clusters {Formatting Citation}. One common aspect of node-like cluster forming neurons is that they are part of the neurons preferentially myelinated. Indeed, the retinal ganglion cell and the Purkinje cells shows a continuous myelination (Skoff et al., 1980; Black et al., 1982; Gianola et al., 2003) and parvalbumin interneurons are preferentially myelinated in the hippocampus (Micheva et al., 2016; Stedehouder et al., 2017, 2019). Lastly, in the zebrafish, commissural primary ascending and circumferential descending neurons are part of the highly myelinated neurons (Auer, 2019). In contrast, in the hippocampus of rodents and in the spinal cord of the zebrafish, neurons on which node-like clusters were not observed show only a sparse myelination (Stedehouder et al., 2017; Auer, 2019; Almeida et al., 2021). Therefore, it would be interesting to study further other axonal projections that are robustly myelinated and investigate whether they form node-like clusters. For instance, in the white matter of the mouse spinal cord, we observed node-like clusters prior to myelination (Figure 42), but the corresponding population(s) of neuron remain to be identified. The fact that node-like clusters are formed on specific neuronal population must be translated in some specificity of the molecular organization of their axons. Further

investigations are necessary to identify these specificities and in particular what are the key elements allowing the formation of node-like clusters.

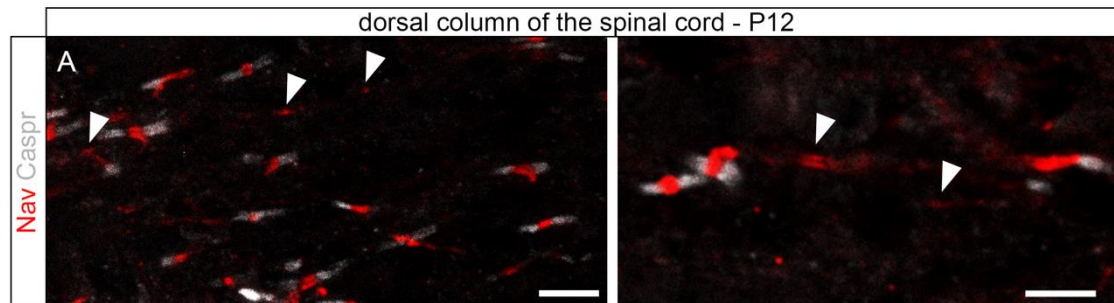


Figure 42: Node-like clusters are formed prior to myelination in the dorsal column of the spinal cord in mouse.

(A-B) Orthogonal projections showing isolated clusters of Nav channels (in red, filled arrowhead) in the dorsal column of the spinal cord from mouse at P12. Scale bars: (A) 5 μm , (B) 4 μm .

3.2 Underlying mechanism(s) of neural activity dependent formation of nodal domains

Both *in vitro* on hippocampal culture and *ex vivo* on Purkinje cell, we observed that neuronal activity modulates the formation of node-like clusters along axons prior to myelination. However, neuronal activity could modulate several mechanisms that may promote the formation of node-like clusters. First, our team observed that the inhibition of protein synthesis in culture of hippocampal neurons inhibit the formation of node-like clusters (Dubessy and Sol-Foulon, unpublished data), in line with previous work performed *in vitro* on retinal ganglion cell (Kaplan et al., 2001). Furthermore, it has been described that neuronal activity modulates the transcriptome of neurons including parvalbumin and somatostatin interneurons (Spiegel et al., 2014; Mardinly et al., 2016; Yap and Greenberg, 2018), that form node-like clusters (Freeman et al., 2015). The formation of node like-clusters starts in particular with the clustering of αNav subunits Nav1.1 and 1.2 (Kaplan et al., 2001; Freeman et al., 2015). *In vitro*, it was shown that neuronal activity tends to upregulate Nav1.1 transcripts (late-response gene, 6 hours) specifically in culture of inhibitory neurons and not in culture of cortical excitatory neurons (Spiegel et al., 2014). Furthermore, it was observed that, in mixed culture and purified neuronal culture treated with OCM, GABAergic neurons forming node-like clusters tend to show a higher firing frequency associated with a higher expression of Nav1.1 transcripts compared to GABAergic neurons in untreated purified neuronal cultures that do not form node-like clusters (Mazuir et al., 2021). Thus, it is possible that the effect of neuronal activity on the formation of node-like clusters is modulated through the upregulation of nodal markers such as Nav1.1.

The activation of node-like clustering by neuronal activity could also act through its effect on nodal proteins transport and targeting. It was shown, by studying the dynamic assembly of node-like clusters, that nodal proteins can partially preassemble prior to membrane targeting along axons of GABAergic neurons *in vitro* (Thetiot et al., 2020). Furthermore, the kinesin-1 family member KIF5A and C were identified as necessary for nodal proteins trafficking prior to node-like cluster formation (Thetiot et al., 2020). Since it was previously shown that the transport of mitochondria by KIF5 along axons is modulated by neuronal activity (Ohno et al., 2011; Chen and Sheng, 2013), neuronal activity might also modulate the transport of nodal protein vesicles. The mitochondrial transport was modulated by calcium rise upon neuronal activity that inhibit the transport and stabilize the cargo (Ohno et al., 2011; Chen and Sheng, 2013). This mechanism was in particular observed at the nodal axolemma along Purkinje cell axons, and was inhibited by Ca^{2+} chelation (Ohno et al., 2011). Therefore, along Purkinje unmyelinated axons that display calcium transients upon stimulation (Callewaert et al., 1996), it is possible that neuronal activity by triggering calcium transients regulates nodal proteins transport by KIF5. The calcium transients may be further amplified locally at Nav channels starting to cluster due to their small calcium permeability (Hanemaaijer et al., 2020). In addition to stabilizing nodal proteins cargo, Ca^{2+} signals triggered by neuronal activity might promote the targeting of nodal proteins at membranes by promoting vesicle exocytosis, a mechanism that was suggested to participate to node of Ranvier formation in the optic nerve (Alix et al., 2008).

Of note, neuronal activity promotes the formation of node-like clusters but is not necessary for their formation, since for instance commissural primary ascending neurons are largely silent but form node-like clusters along their axons prior to myelination (Auer, 2019; Vagionitis et al., 2021). *In vitro*, in hippocampal culture, the complete block of neuronal activity with tetrodotoxin decreases by half the number of GABAergic neurons that forms node-like clusters (Mazuir and Sol-Foulon, unpublished data). Therefore, neuronal activity promotes, but is not necessary, for the formation of node-like clusters.

3.3 Neuronal activity promotes node-like cluster formation: effect on action potential conduction

The formation of node-like clusters along the axon of hippocampal GABAergic neurons is associated with a faster conduction of action potential (Freeman et al., 2015). Thus, in the case of long-projecting neurons such as Purkinje cells or retinal ganglion cells, the formation of node-like clusters prior to myelination might constitute a temporary state with an intermediate conduction speed of the signals between brain structures. The formation of node-like clusters might also change the effect of an action potential, on the activation of some terminal arborizations of the axon. Indeed, an action potential does not necessarily activate all terminals of the axon, and conduction failure, in particular

at branch points, is a process that filter communication with the post-synaptic neurons (Deschênes and Landry, 1980; Wall, 1995; Debanne et al., 1997). The formation of node-like clusters along highly ramified axons such as parvalbumine interneurons may modulate the proportion of branches along which the action potential is propagated. Conduction failure further depends on the firing frequency (Grossman et al., 1979; Meeks et al., 2005), and in fast spiking parvalbumin neurons, the reliability of action potential propagation has been shown to depend on sodium channel density (Hu and Jonas, 2014). Therefore, the formation of node-like clusters by changing the reliability of action potential propagation might affect neural networks functioning. To support this hypothesis, it has been shown in hippocampal culture that β 2Nav, which participates to the early formation of node-like clusters (Thetiot et al., 2020), secures the propagation of action potential at branch points (Cho et al., 2017). Lastly, along neocortical layer 5 axons, the encoding of high frequency burst involves the first node (most proximal)(Kole, 2011). Therefore, the formation of node-like clusters proximally along fast-spiking parvalbumin interneuron axons might also facilitate the generation of high frequency firing pattern, involved in gamma oscillations (40-100Hz) or sharp wave ripples (>140Hz) (Lapray et al., 2012; Hu et al., 2014).

3.4 Neuronal activity promotes node-like clusters formation: effect on myelination

As discussed earlier in the results (part 2), the formation of node-like clusters has been suggested to guide the initiation of myelination *in vitro* and a subset of these clusters were suggested to act as landmarks for the future pattern of myelination *in vivo* in zebrafish (Thetiot et al., 2020; Vagionitis et al., 2021). However, since the inter node-like cluster distance is shorter (40 to 50%) than the inter mature node spacing, not all the node-like clusters predefine the localization of mature node (Freeman et al., 2015; Vagionitis et al., 2021). In line with these observations, it has been described that upon myelination some clusters, are integrated to or become heminodes, and subsequently move along axons to form mature nodes or stable heminodes (Thetiot et al., 2020; Vagionitis et al., 2021). In zebrafish, it was shown that a neurofascin A mutant lacking the transmembrane domain show an alteration of the myelin pattern with longer internode on average (Vagionitis et al., 2021). However, in this study the exact role of neurofascin on the formation or the stability of node-like clusters was not determined (Vagionitis et al., 2021). Since in hippocampal culture from rodents, the absence of neurofascin 186 does not alter the formation of node-like clusters and was suggested to restrict further nodal protein clustering (Freeman et al., 2015; Thetiot et al., 2020), it is likely that neurofascin rather acts as a stop signal that regulates the growth of the myelin sheath facing a node-like cluster. It would be interesting to investigate this mechanism further and in particular assess the molecular differences

between stable vs moving node-like clusters to identify the key parameters responsible for the stability of a subpart of the node-like clusters.

3.5 Node-like clusters are formed prior to remyelination: an impact on repair

Isolated clusters of Nav channels were observed in post-mortem tissues from MS patients. Interestingly, there was a higher density of isolated Nav clusters in partially remyelinated plaques than in periplaques. Thus, these data suggested that Nav channels are clustered prior to remyelination similarly to what was described prior to developmental myelination (Coman et al., 2006). On organotypic cerebellar slices, similarly, it has been observed in our lab that isolated node-like clusters, are observed prior to remyelination (Thetiot and Desmazières, unpublished data, Figure 43). These observations raise the question of the involvement of node-like cluster formation in the process of remyelination. The investigation of the function of these structures in remyelination by modulating their formation would be difficult. Indeed, the inhibition or the activation of the formation of node-like clusters, for instance by a knock-down of AnkyrinG or an overexpression of β 2Nav (Freeman et al., 2015; Thetiot et al., 2020), may inevitably lead to indirect modulations of neuronal activity involved in the modulation of remyelination (Gautier et al., 2015; Jensen et al., 2018; Ortiz et al., 2019; Bacmeister et al., 2020). Nevertheless, it would be interesting to assess whether the stimulation of neuronal activity promotes the formation of node-like clusters and remyelination specifically along stimulated axons similarly to what we have observed during developmental myelination. Furthermore, extrapolating from the results obtained in developmental myelination, it is possible that some of the node-like clusters help to reestablish the original pattern of myelination (as discussed in the results, part 2). Since it has been suggested that node-like clusters may also guide the initiation of myelination (Thetiot et al., 2020), it is also possible that their formation along demyelinated fibers signals axons that are still functional and “should” be remyelinated.

Prior to myelination, the formation of node-like clusters correlates with an higher conduction velocity (Freeman et al., 2015). Following focal demyelination of the ventral spinal root with LPC a conduction block is observed (Smith L et al., 1982). Interestingly, it was shown that the conduction along the demyelinated axons was never continuous but reappeared at specific spatially restrained domains of inward current, notifying the presence of clustered Nav channels named ϕ -nodes (Smith L et al., 1982). Thus, the formation of node-like clusters may be a first step in the restauration of the conduction. If node-like clusters indeed participate to the restauration of action potential conduction their formation might take part to the activation of remyelination by neuronal activity. Indeed, during developmental myelination neuronal activity promotes myelin deposition by synaptic vesicles release (Hines et al., 2015; Mensch et al., 2015; Wake et al., 2015; Koudelka et al., 2016; Almeida et al., 2021),

and synaptic inputs on OPCs were suggested to promote remyelination (Gautier et al., 2015), two mechanisms that require action potential to reach the site of vesicle release. Therefore, it is crucial to better understand the mechanism and the role of node-like cluster formation the process of remyelination.

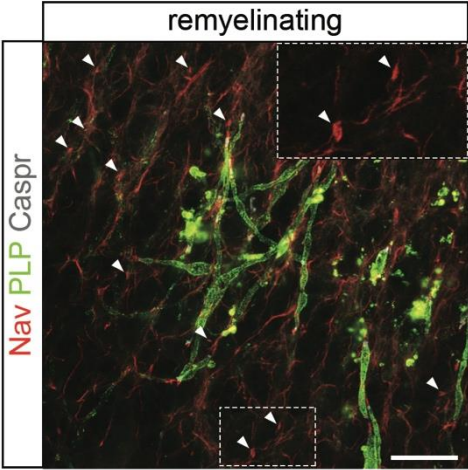


Figure 43: Node-like clusters are observed prior to remyelination in mouse organotypic cerebellar slices. Orthogonal projections showing isolated clusters of Nav channels (in red, filled arrowhead) in a remyelinating cerebellar slices at 11 DIV. Scale bar: (A) 20 μ m.

Concluding remarks

Myelin defects are not restricted to demyelinating diseases, and in some pathologies such as schizophrenia and epilepsy, abnormalities in myelination have been observed (Yang et al., 2012; Du et al., 2013). In these diseases, the abnormal myelination is often associated with defects in circuit activity (Bragin et al., 2004; Knowles et al., 2020), alteration of inhibitory circuits (Selten et al., 2016; Makinson et al., 2017; Maas et al., 2020) and microglia activation (Beach et al., 1995; Morin-Brureau et al., 2018; Sellgren et al., 2019). Thus, in these pathologies, it would be interesting to investigate the formation of the nodes of Ranvier, and their interaction with glial cells. Indeed, the alteration of circuit function and activity might lead to defects in nodal formation or in glia-node interactions which could participate to the development of the pathology.

Furthermore, it would be interesting to study the function of microglia-node interaction and node-like cluster formation in CNS plasticity. As discussed previously, microglial cells may dynamically modulate action potential conduction by regulating the structure of nodes they interact with. Moreover, node-like cluster formation has been studied only in the contexts of developmental myelination and remyelination so far. It would be interesting to assess whether node-like clusters are also formed prior to myelin deposition in adaptive myelination. Indeed, the formation of node-like clusters prior to adaptive myelination, by modulating action potential conduction along unmyelinated axons, or by promoting myelin deposition, might also take part to neuronal circuits plasticity.

References

- A. Privat, C. Jacque, J. M. Bourre, P. Dupouey, and N. Baumann (1979). Absence of the major dense line in myelin of the mutant mouse 'shiverer.' *Neurosci. Lett.*
- Abbott, L. F., and Nelson, S. B. (2000). Synaptic plasticity: taming the beast. *Nat. Neurosci.* 3, 1178–1183. doi:10.1038/81453.
- Absinta, M., Maric, D., Gharagozloo, M., Garton, T., Smith, M. D., Jin, J., et al. (2021). A lymphocyte–microglia–astrocyte axis in chronic active multiple sclerosis. *Nature* 597, 709–714. doi:10.1038/s41586-021-03892-7.
- Adaikkan, C., Middleton, S. J., Marco, A., Pao, P.-C., Mathys, H., Kim, D. N.-W., et al. (2019). Gamma Entrainment Binds Higher-Order Brain Regions and Offers Neuroprotection. *Neuron* 102, 929–943.e8. doi:10.1016/j.neuron.2019.04.011.
- Aggarwal, S., Snaidero, N., Pahler, G., and Frey, S. (2013). Myelin Membrane Assembly Is Driven by a Phase Transition of Myelin Basic Proteins Into a Cohesive Protein Meshwork. 11. doi:10.1371/journal.pbio.1001577.
- Aggarwal, S., Yurlova, L., and Simons, M. (2011a). Central nervous system myelin: Structure, synthesis and assembly. *Trends Cell Biol.* 21, 585–593. doi:10.1016/j.tcb.2011.06.004.
- Aggarwal, S., Yurlova, L., Snaidero, N., Reetz, C., Frey, S., Zimmermann, J., et al. (2011b). A Size Barrier Limits Protein Diffusion at the Cell Surface to Generate Lipid-Rich Myelin-Membrane Sheets. *Dev. Cell* 21, 445–456. doi:10.1016/j.devcel.2011.08.001.
- Akiyoshi, R., Wake, H., Kato, D., Horiuchi, H., Ono, R., Ikegami, A., et al. (2018). Microglia Enhance Synapse Activity to Promote Local Network Synchronization. *eneuro* 5, ENEURO.0088-18.2018. doi:10.1523/ENEURO.0088-18.2018.
- Alix, J. J. P., Dolphin, A. C., and Fern, R. (2008). Vesicular apparatus, including functional calcium channels, are present in developing rodent optic nerve axons and are required for normal node of Ranvier formation. *J. Physiol.* 586, 4069–4089. doi:10.1113/jphysiol.2008.155077.
- Alliot, F., Godin, I., and Pessac, B. (1999). Microglia derive from progenitors, originating from the yolk sac, and which proliferate in the brain. *Dev. Brain Res.* 117, 145–152. doi:10.1016/S0165-3806(99)00113-3.
- Alliot, F., Lecain, E., Grima, B., and Pessac, B. (1991). Microglial progenitors with a high proliferative potential in the embryonic and adult mouse brain. *Proc. Natl. Acad. Sci.* 88, 1541–1545. doi:10.1073/pnas.88.4.1541.
- Almeida, R. G., Pan, S., Cole, K. L. H., Williamson, J. M., Early, J. J., Czopka, T., et al. (2018). Myelination of Neuronal Cell Bodies when Myelin Supply Exceeds Axonal Demand. *Curr. Biol.* 28, 1296–1305.e5. doi:10.1016/j.cub.2018.02.068.
- Almeida, R. G., Williamson, J. M., Madden, M. E., Talbot, W. S., Bianco, I. H., Lyons, D. A., et al. (2021). Myelination induces axonal hotspots of synaptic vesicle fusion that promote sheath growth. *Curr. Biol.*, 1–12. doi:10.1016/j.cub.2021.06.036.
- Amor, V., Zhang, C., Vainshtein, A., Zhang, A., Zollinger, D. R., Eshed-Eisenbach, Y., et al. (2017). The paranodal cytoskeleton clusters Na⁺ channels at nodes of Ranvier. *Elife* 6, 1–15. doi:10.7554/eLife.21392.
- Andoh, M., Shibata, K., Okamoto, K., Onodera, J., Morishita, K., Miura, Y., et al. (2019). Exercise Reverses Behavioral and Synaptic Abnormalities after Maternal Inflammation. *Cell Rep.* 27, 2817–2825.e5. doi:10.1016/j.celrep.2019.05.015.
- Apolloni, S., Fabbrizio, P., Parisi, C., Amadio, S., and Volonté, C. (2016). Clemastine Confers Neuroprotection and Induces an Anti-Inflammatory Phenotype in SOD1G93A Mouse Model of Amyotrophic Lateral Sclerosis. *Mol. Neurobiol.* 53, 518–531. doi:10.1007/s12035-014-9019-8.
- Arancibia-Carcamo, I. L., and Attwell, D. (2014). The node of Ranvier in CNS pathology. *Acta Neuropathol.* 128, 161–175. doi:10.1007/s00401-014-1305-z.

- Arancibia-Cárcamo, I. L., Ford, M. C., Cossell, L., Ishida, K., Tohyama, K., and Attwell, D. (2017). Node of Ranvier length as a potential regulator of myelinated axon conduction speed. *Elife* 6, 1–15. doi:10.7554/eLife.23329.
- Arancillo, M., White, J. J., Lin, T., Stay, T. L., and Sillitoe, R. V. (2015). In vivo analysis of Purkinje cell firing properties during postnatal mouse development. *J. Neurophysiol.* 113, 578–591. doi:10.1152/jn.00586.2014.
- Armbruster, M., Naskar, S., Garcia, J., Sommer, M., Kim, E., Adam, Y., et al. (2021). Neuronal activity drives pathway-specific depolarization of astrocyte distal processes. *bioRxiv*. doi:10.1101/2021.07.03.450922.
- Arnett, H. A. (2004). bHLH Transcription Factor Olig1 Is Required to Repair Demyelinated Lesions in the CNS. *Science (80-)*. 306, 2111–2115. doi:10.1126/science.1103709.
- Arnett, H. A., Mason, J., Marino, M., Suzuki, K., Matsushima, G. K., and Ting, J. P. Y. (2001). TNF α promotes proliferation of oligodendrocyte progenitors and remyelination. *Nat. Neurosci.* 4, 1116–1122. doi:10.1038/nn738.
- Arroyo, E. J., and Scherer, S. S. (2000). On the molecular architecture of myelinated fibers. *Histochem. Cell Biol.* 113, 0001. doi:10.1007/s004180050001.
- Askew, K., Li, K., Olmos-Alonso, A., Garcia-Moreno, F., Liang, Y., Richardson, P., et al. (2017). Coupled Proliferation and Apoptosis Maintain the Rapid Turnover of Microglia in the Adult Brain. *Cell Rep.* 18, 391–405. doi:10.1016/j.celrep.2016.12.041.
- Attwell, D., and Iles, J. F. (1979). Synaptic transmission: ion concentration changes in the synaptic cleft. *Proc. R. Soc. London. Ser. B, Biol. Sci.* 206, 115–31. doi:10.1098/rspb.1979.0095.
- Auer, F. (2019). Investigating mechanisms of myelin sheath length regulation and plasticity.
- Auer, F., Vagionitis, S., and Czopka, T. (2018). Evidence for Myelin Sheath Remodeling in the CNS Revealed by In Vivo Imaging. *Curr. Biol.* 28, 549-559.e3. doi:10.1016/j.cub.2018.01.017.
- Augustine, G. J., Charlton, M. P., and Horn, R. (1988). Role of calcium-activated potassium channels in transmitter release at the squid giant synapse. *J. Physiol.* 398, 149–164. doi:10.1113/jphysiol.1988.sp017035.
- Baalman, K., Marin, M. A., Ho, T. S. Y., Godoy, M., Cherian, L., Robertson, C., et al. (2015). Axon initial segment–associated microglia. *J. Neurosci.* 35, 2283–2292. doi:10.1523/JNEUROSCI.3751-14.2015.
- Bacmeister, C. M., Barr, H. J., McClain, C. R., Thornton, M. A., Nettles, D., Welle, C. G., et al. (2020). Motor learning promotes remyelination via new and surviving oligodendrocytes. *Nat. Neurosci.* 23, 819–831. doi:10.1038/s41593-020-0637-3.
- Bacmeister, C. M., Huang, R., Thornton, M. A., Conant, L., Chavez, A., Poleg-polsky, A., et al. (2021). Motor Learning Drives Dynamic Patterns of Intermittent Myelination on Behaviorally-Activated Axons. *bioRxiv*.
- Badimon, A., Ayata, P., Strasburger, H. J., Chen, X., Ikegami, A., Graves, S. M., et al. (2020). Negative feedback control of neuronal activity by microglia. *Nature*. doi:10.1038/s41586-020-2777-8.
- Bagchi, B., Al-Sabi, A., Kaza, S., Scholz, D., O’Leary, V. B., Dolly, J. O., et al. (2014). Disruption of Myelin Leads to Ectopic Expression of KV1.1 Channels with Abnormal Conductivity of Optic Nerve Axons in a Cuprizone-Induced Model of Demyelination. *PLoS One* 9, e87736. doi:10.1371/journal.pone.0087736.
- Balia, M., Benamer, N., and Angulo, M. C. (2017). A specific GABAergic synapse onto oligodendrocyte precursors does not regulate cortical oligodendrogenesis. *Glia* 65, 1821–1832. doi:10.1002/glia.23197.
- Bansal, R., and Pfeiffer, S. E. (1989). Reversible inhibition of oligodendrocyte progenitor differentiation by a monoclonal antibody against surface galactolipids. *Proc. Natl. Acad. Sci.* 86, 6181–6185. doi:10.1073/pnas.86.16.6181.
- Baraban, M., Koudelka, S., and Lyons, D. A. (2018). Ca²⁺ activity signatures of myelin sheath formation and growth in vivo. *Nat. Neurosci.* 21, 19–25. doi:10.1038/s41593-017-0040-x.
- Barres, B. A., Hart, I. K., Coles, H. S. R., Burne, J. F., Voyvodic, J. T., Richardson, W. D., et al. (1992). Cell death and control of cell survival in the oligodendrocyte lineage. *Cell* 70, 31–46.

- doi:10.1016/0092-8674(92)90531-G.
- Barres, B. A., Koroshetz, W. J., Swartz, K. J., Chun, L. L. Y., and Corey, D. P. (1990). Ion channel expression by white matter glia: The O-2A glial progenitor cell. *Neuron* 4, 507–524. doi:10.1016/0896-6273(90)90109-S.
- Barres, B. A., and Raff, M. C. (1993). Proliferation of oligodendrocyte precursor cells depends on electrical activity in axons. *Nature* 361, 258–260. doi:10.1038/361258a0.
- Barry, J., Gu, Y., Jukkola, P., O’Neill, B., Gu, H., Mohler, P. J., et al. (2014). Ankyrin-G Directly Binds to Kinesin-1 to Transport Voltage-Gated Na⁺ Channels into Axons. *Dev. Cell* 28, 117–131. doi:10.1016/j.devcel.2013.11.023.
- Battefeld, A., Popovic, M. A., de Vries, S. I., and Kole, M. H. P. (2019). High-Frequency Microdomain Ca²⁺ Transients and Waves during Early Myelin Internode Remodeling. *Cell Rep.* 26, 182–191.e5. doi:10.1016/j.celrep.2018.12.039.
- Battefeld, A., Tran, B. T., Gavrilis, J., Cooper, E. C., and Kole, M. H. P. (2014). Heteromeric Kv7.2/7.3 channels differentially regulate action potential initiation and conduction in neocortical myelinated axons. *J. Neurosci.* 34, 3719–3732. doi:10.1523/JNEUROSCI.4206-13.2014.
- Bauer, J., Berkenbosch, F., Van Dam, A.-M., and Dijkstra, C. D. (1993). Demonstration of interleukin-1 β in Lewis rat brain during experimental allergic encephalomyelitis by immunocytochemistry at the light and ultrastructural level. *J. Neuroimmunol.* 48, 13–21. doi:10.1016/0165-5728(93)90053-2.
- Baumgartner, S., Littleton, J. T., Broadie, K., Bhat, M. A., Harbecke, R., Lengyel, J. A., et al. (1996). A Drosophila Neurexin Is Required for Septate Junction and Blood-Nerve Barrier Formation and Function. *Cell* 87, 1059–1068. doi:10.1016/S0092-8674(00)81800-0.
- Beach, T. G., Woodhurst, W. B., MacDonald, D. B., and Jones, M. W. (1995). Reactive microglia in hippocampal sclerosis associated with human temporal lobe epilepsy. *Neurosci. Lett.* 191, 27–30. doi:10.1016/0304-3940(94)11548-1.
- Bekku, Y., Rauch, U., Ninomiya, Y., and Oohashi, T. (2009). Brevican distinctively assembles extracellular components at the large diameter nodes of Ranvier in the CNS. *J. Neurochem.* 108, 1266–1276. doi:10.1111/j.1471-4159.2009.05873.x.
- Bekku, Y., Vargová, L., Goto, Y., Vorísek, I., Dmytrenko, L., Narasaki, M., et al. (2010). Bral1: Its role in diffusion barrier formation and conduction velocity in the CNS. *J. Neurosci.* 30, 3113–3123. doi:10.1523/JNEUROSCI.5598-09.2010.
- Benamer, N., Vidal, M., Balia, M., and Angulo, M. C. (2020). Myelination of parvalbumin interneurons shapes the function of cortical sensory inhibitory circuits. *Nat. Commun.* 11, 1–14. doi:10.1038/s41467-020-18984-7.
- Bennett, M. L., Bennett, F. C., Liddelow, S. A., Ajami, B., Zamanian, J. L., Fernhoff, N. B., et al. (2016). New tools for studying microglia in the mouse and human CNS. *Proc. Natl. Acad. Sci. U. S. A.* 113, E1738–E1746. doi:10.1073/pnas.1525528113.
- Bennett, V., and Lorenzo, D. N. (2016). “An Adaptable Spectrin/Ankyrin-Based Mechanism for Long-Range Organization of Plasma Membranes in Vertebrate Tissues,” in 143–184. doi:10.1016/bs.ctm.2015.10.001.
- Berg, D. A., Kirkham, M., Wang, H., Frisén, J., and Simon, A. (2011). Dopamine Controls Neurogenesis in the Adult Salamander Midbrain in Homeostasis and during Regeneration of Dopamine Neurons. *Cell Stem Cell* 8, 426–433. doi:10.1016/j.stem.2011.02.001.
- Berghoff, S. A., Spieth, L., Sun, T., Hosang, L., Schlaphoff, L., Depp, C., et al. (2021). Microglia facilitate repair of demyelinated lesions via post-squalene sterol synthesis. *Nat. Neurosci.* 24, 47–60. doi:10.1038/s41593-020-00757-6.
- Berghs, S., Aggujaro, D., Dirx, R., Maksimova, E., Stabach, P., Hermel, J.-M., et al. (2000). β iv Spectrin, a New Spectrin Localized at Axon Initial Segments and Nodes of Ranvier in the Central and Peripheral Nervous System. *J. Cell Biol.* 151, 985–1002. doi:10.1083/jcb.151.5.985.
- Bergles, D. E., Roberts, J. D. B., Somogyi, P., and Jahr, C. E. (2000). Glutamatergic synapses on oligodendrocyte precursor cells in the hippocampus. *Nature* 405, 187–191. doi:10.1038/35012083.

- Bernier, L. P., Bohlen, C. J., York, E. M., Choi, H. B., Kamyabi, A., Dissing-Olesen, L., et al. (2019). Nanoscale Surveillance of the Brain by Microglia via cAMP-Regulated Filopodia. *Cell Rep.* 27, 2895–2908.e4. doi:10.1016/j.celrep.2019.05.010.
- Bertrand, J. Y., Jalil, A., Klaine, M., Jung, S., Cumano, A., and Godin, I. (2005). Three pathways to mature macrophages in the early mouse yolk sac. *Blood* 106, 3004–3011. doi:10.1182/blood-2005-02-0461.
- Bhat, M. A., Rios, J. C., Lu, Y., Garcia-Fresco, G. P., Ching, W., Martin, M. St., et al. (2001). Axon-Glia Interactions and the Domain Organization of Myelinated Axons Requires Neurexin IV/Caspr/Paranodin. *Neuron* 30, 369–383. doi:10.1016/S0896-6273(01)00294-X.
- Bian, Z., Gong, Y., Huang, T., Lee, C. Z. W., Bian, L., Bai, Z., et al. (2020). Deciphering human macrophage development at single-cell resolution. *Nature* 582, 571–576. doi:10.1038/s41586-020-2316-7.
- Birgbauer, E., Rao, T. S., and Webb, M. (2004). Lysolecithin induces demyelination in vitro in a cerebellar slice culture system. *J. Neurosci. Res.* 78, 157–166. doi:10.1002/jnr.20248.
- Black, J. A., Dib-Hajj, S., Baker, D., Newcombe, J., Cuzner, M. L., and Waxman, S. G. (2000). Sensory neuron-specific sodium channel SNS is abnormally expressed in the brains of mice with experimental allergic encephalomyelitis and humans with multiple sclerosis. *Proc. Natl. Acad. Sci.* 97, 11598–11602. doi:10.1073/pnas.97.21.11598.
- Black, J. A., Foster, R. E., and Waxman, S. G. (1982). Rat optic nerve: Freeze-fracture studies during development of myelinated axons. *Brain Res.* 250, 1–20. doi:10.1016/0006-8993(82)90948-9.
- Black, J. A., Friedman, B., Waxman, S. G., Elmer, L. W., and Angelides, K. J. (1989). Immunocytochemical localization of sodium channels at nodes of Ranvier and perinodal astrocytes in rat optic nerve. *Proc. R. Soc. London. Ser. B, Biol. Sci.* 238, 39–51. doi:10.1098/rspb.1989.0065.
- Black, J. A., and Waxman, S. G. (1988). The perinodal astrocyte. *Glia* 1, 169–183. doi:10.1002/glia.440010302.
- Blakemore, W. F. (1972). Observations on oligodendrocyte degeneration, the resolution of status spongiosus and remyelination in cuprizone intoxication in mice. *J. Neurocytol.* 1, 413–426. doi:10.1007/BF01102943.
- Blakemore, W. F. (1973). Remyelination of the superior cerebellar peduncle in the mouse following demyelination induced by feeding cuprizone. *J. Neurol. Sci.* 20, 73–83. doi:10.1016/0022-510X(73)90119-6.
- Blakemore, W. F. (1974). Pattern of remyelination in the CNS. *Nature* 249, 577–578. doi:10.1038/249577a0.
- Blinzinger, K., and Kreutzberg, G. (1968). Displacement of synaptic terminals from regenerating motoneurons by microglial cells. *Zeitschrift für Zellforschung und Mikroskopische Anat.* 85, 145–157. doi:10.1007/BF00325030.
- Bliss, T. V. P., and Lømo, T. (1973). Long-lasting potentiation of synaptic transmission in the dentate area of the anaesthetized rabbit following stimulation of the perforant path. *J. Physiol.* 232, 331–356. doi:10.1113/jphysiol.1973.sp010273.
- Bö, L., Mörk, S., Kong, P. A., Nyland, H., Pardo, C. A., and Trapp, B. D. (1994). Detection of MHC class II-antigens on macrophages and microglia, but not on astrocytes and endothelia in active multiple sclerosis lesions. *J. Neuroimmunol.* 51, 135–146. doi:10.1016/0165-5728(94)90075-2.
- Boiko, T., Rasband, M. N., Levinson, S. R., Caldwell, J. H., Mandel, G., Trimmer, J. S., et al. (2001). Compact Myelin Dictates the Differential Targeting of Two Sodium Channel Isoforms in the Same Axon. *Neuron* 30, 91–104. doi:10.1016/S0896-6273(01)00265-3.
- Bolam, J. P., and Pissadaki, E. K. (2012). Living on the edge with too many mouths to feed: Why dopamine neurons die. *Mov. Disord.* 27, 1478–1483. doi:10.1002/mds.25135.
- Bolasco, G., Weinhard, L., Boissonnet, T., Neujahr, R., and Gross, C. T. (2018). Three-Dimensional Nanostructure of an Intact Microglia Cell. *Front. Neuroanat.* 12. doi:10.3389/fnana.2018.00105.
- Bonetto, G., Hivert, B., Goutebroze, L., Karagogeos, D., Crépel, V., and Faivre-Sarrailh, C. (2019). Selective axonal expression of the Kv1 channel complex in pre-myelinated GABAergic hippocampal neurons. *Front. Cell. Neurosci.* 13, 1–17. doi:10.3389/fncel.2019.00222.

- Bonnon, C., Goutebroze, L., Denisenko-Nehrbass, N., Girault, J.-A., and Faivre-Sarrailh, C. (2003). The Paranodal Complex of F3/Contactin and Caspr/Paranodin Traffics to the Cell Surface via a Non-conventional Pathway. *J. Biol. Chem.* 278, 48339–48347. doi:10.1074/jbc.M309120200.
- Bosio, A., Binczek, E., and Stoffel, W. (1996). Functional breakdown of the lipid bilayer of the myelin membrane in central and peripheral nervous system by disrupted galactocerebroside synthesis. *Proc. Natl. Acad. Sci. U. S. A.* 93, 13280–13285. doi:10.1073/pnas.93.23.13280.
- Bostock, H., and Sears, T. A. (1978). The internodal axon membrane: electrical excitability and continuous conduction in segmental demyelination. *J. Physiol.* 280, 273–301. doi:10.1113/jphysiol.1978.sp012384.
- Böttcher, C., Schlickeiser, S., Sneebouer, M. A. M., Kunkel, D., Knop, A., Paza, E., et al. (2019). Human microglia regional heterogeneity and phenotypes determined by multiplexed single-cell mass cytometry. *Nat. Neurosci.* 22, 78–90. doi:10.1038/s41593-018-0290-2.
- Bragin, A., Wilson, C. L., Almajano, J., Mody, I., and Engel, J. (2004). High-frequency Oscillations after Status Epilepticus: Epileptogenesis and Seizure Genesis. *Epilepsia* 45, 1017–1023. doi:10.1111/j.0013-9580.2004.17004.x.
- Braun, N., Sévigny, J., Robson, S. C., Enyoji, K., Guckelberger, O., Hammer, K., et al. (2000). Assignment of ecto-nucleoside triphosphate diphosphohydrolase-1/cd39 expression to microglia and vasculature of the brain. *Eur. J. Neurosci.* 12, 4357–66. Available at: <http://www.ncbi.nlm.nih.gov/pubmed/11122346>.
- Brill, M. H., Waxman, S. G., Moore, J. W., and Joyner, R. W. (1977). Conduction velocity and spike configuration in myelinated fibres: Computed dependence on internode distance. *J. Neurol. Neurosurg. Psychiatry* 40, 769–774. doi:10.1136/jnnp.40.8.769.
- Brohawn, S. G., Wang, W., Handler, A., Campbell, E. B., Schwarz, J. R., and MacKinnon, R. (2019). The mechanosensitive ion channel TRAAK is localized to the mammalian node of Ranvier. *Elife* 8. doi:10.7554/eLife.50403.
- Brown, J. W. L., Cunniffe, N. G., Prados, F., Kanber, B., Jones, J. L., Needham, E., et al. (2021). Safety and efficacy of bexarotene in patients with relapsing-remitting multiple sclerosis (CCMR One): a randomised, double-blind, placebo-controlled, parallel-group, phase 2a study. *Lancet Neurol.* 20, 709–720. doi:10.1016/S1474-4422(21)00179-4.
- Bruce, K. D., Gorkhali, S., Given, K., Coates, A. M., Boyle, K. E., Macklin, W. B., et al. (2018). Lipoprotein Lipase Is a Feature of Alternatively-Activated Microglia and May Facilitate Lipid Uptake in the CNS During Demyelination. *Front. Mol. Neurosci.* 11. doi:10.3389/fnmol.2018.00057.
- Buggen, D. Van, Pohl, F., Langseth, C. M., Kukanja, P., Lee, H., Kabbe, M., et al. (2021). Developmental landscape of human forebrain at a single-cell level unveils early waves of oligodendrogenesis. 1–23.
- Brunoni, A. R., Chaimani, A., Moffa, A. H., Razza, L. B., Gattaz, W. F., Daskalakis, Z. J., et al. (2017). Repetitive Transcranial Magnetic Stimulation for the Acute Treatment of Major Depressive Episodes. *JAMA Psychiatry* 74, 143. doi:10.1001/jamapsychiatry.2016.3644.
- Buffington, S. A., and Rasband, M. N. (2013). Na⁺ Channel-Dependent Recruitment of Nav 4 to Axon Initial Segments and Nodes of Ranvier. *J. Neurosci.* 33, 6191–6202. doi:10.1523/JNEUROSCI.4051-12.2013.
- Bunge, M. B., Bunge, R. P., and Pappas, G. D. (1962). Electron microscopic demonstration of connections between glia and myelin sheaths in the developing mammalian central nervous system. *J. Cell Biol.* 12, 448–453. doi:10.1083/jcb.12.2.448.
- Bunge, M. B., Bunge, R. P., and Ris, H. (1961). ULTRASTRUCTURAL STUDY OF REMYELINATION IN AN EXPERIMENTAL LESION IN ADULT CAT SPINAL CORD. *J. Biophys. Biochem. Cytol.* 10, 67–94. doi:10.1083/jcb.10.1.67.
- Bunge, R. P. (1968). Glial cells and the central myelin sheath. *Physiol. Rev.* 48, 197–251. doi:10.1152/physrev.1968.48.1.197.
- Butovsky, O., Jedrychowski, M. P., Moore, C. S., Cialic, R., Lanser, A. J., Gabriely, G., et al. (2014). Identification of a unique TGF- β -dependent molecular and functional signature in microglia.

- Nat. Neurosci.* 17, 131–143. doi:10.1038/nn.3599.
- Butovsky, O., Landa, G., Kunis, G., Ziv, Y., Avidan, H., Greenberg, N., et al. (2006a). Induction and blockage of oligodendrogenesis by differently activated microglia in an animal model of multiple sclerosis. *J. Clin. Invest.* 116, 905–915. doi:10.1172/JCI26836.
- Butovsky, O., and Weiner, H. L. (2018). Microglial signatures and their role in health and disease. *Nat. Rev. Neurosci.* 19, 622–635. doi:10.1038/s41583-018-0057-5.
- Butovsky, O., Ziv, Y., Schwartz, A., Landa, G., Talpalar, A. E., Pluchino, S., et al. (2006b). Microglia activated by IL-4 or IFN- γ differentially induce neurogenesis and oligodendrogenesis from adult stem/progenitor cells. *Mol. Cell. Neurosci.* 31, 149–160. doi:10.1016/j.mcn.2005.10.006.
- Butt, A. M., Duncan, A., and Berry, M. (1994). Astrocyte associations with nodes of Ranvier: ultrastructural analysis of HRP-filled astrocytes in the mouse optic nerve. *J. Neurocytol.* 23, 486–499. doi:10.1007/BF01184072.
- Butt, A. M., Duncan, A., Hornby, M. F., Kirvell, S. L., Hunter, A., Levine, J. M., et al. (1999). Cells expressing the NG2 antigen contact nodes of ranvier in adult CNS white matter. *Glia* 26, 84–91. doi:10.1002/(SICI)1098-1136(199903)26:1<84::AID-GLIA9>3.0.CO;2-L.
- Cai, J., Qi, Y., Hu, X., Tan, M., Liu, Z., Zhang, J., et al. (2005). Generation of Oligodendrocyte Precursor Cells from Mouse Dorsal Spinal Cord Independent of Nkx6 Regulation and Shh Signaling. *Neuron* 45, 41–53. doi:10.1016/j.neuron.2004.12.028.
- Cajal, S. R. y (1894). La fine structure des centres nerveux. *Proc. R. Soc. London - Biol. Sci.*, 444–468.
- Caldwell, J. H., Schaller, K. L., Lasher, R. S., Peles, E., and Levinson, S. R. (2000). Sodium channel Na(v)1.6 is localized at nodes of ranvier, dendrites, and synapses. *Proc. Natl. Acad. Sci. U. S. A.* 97, 5616–20. doi:10.1073/pnas.090034797.
- Call, C. L., and Bergles, D. E. (2021). Cortical neurons exhibit diverse myelination patterns that scale between mouse brain regions and regenerate after demyelination. *Nat. Commun.* 12, 4767. doi:10.1038/s41467-021-25035-2.
- Callewaert, G., Eilers, J., and Konnerth, A. (1996). Axonal calcium entry during fast “sodium” action potentials in rat cerebellar Purkinje neurones. *J. Physiol.* 495, 641–647.
- Cantaut-Belarif, Y., Antri, M., Pizzarelli, R., Colasse, S., Vaccari, I., Soares, S., et al. (2017). Microglia control the glycinergic but not the GABAergic synapses via prostaglandin E2 in the spinal cord. *J. Cell Biol.* 216, 2979–2989. doi:10.1083/jcb.201607048.
- Cantoni, C., Bollman, B., Licastro, D., Xie, M., Mikesell, R., Schmidt, R., et al. (2015). TREM2 regulates microglial cell activation in response to demyelination in vivo. *Acta Neuropathol.* 129, 429–447. doi:10.1007/s00401-015-1388-1.
- Cantuti-Castelvetri, L., Fitzner, D., Bosch-Queralt, M., Weil, M.-T., Su, M., Sen, P., et al. (2018). Defective cholesterol clearance limits remyelination in the aged central nervous system. *Science (80-.)*. 359, 684–688. doi:10.1126/science.aan4183.
- Carl, A., Frey, B. W., Ward, S. M., Sanders, K. M., and Kenyon, J. L. (1993). Inhibition of slow-wave repolarization and Ca(2+)-activated K⁺ channels by quaternary ammonium ions. *Am. J. Physiol. Physiol.* 264, C625–C631. doi:10.1152/ajpcell.1993.264.3.C625.
- Carré, J.-L., Goetz, B. D., O’Connor, L. T., Bremer, Q., and Duncan, I. D. (2002). Mutations in the rat myelin basic protein gene are associated with specific alterations in other myelin gene expression. *Neurosci. Lett.* 330, 17–20. doi:10.1016/S0304-3940(02)00709-7.
- Carroll, W. (1998). Identification of the adult resting progenitor cell by autoradiographic tracking of oligodendrocyte precursors in experimental CNS demyelination. *Brain* 121, 293–302. doi:10.1093/brain/121.2.293.
- Carroll, W. M., and Jennings, A. R. (1994). Early recruitment of oligodendrocyte precursors in CNS demyelination. *Brain* 117, 563–578. doi:10.1093/brain/117.3.563.
- Chang, A., Nishiyama, A., Peterson, J., Prineas, J., and Trapp, B. D. (2000). NG2-Positive Oligodendrocyte Progenitor Cells in Adult Human Brain and Multiple Sclerosis Lesions. *J. Neurosci.* 20, 6404–6412. doi:10.1523/JNEUROSCI.20-17-06404.2000.
- Chang, A., Tourtellotte, W. W., Rudick, R., and Trapp, B. D. (2002). Premyelinating Oligodendrocytes in Chronic Lesions of Multiple Sclerosis. *N. Engl. J. Med.* 346, 165–173.

doi:10.1056/NEJMoa010994.

- Chang, K.-J., Zollinger, D. R., Susuki, K., Sherman, D. L., Makara, M. A., Brophy, P. J., et al. (2014). Glial ankyrins facilitate paranodal axoglial junction assembly. *Nat. Neurosci.* 17, 1673–1681. doi:10.1038/nn.3858.
- Chang, W., Pedroni, A., Bertuzzi, M., Kizil, C., Simon, A., and Ampatzis, K. (2021). Locomotion dependent neuron-glia interactions control neurogenesis and regeneration in the adult zebrafish spinal cord. *Nat. Commun.* 12, 4857. doi:10.1038/s41467-021-25052-1.
- Charcot, J. M. (1868). *Leçons de 1868; Manuscrits des leçons de JM Charcot*. Fonds numé. Paris.
- Charles, P., Tait, S., Faivre-Sarrailh, C., Barbin, G., Gunn-Moore, F., Denisenko-Nehrbass, N., et al. (2002). Neurofascin Is a Glial Receptor for the Paranodin/Caspr-Contactin Axonal Complex at the Axoglial Junction. *Curr. Biol.* 12, 217–220. doi:10.1016/S0960-9822(01)00680-7.
- Chaumont Joseph, Guyon, N., Valera, A. M., Dugué, G. P., Popa, D., Marcaggi, P., et al. (2013). Clusters of cerebellar Purkinje cells control their afferent climbing fiber discharge. *Proc. Natl. Acad. Sci. U. S. A.* 110, 16223–16228.
- Cheadle, L., Rivera, S. A., Phelps, J. S., Ennis, K. A., Stevens, B., Burkly, L. C., et al. (2020). Sensory Experience Engages Microglia to Shape Neural Connectivity through a Non-Phagocytic Mechanism. *Neuron* 108, 451-468.e9. doi:10.1016/j.neuron.2020.08.002.
- Cheepsunthorn, P., Palmer, C., and Connor, J. R. (1998). Cellular distribution of ferritin subunits in postnatal rat brain. *J. Comp. Neurol.* 400, 73–86. Available at: <http://www.ncbi.nlm.nih.gov/pubmed/9762867>.
- Chen, C. (2004). Mice Lacking Sodium Channel 1 Subunits Display Defects in Neuronal Excitability, Sodium Channel Expression, and Nodal Architecture. *J. Neurosci.* 24, 4030–4042. doi:10.1523/JNEUROSCI.4139-03.2004.
- Chen, C., Bharucha, V., Chen, Y., Westenbroek, R. E., Brown, A., Malhotra, J. D., et al. (2002). Reduced sodium channel density, altered voltage dependence of inactivation, and increased susceptibility to seizures in mice lacking sodium channel β 2-subunits. *Proc. Natl. Acad. Sci. U. S. A.* 99, 17072–17077. doi:10.1073/pnas.212638099.
- Chen, J., Liu, K., Hu, B., Xiao, L., Chan, J. R., Mei, F., et al. (2021). Article Enhancing myelin renewal reverses cognitive dysfunction in a murine model of Alzheimer ' s disease Article Enhancing myelin renewal reverses cognitive dysfunction in a murine model of Alzheimer ' s disease. 1–16. doi:10.1016/j.neuron.2021.05.012.
- Chen, Y., and Sheng, Z.-H. (2013). Kinesin-1–syntaphilin coupling mediates activity-dependent regulation of axonal mitochondrial transport. *J. Cell Biol.* 202, 351–364. doi:10.1083/jcb.201302040.
- Ching, W., Zanazzi, G., Levinson, S. R., and Salzer, J. L. (1999). Clustering of neuronal sodium channels requires contact with myelinating Schwann cells. *J. Neurocytol.* 28, 295–301. doi:10.1023/a:1007053411667.
- Chittajallu, R., Aguirre, A., and Gallo, V. (2004). NG2-positive cells in the mouse white and grey matter display distinct physiological properties. *J. Physiol.* 561, 109–122. doi:10.1113/jphysiol.2004.074252.
- Chiu, S. Y. (1980). Asymmetry currents in the mammalian myelinated nerve. *J. Physiol.* 309, 499–519. doi:10.1113/jphysiol.1980.sp013523.
- Cho, I. H., Panzera, L. C., Chin, M., and Hoppa, M. B. (2017). Sodium channel β 2 subunits prevent action potential propagation failures at axonal branch points. *J. Neurosci.* 37, 9419–9533. doi:10.1523/JNEUROSCI.0891-17.2017.
- Chomiak, T., and Hu, B. (2009). What Is the Optimal Value of the g-Ratio for Myelinated Fibers in the Rat CNS? A Theoretical Approach. *PLoS One* 4, e7754. doi:10.1371/journal.pone.0007754.
- Chong, S. Y. C., Rosenberg, S. S., Fancy, S. P. J., Zhao, C., Shen, Y. A. A., Hahn, A. T., et al. (2012). Neurite outgrowth inhibitor Nogo-A establishes spatial segregation and extent of oligodendrocyte myelination. *Proc. Natl. Acad. Sci. U. S. A.* 109, 1299–1304. doi:10.1073/pnas.1113540109.
- Church, J. S., Kigerl, K. A., Lerch, J. K., Popovich, P. G., and McTigue, D. M. (2016). TLR4 Deficiency

- Impairs Oligodendrocyte Formation in the Injured Spinal Cord. *J. Neurosci.* 36, 6352–6364. doi:10.1523/JNEUROSCI.0353-16.2016.
- Cignarella, F., Filipello, F., Bollman, B., Cantoni, C., Locca, A., Mikesell, R., et al. (2020). TREM2 activation on microglia promotes myelin debris clearance and remyelination in a model of multiple sclerosis. *Acta Neuropathol.* doi:10.1007/s00401-020-02193-z.
- Clark, K. C., Josephson, A., Benusa, S. D., Hartley, R. K., Baer, M., Thummala, S., et al. (2016). Compromised axon initial segment integrity in EAE is preceded by microglial reactivity and contact. *Glia* 64, 1190–1209. doi:10.1002/glia.22991.
- Coetzee, T., Fujita, N., Dupree, J., Shi, R., Blight, A., Suzuki, K., et al. (1996). Myelination in the absence of galactocerebroside and sulfatide: Normal structure with abnormal function and regional instability. *Cell* 86, 209–219. doi:10.1016/S0092-8674(00)80093-8.
- Cohen, C. C. H., Popovic, M. A., Klooster, J., Weil, M., Möbius, W., Nave, K.-A., et al. (2019). Saltatory Conduction along Myelinated Axons Involves a Periaxonal Nanocircuit. *Cell*, 1–12. doi:10.1016/j.cell.2019.11.039.
- Colakoglu, G., Bergstrom-Tyrberg, U., Berglund, E. O., and Ranscht, B. (2014). Contactin-1 regulates myelination and nodal/paranodal domain organization in the central nervous system. *Proc. Natl. Acad. Sci.* 111, E394–E403. doi:10.1073/pnas.1313769110.
- Coman, I., Aigrot, M. S., Seilhean, D., Reynolds, R., Girault, J. A., Zalc, B., et al. (2006). Nodal, paranodal and juxtaparanodal axonal proteins during demyelination and remyelination in multiple sclerosis. *Brain* 129, 3186–3195. doi:10.1093/brain/awl144.
- Connor, J. R., and Menzies, S. L. (1996). Relationship of iron to oligodendrocytes and myelination. *Glia* 17, 83–93. doi:10.1002/(SICI)1098-1136(199606)17:2<83::AID-GLIA1>3.0.CO;2-7.
- Cooper, E. C. (2011). Made for “anchorin”: Kv7.2/7.3 (KCNQ2/KCNQ3) channels and the modulation of neuronal excitability in vertebrate axons. *Semin. Cell Dev. Biol.* 22, 185–192. doi:10.1016/j.semcdb.2010.10.001.
- Corkrum, M., Covelo, A., Lines, J., Bellocchio, L., Pisansky, M., Loke, K., et al. (2020). Dopamine-Evoked Synaptic Regulation in the Nucleus Accumbens Requires Astrocyte Activity. *Neuron* 105, 1036–1047.e5. doi:10.1016/j.neuron.2019.12.026.
- Costello, D. A., Lyons, A., Denieffe, S., Browne, T. C., Cox, F. F., and Lynch, M. A. (2011). Long Term Potentiation Is Impaired in Membrane Glycoprotein CD200-deficient Mice. *J. Biol. Chem.* 286, 34722–34732. doi:10.1074/jbc.M111.280826.
- Crair, M. C., and Malenka, R. C. (1995). A critical period for long-term potentiation at thalamocortical synapses. *Nature* 375, 325–328. doi:10.1038/375325a0.
- Craner, M. J., Hains, B. C., Lo, A. C., Black, J. A., and Waxman, S. G. (2004a). Co-localization of sodium channel Nav1.6 and the sodium-calcium exchanger at sites of axonal injury in the spinal cord in EAE. *Brain* 127, 294–303. doi:10.1093/brain/awh032.
- Craner, M. J., Lo, A. C., Black, J. A., and Waxman, S. G. (2003). Abnormal sodium channel distribution in optic nerve axons in a model of inflammatory demyelination. *Brain* 126, 1552–1561. doi:10.1093/brain/awg153.
- Craner, M. J., Newcombe, J., Black, J. A., Hartle, C., Cuzner, M. L., and Waxman, S. G. (2004b). Molecular changes in neurons in multiple sclerosis: Altered axonal expression of Nav1.2 and Nav1.6 sodium channels and Na⁺/Ca²⁺ exchanger. *Proc. Natl. Acad. Sci.* 101, 8168–8173. doi:10.1073/pnas.0402765101.
- Crawford, D. K., Mangiardi, M., Xia, X., López-Valdés, H. E., and Tiwari-Woodruff, S. K. (2009). Functional recovery of callosal axons following demyelination: a critical window. *Neuroscience* 164, 1407–1421. doi:10.1016/j.neuroscience.2009.09.069.
- Cree, B. A. C., Hollenbach, J. A., Bove, R., Kirkish, G., Sacco, S., Caverzasi, E., et al. (2019). Silent progression in disease activity-free relapsing multiple sclerosis. *Ann. Neurol.* 85, 653–666. doi:10.1002/ana.25463.
- Cserép, C., Pósfai, B., and Dénes, Á. (2021a). Shaping Neuronal Fate: Functional Heterogeneity of Direct Microglia-Neuron Interactions. *Neuron* 109, 222–240. doi:10.1016/j.neuron.2020.11.007.
- Cserép, C., Pósfai, B., Lénárt, N., Fekete, R., László, Z. I., Lele, Z., et al. (2020). Microglia monitor and

- protect neuronal function through specialized somatic purinergic junctions. *Science* (80-.). 367, 528–537. doi:10.1126/science.aax6752.
- Cserép, C., Schwarcz, A. D., Pósfai, B., László, Z. I., Kellermayer, A., Nyerges, M., et al. (2021b). Somatic junctions connect microglia and developing neurons. 1–31. Available at: <https://doi.org/10.1101/2021.03.25.436920>.
- Cullen, C. L., Pepper, R. E., Clutterbuck, M. T., Rodger, J., Jolivet, R. B., Young, K. M., et al. (2021). Periaxonal and nodal plasticities modulate action potential conduction in the adult mouse brain II Periaxonal and nodal plasticities modulate action potential conduction in the adult mouse brain. *CellReports* 34, 108641. doi:10.1016/j.celrep.2020.108641.
- Cumano, A., and Godin, I. (2007). Ontogeny of the Hematopoietic System. *Annu. Rev. Immunol.* 25, 745–785. doi:10.1146/annurev.immunol.25.022106.141538.
- Cunha, M. I., Su, M., Cantuti-Castelvetri, L., Müller, S. A., Schifferer, M., Djannatian, M., et al. (2020). Pro-inflammatory activation following demyelination is required for myelin clearance and oligodendrogenesis. *J. Exp. Med.* 217. doi:10.1084/jem.20191390.
- Cunningham, C. L., Martinez-Cerdeno, V., and Noctor, S. C. (2013). Microglia Regulate the Number of Neural Precursor Cells in the Developing Cerebral Cortex. *J. Neurosci.* 33, 4216–4233. doi:10.1523/JNEUROSCI.3441-12.2013.
- Czopka, T., French-Constant, C., and Lyons, D. A. (2013). Individual oligodendrocytes have only a few hours in which to generate new myelin sheaths *in vivo*. *Dev. Cell* 25, 599–609. doi:10.1016/j.devcel.2013.05.013.
- D’Este, E., Kamin, D., Balzarotti, F., and Hell, S. W. (2017). Ultrastructural anatomy of nodes of Ranvier in the peripheral nervous system as revealed by STED microscopy. *Proc. Natl. Acad. Sci. U. S. A.* 114, E191–E199. doi:10.1073/pnas.1619553114.
- D’Este, E., Kamin, D., Velte, C., Göttfert, F., Simons, M., and Hell, S. W. (2016). Subcortical cytoskeleton periodicity throughout the nervous system. *Sci. Rep.* 6, 1–8. doi:10.1038/srep22741.
- Dai, Z.-M., Sun, S., Wang, C., Huang, H., Hu, X., Zhang, Z., et al. (2014). Stage-Specific Regulation of Oligodendrocyte Development by Wnt/ -Catenin Signaling. *J. Neurosci.* 34, 8467–8473. doi:10.1523/JNEUROSCI.0311-14.2014.
- Davalos, D., Grutzendler, J., Yang, G., Kim, J. V., Zuo, Y., Jung, S., et al. (2005). ATP mediates rapid microglial response to local brain injury *in vivo*. *Nat. Neurosci.* 8, 752–758. doi:10.1038/nn1472.
- Davalos, D., Kyu Ryu, J., Merlini, M., Baeten, K. M., Le Moan, N., Petersen, M. A., et al. (2012). Fibrinogen-induced perivascular microglial clustering is required for the development of axonal damage in neuroinflammation. *Nat. Commun.* 3. doi:10.1038/ncomms2230.
- Davis, J. Q., Lambert, S., and Bennett, V. (1996). Molecular composition of the node of Ranvier: identification of ankyrin-binding cell adhesion molecules neurofascin (mucin+/third FNIII domain-) and NrCAM at nodal axon segments. *J. Cell Biol.* 135, 1355–1367. doi:10.1083/jcb.135.5.1355.
- Dawson, M., Polito, A., Levine, J. M., and Reynolds, R. (2003). NG2-expressing glial progenitor cells: an abundant and widespread population of cycling cells in the adult rat CNS. *Mol. Cell. Neurosci.* 24, 476–488. doi:10.1016/S1044-7431(03)00210-0.
- De Biase, L. M., Nishiyama, A., and Bergles, D. E. (2010). Excitability and Synaptic Communication within the Oligodendrocyte Lineage. *J. Neurosci.* 30, 3600–3611. doi:10.1523/JNEUROSCI.6000-09.2010.
- De Biase, L. M., Schuebel, K. E., Fuschel, Z. H., Jair, K., Hawes, I. A., Cimbri, R., et al. (2017). Local Cues Establish and Maintain Region-Specific Phenotypes of Basal Ganglia Microglia. *Neuron* 95, 341–356.e6. doi:10.1016/j.neuron.2017.06.020.
- Debanne, D., Guérineau, N. C., Gähwiler, B. H., and Thompson, S. M. (1997). Action-potential propagation gated by an axonal IA-like K⁺ conductance in hippocampus. *Nature* 389, 286–289. doi:10.1038/38502.
- Declercq, W., Denecker, G., Fiers, W., and Vandenabeele, P. (1998). Cooperation of both TNF receptors in inducing apoptosis: involvement of the TNF receptor-associated factor binding

- domain of the TNF receptor 75. *J. Immunol.* 161, 390–9. Available at: <http://www.ncbi.nlm.nih.gov/pubmed/9647248>.
- del Río-Hortega, P. (1919a). El “‘Tercer Elemento’” de los Centros Nerviosos. I. La Microglia en Estado Normal. *Bol. la Soc. Esp. Biol.* VIII, 67–82.
- del Río-Hortega, P. (1919b). El “‘Tercer Elemento de los Centros Nerviosos’”. II. Intervencion de la Microglia en los Procesos Patologicos (Celulas en Bastoncito y Cuerpos Granuloadiposos). *Bol. la Soc. Esp. Biol.*, 91–103.
- del Río-Hortega, P. (1919c). El “‘Tercer Elemento’” de los Centros Nerviosos. III. Naturaleza Probable de la Microglia. *Bol. la Soc. Esp. Biol.* VIII.
- del Río-Hortega, P. (1919d). El “‘Tercer Elemento de los Centros Nerviosos’”. IV. Poder Fagocitario y Movilidad de la Microglia. *Bol. la Soc. Esp. Biol.* VIII, 154–171.
- del Río-Hortega, P. (1921). Estudios sobre la neurologia. La glía de escasas radiaciones (oligodendroglía). *Boletín la Real Soc. Española Hist. Nat.* 21, 63–92.
- del Río-Hortega, P. (1922). ¿Son homologables la glía de escasas radiaciones y la célula de Schwann? *Boletín la Soc. Española Biol.* 10, 25–28.
- del Río-Hortega, P. (1928). *Río-Hortega’s third contribution to the morphological knowledge and functional interpretation of the oligodendroglia*. English tr. , ed. Elsevier London.
- del Río-Hortega, P. (1932). “Microglia. In Cytology and cellular pathology of the nervous system,” in (New-York: Hoeber), 483–534.
- del Río-Hortega, P. (1939). The microglia. *Lancet* 233, 1023–1026. doi:10.1016/S0140-6736(00)60571-8.
- Demel, R. A., and De Kruffyff, B. (1976). The function of sterols in membranes. *Biochim. Biophys. Acta - Rev. Biomembr.* 457, 109–132. doi:10.1016/0304-4157(76)90008-3.
- Demerens, C., Stankoff, B., Logak, M., Anglade, P., Allinquant, B., Couraud, F., et al. (1996). Induction of myelination in the central nervous system by electrical activity. *Proc. Natl. Acad. Sci. U. S. A.* 93, 9887–9892. doi:10.1073/pnas.93.18.9887.
- Dendrou, C. A., Fugger, L., and Friese, M. A. (2015). Immunopathology of multiple sclerosis. *Nat. Rev. Immunol.* 15, 545–558. doi:10.1038/nri3871.
- Denisenko-Nehrbass, N., Oguievetskaia, K., Goutebroze, L., Galvez, T., Yamakawa, H., Ohara, O., et al. (2003). Protein 4.1B associates with both Caspr/paranodin and Caspr2 at paranodes and juxtaparanodes of myelinated fibres. *Eur. J. Neurosci.* 17, 411–416. doi:10.1046/j.1460-9568.2003.02441.x.
- Deschênes, M., and Landry, P. (1980). Axonal branch diameter and spacing of nodes in the terminal arborization of identified thalamic and cortical neurons. *Brain Res.* 191, 538–544. doi:10.1016/0006-8993(80)91302-5.
- Desmazieres, A., Zonta, B., Zhang, A., Wu, L. M. N., Sherman, D. L., and Brophy, P. J. (2014). Differential stability of PNS and CNS nodal complexes when neuronal neurofascin is lost. *J. Neurosci.* 34, 5083–5088. doi:10.1523/JNEUROSCI.4662-13.2014.
- Devaux, J., Alcaraz, G., Grinspan, J., Bennett, V., Joho, R., Crest, M., et al. (2003). Kv3.1b is a novel component of CNS nodes. *J. Neurosci.* 23, 4509–4518.
- Devaux, J. J. (2004). KCNQ2 Is a Nodal K⁺ Channel. *J. Neurosci.* 24, 1236–1244. doi:10.1523/JNEUROSCI.4512-03.2004.
- Di Lucente, J., Nguyen, H. M., Wulff, H., Jin, L.-W., and Maezawa, I. (2018). The voltage-gated potassium channel Kv1.3 is required for microglial pro-inflammatory activation in vivo. *Glia* 66, 1881–1895. doi:10.1002/glia.23457.
- Dillenburg, A., Ireland, G., Holloway, R. K., Davies, C. L., Evans, F. L., Swire, M., et al. (2018). Activin receptors regulate the oligodendrocyte lineage in health and disease. *Acta Neuropathol.* 135, 887–906. doi:10.1007/s00401-018-1813-3.
- Dissing-Olesen, L., LeDue, J. M., Rungta, R. L., Hefendehl, J. K., Choi, H. B., and MacVicar, B. A. (2014a). Activation of neuronal NMDA receptors triggers transient ATP-mediated microglial process outgrowth. *J. Neurosci.* 34, 10511–10527. doi:10.1523/JNEUROSCI.0405-14.2014.
- Dissing-Olesen, L., LeDue, J. M., Rungta, R. L., Hefendehl, J. K., Choi, H. B., and MacVicar, B. A.

- (2014b). Activation of Neuronal NMDA Receptors Triggers Transient ATP-Mediated Microglial Process Outgrowth. *J. Neurosci.* 34, 10511–10527. doi:10.1523/JNEUROSCI.0405-14.2014.
- Díaz-Hernández, M., Pintor, J., Castro, E., and Miras-Portugal, M. T. (2002). Co-localisation of functional nicotinic and ionotropic nucleotide receptors in isolated cholinergic synaptic terminals. *Neuropharmacology* 42, 20–33. doi:10.1016/S0028-3908(01)00157-5.
- Djannatian, M., Weikert, U., Safaiyan, S., Wrede, C., Kislinger, G., Ruhwedel, T., et al. (2021). Myelin biogenesis is associated with pathological ultrastructure that is resolved by microglia during development 2 3 4. *bioRxiv*, 2021.02.02.429485. Available at: <https://doi.org/10.1101/2021.02.02.429485>.
- Dolgin, E. (2021). BTK blockers make headway in multiple sclerosis. *Nat. Biotechnol.* 39, 3–5. doi:10.1038/s41587-020-00790-7.
- Donato, A., Kagias, K., Zhang, Y., and Hilliard, M. A. (2019). Neuronal sub-compartmentalization: a strategy to optimize neuronal function. *Biol. Rev.* 94, 1023–1037. doi:10.1111/brv.12487.
- Dours-Zimmermann, M. T., Maurer, K., Rauch, U., Stoffel, W., Fassler, R., and Zimmermann, D. R. (2009). Versican V2 Assembles the Extracellular Matrix Surrounding the Nodes of Ranvier in the CNS. *J. Neurosci.* 29, 7731–7742. doi:10.1523/JNEUROSCI.4158-08.2009.
- Du, F., Cooper, A. J., Thida, T., Shinn, A. K., Cohen, B. M., and Ongür, D. (2013). Myelin and axon abnormalities in schizophrenia measured with magnetic resonance imaging techniques. *Biol. Psychiatry* 74, 451–7. doi:10.1016/j.biopsych.2013.03.003.
- Du, J., Haak, L. L., Phillips-Tansey, E., Russell, J. T., and McBain, C. J. (2000). Frequency-dependent regulation of rat hippocampal somato-dendritic excitability by the K⁺ channel subunit Kv2.1. *J. Physiol.* 522 Pt 1, 19–31. doi:10.1111/j.1469-7793.2000.t01-2-00019.xm.
- Dubessy, A. L., Mazuir, E., Rappeneau, Q., Ou, S., Abi Ghanem, C., Piquand, K., et al. (2019). Role of a Contactin multi-molecular complex secreted by oligodendrocytes in nodal protein clustering in the CNS. *Glia* 67, 2248–2263. doi:10.1002/glia.23681.
- Duflocq, A., Le Bras, B., Bullier, E., Couraud, F., and Davenne, M. (2008). Nav1.1 is predominantly expressed in nodes of Ranvier and axon initial segments. *Mol. Cell. Neurosci.* 39, 180–192. doi:10.1016/j.mcn.2008.06.008.
- Duncan, I. D., Radcliff, A. B., Heidari, M., Kidd, G., August, B. K., and Wierenga, L. A. (2018). The adult oligodendrocyte can participate in remyelination. *Proc. Natl. Acad. Sci. U. S. A.* 115, E11807–E11816. doi:10.1073/pnas.1808064115.
- Dupree, J. L., Mason, J. L., MARCUS, J. R., STULL, M., LEVINSON, R., MATSUSHIMA, G. K., et al. (2004). Oligodendrocytes assist in the maintenance of sodium channel clusters independent of the myelin sheath. *Neuron Glia Biol.* 1, 179–192. doi:10.1017/S1740925X04000304.
- Dutta, D. J., Woo, D. H., Lee, P. R., Pajevic, S., Bukalo, O., Huffman, W. C., et al. (2018). Regulation of myelin structure and conduction velocity by perinodal astrocytes. *Proc. Natl. Acad. Sci. U. S. A.* 115, 11832–11837. doi:10.1073/pnas.1811013115.
- Edgar, J. M., McCulloch, M. C., Thomson, C. E., and Griffiths, I. R. (2008). Distribution of mitochondria along small-diameter myelinated central nervous system axons. *J. Neurosci. Res.* 86, 2250–2257. doi:10.1002/jnr.21672.
- Edgar, J. M., McLaughlin, M., Werner, H. B., McCulloch, M. C., Barrie, J. A., Brown, A., et al. (2009). Early ultrastructural defects of axons and axon-glia junctions in mice lacking expression of Cnp1. *Glia* 57, 1815–1824. doi:10.1002/glia.20893.
- Ehrenberg, C. . (1833). Nothwendigkeit einer feineren mechanischen Zerlegung des Gehirns und der Nerven vor der chemischen, dargestellt aus Beobachtungen. *Ann. Phys.* 28, 449–473.
- Einheber, S., Zanazzi, G., Ching, W., Scherer, S., Milner, T. A., Peles, E., et al. (1997). The Axonal Membrane Protein Caspr, a Homologue of Neurexin IV, Is a Component of the Septate-like Paranodal Junctions That Assemble during Myelination. *J. Cell Biol.* 139, 1495–1506. doi:10.1083/jcb.139.6.1495.
- El Behi, M., Sanson, C., Bachelin, C., Guillot-Noël, L., Fransson, J., Stankoff, B., et al. (2017). Adaptive human immunity drives remyelination in a mouse model of demyelination. *Brain* 140, 967–980. doi:10.1093/brain/awx008.

- Enyedi, P., and Czirják, G. (2010). Molecular Background of Leak K⁺ Currents: Two-Pore Domain Potassium Channels. *Physiol. Rev.* 90, 559–605. doi:10.1152/physrev.00029.2009.
- Eshed-Eisenbach, Y., Devaux, J., Vainshtein, A., Golani, O., Lee, S.-J., Feinberg, K., et al. (2020). Precise Spatiotemporal Control of Nodal Na⁺ Channel Clustering by Bone Morphogenetic Protein-1/Tolloid-like Proteinases. *Neuron* 106, 806–815.e6. doi:10.1016/j.neuron.2020.03.001.
- Eshed, Y., Feinberg, K., Poliak, S., Sabanay, H., Sarig-Nadir, O., Spiegel, I., et al. (2005). Gliomedin Mediates Schwann Cell-Axon Interaction and the Molecular Assembly of the Nodes of Ranvier. *Neuron* 47, 215–229. doi:10.1016/j.neuron.2005.06.026.
- Etxeberria, A., Hokanson, K. C., Dao, D. Q., Mayoral, S. R., Mei, F., Redmond, S. A., et al. (2016). Dynamic modulation of myelination in response to visual stimuli alters optic nerve conduction velocity. *J. Neurosci.* 36, 6937–6948. doi:10.1523/JNEUROSCI.0908-16.2016.
- Eyo, U. B., Mo, M., Yi, M. H., Murugan, M., Liu, J., Yarlagadda, R., et al. (2018). P2Y12R-Dependent Translocation Mechanisms Gate the Changing Microglial Landscape. *Cell Rep.* 23, 959–966. doi:10.1016/j.celrep.2018.04.001.
- Eyo, U. B., Peng, J., Swiatkowski, P., Mukherjee, A., Bispo, A., and Wu, L. J. (2014). Neuronal hyperactivity recruits microglial processes via neuronal NMDA receptors and microglial P2Y12 receptors after status epilepticus. *J. Neurosci.* 34, 10528–10540. doi:10.1523/JNEUROSCI.0416-14.2014.
- Fabricius, C., Berthold, C.-H., and Rydmark, M. (1993). Axoplasmic organelles at nodes of Ranvier. II. Occurrence and distribution in large myelinated spinal cord axons of the adult cat. *J. Neurocytol.* 22, 941–954. doi:10.1007/BF01218352.
- Factor, D. C., Barbeau, A. M., Allan, K. C., Hu, L. R., Madhavan, M., Hoang, A. T., et al. (2020). Cell Type-Specific Intralocus Interactions Reveal Oligodendrocyte Mechanisms in MS. *Cell* 181, 382–395.e21. doi:10.1016/j.cell.2020.03.002.
- Faivre-Sarrailh, C., Gauthier, F., Denisenko-Nehrbass, N., Le Bivic, A., Rougon, G., and Girault, J.-A. (2000). The Glycosylphosphatidyl Inositol-Anchored Adhesion Molecule F3/Contactin Is Required for Surface Transport of Paranodin/Contactin-Associated Protein (Caspr). *J. Cell Biol.* 149, 491–502. doi:10.1083/jcb.149.2.491.
- Fancy, S. P. J., Zhao, C., and Franklin, R. J. M. (2004). Increased expression of Nkx2.2 and Olig2 identifies reactive oligodendrocyte progenitor cells responding to demyelination in the adult CNS. *Mol. Cell. Neurosci.* 27, 247–254. doi:10.1016/j.mcn.2004.06.015.
- Favuzzi, E., Huang, S., Saldi, G. A., Binan, L., Ibrahim, L. A., Fernández-Otero, M., et al. (2021). GABA-receptive microglia selectively sculpt developing inhibitory circuits. *Cell*, 1–16. doi:10.1016/j.cell.2021.06.018.
- Fedoroff, S., Zhai, R., and Novak, J. P. (1997). Microglia and astroglia have a common progenitor cell. *J. Neurosci. Res.* 50, 477–486. doi:10.1002/(SICI)1097-4547(19971101)50:3<477::AID-JNR14>3.0.CO;2-3.
- Feinberg, K., Eshed-Eisenbach, Y., Frechter, S., Amor, V., Salomon, D., Sabanay, H., et al. (2010). A Glial Signal Consisting of Gliomedin and NrCAM Clusters Axonal Na⁺ Channels during the Formation of Nodes of Ranvier. *Neuron* 65, 490–502. doi:10.1016/j.neuron.2010.02.004.
- Feinstein, A., Freeman, J., and Lo, A. C. (2015). Treatment of progressive multiple sclerosis: what works, what does not, and what is needed. *Lancet Neurol.* 14, 194–207. doi:10.1016/S1474-4422(14)70231-5.
- Feldman, D. E. (2012). The Spike-Timing Dependence of Plasticity. *Neuron* 75, 556–571. doi:10.1016/j.neuron.2012.08.001.
- Felts, P. A., Baker, T. A., and Smith, K. J. (1997). Conduction in Segmentally Demyelinated Mammalian Central Axons. *J. Neurosci.* 17, 7267–7277. doi:10.1523/JNEUROSCI.17-19-07267.1997.
- Ferrero, G., Mahony, C. B., Dupuis, E., Yvernogeu, L., Di Ruggiero, E., Miserocchi, M., et al. (2018). Embryonic Microglia Derive from Primitive Macrophages and Are Replaced by cmyb-Dependent Definitive Microglia in Zebrafish. *Cell Rep.* 24, 130–141. doi:10.1016/j.celrep.2018.05.066.
- Ffrench-Constant, C., Miller, R. H., Kruse, J., Schachner, M., and Raff, M. C. (1986). Molecular specialization of astrocyte processes at nodes of Ranvier in rat optic nerve. *J. Cell Biol.* 102,

- 844–852. doi:10.1083/jcb.102.3.844.
- Filipello, F., Morini, R., Corradini, I., Zerbi, V., Canzi, A., Michalski, B., et al. (2018). The Microglial Innate Immune Receptor TREM2 Is Required for Synapse Elimination and Normal Brain Connectivity. *Immunity* 48, 979–991.e8. doi:10.1016/j.immuni.2018.04.016.
- Fontainhas, A. M., Wang, M., Liang, K. J., Chen, S., Mettu, P., Damani, M., et al. (2011). Microglial Morphology and Dynamic Behavior Is Regulated by Ionotropic Glutamatergic and GABAergic Neurotransmission. *PLoS One* 6, e15973. doi:10.1371/journal.pone.0015973.
- Fontana, F. (1781). *Observations sur la structure des nerfs faites à Londres en 1779. Traité sur le Vénin de la Vipere 2*. Florence.
- Foote, A. K., and Blakemore, W. F. (2005). Inflammation stimulates remyelination in areas of chronic demyelination. *Brain* 128, 528–39. doi:10.1093/brain/awh417.
- Ford, M. C., Alexandrova, O., Cossell, L., Stange-Marten, A., Sinclair, J., Kopp-Scheinflug, C., et al. (2015). Tuning of Ranvier node and internode properties in myelinated axons to adjust action potential timing. *Nat. Commun.* 6, 1–14. doi:10.1038/ncomms9073.
- Fourgeaud, L., Través, P. G., Tufail, Y., Leal-Bailey, H., Lew, E. D., Burrola, P. G., et al. (2016). TAM receptors regulate multiple features of microglial physiology. *Nature* 532, 240–244. doi:10.1038/nature17630.
- Frade, J. M., and Barde, Y.-A. (1998). Microglia-Derived Nerve Growth Factor Causes Cell Death in the Developing Retina. *Neuron* 20, 35–41. doi:10.1016/S0896-6273(00)80432-8.
- Frankenhaeuser, B. (1952). Saltatory conduction in myelinated nerve fibers. *J. Physiol.*, 107–112.
- Franklin, R. J. M., and Ffrench-Constant, C. (2008). Remyelination in the CNS: From biology to therapy. *Nat. Rev. Neurosci.* 9, 839–855. doi:10.1038/nrn2480.
- Franklin, R. J. M., Fris, J., and Lyons, D. A. (2020). Seminars in Cell and Developmental Biology Revisiting remyelination : Towards a consensus on the regeneration of CNS myelin. doi:10.1016/j.semcd.2020.09.009.
- Franklin, R. J. M., Gilson, J. M., and Blakemore, W. F. (1997). Local recruitment of remyelinating cells in the repair of demyelination in the central nervous system. *J. Neurosci. Res.* 50, 337–344. doi:10.1002/(SICI)1097-4547(19971015)50:2<337::AID-JNR21>3.0.CO;2-3.
- Freeman, S. A., Desmazières, A., Fricker, D., Lubetzki, C., and Sol-Foulon, N. (2016). Mechanisms of sodium channel clustering and its influence on axonal impulse conduction. *Cell. Mol. Life Sci.* 73, 723–735. doi:10.1007/s00018-015-2081-1.
- Freeman, S. A., Desmazières, A., Simonnet, J., Gatta, M., Pfeiffer, F., Aigrot, M. S., et al. (2015). Acceleration of conduction velocity linked to clustering of nodal components precedes myelination. *Proc. Natl. Acad. Sci. U. S. A.* 112, E321–E328. doi:10.1073/pnas.1419099112.
- Friese, M. A., Schattling, B., and Fugger, L. (2014). Mechanisms of neurodegeneration and axonal dysfunction in multiple sclerosis. *Nat. Rev. Neurol.* 10, 225–238. doi:10.1038/nrneurol.2014.37.
- Frischer, J. M., Weigand, S. D., Guo, Y., Kale, N., Parisi, J. E., Pirko, I., et al. (2015). Clinical and pathological insights into the dynamic nature of the white matter multiple sclerosis plaque. *Ann. Neurol.* 78, 710–721. doi:10.1002/ana.24497.
- Fujii, S., Kato, H., and Kuroda, Y. (2002). Cooperativity between extracellular adenosine 5'-triphosphate and activation of N-methyl-D-aspartate receptors in long-term potentiation induction in hippocampal CA1 neurons. *Neuroscience* 113, 617–628. doi:10.1016/S0306-4522(02)00190-2.
- Fujita, Y., Nakanishi, T., Ueno, M., Itohara, S., and Yamashita, T. (2020). Netrin-G1 Regulates Microglial Accumulation along Axons and Supports the Survival of Layer V Neurons in the Postnatal Mouse Brain. *Cell Rep.* 31, 107580. doi:10.1016/j.celrep.2020.107580.
- Fünfschilling, U., Supplie, L. M., Mahad, D., Boretius, S., Saab, A. S., Edgar, J., et al. (2012). Glycolytic oligodendrocytes maintain myelin and long-term axonal integrity. *Nature* 485, 517–521. doi:10.1038/nature11007.
- Gallego-Delgado, P., James, R., Browne, E., Meng, J., Umashankar, S., Tan, L., et al. (2020). Neuroinflammation in the normal-appearing white matter (NAWM) of the multiple sclerosis brain causes abnormalities at the nodes of Ranvier. doi:10.1371/journal.pbio.3001008.

- Gallo, V., Mangin, J. M., Kukley, M., and Dietrich, D. (2008). Synapses on NG2-expressing progenitors in the brain: Multiple functions? *J. Physiol.* 586, 3767–3781. doi:10.1113/jphysiol.2008.158436.
- Gallo, V., Zhou, J. M., McBain, C. J., Wright, P., Knutson, P. L., and Armstrong, R. C. (1996). Oligodendrocyte progenitor cell proliferation and lineage progression are regulated by glutamate receptor-mediated K⁺ channel block. *J. Neurosci.* 16, 2659–2670. doi:10.1523/jneurosci.16-08-02659.1996.
- Garbay, B., Domec, C., Fournier, M., and Bonnet, J. (1989). Developmental expression of the P0 glycoprotein and basic protein mRNAs in normal and trembler mutant mice. *J. Neurochem.* 53, 907–11. doi:10.1111/j.1471-4159.1989.tb11790.x.
- Garbay, B., Fournier, M., Sallafranque, M. L., Muller, S., Boiron, F., Heape, A., et al. (1988). Po, MBP, histone, and DNA levels in sciatic nerve. Postnatal accumulation studies in normal and trembler mice. *Neurochem. Pathol.* 8, 91–107. doi:10.1007/BF03160138.
- Garbay, B., Heape, A. M., Sargueil, F., and Cassagne, C. (2000). Myelin synthesis in the peripheral nervous system. *Prog. Neurobiol.* 61, 267–304. doi:10.1016/S0301-0082(99)00049-0.
- Garbern, J. Y., Yool, D. A., Moore, G. J., Wilds, I. B., Faulk, M. W., Klugmann, M., et al. (2002). Patients lacking the major CNS myelin protein, proteolipid protein 1, develop length-dependent axonal degeneration in the absence of demyelination and inflammation.
- Garrido, J. J., Giraud, P., Carlier, E., Fernandes, F., Moussif, A., Fache, M.-P., et al. (2003). A Targeting Motif Involved in Sodium Channel Clustering at the Axonal Initial Segment. *Science (80-)*. 300, 2091–2094. doi:10.1126/science.1085167.
- Gasser, A., Ho, T. S.-Y., Cheng, X., Chang, K.-J., Waxman, S. G., Rasband, M. N., et al. (2012). An AnkyrinG-Binding Motif Is Necessary and Sufficient for Targeting Nav1.6 Sodium Channels to Axon Initial Segments and Nodes of Ranvier. *J. Neurosci.* 32, 7232–7243. doi:10.1523/JNEUROSCI.5434-11.2012.
- Gautier, H. O. B., Evans, K. A., Volbracht, K., James, R., Sitnikov, S., Lundgaard, I., et al. (2015). Neuronal activity regulates remyelination via glutamate signalling to oligodendrocyte progenitors. *Nat. Commun.* 6. doi:10.1038/ncomms9518.
- Geha, S., Pallud, J., Junier, M. P., Devaux, B., Leonard, N., Chassoux, F., et al. (2010). NG2+/Olig2+ cells are the major cycle-related cell population of the adult human normal brain. *Brain Pathol.* 20, 399–411. doi:10.1111/j.1750-3639.2009.00295.x.
- Gensert, J. M., and Goldman, J. E. (1997). Endogenous Progenitors Remyelinate Demyelinated Axons in the Adult CNS. *Neuron* 19, 197–203. doi:10.1016/S0896-6273(00)80359-1.
- Geraghty, A. C., Gibson, E. M., Ghanem, R. A., Greene, J. J., Ocampo, A., Goldstein, A. K., et al. (2019). Loss of Adaptive Myelination Contributes to Methotrexate Chemotherapy-Related Cognitive Impairment. *Neuron* 103, 250-265.e8. doi:10.1016/j.neuron.2019.04.032.
- Geren, B. Ben (1954). The formation from the schwann cell surface of myelin in the peripheral nerves of chick embryos. *Exp. Cell Res.* 7, 558–562. doi:10.1016/S0014-4827(54)80098-X.
- Ghasemlou, N., Jeong, S. Y., Lacroix, S., and David, S. (2007). T cells contribute to lysophosphatidylcholine-induced macrophage activation and demyelination in the CNS. *Glia* 55, 294–302. doi:10.1002/glia.20449.
- Gianola, S., Savio, T., Schwab, M. E., and Rossi, F. (2003). Cell-autonomous mechanisms and myelin-associated factors contribute to the development of Purkinje axon intracortical plexus in the rat cerebellum. *J. Neurosci.* 23, 4613–4624. doi:10.1523/jneurosci.23-11-04613.2003.
- Gibson, E. M., Purger, D., Mount, C. W., Goldstein, A. K., Lin, G. L., Wood, L. S., et al. (2014). Neuronal Activity Promotes Oligodendrogenesis and Adaptive Myelination in the Mammalian Brain. *Science (80-)*. 344, 1252304–1252304. doi:10.1126/science.1252304.
- Giera, S., Luo, R., Ying, Y., Ackerman, S. D., Jeong, S. J., Stoveken, H. M., et al. (2018). Microglial transglutaminase-2 drives myelination and myelin repair via GPR56/ADGRG1 in oligodendrocyte precursor cells. *Elife* 7, 1–25. doi:10.7554/eLife.33385.
- Gierten, J., Ficker, E., Bloehs, R., Schlömer, K., Kathöfer, S., Scholz, E., et al. (2008). Regulation of two-pore-domain (K_{2P}) potassium leak channels by the tyrosine kinase inhibitor genistein. *Br. J. Pharmacol.* 154, 1680–1690. doi:10.1038/bjp.2008.213.

- Gilbert, P., Kettenmann, H., and Schachner, M. (1984). gamma-Aminobutyric acid directly depolarizes cultured oligodendrocytes. *J. Neurosci.* 4, 561–569. doi:10.1523/JNEUROSCI.04-02-00561.1984.
- Gilson, J., and Blakemore, W. F. (1993). Failure of remyelination in areas of demyelination produced in the spinal cord of old rats. *Neuropathol. Appl. Neurobiol.* 19, 173–181. doi:10.1111/j.1365-2990.1993.tb00424.x.
- Ginhoux, F., Greter, M., Leboeuf, M., Nandi, S., See, P., Gokhan, S., et al. (2010). Fate Mapping Analysis Reveals That Adult Microglia Derive from Primitive Macrophages. *Science (80-.)*. 701, 841–845. doi:10.1126/science.1194637.
- Giulian, D., and Baker, T. (1986). Characterization of ameboid microglia isolated from developing mammalian brain. *J. Neurosci.* 6, 2163–2178. doi:10.1523/JNEUROSCI.06-08-02163.1986.
- Goldin, A. L., Barchi, R. L., Caldwell, J. H., Hofmann, F., Howe, J. R., Hunter, J. C., et al. (2000). Nomenclature of Voltage-Gated Sodium Channels. *Neuron* 28, 365–368. doi:10.1016/S0896-6273(00)00116-1.
- Goldmann, T., Wieghofer, P., Jordão, M. J. C., Prutek, F., Hagemeyer, N., Frenzel, K., et al. (2016). Origin, fate and dynamics of macrophages at central nervous system interfaces. *Nat. Immunol.* 17, 797–805. doi:10.1038/ni.3423.
- Goldmann, T., Wieghofer, P., Müller, P. F., Wolf, Y., Varol, D., Yona, S., et al. (2013). A new type of microglia gene targeting shows TAK1 to be pivotal in CNS autoimmune inflammation. *Nat. Neurosci.* 16, 1618–1626. doi:10.1038/nn.3531.
- Gollan, L., Sabanay, H., Poliak, S., Berglund, E. O., Ranscht, B., and Peles, E. (2002). Retention of a cell adhesion complex at the paranodal junction requires the cytoplasmic region of Caspr. *J. Cell Biol.* 157, 1247–1256. doi:10.1083/jcb.200203050.
- Gosselin, D., Link, V. M., Romanoski, C. E., Fonseca, G. J., Eichenfield, D. Z., Spann, N. J., et al. (2014). Environment drives selection and function of enhancers controlling tissue-specific macrophage identities. *Cell* 159, 1327–1340. doi:10.1016/j.cell.2014.11.023.
- Graca, D. L., and Blakemore, W. F. (1986). DELAYED REMYELINATION IN RAT SPINAL CORD FOLLOWING ETHIDIUM BROMIDE INJECTION. *Neuropathol. Appl. Neurobiol.* 12, 593–605. doi:10.1111/j.1365-2990.1986.tb00162.x.
- Gravel, M., Peterson, J., Yong, V. W., Kottis, V., Trapp, B., and Braun, P. E. (1996). Overexpression of 2',3'-Cyclic Nucleotide 3'-Phosphodiesterase in Transgenic Mice Alters Oligodendrocyte Development and Produces Aberrant Myelination. *Mol. Cell. Neurosci.* 7, 453–466. doi:10.1006/mcne.1996.0033.
- Green, A. J., Gelfand, J. M., Cree, B. A., Bevan, C., Boscardin, W. J., Mei, F., et al. (2017). Clemastine fumarate as a remyelinating therapy for multiple sclerosis (ReBUILD): a randomised, controlled, double-blind, crossover trial. *Lancet* 390, 2481–2489. doi:10.1016/S0140-6736(17)32346-2.
- Griffiths, I., Klugmann, M., Anderson, T., Yool, D., Thomson, C., Schwab, M. H., et al. (1998). Axonal swellings and degeneration in mice lacking the major proteolipid of myelin.
- Grissmer, S., Nguyen, A. N., Aiyar, J., Hanson, D. C., Mather, R. J., Gutman, G. A., et al. (1994). Pharmacological characterization of five cloned voltage-gated K⁺ channels, types Kv1.1, 1.2, 1.3, 1.5, and 3.1, stably expressed in mammalian cell lines. *Mol. Pharmacol.* 45, 1227–34. doi:7517498.
- Gronski, M. A., Kinchen, J. M., Juncadella, I. J., Franc, N. C., and Ravichandran, K. S. (2009). An essential role for calcium flux in phagocytes for apoptotic cell engulfment and the anti-inflammatory response. *Cell Death Differ.* 16, 1323–1331. doi:10.1038/cdd.2009.55.
- Grossman, Y., Parnas, I., and Spira, M. E. (1979). Mechanisms involved in differential conduction of potentials at high frequency in a branching axon. *J. Physiol.* 295, 307–322. doi:10.1113/jphysiol.1979.sp012970.
- Gründemann, J., and Clark, B. A. (2015). Calcium-Activated Potassium Channels at Nodes of Ranvier Secure Axonal Spike Propagation. *Cell Rep.* 12, 1715–1722. doi:10.1016/j.celrep.2015.08.022.
- Grutzendler, J., Kasthuri, N., and Gan, W.-B. (2002). Long-term dendritic spine stability in the adult cortex. *Nature* 420, 812–816. doi:10.1038/nature01276.
- Gudi, V., Gingele, S., Skripuletz, T., and Stangel, M. (2014). Glial response during cuprizone-induced

- de- and remyelination in the CNS: lessons learned. *Front. Cell. Neurosci.* 8. doi:10.3389/fncel.2014.00073.
- Gyllenstein, L., and Malmfors, T. (1963). Myelination of the optic nerve and its dependence on visual function--a quantitative investigation in mice. *J. Embryol. Exp. Morphol.* 11, 255–266.
- Gyoneva, S., Shapiro, L., Lazo, C., Garnier-Amblard, E., Smith, Y., Miller, G. W., et al. (2014). Adenosine A2A receptor antagonism reverses inflammation-induced impairment of microglial process extension in a model of Parkinson's disease. *Neurobiol. Dis.* 67, 191–202. doi:10.1016/j.nbd.2014.03.004.
- Gyoneva, S., and Traynelis, S. F. (2013). Norepinephrine Modulates the Motility of Resting and Activated Microglia via Different Adrenergic Receptors. *J. Biol. Chem.* 288, 15291–15302. doi:10.1074/jbc.M113.458901.
- Hackett, T. A. (2018). Adenosine A 1 Receptor mRNA Expression by Neurons and Glia in the Auditory Forebrain. *Anat. Rec.* 301, 1882–1905. doi:10.1002/ar.23907.
- Hadley, J. K., Noda, M., Selyanko, A. A., Wood, I. C., Abogadie, F. C., and Brown, D. A. (2000). Differential tetraethylammonium sensitivity of KCNQ1-4 potassium channels. *Br. J. Pharmacol.* 129, 413–415. doi:10.1038/sj.bjp.0703086.
- Hagemeyer, N., Hanft, K. M., Akritidou, M. A., Unger, N., Park, E. S., Stanley, E. R., et al. (2017). Microglia contribute to normal myelinogenesis and to oligodendrocyte progenitor maintenance during adulthood. *Acta Neuropathol.* 134, 441–458. doi:10.1007/s00401-017-1747-1.
- Hall, S. M. (1972). The effect of injections of lysophosphatidyl choline into white matter of the adult mouse spinal cord. *J. Cell Sci.* 10, 535–46. Available at: <http://www.ncbi.nlm.nih.gov/pubmed/5018033>.
- Hamada, M. S., and Kole, M. H. P. (2015). Myelin Loss and Axonal Ion Channel Adaptations Associated with Gray Matter Neuronal Hyperexcitability. *J. Neurosci.* 35, 7272–7286. doi:10.1523/JNEUROSCI.4747-14.2015.
- Hamada, M. S., Popovic, M. A., and Kole, M. H. P. (2017). Loss of saltation and presynaptic action potential failure in demyelinated axons. *Front. Cell. Neurosci.* 11, 1–11. doi:10.3389/fncel.2017.00045.
- Hamilton, N. B., Kolodziejczyk, K., Kougioumtzidou, E., and Attwell, D. (2016). Proton-gated Ca²⁺-permeable TRP channels damage myelin in conditions mimicking ischaemia. *Nature* 529, 523–527. doi:10.1038/nature16519.
- Hamilton, N., Vayro, S., Wigley, R., and Butt, A. M. (2010). Axons and astrocytes release ATP and glutamate to evoke calcium signals in NG2-glia. *Glia* 58, 66–79. doi:10.1002/glia.20902.
- Hammond, T. R., Dufort, C., Dissing-Olesen, L., Giera, S., Young, A., Wysoker, A., et al. (2019). Single-Cell RNA Sequencing of Microglia throughout the Mouse Lifespan and in the Injured Brain Reveals Complex Cell-State Changes. *Immunity* 50, 253–271.e6. doi:10.1016/j.immuni.2018.11.004.
- Hanemaaijer, N. A. K., Popovic, M. A., Wilders, X., Grasman, S., Arocas, O. P., and Kole, M. H. P. (2020). Ca²⁺ entry through nav channels generates submillisecond axonal ca²⁺ signaling. *Elife* 9, 1–75. doi:10.7554/eLife.54566.
- Hanson, M. G., and Landmesser, L. T. (2004). Normal Patterns of Spontaneous Activity Are Required for Correct Motor Axon Guidance and the Expression of Specific Guidance Molecules. *Neuron* 43, 687–701. doi:10.1016/j.neuron.2004.08.018.
- Hao, C., Richardson, A., and Fedoroff, S. (1991). Macrophage-like cells originate from neuroepithelium in culture: Characterization and properties of the macrophage-like cells. *Int. J. Dev. Neurosci.* 9, 1–14. doi:10.1016/0736-5748(91)90067-V.
- Hao, J., Padilla, F., Dandonneau, M., Lavebratt, C., Lesage, F., Noël, J., et al. (2013). Kv1.1 Channels Act as Mechanical Brake in the Senses of Touch and Pain. *Neuron* 77, 899–914. doi:10.1016/j.neuron.2012.12.035.
- Harris, T. H., Banigan, E. J., Christian, D. A., Konradt, C., Tait Wojno, E. D., Norose, K., et al. (2012). Generalized Lévy walks and the role of chemokines in migration of effector CD8⁺ T cells. *Nature* 486, 545–548. doi:10.1038/nature11098.

- Hartley, M. D., Banerji, T., Tagge, I. J., Kirkemo, L. L., Chaudhary, P., Calkins, E., et al. (2019). Myelin repair stimulated by CNS-selective thyroid hormone action. *JCI Insight* 4. doi:10.1172/jci.insight.126329.
- Hartline, D. K. (2011). The evolutionary origins of glia. *Glia* 59, 1215–1236. doi:10.1002/glia.21149.
- Hartline, D. K., and Colman, D. R. (2007). Rapid Conduction and the Evolution of Giant Axons and Myelinated Fibers. *Curr. Biol.* 17, 29–35. doi:10.1016/j.cub.2006.11.042.
- Hassel, B., Rathjen, F. G., and Volkmer, H. (1997). Organization of the neurofascin gene and analysis of developmentally regulated alternative splicing. *J. Biol. Chem.* 272, 28742–28749. doi:10.1074/jbc.272.45.28742.
- Hawkins, R., Abrams, T., Carew, T., and Kandel, E. (1983). A cellular mechanism of classical conditioning in Aplysia: activity-dependent amplification of presynaptic facilitation. *Science* (80- .). 219, 400–405. doi:10.1126/science.6294833.
- Haynes, S. E., Hollopeter, G., Yang, G., Kurpius, D., Dailey, M. E., Gan, W. B., et al. (2006). The P2Y12 receptor regulates microglial activation by extracellular nucleotides. *Nat. Neurosci.* 9, 1512–1519. doi:10.1038/nn1805.
- Healy, L. M., Perron, G., Won, S.-Y., Michell-Robinson, M. A., Rezk, A., Ludwin, S. K., et al. (2016). MerTK Is a Functional Regulator of Myelin Phagocytosis by Human Myeloid Cells. *J. Immunol.* 196, 3375–84. doi:10.4049/jimmunol.1502562.
- Hedstrom, K. L., Xu, X., Ogawa, Y., Frischknecht, R., Seidenbecher, C. I., Shrager, P., et al. (2007). Neurofascin assembles a specialized extracellular matrix at the axon initial segment. *J. Cell Biol.* 178, 875–886. doi:10.1083/jcb.200705119.
- Hetier, E., Ayala, J., Denèfle, P., Bousseau, A., Rouget, P., Mallat, M., et al. (1988). Brain macrophages synthesize interleukin-1 and interleukin-1 mRNAs in vitro. *J. Neurosci. Res.* 21, 391–397. doi:10.1002/jnr.490210230.
- Hickman, S., Izzy, S., Sen, P., Morsett, L., and El Khoury, J. (2018). Microglia in neurodegeneration. *Nat. Neurosci.* 21, 1359–1369. doi:10.1038/s41593-018-0242-x.
- Hildebrand, C. (1971). Ultrastructural and light-microscopic studies of the developing feline spinal cord white matter. I. The nodes of Ranvier. *Acta Physiol. Scand. Suppl.* 364, 81–109. Available at: <http://www.ncbi.nlm.nih.gov/pubmed/4109396> [Accessed September 2, 2019].
- Hildebrand, C., Bowe, C. M., and Remahl, I. N. (1994). Myelination and myelin sheath remodelling in normal and pathological PNS nerve fibres. *Prog. Neurobiol.* 43, 85–141. doi:10.1016/0301-0082(94)90010-8.
- Hildebrand, C., Remahl, S., Persson, H., and Bjartmar, C. (1993). Myelinated nerve fibres in the CNS. *Prog. Neurobiol.* 40, 319–384. doi:10.1016/0301-0082(93)90015-K.
- Hildebrand, C., and Waxman, S. G. (1983). Regional node-like membrane specializations in non-myelinated axons of rat retinal nerve fiber layer. *Brain Res.* 258, 23–32. doi:10.1016/0006-8993(83)91222-2.
- Hill, R. A., Li, A. M., and Grutzendler, J. (2018). Lifelong cortical myelin plasticity and age-related degeneration in the live mammalian brain. *Nat. Neurosci.* 21, 683–695. doi:10.1038/s41593-018-0120-6.
- Hines, J. H., Ravanelli, A. M., Schwindt, R., Scott, E. K., and Appel, B. (2015). Neuronal activity biases axon selection for myelination in vivo. *Nat. Neurosci.* 18, 683–689. doi:10.1038/nn.3992.
- Hirase, H., Qian, L., Barthó, P., and Buzsáki, G. (2004). Calcium Dynamics of Cortical Astrocytic Networks In Vivo. *PLoS Biol.* 2, e96. doi:10.1371/journal.pbio.0020096.
- Hirono, M., Ogawa, Y., Misono, K., Zollinger, D. R., Trimmer, J. S., Rasband, M. N., et al. (2015). BK channels localize to the paranodal junction and regulate action potentials in myelinated axons of cerebellar Purkinje cells. *J. Neurosci.* 35, 7082–7094. doi:10.1523/JNEUROSCI.3778-14.2015.
- Hlavica, M., Delparente, A., Good, A., Good, N., Plattner, P. S., Seyedsadr, M. S., et al. (2017). Intrathecal insulin-like growth factor 1 but not insulin enhances myelin repair in young and aged rats. *Neurosci. Lett.* 648, 41–46. doi:10.1016/j.neulet.2017.03.047.
- Ho, T. S.-Y., Zollinger, D. R., Chang, K.-J., Xu, M., Cooper, E. C., Stankewich, M. C., et al. (2014). A hierarchy of ankyrin-spectrin complexes clusters sodium channels at nodes of Ranvier. *Nat.*

- Neurosci.* 17, 1664–1672. doi:10.1038/nn.3859.
- Hodgkin, A. L., and Huxley, A. F. (1952). A quantitative description of membrane current and its application to conduction and excitation in nerve. *J. Physiol.* 117, 500–544. doi:10.1113/jphysiol.1952.sp004764.
- Hoehn, H. J., Kress, Y., Sohn, A., Brosnan, C. F., Bourdon, S., and Shafit-Zagardo, B. (2008). Axl^{-/-} mice have delayed recovery and prolonged axonal damage following cuprizone toxicity. *Brain Res.* 1240, 1–11. doi:10.1016/j.brainres.2008.08.076.
- Holtman, I. R., Raj, D. D., Miller, J. A., Schaafsma, W., Yin, Z., Brouwer, N., et al. (2015). Induction of a common microglia gene expression signature by aging and neurodegenerative conditions: a co-expression meta-analysis. *Acta Neuropathol. Commun.* 3, 31. doi:10.1186/s40478-015-0203-5.
- Honda, S., Sasaki, Y., Ohsawa, K., Imai, Y., Nakamura, Y., Inoue, K., et al. (2001). Extracellular ATP or ADP Induce Chemotaxis of Cultured Microglia through G_{i/o}-Coupled P2Y Receptors. *J. Neurosci.* 21, 1975–1982. doi:10.1523/JNEUROSCI.21-06-01975.2001.
- Hooks, B. M., and Chen, C. (2006). Distinct Roles for Spontaneous and Visual Activity in Remodeling of the Retinogeniculate Synapse. *Neuron* 52, 281–291. doi:10.1016/j.neuron.2006.07.007.
- Horner, P. J., Power, A. E., Kempermann, G., Kuhn, H. G., Palmer, T. D., Winkler, J., et al. (2000). Proliferation and Differentiation of Progenitor Cells Throughout the Intact Adult Rat Spinal Cord. *J. Neurosci.* 20, 2218–2228. doi:10.1523/JNEUROSCI.20-06-02218.2000.
- Horton, L., Conger, A., Conger, D., Remington, G., Frohman, T., Frohman, E., et al. (2013). Effect of 4-aminopyridine on vision in multiple sclerosis patients with optic neuropathy. *Neurology* 80, 1862–1866. doi:10.1212/WNL.0b013e3182929fd5.
- Hortsch, M., Nagaraj, K., and Godenschwege, T. (2009). The interaction between L1-type proteins and ankyrins - a master switch for L1-type CAM function. *Cell. Mol. Biol. Lett.* 14. doi:10.2478/s11658-008-0035-4.
- Hoshiko, M., Arnoux, I., Avignone, E., Yamamoto, N., and Audinat, E. (2012). Deficiency of the microglial receptor CX3CR1 impairs postnatal functional development of thalamocortical synapses in the barrel cortex. *J. Neurosci.* 32, 15106–15111. doi:10.1523/JNEUROSCI.1167-12.2012.
- Howell, O. W., Rundle, J. L., Garg, A., Komada, M., Brophy, P. J., and Reynolds, R. (2010). Activated Microglia Mediate Axoglial Disruption That Contributes to Axonal Injury in Multiple Sclerosis. *J. Neuropathol. Exp. Neurol.* 69, 1017–1033. doi:10.1097/NEN.0b013e3181f3a5b1.
- Hoyos, H. C., Rinaldi, M., Mendez-Huergo, S. P., Marder, M., Rabinovich, G. A., Pasquini, J. M., et al. (2014). Galectin-3 controls the response of microglial cells to limit cuprizone-induced demyelination. *Neurobiol. Dis.* 62, 441–455. doi:10.1016/j.nbd.2013.10.023.
- Hrvatin, S., Hochbaum, D. R., Nagy, M. A., Cicconet, M., Robertson, K., Cheadle, L., et al. (2018). Single-cell analysis of experience-dependent transcriptomic states in the mouse visual cortex. *Nat. Neurosci.* 21, 120–129. doi:10.1038/s41593-017-0029-5.
- Hu, H., Gan, J., and Jonas, P. (2014). Fast-spiking, parvalbumin⁺ GABAergic interneurons: From cellular design to microcircuit function. *Science (80-)*. 345. doi:10.1126/science.1255263.
- Hu, H., and Jonas, P. (2014). A supercritical density of Na⁺ channels ensures fast signaling in GABAergic interneuron axons. *Nat. Neurosci.* 17, 686–693. doi:10.1038/nn.3678.
- Hu, P., Fabyanic, E., Kwon, D. Y., Tang, S., Zhou, Z., and Wu, H. (2017). Dissecting Cell-Type Composition and Activity-Dependent Transcriptional State in Mammalian Brains by Massively Parallel Single-Nucleus RNA-Seq. *Mol. Cell* 68, 1006–1015.e7. doi:10.1016/j.molcel.2017.11.017.
- Hu, W., Tian, C., Li, T., Yang, M., Hou, H., and Shu, Y. (2009). Distinct contributions of Nav1.6 and Nav1.2 in action potential initiation and backpropagation. *Nat. Neurosci.* 12, 996–1002. doi:10.1038/nn.2359.
- Huang, C. Y.-M., and Rasband, M. N. (2018). Axon initial segments: structure, function, and disease. *Ann. N. Y. Acad. Sci.* 1420, 46–61. doi:10.1111/nyas.13718.
- Huang, J. K., Jarjour, A. A., Nait Oumesmar, B., Kerninon, C., Williams, A., Krezel, W., et al. (2011). Retinoid X receptor gamma signaling accelerates CNS remyelination. *Nat. Neurosci.* 14, 45–53. doi:10.1038/nn.2702.

- Huang, J. K., Phillips, G. R., Roth, A. D., Pedraza, L., Shan, W., Belkaid, W., et al. (2005). Glial Membranes at the Node of Ranvier Prevent Neurite Outgrowth. *Science* (80-.). 310, 1813–1817. doi:10.1126/science.1118313.
- Hughes, A. N. (2021). Glial Cells Promote Myelin Formation and Elimination. *Front. Cell Dev. Biol.* 9, 1–16. doi:10.3389/fcell.2021.661486.
- Hughes, A. N., and Appel, B. (2020). Microglia phagocytose myelin sheaths to modify developmental myelination. *Nat. Neurosci.* 215, 41–47. doi:10.1038/s41593-020-0654-2.
- Hughes, E. G., Orthmann-Murphy, J. L., Langseth, A. J., and Bergles, D. E. (2018). Myelin remodeling through experience-dependent oligodendrogenesis in the adult somatosensory cortex. *Nat. Neurosci.* 21, 696–706. doi:10.1038/s41593-018-0121-5.
- Hume, D. A., Perry, V. H., and Gordon, S. (1983). Immunohistochemical localization of a macrophage-specific antigen in developing mouse retina: phagocytosis of dying neurons and differentiation of microglial cells to form a regular array in the plexiform layers. *J. Cell Biol.* 97, 253–257. doi:10.1083/jcb.97.1.253.
- Hunter, G. K., Wong, K. S., and Kim, J. J. (1988). Binding of calcium to glycosaminoglycans: An equilibrium dialysis study. *Arch. Biochem. Biophys.* 260, 161–167. doi:10.1016/0003-9861(88)90437-7.
- Huxley, B. Y. A. F., and Stampfli, A. D. R. (1949). Evidence for Saltatory Conduction in peripheral myelinated nerves fibers. *J. Physiol.* 108, 315–339.
- Iaccarino, H. F., Singer, A. C., Martorell, A. J., Rudenko, A., Gao, F., Gillingham, T. Z., et al. (2016). Gamma frequency entrainment attenuates amyloid load and modifies microglia. *Nature* 540, 230–235. doi:10.1038/nature20587.
- Imamoto, K., and Leblond, C. P. (1978). Radioautographic investigation of gliogenesis in the corpus callosum of young rats II. Origin of microglial cells. *J. Comp. Neurol.* 180, 139–163. doi:10.1002/cne.901800109.
- Irvine, K. A., and Blakemore, W. F. (2008). Remyelination protects axons from demyelination-associated axon degeneration. *Brain* 131, 1464–1477. doi:10.1093/brain/awn080.
- Ito, D., Imai, Y., Ohsawa, K., Nakajima, K., Fukuuchi, Y., and Kohsaka, S. (1998). Microglia-specific localisation of a novel calcium binding protein, Iba1. *Mol. Brain Res.* 57, 1–9. doi:10.1016/S0169-328X(98)00040-0.
- Izquierdo, P., Shiina, H., Hirunpattarasilp, C., Gillis, G., and Attwell, D. (2021a). Synapse development is regulated by microglial THIK-1 K⁺ channels. *Proc. Natl. Acad. Sci. U. S. A.* 118, 6. doi:10.1073/pnas.2106294118.
- Izquierdo, P., Shiina, H., Hirunpattarasilp, C., Sethi, H., and Attwell, D. (2021b). Synapse development is regulated by microglial THIK-1 K⁺ channels. *bioRxiv*, 6. doi:https://doi.org/10.1101/2021.04.05.438436.
- Jahn, O., Siems, S. B., Kusch, K., Hesse, D., Jung, R. B., Liepold, T., et al. (2020). The CNS Myelin Proteome: Deep Profile and Persistence After Post-mortem Delay. *Front. Cell. Neurosci.* 14. doi:10.3389/fncel.2020.00239.
- Jahn, O., Tenzer, S., and Werner, H. B. (2009). Myelin Proteomics: Molecular Anatomy of an Insulating Sheath. *Mol. Neurobiol.* 40, 55–72. doi:10.1007/s12035-009-8071-2.
- Jarolimek, W., Soman, K. V., Alam, M., and Brown, A. M. (1995). The selectivity of different external binding sites for quaternary ammonium ions in cloned potassium channels. *Pflügers Arch. Eur. J. Physiol.* 430, 672–681. doi:10.1007/BF00386161.
- Jeffery, N. D., and Blakemore, W. F. (1995). Remyelination of mouse spinal cord axons demyelinated by local injection of lysolecithin. *J. Neurocytol.* 24, 775–781. doi:10.1007/BF01191213.
- Jenkins, S. M., and Bennett, V. (2002). Developing nodes of Ranvier are defined by ankyrin-G clustering and are independent of paranodal axoglial adhesion. *Proc. Natl. Acad. Sci.* 99, 2303–2308. doi:10.1073/pnas.042601799.
- Jensen, S. K., Michaels, N. J., Ilyntskyy, S., Keough, M. B., Kovalchuk, O., and Yong, V. W. (2018). Multimodal Enhancement of Remyelination by Exercise with a Pivotal Role for Oligodendroglial PGC1 α . *Cell Rep.* 24, 3167–3179. doi:10.1016/j.celrep.2018.08.060.

- Jiang, B., Sun, X., Cao, K., and Wang, R. (2002). Endogenous Kv channels in human embryonic kidney (HEK-293) cells. *Mol. Cell. Biochem.* 238, 69–79. doi:10.1023/a:1019907104763.
- Jinno, S., Fleischer, F., Eckel, S., Schmidt, V., and Kosaka, T. (2007). Spatial arrangement of microglia in the mouse hippocampus: A stereological study in comparison with astrocytes. *Glia* 55, 1334–1347. doi:10.1002/glia.20552.
- Jo, Y.-H., and Role, L. W. (2002). Coordinate Release of ATP and GABA at In Vitro Synapses of Lateral Hypothalamic Neurons. *J. Neurosci.* 22, 4794–4804. doi:10.1523/JNEUROSCI.22-12-04794.2002.
- Johnston, W. L., Dyer, J. R., Castellucci, V. F., and Dunn, R. J. (1996). Clustered voltage-gated Na⁺ channels in Aplysia axons. *J. Neurosci.* 16, 1730–1739. doi:10.1523/jneurosci.16-05-01730.1996.
- Jordão, M. J. C., Sankowski, R., Brendecke, S. M., Sagar, Locatelli, G., Tai, Y. H., et al. (2019). Neuroimmunology: Single-cell profiling identifies myeloid cell subsets with distinct fates during neuroinflammation. *Science (80-.)*. 363. doi:10.1126/science.aat7554.
- Jukkola, P. I., Lovett-Racke, A. E., Zamvil, S. S., and Gu, C. (2012). K⁺ channel alterations in the progression of experimental autoimmune encephalomyelitis. *Neurobiol. Dis.* 47, 280–293. doi:10.1016/j.nbd.2012.04.012.
- Julio-Kalajzić, F., Villanueva, S., Burgos, J., Ojeda, M., Cid, L. P., Jentsch, T. J., et al. (2018). K⁺ TASK-2 and KCNQ1-KCNE3 K⁺ channels are major players contributing to intestinal anion and fluid secretion. *J. Physiol.* 596, 393–407. doi:10.1113/JP275178.
- Jung, S., Aliberti, J., Graemmel, P., Sunshine, M. J., Kreutzberg, G. W., Sher, A., et al. (2000). Analysis of Fractalkine Receptor CX3CR1 Function by Targeted Deletion and Green Fluorescent Protein Reporter Gene Insertion. *Mol. Cell. Biol.* 20, 4106–4114. doi:10.1128/MCB.20.11.4106-4114.2000.
- Kabat, E. A., Wolf, A., Bezer, A. E., and Murray, J. P. (1951). STUDIES ON ACUTE DISSEMINATED ENCEPHALOMYELITIS PRODUCED EXPERIMENTALLY IN RHESUS MONKEYS. *J. Exp. Med.* 93, 615–633. doi:10.1084/jem.93.6.615.
- Kalla, R., Bohatschek, M., Kloss, C. U. A., Krol, J., Von Maltzan, X., and Raivich, G. (2003). Loss of microglial ramification in microglia-astrocyte cocultures: Involvement of adenylate cyclase, calcium, phosphatase, and Gi-protein systems. *Glia* 41, 50–63. doi:10.1002/glia.10176.
- Kanda, H., Ling, J., Tonomura, S., Noguchi, K., Matalon, S., and Gu, J. G. (2019). TREK-1 and TRAAK Are Principal K⁺ Channels at the Nodes of Ranvier for Rapid Action Potential Conduction on Mammalian Myelinated Afferent Nerves. *Neuron* 104, 960-971.e7. doi:10.1016/j.neuron.2019.08.042.
- Kandel, E. R., Dudai, Y., and Mayford, M. R. (2014). The molecular and systems biology of memory. *Cell* 157, 163–186. doi:10.1016/j.cell.2014.03.001.
- Kang, S. H., Fukaya, M., Yang, J. K., Rothstein, J. D., and Bergles, D. E. (2010). NG2⁺ CNS glial progenitors remain committed to the oligodendrocyte lineage in postnatal life and following neurodegeneration. *Neuron* 68, 668–681. doi:10.1016/j.neuron.2010.09.009.
- Kaplan, M. R., Cho, M. H., Ullian, E. M., Isom, L. L., Levinson, S. R., and Barres, B. A. (2001). Differential control of clustering of the sodium channels Nav1.2 and Nav1.6 at developing CNS nodes of Ranvier. *Neuron* 30, 105–119. doi:10.1016/S0896-6273(01)00266-5.
- Kaplan, M. R., Meyer-Franke, A., Lambert, S., Bennett, V., Duncan, I. D., Levinson, S. R., et al. (1997). Induction of sodium channel clustering by oligodendrocytes. *Nature* 386, 724–728. doi:10.1038/386724a0.
- Káradóttir, R., Cavalier, P., Bergersen, L. H., and Attwell, D. (2005). NMDA receptors are expressed in oligodendrocytes and activated in ischaemia. *Nature* 438, 1162–1166. doi:10.1038/nature04302.
- Káradóttir, R., Hamilton, N. B., Bakiri, Y., and Attwell, D. (2008). Spiking and nonspiking classes of oligodendrocyte precursor glia in CNS white matter. *Nat. Neurosci.* 11, 450–456. doi:10.1038/nn2060.
- Kato, G., Inada, H., Wake, H., Akiyoshi, R., Miyamoto, A., Eto, K., et al. (2016). Microglial Contact Prevents Excess Depolarization and Rescues Neurons from Excitotoxicity. *eneuro* 3, ENEURO.0004-16.2016. doi:10.1523/ENEURO.0004-16.2016.

- Katz, L. C., and Shatz, C. J. (1996). Synaptic Activity and the Construction of Cortical Circuits. *Science* (80-.). 274, 1133–1138. doi:10.1126/science.274.5290.1133.
- Kawai, T., and Akira, S. (2007). TLR signaling. *Semin. Immunol.* 19, 24–32. doi:10.1016/j.smim.2006.12.004.
- Kazarinova-Noyes, K., Malhotra, J. D., McEwen, D. P., Mattei, L. N., Berglund, E. O., Ranscht, B., et al. (2001). Contactin Associates with Na⁺ Channels and Increases Their Functional Expression. *J. Neurosci.* 21, 7517–7525. doi:10.1523/JNEUROSCI.21-19-07517.2001.
- Kershman, K. (1939). Genesis of microglia in the human brain. *Arch. Neurol. Psychiatr.* 24–50.
- Kessarar, N., Fogarty, M., Iannarelli, P., Grist, M., Wegner, M., and Richardson, W. D. (2006). Competing waves of oligodendrocytes in the forebrain and postnatal elimination of an embryonic lineage. *Nat. Neurosci.* 9, 173–179. doi:10.1038/nn1620.
- Kettenmann, H., Hoppe, D., Gottmann, K., Banati, R., and Kreutzberg, G. (1990). Cultured microglial cells have a distinct pattern of membrane channels different from peritoneal macrophages. *J. Neurosci. Res.* 26, 278–287. doi:10.1002/jnr.490260303.
- Khaliq, Z. M., and Raman, I. M. (2006). Relative contributions of axonal and somatic Na channels to action potential initiation in cerebellar purkinje neurons. *J. Neurosci.* 26, 1935–1944. doi:10.1523/JNEUROSCI.4664-05.2006.
- Kierdorf, K., Erny, D., Goldmann, T., Sander, V., Schulz, C., Perdiguero, E. G., et al. (2013). Microglia emerge from erythromyeloid precursors via Pu.1- and Irf8-dependent pathways. *Nat. Neurosci.* 16, 273–280. doi:10.1038/nn.3318.
- Kierdorf, K., Masuda, T., Jordão, M. J. C., and Prinz, M. (2019). Macrophages at CNS interfaces: ontogeny and function in health and disease. *Nat. Rev. Neurosci.* 20. doi:10.1038/s41583-019-0201-x.
- Kitamura, T., Miyake, T., and Fujita, S. (1984). Genesis of resting microglia in the gray matter of mouse hippocampus. *J. Comp. Neurol.* 226, 421–433. doi:10.1002/cne.902260310.
- Klingseisen, A., Ristoiu, A., Kegel, L., Sherman, D. L., Rubio-Brotons, M., Almeida, R. G., et al. (2019). Oligodendrocyte Neurofascin Independently Regulates Both Myelin Targeting and Sheath Growth in the CNS. *Dev. Cell* 51, 730-744.e6. doi:10.1016/j.devcel.2019.10.016.
- Klugmann, M., Schwab, M. H., Schneider, A., Zimmermann, F., Griffiths, I. R., and Nave, K. (1997). Assembly of CNS Myelin in the Absence of Proteolipid Protein. 18, 59–70.
- Knowles, J. K., Soane, C., Frost, E., Tam, L. T., Fraga, D., Xu, H., et al. (2020). Maladaptive myelination promotes epileptogenesis in absence epilepsy. *bioRxiv*. doi:10.1101/2020.08.20.260083.
- Koch, T., Brugger, T., Bach, A., Gennarini, G., and Trotter, J. (1997). Expression of the immunoglobulin superfamily cell adhesion molecule F3 by oligodendrocyte-lineage cells. *Glia* 19, 199–212. doi:10.1002/(SICI)1098-1136(199703)19:3<199::AID-GLIA3>3.0.CO;2-V.
- Kole, M. (2011). First node of ranvier facilitates high-frequency burst encoding. *Neuron* 71, 671–682. doi:10.1016/j.neuron.2011.06.024.
- Koles, Z. J., and Rasminsky, M. (1972). A computer simulation of conduction in demyelinated nerve fibres. *J. Physiol.* 227, 351–364. doi:10.1113/jphysiol.1972.sp010036.
- Komuro, H., and Rakic, P. (1993). Modulation of neuronal migration by NMDA receptors. *Science* (80-.). 260, 95–97. doi:10.1126/science.8096653.
- Kordeli, E., Lambert, S., and Bennett, V. (1995). Ankyrin. *J. Biol. Chem.* 270, 2352–2359. doi:10.1074/jbc.270.5.2352.
- Kotter, M. R., Li, W.-W., Zhao, C., and Franklin, R. J. M. (2006). Myelin impairs CNS remyelination by inhibiting oligodendrocyte precursor cell differentiation. *J. Neurosci.* 26, 328–32. doi:10.1523/JNEUROSCI.2615-05.2006.
- Kotter, M. R., Zhao, C., van Rooijen, N., and Franklin, R. J. M. (2005). Macrophage-depletion induced impairment of experimental CNS remyelination is associated with a reduced oligodendrocyte progenitor cell response and altered growth factor expression. *Neurobiol. Dis.* 18, 166–175. doi:10.1016/j.nbd.2004.09.019.
- Koudelka, S., Voas, M. G. G., Almeida, R. G. G., Baraban, M., Soetaert, J., Meyer, M. P. P., et al. (2016). Individual Neuronal Subtypes Exhibit Diversity in CNS Myelination Mediated by Synaptic

- Vesicle Release. *Curr. Biol.* 26, 1447–1455. doi:10.1016/j.cub.2016.03.070.
- Kougioumtzidou, E., Shimizu, T., Hamilton, N. B., Tohyama, K., Sprengel, R., Monyer, H., et al. (2017). Signalling through AMPA receptors on oligodendrocyte precursors promotes myelination by enhancing oligodendrocyte survival. *Elife* 6, 1–31. doi:10.7554/eLife.28080.
- Krasemann, S., Madore, C., Cialic, R., Baufeld, C., Calcagno, N., El Fatimy, R., et al. (2017). The TREM2-APOE Pathway Drives the Transcriptional Phenotype of Dysfunctional Microglia in Neurodegenerative Diseases. *Immunity* 47, 566–581.e9. doi:10.1016/j.immuni.2017.08.008.
- Krasnow, A. M., Ford, M. C., Valdivia, L. E., Wilson, S. W., and Attwell, D. (2018). Regulation of developing myelin sheath elongation by oligodendrocyte calcium transients in vivo. *Nat. Neurosci.* 21, 24–30. doi:10.1038/s41593-017-0031-y.
- Kukley, M., Capetillo-Zarate, E., and Dietrich, D. (2007). Vesicular glutamate release from axons in white matter. *Nat. Neurosci.* 10, 311–320. doi:10.1038/nn1850.
- Kukley, M., and Dietrich, D. (2009). Kainate receptors and signal integration by NG2 glial cells. *Neuron Glia Biol.* 5, 13–20. doi:10.1017/S1740925X09990081.
- Kukley, M., Kiladze, M., Tognatta, R., Hans, M., Swandulla, D., Schramm, J., et al. (2008). Glial cells are born with synapses. *FASEB J.* 22, 2957–2969. doi:10.1096/fj.07-090985.
- Kukley, M., Nishiyama, A., and Dietrich, D. (2010). The Fate of Synaptic Input to NG2 Glial Cells: Neurons Specifically Downregulate Transmitter Release onto Differentiating Oligodendroglial Cells. *J. Neurosci.* 30, 8320–8331. doi:10.1523/JNEUROSCI.0854-10.2010.
- Kurpius, D., Nolley, E. P., and Dailey, M. E. (2007). Purines induce directed migration and rapid homing of microglia to injured pyramidal neurons in developing hippocampus. *Glia* 55, 873–884. doi:10.1002/glia.20509.
- Kutzelnigg, A., Lucchinetti, C. F., Stadelmann, C., Brück, W., Rauschka, H., Bergmann, M., et al. (2005). Cortical demyelination and diffuse white matter injury in multiple sclerosis. *Brain* 128, 2705–2712. doi:10.1093/brain/awh641.
- Kyrargyri, V., Madry, C., Rifat, A., Arancibia-Carcamo, I. L., Jones, S. P., Chan, V. T. T., et al. (2019). P2Y₁₃ receptors regulate microglial morphology, surveillance, and resting levels of interleukin 1 β release. *Glia*, glia.23719. doi:10.1002/glia.23719.
- Labasque, M., and Faivre-Sarrailh, C. (2010). GPI-anchored proteins at the node of Ranvier. *FEBS Lett.* 584, 1787–1792. doi:10.1016/j.febslet.2009.08.025.
- Lacar, B., Linker, S. B., Jaeger, B. N., Krishnaswami, S. R., Barron, J. J., Kelder, M. J. E., et al. (2016). Nuclear RNA-seq of single neurons reveals molecular signatures of activation. *Nat. Commun.* 7, 11022. doi:10.1038/ncomms11022.
- Lacas-Gervais, S., Guo, J., Strenzke, N., Scarfone, E., Kolpe, M., Jahkel, M., et al. (2004). β IV Σ 1 spectrin stabilizes the nodes of Ranvier and axon initial segments. *J. Cell Biol.* 166, 983–990. doi:10.1083/jcb.200408007.
- Lambert, S., Davis, J. Q., and Bennett, V. (1997). Morphogenesis of the Node of Ranvier: Co-Clusters of Ankyrin and Ankyrin-Binding Integral Proteins Define Early Developmental Intermediates. *J. Neurosci.* 17, 7025–7036. doi:10.1523/JNEUROSCI.17-18-07025.1997.
- Lampron, A., Laroche, A., Laflamme, N., Préfontaine, P., Plante, M. M., Sánchez, M. G., et al. (2015). Inefficient clearance of myelin debris by microglia impairs remyelinating processes. *J. Exp. Med.* 212, 481–495. doi:10.1084/jem.20141656.
- Landon, D. N., and Williams, P. L. (1963). Ultrastructure of the Node of Ranvier. *Nature* 199, 575–577. doi:10.1038/199575a0.
- Lang, D. G., and Ritchie, A. K. (1990). Tetraethylammonium blockade of apamin-sensitive and insensitive Ca²⁺-activated K⁺ channels in a pituitary cell line. *J. Physiol.* 425, 117–132. doi:10.1113/jphysiol.1990.sp018095.
- Lappe-Siefke, C., Goebbels, S., Gravel, M., Nicksch, E., Lee, J., Braun, P. E., et al. (2003). Disruption of Cnp1 uncouples oligodendroglial functions in axonal support and myelination. *Nat. Genet.* 33, 366–374. doi:10.1038/ng1095.
- Lapray, D., Lasztozci, B., Lagler, M., Viney, T. J., Katona, L., Valenti, O., et al. (2012). Behavior-dependent specialization of identified hippocampal interneurons. *Nat. Neurosci.* 15, 1265–71.

- doi:10.1038/nn.3176.
- Larson, V. A., Mironova, Y., Vanderpool, K. G., Waisman, A., Rash, J. E., Agarwal, A., et al. (2018). Oligodendrocytes control potassium accumulation in white matter and seizure susceptibility. *Elife* 7, 1–33. doi:10.7554/eLife.34829.
- Lassmann, H. (1979). Chronic Relapsing Experimental Allergic Encephalomyelitis. *Arch. Neurol.* 36, 490. doi:10.1001/archneur.1979.00500440060011.
- Lassmann, H., and Bradl, M. (2017). Multiple sclerosis: experimental models and reality. *Acta Neuropathol.* 133, 223–244. doi:10.1007/s00401-016-1631-4.
- Lauritzen, M., Dreier, J. P., Fabricius, M., Hartings, J. A., Graf, R., and Strong, A. J. (2011). Clinical Relevance of Cortical Spreading Depression in Neurological Disorders: Migraine, Malignant Stroke, Subarachnoid and Intracranial Hemorrhage, and Traumatic Brain Injury. *J. Cereb. Blood Flow Metab.* 31, 17–35. doi:10.1038/jcbfm.2010.191.
- Lee, S., Leach, M. K., Redmond, S. A., Chong, S. Y. C., Mellon, S. H., Tuck, S. J., et al. (2012a). A culture system to study oligodendrocyte myelination processes using engineered nanofibers. *Nat. Methods* 9, 917–922. doi:10.1038/nmeth.2105.
- Lee, Y., Morrison, B. M., Li, Y., Lengacher, S., Farah, M. H., Hoffman, P. N., et al. (2012b). Oligodendroglia metabolically support axons and contribute to neurodegeneration. *Nature* 487, 443–448. doi:10.1038/nature11314.
- Lehrman, E. K., Wilton, D. K., Litvina, E. Y., Welsh, C. A., Chang, S. T., Frouin, A., et al. (2018). CD47 Protects Synapses from Excess Microglia-Mediated Pruning during Development. *Neuron* 100, 120–134.e6. doi:10.1016/j.neuron.2018.09.017.
- Lemaillet, G., Walker, B., and Lambert, S. (2003). Identification of a Conserved Ankyrin-binding Motif in the Family of Sodium Channel α Subunits. *J. Biol. Chem.* 278, 27333–27339. doi:10.1074/jbc.M303327200.
- Lessig, J., and Fuchs, B. (2009). Plasmalogens in Biological Systems: Their Role in Oxidative Processes in Biological Membranes, their Contribution to Pathological Processes and Aging and Plasmalogen Analysis. *Curr. Med. Chem.* 16, 2021–2041. doi:10.2174/092986709788682164.
- Levay, S., Stryker, M. P., and Shatz, C. J. (1978). Ocular dominance columns and their development in layer IV of the cat's visual cortex: A quantitative study. *J. Comp. Neurol.* 179, 223–244. doi:10.1002/cne.901790113.
- Lezmy, J., Arancibia-Cárcamo, I. L., Quintela-López, T., Sherman, D. L., Brophy, P. J., and Attwell, D. (2021). Astrocyte Ca²⁺-evoked ATP release regulates myelinated axon excitability and conduction speed. *Science* 374, eabh2858. doi:10.1126/science.abh2858.
- Li, Q., Cheng, Z., Zhou, L., Darmanis, S., Neff, N. F., Okamoto, J., et al. (2019). Developmental Heterogeneity of Microglia and Brain Myeloid Cells Revealed by Deep Single-Cell RNA Sequencing. *Neuron* 101, 207–223.e10. doi:10.1016/j.neuron.2018.12.006.
- Li, Y., Du, X. F., Liu, C. S., Wen, Z. L., and Du, J. L. (2012). Reciprocal Regulation between Resting Microglial Dynamics and Neuronal Activity In Vivo. *Dev. Cell* 23, 1189–1202. doi:10.1016/j.devcel.2012.10.027.
- Liang, K. J., Lee, J. E., Wang, Y. D., Ma, W., Fontainhas, A. M., Fariss, R. N., et al. (2009). Regulation of Dynamic Behavior of Retinal Microglia by CX3CR1 Signaling. *Investig. Ophthalmology Vis. Sci.* 50, 4444. doi:10.1167/iovs.08-3357.
- Liddelow, S. A., Guttenplan, K. A., Clarke, L. E., Bennett, F. C., Bohlen, C. J., Schirmer, L., et al. (2017). Neurotoxic reactive astrocytes are induced by activated microglia. *Nature* 541, 481–487. doi:10.1038/nature21029.
- Lillie, R. S. (1925). Factors affecting transmission and recovery in the passive iron nerve model. *J. Gen. Physiol.* 7, 473–507. doi:10.1085/jgp.7.4.473.
- Lin, S. C., and Bergles, D. E. (2004). Synaptic signaling between GABAergic interneurons and oligodendrocyte precursor cells in the hippocampus. *Nat. Neurosci.* 7, 24–32. doi:10.1038/nn1162.
- Lin, S., Huck, J. H. J., Roberts, J. D. B., Macklin, W. B., Somogyi, P., and Bergles, D. E. (2005). Climbing Fiber Innervation of NG2-Expressing Glia in the Mammalian Cerebellum. *Neuron* 46, 773–785.

doi:10.1016/j.neuron.2005.04.025.

- Lindsay M. De Biase, Michele L. Pucak, Kang, S. H., Rodriguez, S. N., and Bergles, D. E. (2017). Sparse interaction between oligodendrocyte precursor cells (NG2 + cells) and nodes of Ranvier in the central nervous system. *bioRxiv*.
- Ling, E.-A., and Wong, W.-C. (1993). The origin and nature of ramified and amoeboid microglia: A historical review and current concepts. *Glia* 7, 9–18. doi:10.1002/glia.440070105.
- Ling, E. A. (1979). Transformation of monocytes into amoeboid microglia in the corpus callosum of postnatal rats, as shown by labelling monocytes by carbon particles. *J. Anat.* 128, 847–58. Available at: <http://www.ncbi.nlm.nih.gov/pubmed/489472>.
- Liodis, P., Denaxa, M., Grigoriou, M., Akufo-Addo, C., Yanagawa, Y., and Pachnis, V. (2007). Lhx6 Activity Is Required for the Normal Migration and Specification of Cortical Interneuron Subtypes. *J. Neurosci.* 27, 3078–3089. doi:10.1523/JNEUROSCI.3055-06.2007.
- Liu, C.-H., Seo, R., Ho, T. S.-Y., Stankewich, M., Mohler, P. J., Hund, T. J., et al. (2020). β spectrin-dependent and domain specific mechanisms for Na⁺ channel clustering. *Elife* 9. doi:10.7554/eLife.56629.
- Liu, J., Dietz, K., Deloyht, J. M., Pedre, X., Kelkar, D., Kaur, J., et al. (2012). Impaired adult myelination in the prefrontal cortex of socially isolated mice. *Nat. Neurosci.* 15, 1621–1623. doi:10.1038/nn.3263.
- Liu, Y. U., Ying, Y., Li, Y., Eyo, U. B., Chen, T., Zheng, J., et al. (2019). Neuronal network activity controls microglial process surveillance in awake mice via norepinephrine signaling. *Nat. Neurosci.* 22, 1771–1781. doi:10.1038/s41593-019-0511-3.
- Lloyd, A. F., Davies, C. L., Holloway, R. K., Labrak, Y., Ireland, G., Carradori, D., et al. (2019). Central nervous system regeneration is driven by microglia necroptosis and repopulation. *Nat. Neurosci.* 22, 1046–1052. doi:10.1038/s41593-019-0418-z.
- Lloyd, A. F., and Miron, V. E. (2019). The pro-remyelination properties of microglia in the central nervous system. *Nat. Rev. Neurol.*, 29–34. doi:10.1038/s41582-019-0184-2.
- Locatelli, G., Theodorou, D., Kendirli, A., Jordão, M. J. C., Staszewski, O., Phulphagar, K., et al. (2018). Mononuclear phagocytes locally specify and adapt their phenotype in a multiple sclerosis model. *Nat. Neurosci.* 21, 1196–1208. doi:10.1038/s41593-018-0212-3.
- Locksley, R. M., Killeen, N., and Lenardo, M. J. (2001). The TNF and TNF Receptor Superfamilies. *Cell* 104, 487–501. doi:10.1016/S0092-8674(01)00237-9.
- Lopreore, C. L., Bartol, T. M., Coggan, J. S., Keller, D. X., Sosinsky, G. E., Ellisman, M. H., et al. (2008). Computational modeling of three-dimensional electrodiffusion in biological systems: Application to the node of Ranvier. *Biophys. J.* 95, 2624–2635. doi:10.1529/biophysj.108.132167.
- Lorenzo-Ceballos, Y., Carrasquel-Ursulaez, W., Castillo, K., Alvarez, O., and Latorre, R. (2019). Calcium-driven regulation of voltage-sensing domains in BK channels. *Elife* 2, 520429. doi:10.1101/520429.
- Lubetzki, C., Sol-Foulon, N., and Desmazières, A. (2020a). Nodes of Ranvier during development and repair in the CNS. *Nat. Rev. Neurol.* 16, 426–439. doi:10.1038/s41582-020-0375-x.
- Lubetzki, C., Zalc, B., Williams, A., Stadelmann, C., and Stankoff, B. (2020b). Remyelination in multiple sclerosis: from basic science to clinical translation. *Lancet Neurol.* 19, 678–688. doi:10.1016/S1474-4422(20)30140-X.
- Lublin, F. D., and Reingold, S. C. (1996). Defining the clinical course of multiple sclerosis: Results of an international survey. *Neurology* 46, 907–911. doi:10.1212/WNL.46.4.907.
- Ludwin, S. K. (1980). Chronic demyelination inhibits remyelination in the central nervous system. An analysis of contributing factors. *Lab. Invest.* 43, 382–7. Available at: <http://www.ncbi.nlm.nih.gov/pubmed/7442125>.
- Lundgaard, I., Luzhynskaya, A., Stockley, J. H., Wang, Z., Evans, K. A., Swire, M., et al. (2013). Neuregulin and BDNF Induce a Switch to NMDA Receptor-Dependent Myelination by Oligodendrocytes. *PLoS Biol.* 11. doi:10.1371/journal.pbio.1001743.
- Lustig, M., Zanazzi, G., Sakurai, T., Blanco, C., Levinson, S. R., Lambert, S., et al. (2001). Nr-CAM and

- neurofascin interactions regulate ankyrin G and sodium channel clustering at the node of Ranvier. *Curr. Biol.* 11, 1864–1869. doi:10.1016/S0960-9822(01)00586-3.
- Lux, H. D., and Heinemann, U. (1978). Ionic changes during experimentally induced seizure activity. *Electroencephalogr. Clin. Neurophysiol. Suppl.*, 289–97. Available at: <http://www.ncbi.nlm.nih.gov/pubmed/285839>.
- Ma, D. K., Kim, W. R., Ming, G., and Song, H. (2009). Activity-dependent Extrinsic Regulation of Adult Olfactory Bulb and Hippocampal Neurogenesis. *Ann. N. Y. Acad. Sci.* 1170, 664–673. doi:10.1111/j.1749-6632.2009.04373.x.
- Maas, D. A., Eijnsink, V. D., Spoelder, M., van Hulten, J. A., De Weerd, P., Homberg, J. R., et al. (2020). Interneuron hypomyelination is associated with cognitive inflexibility in a rat model of schizophrenia. *Nat. Commun.* 11, 2329. doi:10.1038/s41467-020-16218-4.
- Madry, C., Arancibia-Cárcamo, I. L., Kyrargyri, V., Chan, V. T. T., Hamilton, N. B., and Attwell, D. (2018a). Effects of the ecto-ATPase apyrase on microglial ramification and surveillance reflect cell depolarization, not ATP depletion. *Proc. Natl. Acad. Sci. U. S. A.* 115, E1608–E1617. doi:10.1073/pnas.1715354115.
- Madry, C., and Attwell, D. (2015). Receptors, ion channels, and signaling mechanisms underlying Microglial dynamics. *J. Biol. Chem.* 290, 12443–12450. doi:10.1074/jbc.R115.637157.
- Madry, C., Kyrargyri, V., Arancibia-Cárcamo, I. L., Jolivet, R., Kohsaka, S., Bryan, R. M., et al. (2018b). Microglial Ramification, Surveillance, and Interleukin-1 β Release Are Regulated by the Two-Pore Domain K⁺ Channel THIK-1. *Neuron* 97, 299–312.e6. doi:10.1016/j.neuron.2017.12.002.
- Maingret, N., Girardeau, G., Todorova, R., Goutier, M., and Zugaro, M. (2016). Hippocampo-cortical coupling mediates memory consolidation during sleep. *Nat. Neurosci.* 19, 959–964. doi:10.1038/nn.4304.
- Makinson, C. D., Tanaka, B. S., Sorokin, J. M., Wong, J. C., Christian, C. A., Goldin, A. L., et al. (2017). Regulation of Thalamic and Cortical Network Synchrony by Scn8a. *Neuron* 93, 1165–1179.e6. doi:10.1016/j.neuron.2017.01.031.
- Malavasi, E. L., Ghosh, A., Booth, D. G., Zagnoni, M., Sherman, D. L., and Brophy, P. J. (2021). Dynamic early clusters of nodal proteins contribute to node of Ranvier assembly during myelination of peripheral neurons. *Elife* 10. doi:10.7554/eLife.68089.
- Malhotra, J. D., Kazen-Gillespie, K., Hortsch, M., and Isom, L. L. (2000). Sodium Channel β Subunits Mediate Homophilic Cell Adhesion and Recruit Ankyrin to Points of Cell-Cell Contact. *J. Biol. Chem.* 275, 11383–11388. doi:10.1074/jbc.275.15.11383.
- Malhotra, J. D., Koopmann, M. C., Kazen-Gillespie, K. A., Fettman, N., Hortsch, M., and Isom, L. L. (2002). Structural Requirements for Interaction of Sodium Channel β 1 Subunits with Ankyrin. *J. Biol. Chem.* 277, 26681–26688. doi:10.1074/jbc.M202354200.
- Mangin, J. M., Li, P., Scafidi, J., and Gallo, V. (2012). Experience-dependent regulation of NG2 progenitors in the developing barrel cortex. *Nat. Neurosci.* 15, 1192–1194. doi:10.1038/nn.3190.
- Mardinly, A. R., Spiegel, I., Patrizi, A., Centofante, E., Bazinet, J. E., Tzeng, C. P., et al. (2016). Sensory experience regulates cortical inhibition by inducing IGF1 in VIP neurons. *Nature* 531, 371–5. doi:10.1038/nature17187.
- Marín-Teva, J. L., Dusart, I., Colin, C., Gervais, A., Van Rooijen, N., and Mallat, M. (2004). Microglia Promote the Death of Developing Purkinje Cells. *Neuron* 41, 535–547. doi:10.1016/S0896-6273(04)00069-8.
- Marisca, R., Hoche, T., Agirre, E., Hoodless, L. J., Barkey, W., Auer, F., et al. (2020). Functionally distinct subgroups of oligodendrocyte precursor cells integrate neural activity and execute myelin formation. *Nat. Neurosci.*, 1–12. doi:10.1038/s41593-019-0581-2.
- Marques, S., Zeisel, A., Codeluppi, S., van Bruggen, D., Mendanha Falcao, A., Xiao, L., et al. (2016). Oligodendrocyte heterogeneity in the mouse juvenile and adult central nervous system. *Science (80-.)*. 352, 1326–1329. doi:10.1126/science.aaf6463.
- Marschallinger, J., Iram, T., Zardeneta, M., Lee, S. E., Lehallier, B., Haney, M. S., et al. (2020). Author Correction: Lipid-droplet-accumulating microglia represent a dysfunctional and

- proinflammatory state in the aging brain. *Nat. Neurosci.* 23, 1308–1308. doi:10.1038/s41593-020-0682-y.
- Marshall-Phelps, K. L. H., Kegel, L., Baraban, M., Ruhwedel, T., Almeida, R. G., Rubio-Brotons, M., et al. (2020). Neuronal activity disrupts myelinated axon integrity in the absence of NKCC1b. *J. Cell Biol.* 219. doi:10.1083/jcb.201909022.
- Martín-Partido, G., Rodríguez-Gallardo, L., Alvarez, I. S., and Navascués, J. (1988). Cell death in the ventral region of the neural retina during the early development of the chick embryo eye. *Anat. Rec.* 222, 272–281. doi:10.1002/ar.1092220308.
- Martini, F. J., Guillamón-Vivancos, T., Moreno-Juan, V., Valdeolmillos, M., and López-Bendito, G. (2021). Spontaneous activity in developing thalamic and cortical sensory networks. *Neuron* 109, 2519–2534. doi:10.1016/j.neuron.2021.06.026.
- Martorell, A. J., Paulson, A. L., Suk, H. J., Abdurrob, F., Drummond, G. T., Guan, W., et al. (2019). Multi-sensory Gamma Stimulation Ameliorates Alzheimer’s-Associated Pathology and Improves Cognition. *Cell* 177, 256–271.e22. doi:10.1016/j.cell.2019.02.014.
- Mason, J. L., Suzuki, K., Chaplin, D. D., and Matsushima, G. K. (2001). Interleukin-1 β Promotes Repair of the CNS. *J. Neurosci.* 21, 7046–7052. doi:10.1523/JNEUROSCI.21-18-07046.2001.
- Mason, J. L., Ye, P., Suzuki, K., D’Ercole, A. J., and Matsushima, G. K. (2000). Insulin-Like Growth Factor-1 Inhibits Mature Oligodendrocyte Apoptosis during Primary Demyelination. *J. Neurosci.* 20, 5703–5708. doi:10.1523/JNEUROSCI.20-15-05703.2000.
- Masuda, T., Amann, L., Sankowski, R., Staszewski, O., Lenz, M., D’Errico, P., et al. (2020). Novel Hexb-based tools for studying microglia in the CNS. *Nat. Immunol.* 21, 802–815. doi:10.1038/s41590-020-0707-4.
- Masuda, T., Sankowski, R., Staszewski, O., Böttcher, C., Amann, L., Scheiwe, C., et al. (2019). Spatial and temporal heterogeneity of mouse and human microglia at single-cell resolution. *Nature* 566, 388–392. doi:10.1038/s41586-019-0924-x.
- Mathews, E. S., Mawdsley, D. J., Walker, M., Hines, J. H., Pozzoli, M., and Appel, B. (2014). Mutation of 3-hydroxy-3-methylglutaryl CoA synthase I reveals requirements for isoprenoid and cholesterol synthesis in oligodendrocyte migration arrest, axon wrapping, and myelin gene expression. *J. Neurosci.* 34, 3402–3412. doi:10.1523/JNEUROSCI.4587-13.2014.
- Mathieu, P. A., Almeida Gubiani, M. F., Rodríguez, D., Gómez Pinto, L. I., Calcagno, M. de L., and Adamo, A. M. (2019). Demyelination-remyelination in the Central Nervous System: Ligand-dependent Participation of the Notch Signaling Pathway. *Toxicol. Sci.* 171, 172–192. doi:10.1093/toxsci/kfz130.
- Matsuda, W., Furuta, T., Nakamura, K. C., Hioki, H., Fujiyama, F., Arai, R., et al. (2009). Single Nigrostriatal Dopaminergic Neurons Form Widely Spread and Highly Dense Axonal Arborizations in the Neostriatum. *J. Neurosci.* 29, 444–453. doi:10.1523/JNEUROSCI.4029-08.2009.
- Matsushima, G. K., and Morell, P. (2006). The Neurotoxicant, Cuprizone, as a Model to Study Demyelination and Remyelination in the Central Nervous System. *Brain Pathol.* 11, 107–116. doi:10.1111/j.1750-3639.2001.tb00385.x.
- Matthews, M. A., and Duncan, D. (1971). A quantitative study of morphological changes accompanying the initiation and progress of myelin production in the dorsal funiculus of the rat spinal cord. *J. Comp. Neurol.* 142, 1–22. doi:10.1002/cne.901420102.
- Mayoral, S. R., Etxeberria, A., Shen, Y. A. A., and Chan, J. R. (2018). Initiation of CNS Myelination in the Optic Nerve Is Dependent on Axon Caliber. *Cell Rep.* 25, 544–550.e3. doi:10.1016/j.celrep.2018.09.052.
- Mazaheri, F., Snaidero, N., Kleinberger, G., Madore, C., Daria, A., Werner, G., et al. (2017). TREM2 deficiency impairs chemotaxis and microglial responses to neuronal injury. *EMBO Rep.* 18, 1186–1198. doi:10.15252/embr.201743922.
- Mazuir, E., Richevaux, L., Nassar, M., Robil, N., de la Grange, P., Lubetzki, C., et al. (2021). Oligodendrocyte Secreted Factors Shape Hippocampal GABAergic Neuron Transcriptome and Physiology. *Cereb. Cortex*, 1–18. doi:10.1093/cercor/bhab139.

- McDonald, W. I., and Sears, T. A. (1970). FOCAL EXPERIMENTAL DEMYELINATION IN THE CENTRAL NERVOUS SYSTEM. *Brain* 93, 575–582. doi:10.1093/brain/93.3.575.
- McEwen, D. P., and Isom, L. L. (2004). Heterophilic Interactions of Sodium Channel β 1 Subunits with Axonal and Glial Cell Adhesion Molecules. *J. Biol. Chem.* 279, 52744–52752. doi:10.1074/jbc.M405990200.
- McKenzie, I. A., Ohayon, D., Li, H., De Faria, J. P., Emery, B., Tohyama, K., et al. (2014). Motor skill learning requires active central myelination. *Science* (80-.). 346, 318–322. doi:10.1126/science.1254960.
- McMahon, E. J., Suzuki, K., and Matsushima, G. K. (2002). Peripheral macrophage recruitment in cuprizone-induced CNS demyelination despite an intact blood–brain barrier. *J. Neuroimmunol.* 130, 32–45. doi:10.1016/S0165-5728(02)00205-9.
- Meeks, J. P., Jiang, X., and Mennerick, S. (2005). Action potential fidelity during normal and epileptiform activity in paired soma-axon recordings from rat hippocampus. *J. Physiol.* 566, 425–441. doi:10.1113/jphysiol.2005.089086.
- Mei, F., Fancy, S. P. J., Shen, Y.-A. A., Niu, J., Zhao, C., Presley, B., et al. (2014). Micropillar arrays as a high-throughput screening platform for therapeutics in multiple sclerosis. *Nat. Med.* 20, 954–960. doi:10.1038/nm.3618.
- Mei, F., Lehmann-Horn, K., Shen, Y.-A. A., Rankin, K. A., Stebbins, K. J., Lorrain, D. S., et al. (2016). Accelerated remyelination during inflammatory demyelination prevents axonal loss and improves functional recovery. *Elife* 5. doi:10.7554/eLife.18246.
- Meller, J., Chen, Z., Dudiki, T., Cull, R. M., Murtazina, R., Bal, S. K., et al. (2017). Integrin-Kindlin3 requirements for microglial motility in vivo are distinct from those for macrophages. *JCI Insight* 2. doi:10.1172/jci.insight.93002.
- Mendel, I., de Rosbo, N. K., and Ben-Nun, A. (1995). A myelin oligodendrocyte glycoprotein peptide induces typical chronic experimental autoimmune encephalomyelitis in H-2b mice: Fine specificity and T cell receptor V β expression of encephalitogenic T cells. *Eur. J. Immunol.* 25, 1951–1959. doi:10.1002/eji.1830250723.
- Menegoz, M., Gaspar, P., Le Bert, M., Galvez, T., Burgaya, F., Palfrey, C., et al. (1997). Paranodin, a Glycoprotein of Neuronal Paranodal Membranes. *Neuron* 19, 319–331. doi:10.1016/S0896-6273(00)80942-3.
- Mensch, S., Baraban, M., Almeida, R., Czopka, T., Ausborn, J., El Manira, A., et al. (2015). Synaptic vesicle release regulates myelin sheath number of individual oligodendrocytes in vivo. *Nat. Neurosci.* 18, 628–630. doi:10.1038/nn.3991.
- Merlini, M., Rafalski, V. A., Ma, K., Kim, K., Bushong, E. A., Coronado, P. E. R., et al. (2021). Microglial G β 1-dependent dynamics regulate brain network hyperexcitability. *Nat. Neurosci.* 24. doi:10.1038/s41593-020-00756-7.
- Meyer-Franke, A., Kaplan, M. R., Pfeifer, F. W., and Barres, B. A. (1995). Characterization of the signaling interactions that promote the survival and growth of developing retinal ganglion cells in culture. *Neuron* 15, 805–819. doi:10.1016/0896-6273(95)90172-8.
- Meyer, N., Richter, N., Fan, Z., Siemonsmeier, G., Pivneva, T., Jordan, P., et al. (2018). Oligodendrocytes in the Mouse Corpus Callosum Maintain Axonal Function by Delivery of Glucose. *Cell Rep.* 22, 2383–2394. doi:10.1016/j.celrep.2018.02.022.
- Micheva, K. D., Chang, E. F., Nana, A. L., Seeley, W. W., Ting, J. T., Cobbs, C., et al. (2018). Distinctive structural and molecular features of myelinated inhibitory axons in human neocortex. *eNeuro* 5, 1–12. doi:10.1523/ENEURO.0297-18.2018.
- Micheva, K. D., Wolman, D., Mensch, B. D., Pax, E., Buchanan, J., Smith, S. J., et al. (2016). A large fraction of neocortical myelin ensheathes axons of local inhibitory neurons. *Elife* 5, 1–29. doi:10.7554/eLife.15784.
- Micu, I., Jiang, Q., Coderre, E., Ridsdale, A., Zhang, L., Woulfe, J., et al. (2006). NMDA receptors mediate calcium accumulation in myelin during chemical ischaemia. *Nature* 439, 988–992. doi:10.1038/nature04474.
- Miron, V. E., Boyd, A., Zhao, J. W., Yuen, T. J., Ruckh, J. M., Shadrach, J. L., et al. (2013). M2 microglia

- and macrophages drive oligodendrocyte differentiation during CNS remyelination. *Nat. Neurosci.* 16, 1211–1218. doi:10.1038/nn.3469.
- Mitew, S., Gobius, I., Fenlon, L. R., McDougall, S. J., Hawkes, D., Xing, Y. L., et al. (2018). Pharmacogenetic stimulation of neuronal activity increases myelination in an axon-specific manner. *Nat. Commun.* 9, 1–16. doi:10.1038/s41467-017-02719-2.
- Miyamoto, A., Wake, H., Ishikawa, A. W., Eto, K., Shibata, K., Murakoshi, H., et al. (2016). Microglia contact induces synapse formation in developing somatosensory cortex. *Nat. Commun.* 7, 12540. doi:10.1038/ncomms12540.
- Möbius, W., Cooper, B., Kaufmann, W. A., Imig, C., Ruhwedel, T., Snaidero, N., et al. (2010). *Electron microscopy of the mouse central nervous system*. doi:10.1016/S0091-679X(10)96020-2.
- Monsivais, P., Clark, B. A., Roth, A., and Häusser, M. (2005). Determinants of Action Potential Propagation in Cerebellar Purkinje Cell Axons. *J. Neurosci.* 25, 464–472. doi:10.1523/JNEUROSCI.3871-04.2005.
- Montalban, X., Arnold, D. L., Weber, M. S., Staikov, I., Piasecka-Stryczynska, K., Willmer, J., et al. (2019). Placebo-Controlled Trial of an Oral BTK Inhibitor in Multiple Sclerosis. *N. Engl. J. Med.* 380, 2406–2417. doi:10.1056/NEJMoa1901981.
- Moore, J. W., Joyner, R. W., Brill, M. H., Waxman, S. D., and Najar-Joa, M. (1978). Simulations of conduction in uniform myelinated fibers. Relative sensitivity to changes in nodal and internodal parameters. *Biophys. J.* 21, 147–160. doi:10.1016/S0006-3495(78)85515-5.
- Moore, S., Meschkat, M., Ruhwedel, T., Trevisiol, A., Tzvetanova, I. D., Battefeld, A., et al. (2020). A role of oligodendrocytes in information processing. *Nat. Commun.* 11, 5497. doi:10.1038/s41467-020-19152-7.
- Morganti, J. M., Riparip, L.-K., and Rosi, S. (2016). Call Off the Dog(ma): M1/M2 Polarization Is Concurrent following Traumatic Brain Injury. *PLoS One* 11, e0148001. doi:10.1371/journal.pone.0148001.
- Morin-Brureau, M., Milior, G., Royer, J., Chali, F., Le Duigou, C., Savary, E., et al. (2018). Microglial phenotypes in the human epileptic temporal lobe. *Brain* 141, 3343–3360. doi:10.1093/brain/awy276.
- Mount, C. W., Yalçın, B., Cunliffe-Koehler, K., Sundaresh, S., and Monje, M. (2019). Monosynaptic tracing maps brain-wide afferent oligodendrocyte precursor cell connectivity. *Elife*, 669572. doi:10.1101/669572.
- Mrdjen, D., Pavlovic, A., Hartmann, F. J., Schreiner, B., Utz, S. G., Leung, B. P., et al. (2018). High-Dimensional Single-Cell Mapping of Central Nervous System Immune Cells Reveals Distinct Myeloid Subsets in Health, Aging, and Disease. *Immunity* 48, 380-395.e6. doi:10.1016/j.immuni.2018.01.011.
- Mu, Y., Bennett, D. V., Rubinov, M., Narayan, S., Yang, C. T., Tanimoto, M., et al. (2019). Glia Accumulate Evidence that Actions Are Futile and Suppress Unsuccessful Behavior. *Cell* 178, 27-43.e19. doi:10.1016/j.cell.2019.05.050.
- Muñoz-Planillo, R., Kuffa, P., Martínez-Colón, G., Smith, B. L., Rajendiran, T. M., and Núñez, G. (2013). K⁺ Efflux Is the Common Trigger of NLRP3 Inflammasome Activation by Bacterial Toxins and Particulate Matter. *Immunity* 38, 1142–1153. doi:10.1016/j.immuni.2013.05.016.
- Murabe, Y., and Sano, Y. (1982). Morphological studies on neuroglia. *Cell Tissue Res.* 225. doi:10.1007/BF00214798.
- Murabe, Y., and Sano, Y. (1983). Morphological studies on neuroglia. *Cell Tissue Res.* 229. doi:10.1007/BF00217882.
- Myllykoski, M., Seidel, L., Muruganandam, G., Raasakka, A., Torda, A. E., and Kursula, P. (2016). Structural and functional evolution of 2',3'-cyclic nucleotide 3'-phosphodiesterase. *Brain Res.* 1641, 64–78. doi:10.1016/j.brainres.2015.09.004.
- Nagy, B., Hovhannisyann, A., Barzan, R., Chen, T.-J., and Kukley, M. (2017). Different patterns of neuronal activity trigger distinct responses of oligodendrocyte precursor cells in the corpus callosum. *PLOS Biol.* 15, e2001993. doi:10.1371/journal.pbio.2001993.
- Namadurai, S., Yereddi, N. R., Cusdin, F. S., Huang, C. L.-H., Chirgadze, D. Y., and Jackson, A. P. (2015).

- A new look at sodium channel β subunits. *Open Biol.* 5, 140192. doi:10.1098/rsob.140192.
- Nans, A., Einheber, S., Salzer, J. L., and Stokes, D. L. (2011). Electron tomography of paranodal septate-like junctions and the associated axonal and glial cytoskeletons in the central nervous system. *J. Neurosci. Res.* 89, 310–319. doi:10.1002/jnr.22561.
- Natrajan, M. S., de la Fuente, A. G., Crawford, A. H., Linehan, E., Nuñez, V., Johnson, K. R., et al. (2015). Retinoid X receptor activation reverses age-related deficiencies in myelin debris phagocytosis and remyelination. *Brain* 138, 3581–3597. doi:10.1093/brain/awv289.
- Nave, K.-A., and Werner, H. B. (2014). Myelination of the Nervous System: Mechanisms and Functions. *Annu. Rev. Cell Dev. Biol.* 30, 503–533. doi:10.1146/annurev-cellbio-100913-013101.
- Neely, S. A., Williamson, J. M., Klingseisen, A., Zoupi, L., Early, J. J., Williams, A., et al. (2020). New oligodendrocytes exhibit more abundant and accurate myelin regeneration than those that survive demyelination. *bioRxiv*, 1–14. doi:10.1101/2020.05.22.110551.
- Nelson, A. D., and Jenkins, P. M. (2017). Axonal Membranes and Their Domains: Assembly and Function of the Axon Initial Segment and Node of Ranvier. *Front. Cell. Neurosci.* 11. doi:10.3389/fncel.2017.00136.
- Nelson, H. N., Treichel, A. J., Eggum, E. N., Martell, M. R., Kaiser, A. J., Trudel, A. G., et al. (2019). Individual neuronal subtypes control initial myelin sheath growth and stabilization. *bioRxiv*, 809996. doi:10.1101/809996.
- Nemes-baran, A. D., White, D. R., Desilva, T. M., Nemes-baran, A. D., White, D. R., and Desilva, T. M. (2020). Article Fractalkine-Dependent Microglial Pruning of Viable Oligodendrocyte Progenitor Cells Regulates Myelination II II Fractalkine-Dependent Microglial Pruning of Viable Oligodendrocyte Progenitor Cells Regulates Myelination. *CellReports* 32, 108047. doi:10.1016/j.celrep.2020.108047.
- Nguyen, P. T., Dorman, L. C., Pan, S., Vainchtein, I. D., Han, R. T., Nakao-Inoue, H., et al. (2020). Microglial Remodeling of the Extracellular Matrix Promotes Synapse Plasticity. *Cell*, 1–16. doi:10.1016/j.cell.2020.05.050.
- Nicoll, R. A. (2017). A Brief History of Long-Term Potentiation. *Neuron* 93, 281–290. doi:10.1016/j.neuron.2016.12.015.
- Nikić, I., Merkler, D., Sorbara, C., Brinkoetter, M., Kreutzfeldt, M., Bareyre, F. M., et al. (2011). A reversible form of axon damage in experimental autoimmune encephalomyelitis and multiple sclerosis. *Nat. Med.* 17, 495–499. doi:10.1038/nm.2324.
- Nimmerjahn, A., Kirchhoff, F., and Helmchen, F. (2005). Resting microglial cells are highly dynamic surveillants of brain parenchyma in vivo. *Science (80-)*. 308, 1314–1318. doi:10.1126/science.1110647.
- Norton, W. T., and Cammer, W. (1984). *Isolation and characterization of myelin*. Morell, P. , ed. P. Morell Boston, MA: Springer US doi:10.1007/978-1-4615-7514-6.
- Norton, W. T., and Poduslo, S. E. (1973). Myelination in Rat Brain: Method of Myelin Isolation. *J. Neurochem.* 21, 749–757. doi:10.1111/j.1471-4159.1973.tb07519.x.
- Notterpek, L., Snipes, G. J., and Shooter, E. M. (1999). Temporal expression pattern of peripheral myelin protein 22 during in vivo and in vitro myelination. *Glia* 25, 358–69. Available at: <http://www.ncbi.nlm.nih.gov/pubmed/10028918>.
- Nunes, P., and Demarex, N. (2010). The role of calcium signaling in phagocytosis. *J. Leukoc. Biol.* 88, 57–68. doi:10.1189/jlb.0110028.
- O'Brien, J. S., and Sampson, E. L. (1965). Myelin Membrane: A Molecular Abnormality. *Science (80-)*. 150, 1613–1614. doi:10.1126/science.150.3703.1613.
- O'Koren, E. G., Mathew, R., and Saban, D. R. (2016). Fate mapping reveals that microglia and recruited monocyte-derived macrophages are definitively distinguishable by phenotype in the retina. *Sci. Rep.* 6, 20636. doi:10.1038/srep20636.
- O'Malley, H. A., and Isom, L. L. (2015). Sodium Channel β Subunits: Emerging Targets in Channelopathies. *Annu. Rev. Physiol.* 77, 481–504. doi:10.1146/annurev-physiol-021014-071846.
- Ochiishi, T., Chen, L., Yukawa, A., Saitoh, Y., Sekino, Y., Arai, T., et al. (1999). Cellular localization of

- adenosine A1 receptors in rat forebrain: immunohistochemical analysis using adenosine A1 receptor-specific monoclonal antibody. *J. Comp. Neurol.* 411, 301–16. Available at: <http://www.ncbi.nlm.nih.gov/pubmed/10404255>.
- Ogawa, Y. (2006). Spectrins and AnkyrinB Constitute a Specialized Paranodal Cytoskeleton. *J. Neurosci.* 26, 5230–5239. doi:10.1523/JNEUROSCI.0425-06.2006.
- Ogiwara, I., Miyamoto, H., Morita, N., Atapour, N., Mazaki, E., Inoue, I., et al. (2007). Nav1.1 Localizes to Axons of Parvalbumin-Positive Inhibitory Interneurons: A Circuit Basis for Epileptic Seizures in Mice Carrying an Scn1a Gene Mutation. *J. Neurosci.* 27, 5903–5914. doi:10.1523/JNEUROSCI.5270-06.2007.
- Ohno, N., Kidd, G. J., Mahad, D., Kiryu-Seo, S., Avishai, A., Komuro, H., et al. (2011). Myelination and axonal electrical activity modulate the distribution and motility of mitochondria at CNS nodes of Ranvier. *J. Neurosci.* 31, 7249–7258. doi:10.1523/JNEUROSCI.0095-11.2011.
- Ohsawa, K., Irino, Y., Sanagi, T., Nakamura, Y., Suzuki, E., Inoue, K., et al. (2010). P2Y₁₂ receptor-mediated integrin- β 1 activation regulates microglial process extension induced by ATP. *Glia*, NA-NA. doi:10.1002/glia.20963.
- Oohashi, T., Hirakawa, S., Bekku, Y., Rauch, U., Zimmermann, D. R., Su, W.-D., et al. (2002). Bral1, a Brain-Specific Link Protein, Colocalizing with the Versican V2 Isoform at the Nodes of Ranvier in Developing and Adult Mouse Central Nervous Systems. *Mol. Cell. Neurosci.* 19, 43–57. doi:10.1006/mcne.2001.1061.
- Orduz, D., Maldonado, P. P., Balia, M., Vélez-Fort, M., de Sars, V., Yanagawa, Y., et al. (2015). Interneurons and oligodendrocyte progenitors form a structured synaptic network in the developing neocortex. *Elife* 4. doi:10.7554/eLife.06953.
- Orr, A. G., Orr, A. L., Li, X.-J., Gross, R. E., and Traynelis, S. F. (2009). Adenosine A_{2A} receptor mediates microglial process retraction. *Nat. Neurosci.* 12, 872–878. doi:10.1038/nn.2341.
- Orthmann-Murphy, J., Call, C. L., Molina-Castro, G. C., Hsieh, Y. C., Rasband, M. N., Calabresi, P. A., et al. (2020). Remyelination alters the pattern of myelin in the cerebral cortex. *Elife* 9, 1–61. doi:10.7554/eLife.56621.
- Ortiz, F. C., Habermacher, C., Graciarena, M., Houry, P.-Y., Nishiyama, A., Oumesmar, B. N., et al. (2019). Neuronal activity in vivo enhances functional myelin repair. *JCI Insight* 4. doi:10.1172/jci.insight.123434.
- Ousman, S. S., and David, S. (2000). Lysophosphatidylcholine induces rapid recruitment and activation of macrophages in the adult mouse spinal cord. *Glia* 30, 92–104. Available at: <http://www.ncbi.nlm.nih.gov/pubmed/10696148>.
- Pagani, F., Paolicelli, R. C., Murana, E., Cortese, B., Angelantonio, S. Di, Zurolo, E., et al. (2015). Defective microglial development in the hippocampus of Cx3cr1 deficient mice. *Front. Cell. Neurosci.* 09. doi:10.3389/fncel.2015.00111.
- Pajevic, S., Basser, P. J., and Fields, R. D. (2014). Role of myelin plasticity in oscillations and synchrony of neuronal activity. *Neuroscience* 276, 135–147. doi:10.1016/j.neuroscience.2013.11.007.
- Palacio, S., Chevaleyre, V., Brann, D. H., Murray, K. D., Piskorowski, R. A., and Trimmer, J. S. (2017). Heterogeneity in Kv2 Channel Expression Shapes Action Potential Characteristics and Firing Patterns in CA1 versus CA2 Hippocampal Pyramidal Neurons. *eneuro* 4, ENEURO.0267-17.2017. doi:10.1523/ENEURO.0267-17.2017.
- Pan, S., Mayoral, S. R., Choi, H. S., Chan, J. R., and Kheirbek, M. A. (2020). Preservation of a remote fear memory requires new myelin formation. *Nat. Neurosci.* 23, 487–499. doi:10.1038/s41593-019-0582-1.
- Pan, Z., Kao, T., Horvath, Z., Lemos, J., Sul, J. Y., Cranstoun, S. D., et al. (2006). A common ankyrin-G-based mechanism retains KCNQ and Na⁺ V channels at electrically active domains of the axon. *J. Neurosci.* 26, 2599–2613. doi:10.1523/JNEUROSCI.4314-05.2006.
- Pankratov, Y., Lalo, U., Verkhratsky, A., and North, R. A. (2006). Vesicular release of ATP at central synapses. *Pflügers Arch. - Eur. J. Physiol.* 452, 589–597. doi:10.1007/s00424-006-0061-x.
- Paolicelli, R. C., Bolasco, G., Pagani, F., Maggi, L., Scianni, M., Panzanelli, P., et al. (2011). Synaptic Pruning by Microglia Is Necessary for Normal Brain Development. *Science (80-)*. 333, 1456–

1458. doi:10.1126/science.1202529.
- Parkhurst, C. N., Yang, G., Ninan, I., Savas, J. N., Yates, J. R., Lafaille, J. J., et al. (2013). Microglia promote learning-dependent synapse formation through brain-derived neurotrophic factor. *Cell* 155, 1596–1609. doi:10.1016/j.cell.2013.11.030.
- Pascual, O., Ben Achour, S., Rostaing, P., Triller, A., and Bessis, A. (2012). Microglia activation triggers astrocyte-mediated modulation of excitatory neurotransmission. *Proc. Natl. Acad. Sci.* 109, E197–E205. doi:10.1073/pnas.1111098109.
- Pascual, O., Casper, K. B., Kubera, C., Zhang, J., Revilla-Sanchez, R., Sul, J.-Y., et al. (2005). Astrocytic purinergic signaling coordinates synaptic networks. *Science* 310, 113–6. doi:10.1126/science.1116916.
- Pasquini, L. A., Millet, V., Hoyos, H. C., Giannoni, J. P., Croci, D. O., Marder, M., et al. (2011). Galectin-3 drives oligodendrocyte differentiation to control myelin integrity and function. *Cell Death Differ.* 18, 1746–1756. doi:10.1038/cdd.2011.40.
- Pedraza, L., Huang, J. K., and Colman, D. R. (2001). Organizing Principles of the Axoglial Apparatus. *Neuron* 30, 335–344. doi:10.1016/S0896-6273(01)00306-3.
- Peles, E., Joho, K., Plowman, G. D., and Schlessinger, J. (1997a). Close Similarity between Drosophila Neurexin IV and Mammalian Caspr Protein Suggests a Conserved Mechanism for Cellular Interactions. *Cell* 88, 745–746. doi:10.1016/S0092-8674(00)81920-0.
- Peles, E., Nativ, M., Lustig, M., Grumet, M., Schilling, J., Martinez, R., et al. (1997b). Identification of a novel contactin-associated transmembrane receptor with multiple domains implicated in protein-protein interactions. *EMBO J.* 16, 978–988. doi:10.1093/emboj/16.5.978.
- Penfield, W. (1924). Oligodendroglia and its relation to classical neuroglia. *Brain* 47, 430–452.
- Peng, J., Liu, Y., Umpierre, A. D., Xie, M., Tian, D.-S., Richardson, J. R., et al. (2019). Microglial P2Y12 receptor regulates ventral hippocampal CA1 neuronal excitability and innate fear in mice. *Mol. Brain* 12, 71. doi:10.1186/s13041-019-0492-x.
- Penn, A. A., Riquelme, P. A., Feller, M. B., and Shatz, C. J. (1998). Competition in retinogeniculate patterning driven by spontaneous activity. *Science* 279, 2108–12. doi:10.1126/science.279.5359.2108.
- Pérez-Sen, R., Gómez-Villafuertes, R., Ortega, F., Gualix, J., Delicado, E. G., and Miras-Portugal, M. T. (2017). “An Update on P2Y13 Receptor Signalling and Function,” in 139–168. doi:10.1007/5584_2017_91.
- Perkins, G. A., and Ellisman, M. H. (2011). Mitochondrial configurations in peripheral nerve suggest differential ATP production. *J. Struct. Biol.* 173, 117–127. doi:10.1016/j.jsb.2010.06.017.
- Perkins, K. L. (2006). Cell-attached voltage-clamp and current-clamp recording and stimulation techniques in brain slices. *J. Neurosci. Methods* 154, 1–18. doi:10.1016/j.jneumeth.2006.02.010.
- Perry, V. H., Hume, D. A., and Gordon, S. (1985). Immunohistochemical localization of macrophages and microglia in the adult and developing mouse brain. *Neuroscience* 15, 313–326. doi:10.1016/0306-4522(85)90215-5.
- Peters, A., Palay, S. ., and Webster, H. (1991). *The Fine Structure of the Nervous System, Third Edition* . Third Edit. , ed. O. U. Press New-York.
- Petersen, M. A., Ryu, J. K., Chang, K. J., Etxeberria, A., Bardehle, S., Mendiola, A. S., et al. (2017). Fibrinogen Activates BMP Signaling in Oligodendrocyte Progenitor Cells and Inhibits Remyelination after Vascular Damage. *Neuron* 96, 1003-1012.e7. doi:10.1016/j.neuron.2017.10.008.
- Pfeiffer, F., Frommer-Kaestle, G., and Fallier-Becker, P. (2019). Structural adaption of axons during de- and remyelination in the Cuprizone mouse model. *Brain Pathol.* 29, 675–692. doi:10.1111/bpa.12748.
- Pfeiffer, T., Avignone, E., and Nägerl, U. V. (2016). Induction of hippocampal long-term potentiation increases the morphological dynamics of microglial processes and prolongs their contacts with dendritic spines. *Sci. Rep.* 6, 1–9. doi:10.1038/srep32422.
- Piaton, G., Aigrot, M.-S., Williams, A., Moyon, S., Tepavcevic, V., Moutkine, I., et al. (2011). Class 3 semaphorins influence oligodendrocyte precursor recruitment and remyelination in adult

- central nervous system. *Brain* 134, 1156–1167. doi:10.1093/brain/awr022.
- Pillai, A. M., Thaxton, C., Pribisko, A. L., Cheng, J.-G., Dupree, J. L., and Bhat, M. A. (2009). Spatiotemporal ablation of myelinating glia-specific neurofascin (Nfasc NF155) in mice reveals gradual loss of paranodal axoglial junctions and concomitant disorganization of axonal domains. *J. Neurosci. Res.* 87, 1773–1793. doi:10.1002/jnr.22015.
- Plemel, J. R., Stratton, J. A., Michaels, N. J., Rawji, K. S., Zhang, E., Sinha, S., et al. (2020). Microglia response following acute demyelination is heterogeneous and limits infiltrating macrophage dispersion. *Sci. Adv.* 6, 1–16. doi:10.1126/sciadv.aay6324.
- Poliak, S., Salomon, D., Elhanany, H., Sabanay, H., Kiernan, B., Pevny, L., et al. (2003). Juxtaparanodal clustering of Shaker-like K⁺ channels in myelinated axons depends on Caspr2 and TAG-1. *J. Cell Biol.* 162, 1149–1160. doi:10.1083/jcb.200305018.
- Poliani, P. L., Wang, Y., Fontana, E., Robinette, M. L., Yamanishi, Y., Gilfillan, S., et al. (2015). TREM2 sustains microglial expansion during aging and response to demyelination. *J. Clin. Invest.* 125, 2161–2170. doi:10.1172/JCI77983.
- Pont-Lezica, L., Beumer, W., Colasse, S., Drexhage, H., Versnel, M., and Bessis, A. (2014). Microglia shape corpus callosum axon tract fasciculation: Functional impact of prenatal inflammation. *Eur. J. Neurosci.* 39, 1551–1557. doi:10.1111/ejn.12508.
- Prineas, J. W., Barnard, R. O., Kwon, E. E., Sharer, L. R., and Cho, E.-S. (1993). Multiple sclerosis: Remyelination of nascent lesions: Remyelination of nascent lesions. *Ann. Neurol.* 33, 137–151. doi:10.1002/ana.410330203.
- Pringle, N. P., and Richardson, W. D. (1993). A singularity of PDGF alpha-receptor expression in the dorsoventral axis of the neural tube may define the origin of the oligodendrocyte lineage. *Development* 117, 525–533. doi:10.1242/dev.117.2.525.
- Prinz, M., Jung, S., and Priller, J. (2019). Microglia Biology: One Century of Evolving Concepts. *Cell* 179, 292–311. doi:10.1016/j.cell.2019.08.053.
- Rakic, P. (1976). Prenatal genesis of connections subserving ocular dominance in the rhesus monkey. *Nature* 261, 467–471. doi:10.1038/261467a0.
- Ramaglia, V., Hughes, T. R., Donev, R. M., Ruseva, M. M., Wu, X., Huitinga, I., et al. (2012). C3-dependent mechanism of microglial priming relevant to multiple sclerosis. *Proc. Natl. Acad. Sci. U. S. A.* 109, 965–970. doi:10.1073/pnas.1111924109.
- Ramón y Cajal, S. (1909). *Histologie du système nerveux de l'homme et des vertébrés*. Maloine.
- Ramón y Cajal, S. (1911). *Histologie du système nerveux de l'homme & des vertébrés: Cervelet, cerveau moyen, rétine, couche optique, corps strié, écorce cérébrale générale & régionale, grand sympathique (Vol. 2)*. , ed. A. Maloine.
- Ransohoff, R. M. (2016). A polarizing question: do M1 and M2 microglia exist? *Nat. Neurosci.* 19, 987–991. doi:10.1038/nn.4338.
- Ranvier, L.-A. (1878). *Leçons sur l'Histologie du Système Nerveux*. Librairie F. Savy.
- Ranvier, L. (1872). Recherches sur l'histologie et la physiologie des nerfs. *Arch. Physiol. Norm. Pathol.* 4, 129–149.
- Rasband, M. N., Kagawa, T., Park, E. W., Ikenaka, K., and Trimmer, J. S. (2003). Dysregulation of axonal sodium channel isoforms after adult-onset chronic demyelination. *J. Neurosci. Res.* 73, 465–470. doi:10.1002/jnr.10675.
- Rasband, M. N., and Peles, E. (2021). Mechanisms of node of Ranvier assembly. *Nat. Rev. Neurosci.* 22, 7–20. doi:10.1038/s41583-020-00406-8.
- Rasband, M. N., Peles, E., Trimmer, J. S., Levinson, S. R., Lux, S. E., and Shrager, P. (1999). Dependence of nodal sodium channel clustering on paranodal axoglial contact in the developing CNS. *J. Neurosci.* 19, 7516–7528. doi:10.1523/jneurosci.19-17-07516.1999.
- Rasband, M. N., Trimmer, J. S., Schwarz, T. L., Levinson, S. R., Ellisman, M. H., Schachner, M., et al. (1998). Potassium channel distribution, clustering, and function in remyelinating rat axons. *J. Neurosci.* 18, 36–47. Available at: <http://www.ncbi.nlm.nih.gov/pubmed/9412484>.
- Ratcliffe, C. F., Westenbroek, R. E., Curtis, R., and Catterall, W. A. (2001). Sodium channel β 1 and β 3 subunits associate with neurofascin through their extracellular immunoglobulin-like domain. *J.*

- Cell Biol.* 154, 427–434. doi:10.1083/jcb.200102086.
- Rawlins, F. A. (1973). A time-sequence auto radiographic study of the in vivo incorporation of [1, 2-³H] cholesterol into peripheral nerve myelin. *J. Cell Biol.* 58, 42–53. doi:10.1083/jcb.58.1.42.
- Redmond, S. A., Mei, F., Eshed-Eisenbach, Y., Osso, L. A., Leshkowitz, D., Shen, Y. A. A., et al. (2016). Somatodendritic Expression of JAM2 Inhibits Oligodendrocyte Myelination. *Neuron* 91, 824–836. doi:10.1016/j.neuron.2016.07.021.
- Reich, D. S., Arnold, D. L., Vermersch, P., Bar-Or, A., Fox, R. J., Matta, A., et al. (2021). Safety and efficacy of tolebrutinib, an oral brain-penetrant BTK inhibitor, in relapsing multiple sclerosis: a phase 2b, randomised, double-blind, placebo-controlled trial. *Lancet Neurol.* 20, 729–738. doi:10.1016/S1474-4422(21)00237-4.
- Remak, R. (1836). Vorläufige Mittheilung microscopischer Beobachtungen über den innern Bau der Cerebrospinalnerven und über die Entwicklung ihrer Formelemente. *Müller's Arch. für Anat. Physiol. und wissenschaftliche Med.*, 145–161.
- Remington, L. T., Babcock, A. A., Zehntner, S. P., and Owens, T. (2007). Microglial Recruitment, Activation, and Proliferation in Response to Primary Demyelination. *Am. J. Pathol.* 170, 1713–1724. doi:10.2353/ajpath.2007.060783.
- Renigunta, V., Schlichthörl, G., and Daut, J. (2015). Much more than a leak: Structure and function of K2P-channels. *Pflugers Arch. Eur. J. Physiol.* 467, 867–894. doi:10.1007/s00424-015-1703-7.
- Réu, P., Khosravi, A., Bernard, S., Mold, J. E., Salehpour, M., Alkass, K., et al. (2017). The Lifespan and Turnover of Microglia in the Human Brain. *Cell Rep.* 20, 779–784. doi:10.1016/j.celrep.2017.07.004.
- Richardson, W. D., Kessaris, N., and Pringle, N. (2006). Oligodendrocyte wars. *Nat. Rev. Neurosci.* 7, 11–18. doi:10.1038/nrn1826.
- Richardson, W. D., Smith, H. K., Sun, T., Pringle, N. P., Hall, A., and Woodruff, R. (2000). Oligodendrocyte lineage and the motor neuron connection. *Glia* 29, 136–142. doi:10.1002/(SICI)1098-1136(20000115)29:2<136::AID-GLIA6>3.0.CO;2-G.
- Rinaldi, F., Calabrese, M., Grossi, P., Puthenparampil, M., Perini, P., and Gallo, P. (2010). Cortical lesions and cognitive impairment in multiple sclerosis. *Neurol. Sci.* 31, 235–237. doi:10.1007/s10072-010-0368-4.
- Rinner, W. A., Bauer, J., Schmidts, M., Lassmann, H., and Hickey, W. F. (1995). Resident microglia and hematogenous macrophages as phagocytes in adoptively transferred experimental autoimmune transferred experimental autoimmune encephalomyelitis: An investigation using rat radiation bone marrow chimeras. *Glia* 14, 257–266. doi:10.1002/glia.440140403.
- Rios, J. C., Melendez-Vasquez, C. V., Einheber, S., Lustig, M., Grumet, M., Hemperly, J., et al. (2000). Contactin-Associated Protein (Caspr) and Contactin Form a Complex That Is Targeted to the Paranodal Junctions during Myelination. *J. Neurosci.* 20, 8354–8364. doi:10.1523/JNEUROSCI.20-22-08354.2000.
- Rios, J. C., Rubin, M., Martin, M. St., Downey, R. T., Einheber, S., Rosenbluth, J., et al. (2003). Paranodal Interactions Regulate Expression of Sodium Channel Subtypes and Provide a Diffusion Barrier for the Node of Ranvier. *J. Neurosci.* 23, 7001–7011. doi:10.1523/JNEUROSCI.23-18-07001.2003.
- Rivers, L. E., Young, K. M., Rizzi, M., Jamen, F., Psachoulia, K., Wade, A., et al. (2008). PDGFRA/NG2 glia generate myelinating oligodendrocytes and piriform projection neurons in adult mice. *Nat. Neurosci.* 11, 1392–1401. doi:10.1038/nn.2220.
- Rodemer, C., Thai, T.-P., Brugger, B., Kaercher, T., Werner, H., Nave, K.-A., et al. (2003). Inactivation of ether lipid biosynthesis causes male infertility, defects in eye development and optic nerve hypoplasia in mice. *Hum. Mol. Genet.* 12, 1881–1895. doi:10.1093/hmg/ddg191.
- Rogers, J. T., Morganti, J. M., Bachstetter, A. D., Hudson, C. E., Peters, M. M., Grimmig, B. A., et al. (2011). CX3CR1 Deficiency Leads to Impairment of Hippocampal Cognitive Function and Synaptic Plasticity. *J. Neurosci.* 31, 16241–16250. doi:10.1523/JNEUROSCI.3667-11.2011.
- Ronzano, R., Roux, T., Thetiot, M., Aigrot, M. S., Richard, L., Lejeune, F. X., et al. (2021). Microglia-neuron interaction at nodes of Ranvier depends on neuronal activity through potassium release

- and contributes to remyelination. *Nat. Commun.* 12, 5219. doi:10.1038/s41467-021-25486-7.
- Rosenberg, S. S., Kelland, E. E., Tokar, E., De La Torre, A. R., and Chan, J. R. (2008). The geometric and spatial constraints of the microenvironment induce oligodendrocyte differentiation. *Proc. Natl. Acad. Sci. U. S. A.* 105, 14662–14667. doi:10.1073/pnas.0805640105.
- Rosenbluth, J. (1976). Intramembranous particle distribution at the node of Ranvier and adjacent axolemma in myelinated axons of the frog brain. *J. Neurocytol.* 5, 731–745. doi:10.1007/BF01181584.
- Rosenbluth, J. (1980). Central Myelin in the Mouse Mutant Shiverer. 648, 639–648.
- Rosenbluth, J. (1983). Intramembranous particle distribution in nerve fiber membranes. *Experientia* 39, 953–963. doi:10.1007/BF01989760.
- Rosenbluth, J. (2009). Multiple functions of the paranodal junction of myelinated nerve fibers. *J. Neurosci. Res.* 87, 3250–3258. doi:10.1002/jnr.22013.
- Roth, B. L. (2016). DREADDs for Neuroscientists. *Neuron* 89, 683–694. doi:10.1016/j.neuron.2016.01.040.
- Roumier, A., Béchade, C., Poncer, J.-C., Smalla, K.-H., Tomasello, E., Vivier, E., et al. (2004). Impaired synaptic function in the microglial KARAP/DAP12-deficient mouse. *J. Neurosci.* 24, 11421–8. doi:10.1523/JNEUROSCI.2251-04.2004.
- Rush, A. M., Dib-Hajj, S. D., and Waxman, S. G. (2005). Electrophysiological properties of two axonal sodium channels, Na_v 1.2 and Na_v 1.6, expressed in mouse spinal sensory neurones. *J. Physiol.* 564, 803–815. doi:10.1113/jphysiol.2005.083089.
- Saab, A. S., and Nave, K. A. (2017). Myelin dynamics: protecting and shaping neuronal functions. *Curr. Opin. Neurobiol.* 47, 104–112. doi:10.1016/j.conb.2017.09.013.
- Saab, A. S., Tzvetavona, I. D., Trevisiol, A., Baltan, S., Dibaj, P., Kusch, K., et al. (2016). Oligodendroglial NMDA Receptors Regulate Glucose Import and Axonal Energy Metabolism. *Neuron* 91, 119–132. doi:10.1016/j.neuron.2016.05.016.
- Saab, C. Y., Craner, M. J., Kataoka, Y., and Waxman, S. G. (2004). Abnormal Purkinje cell activity in vivo in experimental allergic encephalomyelitis. *Exp. Brain Res.* 158, 1–8. doi:10.1007/s00221-004-1867-4.
- Saederup, N., Cardona, A. E., Croft, K., Mizutani, M., Coteleur, A. C., Tsou, C.-L., et al. (2010). Selective Chemokine Receptor Usage by Central Nervous System Myeloid Cells in CCR2-Red Fluorescent Protein Knock-In Mice. *PLoS One* 5, e13693. doi:10.1371/journal.pone.0013693.
- Safaiyan, S., Kannaiyan, N., Snaidero, N., Brioschi, S., Biber, K., Yona, S., et al. (2016). Age-related myelin degradation burdens the clearance function of microglia during aging. *Nat. Neurosci.* 19, 995–998. doi:10.1038/nn.4325.
- Saher, G., Brügger, B., Lappe-Siefke, C., Möbius, W., Tozawa, R. I., Wehr, M. C., et al. (2005). High cholesterol level is essential for myelin membrane growth. *Nat. Neurosci.* 8, 468–475. doi:10.1038/nn1426.
- Saher, G., Quintes, S., Möbius, W., Wehr, M. C., Kramer-Albers, E.-M., Brügger, B., et al. (2009). Cholesterol Regulates the Endoplasmic Reticulum Exit of the Major Membrane Protein P0 Required for Peripheral Myelin Compaction. *J. Neurosci.* 29, 6094–6104. doi:10.1523/JNEUROSCI.0686-09.2009.
- Salter, M. G., and Fern, R. (2005). NMDA receptors are expressed in developing oligodendrocyte processes and mediate injury. *Nature* 438, 1167–1171. doi:10.1038/nature04301.
- Salzer, J. L. (2003). Polarized domains of myelinated axons. *Neuron* 40, 297–318. doi:10.1016/S0896-6273(03)00628-7.
- Salzer, J. L., and Zalc, B. (2016). Myelination. *Curr. Biol.* 26, R971–R975. doi:10.1016/j.cub.2016.07.074.
- Sampaio-Baptista, C., Khrapitchev, A. A., Foxley, S., Schlagheck, T., Scholz, J., Jbabdi, S., et al. (2013). Motor skill learning induces changes in white matter microstructure and myelination. *J. Neurosci.* 33, 19499–19503. doi:10.1523/JNEUROSCI.3048-13.2013.
- Sarkar, S., Nguyen, H. M., Malovic, E., Luo, J., Langley, M., Palanisamy, B. N., et al. (2020). Kv1.3 modulates neuroinflammation and neurodegeneration in Parkinson's disease. *J. Clin. Invest.*

doi:10.1172/JCI136174.

- Sasaki, Y., Hoshi, M., Akazawa, C., Nakamura, Y., Tsuzuki, H., Inoue, K., et al. (2003). Selective expression of Gi/o-coupled ATP receptor P2Y₁₂ in microglia in rat brain. *Glia* 44, 242–250. doi:10.1002/glia.10293.
- Sausbier, U., Sausbier, M., Sailer, C. A., Arntz, C., Knaus, H.-G., Neuhuber, W., et al. (2006). Ca²⁺-activated K⁺ channels of the BK-type in the mouse brain. *Histochem. Cell Biol.* 125, 725–741. doi:10.1007/s00418-005-0124-7.
- Sawada, M., Kondo, N., Suzumura, A., and Marunouchi, T. (1989). Production of tumor necrosis factor-alpha by microglia and astrocytes in culture. *Brain Res.* 491, 394–397. doi:10.1016/0006-8993(89)90078-4.
- Schafer, D. P., Custer, A. W., Shrager, P., and Rasband, M. N. (2006). Early events in node of Ranvier formation during myelination and remyelination in the PNS. *Neuron Glia Biol.* 2, 69–79. doi:10.1017/S1740925X06000093.
- Schafer, D. P., Lehrman, E. K., Kautzman, A. G., Koyama, R., Mardinly, A. R., Yamasaki, R., et al. (2012). Microglia Sculpt Postnatal Neural Circuits in an Activity and Complement-Dependent Manner. *Neuron* 74, 691–705. doi:10.1016/j.neuron.2012.03.026.
- Schilling, T., and Eder, C. (2007). Ion channel expression in resting and activated microglia of hippocampal slices from juvenile mice. *Brain Res.* 1186, 21–8. doi:10.1016/j.brainres.2007.10.027.
- Schilling, T., and Eder, C. (2015). Microglial K⁺ channel expression in young adult and aged mice. *Glia* 63, 664–672. doi:10.1002/glia.22776.
- Schirmer, L., Srivastava, R., Kalluri, S. R., Böttinger, S., Herwerth, M., Carassiti, D., et al. (2014). Differential loss of KIR4.1 immunoreactivity in multiple sclerosis lesions. *Ann. Neurol.* 75, 810–828. doi:10.1002/ana.24168.
- Schniepp, R., Jakl, V., Wuehr, M., Havla, J., Kümpfel, T., Dieterich, M., et al. (2013). Treatment with 4-aminopyridine improves upper limb tremor of a patient with multiple sclerosis: a video case report. *Mult. Scler. J.* 19, 506–508. doi:10.1177/1352458512461394.
- Scholle, A., Dugarmaa, S., Zimmer, T., Leonhardt, M., Koopmann, R., Engeland, B., et al. (2004). Rate-limiting Reactions Determining Different Activation Kinetics of Kv1.2 and Kv2.1 Channels. *J. Membr. Biol.* 198. doi:10.1007/s00232-004-0664-0.
- Scholz, J., Klein, M. C., Behrens, T. E. J., and Johansen-Berg, H. (2009). Training induces changes in white-matter architecture. *Nat. Neurosci.* 12, 1370–1371. doi:10.1038/nn.2412.
- Schulz, C., Perdiguero, E. G., Chorro, L., Szabo-Rogers, H., Cagnard, N., Kierdorf, K., et al. (2012). A Lineage of Myeloid Cells Independent of Myb and Hematopoietic Stem Cells. *Science (80-)*. 336, 86–90. doi:10.1126/science.1219179.
- Schwann, T. (1839). *Mikroskopische Untersuchungen über die Uebereinstimmung in der Struktur und dem Wachsthum der Thiere und Pflanzen*, Reimer. Translated. , ed. L. Sydenham Society Berlin.
- Schwarz, J. R., Glassmeier, G., Cooper, E. C., Kao, T. C., Nodera, H., Tabuena, D., et al. (2006). KCNQ channels mediate IKs, a slow K⁺ current regulating excitability in the rat node of Ranvier. *J. Physiol.* 573, 17–34. doi:10.1113/jphysiol.2006.106815.
- Sellgren, C. M., Gracias, J., Watmuff, B., Biag, J. D., Thanos, J. M., Whittredge, P. B., et al. (2019). Increased synapse elimination by microglia in schizophrenia patient-derived models of synaptic pruning. *Nat. Neurosci.* 22, 374–385. doi:10.1038/s41593-018-0334-7.
- Selten, M. M., Meyer, F., Ba, W., Vallès, A., Maas, D. A., Negwer, M., et al. (2016). Increased GABAB receptor signaling in a rat model for schizophrenia. *Sci. Rep.* 6, 34240. doi:10.1038/srep34240.
- Semyanov, A., Henneberger, C., and Agarwal, A. (2020). Making sense of astrocytic calcium signals — from acquisition to interpretation. *Nat. Rev. Neurosci.* 21, 551–564. doi:10.1038/s41583-020-0361-8.
- Serwanski, D. R., Jukkola, P., and Nishiyama, A. (2016). Heterogeneity of astrocyte and NG2 cell insertion at the node of Ranvier. *J. Comp. Neurol.*, 1–10. doi:10.1002/cne.
- Sharma, K., Bisht, K., and Eyo, U. B. (2021). A Comparative Biology of Microglia Across Species. *Front. Cell Dev. Biol.* 9, 1–15. doi:10.3389/fcell.2021.652748.

- Shatz, C. J. (1990). Impulse activity and the patterning of connections during CNS development. *Neuron* 5, 745–756. doi:10.1016/0896-6273(90)90333-B.
- Shen, S., Sandoval, J., Swiss, V. A., Li, J., Dupree, J., Franklin, R. J. M., et al. (2008). Age-dependent epigenetic control of differentiation inhibitors is critical for remyelination efficiency. *Nat. Neurosci.* 11, 1024–1034. doi:10.1038/nn.2172.
- Sherman, D. L., Tait, S., Melrose, S., Johnson, R., Zonta, B., Court, F. A., et al. (2005). Neurofascins are required to establish axonal domains for saltatory conduction. *Neuron* 48, 737–742. doi:10.1016/j.neuron.2005.10.019.
- Shields, S. A., Gilson, J. M., Blakemore, W., and Franklin, R. J. (2000). Remyelination occurs as extensively but more slowly in old rats compared to young rats following flitoxin-induced CNS demyelination. *Glia* 29, 102. doi:10.1002/(sici)1098-1136(20000101)29:1<102::aid-glia12>3.0.co;2-1.
- Shigemoto-Mogami, Y., Hoshikawa, K., Goldman, J. E., Sekino, Y., and Sato, K. (2014a). Microglia Enhance Neurogenesis and Oligodendrogenesis in the Early Postnatal Subventricular Zone. *J. Neurosci.* 34, 2231–2243. doi:10.1523/JNEUROSCI.1619-13.2014.
- Shigemoto-Mogami, Y., Hoshikawa, K., Goldman, J. E., Sekino, Y., and Sato, K. (2014b). Microglia Enhance Neurogenesis and Oligodendrogenesis in the Early Postnatal Subventricular Zone. *J. Neurosci.* 34, 2231–2243. doi:10.1523/JNEUROSCI.1619-13.2014.
- Shlesinger, M. F. (2006). Search research. *Nature* 443, 281–282. doi:10.1038/443281a.
- Siapas, A. G., and Wilson, M. A. (1998). Coordinated Interactions between Hippocampal Ripples and Cortical Spindles during Slow-Wave Sleep. *Neuron* 21, 1123–1128. doi:10.1016/S0896-6273(00)80629-7.
- Siems, S. B., Jahn, O., Eichel, M. A., Kannaiyan, N., Wu, L. M. N., Sherman, D. L., et al. (2020). Proteome profile of peripheral myelin in healthy mice and in a neuropathy model. *Elife* 9. doi:10.7554/eLife.51406.
- Siems, S. B., Jahn, O., Hoodless, L. J., Jung, R. B., Hesse, D., Möbius, W., et al. (2021). Proteome Profile of Myelin in the Zebrafish Brain. *Front. Cell Dev. Biol.* 9, 1–17. doi:10.3389/fcell.2021.640169.
- Sierra, A., de Castro, F., del Río-Hortega, J., Rafael Iglesias-Rozas, J., Garrosa, M., and Kettenmann, H. (2016). The “Big-Bang” for modern glial biology: Translation and comments on Pío del Río-Hortega 1919 series of papers on microglia. *Glia* 64, 1801–1840. doi:10.1002/glia.23046.
- Sierra, A., Encinas, J. M., Deudero, J. J. P., Chancey, J. H., Enikolopov, G., Overstreet-Wadiche, L. S., et al. (2010). Microglia shape adult hippocampal neurogenesis through apoptosis-coupled phagocytosis. *Cell Stem Cell* 7, 483–495. doi:10.1016/j.stem.2010.08.014.
- Simon, C., Götz, M., and Dimou, L. (2011). Progenitors in the adult cerebral cortex: Cell cycle properties and regulation by physiological stimuli and injury. *Glia* 59, 869–881. doi:10.1002/glia.21156.
- Simons, M., Krämer, E.-M., Thiele, C., Stoffel, W., and Trotter, J. (2000). Assembly of Myelin by Association of Proteolipid Protein with Cholesterol- and Galactosylceramide-Rich Membrane Domains. *J. Cell Biol.* 151, 143–154. doi:10.1083/jcb.151.1.143.
- Simons, M., and Nave, K. A. (2016). Oligodendrocytes: Myelination and axonal support. *Cold Spring Harb. Perspect. Biol.* 8, 1–16. doi:10.1101/cshperspect.a020479.
- Sipe, G. O., Lowery, R. L., Tremblay, M., Kelly, E. A., Lamantia, C. E., and Majewska, A. K. (2016). Microglial P2Y₁₂ is necessary for synaptic plasticity in mouse visual cortex. *Nat. Commun.* 7. doi:10.1038/ncomms10905.
- Skoff, R. P., Price, D. L., and Stocks, A. (1976). Electron microscopic autoradiographic studies of gliogenesis in rat optic nerve. II. Time of origin. *J. Comp. Neurol.* 169, 313–333. doi:10.1002/cne.901690304.
- Skoff, R. P., Toland, D., and Nast, E. (1980). Pattern of myelination and distribution of neuroglial cells along the developing optic system of the rat and rabbit. *J. Comp. Neurol.* 191, 237–253. doi:10.1002/cne.901910207.
- Skripuletz, T., Hackstette, D., Bauer, K., Gudi, V., Pul, R., Voss, E., et al. (2013). Astrocytes regulate myelin clearance through recruitment of microglia during cuprizone-induced demyelination.

- Brain* 136, 147–167. doi:10.1093/brain/aws262.
- Smith L, K. J., Bostock L, H., and Hall S, M. (1982). Saltatory Conduction Precedes Remyelination in Axons demyelinated with lysophosphatidyl choline. *Methods*, 13–31.
- Smith, R. S., and Koles, Z. J. (1970). Myelinated nerve fibers: computed effect of myelin thickness on conduction velocity. *Am. J. Physiol.* 219, 1256–1258. doi:10.1152/ajplegacy.1970.219.5.1256.
- Snaidero, N., Möbius, W., Czopka, T., Hekking, L. H. P., Mathisen, C., Verkleij, D., et al. (2014). Myelin membrane wrapping of CNS axons by PI(3,4,5)P3-dependent polarized growth at the inner tongue. *Cell* 156, 277–290. doi:10.1016/j.cell.2013.11.044.
- Snaidero, N., Schifferer, M., Mezydło, A., Zalc, B., Kerschensteiner, M., and Misgeld, T. (2020). Myelin replacement triggered by single-cell demyelination in mouse cortex. *Nat. Commun.* 11. doi:10.1038/s41467-020-18632-0.
- Snaidero, N., Velte, C., Myllykoski, M., Raasakka, A., Ignatev, A., Werner, H. B., et al. (2017). Antagonistic Functions of MBP and CNP Establish Cytosolic Channels in CNS Myelin. *Cell Rep.* 18, 314–323. doi:10.1016/j.celrep.2016.12.053.
- Snipes, G. J., Suter, U., Welcher, A. A., and Shooter, E. M. (1992). Characterization of a novel peripheral nervous system myelin protein (PMP-22/SR13). *J. Cell Biol.* 117, 225–38. doi:10.1083/jcb.117.1.225.
- Sogn, C. J. L., Puchades, M., and Gundersen, V. (2013). Rare contacts between synapses and microglial processes containing high levels of Iba1 and actin - a postembedding immunogold study in the healthy rat brain. *Eur. J. Neurosci.* 38, 2030–2040. doi:10.1111/ejn.12213.
- Solly, S. K., Thomas, J.-L., Monge, M., Demerens, C., Lubetzki, C., Gardinier, M. V., et al. (1996). Myelin/oligodendrocyte glycoprotein (MOG) expression is associated with myelin deposition. *Glia* 18, 39–48. doi:10.1002/(SICI)1098-1136(199609)18:1<39::AID-GLIA4>3.0.CO;2-Z.
- Somjen, G. G. (1988). Nervenkitz: Notes on the history of the concept of neuroglia. *Glia* 1, 2–9. doi:10.1002/glia.440010103.
- Soulika, A. M., Lee, E., McCauley, E., Miers, L., Bannerman, P., and Pleasure, D. (2009). Initiation and Progression of Axonopathy in Experimental Autoimmune Encephalomyelitis. *J. Neurosci.* 29, 14965–14979. doi:10.1523/JNEUROSCI.3794-09.2009.
- Spassky, N., Goujet-Zalc, C., Parmantier, E., Olivier, C., Martinez, S., Ivanova, A., et al. (1998). Multiple Restricted Origin of Oligodendrocytes. *J. Neurosci.* 18, 8331–8343. doi:10.1523/JNEUROSCI.18-20-08331.1998.
- Spassky, N., Olivier, C., Cobos, I., LeBras, B., Goujet-Zalc, C., Martinez, S., et al. (2001). The Early Steps of Oligodendrogenesis : Insights from the Study of the plp Lineage in the Brain of Chicks and Rodents. 23, 318–326. doi:10.1159/000048715.
- Spassky, N., Olivier, C., Perez-Villegas, E., Goujet-Zalc, C., Martinez, S., Thomas, J., et al. (2000). Single or multiple oligodendroglial lineages: A controversy. *Glia* 29, 143–148. doi:10.1002/(SICI)1098-1136(20000115)29:2<143::AID-GLIA7>3.0.CO;2-D.
- Spiegel, I., Mardinly, A. R., Gabel, H. W., Bazinet, J. E., Couch, C. H., Tzeng, C. P., et al. (2014). Npas4 Regulates Excitatory-Inhibitory Balance within Neural Circuits through Cell-Type-Specific Gene Programs. *Cell* 157, 1216–1229. doi:10.1016/j.cell.2014.03.058.
- Spitzer, S. O., Sitnikov, S., Kamen, Y., Evans, K. A., Kronenberg-Versteeg, D., Dietmann, S., et al. (2019). Oligodendrocyte Progenitor Cells Become Regionally Diverse and Heterogeneous with Age. *Neuron* 101, 459-471.e5. doi:10.1016/j.neuron.2018.12.020.
- Squarzoni, P., Oller, G., Hoeffel, G., Pont-Lezica, L., Rostaing, P., Low, D., et al. (2014). Microglia Modulate Wiring of the Embryonic Forebrain. *Cell Rep.* 8, 1271–1279. doi:10.1016/j.celrep.2014.07.042.
- Srinivasan, J., Schachner, M., and Catterall, W. A. (1998). Interaction of voltage-gated sodium channels with the extracellular matrix molecules tenascin-C and tenascin-R. *Proc. Natl. Acad. Sci.* 95, 15753–15757. doi:10.1073/pnas.95.26.15753.
- Stange-Marten, A., Nabel, A. L., Sinclair, J. L., Fischl, M., Alexandrova, O., Wohlfrom, H., et al. (2017). Input timing for spatial processing is precisely tuned via constant synaptic delays and myelination patterns in the auditory brainstem. *Proc. Natl. Acad. Sci. U. S. A.* 114, E4851–E4858.

- doi:10.1073/pnas.1702290114.
- Stangel, M., Kuhlmann, T., Matthews, P. M., and Kilpatrick, T. J. (2017). Achievements and obstacles of remyelinating therapies in multiple sclerosis. *Nat. Rev. Neurol.* 13, 742–754. doi:10.1038/nrneurol.2017.139.
- Steadman, P. E., Xia, F., Ahmed, M., Mocle, A. J., Penning, A. R. A., Geraghty, A. C., et al. (2020). Disruption of Oligodendrogenesis Impairs Memory Consolidation in Adult Mice. *Neuron* 105, 150–164.e6. doi:10.1016/j.neuron.2019.10.013.
- Stedehouder, J., Brizee, D., Shpak, G., and Kushner, S. A. (2018). Activity-dependent myelination of parvalbumin interneurons mediated by axonal morphological plasticity. *J. Neurosci.* 38, 3631–3642. doi:10.1523/JNEUROSCI.0074-18.2018.
- Stedehouder, J., Brizee, D., Slotman, J. A., Pascual-Garcia, M., Leyrer, M. L., Bouwen, B. L., et al. (2019). Local axonal morphology guides the topography of interneuron myelination in mouse and human neocortex. *Elife* 8. doi:10.7554/eLife.48615.
- Stedehouder, J., Couey, J. J., Brizee, D., Hosseini, B., Slotman, J. A., Dirven, C. M. F., et al. (2017). Fast-spiking Parvalbumin Interneurons are Frequently Myelinated in the Cerebral Cortex of Mice and Humans. *Cereb. Cortex* 27, 5001–5013. doi:10.1093/cercor/bhx203.
- Steinhäser, C., Jabs, R., and Kettenmann, H. (1994). Properties of GABA and glutamate responses in identified glial cells of the mouse hippocampal slice. *Hippocampus* 4, 19–35. doi:10.1002/hipo.450040105.
- Stellwagen, D., and Malenka, R. C. (2006). Synaptic scaling mediated by glial TNF- α . *Nature* 440, 1054–1059. doi:10.1038/nature04671.
- Sternson, S. M., and Roth, B. L. (2014). Chemogenetic Tools to Interrogate Brain Functions. *Annu. Rev. Neurosci.* 37, 387–407. doi:10.1146/annurev-neuro-071013-014048.
- Stevens, B., Porta, S., Haak, L. L., Gallo, V., and Fields, R. D. (2002). Adenosine: A neuron-glial transmitter promoting myelination in the CNS in response to action potentials. *Neuron* 36, 855–868. doi:10.1016/S0896-6273(02)01067-X.
- Stobart, J. L., Ferrari, K. D., Barrett, M. J. P., Glück, C., Stobart, M. J., Zuend, M., et al. (2018). Cortical Circuit Activity Evokes Rapid Astrocyte Calcium Signals on a Similar Timescale to Neurons. *Neuron* 98, 726–735.e4. doi:10.1016/j.neuron.2018.03.050.
- Storch, M. K., Stefferl, A., Brehm, U., Weissert, R., Wallström, E., Kerschensteiner, M., et al. (1998). Autoimmunity to Myelin Oligodendrocyte Glycoprotein in Rats Mimics the Spectrum of Multiple Sclerosis Pathology. *Brain Pathol.* 8, 681–694. doi:10.1111/j.1750-3639.1998.tb00194.x.
- Stowell, R. D., Sipe, G. O., Dawes, R. P., Batchelor, H. N., Lordy, K. A., Whitelaw, B. S., et al. (2019). Noradrenergic signaling in the wakeful state inhibits microglial surveillance and synaptic plasticity in the mouse visual cortex. *Nat. Neurosci.* 22, 1782–1792. doi:10.1038/s41593-019-0514-0.
- Stowell, R. D., Wong, E. L., Batchelor, H. N., Mendes, M. S., Lamantia, C. E., Whitelaw, B. S., et al. (2018). Cerebellar microglia are dynamically unique and survey Purkinje neurons in vivo. *Dev. Neurobiol.* 78, 627–644. doi:10.1002/dneu.22572.
- Susuki, K., Chang, K. J., Zollinger, D. R., Liu, Y., Ogawa, Y., Eshed-Eisenbach, Y., et al. (2013). Three mechanisms assemble central nervous system nodes of ranvier. *Neuron* 78, 469–482. doi:10.1016/j.neuron.2013.03.005.
- Svoboda, K., Denk, W., Kleinfeld, D., and Tank, D. W. (1997). In vivo dendritic calcium dynamics in neocortical pyramidal neurons. *Nature* 385, 161–165. doi:10.1038/385161a0.
- Swire, M., Assinck, P., McNaughton, P. A., Lyons, D. A., French-Constant, C., and Livesey, M. R. (2021). Oligodendrocyte HCN2 Channels Regulate Myelin Sheath Length. *J. Neurosci.* 41, 7954–7964. doi:10.1523/jneurosci.2463-20.2021.
- Tait, S., Gunn-Moore, F., Collinson, J. M., Huang, J., Lubetzki, C., Pedraza, L., et al. (2000). An Oligodendrocyte Cell Adhesion Molecule at the Site of Assembly of the Paranodal Axo-Glial Junction. *J. Cell Biol.* 150, 657–666. doi:10.1083/jcb.150.3.657.
- Takahashi, K., Rochford, C. D. P., and Neumann, H. (2005). Clearance of apoptotic neurons without inflammation by microglial triggering receptor expressed on myeloid cells-2. *J. Exp. Med.* 201,

- 647–657. doi:10.1084/jem.20041611.
- Takeuchi, H., Sekiguchi, A., Taki, Y., Yokoyama, S., Yomogida, Y., Komuro, N., et al. (2010). Training of working memory impacts structural connectivity. *J. Neurosci.* 30, 3297–3303. doi:10.1523/JNEUROSCI.4611-09.2010.
- Tanaka, Y., Tozuka, Y., Takata, T., Shimazu, N., Matsumura, N., Ohta, A., et al. (2009). Excitatory GABAergic activation of cortical dividing glial cells. *Cereb. Cortex* 19, 2181–2195. doi:10.1093/cercor/bhn238.
- Tasaki, I. (1939). The electro-saltatory transmission of the nerve impulse and the effect of narcosis upon the nerve fiber. *Am. J. Phys.*, 211–227.
- Tay, T. L., Mai, D., Dautzenberg, J., Fernández-Klett, F., Lin, G., Sagar, S., et al. (2017). A new fate mapping system reveals context-dependent random or clonal expansion of microglia. *Nat. Neurosci.* 20, 793–803. doi:10.1038/nn.4547.
- Teissier, A., Le Magueresse, C., Olusakin, J., Andrade da Costa, B. L. S., De Stasi, A. M., Bacci, A., et al. (2020). Early-life stress impairs postnatal oligodendrogenesis and adult emotional behaviour through activity-dependent mechanisms. *Mol. Psychiatry* 25, 1159–1174. doi:10.1038/s41380-019-0493-2.
- Thetiot, M., Freeman, S. A., Roux, T., Dubessy, A., Aigrot, M., Rappeneau, Q., et al. (2020). An alternative mechanism of early nodal clustering and myelination onset in GABAergic neurons of the central nervous system. *Glia* 68, 1891–1909. doi:10.1002/glia.23812.
- Thetiot, M., Ronzano, R., Aigrot, M. S., Lubetzki, C., and Desmazières, A. (2019). Preparation and Immunostaining of Myelinating Organotypic Cerebellar Slice Cultures. *J. Vis. Exp.*, 1–7. doi:10.3791/59163.
- Thompson, A. J., Baranzini, S. E., Geurts, J., Hemmer, B., and Ciccarelli, O. (2018). Multiple sclerosis. *Lancet* 391, 1622–1636. doi:10.1016/S0140-6736(18)30481-1.
- Timsit, S., Martinez, S., Allinquant, B., Peyron, F., Puellas, L., and Zalc, B. (1995). Oligodendrocytes originate in a restricted zone of the embryonic ventral neural tube defined by DM-20 mRNA expression. *J. Neurosci.* 15, 1012–1024. doi:10.1523/JNEUROSCI.15-02-01012.1995.
- Todorich, B., Pasquini, J. M., Garcia, C. I., Paez, P. M., and Connor, J. R. (2009). Oligodendrocytes and myelination: The role of iron. *Glia* 57, 467–478. doi:10.1002/glia.20784.
- Tomassy, G. S., Berger, D. R., Chen, H.-H., Kasthuri, N., Hayworth, K. J., Vercelli, A., et al. (2014). Distinct Profiles of Myelin Distribution Along Single Axons of Pyramidal Neurons in the Neocortex. *Science (80-.)*. 344, 319–324. doi:10.1126/science.1249766.
- Tourneux, F., and Le Goff, R. (1875). Les étranglements des tubes nerveux de la moelle épinière. *J. Anat. Physiol. Norm. Pathol.* 11, 403–404.
- Traka, M., Goutebroze, L., Denisenko, N., Bessa, M., Nifli, A., Havaki, S., et al. (2003). Association of TAG-1 with Caspr2 is essential for the molecular organization of juxtaparanodal regions of myelinated fibers. *J. Cell Biol.* 162, 1161–1172. doi:10.1083/jcb.200305078.
- Trapp, B. D., Bernier, L., Andrews, S. B., and Colman, D. R. (1988). Cellular and Subcellular Distribution of 2',3'-Cyclic Nucleotide 3'-Phosphodiesterase and Its mRNA in the Rat Central Nervous System. *J. Neurochem.* 51, 859–868. doi:10.1111/j.1471-4159.1988.tb01822.x.
- Trapp, B. D., and Nave, K.-A. (2008). Multiple Sclerosis: An Immune or Neurodegenerative Disorder? *Annu. Rev. Neurosci.* 31, 247–269. doi:10.1146/annurev.neuro.30.051606.094313.
- Trapp, B. D., Nishiyama, A., Cheng, D., and Macklin, W. (1997). Differentiation and Death of Premyelinating Oligodendrocytes in Developing Rodent Brain. *J. Cell Biol.* 137, 459–468. doi:10.1083/jcb.137.2.459.
- Trapp, B. D., Wujek, J. R., Criste, G. A., Jalabi, W., Yin, X., Kidd, G. J., et al. (2007). Evidence for synaptic stripping by cortical microglia. *Glia* 55, 360–368. doi:10.1002/glia.20462.
- Tremblay, M. E., Lowery, R. L., and Majewska, A. K. (2010). Microglial interactions with synapses are modulated by visual experience. *PLoS Biol.* 8. doi:10.1371/journal.pbio.1000527.
- Trimmer, J. S. (2015). Subcellular localization of K⁺ channels in mammalian brain neurons: Remarkable precision in the midst of extraordinary complexity. *Neuron* 85, 238–256. doi:10.1016/j.neuron.2014.12.042.

- Tripathi, R. B., Jackiewicz, M., McKenzie, I. A., Kougioumtzidou, E., Grist, M., and Richardson, W. D. (2017). Remarkable Stability of Myelinating Oligodendrocytes in Mice. *Cell Rep.* 21, 316–323. doi:10.1016/j.celrep.2017.09.050.
- Tripathi, R. B., Rivers, L. E., Young, K. M., Jamen, F., and Richardson, W. D. (2010). NG2 Glia Generate New Oligodendrocytes But Few Astrocytes in a Murine Experimental Autoimmune Encephalomyelitis Model of Demyelinating Disease. *J. Neurosci.* 30, 16383–16390. doi:10.1523/JNEUROSCI.3411-10.2010.
- Turrigiano, G. (2012). Homeostatic Synaptic Plasticity: Local and Global Mechanisms for Stabilizing Neuronal Function. *Cold Spring Harb. Perspect. Biol.* 4, a005736–a005736. doi:10.1101/cshperspect.a005736.
- Turrigiano, G. G., Leslie, K. R., Desai, N. S., Rutherford, L. C., and Nelson, S. B. (1998). Activity-dependent scaling of quantal amplitude in neocortical neurons. *Nature* 391, 892–896. doi:10.1038/36103.
- Uemoto, Y., Suzuki, S., Terada, N., Ohno, N., Ohno, S., Yamanaka, S., et al. (2007). Specific Role of the Truncated β IV-Spectrin Σ 6 in Sodium Channel Clustering at Axon Initial Segments and Nodes of Ranvier. *J. Biol. Chem.* 282, 6548–6555. doi:10.1074/jbc.M609223200.
- Ueno, M., Fujita, Y., Tanaka, T., Nakamura, Y., Kikuta, J., Ishii, M., et al. (2013). Layer V cortical neurons require microglial support for survival during postnatal development. *Nat. Neurosci.* 16, 543–551. doi:10.1038/nn.3358.
- Umpierre, A. D., Bystrom, L. L., Ying, Y., Liu, Y. U., Worrell, G., and Wu, L.-J. (2020). Microglial calcium signaling is attuned to neuronal activity in awake mice. *Elife* 9. doi:10.7554/eLife.56502.
- Uweru, J. O., and Eyo, U. B. (2019). A decade of diverse microglial-neuronal physical interactions in the brain (2008–2018). *Neurosci. Lett.* 698, 33–38. doi:10.1016/j.neulet.2019.01.001.
- Vabnick, I., Novaković, S. D., Levinson, S. R., Schachner, M., and Shrager, P. (1996). The Clustering of Axonal Sodium Channels during Development of the Peripheral Nervous System. *J. Neurosci.* 16, 4914–4922. doi:10.1523/JNEUROSCI.16-16-04914.1996.
- Vagionitis, S., Auer, F., Xiao, Y., Almeida, R. G., Lyons, D. A., and Czopka, T. (2021). Clusters of neuronal Neurofascin prefigure node of Ranvier position along single axons. *bioRxiv*, 1–29.
- Vainchtein, I. D., Chin, G., Cho, F. S., Kelley, K. W., Miller, J. G., Chien, E. C., et al. (2018). Astrocyte-derived interleukin-33 promotes microglial synapse engulfment and neural circuit development. *Science (80-)*. 359, 1269–1273. doi:10.1126/science.aal3589.
- Valerio, A., Ferrario, M., Dreano, M., Garotta, G., Spano, P., and Pizzi, M. (2002). Soluble interleukin-6 (IL-6) receptor/IL-6 fusion protein enhances in vitro differentiation of purified rat oligodendroglial lineage cells. *Mol. Cell. Neurosci.* 21, 602–15. doi:10.1006/mcne.2002.1208.
- Vallstedt, A., Klos, J. M., and Ericson, J. (2005). Multiple Dorsoventral Origins of Oligodendrocyte Generation in the Spinal Cord and Hindbrain. *Neuron* 45, 55–67. doi:10.1016/j.neuron.2004.12.026.
- van Leeuwenhoek, A. (1719). *Epistola XXXII. Epistolae Physiologicae Super Compluribus Naturae Arcanis*. Delft, Adr.
- Van Strien, M. E., Baron, W., Bakker, E. N. T. P., Bauer, J., Bol, J. G. J. M., Brevé, J. J. P., et al. (2011). Tissue transglutaminase activity is involved in the differentiation of oligodendrocyte precursor cells into myelin-forming oligodendrocytes during CNS remyelination. *Glia* 59, 1622–1634. doi:10.1002/glia.21204.
- Varga, D. P., Menyhárt, Á., Pósfai, B., Császár, E., Lénárt, N., Cserép, C., et al. (2020). Microglia alter the threshold of spreading depolarization and related potassium uptake in the mouse brain. *J. Cereb. Blood Flow Metab.* doi:10.1177/0271678X19900097.
- Vela, J. M., Molina-Holgado, E., Arévalo-Martín, A., Almazán, G., and Guaza, C. (2002). Interleukin-1 regulates proliferation and differentiation of oligodendrocyte progenitor cells. *Mol. Cell. Neurosci.* 20, 489–502. doi:10.1006/mcne.2002.1127.
- Velez-Fort, M., Maldonado, P. P., Butt, A. M., Audinat, E., and Angulo, M. C. (2010). Postnatal Switch from Synaptic to Extrasynaptic Transmission between Interneurons and NG2 Cells. *J. Neurosci.* 30, 6921–6929. doi:10.1523/JNEUROSCI.0238-10.2010.

- Vesalius, A. (1543). *De Humani Corporis Fabrica Libri Septem*.
- Virchow, R. (1858). *Die Cellularpathologie in ihrer Begründung auf physiologische und pathologische Gewebelehre*. August Hir., ed. 1860. Translated in English by F. Chance Berlin: Cellular Pathology, John Churchill, London.
- Viswanathan, G. M., Buldyrev, S. V., Havlin, S., da Luz, M. G. E., Raposo, E. P., and Stanley, H. E. (1999). Optimizing the success of random searches. *Nature* 401, 911–914. doi:10.1038/44831.
- von Bartheld, C. S., Bahney, J., and Herculano-Houzel, S. (2016). The search for true numbers of neurons and glial cells in the human brain: A review of 150 years of cell counting. *J. Comp. Neurol.* 524, 3865–3895. doi:10.1002/cne.24040.
- Voss, E. V., Škuljec, J., Gudi, V., Skripuletz, T., Pul, R., Trebst, C., et al. (2012). Characterisation of microglia during de- and remyelination: Can they create a repair promoting environment? *Neurobiol. Dis.* 45, 519–528. doi:10.1016/j.nbd.2011.09.008.
- Wake, H., Lee, P. R., and Fields, R. D. (2011). Control of local protein synthesis and initial events in myelination by action potentials. *Science (80-)*. 333, 1647–1651. doi:10.1126/science.1206998.
- Wake, H., Moorhouse, A. J., Jinno, S., Kohsaka, S., and Nabekura, J. (2009). Resting microglia directly monitor the functional state of synapses in vivo and determine the fate of ischemic terminals. *J. Neurosci.* 29, 3974–3980. doi:10.1523/JNEUROSCI.4363-08.2009.
- Wake, H., Ortiz, F. C., Woo, D. H., Lee, P. R., Angulo, M. C., and Fields, R. D. (2015). Nonsynaptic junctions on myelinating glia promote preferential myelination of electrically active axons. *Nat. Commun.* 6. doi:10.1038/ncomms8844.
- Wakselman, S., Béchade, C., Roumier, A., Bernard, D., Triller, A., and Bessis, A. (2008). Developmental neuronal death in hippocampus requires the microglial CD11b integrin and DAP12 immunoreceptor. *J. Neurosci.* 28, 8138–8143. doi:10.1523/JNEUROSCI.1006-08.2008.
- Walker, B. A., Hengst, U., Kim, H. J., Jeon, N. L., Schmidt, E. F., Heintz, N., et al. (2012). Reprogramming axonal behavior by axon-specific viral transduction. *Gene Ther.* 19, 947–955. doi:10.1038/gt.2011.217.
- Wall, P. (1995). Do nerve impulses penetrate terminal arborizations? A pre-presynaptic control mechanism. *Trends Neurosci.* 18, 99–103. doi:10.1016/0166-2236(95)93883-Y.
- Wallner, S., and Schmitz, G. (2011). Plasmalogens the neglected regulatory and scavenging lipid species. *Chem. Phys. Lipids* 164, 573–589. doi:10.1016/j.chemphyslip.2011.06.008.
- Wang, C., Yue, H., Hu, Z., Shen, Y., Ma, J., Li, J., et al. (2020a). Microglia mediate forgetting via complement-dependent synaptic elimination. *Science (80-)*. 367, 688–694. doi:10.1126/science.aaz2288.
- Wang, F., Ren, S., Chen, J., Liu, K., Li, R.-X., Li, Z., et al. (2020b). Myelin degeneration and diminished myelin renewal contribute to age-related deficits in memory. *Nat. Neurosci.* 23, 481–486. doi:10.1038/s41593-020-0588-8.
- Wang, H., Kunkel, D. D., Martin, T. M., Schwartzkroin, P. A., and Tempel, B. L. (1993). Heteromultimeric K⁺ channels in terminal and juxtaparanodal regions of neurons. *Nature* 365, 75–9. doi:10.1038/365075a0.
- Wang, H. S., Brown, B. S., McKinnon, D., and Cohen, I. S. (2000). Molecular basis for differential sensitivity of KCNQ and I(Ks) channels to the cognitive enhancer XE991. *Mol. Pharmacol.* 57, 1218–23. Available at: <http://www.ncbi.nlm.nih.gov/pubmed/10825393>.
- Wang, H. S., Pan, Z., Shi, W., Brown, B. S., Wymore, R. S., Cohen, I. S., et al. (1998). KCNQ2 and KCNQ3 potassium channel subunits: molecular correlates of the M-channel. *Science* 282, 1890–3. doi:10.1126/science.282.5395.1890.
- Watanabe, M., Hadzic, T., and Nishiyama, A. (2004). Transient upregulation of Nkx2.2 expression in oligodendrocyte lineage cells during remyelination. *Glia* 46, 311–322. doi:10.1002/glia.20006.
- Watkins, T. A., Emery, B., Mulinyawe, S., and Barres, B. A. (2008). Distinct Stages of Myelination Regulated by γ -Secretase and Astrocytes in a Rapidly Myelinating CNS Coculture System. *Neuron* 60, 555–569. doi:10.1016/j.neuron.2008.09.011.
- Waxman, S. G. (2006). Axonal conduction and injury in multiple sclerosis: The role of sodium channels. *Nat. Rev. Neurosci.* 7, 932–941. doi:10.1038/nrn2023.

- Waxman, S. G., and Bennett, M. V. L. (1972). Relative Conduction Velocities of Small Myelinated and Non-myelinated Fibres in the Central Nervous System. *Nat. New Biol.* 238, 217–219. doi:10.1038/newbio238217a0.
- Waxman, S. G., Craner, M. J., and Black, J. A. (2004). Na⁺ channel expression along axons in multiple sclerosis and its models. *Trends Pharmacol. Sci.* 25, 584–591. doi:10.1016/j.tips.2004.09.001.
- Waxman, S. G., and Ritchie, J. M. (1993). Molecular dissection of the myelinated axon. *Ann. Neurol.* 33, 121–136. doi:10.1002/ana.410330202.
- Waxman, S. G., and Swadlow, H. A. (1976). Ultrastructure of visual callosal axons in the rabbit. *Exp. Neurol.* 53, 115–127. doi:10.1016/0014-4886(76)90287-9.
- Weber, P., Bartsch, U., Rasband, M. N., Czaniara, R., Lang, Y., Bluethmann, H., et al. (1999). Mice Deficient for Tenascin-R Display Alterations of the Extracellular Matrix and Decreased Axonal Conduction Velocities in the CNS. *J. Neurosci.* 19, 4245–4262. doi:10.1523/JNEUROSCI.19-11-04245.1999.
- Wei, A. D., Gutman, G. A., Aldrich, R., Chandy, K. G., Grissmer, S., and Wulff, H. (2005). International Union of Pharmacology. LII. Nomenclature and Molecular Relationships of Calcium-Activated Potassium Channels. *Pharmacol. Rev.* 57, 463–472. doi:10.1124/pr.57.4.9.
- Weinhard, L., di Bartolomei, G., Bolasco, G., Machado, P., Schieber, N. L., Neniskyte, U., et al. (2018). Microglia remodel synapses by presynaptic trogocytosis and spine head filopodia induction. *Nat. Commun.* 9, 1228. doi:10.1038/s41467-018-03566-5.
- Wellbourne-Wood, J., Rimmele, T. S., and Chatton, J.-Y. (2017). Imaging extracellular potassium dynamics in brain tissue using a potassium-sensitive nanosensor. *Neurophotonics* 4, 015002. doi:10.1117/1.nph.4.1.015002.
- Werneburg, S., Jung, J., Kunjamma, R. B., Ha, S.-K., Luciano, N. J., Willis, C. M., et al. (2019). Targeted Complement Inhibition at Synapses Prevents Microglial Synaptic Engulfment and Synapse Loss in Demyelinating Disease. *Immunity*, 1–16. doi:10.1016/j.immuni.2019.12.004.
- Werner, H. B., Krämer-Albers, E.-M., Strenzke, N., Saher, G., Tenzer, S., Ohno-Iwashita, Y., et al. (2013). A critical role for the cholesterol-associated proteolipids PLP and M6B in myelination of the central nervous system. *Glia* 61, 567–586. doi:10.1002/glia.22456.
- William A. Catterall (2000). From Ionic Currents to Molecular Review Mechanisms: The Structure and Function of Voltage-Gated Sodium Channels. *Neuron* 26, 13–25. Available at: [https://www.cell.com/neuron/pdf/S0896-6273\(00\)81133-2.pdf](https://www.cell.com/neuron/pdf/S0896-6273(00)81133-2.pdf).
- Williams, A., Piaton, G., Aigrot, M.-S., Belhadi, A., Theaudin, M., Petermann, F., et al. (2007). Semaphorin 3A and 3F: key players in myelin repair in multiple sclerosis? *Brain* 130, 2554–2565. doi:10.1093/brain/awm202.
- Winkler, C. C., Yabut, O. R., Fregoso, S. P., Gomez, H. G., Dwyer, B. E., Pleasure, S. J., et al. (2018). The Dorsal Wave of Neocortical Oligodendrogenesis Begins Embryonically and Requires Multiple Sources of Sonic Hedgehog. *J. Neurosci.* 38, 5237–5250. doi:10.1523/JNEUROSCI.3392-17.2018.
- Wlodarczyk, A., Cédile, O., Jensen, K. N., Jasson, A., Mony, J. T., Khorooshi, R., et al. (2015). Pathologic and Protective Roles for Microglial Subsets and Bone Marrow- and Blood-Derived Myeloid Cells in Central Nervous System Inflammation. *Front. Immunol.* 6. doi:10.3389/fimmu.2015.00463.
- Wlodarczyk, A., Holtman, I. R., Krueger, M., Yogev, N., Bruttger, J., Khorooshi, R., et al. (2017). A novel microglial subset plays a key role in myelinogenesis in developing brain. *EMBO J.* 36, 3292–3308. doi:10.15252/embj.201696056.
- Woodruff, R. H., and Franklin, R. J. M. (1999). Demyelination and remyelination of the caudal cerebellar peduncle of adult rats following stereotaxic injections of lysolecithin, ethidium bromide, and complement/anti-galactocerebroside: A comparative study. *Glia* 25, 216–228. doi:10.1002/(SICI)1098-1136(19990201)25:3<216::AID-GLIA2>3.0.CO;2-L.
- Wulff, H., Miller, M. J., Hansel, W., Grissmer, S., Cahalan, M. D., and Chandy, K. G. (2000). Design of a potent and selective inhibitor of the intermediate-conductance Ca²⁺-activated K⁺ channel, IKCa1: A potential immunosuppressant. *Proc. Natl. Acad. Sci.* 97, 8151–8156. doi:10.1073/pnas.97.14.8151.

- Xiao, L., Ohayon, D., McKenzie, I. A., Sinclair-Wilson, A., Wright, J. L., Fudge, A. D., et al. (2016). Rapid production of new oligodendrocytes is required in the earliest stages of motor-skill learning. *Nat. Neurosci.* 19, 1210–1217. doi:10.1038/nn.4351.
- Xu, J., Zhu, L., He, S., Wu, Y., Jin, W., Yu, T., et al. (2015). Temporal-Spatial Resolution Fate Mapping Reveals Distinct Origins for Embryonic and Adult Microglia in Zebrafish. *Dev. Cell* 34, 632–641. doi:10.1016/j.devcel.2015.08.018.
- Yamasaki, R., Lu, H., Butovsky, O., Ohno, N., Rietsch, A. M., Cialic, R., et al. (2014). Differential roles of microglia and monocytes in the inflamed central nervous system. *J. Exp. Med.* 211, 1533–1549. doi:10.1084/jem.20132477.
- Yang, S. M., Michel, K., Jokhi, V., Nedivi, E., and Arlotta, P. (2020). Neuron class-specific responses govern adaptive myelin remodeling in the neocortex. *Science* (80-.). 370. doi:10.1126/science.abd2109.
- Yang, T., Guo, Z., Luo, C., Li, Q., Yan, B., Liu, L., et al. (2012). White matter impairment in the basal ganglia-thalamocortical circuit of drug-naïve childhood absence epilepsy. *Epilepsy Res.* 99, 267–73. doi:10.1016/j.eplepsyres.2011.12.006.
- Yang, Y. (2004). IV Spectrins Are Essential for Membrane Stability and the Molecular Organization of Nodes of Ranvier. *J. Neurosci.* 24, 7230–7240. doi:10.1523/JNEUROSCI.2125-04.2004.
- Yang, Y., Ogawa, Y., Hedstrom, K. L., and Rasband, M. N. (2007). β IV spectrin is recruited to axon initial segments and nodes of Ranvier by ankyrinG. *J. Cell Biol.* 176, 509–519. doi:10.1083/jcb.200610128.
- Yap, E.-L., and Greenberg, M. E. (2018). Activity-Regulated Transcription: Bridging the Gap between Neural Activity and Behavior. *Neuron* 100, 330–348. doi:10.1016/j.neuron.2018.10.013.
- Yeung, M. S. Y., Djelloul, M., Steiner, E., Bernard, S., Salehpour, M., Possnert, G., et al. (2019). Dynamics of oligodendrocyte generation in multiple sclerosis. *Nature* 566, 538–542. doi:10.1038/s41586-018-0842-3.
- Yeung, M. S. Y., Zdunek, S., Bergmann, O., Bernard, S., Salehpour, M., Alkass, K., et al. (2014). Dynamics of oligodendrocyte generation and myelination in the human brain. *Cell* 159, 766–774. doi:10.1016/j.cell.2014.10.011.
- Yin, X., Peterson, J., Gravel, M., Braun, P. E., and Trapp, B. D. (1997). CNP overexpression induces aberrant oligodendrocyte membranes and inhibits MBP accumulation and myelin compaction. *J. Neurosci. Res.* 50, 238–247. doi:10.1002/(SICI)1097-4547(19971015)50:2<238::AID-JNR12>3.0.CO;2-4.
- Young, K. M., Psachoulia, K., Tripathi, R. B., Dunn, S. J., Cossell, L., Attwell, D., et al. (2013). Oligodendrocyte dynamics in the healthy adult CNS: Evidence for myelin remodeling. *Neuron* 77, 873–885. doi:10.1016/j.neuron.2013.01.006.
- Yu, Z., Sun, D., Feng, J., Tan, W., Fang, X., Zhao, M., et al. (2015). MSX3 Switches Microglia Polarization and Protects from Inflammation-Induced Demyelination. *J. Neurosci.* 35, 6350–6365. doi:10.1523/JNEUROSCI.2468-14.2015.
- Zabala, A., Vazquez-Villoldo, N., Rissiek, B., Gejo, J., Martin, A., Palomino, A., et al. (2018). P2X4 receptor controls microglia activation and favors remyelination in autoimmune encephalitis. *EMBO Mol. Med.* 10, 1–20. doi:10.15252/emmm.201708743.
- Zalc, B., Goujet, D., and Colman, D. (2008). The origin of the myelination program in vertebrates. *Curr. Biol.* 18, 511–512. doi:10.1016/j.cub.2008.04.010.
- Zalc, B., Monge, M., Dupouey, P., Hauw, J. J., and Baumann, N. A. (1981). Immunohistochemical localization of galactosyl and sulfogalactosyl ceramide in the brain of the 30-day-old mouse. *Brain Res.* 211, 341–354. doi:10.1016/0006-8993(81)90706-X.
- Zatorre, R. J., Fields, R. D., and Johansen-Berg, H. (2012). Plasticity in gray and white: Neuroimaging changes in brain structure during learning. *Nat. Neurosci.* 15, 528–536. doi:10.1038/nn.3045.
- Zawadzka, M., Rivers, L. E., Fancy, S. P. J., Zhao, C., Tripathi, R., Jamen, F., et al. (2010). CNS-Resident Glial Progenitor/Stem Cells Produce Schwann Cells as well as Oligodendrocytes during Repair of CNS Demyelination. *Cell Stem Cell* 6, 578–590. doi:10.1016/j.stem.2010.04.002.
- Zeger, M., Popken, G., Zhang, J., Xuan, S., Lu, Q. R., Schwab, M. H., et al. (2007). Insulin-like growth

- factor type 1 receptor signaling in the cells of oligodendrocyte lineage is required for normal in vivo oligodendrocyte development and myelination. *Glia* 55, 400–411. doi:10.1002/glia.20469.
- Zhang, A., Desmazieres, A., Zonta, B., Melrose, S., Campbell, G., Mahad, D., et al. (2015). Neurofascin 140 Is an Embryonic Neuronal Neurofascin Isoform That Promotes the Assembly of the Node of Ranvier. *J. Neurosci.* 35, 2246–2254. doi:10.1523/JNEUROSCI.3552-14.2015.
- Zhang, C. L., Ho, P. L., Kintner, D. B., Sun, D., and Chiu, S. Y. (2010). Activity-dependent regulation of mitochondrial motility by calcium and Na/K-ATPase at nodes of ranvier of myelinated nerves. *J. Neurosci.* 30, 3555–3566. doi:10.1523/JNEUROSCI.4551-09.2010.
- Zhang, J., Yang, X., Zhou, Y., Fox, H., and Xiong, H. (2019). Direct contacts of microglia on myelin sheath and Ranvier’s node in the corpus callosum in rats. *J. Biomed. Res.* 33, 192–200. doi:10.7555/JBR.32.20180019.
- Zhang, S.-C., Goetz, B. D., Carré, J.-L., and Duncan, I. D. (2001). Reactive microglia in dysmyelination and demyelination. *Glia* 34, 101–109. doi:10.1002/glia.1045.
- Zhang, X., and Bennett, V. (1998). Restriction of 480/270-kD Ankyrin G to Axon Proximal Segments Requires Multiple Ankyrin G-specific Domains. *J. Cell Biol.* 142, 1571–1581. doi:10.1083/jcb.142.6.1571.
- Zhang, X., Surguladze, N., Slagle-Webb, B., Cozzi, A., and Connor, J. R. (2006). Cellular iron status influences the functional relationship between microglia and oligodendrocytes. *Glia* 54, 795–804. doi:10.1002/glia.20416.
- Zhang, Y., Chen, K., Sloan, S. A., Bennett, M. L., Scholze, A. R., O’Keeffe, S., et al. (2014). An RNA-sequencing transcriptome and splicing database of glia, neurons, and vascular cells of the cerebral cortex. *J. Neurosci.* 34, 11929–11947. doi:10.1523/JNEUROSCI.1860-14.2014.
- Zhang, Y., Sloan, S. A., Clarke, L. E., Caneda, C., Plaza, C. A., Blumenthal, P. D., et al. (2016). Purification and Characterization of Progenitor and Mature Human Astrocytes Reveals Transcriptional and Functional Differences with Mouse. *Neuron* 89, 37–53. doi:10.1016/j.neuron.2015.11.013.
- Zhu, X., Hill, R. A., Dietrich, D., Komitova, M., Suzuki, R., and Nishiyama, A. (2011). Age-dependent fate and lineage restriction of single NG2 cells. *Development* 138, 745–753. doi:10.1242/dev.047951.
- Zhu, Y., Xu, J., and Heinemann, S. F. (2009). Two Pathways of Synaptic Vesicle Retrieval Revealed by Single-Vesicle Imaging. *Neuron* 61, 397–411. doi:10.1016/j.neuron.2008.12.024.
- Ziskin, J. L., Nishiyama, A., Rubio, M., Fukaya, M., and Bergles, D. E. (2007). Vesicular release of glutamate from unmyelinated axons in white matter. *Nat. Neurosci.* 10, 321–330. doi:10.1038/nn1854.
- Zonouzi, M., Scafidi, J., Li, P., McEllin, B., Edwards, J., Dupree, J. L., et al. (2015). GABAergic regulation of cerebellar NG2 cell development is altered in perinatal white matter injury. *Nat. Neurosci.* 18, 674–682. doi:10.1038/nn.3990.
- Zonta, B., Tait, S., Melrose, S., Anderson, H., Harroch, S., Higginson, J., et al. (2008). Glial and neuronal isoforms of Neurofascin have distinct roles in the assembly of nodes of Ranvier in the central nervous system. *J. Cell Biol.* 181, 1169–1177. doi:10.1083/jcb.200712154.
- Zoupi, L., Markoullis, K., Kleopa, K. A., and Karagogeos, D. (2013). Alterations of juxtapanodal domains in two rodent models of CNS demyelination. *Glia* 61, 1236–1249. doi:10.1002/glia.22511.
- Zrzavy, T., Hametner, S., Wimmer, I., Butovsky, O., Weiner, H. L., and Lassmann, H. (2017). Loss of ‘homeostatic’ microglia and patterns of their activation in active multiple sclerosis. *Brain* 140, 1900–1913. doi:10.1093/brain/awx113.
- Zuchero, J. B., Fu, M. meng, Sloan, S. A., Ibrahim, A., Olson, A., Zaremba, A., et al. (2015). CNS Myelin Wrapping Is Driven by Actin Disassembly. *Dev. Cell* 34, 152–167. doi:10.1016/j.devcel.2015.06.011.

Résumé

La conduction saltatoire le long des fibres myélinisées repose sur l'alternance de segments myélinisés, les internœuds, et de petits domaines amyéliniques enrichis en canaux sodiques voltage dépendants, les nœuds de Ranvier. Dans la sclérose en plaques (SEP), pathologie inflammatoire démyélinisante du système nerveux central, il y a une démyélinisation, qui conduit à des déficits fonctionnels et à une perte neuronale. Il n'existe à ce jour aucun traitement permettant de promouvoir efficacement la remyélinisation et de prévenir la neurodégénération. La compréhension des mécanismes sous-jacents à la remyélinisation et l'identification de cibles thérapeutiques potentielles permettant de limiter la progression de la pathologie sont donc des enjeux majeurs dans la SEP. Lors de la démyélinisation, l'organisation des protéines nodales est altérée, ce qui participe aux défauts de conduction axonale. Il a par ailleurs été montré que des structures nodales, nommées prénoeuds, peuvent se reformer précocement, avant même la remyélinisation, un mécanisme également observé lors de la myélinisation développementale. Ces résultats suggèrent que les prénoeuds pourraient participer au processus de réparation dans la SEP. De plus, les cellules microgliales, qui sont les cellules immunes résidentes du système nerveux central, ont été identifiées comme des acteurs majeurs de la remyélinisation. Le dialogue entre microglie et neurone lors de la remyélinisation reste cependant à décrire.

Au cours de ma thèse, nous avons montré que la microglie contacte les nœuds de Ranvier dans l'ensemble du système nerveux central et que ces contacts sont renforcés au cours de la remyélinisation. Nous avons identifié les nœuds comme des sites préférentiels d'interaction le long des axones myélinisés et avons montré que l'activité neuronale permet de stabiliser ces interactions, via les flux potassiques qu'elle induit. Lors de la remyélinisation, la perturbation de ce signal potassique induit une diminution de l'interaction microglie-nœud, associée à une altération du passage de la microglie vers un phénotype pro-régénératif et à une réduction de la remyélinisation. Ces derniers résultats suggèrent que l'interaction entre cellules microgliales et nœuds de Ranvier pourrait donc moduler la remyélinisation.

Dans la seconde partie de ma thèse, qui correspond à un travail en cours, nous avons montré que l'activité neuronale favorise la formation des prénoeuds. Ce mécanisme, qui pourrait être conservé durant la remyélinisation, pourrait avoir un rôle important dans la réparation.

L'ensemble de ces résultats identifie le nœud de Ranvier comme un acteur important dans le processus de (re)myélinisation. Par ailleurs, ils montrent que l'activité neuronale pourrait promouvoir la (re)myélinisation, non seulement par des effets directs sur le lignage oligodendrocytaire, mais aussi indirectement en modulant les fonctions microgliales et la formation des domaines nodaux.

Summary

Fast saltatory conduction along myelinated axons is based on insulated segments, the internodes, alternating with small myelinic domains enriched in voltage-gated sodium channels, the nodes of Ranvier. In Multiple Sclerosis (MS), an inflammatory demyelinating disease of the central nervous system, there is a primary demyelination leading to axonal conduction alteration, and with time to neurodegeneration. So far, there is a lack of efficient treatment to promote remyelination, enhance neuroprotection and slow handicap progression in MS. In this context, it is of paramount importance to better understand the underlying mechanisms promoting an efficient remyelination and to identify potential targets for future treatments.

The nodes of Ranvier have been identified as an early target of monocyte derived macrophages in demyelinating lesions. It was further shown that voltage-gated channels can form clusters, named node-like clusters, prior to remyelination in MS, a mechanism also observed during developmental myelination. Therefore, nodal structures might modulate remyelination. Microglia, the resident immune cells of the central nervous system have been shown to interact with neurons and were identified as major regulator of remyelination. However, the crosstalk between microglia and neurons during remyelination and how it could affect repair remained unknown.

During my thesis, we showed that microglia contact node of Ranvier throughout the central nervous system and that this interaction is reinforced in remyelination. We further showed that the node of Ranvier is a preferential domain of interaction with microglia along myelinated axons, and that this interaction is modulated by neuronal activity stimulation and in particular by potassium fluxes at nodes. Inhibiting potassium fluxes at nodes alters microglia-node interaction and leads during remyelination to an alteration of microglial switch toward a pro-regenerative phenotype and to a reduced remyelination. These results suggest that microglia-neuron interaction at the node of Ranvier may modulate the pro-remyelinating effect of microglia in repair.

The second part of my thesis which is currently carried on, showed that neuronal activity promotes the formation of node-like clusters prior to myelination, a mechanism that may be conserved in remyelination and may modulate repair.

Taken together the results of my thesis identify the node of Ranvier as an important player in the modulation of (re)myelination. Furthermore, it shows that neuronal activity may promote (re)myelination not only through its effect on oligodendroglial cells but also indirectly through modulation of microglia and nodal domain formation.